AD NUMBER

ADB013240

LIMITATION CHANGES

TO:

Approved for public release; distribution is unlimited. Document partially illegible.

FROM:

Distribution authorized to U.S. Gov't. agencies only; Test and Evaluation; FEB 1976. Other requests shall be referred to Air Force Flight Dynamic Laboratory, Structures Division, FBS, Wright-Patterson AFB, OH 45433. Document partially illegible.

AUTHORITY

afal ltr, 22 may 1978

AFFDL-TR-76-10

ADVANCED DESIGN COMPOSITE AIRCRAFT

ROCKWELL INTERNATIONAL
5701 W. IMPERIAL HWY.
LOS ANGELES, CA 90009

APRIL 1976

TECHNICAL REPORT AFFDL-TR-76-10
FINAL REPORT FOR PERIOD JULY – DECEMBER 1975

AIR FORCE FLIGHT DYNAMICS LABORATORIES
AIR FORCE WRIGHT AERONAUTICAL LABORATORIES
AIR FORCE SYSTEMS COMMAND
WRIGHT-PATTERSON AIR FORCE BASE, OHIO 45433

NOTICES

When Government drawings, specifications, or other data are used for any purpose other than in connection with a definitely related Government procurement operation, the United States Government thereby incurs no responsibility nor any obligation whatsoever, and the fact that the Government may have formulated, furnished, or in any way supplied the said drawings, specifications, or other data is not to be regarded by implication or otherwise as in any manner licensing the holder or any other person or corporation, or conveying any rights or permission to manufacture, use, or sell any patented invention that may in any way be related thereto.

This technical report has been reviewed and is approved for publication.

Engbert T. Bannink

Engbert T. Bannink, Jr.
Aerospace Engineer
Structural Mechanics Division
Air Force Flight Dynamics Laboratory

Larry G. Kelly

Larry G. Kelly, Acting Chief
Advanced Structures Development Branch
Structural Mechanics Division
Air Force Flight Dynamics Laboratory

FOR THE COMMANDER

Gerald G. Leigh

GERALD G. LEIGH, Lt Col, USAF
Chief, Structures Division

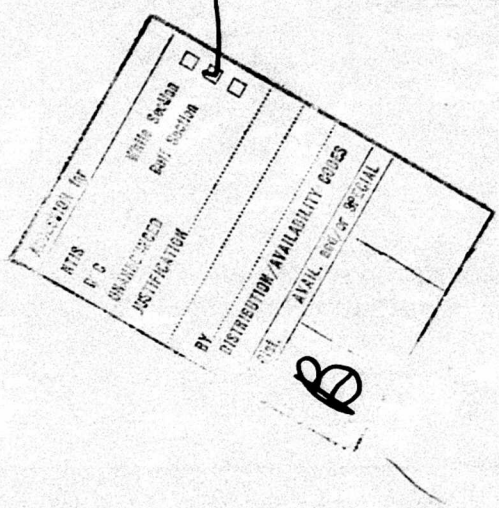

Copies of this report should not be returned unless return is required by security considerations, contractual obligations, or notice on a specific document.

AIR FORCE - 20 AUGUST 76 - 100

(9) Final technical rept. 25 Jun – 19 Dec 75

UNCLASSIFIED

SECURITY CLASSIFICATION OF THIS PAGE (When Data Entered)

(19) REPORT DOCUMENTATION PAGE		READ INSTRUCTIONS BEFORE COMPLETING FORM
(18) 1. REPORT NUMBER: AFFDL-TR-76-10	2. GOVT ACCESSION NO.	3. RECIPIENT'S CATALOG NUMBER
(6) 4. TITLE (and Subtitle): ADVANCED DESIGN COMPOSITE AIRCRAFT		5. TYPE OF REPORT & PERIOD COVERED: Final Technical Report July-September 1975
		(14) 6. PERFORMING ORG. REPORT NUMBER: NA-75-536-1
(10) 7. AUTHOR(s): B.F. Baumann, T. Goebel, E. Jaffe, F. McQuilkin, G. Minnick, M. Nadler, F. Reimer, D. Robinson, R. Wykes, L. Young		(15) 8. CONTRACT OR GRANT NUMBER(s): F33615-75-C-3157
9. PERFORMING ORGANIZATION NAME AND ADDRESS: Rockwell International, Los Angeles, Aircraft Division, International Airport, Los Angeles, California 90009		10. PROGRAM ELEMENT, PROJECT, TASK AREA & WORK UNIT NUMBERS: FY1456-75-00516/1368-01-35
(12) 378 p. 11. CONTROLLING OFFICE NAME AND ADDRESS: Air Force Flight Dynamics Laboratory, Attn: AFFDL/FBS - Contract No.F33615-75-C-3157, Item No. 0002, Sequence No. A00B, Wright-Patterson AFB, Ohio 45433		(11) 12. REPORT DATE: Feb[illegible]976; 13. NUMBER OF PAGES: 341
14. MONITORING AGENCY NAME & ADDRESS (if different from Controlling Office): Air Force Flight Dynamics Laboratory, Attn: AFFDL/FBS - Contract No.F33615-75-C-3157, Item No. 0002, Sequence No. A00B, Wright-Patterson AFB, Ohio 45433		15. SECURITY CLASS. (of this report): Unclassified; 15a. DECLASSIFICATION/DOWNGRADING SCHEDULE

16. DISTRIBUTION STATEMENT (of this Report)

Distribution limited to U.S. Government agencies only; test and evaluation data, February 1976. Other requests for this document must be referred to the Structures Division (FBS), Air Force Flight Dynamics Laboratory, Wright-Patterson AFB, Ohio 45433.

17. DISTRIBUTION STATEMENT (of the abstract entered in Block 20, if different from Report)

(16) AF-1368 (17) 136801

Approved for public release, distribution unlimited.

18. SUPPLEMENTARY NOTES

19. KEY WORDS (Continue on reverse side if necessary and identify by block number)

advanced composites, all-composite aircraft

20. ABSTRACT (Continue on reverse side if necessary and identify by block number)

This study was conducted to identify the payoff of advanced composite materials, in comparison to advanced metallic materials, for design of future fighter aircraft in the early 1980 time period. A mission, typical of a deep-strike, supersonic penetration, interdiction fighter, is selected for use in the design of an all-composite fighter incorporating advanced composite materials into 70 to 80 percent of its empty weight. The cost, weight, and performance

DD FORM 1 JAN 73 1473 EDITION OF 1 NOV 65 IS OBSOLETE

UNCLASSIFIED

SECURITY CLASSIFICATION OF THIS PAGE (When Data Entered)

408245 LB

20. ABSTRACT (Continued)

characteristics of this aircraft are compared to a fighter, designed to the same mission, which utilizes advanced metallic structure and about 10 percent of advanced composite materials.

FOREWORD

This report was prepared for the Air Force Flight Dynamics Laboratory (AFFDL) by the Los Angeles Aircraft Division of Rockwell International. This is the final technical report for the Advanced Design Composite Aircraft (ADCA) study program, conducted under contract F33615-75-C-3157, project task No. 1368-01-35. The period of contract performance is 25 June 1975 to 19 December 1975. Submittal date of the final report is February 1976. Mr. Larry Kelly, AFFDL/FBSC, is group leader, Advanced Structure Technology Group, Structure Division of the AFDL, and Capt. E. T. Bannink, AFFDL/FBSC, is the ADCA project engineer for the USAF. Mr. B. F. Baumann is program manager for Rockwell. Key assistants are Mr. E. Jaffe, deputy program manager; Mr. D. Robinson, configuration development and mission trade studies; Mr. F. McQuilkin, structural design; Mr. T. Goebel, aerodynamics; Mr. P. Jesse and Mr. M. Nadler, manufacturing; Mr. G. Minnick, mass properties; Mr. L. Young, propulsion; Mr. F. Reimer, operations and cost analysis; Mr. T. Matoi, structure analysis; and Mr. C. Crother, flight controls.

TABLE OF CONTENTS

TABLE OF CONTENTS (Continued)

TABLE OF CONTENTS (Concluded)

LIST OF ILLUSTRATIONS

LIST OF ILLUSTRATIONS (Continued)

LIST OF ILLUSTRATIONS (Continued)

LIST OF ILLUSTRATIONS (Continued)

LIST OF ILLUSTRATIONS (Concluded)

LIST OF TABLES

LIST OF SYMBOLS

A	Area sq in., sq meters
a (in.)	Panel dimension
A (in.^{2})	Area
a.c.	Aerodynamic center
A_o/A_c	- Inlet mass flow ratio
AR	Aspect ratio of reference trapezoidal wing
b (in.)	Panel dimension subscript, bending
BSTR	Stringer or spar spacing, in.
c (in.)	Core height subscript, core subscript, compression
$\bar{c}$	Mean aerodynamic chord of reference trapezoidal wing, in.
C_D	Drag coefficient, D/qS_w
C_{d_β}	- $\frac{\text{Boattail drag coefficient}}{D_\beta/q_o A_{max}}$,
C_{d_i}	- Inlet drag coefficient, $D_i/q_o A_c$
C_{D_O}	Zero-lift-drag coefficient
C_{f_g}	- Nozzle thrust coefficient
C_L	Lift coefficient, L/qS_w
C_l	Rolling/Moment coefficient, $l/qS_w b$
C_M	Pitching/Moment coefficient, $M/qS_w \bar{c}$
C_n	Yawing/Moment coefficient, $n/qS_w b$

cr	Subscript, critical subscript, crushing
C_y	Side Force coefficient, Y/qS_w
E_x^c (Msi)	Longitudinal compression modulus
E_x^t (Msi)	Longitudinal tension modulus
E_y^c (Msi)	Transverse compression modulus
E_y^t (Msi)	Transverse tension modulus
F (psi)	Allowable stress
f(psi)	Applied stress
$(\ )_F$	Flexible or flap
f_b (psi)	Applied bending stress
f_c (psi)	Applied compressive stress
FCL	Applied compression stress in lower cover for negative vertical load factor, $lb/in.^2$
FCU	Applied compression stress in upper cover for positive vertical load factor, $lb/in.^2$
$F - D/F_{gi}$	$-\frac{\text{Thrust - drag}}{\text{Ideal gross thrust}}$
Fg/F_i, Fg/F_{g_i}	$-\frac{\text{Measured gross thrust}}{\text{Ideal gross thrust}}$
F^{isu} (ksi)	Interlaminar shear ultimate
$(F_j - Fa,_p)/F_i$	$-\frac{\text{Thrust - pressure drag}}{\text{Ideal gross thrust}}$ (NASA TN P-7906
f_s (psi)	Applied shear stress

FTU	Applied tension stress in upper cover for negative vertical load factor, $lb/in.^2$
F_x^{cu} (ksi)	Compression ultimate
F_x^{tu}	Longitudinal tensile ultimate
F_{xy}^{su}	In-plane shear ultimate
F_y^{cu} (ksi)	Transverse compression ultimate
F_y^{tu} (ksi)	Transverse tensile ultimate
g	Gravitational constant, 32 ft/sec^2
G_{xy} (Msi)	In-plane shear modulus
G'_{cx} (psi)	Core shear modulus (longitudinal)
G'_{cy} (psi)	Core shear modulus (transverse)
I ($in.^4$)	Inertia
K	Buckling coefficient
K_g	Coefficient (panel shear for p loading)
K_M	Coefficient (panel moment for p loading)
L (in.)	Length

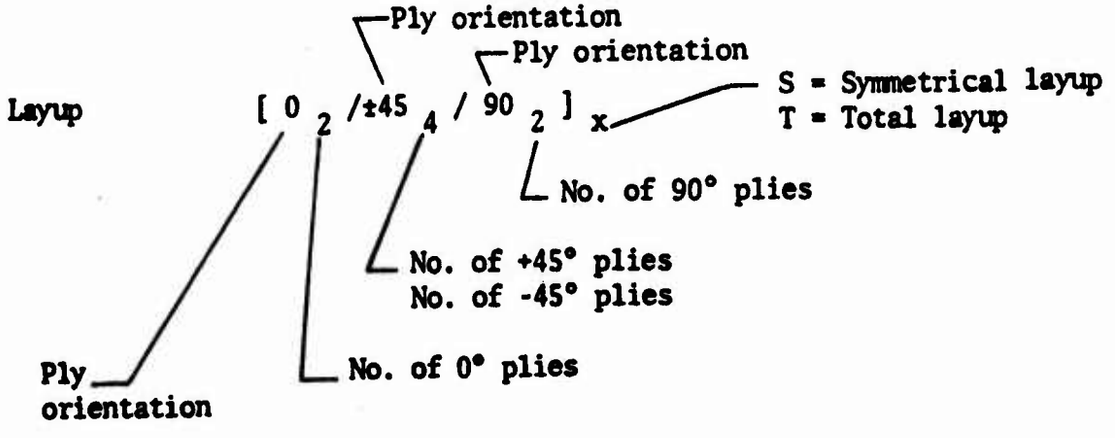

M	Mach number
M (in.-lb)	Bending moment
MAX	Subscript, maximum
M_o	Free-stream mach number
M.S.	Margin of safety
N(lb/in.)	In-plane load
n_c (in.)	Core height
N_{cr} (lb/in.)	Critical in-plane load
NMI	Nautical miles
NOS	Number of stringers or intermediate spars
N^t_{xy}	Longitudinal Poisson's ratio
$-N_x$	Cover load for negative vertical load factor, lb/in.
$+N_x$	Cover load for positive vertical load factor, lb/in.
P (lb)	Axial load
P (psi)	- Pressure
p (psi)	Uniformaly distributed normal load (pressure)
p	Roll rate, rad/sec
P_2	Steady-state static pressure at engine face, psig
PHS	Hammershock pressure, psig
P_t (psi)	- Total pressure
P_{t_2}/P_t	- Inlet pressure recovery
P_{t8}/P_o	- Nozzle pressure ratio

Q (lb/in.)	Allowable transverse shear
q	Dynamic pressure, lb/ft^2
q (lb/in.)	Applied transverse shear force
R (in.)	Radius
$(\ )_R$	Rigid or rudder
r	Yaw rate, rad/sec
R_C	Ratio applied stress/allowable stress (comp)
R_{PEN}	Radius of penetration leg, mautical miles
R_S	Ratio applied stress/allowable stress (shear)
SFC (lb/hr/lb thrust)	- Specific fuel consumption
s.s	Simple support
S_w	Planform area of reference trapezoidal wing, ft^2
t (in.)	Thickness
t/c	Wing thickness ratio
t_f (in.)	Face sheet thickness
T-L	Lower cover equivalent gage for total skin, stringers, and intermediate spar caps, in.
TSKL	Lower cover skin gage, in.
TSKU	Upper cover skin gage, in.
TSTR	Stringer or intermediate spar cap gage, in.
T-U	Upper cover equivalent gage for total skin, stringers, and intermediate spar caps, in.
V_H	Level-flight maximum speed, nautical miles

V_L	Limit speed, nautical miles
V_s (lb)	Vertical shear
V_{yx}	Transverse Poisson's ratio
W	- Weight flow, lb/sec
W_f (lb/hr)	- Fuel consumption
W_o	Takeoff gross weight
W/S	Wingloading, psf
$W\sqrt{\theta}/\delta t_2$ (lb/sec)	- Engine inlet airflow corrected to sea-level standard
X	Cartesian coordinate - subscript, x-direction
Y	Cartesian coordinate - subscript, y-direction
α	Angle of attack, deg
β	Angle of sideslip, deg
ΔC_{d_β}	- Boattail drag / Ideal gross thrust
ΔC_{d_q}	- Plug drag / Ideal gross thrust
ΔC_{f_e}	- External nozzle friction drag / Ideal gross thrust
ΔC_{in}	- Internal nozzle friction drag / Ideal gross thrust
ΛLE	Leading edge sweep of reference trapezoidal wing, deg
δ_f	Flap deflection, deg
δ_f, δ_R	Deflection of trailing edge flap or rudder, deg

ϵ_x^{tu} (μin./in.)	Ultimate longitudinal strain
ϵ_y^{tu} (μin./in.)	Ultimate transverse strain
0	Free stream engine station
2	Engine inlet engine station
8	Nozzle throat engine station
9	Nozzle exit engine station

Section I

INTRODUCTION AND SUMMARY

PROGRAM OVERVIEW

OBJECTIVE

The objective of the ADCA study program was to exploit the benefits of advanced composite materials at the conceptual design phase of an advanced high-performance fighter. The study was to utilize the high specific strength properties (thin wings, higher aspect ratio) and variable anisotropic properties (aeroelastic tailoring) of advanced composite materials in the design of a credible, realistic, lightweight, and reliable future fighter aircraft. The design was to incorporate unitized construction and low-cost assembly techniques to achieve cost reduction through a lower weight, smaller airframe design. The integration of composite material structural components with air vehicle subsystems was to be assessed. The cost and performance payoffs of advanced composite materials were to be assessed relative to advanced metallic structure. In addition, technology gaps were to be identified in the categories of structure analysis, design, manufacture, maintainability, and service life, and development programs were to be defined that would allow low-risk system application of advanced composite materials in the early 1980 time period.

APPROACH AND STUDY PAYOFF

The approach to conducting the study was to first select a design mission and define an all-composite (70 to 80 percent of the structural weight) baseline configuration which met these mission requirements. Then, using the same configuration concept, mission, and design requirements, a baseline configuration was defined which utilized advanced metallic structure. Since some use of composite materials in aircraft design is now considered state-of-the-art, the advanced metallic configuration was permitted by study ground rules to incorporate advanced composite materials up to 20 percent of its structural weight. This was interpreted to be secondary type of structural components such as leading and trailing edge high-lift devices, control surfaces, and weapon bay doors.

These two aircraft designs were to be compared in the categories of:

- Takeoff gross weight
- Empty weight

- Flyaway cost
- Life cycle cost
- Aircraft performance characteristics
- Fuel consumption

The study payoffs, however, go beyond just identification of payoffs for advanced composite materials in the aforementioned categories. The study calls for rigorous application of 1980 advanced composite technology level in the design of a future fighter at the conceptual design phase. This is an entirely different problem than designing composite component substitutions for metal counterparts. The payoffs of this design exercise would, therefore, result in the development of methods to apply composite materials at the point in the design cycle of an aircraft development when the benefits of composite materials could be maximized. The study payoffs would also include identification of technology gaps and definition of required development programs.

PROGRAM TASK DESCRIPTIONS

The program was organized into four technical tasks with subtasks, as shown in Figure 1, plus reporting.

Task I set the stage for the ADCA study by defining the mission and design requirements of the air vehicle, by sizing the two configurations, and by formulating a payoff assessment method (and exercising it at a preliminary level) which would properly compare metal and composite aircraft. The initial configurations, at the start of task I, were refined at the conclusion of task I, based on evaluation of mission and design trade studies, composite application trade studies, manufacturing assessment of and influence on the initial configuration, and aerodynamic development and analysis.

At the conclusion of task I, 12 weeks after contract go-ahead, a formal briefing was presented at WPAFB. The purpose of the briefing was to establish the viability of the configuration concept. Following this presentation, the Air Force was to make a decision whether the program was to be terminated or continued, and if continued whether it would proceed as planned or modified to reexamine the configuration or some other program variation.

The purpose of task II was to develop vehicle structural and configuration definitions which would provide the basis for further detail design and payoff analysis in tasks III and IV. In line with the major thrust of the program, emphasis was to be placed on maximum exploitation of composites

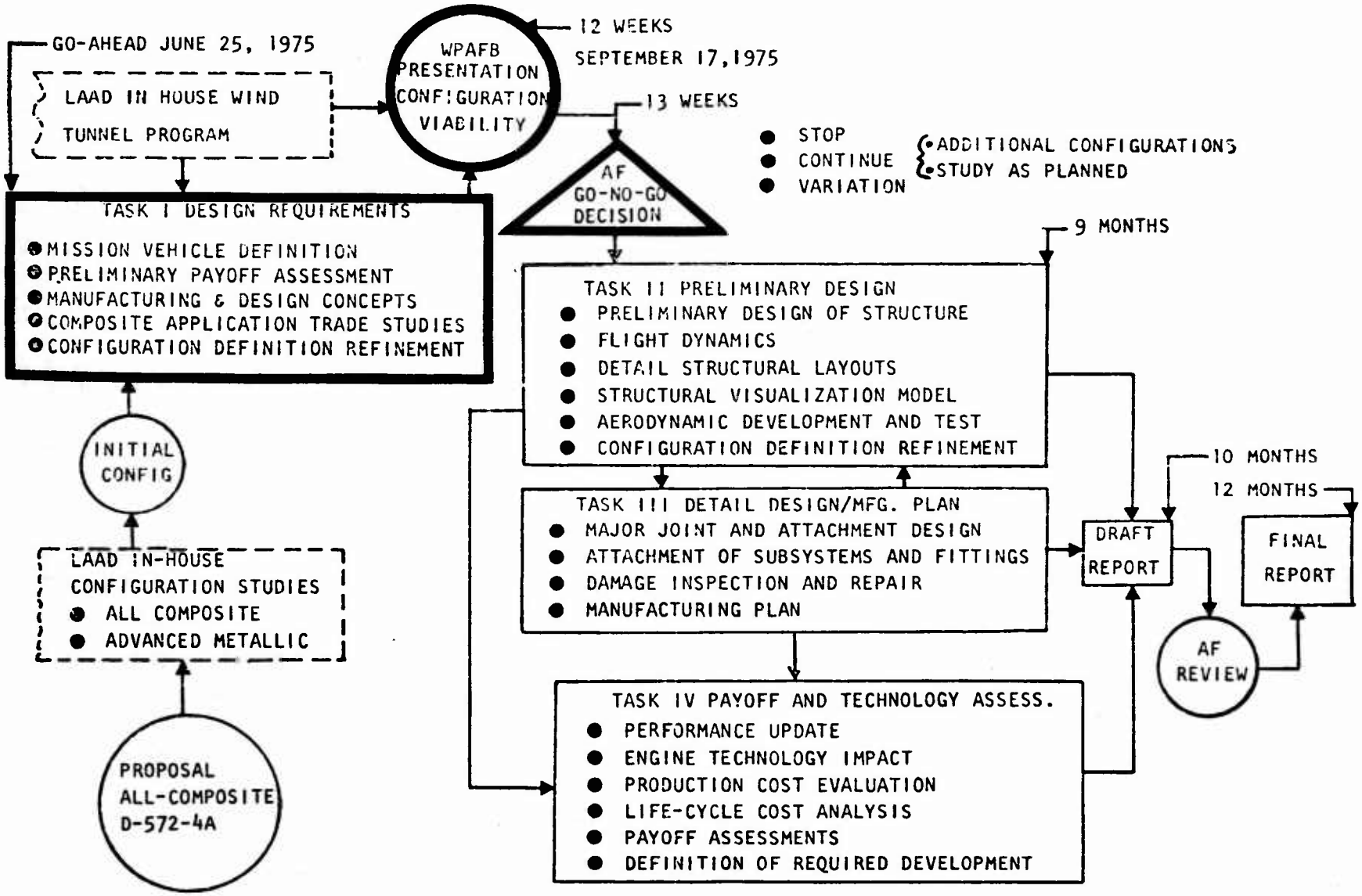

Figure 1. Program tasks.

to produce a minimum-cost aircraft meeting mission requirements. Emphasis was also to be placed on credibility through the detailed development of designs and analysis and a concurrent, closely integrated, manufacturing development.

The purpose of task III was to examine certain areas of the preliminary design which were known trouble spots for application of the all-composite approach, and to create a manufacturing plan which would show that the design being evolved in task II could be built with low-cost techniques. In particular, the joint interface design problems associated with the joining of major airframe components were to be addressed to optimize these connections to minimize the associated cost/weight penalties to the composite airframe. The airframe components were to be assessed for in-process and service damage vulnerability. These assessments were to lead to classification of the types of damage expected to occur, and proposed depot and field repair methods to restore the damaged hardware to its design strength. The task was to define inspection procedures and techniques required to insure quality and reliability assurance for the proposed manufacturing and tooling concepts proposed to support the high-rate production of the composite airplane.

The first purpose of task IV was to compare the all-composite baseline from tasks II and III with the metal baseline developed in task I. The principal payoff index was to be lower cost to perform the same mission role and the second index was to be increased performance. The second purpose of task IV was to identify the key assumptions which support the payoff assessment, and to determine what must be done to accomplish the necessary advances in the state-of-the-art by 1980. Advanced development plans (ADP's) needed by the all-composite design were to be formulated. The focus of these ADP's were to be toward the developments which must be accomplished before an all-composite airplane could be built with acceptable risk.

A similar contract was awarded to Grumman Aircraft Corporation and, following contract award, it became apparent the AFFDL, as a result of budget cuts within the structural division, did not have sufficient funds to continue both Grumman and LAAD contracts. It became necessary to stop one contractor at the conclusion of task I. The contract with LAAD was terminated after completion of task I. This report thus includes the results of task I activities only.

MASTER PHASING SCHEDULE

Each subtask activity shown in the task flow diagram is shown on the master phasing schedule in Figure 2 plus significant reporting milestones. The vertical scale on the right side of the schedule indicates program dollars. The dashed line running diagonally across the schedule shows scheduled expenditures. As the program progressed, actual expenses were shown as a solid line on a weekly basis. The value of work performed is shown as a third coded line.

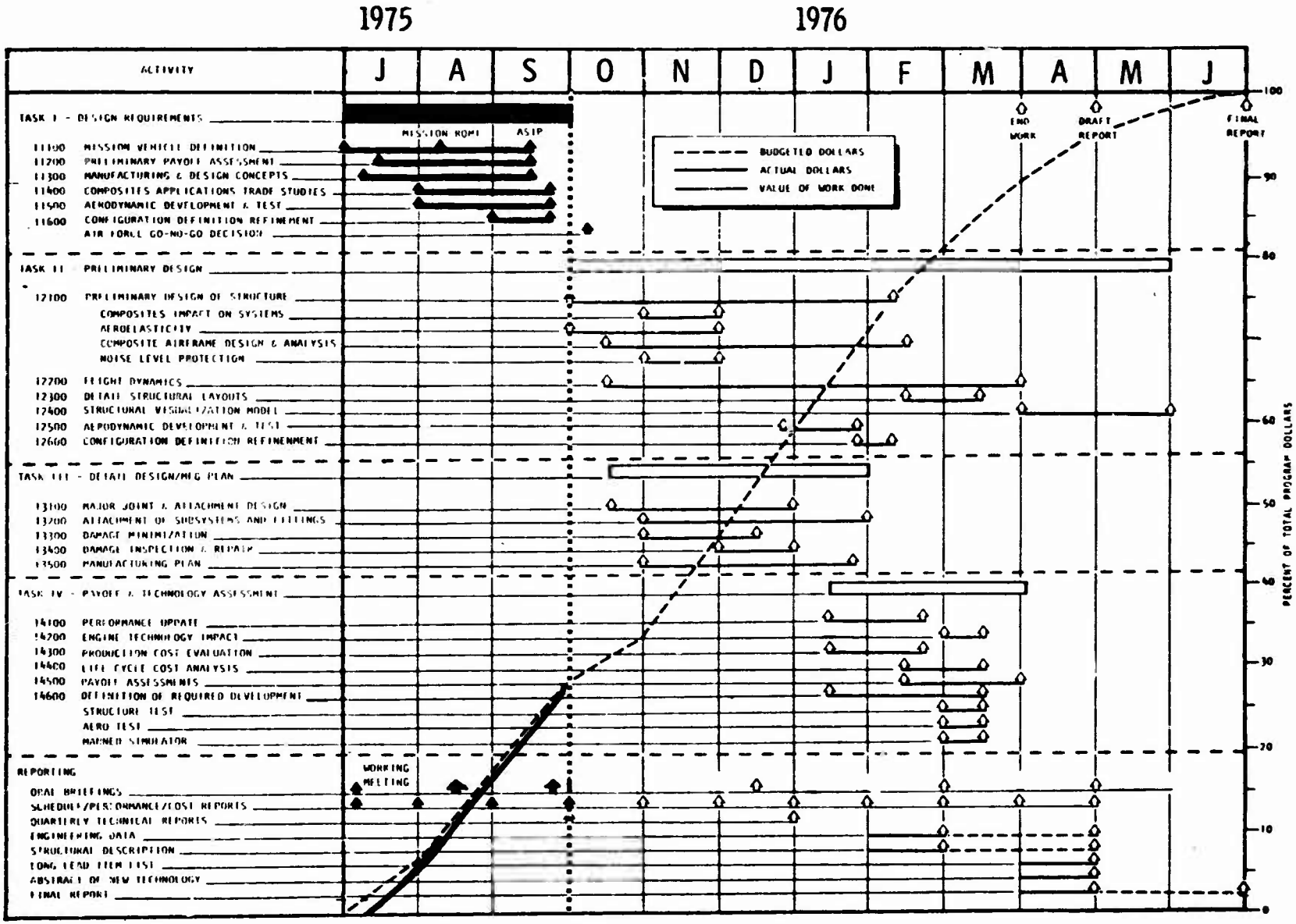

Figure 2. ADCA master schedule.

TASK I SUMMARY

Task I activities were conducted as shown on the work flow diagram in Figure 3. The ADCA point design mission was selected from representative tactical fighters mission desires (discussed in Section II) and used for sizing the initial contract configurations for both the all-composite basepoint and advanced metallic basepoint shown in Figures 4 and 5. Using these two basepoint aircraft, trade studies were conducted on a family of wing geometry variations (aspect ratio, thickness, wing loading, and sweep) and sensitivity studies were conducted for drag, weight, and mission parameters.

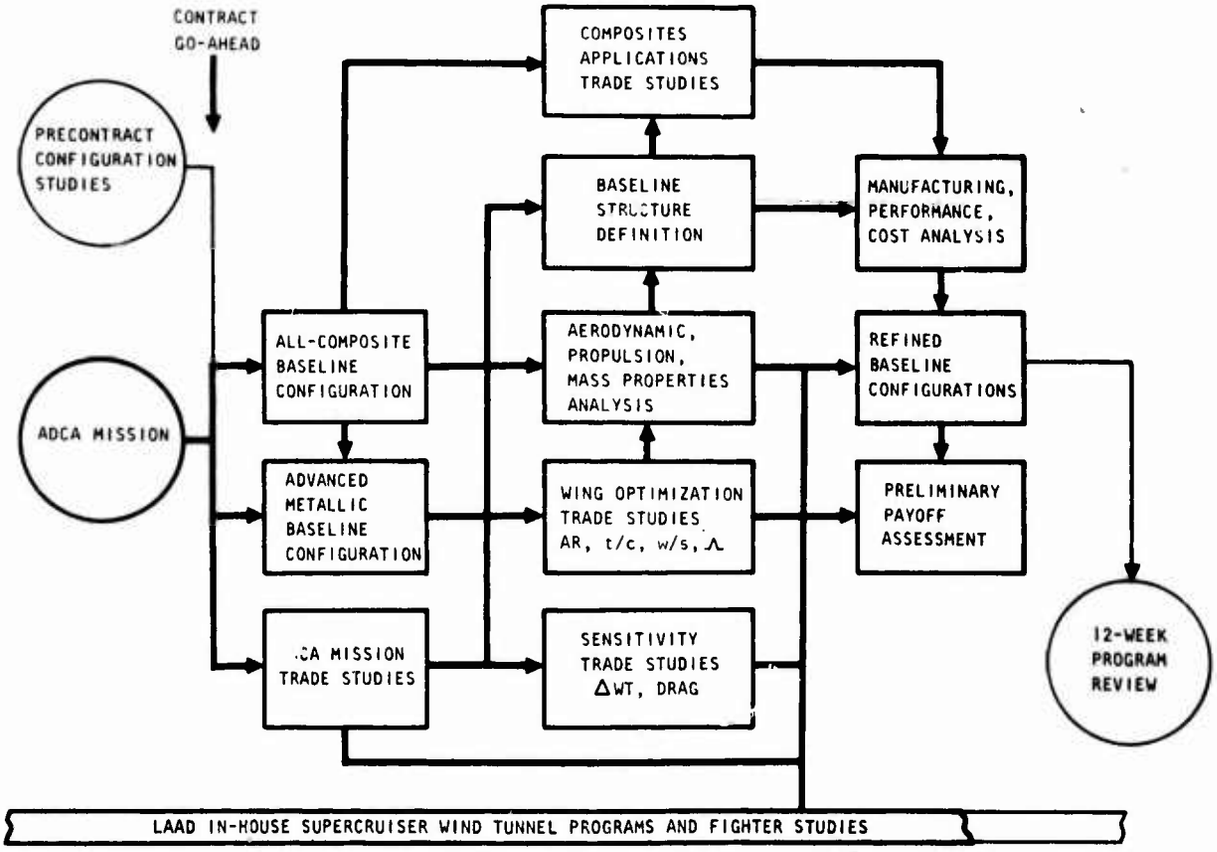

Figure 3. Task I activities.

- TOGW 31,303 LB
  - EMPTY WEIGHT 20,331 LB
  - FUEL 6,852 LB
- ENGINES (2)
  F404-GE-400 (F-18)
- ARMAMENT
  (2) MK84LGB (4,120 LB)
  (1) M61 GUN
- AVIONICS 1,000 LB

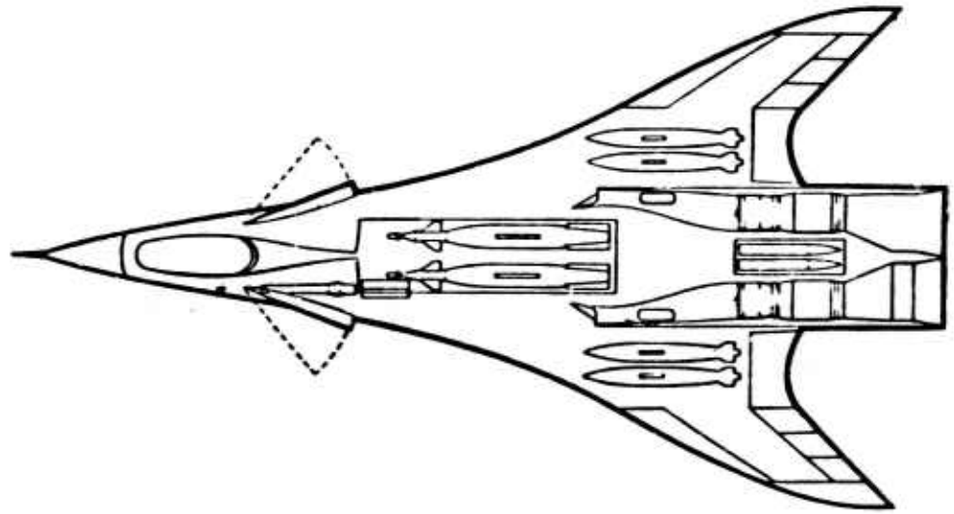

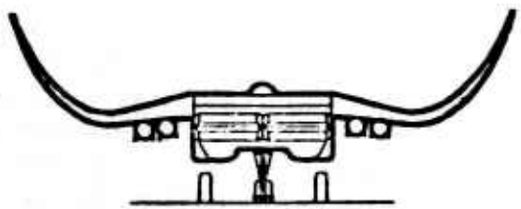

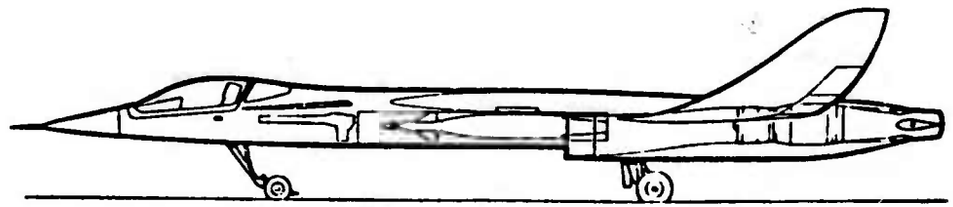

Figure 4. All-composite baseline configuration D572-4B.

- TOGW 35,108 LB
  - EMPTY WEIGHT 22,763 LB
  - FUEL WEIGHT 7,642 LB
- ENGINES (2) F404-GE-400 (F-18)
- ARMAMENT
  (2) MK84 LGB (4,120)
  (1) M61 GUN
- AVIONICS 1,000 LB

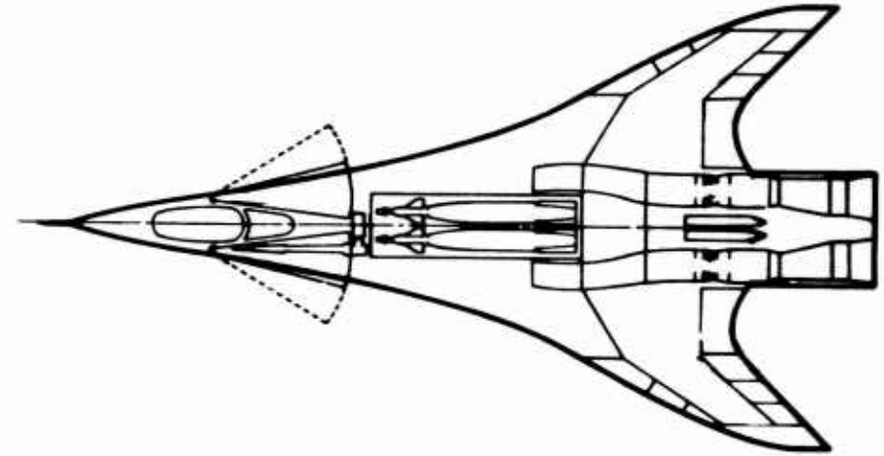

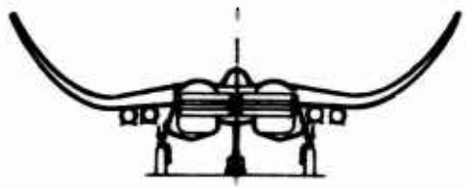

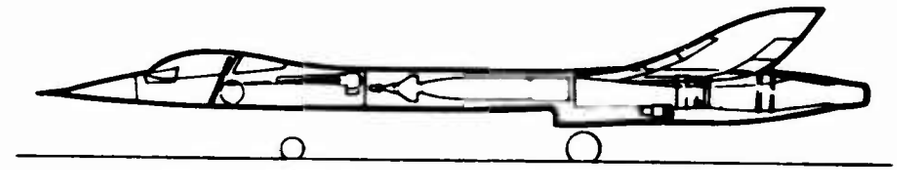

Figure 5. Advanced metallic baseline configuration D572-5A.

The two initial baseline configurations were also subjected to detailed aerodynamic, propulsion, and mass properties analysis. Baseline structure diagrams plus material and structural concept drawings were also prepared for both baseline configurations. Trade studies on the all-composite configuration included variations in structural concepts for the outer wing panel, wing carry-through structure and fuselage. Manufacturing analysis included an interface with engineering to influence structure design toward low-cost fabrication methods and also included development of preliminary tooling concepts, manufacturing breaks for few components and unitized construction, and development of a preliminary assembly sequence. Following the analysis and trade study activities, the data was evaluated for selection of design parameters to be used for a design iteration of the initial baseline configurations into refined baseline configurations to be recommended for subsequent task II, III, and IV studies.

Sections II through IV of this document include details of the aforementioned task I activities. A three-view drawing is shown in figure 6 of the baseline all-composite configuration. This is the baseline which was recommended for further study in tasks II, III, and IV.

CONCLUSIONS

Preliminary assessment indicates that the composite baseline aircraft provides significant payoff in comparison to the metallic baseline in terms of both weight and cost. Performance is identical for the two airplanes in terms of radius, payload, and cruise speed but there are advantages for the composite baseline in maneuver performance. The two airplanes are compared in Table 1. The cost of the all-composite aircraft was calculated at two values for cost of composite material. One value was 20 dollars per pound, generally believed by the industry to be achievable by the early 1980 time period. However, since there is some doubt that this value will be achieved, a second cost comparison was made using a value of 35 dollars per pound for composite materials. This compares to 39 dollars per pound actually being paid today for composite materials.

Weight differences between the two airplanes are at a lower percentage than ordinarily seen in earlier similar studies. The reason for this is that both of these airplanes use the same engine, and off-design performance capability (transonic and supersonic maneuver) is allowed to be a variable. If maneuver were held constant and rubberized engines were used the differences of weight between the two airplanes would be substantially increased.

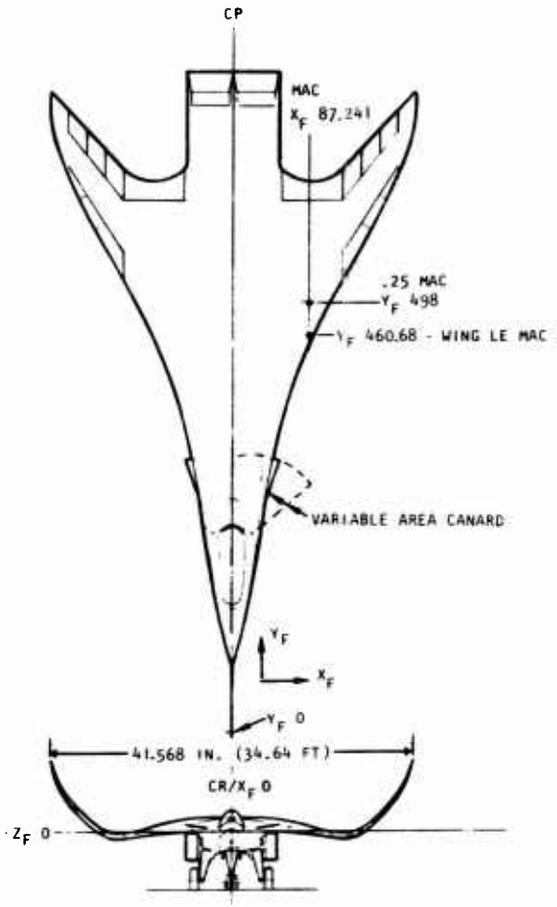

GEOMETRIC DATA

ITEM	WING (TRAPEZOID)	CANARD (MAX EXTEND.)
AREA - SQ FT	400	35 TRUE EXPOSED
ASPECT RATIO	3.0	2.53
TAPER RATIO	0.35	0
LE SWEEP - DEGREES	60°	40°
DIHEDRAL - DEGREES	AS SHOWN	10°
AIRFOIL	AERODYNAMIC DEFINITION VARIABLE	64A004
SPAN - IN.	415.68	113.0
ROOT CHORD - IN.	205.284	900
TIP CHORD - IN.	71.849	0
MAC - IN.	149.273	600
$\bar{X}$ OR $\bar{Z}$ - IN.	87.241	18.83

WEIGHT DATA

CONDITION	WEIGHT - POUNDS
GROSS TAKEOFF	34,069
FUEL	6,962
PAYLOAD	5,770

PROPULSION DATA

TWO F404-GE-400 TURBOJET ENGINES WITH TWO-DIMENSIONAL PLUG NOZZLES INCORPORATING THRUST VECTORING, THRUST SPOILAGE, AND THRUST REVERSING.

TWO-DIMENSIONAL EXTERNAL COMPRESSION INLETS WITH FIXED VERTICAL RAMPS
A_C = 525² IN. EACH

LANDING GEAR DATA

ITEM	NOSE	MAIN
TYPE	18 DIA X 44 TWIN WHEELS	28 DIA X 90-12 SINGLE WHEEL
STROKE	12 IN.	12 IN.

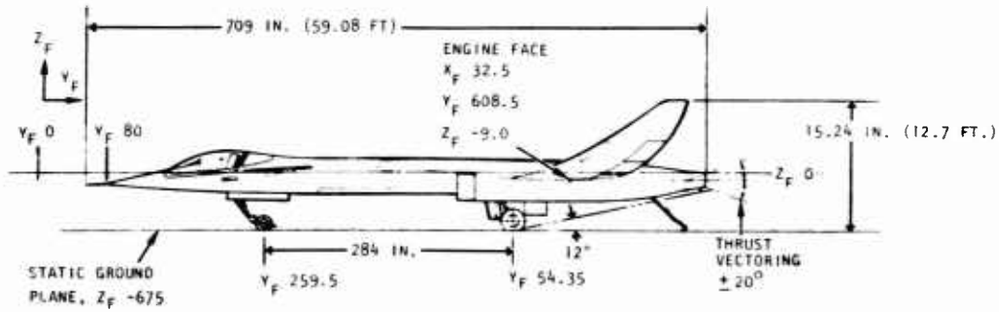

Figure 6. Recommended composite baseline configuration.

TABLE 1. COMPARISON, ALL-COMPOSITE VS ADVANCED METALLIC BASELINE CONFIGURATIONS

Parameter	-4B Composite	-5A Metallic	Composite Payoff
Total Program Cost, 300 Units[a, b]	823.84	1263.77	439.93
Average Unit Cost[a, b]	2.746	4.213	1.467
Total Program Cost, 300 Units[a, c]	951.90	1263.77	311.87
Average Unit Cost[a]	3.173	4.213	1.040
Takeoff Gross Weight	31303	35108	12.1%
Wing Area	400 Ft^2	500 Ft^2	--
Wing Loading (PSF)	78.3	70.2	--
Engines	F404-GE-400	F404-GE-400	--
Installed Thrust-to-Weight	0.763	0.680	10.8%
Structural Weight	8300	11346	36.7%
Empty Weight	20331	22763	12%
Fuel Weight	6852	7642	11.5%
Design Mission Radius	400 NM	400 NM	--
Battlefield Mission Radius	252 NM	257 NM	-5 NM
Ferry Mission Range (no auxiliary)	2563 NM	2037 NM	526 NM
Takeoff Distance	2251 Ft	2460 Ft	209 Ft
Landing Distance	2505 Ft	2632 Ft	127 Ft
P_s - 0.9M/30,000 Ft/5g	-5 FPS	-9 FPS	4 FPS
P_s - 1.2M/30,000 Ft/5g	266 FPS	172 FPS	94 FPS

[a]Cost in million dollars - does not include RDT&E, avionics, or engines.
[b]Cost based on $20 per pound for composite materials.
[c]Cost based on $35 per pound for composite materials.

RECOMMENDATIONS

Because of the very substantial potential cost payoffs in the use of composite materials, it is strongly recommended that programs be formulated to continue the development of these materials, with emphasis on known problem areas, critical design areas, and manufacturing development. These include the development of materials to be used as core structure in honeycomb panels to eliminate corrosion problems currently being experienced. It also includes the detail design, test article fabrication and strength and fatigue testing of typical highly loaded joints such as wing to fuselage, fuselage break points, outer panel to wing center section, and landing gear carry-through structure. Testing is required at the element and subcomponent level to ascertain combined fatigue/environment effect on long-term durability. These are long-running, expensive tests which should be undertaken now.

In addition, development of matrix materials should emphasize higher temperature resistance to provide for future aircraft operating at higher mach numbers and to provide greater protection against combined effects of temperature and moisture at today's operating temperatures.

Development of thermoplastic matrices is required to reduce moisture degradation and fabrication costs.

Immediate development of manufacturing methods for integrated substructure/cover structure is necessary to insure readiness in the 1980-85 time period.

Section II

CONFIGURATION DEVELOPMENT

INTRODUCTION

The two baseline configurations, D579-4B and -5A, respectively composite and advanced metallic designs, are the result of iterative design and mission changes which began before the Advanced Design Composite Aircraft (ADCA) request for proposal (RFP) was received. Rockwell International's supersonic cruise vehicle, or "supercruiser," concept was selected as an ideal demonstration vehicle for use of composite materials. Preliminary vehicle synthesis was based on the RFP mission and the initial ADCA configuration design cycle was started. Aerodynamic, mass properties, and propulsion analyses were made and vehicle sizing and performance were calculated at an approximate level of effort encompassed by the heavy dark lines as shown in Figure 7. The resulting vehicle became the proposal vehicle (-4) shown in Figure 8. Changes in mission and/or vehicle requirements led to the -4A and -4B vehicles shown on the same figure. Parametric changes in the -4A vehicle led to the design of the advanced metallic vehicle, -5, and in a similar fashion, analysis produced the -5A vehicle. Level of analyses of effort of the -4B and -5A vehicles in general was represented by the lighter solid lines of Figure 7. Parametric vehicles and mission trades were conducted on these vehicles and the resulting changes were incorporated in the task II basepoint vehicles -4C and -5B. These analysis levels in task II for these vehicles is expected to be nearly the maximum scope shown on Figure 7.

This section will present only propulsion, mass properties, and analysis used to define these configurations. Aerodynamics characteristic will be discussed in Section III.

Details of the vehicle definition presented within this section are primarily those of -4B and -5A, with the resulting -4C and -5B discussed briefly.

SIZING GROUND RULES

Vehicle sizing and development for the baseline aircraft was done through use of the Rockwell-developed Vehicle Sizing and Performance Estimation Program (VSPEP). This computer program utilizes baseline aero, propulsion, and mass property data coupled with a vehicle geometry representation to effect the scaling of the baseline aircraft to accomplish some specified criteria. For the ADCA contract, the primary criterion is the Deep-Strike Mission radius (defined in the next section). The performance of this vehicle was then measured against alternate criteria (i.e., the Battlefield Interdiction Mission and the Ferry Mission requirements) with variations made only in payload and fuel

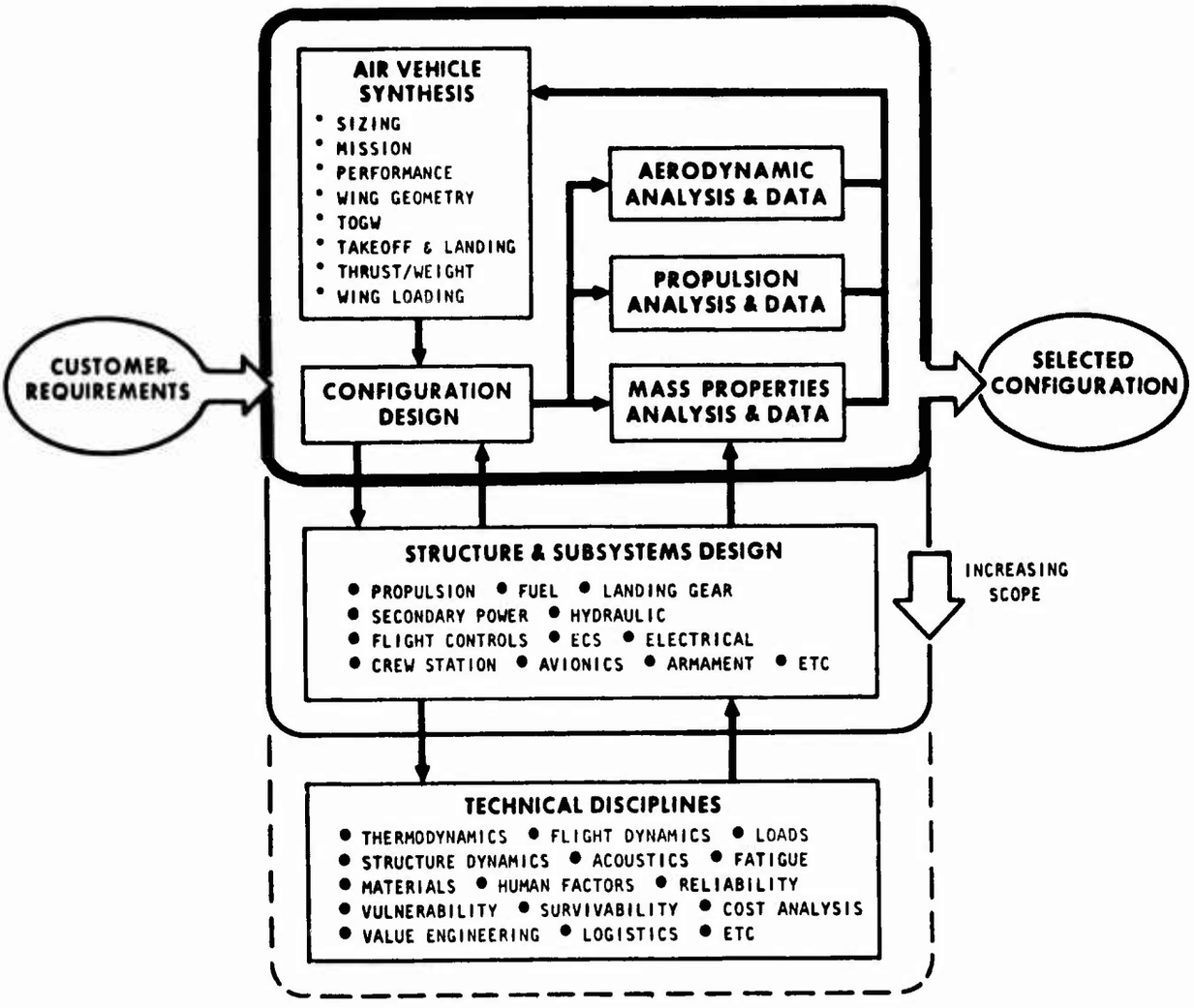

Figure 7. Configuration development process.

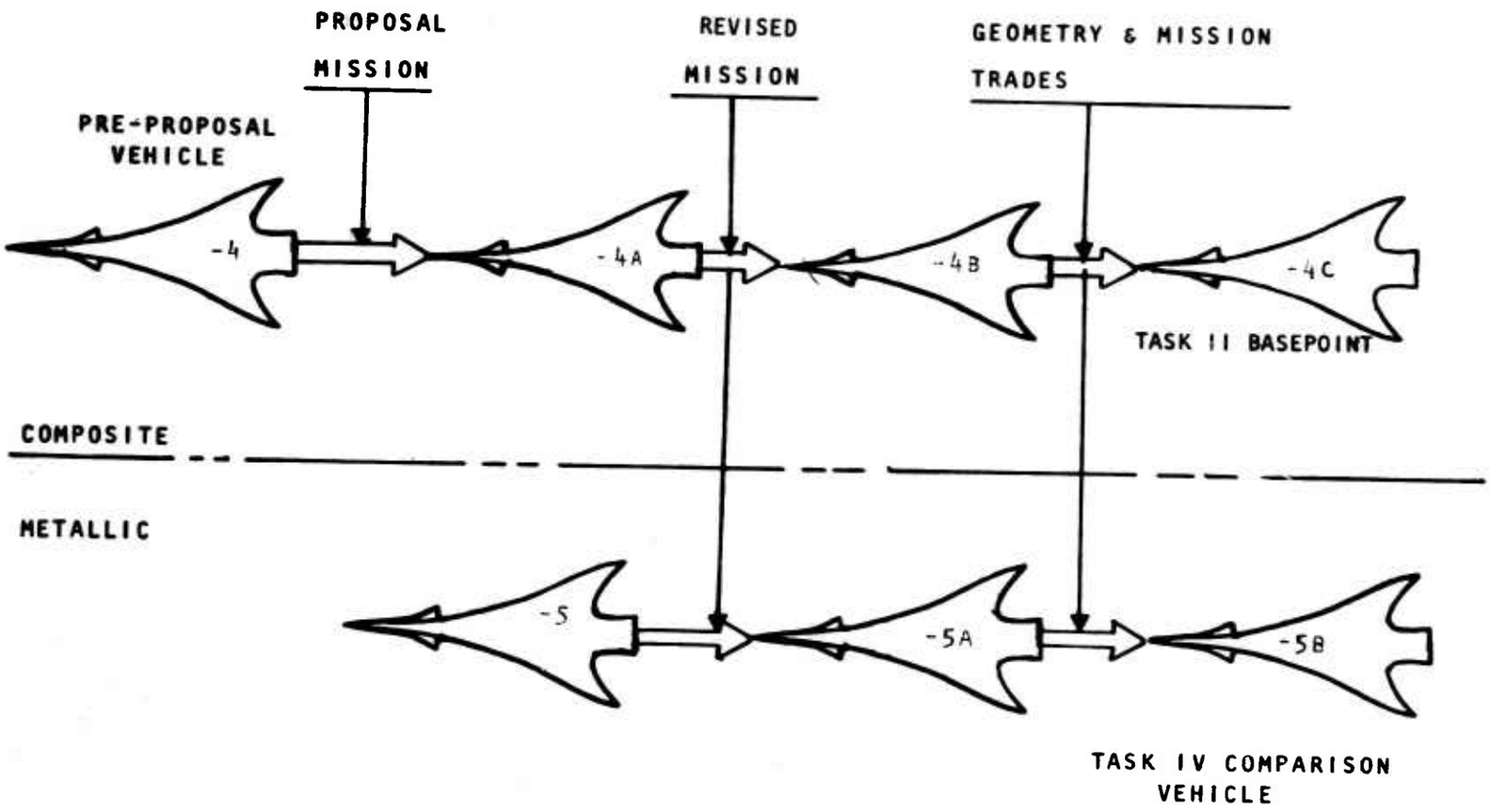

Figure 8. Configuration development.

available, and the resulting takeoff weight, due to different alternate mission design criteria. In addition, the vehicle performance was computed for takeoff utilizing various flap settings and power settings, landing with and without thrust reversing, and acceleration ability at an altitude of 35,000 feet. The maneuverability of the aircraft at various mach, altitude, and load factor conditions was calculated, as was the variation in the Breguet range parameter ((M * L/D)/SFC). All of these parameters were also computed when the wing loading was parametrically varied, and the results are presented in the section titled "Mission and Design Trade Studies."

Payload ground rules were a function of mission. For the deep-strike mission, the assumed payload was two MK-84 laser-guided bombs carried internally and, although the M-61 cannon was carried, no ammunition was provided, nor were any self-defense missiles. For the battlefield interdiction mission, two self-defense missiles of configuration similar to the AGILE were included, as was 300 rounds of ammunition for the M-61 cannon. Although the current version of the MK-84-LGB is not compatible with external carriage at 1.5 mach number, two weapons of that configuration were added to the two carried internally, as weight and drag characteristics were assumed to be representative. No weapons except the M-61 cannon were carried for the ferry mission. The maximum fuel volume of the vehicles was utilized, and additional tanks and fuel were added to the armament bays. The armament bay contained 3,000 pounds in 300 pounds of tanks, supporting structure, and attachments.

Maximum allowable takeoff and landing distance was set at 3,000 feet and a desired maneuverability level for the 0.9 mach, 30,000-foot, 5-G load factor case was assumed as approximately equal to a lightweight fighter class of vehicle (i.e., $P_s = 0$).

DESIGN MISSION

The ADCA was designed for the primary mission, a deep-strike mission, and two alternate missions; a battlefield interdiction mission and a ferry mission (see Figure 9).

The deep-strike mission was based upon the requirement for an operational radius of at least 400 nautical miles, including a supersonic penetration of 200 nautical miles beyond the FEBA. The weaponry compliment carried on the deep-strike mission includes two MK-84 laser-guided bombs and an improved M-61 cannon.

The mission consists of a warmup and takeoff, a minimum-fuel climb to best cruise altitude, cruise at optimum mach and altitude to the FEBA, climb and accelerate to 1.5 mach number and optimum altitude, penetrate at 1.5 mach to the point of weapons delivery, drop stores, execute a 180° turn, egress at 1.5 mach and optimum altitude, descend and decelerate (no time or fuel) to subsonic optimum mach and altitude, and loiter for 20 minutes at sea level.

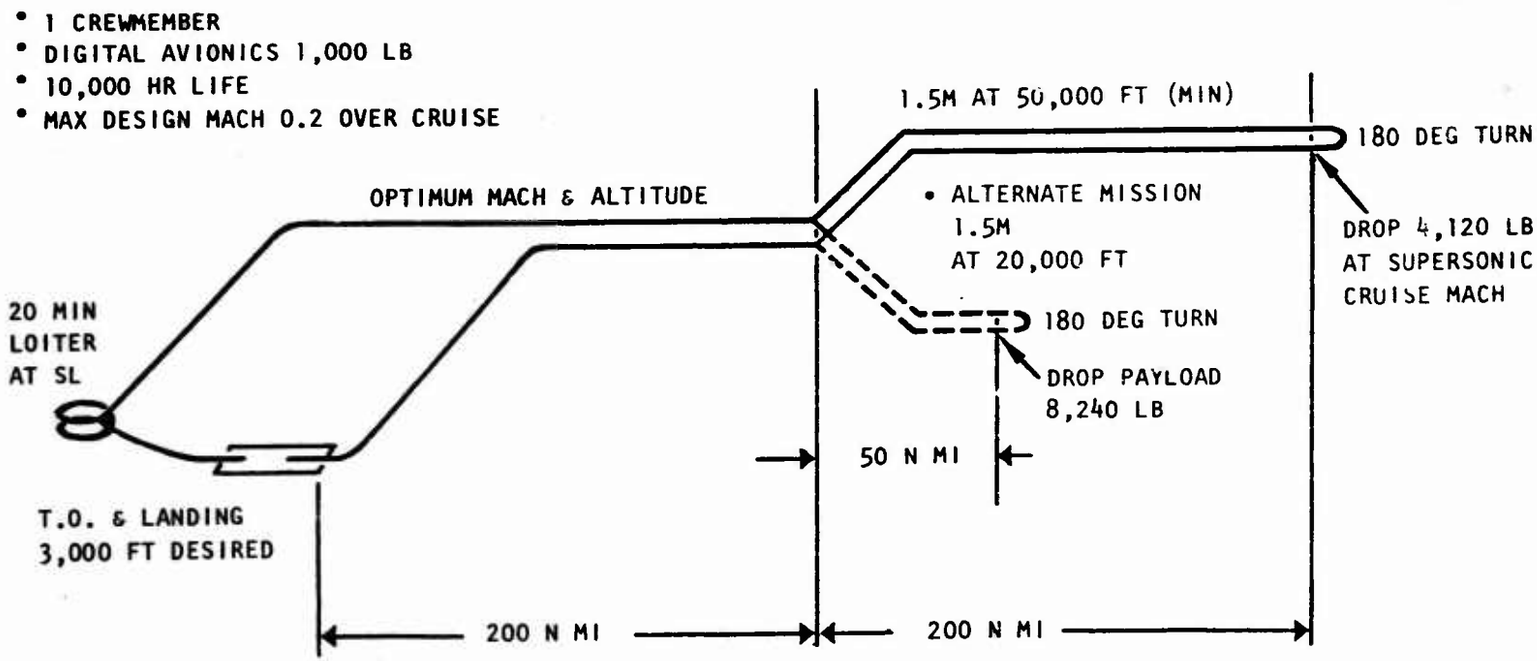

- 1.2M SL CAPABILITY
- 2,800 N MI FERRY WITHOUT REFUELING
- FWD FIRING GUN IN BOTH MISSIONS
- AMMO & 2 A-A MISSILES IN ALTERNATE MISSION ONLY
- ACCEL FROM 0.8M TO 1.6M AT 35,000 FT IN 80 SEC MAX
- INSTANTANEOUS 4G CAPABILITY MINIMUM

Figure 9. ADCA point design mission.

The battlefield mission consists of the same outbound and return legs as the deep-strike mission up to the FEBA. From the FEBA, the vehicle descends to 20,000 feet and penetrates at 1.5 mach for 50 nautical miles to a point where the weapons are delivered. The payload for the battlefield mission includes four MK-84 laser-guided bombs, two self-defense missiles, and one M-61 cannon with 300 rounds of ammunition.

The ferry mission features a 2,800-nautical-mile range without refueling. In order to meet the range requirement, the weapons bay was fitted with a fuel tank and the excess volume in the wing tank was utilized. The total additional fuel was 8,900 pounds, 3,000 pounds in the weapons bay, and 5,900 additional in the wing tank.

The desired requirements for the takeoff is to design the aircraft to a 3,000-foot takeoff over a 50-foot obstacle.

ALL-COMPOSITE BASELINE CONFIGURATION

The baseline composite aircraft configuration D572-4B is illustrated in Figure 10. This vehicle is designed to the mission requirements outlined in the paragraph "Design Mission." Briefly summarized, these include a 3,000-foot takeoff over a 50-foot obstacle, deep-strike mission radius of 400 nautical miles, unrefueled ferry mission range of 2,800 nautical miles, and battlefield mission radius of 250 nautical miles with a 50-nautical-mile penetration. The takeoff gross weight for the primary design mission was 31,845 pounds, and the resulting wingloading was 79.6. The installed thrust-to-weight for static sea level conditions is 0.751.

The basepoint configuration features a one man crew situated in a 65-degree "laydown" high-acceleration cockpit. This arrangement results in lower wave drag due to reduced cross-sectional area and provides for increased G-level tolerance for this pilot. The design features that contribute most significantly to the low total drag are (1) minimum control surface size, (2) high degree of propulsion integration, (3) aerodynamic shaping to produce isobars that fall behind the mach cone, (4) low profile cockpit, and (5) minimum wetted area. An assumption inherent in this design is the strong requirement imposed by aeroelasticity that requires the wing torsional deflections are minimized as the wing bends.

The wing has an aspect ratio of 2.5 and a leading edge sweep of 60 degrees, and is shaped to generate vortex lift to improve the off-design high-lift capability. The wing incorporate elevons and powered droop leading edge devices for mechanical camber control as well as structural design for dynamically controlled bending. The primary material of the wing is graphite/epoxy.

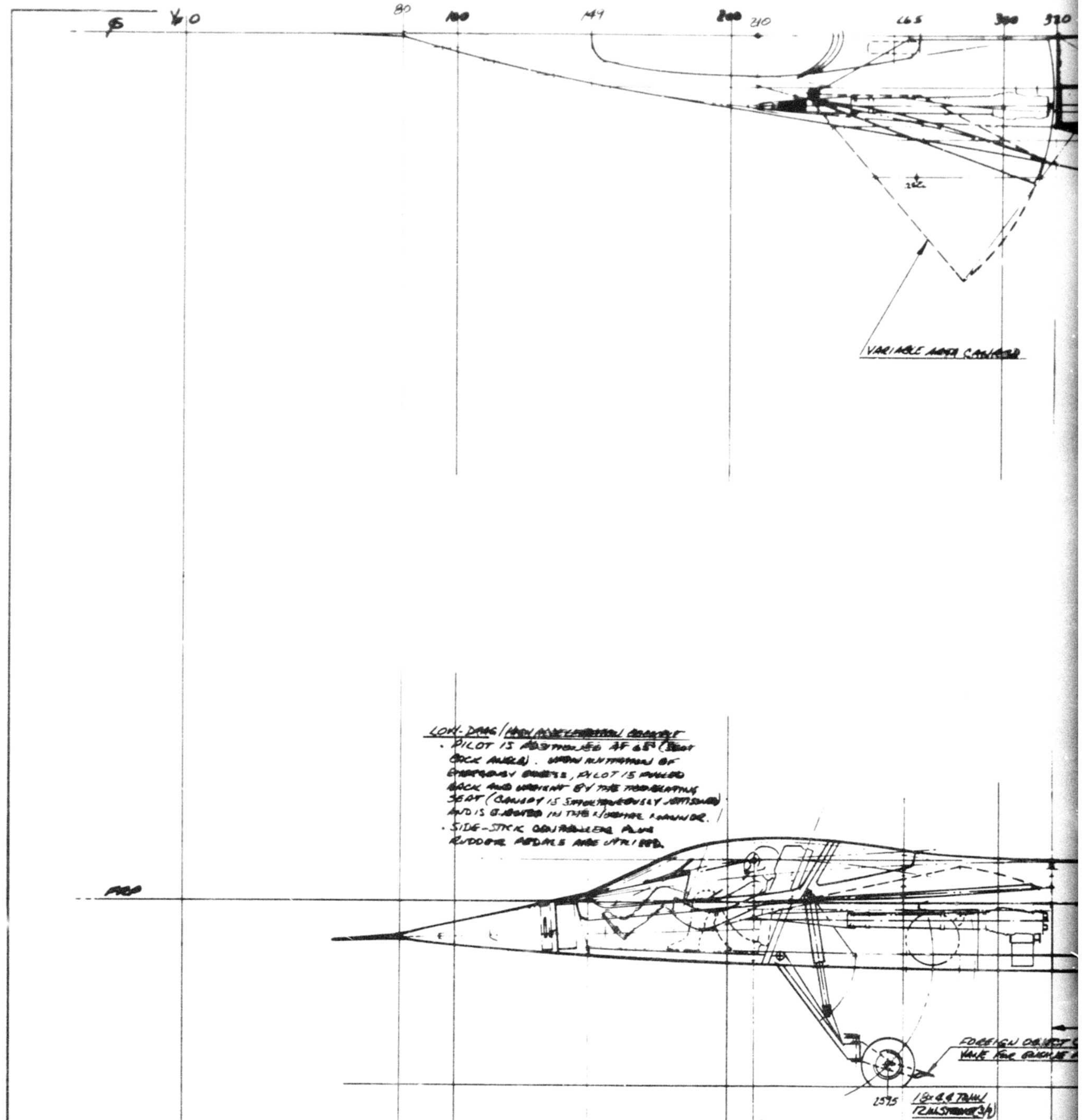

80
149
210
265
320
2575
LOW-DRAG
PILOT IS
PILOT IS
SIDE-STICK

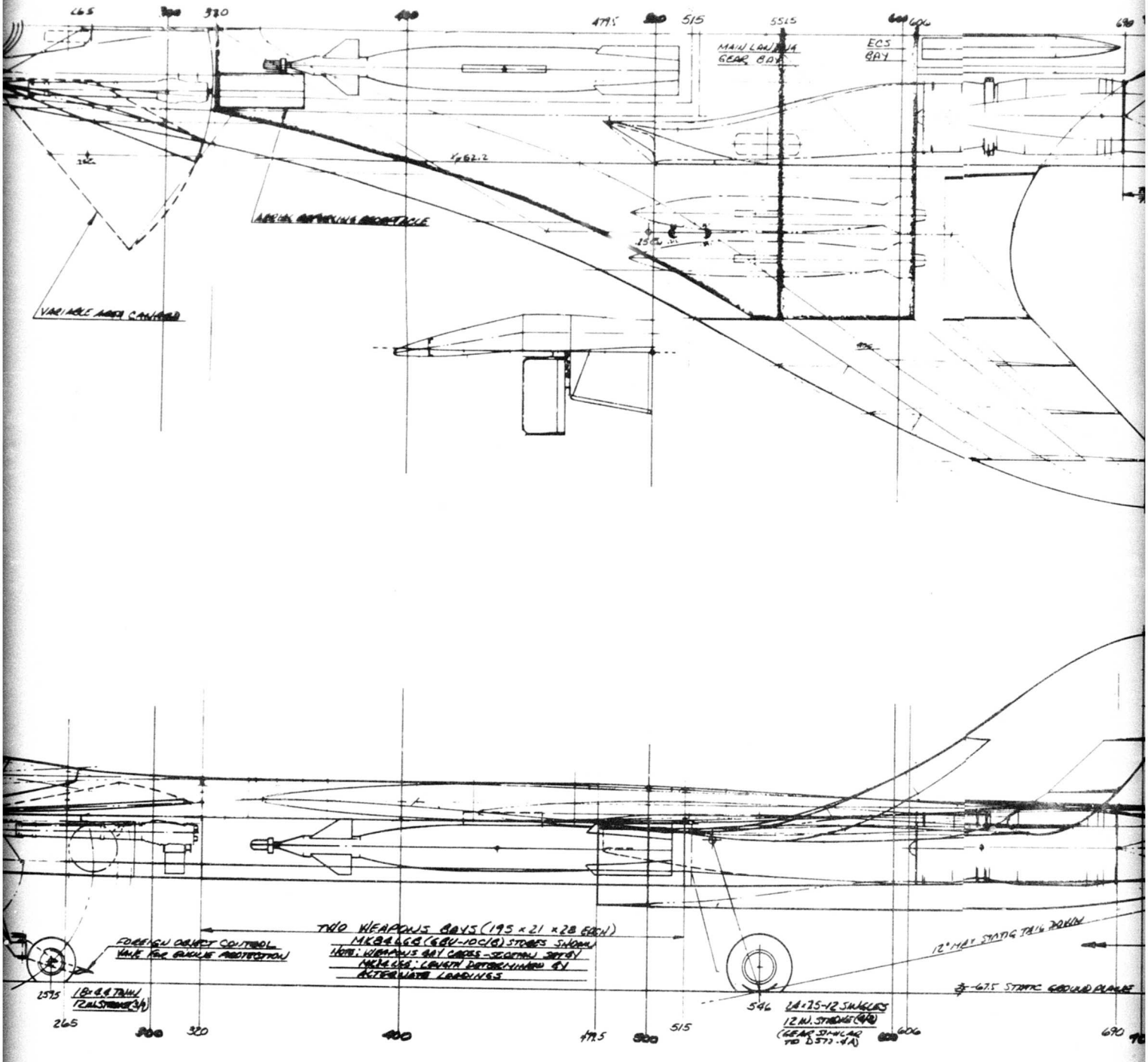
MAIN LANDING GEAR BAY
ECS BAY
VARIABLE AREA CANARD
TWO WEAPONS BAYS (195 x 21 x 28 EACH)
MK82 LGB (6BV-10C/B) STORES SHOWN
NOTE: WEAPONS BAY CARES - SEVERAL OPTION
MK84 LGB: LENGTH DETERMINING BAY
ALTERNATE LOADINGS
FOREIGN OBJECT CONTROL VALVE FOR RUNWAY PROTECTION
12° MAX STATIC TAIL DOWN
-67.5 STATIC GROUND PLANE
24 x 35-12 SINGLES
(12 M. STRONGS (4/2)
(GEAR SHOWN TO SCALE)
265
320
400
479.5
515
546
606
690

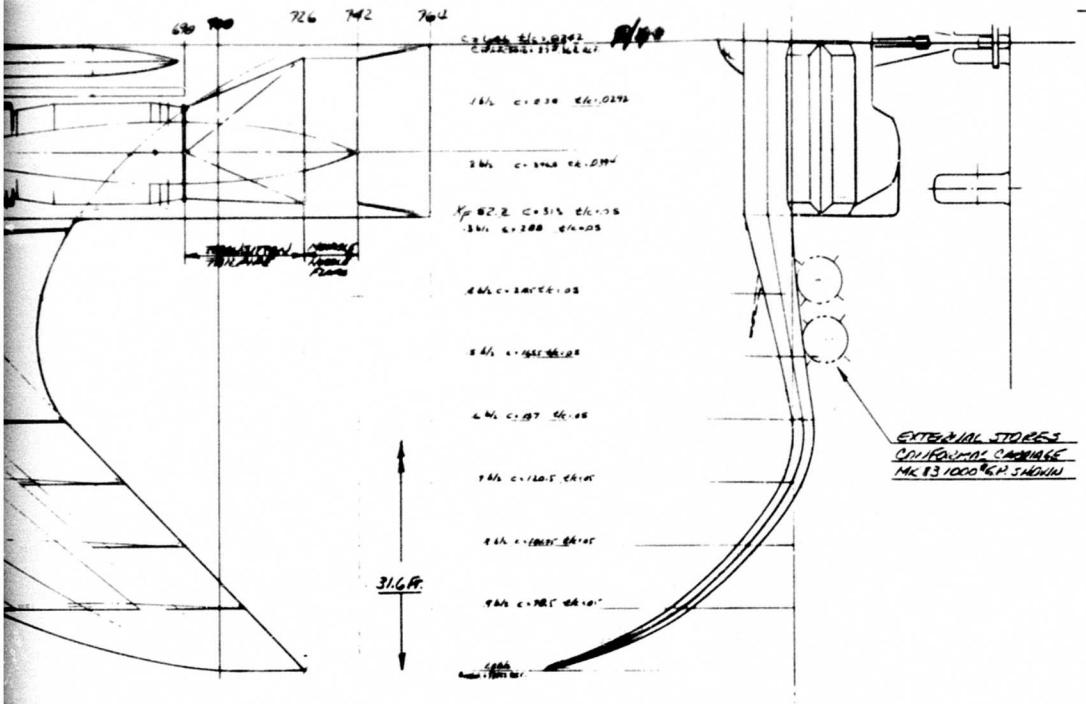

PROPULSION

- TWO F404-GE-400 TURBOJET ENGINES WITH TWO-DIMENSIONAL PLUG NOZZLES W/COMBINATING THRUST VECTORING, THRUST SPOILAGE AND THRUST REVERSING.
- TWO-DIMENSIONAL EXTERNAL COMPRESSION INLETS W/ 74 FT² AREAS. A_C = 525 SQ IN EACH

TARGET WEIGHTS

W_O = 31200 LBS.
W_F = 7300 LBS.
W_{PL} = 5200 LBS.
- TWO MK 84 LGB (GBU-10C/B)
- TWO THRUST VECTORED TAIL ZERO-LOC MISSILES
- M61 6 mm W/ 1200 RDS. AMMO.

NOTES

- THIS CONFIGURATION IS SIMILAR TO DS72-400 EXPANSIONS TO PROPULSION SYSTEM, WING AND WEAPONS BAY HAVE BEEN INCORPORATED.

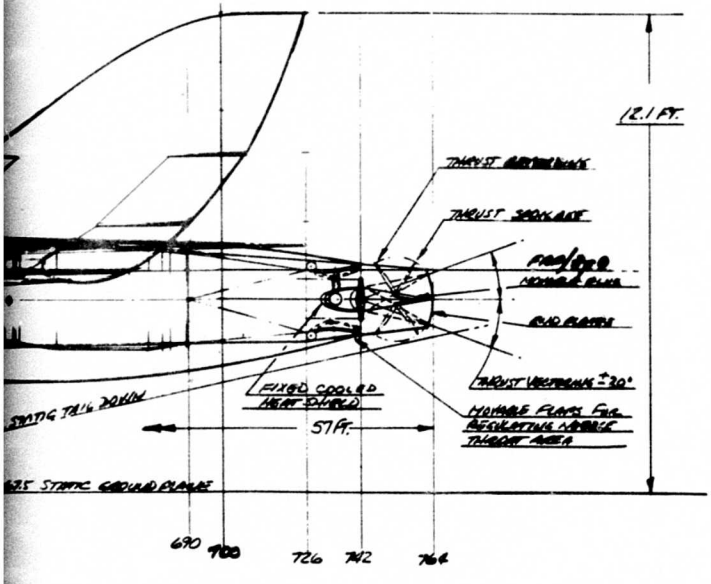

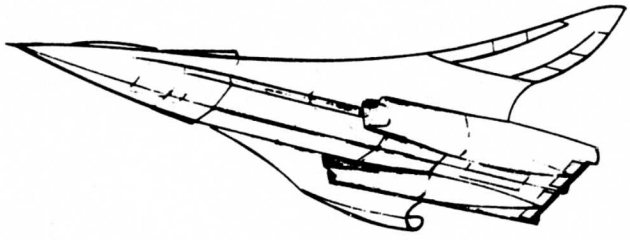

Figure 10. Advanced design composite aircraft su
penetration interdiction fighter.

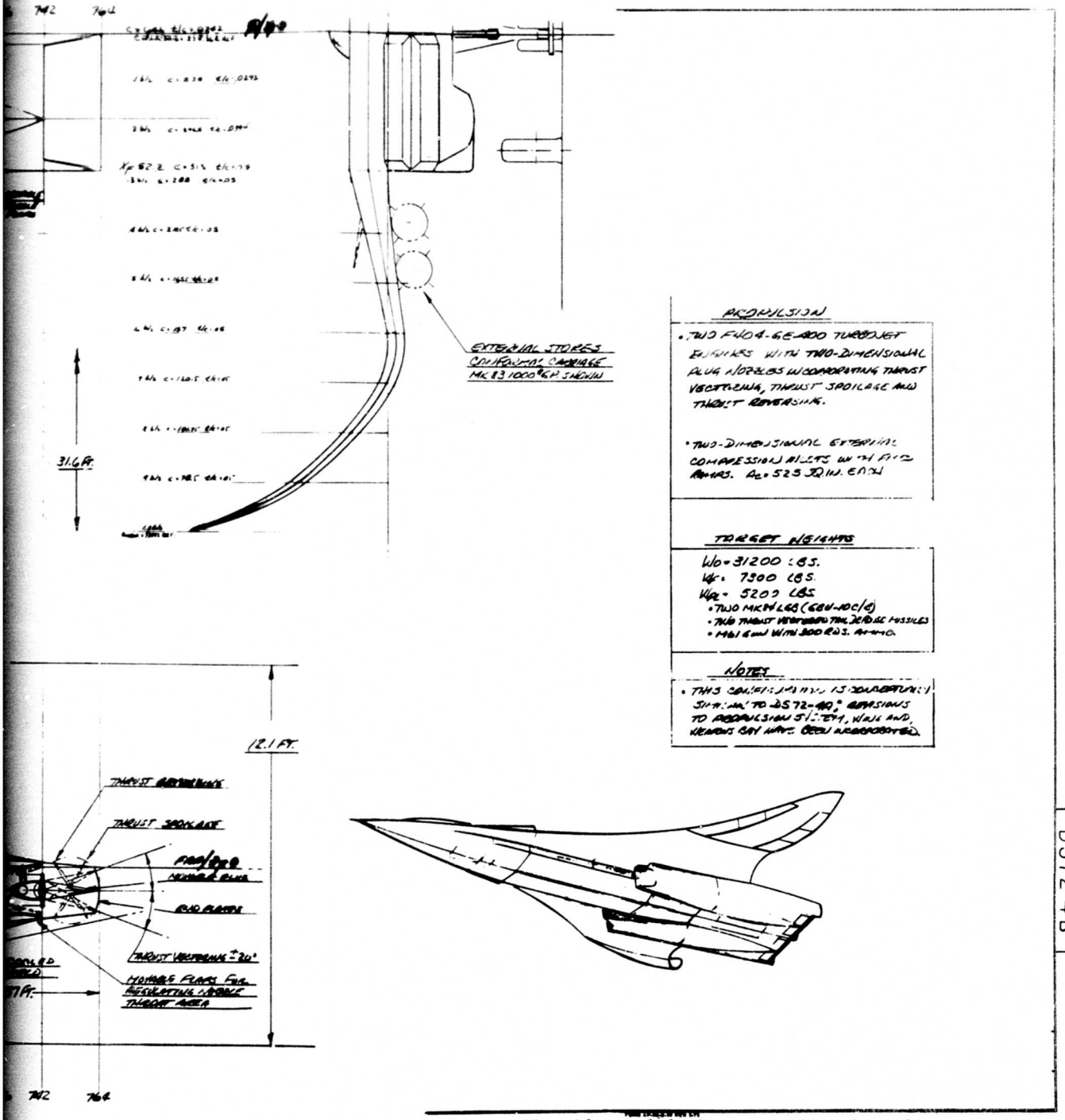

Figure 10. Advanced design composite aircraft supersonic penetration interdiction fighter.

The basepoint aircraft is powered by two General Electric F404-GE-400 engines. Each engine is equipped with remote afterburning, thrust reversing, thrust spoilage, and thrust vector control. The installation includes a 2-D fixed-ramp inlet designed for 1.6 mach number and an aerodynamically integrated exhaust system with a 2-D plug nozzle. Details of the propulsion system are included in a later section.

ADVANCED METALLIC BASELINE CONFIGURATION

The baseline metallic aircraft D572-5A is shown in Figure 11. The vehicle design requirements and design missions are identical to the D572-4B presented previously. The takeoff gross weight for the summary design mission was 35,385 pounds, and the resulting wing loading is 70.7. The installed thrust-to-weight ratio for static sea-level conditions and gross weight was 0.676.

The basepoint metallic airplane configuration features and design assumptions are identical to the -4B airplane, with the exception that the majority structure is metallic with composites used only on the armament bay doors and the wing leading and trailing edge devices.

PROPULSION SYSTEM SUBSTANTIATION

INTRODUCTION

The ADCA propulsion system is keyed to the use of a rectangular 2-D plug nozzle. The 2-D plug nozzle minimizes afterbody and wave drag. Thrust vectoring is used to capitalize upon propulsive lift enhancement for maneuvers. The plug nozzle also incorporates a lightweight thrust reverser installation.

A fixed-geometry inlet was selected for a 1.6 mach number design. The inlet is designed to maintain high performance while minimizing the use of cutouts or variable-geometry panels. However, an inlet bypass system is employed to improve the inlet-engine match during supersonic penetration at 20,000 feet.

This section presents the propulsion system design guides and criteria and substantiation data for the installed performance data input for the mission analyses of the ADCA.

Engine Description

The Statement of Work specified the use of a 1980 production engine for the ADCA study. The selected engine is the General Electric F404-GE-400 (company designation J101-J7A9) with a rectangular augmentor and plug nozzle replacing the axisymmetric augmentor and nozzle used in the F-18 fighter

installation. The F404-GE-400 sea-level static, Standard Day ratings are: thrust - 15,950 pounds at maximum power, 11,480 pounds at intermediate power, 142.5 pounds-per-second airflow, bypass ratio 0.34, cycle pressure ratio 24.4.

The Rockwell cycle analyses were conducted using the GE Source Deck J101/J7A9 75015 to modify the F404 engine performance for the installation of the 2-D augmentor and nozzle. This resulted in reducing the maximum augmentor temperature, and a revised thrust coefficient schedule. The resultant rated thrust, adjusted to a 100-percent inlet recovery, is about 2 percent lower than the -400 engine. However, the ADCA is not takeoff limited, and maximum thrust is not critical.

The transition from the basic axisymmetric to a rectangular augmentor cross section begins at the -400 augmentor fuel manifold; engine station 271, and air vehicle station 690. (See Figures 19 and 20.) The augmentor/nozzle modification will increase the base engine weight from 2,020 pounds (-400) to 2,673 pounds (Rockwell estimates based on GE and PWA contributions to the AFTI program).

Inlet Selection

The engine flight limits and corrected airflow demand are given in Figure 12. The maximum corrected flow is 145 pounds per second, which results in a maximum inlet throat area of 428 square inches for efficient transonic acceleration. The airflow curves in Figure 12 show a significant corrected airflow decay with increasing ram temperature which will require variable-geometry provisions for proper inlet engine match during supersonic flight at low altitudes.

The pressure recovery versus mach number capabilities of several inlet configurations are compared in Figure 13. A fixed ramp or fixed cone inlet can achieve good recoveries up to M1.6. A variable ramp or translating cone is required for good performance for a M2.0 design. The M1.5 penetration design D572-4B air vehicle has the vertical wall of the weapons bay forward of the inlet. A vertical ramp inlet at the wing fuselage juncture provides the optimum diffuser contours and lightest weight for the ADCA application. The inlet is designed for shock-on-cowl at M1.8 to provide maneuvering stability at M1.6. The inlet has a 6-degree fixed ramp, a 0.5-inch cowl thickness, and a capture area of 525 square inches.

Both top and bottom inlet locations were considered for this air vehicle. The ideal location of the inlet for a penetration air vehicle is the upper aft fuselage, to shield the cavity reflector from ground-based radar. Unfortunately, the local mach numbers at this location are normally above freestream and become progressively higher with angle of attack. The result would be a progressively decreasing thrust and inlet stability margin during air vehicle maneuvers; i.e., SAM avoidance. Figure 14 presents experimental flow field

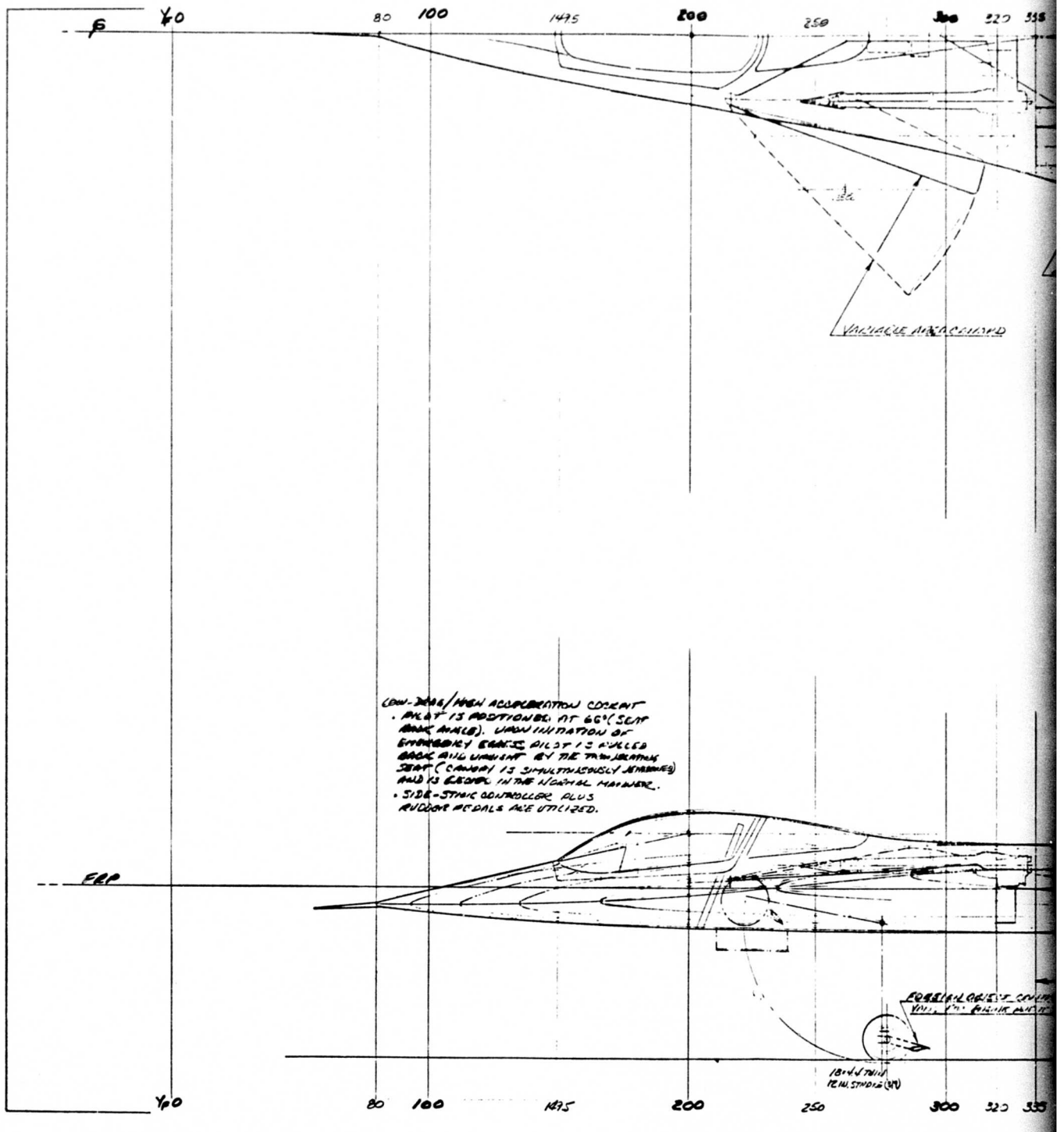
80
100
1495
200
250
300
320
335
FRP
(LOW-G/HIGH ACCELERATION CONCEPT
• PILOT IS POSITIONED AT 60° (SEAT BACK ANGLE). UPON INITIATION OF EMERGENCY EGRESS, PILOT IS PULLED BACK AND UPWARD BY THE TRANSLATING SEAT (CANOPY IS SIMULTANEOUSLY REMOVED) AND IS EJECTED IN THE NORMAL MANNER.
• SIDE-STICK CONTROLLER PLUS RUDDER PEDALS ARE UTILIZED.

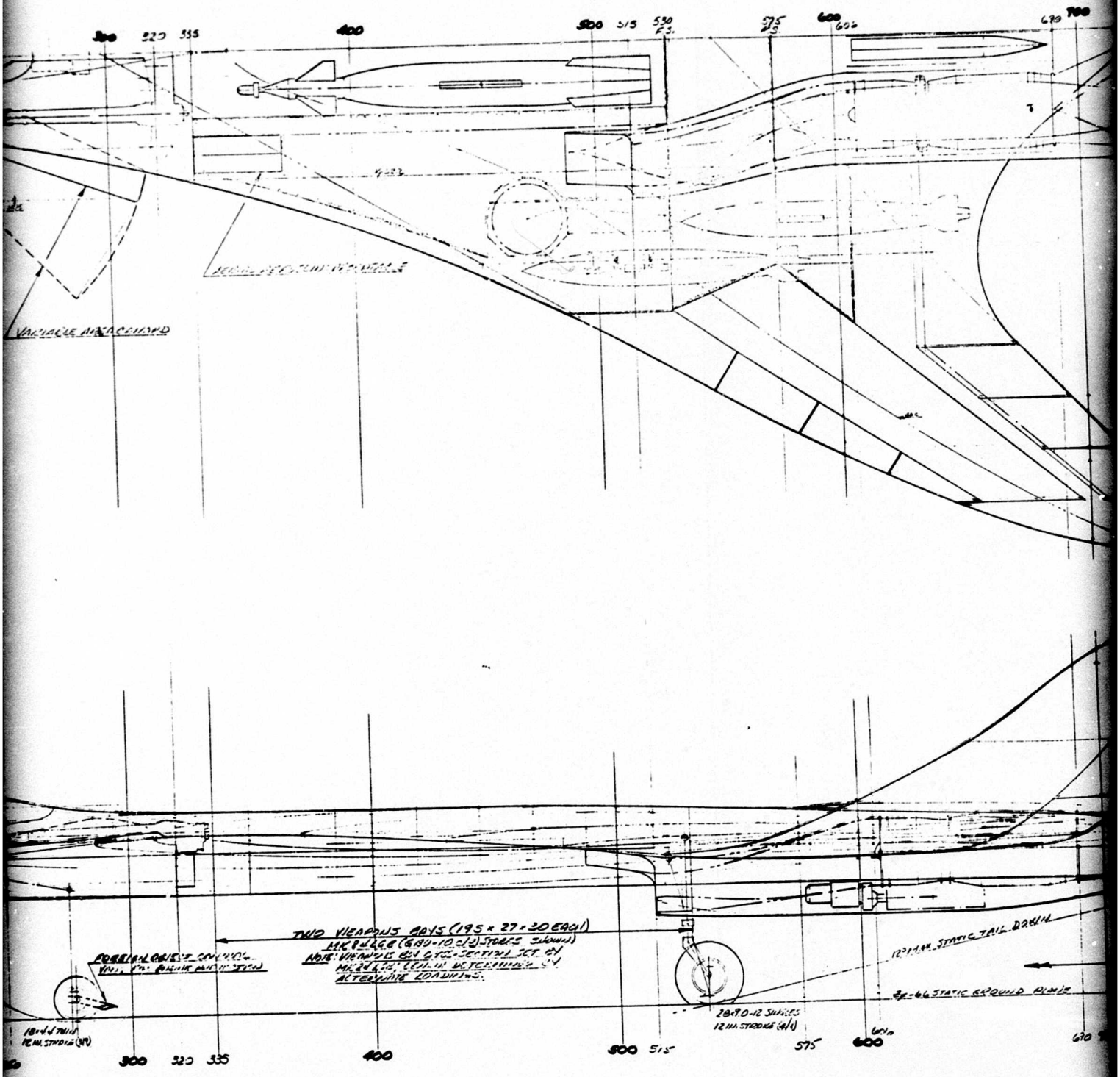
300
320
335
400
500
515
530
F.S.
575
600
620
700
TWO WEAPONS BAYS (19.5 × 27 × 30 EACH)
MK 82 LGB (GBU-10 2/2) STORES SHOWN)
NOTE: WEAPONS BAY CROSS-SECTIONAL SET BY
MK 82 LGB CELL IN DETERMINING
ALTERNATE LOADINGS.
28×9.0-12 SINGLES
12 PLY STRENGTH (4/4)
12'1.1 IN. STATIC TAIL DOWN
3'-6.6 STATIC GROUND CLEAR

2

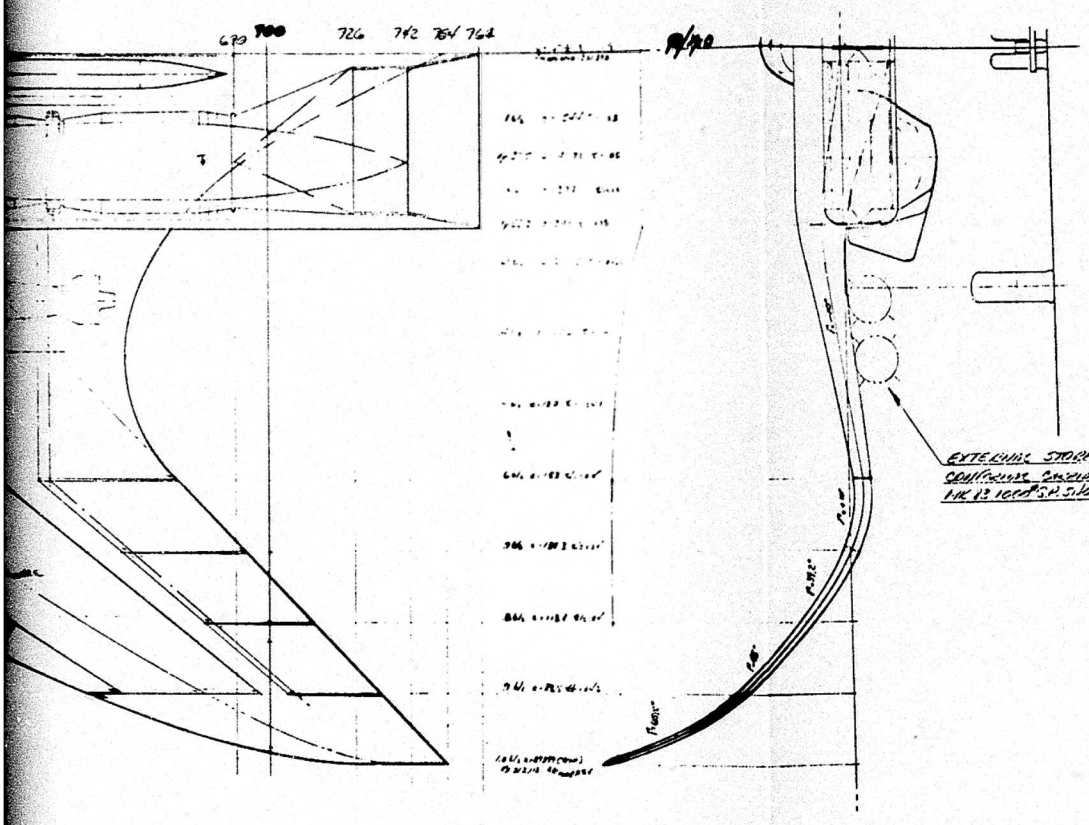

GEOMETRIC DATA

ITEM	WING (PLANE 2010)	CANARD (EXPOSED)
S	500 FT²	42 FT² EXPOSED
AR	2.5	2.4
λ	0.35	0
Λ LE	60°	40°
AIRFOIL	[illegible]	GAMMA 4
b	43.0.227	132.0
C_r	251.393	100.0
C_t	87.937	0
$\bar{C}$	182.206	64.57
$\bar{R}$	77.023	20.33
Γ	AS THICKNESS	10°

ASSUMPTIONS

- TWO F404-GE-400 TURBOJET ENGINES WITH TWO-DIMENSIONAL PLUG NOZZLES INCORPORATING THRUST VECTORING, THRUST SPOILAGE AND THRUST REVERSING.
- TWO-DIMENSIONAL EXTERNAL COMPRESSION INLETS WITH FIXED RAMPS. A_C = 525 SQ.IN. EACH

TARGET WEIGHTS

W_0 = 35000 LBS.
W_f = 7900 LBS.
W_{PL} = 5200 LBS.
- TWO MK84 LGB (GBU-10 C/C)
- TWO THRUST VECTORED TAIL MTD. SIDEWINDER
- M61 GUN WITH 200 RDS. AMMO.

NOTES

- THIS CONCEPT ILLUSTRATES AN ALL-METAL VEHICLE TO BE USED FOR COMPARISON PURPOSES WITH THE ADVANCED COMPOSITES CONFIGURATION DS72-44.

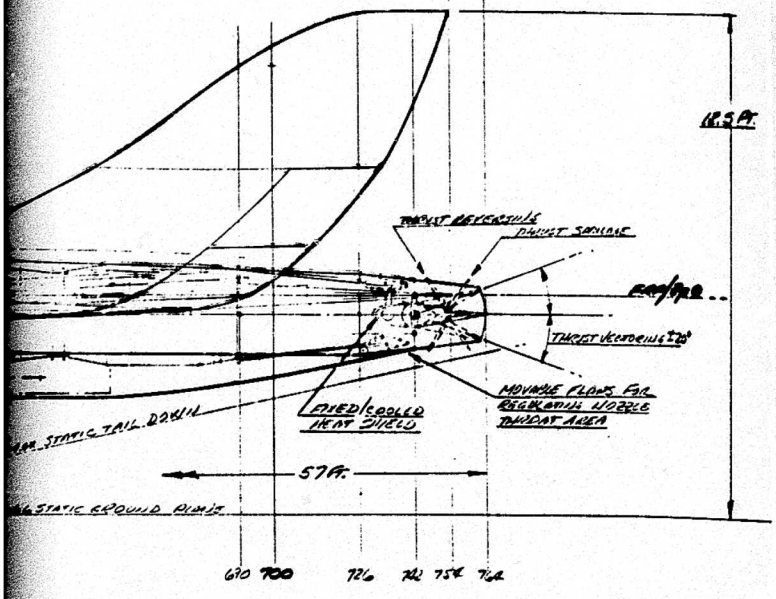

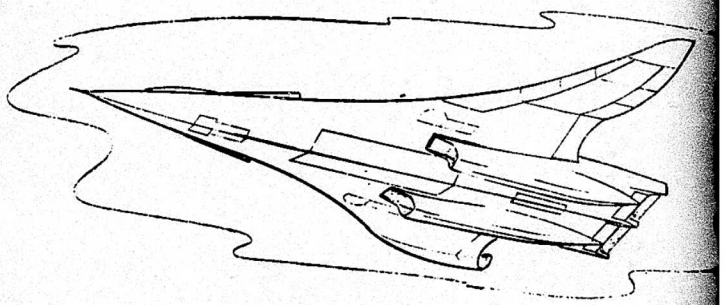

Figure 11. Advanced design composite aircraft study baseline comparison configuration.

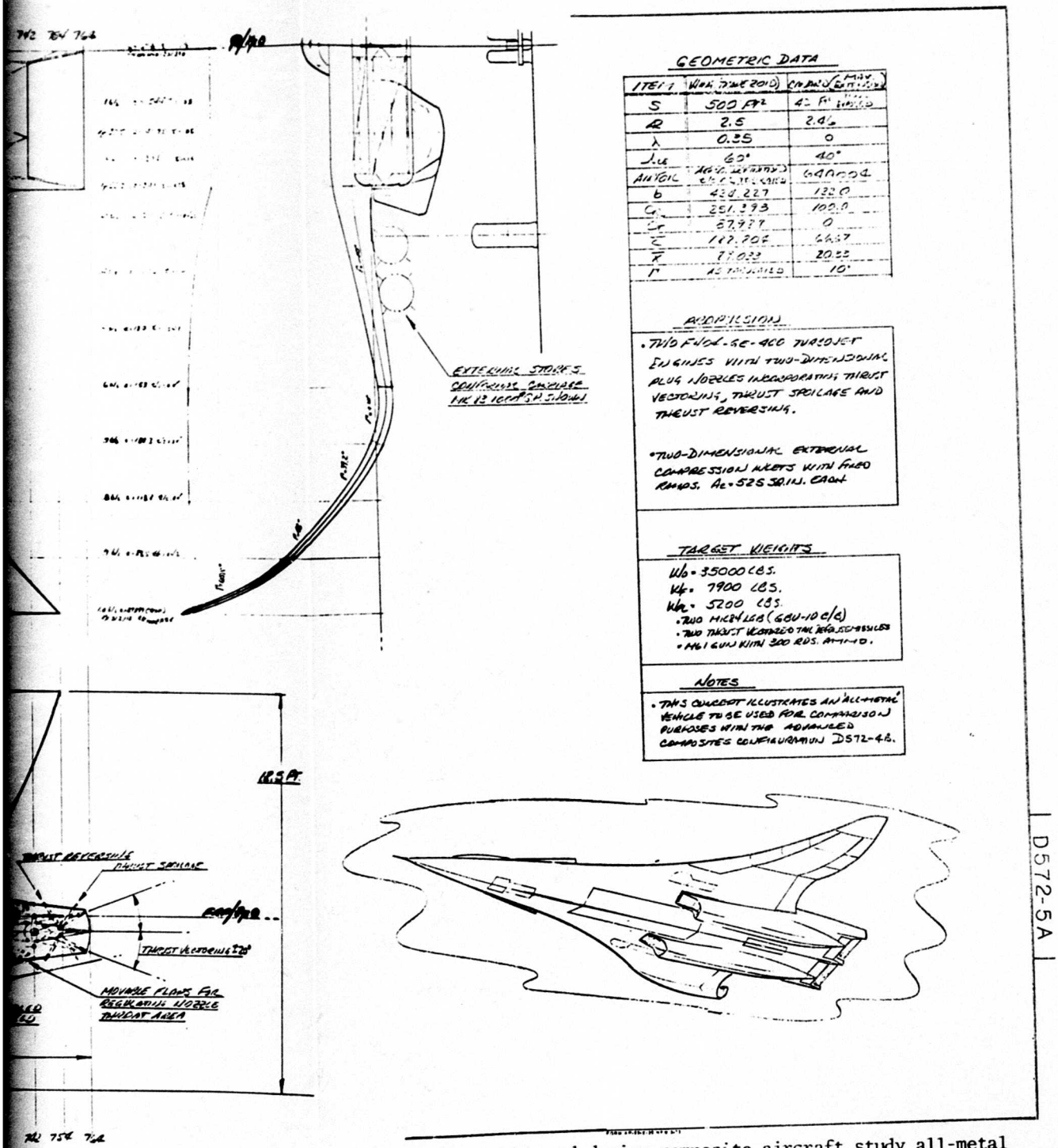

Figure 11. Advanced design composite aircraft study all-metal baseline comparison configuration.

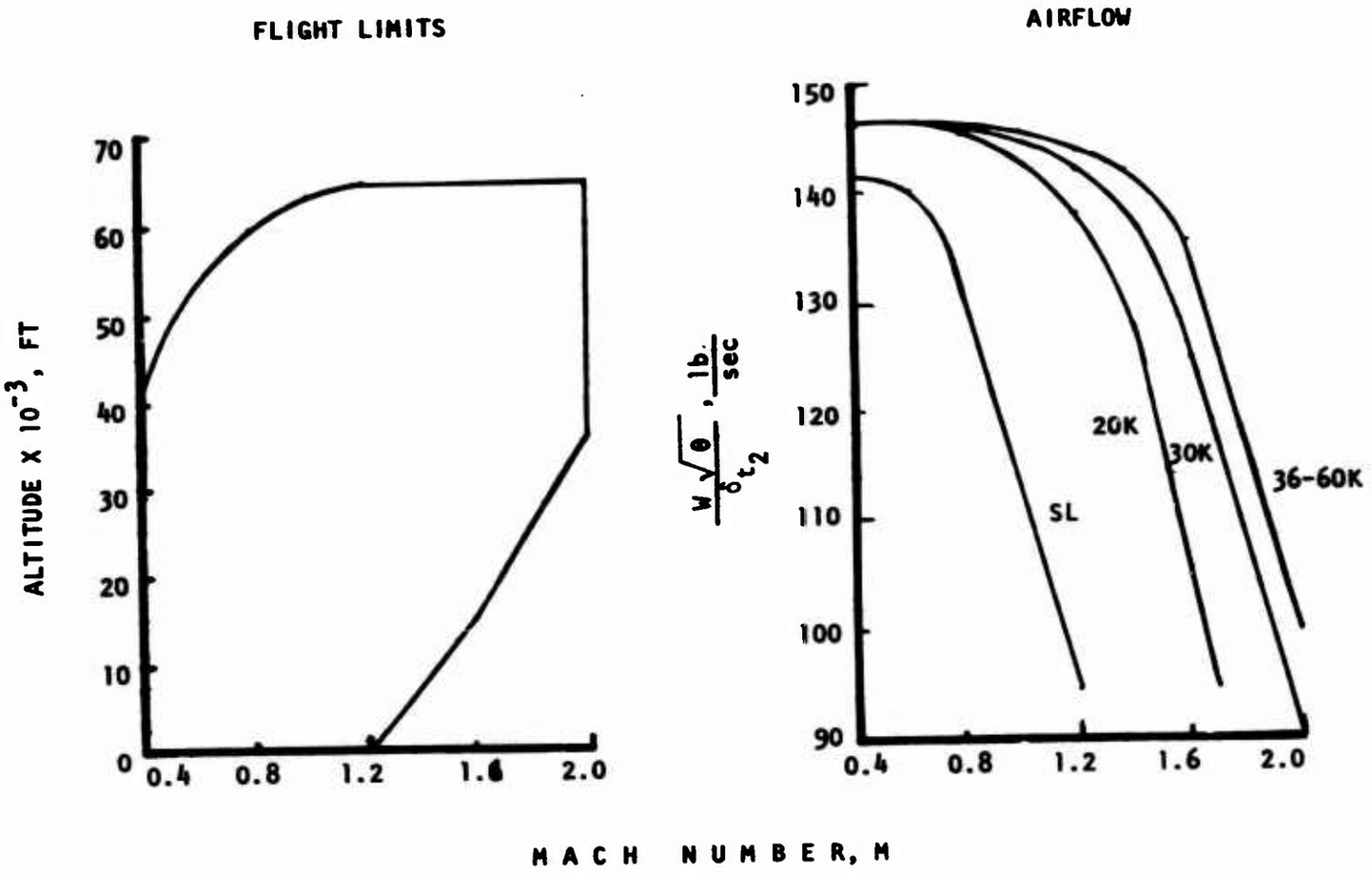

Figure 12. F404-GE-400 engine parameters.

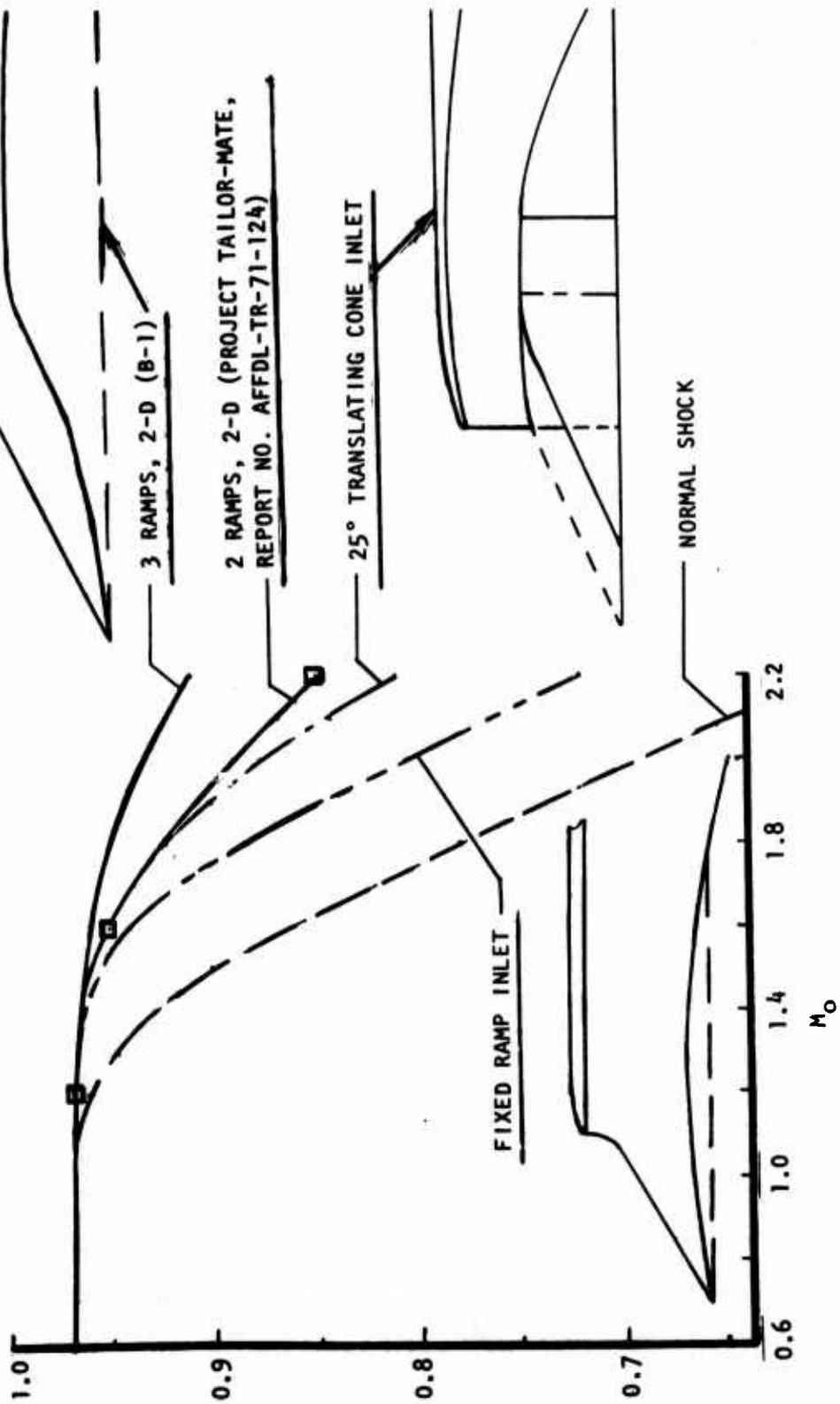

Figure 13. Inlet geometry comparison.

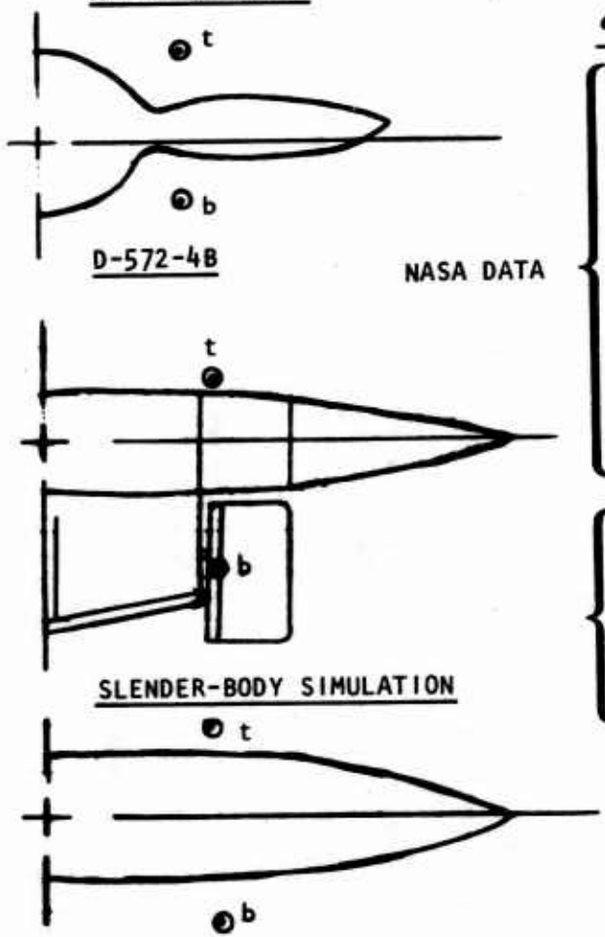

$M_o = 1.6$

		INLET STATION					
		LOCAL M		α		β	
α_o	β_o	t	b	t	b	t	b
3	0	1.70	1.60	2.0	2.5	2.0	2.0
3	5	1.71	1.59	-0.5	1.0	6.5	4.0
3	-5	1.68	1.52	-4.5	5.0	-3.5	-5.0
6	0	1.72	1.55	-3.5	3.0	3.0	-2.5
9	0	1.83	1.50	5.0	2.5	-7.5	-4.0
		SIMULATION					
4	0	1.61	1.59	-3.1	-1.6	-3.6	1.4
4	4	1.61	1.59	-2.8	-1.9	-3.7	1.2
4	-4	1.61	1.59	-3.7	-1.2	-3.4	1.8

NOTE: SLENDER BODY HAS 9:1 ELLIPSE RATIO.

Figure 14. ADCA inlet flow field survey.

data from NASA TN D-4809, "Flow Field Properties Near an Arrow-Wing-Body Model at Mach Numbers of 1.60, 2.36, and 2.96." This test showed unacceptable flow gradients in both pitch and yaw for a top inlet location. The figure also shows cross sections for both the D572-4B configuration and the 9:1 ellipse used in a Slender Body Simulation program. The simulation data show mild flow transients, however: (1) attempts to input a more representative body shape into the simulation were unsuccessful, and (2) the program accuracy is limited to about 5-degree pitch or yaw variations. More work is needed in this area.

The ADCA diffuser loss coefficient is estimated to be 8 percent of the throat dynamic pressure with good entrance flow. A perforated surface bleed region on the ramp at the inlet lip station will remove a boundary layer bleed flow equivalent to 1.5 percent of the inlet capture area at 1.6 mach number to minimize shock-boundary layer interaction and to achieve good diffuser entrance flow. The boundary layer bleed also helps to lower the mass flow ratios at which buzz instability occurs. Figure 15 presents B-1 inlet test data with the inlet ramps in the minimum angle, maximum throat area position (7° ramp angle vs 6° ramp for ADCA). For this off-design geometry, the B-1 inlet shows high performance at 1.4 mach number, but the pressure distortion (max-min/P_{t2}) and turbulence ($\Delta P_{RMS}/P_{t2}$) are unsatisfactory at 1.8 mach number. The combined effects of this distortion and turbulence exceed the inlet flow quality limits for the F101 engine. The B-1 inlet bleed pattern was optimized for four-shock operation. Improved performance with a low ramp angle will be achieved with future tests of the fixed ramp B-1 inlet with the boundary layer bleed configuration modified for fixed, single, ramp operation.

The above data, plus a survey of other inlet buzz margins, were used for the estimated buzz margin schedules of Figure 16. The aforementioned depressed engine air demand during the 20,000 feet penetration results in inlet-engine matching very near the buzz limit at 1.5 mach number. A decrease in engine air demand by an engine deficiency or a step increase in ambient temperature, a mach number overshoot, a decrease in angle of attack, or an air vehicle sideslip maneuver could rapidly use up the inlet stability margin, without bypass provisions. The effect of the inlet bypass system on maneuvering margin is shown on the right side of the figure. This bypass will be controlled by the inlet throat mach number at flight mach numbers above 1.4. Both the B-1 type of hinged door and a sliding block type of bypass exit will be studied during the structural design phase. The concept most compatible with composite construction will be employed.

The estimated inlet performance data used in the installed performance calculations are shown on Figures 17 and 18. These performance estimates were supported by the extensive B-1 inlet test data.

AEDC TESTS S316, T164

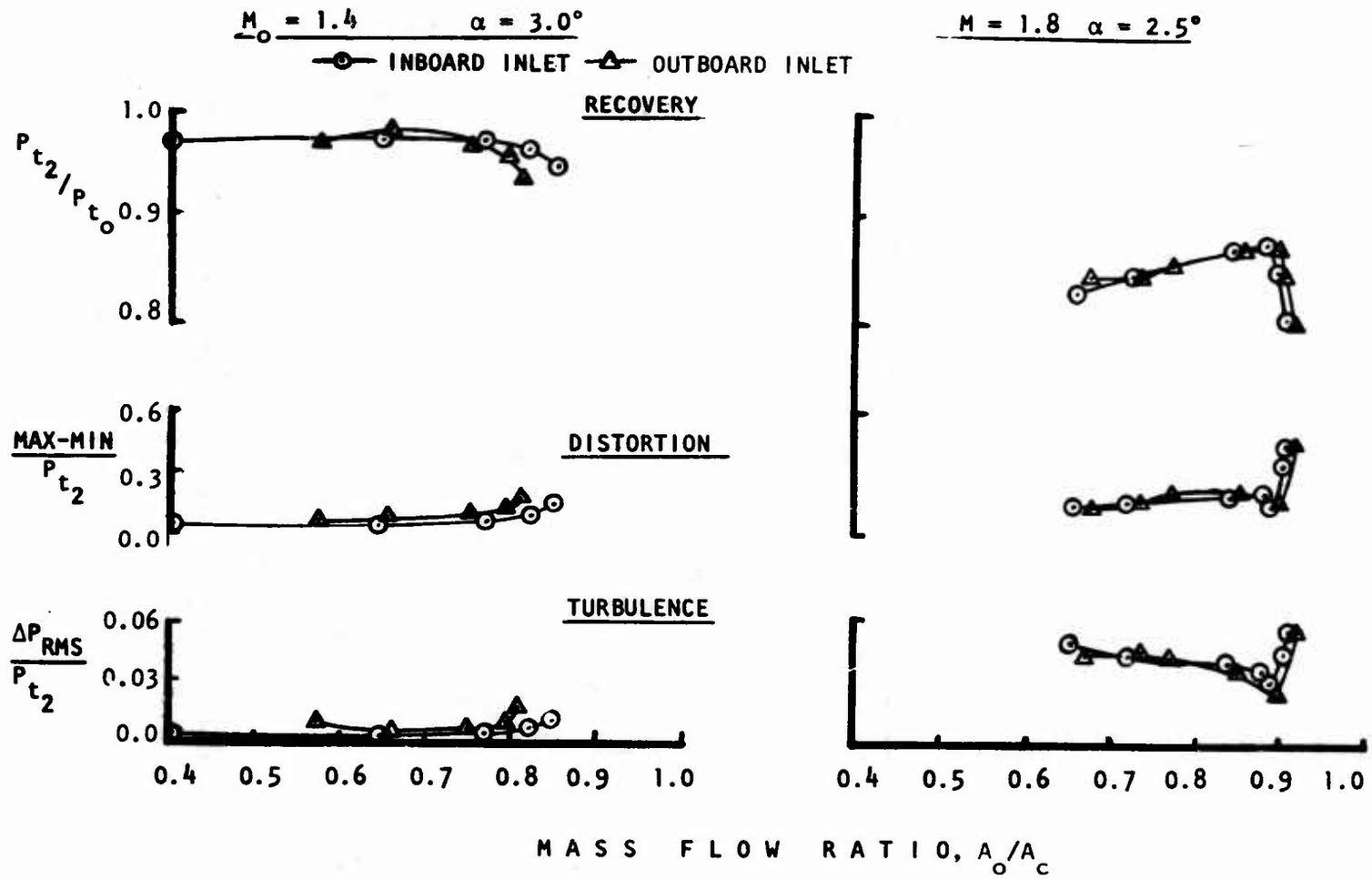

Figure 15. Fixed-geometry B-1 inlet operation - AEDC tests S316, T164.

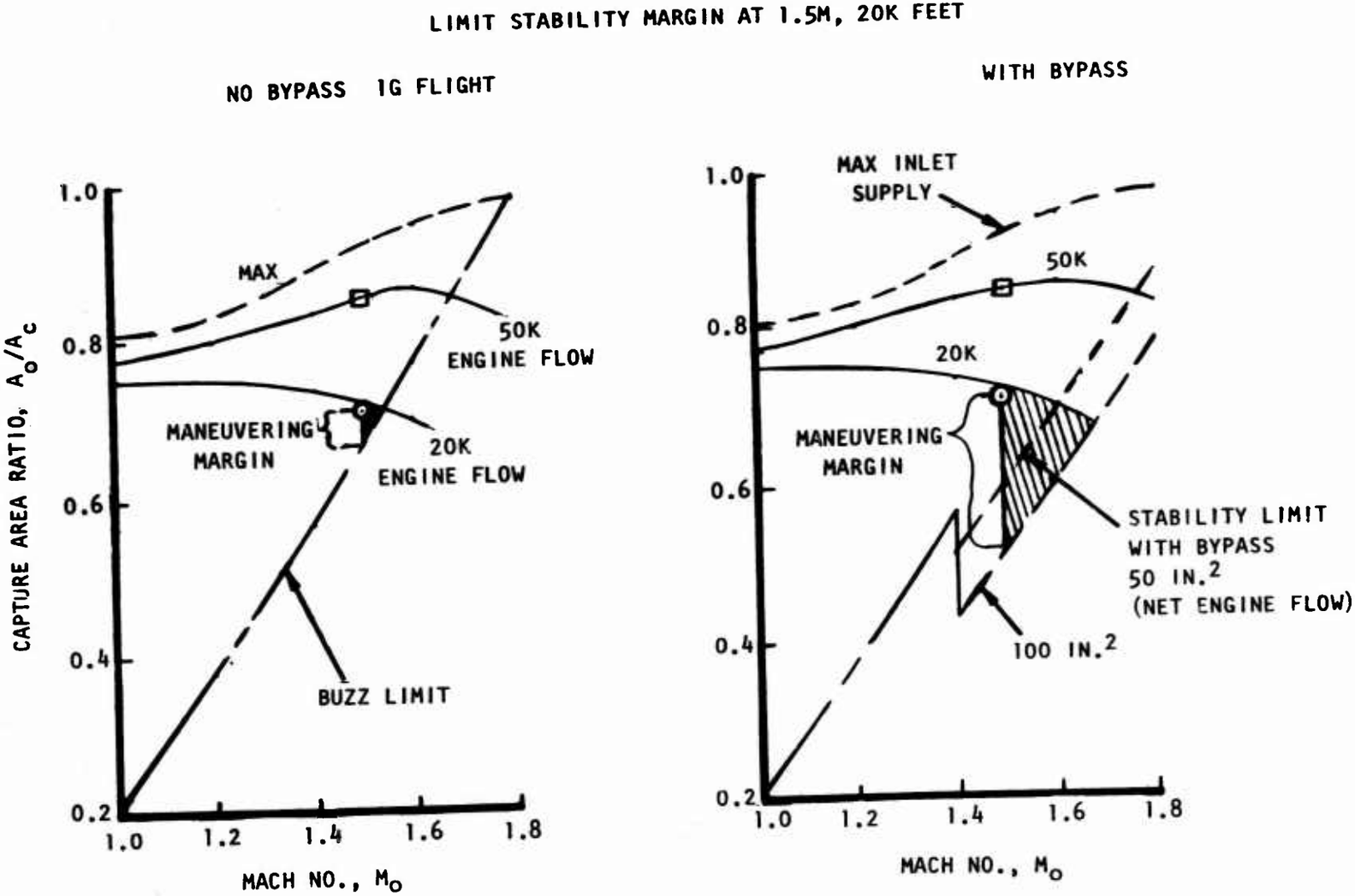

Figure 16. ADCA inlet bypass sizing.

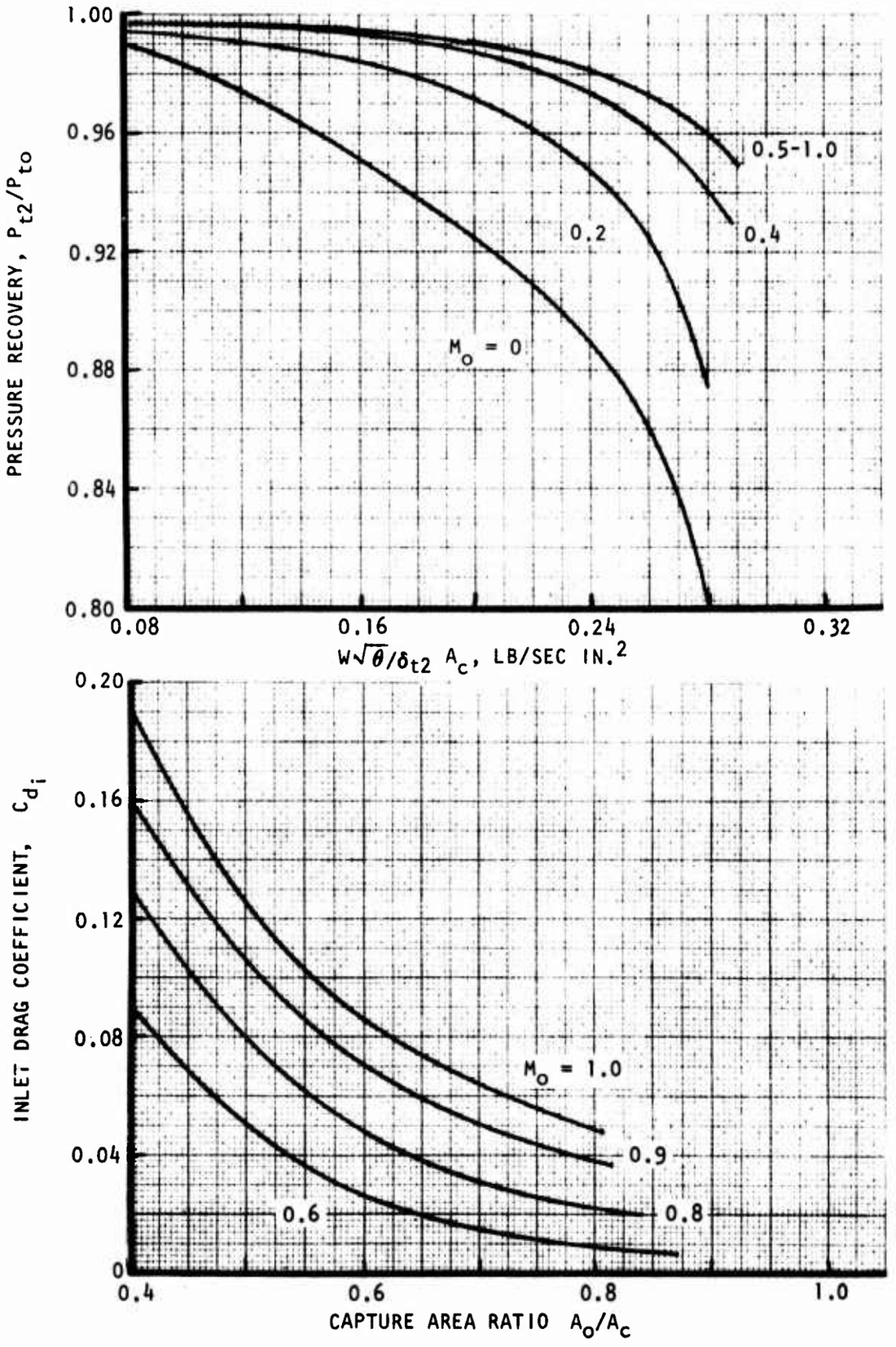

Figure 17. Inlet performance - subsonic.

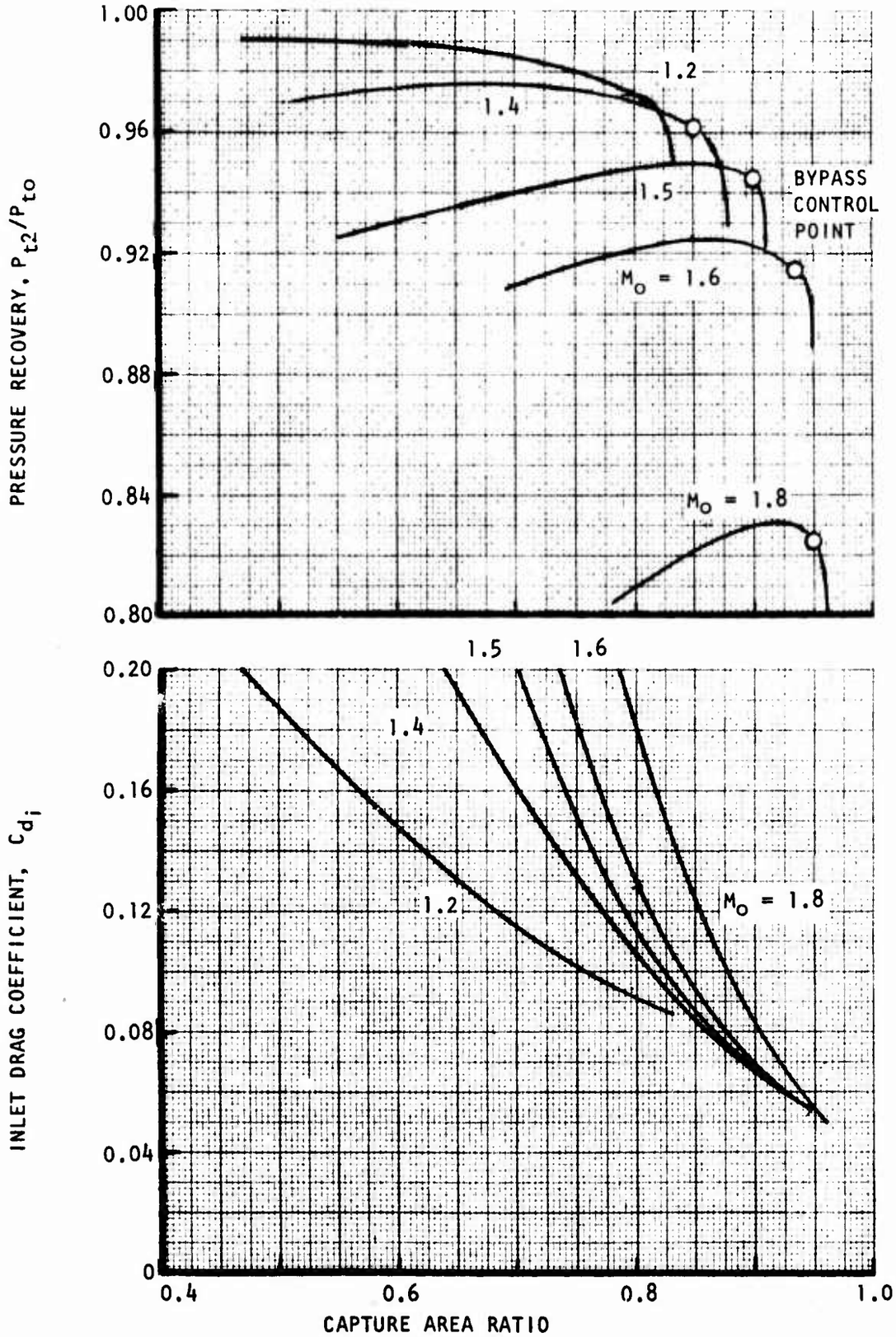

Figure 18. Inlet performance - supersonic.

Exhaust Nozzle Selection

The F404-GE-400 axisymmetric augmentor and nozzle and the 2-D plug nozzle with both a high intensity "Vee" gutter and the PWA swirl burner augmentors are depicted on Figure 19. The swirl burners have demonstrated efficient combustion in a short length, and the burner can surface provides an intermediate heat shield for the augmentor walls and thus minimizes the augmentor shroud cooling airflow, pressure drop, and thrust penalty for cooling. The high-intensity "V" gutter will create high-pressure losses and will result in high heat transfer to the augmentor walls. Therefore, the swirl burner augmentor design will produce the best fuel consumption for this application due to reduced cooling airflow and pressure losses. To determine the most critical flight conditions for nozzle performance, the ADCA fuel usage versus range for both the basic and alternate missions are plotted on Figure 20. The mission segments of greatest significance are 3, 5, 7, and 8. The nozzle/afterbody performance for these segments is analyzed in detail in the following sections. Figure 21 compares the nozzle area ratio schedules, i.e., exit area, A_9, versus throat area A_8, for both the GE axisymmetric nozzle and the Rockwell 2-D plug nozzles, and the resulting isentropic thrust coefficients for the significant cruise points. The GE nozzle is optimized for the F-18 air vehicle but is not the best choice for supersonic cruise at Intermediate Power due to its low expansion ratio at minimum A_8.

The ADCA nozzle/afterbody is shown on Figure 22. Significant cross-section areas are noted on the figure. The cross-hatched regions on the rear view illustrates the expansion areas on the plug and sidewalls. As shown on Figure 26, the nozzle throat area between the flaps and plug and the nozzle flap contour is controlled by a pair of actuators mounted in the sidewalls. The A_9/A_8 ratio is 1.5 at Intermediate Power and decreases to 1.2 at Maximum Power, Figure 21. At supersonic speeds an additional external expansion thrust is created on the plug surface. As will be shown later, a 2-D plug nozzle does not incur significant overexpansion losses at subsonic cruise conditions. Data to be presented in AIAA 75-1317, "Investigation of Two-Dimensional Wedge Nozzles for Advanced Aircraft," show that internal-external expansion 2-D nozzles show very high thrust minus drag transonic speeds.

The plug nozzle thrust bookkeeping is shown on Figure 23. The Rockwell procedure used for ADCA divides the external aerodynamics and propulsion drag responsibilities at Station 726. The nozzle/afterbody performance is expressed as gross thrust minus drag (F_g-D) divided by the ideal gross thrust potential for gas properties measured at the augmentor exit, F_{gi}. The nozzle/afterbody forces are:

1. expansion decrement - $\Delta F_{isen}/F_{gi}$, due to a non-optimum nozzle area ratio

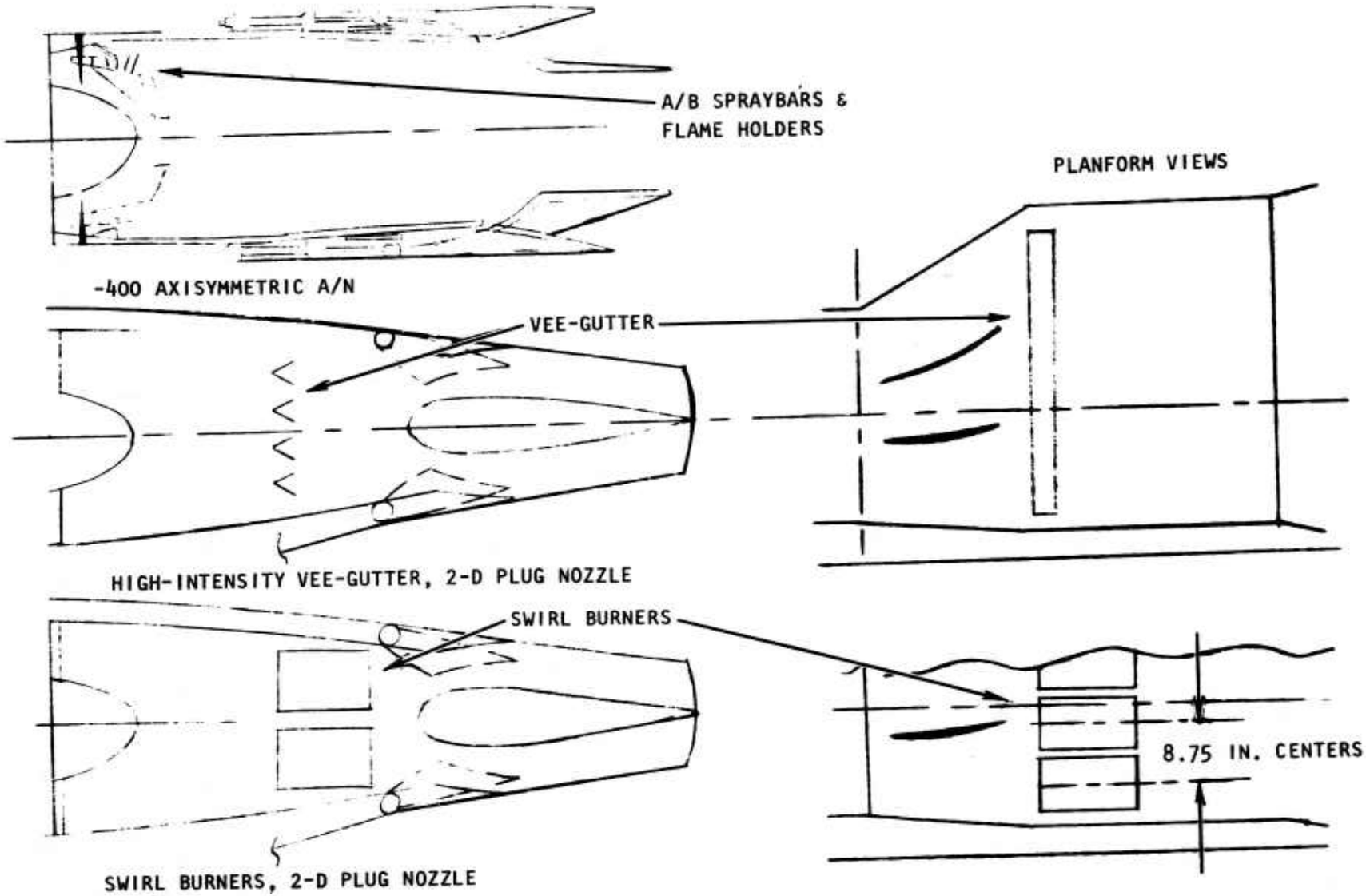

Figure 19. F404 augmentor/nozzle variants.

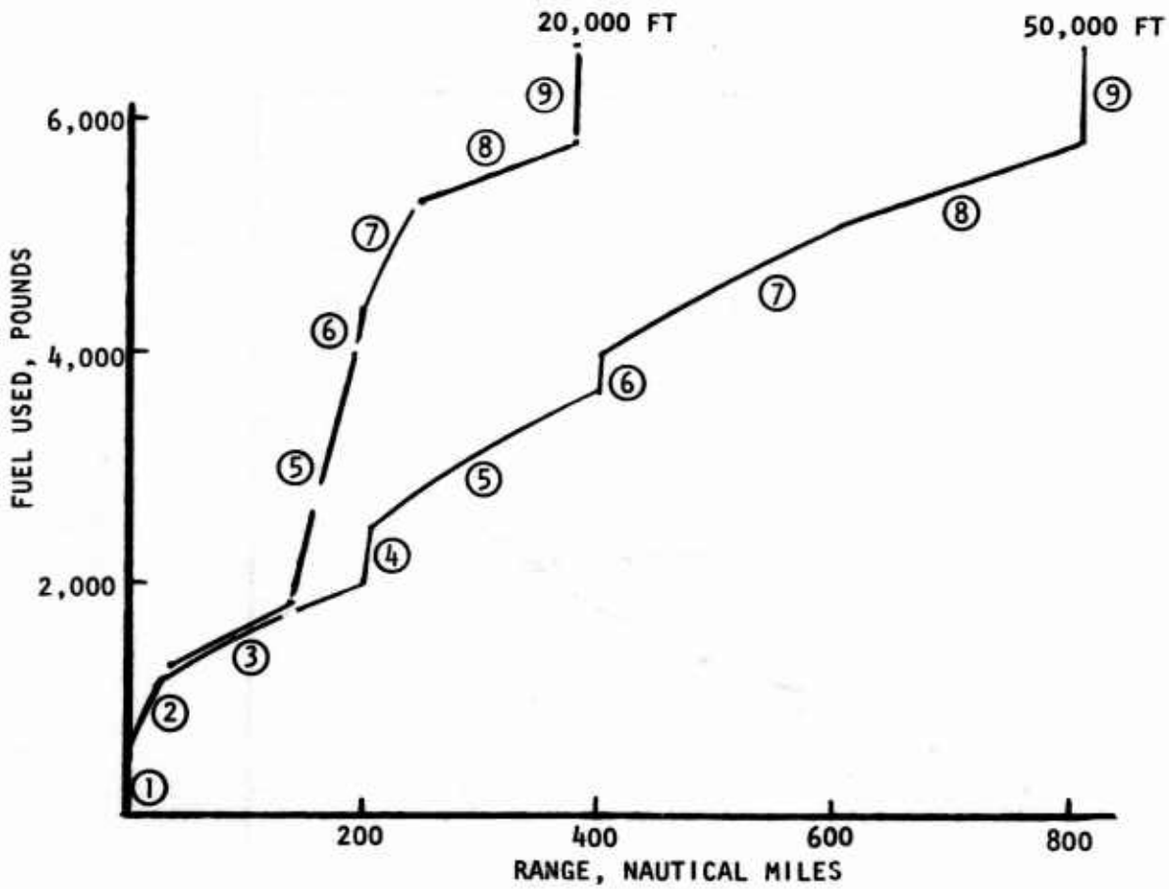

	MODE	M_o
①	T.O.	
②	CLIMB	0.9
③	CRUISE	0.95
④	CL - ACCEL	1.5
⑤	CRUISE	1.5
⑥	TURN	1.5
⑦	CRUISE	1.5
⑧	CRUISE	0.92
⑨	LOITER	0.3

Figure 20. ADCA mission profiles.

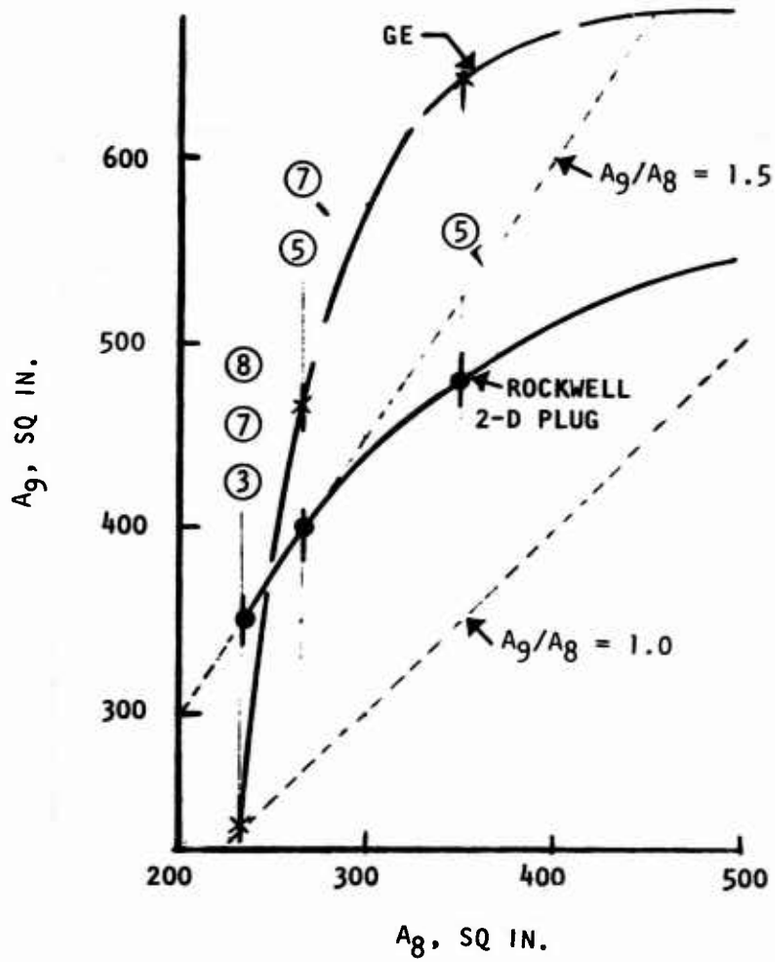

MODE	M_o	P_{t8}/P_o	F_{isen}/F_{gi} GE	F_{isen}/F_{gi} ROCKWELL
20,000 FT MISSION				
③	0.95	4.4	0.975	0.993
⑤	1.5	7.0	0.993	0.995
⑦	1.5	7.3	0.997	0.997
⑧	0.95	4.1	0.981	0.992
50,000 FT MISSION				
③	0.95	4.4	0.975	0.993
⑤	1.5	9.0	0.997	0.981
⑦	1.5	8.6	0.929	0.993
⑧	0.95	4.1	0.981	0.992

Figure 21. F404 nozzle comparison, ADCA mission.

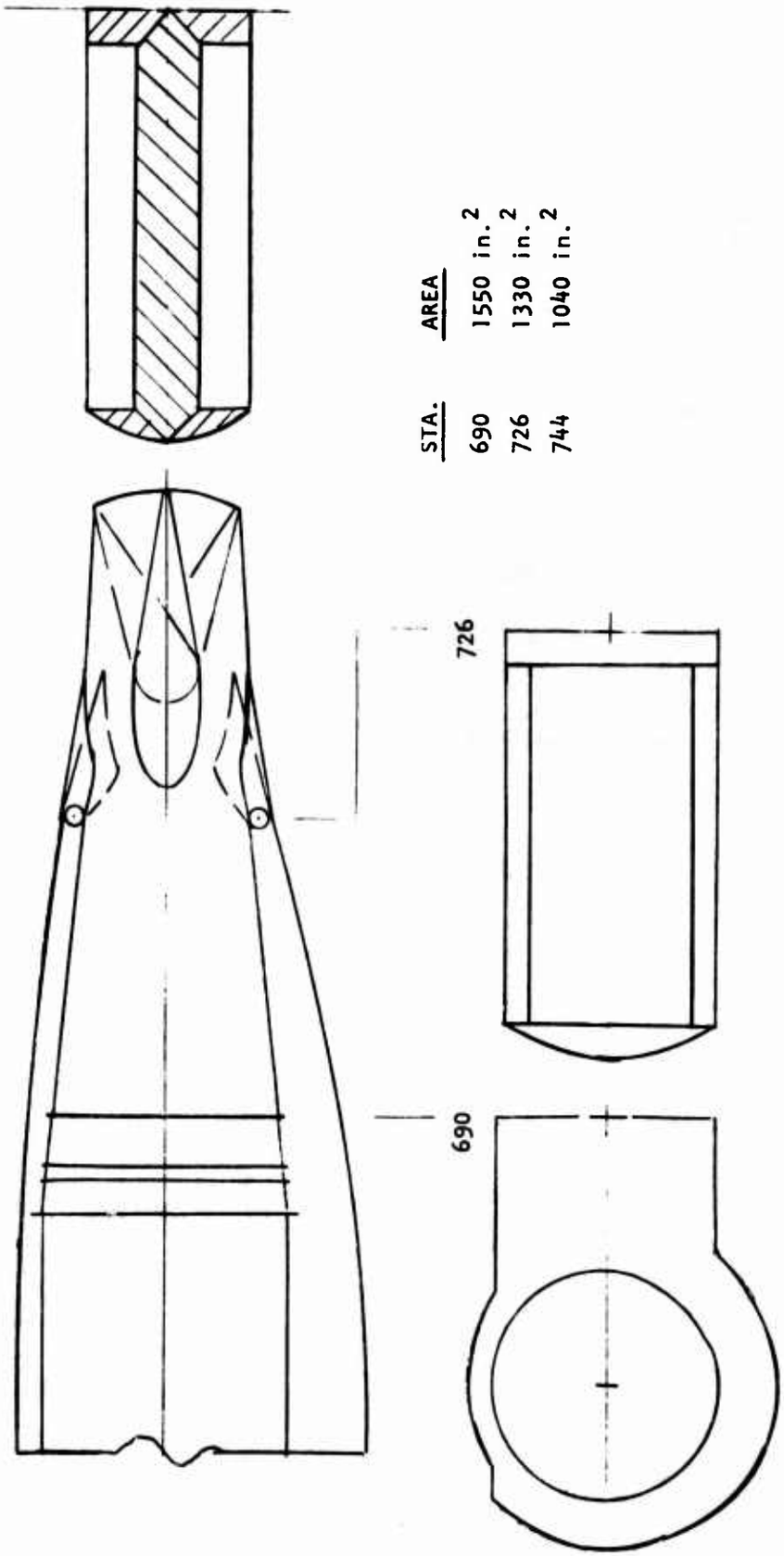

Figure 22. ADCA nozzle/afterbody.

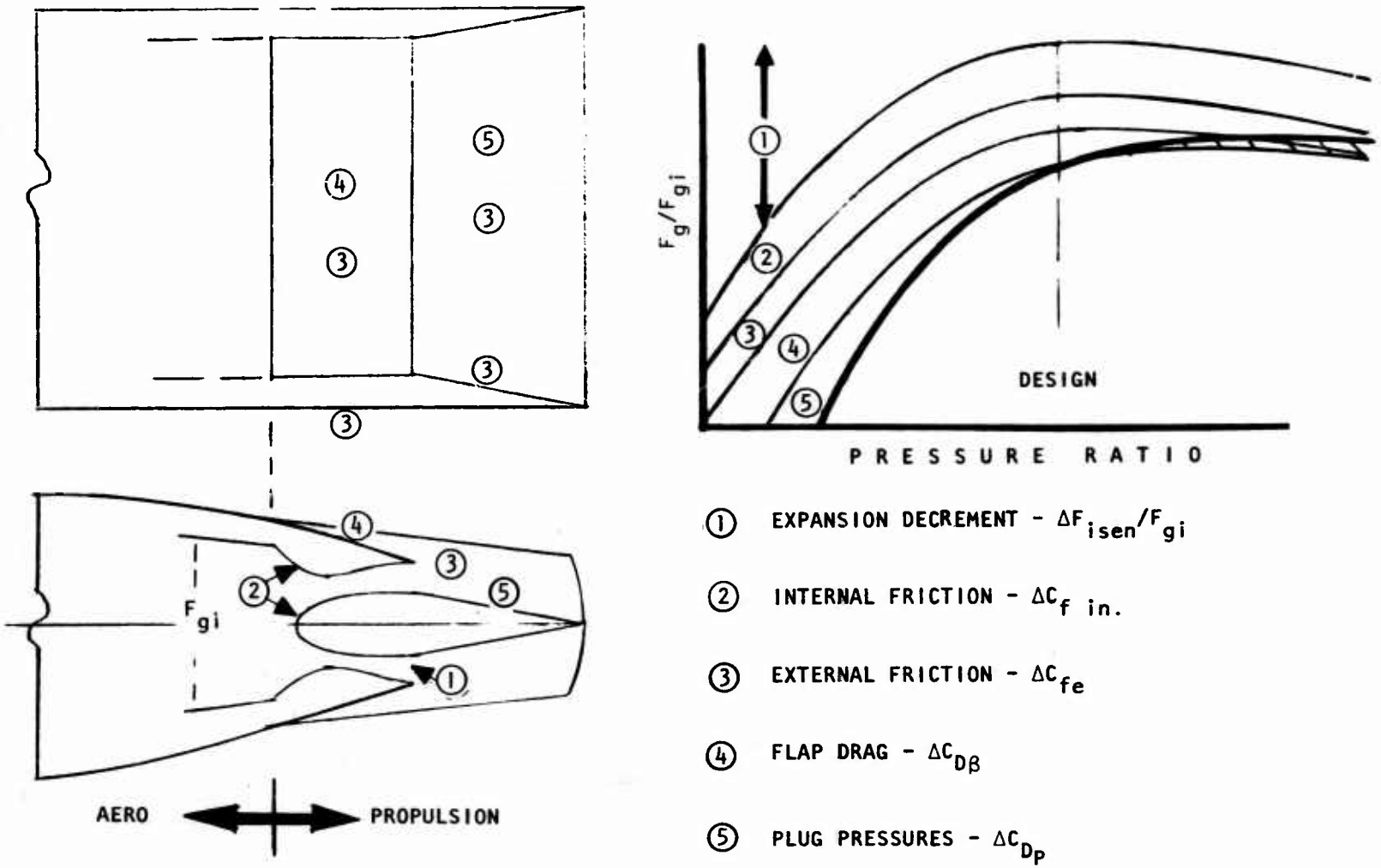

Figure 23. Plug nozzle thrust bookkeeping.

2. internal nozzle friction - $\Delta C_{f\ in}$

3. external friction aft of Station 744, sidewalls and plug surface scrubbed by exhaust gases - ΔC_{fe}

4. pressure drag on the external flap surface - ΔC_{D_β}

5. the pressure drag or thrust on the plug and sidewall surface - ΔC_{D_P}

The plots on the right of the figure illustrate typical trends of these nozzle/afterbody thrust and drag components versus nozzle pressure ratio. Note that item 5 becomes a thrust increment at nozzle pressure ratios above design.

Figure 24 compares the ADCA afterbody and the plug nozzle test model reported in NASA TN D-7906, "Performance of an Isolated Two-Dimensional Variable-Geometry Wedge Nozzle with Translating Shroud and Collapsing Wedge at Speeds Up to Mach 2.01." The afterbody drag estimates on the right side of the figure were based upon boattail drag versus area ratio trends from L/D = 1 models, NASA TN D-7163, "Effects of Fineness and Closure Ratios on Boattail Drag of Circular-Arc Afterbody Models With Jet Exhaust at Mach Numbers Up to 1.3," at mach numbers below 1.2 and Prandtl-Meyer expansion calculations at mach numbers above 1.2. These calculations were based on jet exit conditions which result in ambient pressure at the junction of the jet and external flow. The solid curve represents the afterbody drag forward of Station 726 that is buried in the air vehicle wave drag computations. The ΔC_d between stations 726 and 744 is part of the propulsion bookeeping, item (4) of the preceding figure, assuming a continuing Prandtl-Meyer expansion aft of station 726, at $M_o > 1$, and no interaction with the nozzle exhaust for this case.

Test data in TN D-7906 were used to extrapolate and interpolate nozzle/afterbody performance at mach 1.5 cruise conditions. Selected NASA data are shown on Figures 2-19 (simulated dry power nozzle) and 2-20 (simulated maximum power nozzle). The circular symbols denote static test thrust coefficients; a 0.985 F_{isen}/F_i (items 1 and 2 of Figure 23) is included for comparison and extrapolation. The diamond symbols denote the NASA test $(F_j - F_a, ap)/Fi$ (model thrust minus drag adjusted for afterbody friction drag). Afterbody pressure data were not shown in the NASA report. The "X" symbols show a Rockwell correction for the estimated afterbody drag from Figure 24 - $\Delta C_{f_\beta} = C_{D_\beta}/F_i$. Thus, the $\Delta C_{f\ ex}$ is the combined plug pressure force and friction drag on the plug and sidewalls (items 3 and 5 on Figure 23) plus interaction between the exhaust jet and boattail).

The dry power nozzle with an internal expansion ratio of 1.53 (design pressure ratio = 6.05) is examined on Figure 25. The $M_o = 0.95$ data show a high $\Delta C_{f\ ex}$ at low nozzle pressure ratio but this increment decreases to little more than plug and sidewall friction drag at pressure ratios of 3 to 4. At very low pressure ratios the overexpanded jet probably sucked down the

M_o < 1.2 (TN-D-7163), M_o > 1.2 (P-M EXPANSION)

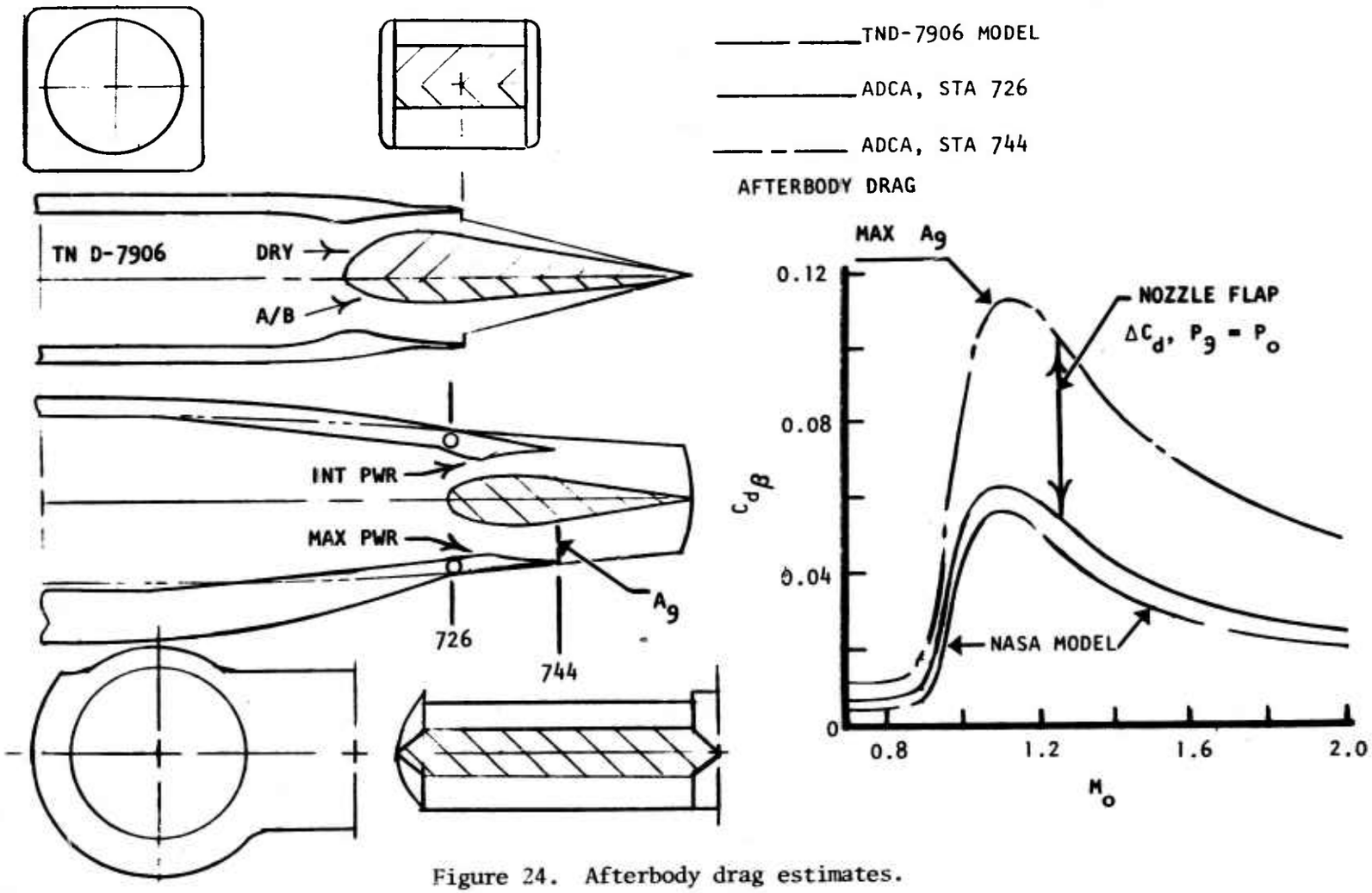

Figure 24. Afterbody drag estimates.

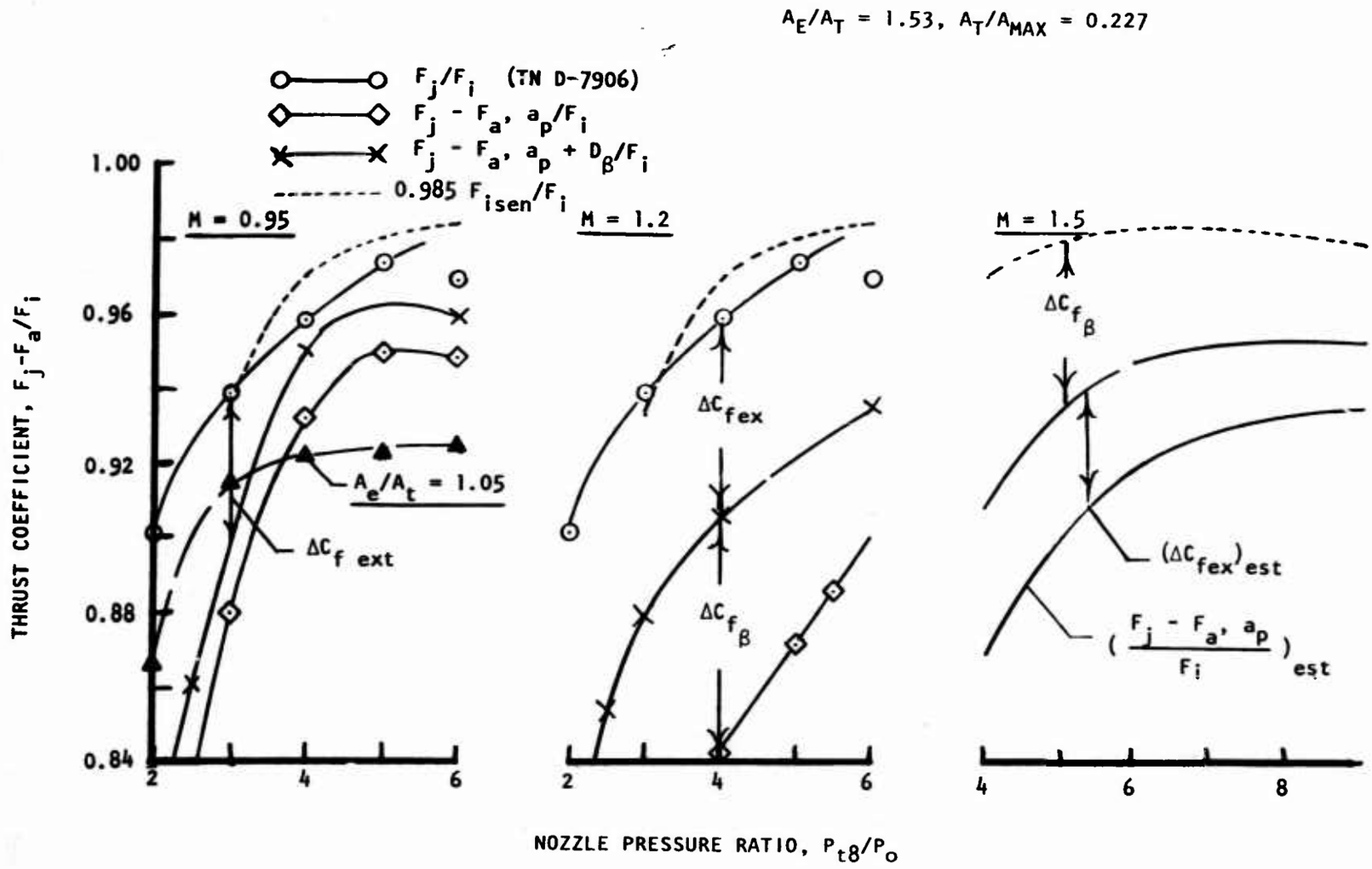

Figure 25. Review of NASA TN D-7906 data-I.

boattail surfaces and may have further overexpanded on the plug. The A_e/A_c = 1.05 nozzle (design pressure ratio = 2.6) showed better performance at pressure ratios below 3.5. At mach 1.2 the $\Delta C_{f\ ex}$ was about 6 points at all nozzle pressure ratios. At mach 1.5 the $\Delta C_{f\ ex}$ was estimated to be about 2 points in the anticipated operating pressure ratios of 7 to 9. The $\Delta C_{f\ ex}$ increment is much smaller with the maximum power nozzle at 1.2M (Figure 26) due to the lower internal expansion ratio and smaller plug/nozzle area ratio. At mach 2.0 a substantial plug thrust is indicated. Interpolation indicates a small external force penalty at mach 1.5.

The data from NASA TN D-7906 and AIAA 75-1317 show that twin 2-D plug nozzles will provide significantly higher thrust minus drag than axisymmetric nozzles. Experimental data at mach 1.2 and 2.0 indicate that efficient supersonic cruise with 2-D nozzles can be achieved. It also appears that the plug forces approach friction drag at subsonic speeds and 75 to 100 percent of the design internal expansion pressure ratio.

One of the major unknown factors of supersonic cruise performance is the effect of boattail flow-exhaust jet interaction. The local mach numbers on the basic body will be above freestream due to the progressive reduction in cross section to station 726. Prandtl-Meyer expansions at the nozzle flap hinge can create even more sub-ambient pressure and drag. Tests of axially symmetric boattails show that a positive exit static pressure of an underexpanded jet will initiate a shock-induced separation of the boattail boundary and create a region of ambient or positive pressures over a part of the boattail. This is illustrated on Figure 27; the scheduled geometry operation results in a jet exit static-pressure ratio of 1.6 and an 8-degree turning of the jet boundary. The flap angle was 14 degrees at this point; therefore, it was assumed that 8/14 of the theoretical flap drag was cancelled by ambient pressure on the flap. As shown by the bar chart on the right side of the figure, the thrust minus drag is within two points of the complete expansion geometry configuration.

The thrust coefficients used for the installed performance calculations in May 1975, were developed in TFD-75-573, "Inlet and 2-D Plug Nozzle Design and Performance, ADCA Supersonic Penetration Interdiction Fighter," from a brief review of the aforementioned NASA TN D-7906. The nozzle pressure ratio versus mach number trends at part power cruise conditions were unknown at that point so the simple C_{fg} versus P_{t8}/P_o was employed. Figure 28 presents a recap of both the 20,000 and 50,000 feet penetration missions.

The C_{fg} versus P_{t8}/P_o data on the left present the simplified data inputs used for the initial propulsion inputs for the ADCA mission analyses and several detailed spot point analyses of cruise segments. The ΔC_{fg} increments between the curves and specific points were utilized to compute the change in specific fuel consumption, ΔSFC, and the resulting errors in mission fuel usage, ΔW_f, shown on the table to the right side of Figure 28. The points (3) and (8) show that a detailed analysis assigned a larger boattail drag penalty during

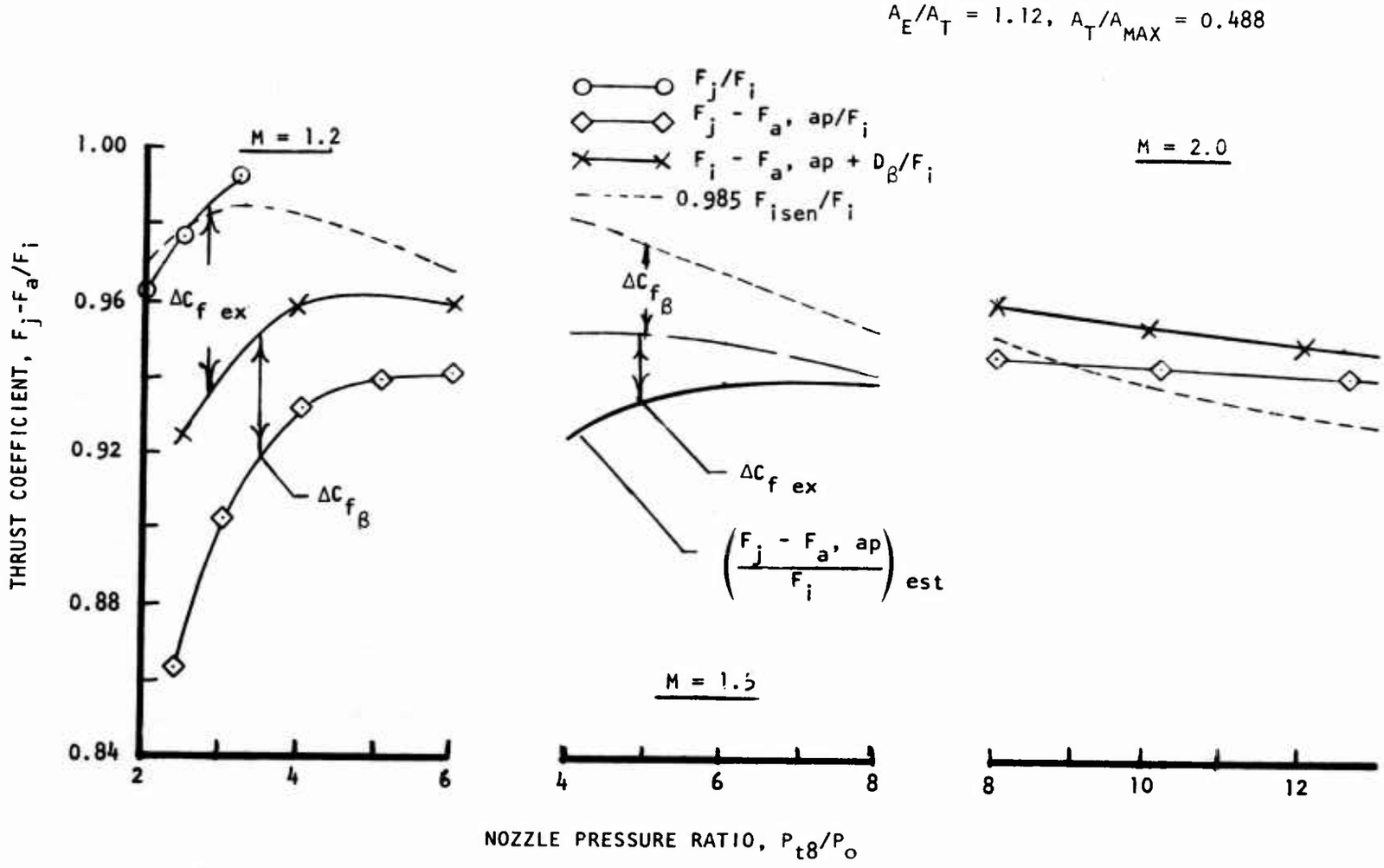

Figure 26. Review of NASA TN D-7906 data-II.

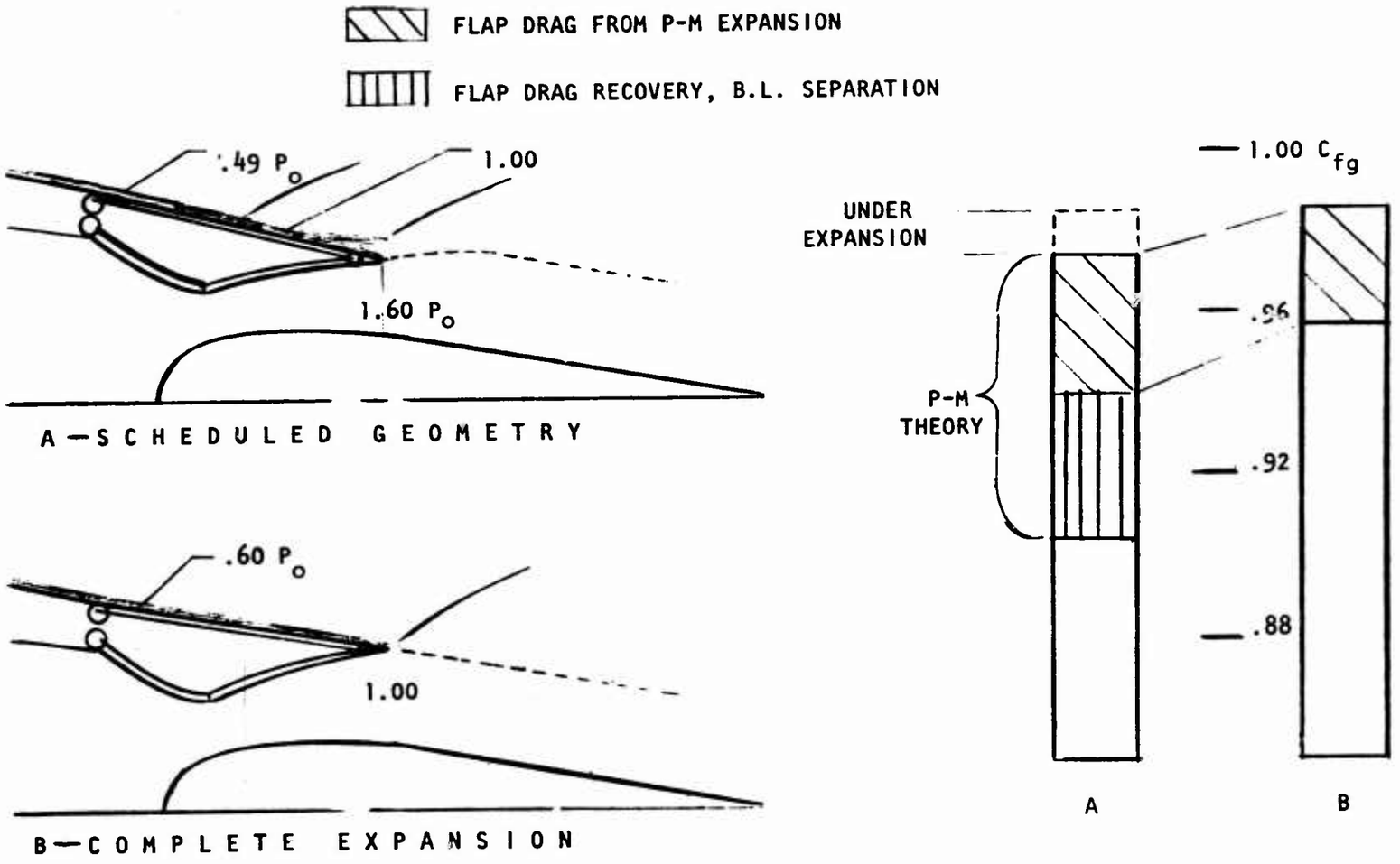

Figure 27. Exhaust nozzle flow - M_o = 1.5 intermediate power.

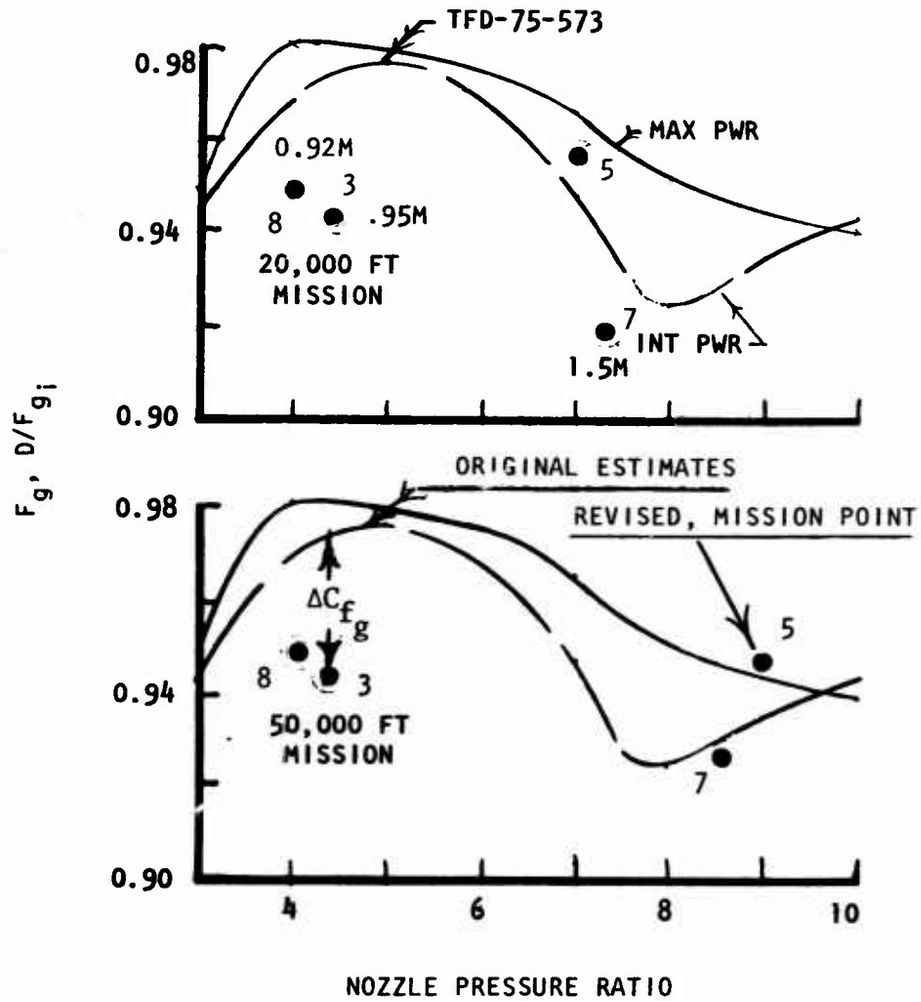

FUEL CONSUMPTION

20,000 FT MISSION

	ΔSFC %	W_f lb	ΔW_f lb	$\Sigma\Delta W_f$ lb	
③	4.9	603	+29	+85	
⑤	-0.6	1979	-12		
⑦	5.1	979	+50		-6 MILES RADIUS
⑧	3.6	489	+18		

50,000 FT MISSION

③	4.9	837	+41	+54	
⑤	-3.0	1226	-37		
⑦	2.2	1074	+24		-7 MILES RADIUS
⑧	3.6	724	+26		

Figure 28. ADCA nozzle performance recap.

operation at 50 to 60 percent of Intermediate Power. The initial optimism was due to (1) an anticipated higher power level and nozzle pressure ratio at subsonic cruise, and (2) an under estimation of the flap drag penalty at M_0 = 0.92 - 0.95, see Figure 24. The original flap drag estimates were more conservative and realistic at M_0 = 1.5. The fuel consumption table on the right side of the figure shows that the cruise fuel consumption was off by 85 pounds for the low-altitude mission and 54 pounds for the high-altitude mission. The 6-and-7 mile losses in radius could be partially cancelled by reducing the subsonic cruise mach numbers and boattail drag. For future performance computations a more complex input matrix of thrust coefficient versus nozzle pressure ratio at constant mach number for several nozzle positions will be used.

Nozzle Configuration Details

The nozzle cooling concept is shown on Figure 29. This concept uses trends from the report P&WA FR-6634, "Afterburning Jet Flap Exhaust System for F100/AFTI." Eight percent of the augmentor entrance flow will be diverted to the cooling liner for film cooling of the augmentor and primary nozzle flap. An additional 3-percent flow will be ducted into the nozzle flap and sidewalls in the throat region. Another 4-percent cooling flow will be ducted into the plug cavity for film cooling of the plug surface. Most of the plug cooling flow will be concentrated at the plug leading edge and nozzle throat region. A small flow through the vectoring pivot tube will pressurize and ventilate the plug cavity. This air will exhaust through the slots at the plug vectoring and reverser hinge gaps.

Figure 30 shows the ADCA thrust reverser for minimizing landing distance. For this simple, lightweight geometry the reversed thrust vector is limited by flow choking between the nozzle flaps and reverser doors, A_r = reversed gas throat. A higher reversed thrust could be achieved with a longer, articulated door and a longer plug. This configuration could be beefed up to an in-flight reverser if studies indicate desire for an in-flight thrust reverser for SAM avoidance maneuvers.

A more detailed drawing of the ADCA augmentor and nozzle is shown on Figure 31. The nozzle throat area, A_8, and exit area, A_9, will be controlled by actuators in the sidewalls and connecting linkage to assure both vertical and horizontal symmetry. The thrust vectoring and reversing functions will be accomplished by actuators located in the plug cavity.

Summary

The D572-4B propulsion system design is based on proven inlet technology and F404 engines modified for rectangular, vectoring plug, and exhaust nozzles. An inlet bypass system will be needed to insure inlet-engine compatibility for the 20,000-foot supersonic mission. The initial 2-D plug nozzle performance

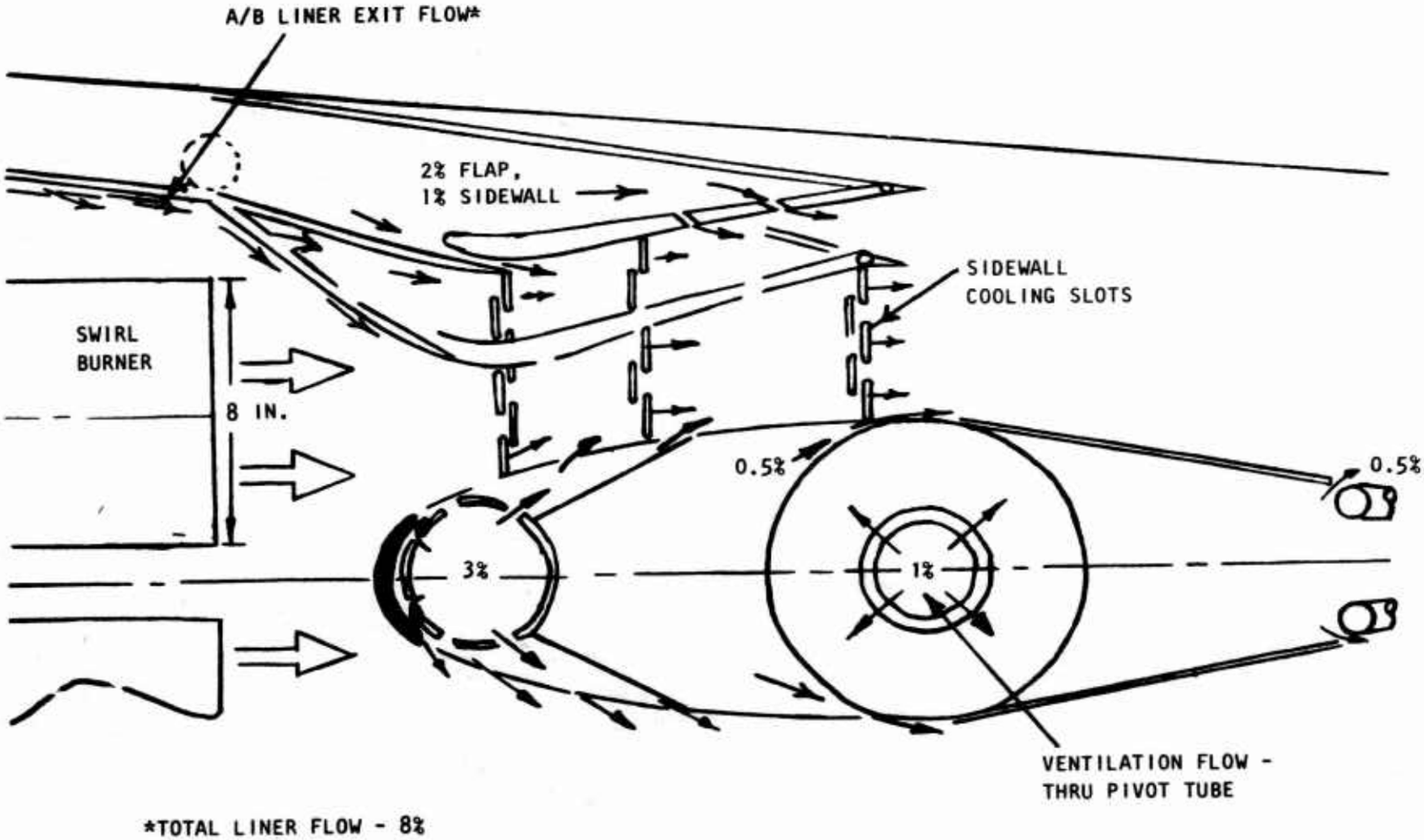

Figure 29. Nozzle cooling concept.

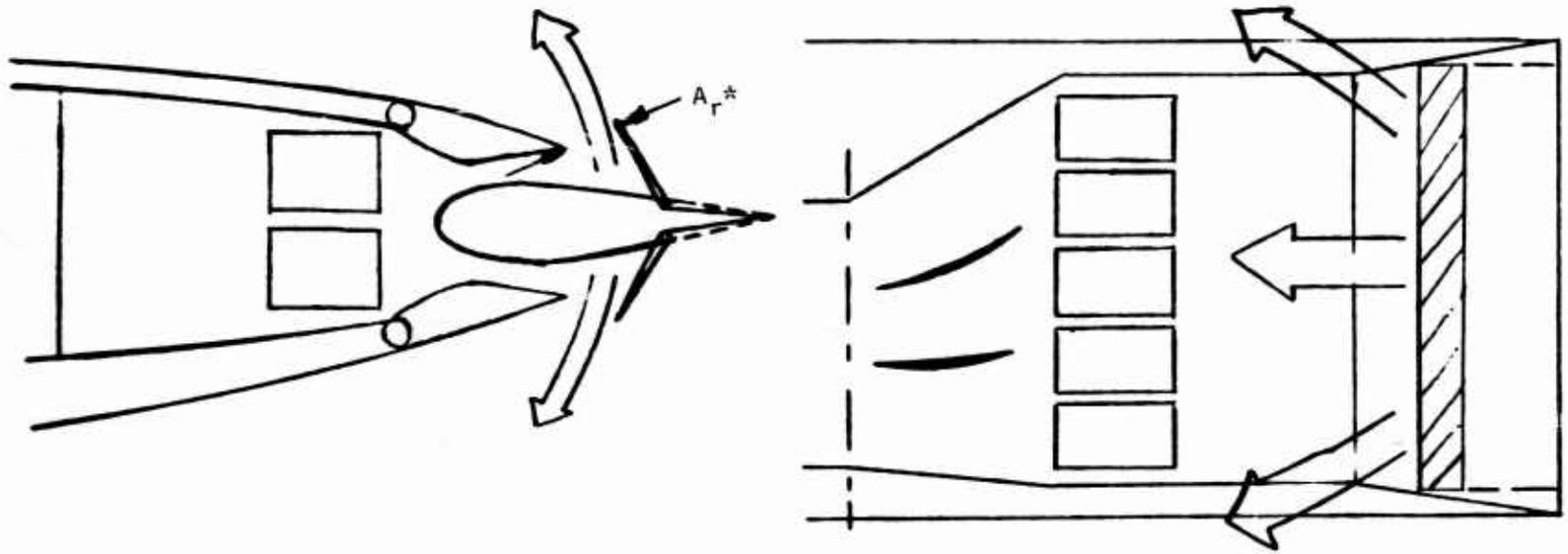

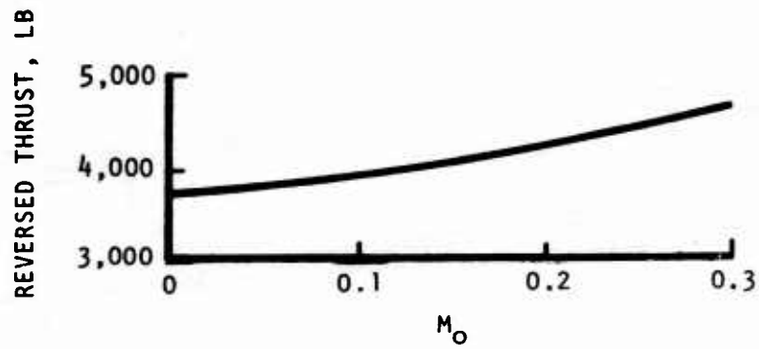

ASSUMPTIONS

- INTERMEDIATE POWER
- ΔP_T = 24-26% IN REVERSER
- A_r* - REVERSED GAS THROAT
- REVERSING ANGLE = 30°

Figure 30. ADCA reversed thrust.

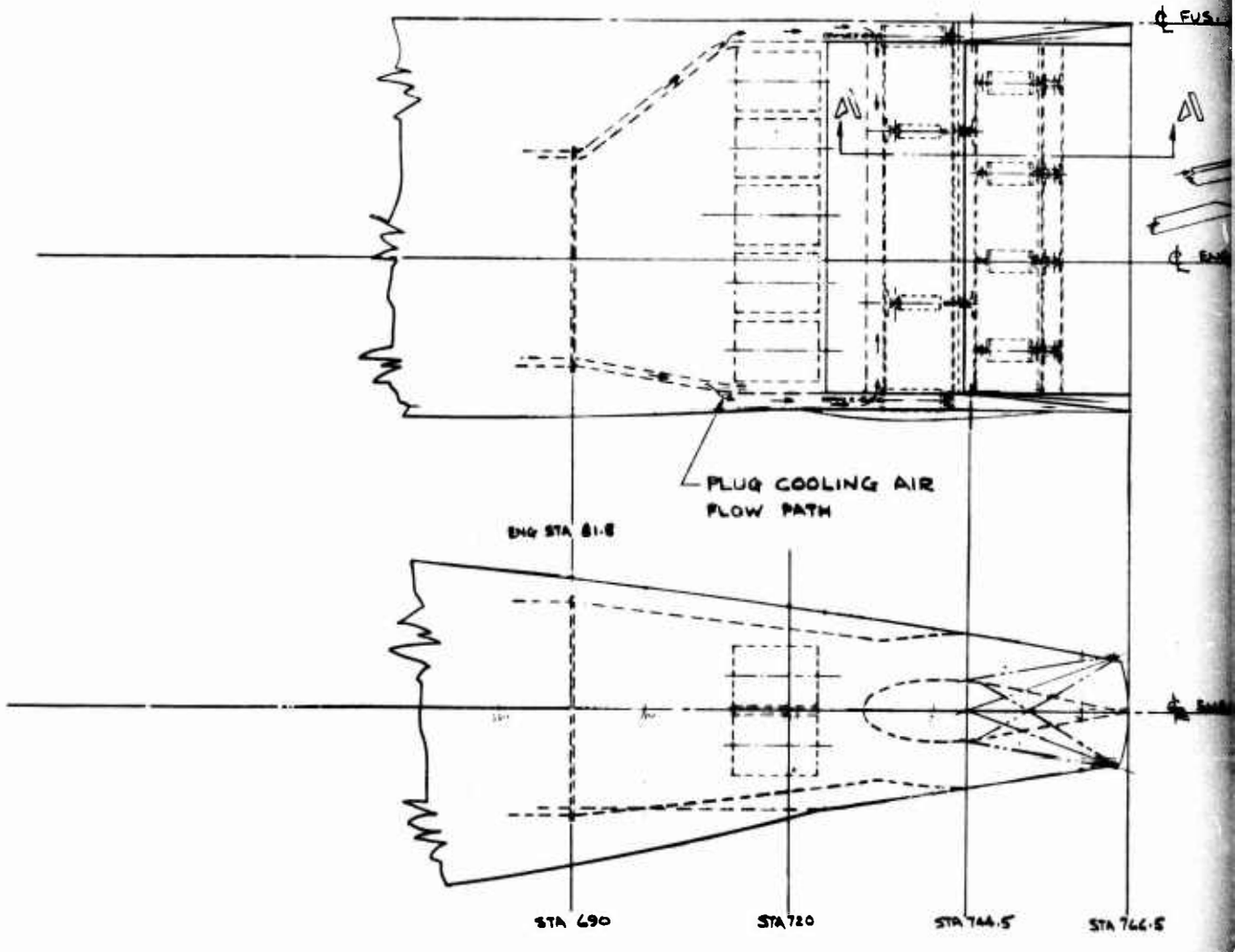
PLUG COOLING AIR
FLOW PATH
ENG STA 81.8
STA 690
STA 720
STA 744.5
STA 766.5

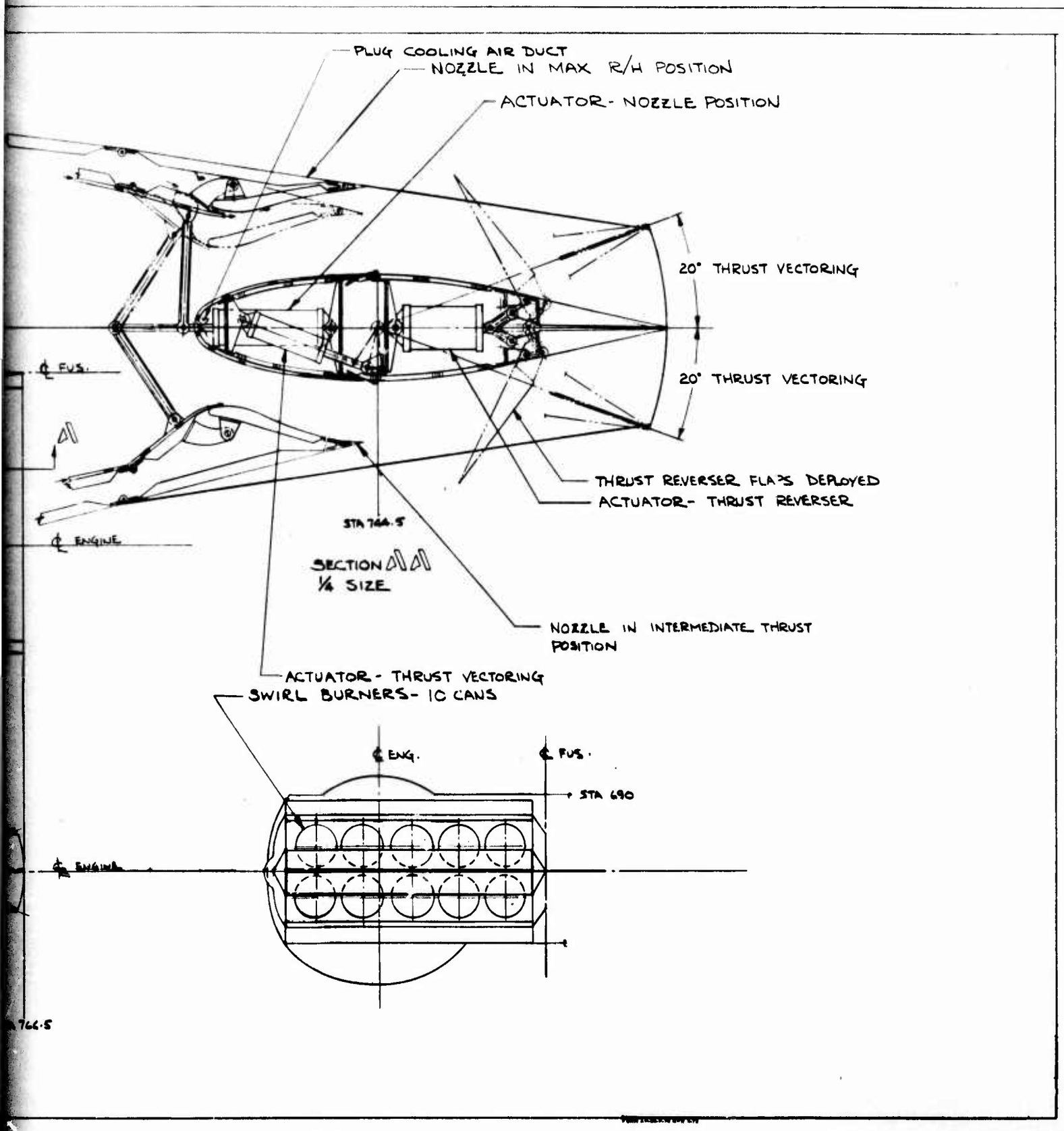

Figure 31. Design study - 2-D nozzle configuration ADCA.

estimates have been revised for the subsonic cruise mode. The NASA wind tunnel tests discussed previously show a significant advantage for 2-D nozzles for multi-engine supersonic cruise vehicles. Future programs such as the USAF FDL Non-Axisymmetric Nozzle Follow-On program and the USAF APL Turbine Engine Survivability Criteria program will establish a firm data base for use of 2-D nozzles in the ADCA.

MASS PROPERTIES DATA

WEIGHT AND BALANCE

Basepoint weights for the composite configuration (D572-4B) and the metal configuration (D572-5A) were derived using a combination of analytical, statistical, and comparative methods. Structural components were primarily estimated through the use of the Structural Weight Estimation Program (SWEEP), Reference 13. The propulsion and equipment group weights estimates reflect all three methods.

SWEEP was also used to develop a wing weight matrix for both composite and metal vehicles to be used in the vehicle sizing efforts. Wing weights which reflect the structural concept, material properties, vehicle speed profile, and flutter requirement were calculated for variations in aspect ratio, wing area, leading edge sweep, thickness ratio, and gross weight.

The range of values investigated in this study are shown in the following paragraph.

Gross Weight Pounds	Wing Area Sq. Ft.	Leading Edge Sweep Degrees	Aspect Ratio	Wing Thickness Ratio
30,000	300	50	2.5	0.050
37,000	400	60	3.0	0.055
44,000	500	70	3.5	0.060

This matrix resulted in 243 wing weights for both composite and metal concepts. The actual number calculated by using SWEEP was reduced to 90 and the remainder extrapolated statistically from the calculated points. Wing weight matrix data reflected initial estimates for flutter solutions. Surface flutter studies incorporating aerodynamic forces, revised mass distributions, and elastic axis data were used to refine the basepoint weights.

The weight and balance summaries for the final iterated composite and metal basepoint vehicles are presented in Tables 2 and 3. Figures 32 and 33 give the center-of-gravity variation with gross weight for the basic mission

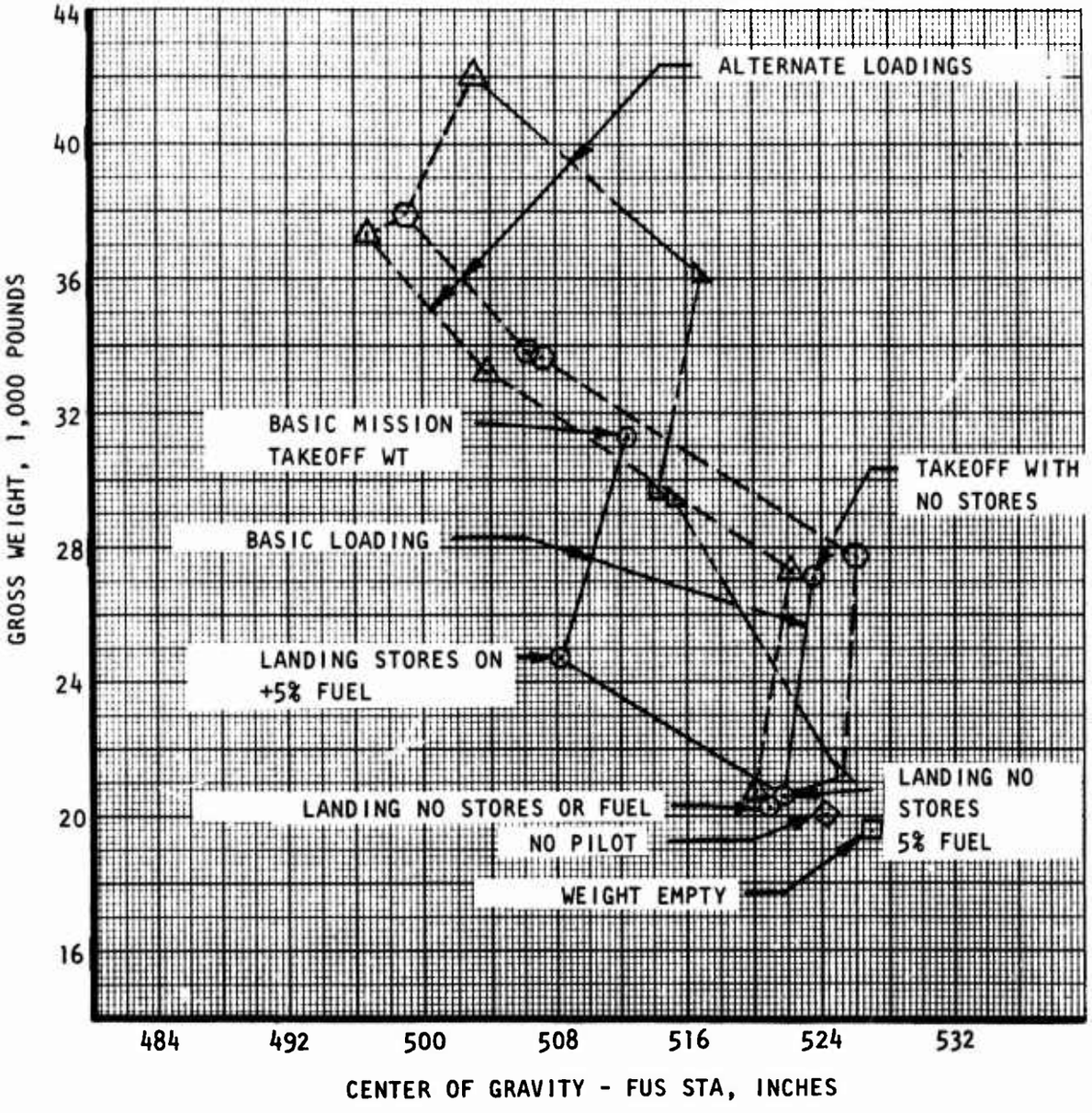

Figure 32. Gross weight versus CG for D572-4B.

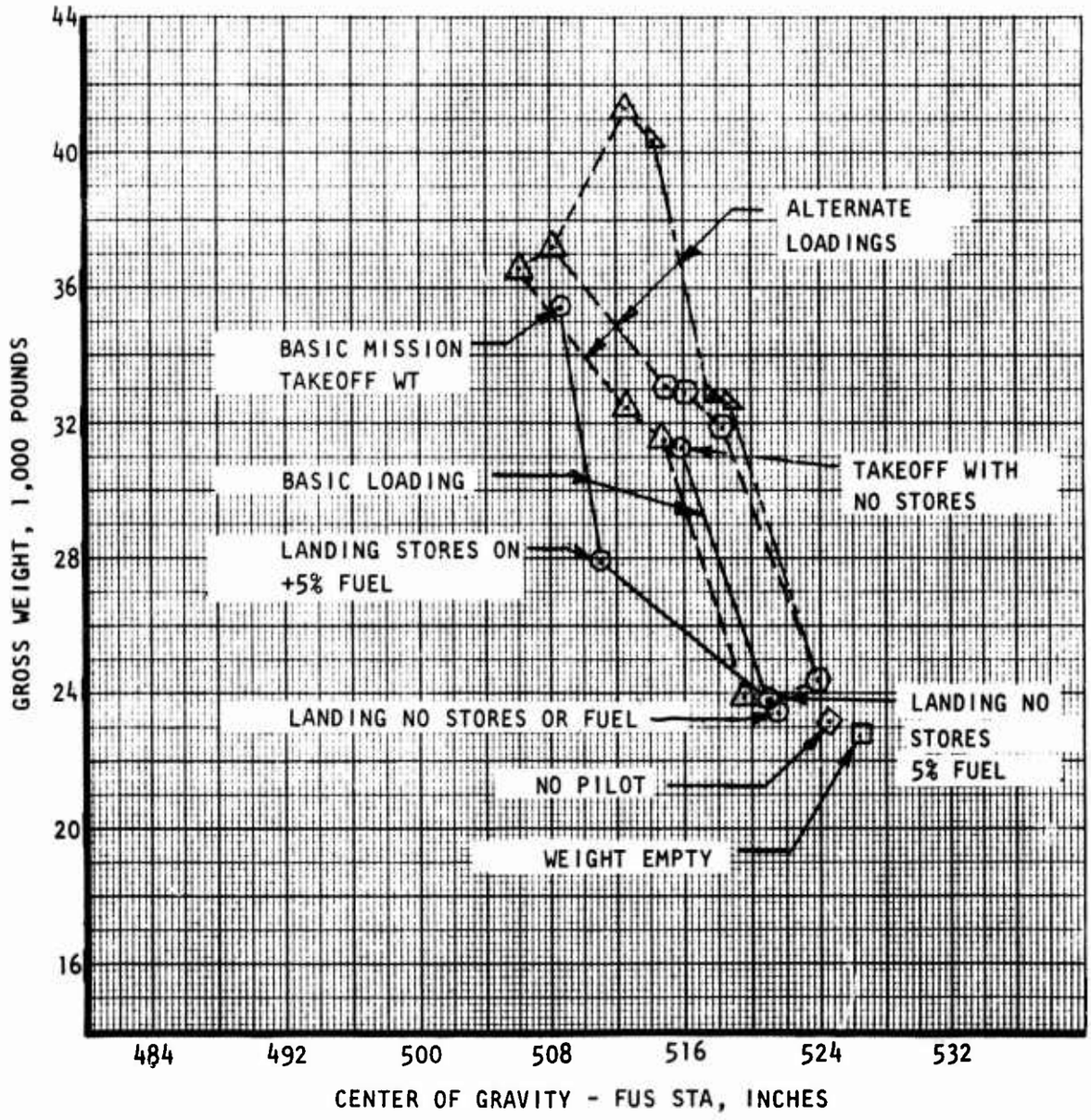

Figure 33. Gross weight versus CG for D572-5A.

TABLE 2. D572-4B WEIGHT SUMMARY (COMPOSITE VEHICLE)

	BASIC WT.	C.G.'S	MOMENT	MAX. WT.	C.G.'s	MOMENT
STRUCTURE GROUPS	(7885)	500.4	(3945990)			
WING GROUP	2890	577				
TAIL GROUP - HORIZONTAL	165	270				
- VERTICAL						
BODY GROUP	3130	432				
ALIGHTING GEAR GROUP - MAIN	1095	540				
- AUXILIARY	185	250				
ENGINE SECTION OR NACELLE GROUP	120	660				
AIR INDUCTION SYSTEM	300	550				
PROPULSION GROUP	(6435)	642.2	(4158525)			
ENGINE (AS INSTALLED)	3690	652				
ACCESSORY GEAR BOXES & DRIVES	190	585				
EXHAUST SYSTEM	1655	729				
COOLING & DRAIN PROVISIONS	30	630				
ENGINE CONTROLS	40	345				
STARTING SYSTEM	80	585				
FUEL SYSTEM	750	474				
FAN (AS INSTALLED)						
HOT GAS DUCT SYSTEM						
EQUIPMENT GROUPS	(4945)	410.9	(2032000)			
FLIGHT CONTROLS GROUP	830	470				
AUXILIARY POWER PLANT GROUP	120	575				
INSTRUMENTS GROUP	120	317				
HYDRAULIC & PNEUMATIC GROUP	430	532				
ELECTRICAL GROUP	680	410				
AVIONICS GROUP	1350	358				
ARMAMENT GROUP INCLUDES RACKS	560	355				
FURNISHINGS AND EQUIPMENT GROUP	320	235				
AIR CONDITIONING GROUP	530	505				
ANTI-ICING GROUP						
PHOTOGRAPHIC GROUP						
LOAD & HANDLING GROUP	5	470				
TOTAL WEIGHT EMPTY	(19265)	526.2	10136515	19265	526.2	10136515
CREW	215	203		215	203	
FUEL - UNUSABLE	190	474		190	474	
FUEL - USABLE	6850	531		12800	490	
OIL - ENGINE	20	652		20	652	
PASSENGERS / CARGO						
ARMAMENT 2-MK84 LGB	4120	440		8240	479	
2-SELF DEFENSE MISSILE				600	640	
M-61 GUN (IMPROVED)	192	288		192	288	
AMMO - 300 RDS				170	310	
EQUIPMENT LIQUID N_2	20	484		20	484	
EPU FUEL	60	575		60	575	
TOTAL USEFUL LOAD	11667	488.2	5696371	22507	482.3	10854902
TAKEOFF GROSS WEIGHT	30932	511.9	15832886	41772	502.5	20991417
FLIGHT DESIGN GROSS WEIGHT	29562	510.9				
LANDING DESIGN GROSS WEIGHT	26822	509.3				

FORM 1034-C-9 REV. 12-74

TABLE 3. D572-5A WEIGHT SUMMARY (METAL VEHICLE)

	BASIC WT.	C.G.	MOMENT	MAX. WT.	C.G.	MOMENT
STRUCTURE GROUPS	(11370)	509.2	(5789642)			
WING GROUP	4834	585				
TAIL GROUP - HORIZONTAL	250	266				
- VERTICAL						
BODY GROUP	4117	448				
ALIGHTING GEAR GROUP - MAIN	1530	490				
- AUXILIARY	214	239				
ENGINE SECTION OR NACELLE GROUP	120	665				
AIR INDUCTION SYSTEM	305	558				
PROPULSION GROUP	(6255)	650.5	(4068715)			
ENGINE (AS INSTALLED)	3690	648				
ACCESSORY GEAR BOXES & DRIVES	190	596				
EXHAUST SYSTEM	1655	727				
COOLING & DRAIN PROVISIONS	30	636				
ENGINE CONTROLS	40	345				
STARTING SYSTEM	80	591				
FUEL SYSTEM	570	493				
FAN (AS INSTALLED)						
HOT GAS DUCT SYSTEM						
EQUIPMENT GROUPS	(5120)	413.0	(2114500)			
FLIGHT CONTROLS GROUP	1005	470				
AUXILIARY POWER PLANT GROUP	120	481				
INSTRUMENTS GROUP	120	317				
HYDRAULIC & PNEUMATIC GROUP	430	537				
ELECTRICAL GROUP	680	412				
AVIONICS GROUP	1350	360				
ARMAMENT GROUP INCLUDES RACK	560	345				
FURNISHINGS AND EQUIPMENT GROUP	320	225				
AIR CONDITIONING GROUP	530	509				
ANTI-ICING GROUP						
PHOTOGRAPHIC GROUP						
LOAD & HANDLING GROUP	5	470				
TOTAL WEIGHT EMPTY	22745	526.4	11972857	22745	526.4	11972857
CREW	215	187		215	187	
FUEL - UNUSABLE	135	493		135	493	
FUEL - USABLE	7878	499		8900	493	
OIL - ENGINE	20	656		20	656	
PASSENGERS / CARGO						
ARMAMENT 2-MK84 LGB	4120	454		8240	503	
2-SELF DEFENSE MISSILE				600	638	
M-61 GUN (IMPROVED)	192	304		192	304	
AMMO - 300RDS				170	324	
EQUIPMENT LIQUID N_2	20	490		20	490	
EPU FUEL	60	581		60	581	
TOTAL USEFUL LOAD	12640	476.6	6024510	18552	495.7	9196118
TAKEOFF GROSS WEIGHT	35385	508.6	17997367	41297	512.6	21168975
FLIGHT DESIGN GROSS WEIGHT	33809	509.2				
LANDING DESIGN GROSS WEIGHT	30658	510.1				

FORM 1034-C-8 REV. 12-74

loading and the alternate maximum loading for both vehicles. Table 4 summarizes the design weight and center-of-gravity data assumed to derive structural loads and weights. The definition of flight design weight is basic mission takeoff weight less 20 percent of mission required fuel. The definition of landing design weight is basic mission takeoff weight less 60 percent of mission required fuel. Maximum design weight is defined as four MK-84 LGB (GBU-10C/B), full ammo, self-defense missiles and full internal fuel. The basic mission takeoff weight does not include ammo and self-defense missiles but the final designs (D572-4C and D572-5B) which resulted from this sizing study will, because of a change in mission ground rules.

WEIGHT DERIVATION

Structure Group

SWEEP was used to derive structure weight estimates for both the composite and metal vehicles. SWEEP does not lend itself well to analyzing nonplanar wing configurations. Therefore, modifications were made to the basic program and computer programs were developed to support SWEEP activities. Additional process amendments were required to simulate geometry, develop design loads, and analysis limitations. The major assumptions made to implement the use of SWEEP are discussed in the following text.

TABLE 4. VEHICLE DESIGN WEIGHTS AND CENTERS OF GRAVITY

Composite Vehicle (D572-4B)		
Description	Weight (Pounds)	Center of Gravity (Fus. Sta.)
Flight Design	29562	510.9
Landing Design	26822	509.3
Maximum Design	41772	502.5
Metal Vehicle (D572-5A)		
Flight Design	33809	509.2
Landing Design	30658	510.1
Maximum Design	41297	512.6

SWEEP Geometry Model

Wing geometry of both configurations is non-planar and blended. Because of the unique wing configuration, an unconventional approach was used in the SWEEP analysis. The wing structure was estimated in two separate analysis steps, one being the outboard panel from 60 percent span to the tip, and the second being from buttock line 33 to 60 percent span.

In modeling the outboard panel, a planar wing was developed from the non-planar geometry. In the planar simulation, the sweep of the 45 percent element line was assumed equal to that of the non-planar line and true wing chords developed around this reference line. Using the true box chord at the 60 and 90 percent spanwise locations on the non-planar geometry (49.2 and 80 percent on a planar planform) as the definition for the box taper ratio gave a reasonable approximation of the spanwise variation of box width. This approach was used for both metal and composite wings. Since the wing chords were made true it follows that the thicknesses are true.

The assumed effective torque box for the inboard panel is different between the metal and composite designs. On the composite design the leading edge (front spar) was defined by a straight line connecting the points defined by 1, the 45 percent element at 60 percent of the non-planar span and 2, buttock line 33 at fuselage station 481. The box inboard trailing edge intercept (rear spar) was defined to be buttock line 33 at fuselage station 606. Figure 34 shows the assumed torque box on a non-planar planform. On the metal design, the box inboard leading edge intercept was defined to be buttock line 33 at fuselage station 530, and the box inboard trailing edge intercept was defined to be buttock line 33 at fuselage station 575. Figure 35 shows the assumed torque box on a non-planar planform. These two torque box models provide reasonable structural definition to develop sizing studies and weight estimates. The numbers on Figures 34 and 35 represent the wing station cuts for SWEEP analysis.

The fuselage structural perimeter for the two configurations are shown in Figures 36 and 37. They were developed by using the following ground rules:

1. Fuselage width between stations 80 and 500 (80 and 520 for metal version) limited to 66 inches.

2. Fuselage width is 104.4 inches aft of station 500 (520 for metal version).

3. The upper moldline of fuselage coincide with upper wing cover where common structure occurs.

4. The canopy bump is not included in the perimeter data.

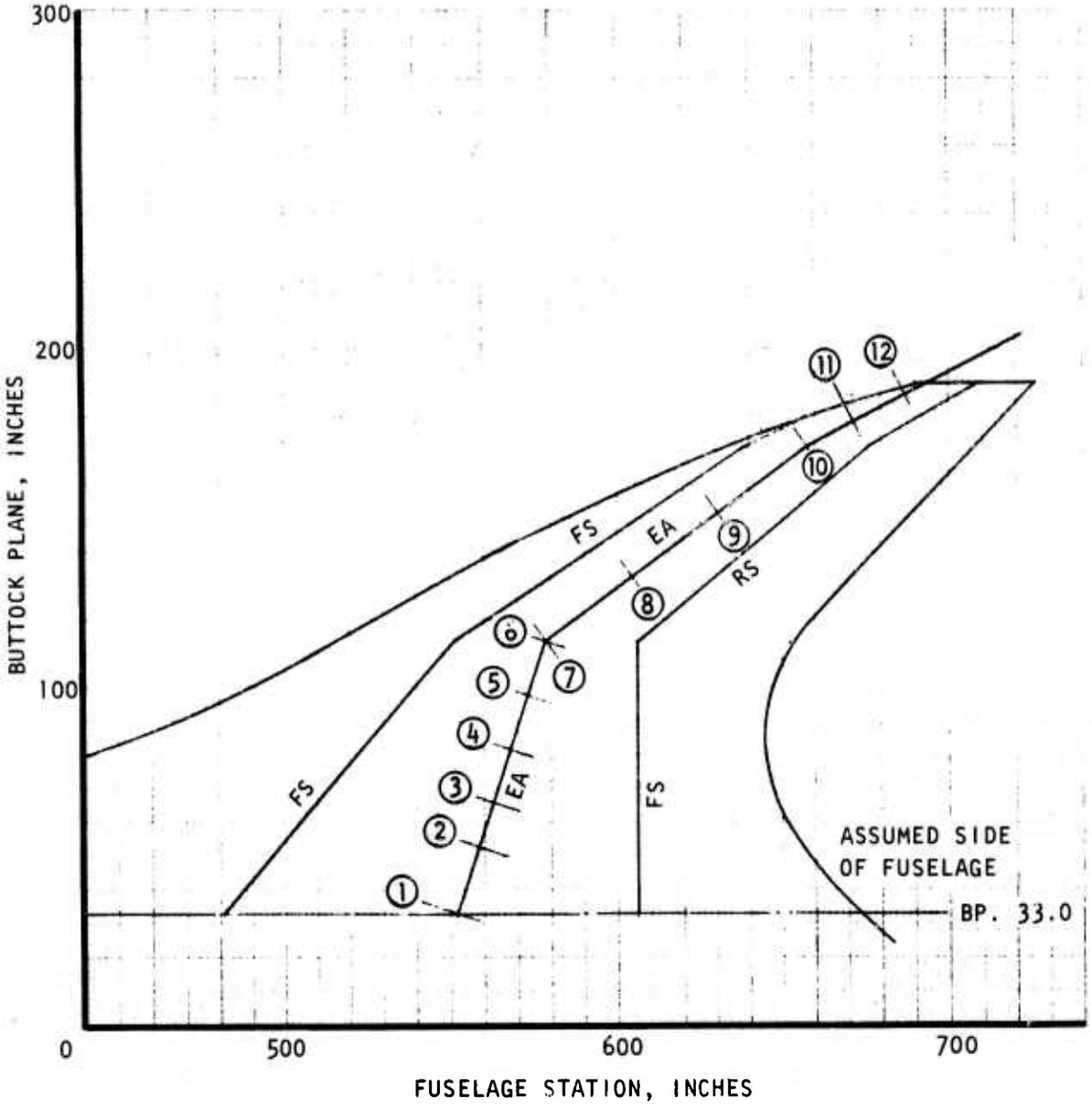

Figure 34. D572-4B wing torque box geometry model.

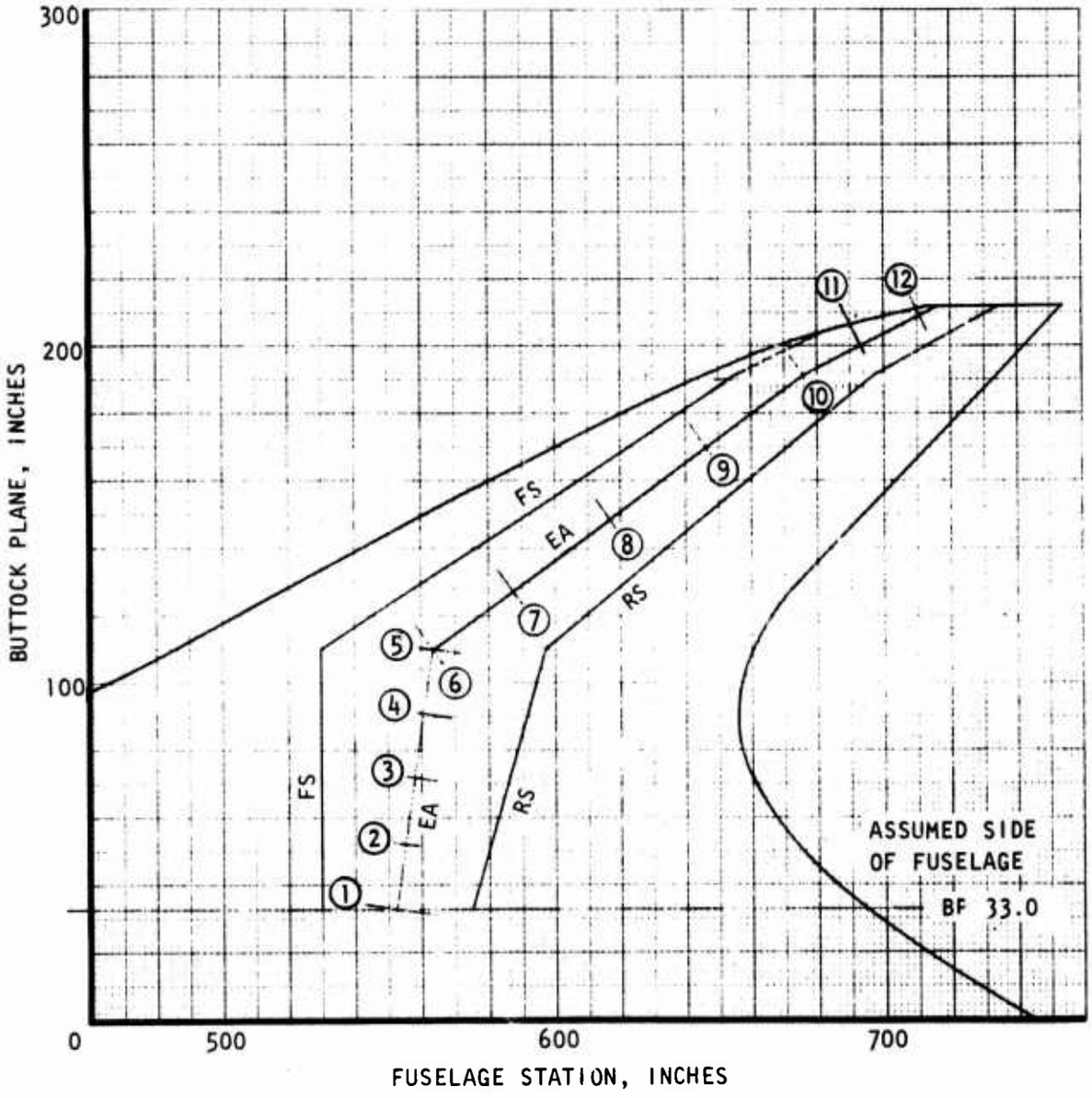

Figure 35. D572-5A wing torque box geometry model.

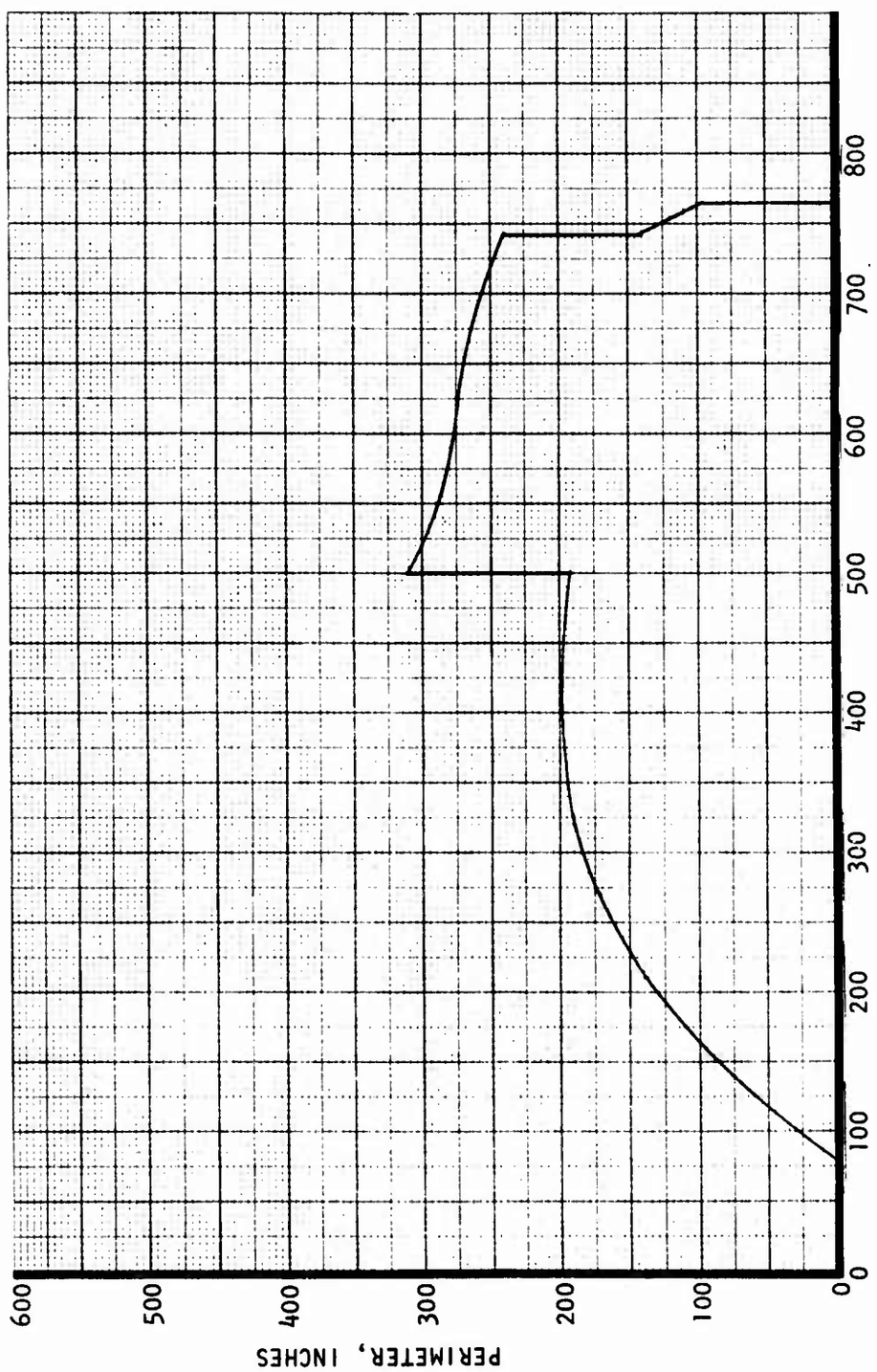

Figure 36. D572-4B fuselage structural perimeter plot.

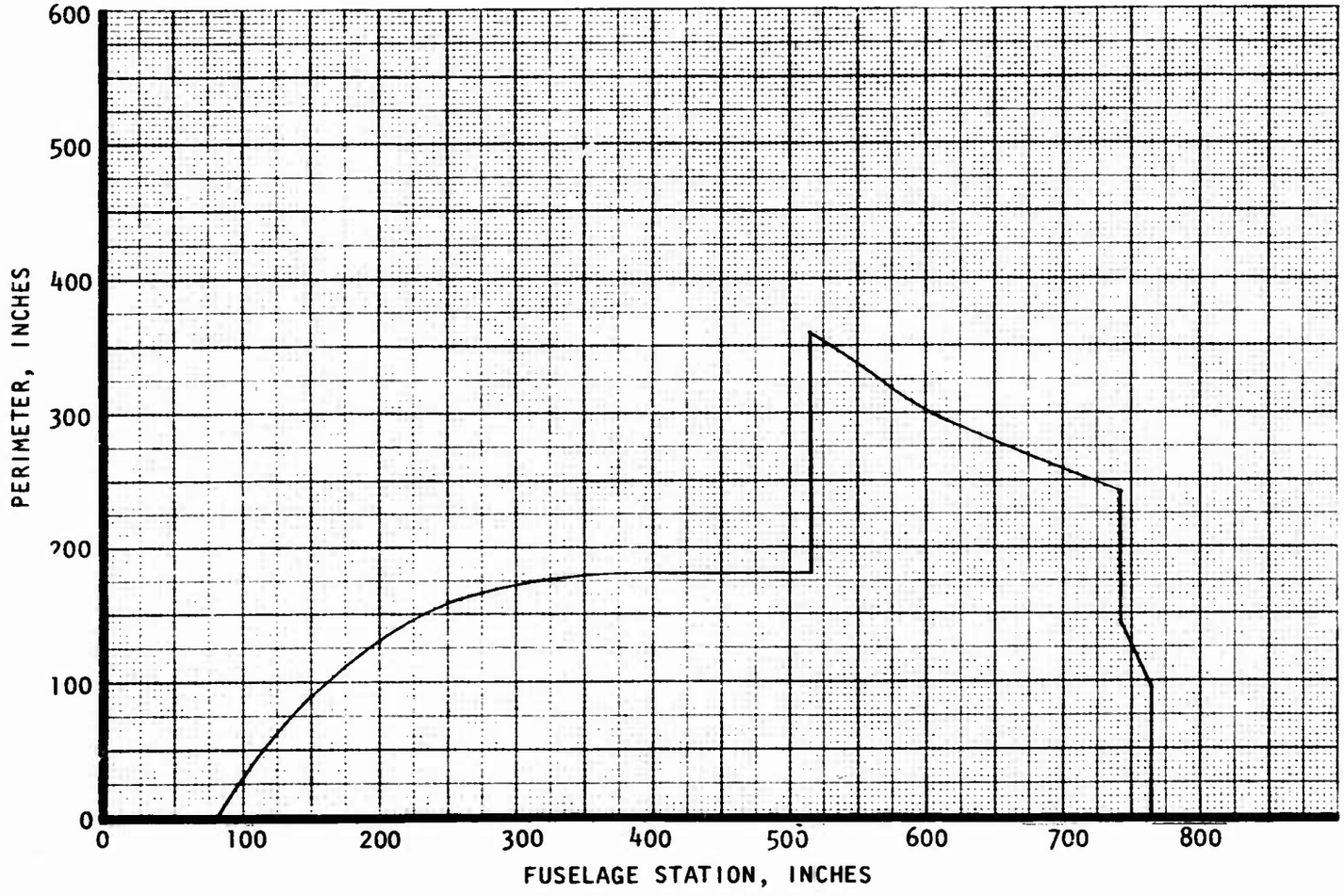

Figure 37. D572-5A fuselage structural perimeter plot.

SWEEP Type Construction Model (Advanced Composite)

The outboard wing torque box is full-depth honeycomb with graphite/epoxy face sheets. The honeycomb core is also graphite/epoxy. It was assumed for SWEEP analysis that the density of the core would be 4 pounds per cubic foot with design allowables equivalent to that for aluminum core of the same density. Recent checks by the Stress Group indicate that a 4-pound core would probably be sufficient to support crushing loads resulting from the spanwise curvature of the wing. Succeeding SWEEP analysis will reflect this detail check.

The inboard wing torque box is multi-spar with honeycomb panel skins. Honeycomb core in the SWEEP analysis was assumed to be the same as that used for the outboard panel. The face sheets are graphite/epoxy. Spar webs are also a honeycomb panel design. The wing skin panels were 0.75 inch thick while spar web panels were assumed to be 0.25 inch. It was determined from the SWEEP analysis that the required ±45-degree fiber layups were critical from a torsional rigidity requirement for flutter speeds rather than a panel stability requirement. This was also true for the outboard wing box. SWEEP does not check wing skins for fuel pressure but estimates the number of 90 degree directional fibers as a fraction of the zero directional fibers. Studies have indicated that the 10 percent used in the analysis is low and should be increased to 40 percent. Subsequent analysis will incorporate this data.

The canard was full-depth honeycomb with graphite/epoxy face sheets. The core was graphite/epoxy. The same assumptions for density and properties were made as that used for the outboard wing panel.

The fuselage construction model used to derive the basic shell weight requires additional design verification to establish the same confidence level as that obtained in the lifting surface analysis process. SWEEP fuselage estimating methods have no composite or honeycomb panel analysis capabilities at the present time. In order to simulate composite construction, skin-frame-longeron fuselage design procedures, coupled with derived isotropic graphite material properties were used to establish the fuselage shell weight. The frame spacing was selected at 10 inches to prevent excessive skin weight due to panel flutter criteria. The skin material properties were derived for symmetrical layups of 25 percent of the thickness composed of both zero and ninety degree fibers and 50 percent ±45 degree fibers which were allowed to have diagonal tension fields. The same applied to frame material. The longerons properties were based on 70 percent zero degrees and 30 percent ±45 degree fibers. This approach was used in lieu of fractions of metal weight in order to make fuselage weight sensitive to advanced composite material properties. These assumption will be verified and changed as required as the design analysis progresses.

SWEEP Type Construction Model (Metal)

The wing torque box estimate was based on multi-spar plate construction. The inboard torque box was analyzed with a constant spar spacing of 9 inches; the outboard torque box was based on a constant number of spars (2 intermediate spars). Subsequent analysis by the Stress Group of outboard wing curvature effects indicated that three additional spars were required to stabilize the covers and react the crushing loads. These results will be incorporated in succeeding SWEEP analysis.

The canard was designed with full-depth aluminum honeycomb core and face sheets. Core density was assumed to be 4 pounds per cubic foot.

The fuselage shell structure estimate was based on skin-frame-longeron construction. The shell was constructed primarily of aluminum alloy with titanium used in the engine compartment.

Materials used in the analysis of each of the structural components are tabulated in the next paragraph.

Component	Material
Wing Torque Box	X7475-T76 Aluminum Alloy
Canard Torque Box	X2048-T851 Aluminum Alloy
Forward and Mid Fuselage	
Cover	X2048-T851 Aluminum Alloy
Longeron	X7475-T76 Aluminum Alloy
Minor Frames	X2048-T851 Aluminum Alloy
Major Frames	X7475-T76 Aluminum Alloy
Aft Fuselage	Ti-6Al-4V (Annealed) Titanium

SWEEP Load Model

Because of the unique wing design, the SWEEP load analysis methods were not used to derive vehicle airloads. Recently Rockwell International/LAAD has developed under IR&D funding new computer programs and procedures to verify and evaluate aeroelastic tailoring requirements. The procedure uses the box beam theory of SWEEP as its initial structural model. Along with this development new load routines were created to supply SWEEP input loads. Revisions to SWEEP were also made to accept and process these loads.

Trimmed pressure distributions for a rigid vehicle were supplied by a modified version of the Non-planar Unified Distributed Panel Wing-Body Program used by the Aerodynamics Group. This program computes subsonic and supersonic aerodynamic characteristics of wing-body configurations, surface pressures, load distribution, and total component and configuration loads. Data sets of

pressure distributions, normalized to dynamic pressure and for a trimmed lift coefficient of one, were created for various mach numbers. Unit shears, moments, and torques were calculated with a new computer program called Load Influence Coefficient Program. The unit loads were then converted to limit loads at the design load factors, gross weight and dynamic pressures at the given mach numbers and altitudes by another new program called Design Loads Program. The resulting loads sets were inputted into SWEEP for corresponding design synthesis points on the planar planform. Four flight conditions were used to represent a reasonable sample of loads for designing components and estimating structure weights.

These flight conditions at the flight design gross weight for each of the configurations are listed in the following paragraph.

Mach No.	Altitude	Canard Position	Vertical Load Factor
0.9	Sea Level	Retracted	8.0
1.2	Sea Level	Retracted	9.0
1.2	Sea Level	Retracted	-3.0
1.71	20,000 Ft.	Retracted	6.5

Canard loads for ADCA were estimated by using the airloads module of SWEEP with the planar wing model and trimming with the canard. This was done to expedite the load process. This method gives conservative canard loads which will be reviewed and corrected in the next design phase.

Figures 59 through 74 and Tables 12 through 15 of Section IV present the net ultimate wing and fuselage loads which resulted from the above described procedures.

SWEEP Structural Weights

Lifting surface torque box weights were calculated from SWEEP derived theoretical sizing. Provisions have been programmed so that multiplication factors can be applied to the SWEEP weight results. These scaling numbers bridge the gap between the theoretical early preliminary design and the more rigorous downstream layout phases. Table 5 gives the weight index factors used to obtain the weight estimates. The leading and trailing edge weights were derived from statistical equations based on metal design data. Therefore, the composite construction leading and trailing edge weights were derived by assuming that composite weights were a percent of the statistical metal weights. The track and pivot weight for the canard was assumed to equal 40 percent of the torque box (note the last number in the last column of Table 5).

TABLE 5. WEIGHT INDICES FOR LIFTING SURFACES

Description	Wing				Canard
	Composite		Metal		Composite
	Inbd	Outbd	Inbd	Outbd	and Metal
Total Upper Cover	1.13	1.13	1.13	1.13	1.13
Skin	1.10	1.10	1.10	1.10	1.10
Spar Caps, Adhesive, or Inserts	1.5	1.50	1.5	1.50	1.50
Total Lower Cover	1.16	1.16	1.16	1.16	1.16
Skin	1.10	1.10	1.10	1.10	1.10
Spar Caps, Adhesive, or Inserts	1.50	1.50	1.50	1.50	1.50
Upper and Lower Miscellaneous Skin	1.20	1.20	1.20	1.20	1.20
Upper and Lower Skin Fasteners	1.00	1.00	1.00	1.00	1.0
Total Interm. Ribs, Spars, or Core	1.20	1.00	1.20	1.20	1.0
Webs or Core	1.25	1.25	1.25	1.25	1.0
Miscellaneous	1.25	1.25	1.25	1.25	1.25
Joint Attachments & Bulkheads	1.25	1.25	1.25	1.25	1.25
Total Front Spar	1.10	1.10	1.10	1.10	1.10
Caps	1.15	1.15	1.15	1.15	1.15
Web	1.25	1.25	1.25	1.25	1.25
Miscellaneous	1.15	1.15	1.15	1.15	1.15
Total Rear Spar	1.10	1.10	1.10	1.10	1.10
Caps	1.15	1.15	1.15	1.15	1.15
Web	1.25	1.25	1.25	1.25	1.25
Miscellaneous	1.15	1.15	1.15	1.15	1.15
Total Root Rib	1.00	1.00	1.00	1.00	1.00
Caps	1.00	1.00	1.00	1.00	1.00
Web	0.75	1.00	0.75	1.00	1.00
Miscellaneous	1.0	1.00	1.00	1.00	1.00
Total Torque Box	1.00	1.00	1.00	1.00	1.40

Composite construction secondary structure component weights, except for glass, radome, and external finish, were assumed to be 80 percent of the statistical metal weights.

The landing gear weights were derived from SWEEP results. The gear was analyzed as if it were made of metal. The metal weight was then corrected to reflect composite material. The assumption for deriving the composite weight was that 40 percent of the strut weight could be saved with composites. This

results in a total alighting gear weight reduction of 10 percent. The weight indices used in SWEEP gear analysis to derive the total metal gear weight are as follows:

	Main Gear	Nose Gear
Total Gear	1.0	1.1
Outer Cylinder	2.0	2.0
Inner Cylinder	2.0	2.0
Drag Strut	5.0	4.0
Side Strut	5.0	0.0

The engine section weight consists of engine mounts, firewall and insulation. The engine mounts are SWEEP derived. The firewall is assumed to be 0.02-inch titanium. The insulation was assumed to be 1-inch thick with a density of 4 pounds per cubic foot. A summary of the engine section weight is listed as follows:

	Weight (Pounds)
Engine Mounts	55
Firewall	40
Insulation	25

The inlet duct weight estimate for air induction system is based on inlet pressures defined by the speed/altitude profile in Appendix A. The duct design point is a hammershock condition occuring at 1.39M/8,000 feet. The limit pressure for this condition is 45.1 psig (ultimate = 67.7 psig) and temperature is 220° F. In deriving the critical pressure/temperature design point a reduced safety factor of 1.15 was applied to the hammershock pressures on the V_L curve and the standard 1.5 was used for all other points on both the V_L and V_H curves. Table 6 gives the inlet pressures and temperatures for the points investigated.

TABLE 6. INLET PRESSURES AND TEMPERATURES

M_o	Altitude (Feet)	°F	P_2 (Psig) (Limit)	P_{HS} (Psig) (Limit)
1.20	0	208	17.4	45.3
1.31 (V_H)	5000	214	18.4	43.9
1.41 (V_L)	5000	241	23.4	51.6
1.39 (V_H)	8000	220	19.6	45.1
1.49 (V_L)	8000	248	24.3	52.1
1 64 (V_H)	22000	217	18.3	38.7
1.74 (V_L)	22000	247	22.3	44.7

The metal configuration components were obtained directly from statistical weight calculations. Percentages used to estimate the composite leading and trailing edge components are listed in the next paragraph.

Leading and Trailing Composite Weights as Percent of Metal		
	Wing	Canard
Fixed Leading Edge	80	80
Leading Edge Control Device	70	--
Fixed Trailing Edge	80	80
Trailing Edge Control Device	65	--

The fuselage shell weight was derived using the theoretical sizing with weight index factor to reflect actual weight. These index factors, used for both composite and metal concepts, are listed as the following:

Fuselage Weight Indices	
Description	Index
Covers	1.20
Longerons	1.25
Joints	1.10
Minor Frames	1.15
Major Frames	1.20
Bulkheads	1.20

The duct weight estimate was obtained by analytically deriving a unit weight for the design pressure/temperature condition (45.1 psig/220°F). Based on assuming a typical aluminum skin/frame construction, an assumed 15-percent reduction factor was applied to metal unit weights for a composite constructed duct. The unit weights for the metal and composite ducts are 2.23 and 1.90 pounds per square foot, respectively. These unit weights were applied to the duct surface areas for total duct weights of 250 and 255 pounds. The inlet duct of the metal configuration (D572-5A) is 15 inches shorter than its composite material counterpart. The duct length difference was brought about by configuration differences in the armament bay location. The shorter duct length accounts for an approximate 15-percent reduction in duct surface area.

The inlet air bypass system weight was empirically derived by assuming a door area at 35 percent of the inlet capture area and a door unit weight of 20 pounds/foot^2. This unit weight includes actuation and controls.

	Composite D572-4B (pounds)	Metal D572-5A (pounds)
Ducts	250	255
Bypass System	50	50
Total Air Induction	300	305

Propulsion Group

The estimated weights of the propulsion systems were based primarily on statistical and empirical weight estimating methods. Vendor data were used when applicable. The propulsion weights are identical for both the metal and composite airplanes except for the fuel system, which is outlined later in the text.

Engine

The engines are modified F404-GE-400 turbofans. The standard engine has a bare dry weight of 2020 pounds. The engine weight without the afterburner casing and nozzle as configured for use in conjunction with a two-dimensional plug nozzle weighs 1770 pounds. The nozzle weight with the afterburner casing/transition duct is included with the exhaust system weight. The modified engine weight is based on data supplied by General Electric for a J101 engine similarly reconfigured. The F404-GE-400 is a derivative of the J101.

The installed engine weight includes an allowance of 75 pounds per engine for residual fluids and miscellaneous airframe/engine interfacting provisions. This allowance is based on data from the YF-17 air vehicle, which has YJ101 engines.

	Pounds
Engines (less transition duct and nozzles) (2)	3540
Residual fluids	150
Miscellaneous Installation provisions	
Engines (As Installed)	3690

Accessory Gearbox and Drives

The accessory gearbox system weight was estimated from statistical/empirical data. The gearbox weights were based on vendor data for the YF-17 gearboxes. The weights of the installation provisions were empirically estimated.

The YF-17 gearbox drives one hydraulic pump and one integrated drive generator and has a starter input pad and drive train. This box weighs 42 pounds. The box for the ADCA vehicle drives an additional hydraulic pump and is estimated at 52 pounds.

	Pounds
Gearboxes (2)	104
Power Takeoff Shafts (2)	16
Cooling and Lubrication System	40
Mounting Provisions	15
Miscellaneous	15
Accessory Gearboxes and Drives	190

Exhaust System

The exhaust system weight consists of the two-dimensional afterburner casing/transition duct and nozzles (Figure 38). The weight estimate of the transition ducts with the movable flaps for regulating nozzle throat area was based on data supplied by General Electric (Reference 11). The data was

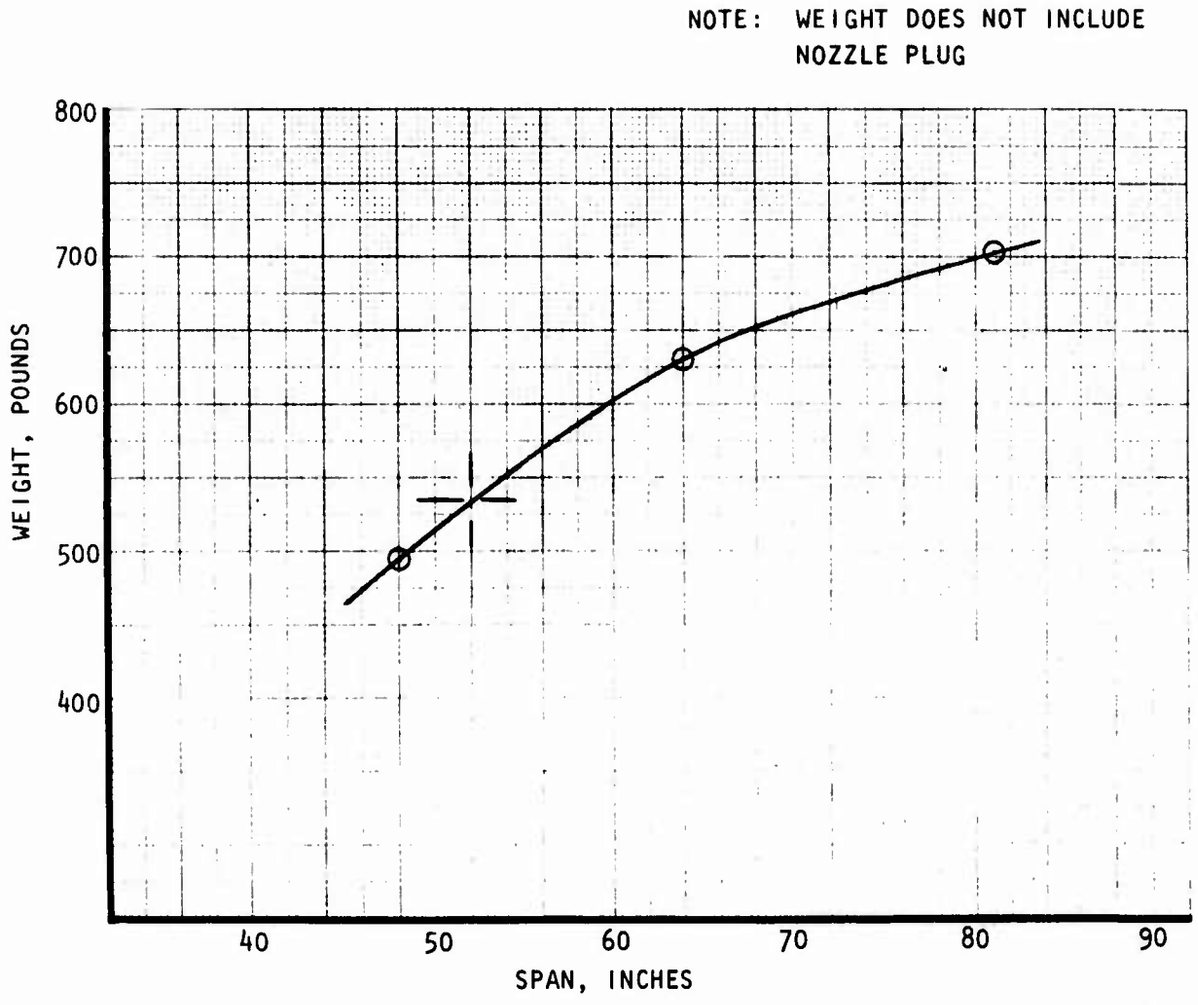

Figure 38. Jet flap weight.

for a jet flap exhaust system used in conjunction with a J101 engine and supplied under contract in support of Rockwell International's Advanced Fighter Technology Integrator Program.

This data was used as a basis to develop the curve of jet flap weight versus flap span (Figure 38). The curve does not include the weight of the nozzle plug and its systems. The weight of a 52-inch flap span exhaust system for the ADCA less the nozzle plugs is 1070 pounds per vehicle. The weight of the plugs and their systems is estimated at 585 pounds. The total exhaust system weight is 1655 pounds. The comparable exhaust system weight if a standard F404-GE-400 system was used is 500 pounds.

Starting System

The engines are started by air turbine starters mounted on the air vehicle accessory gearboxes. The turbines are powered by either an external power source or cross ship bleed air from a started engine.

	Pounds
Starter Turbines and Valves (2)	60
External Receptacle	5
Ducting	10
Wiring and Misc	5
Total Starting System	80

Fuel System

The fuel system weight estimates are based on statistical/empirical data. The fuel system weights for the composite and metal vehicles are a function of their respective maximum fuel volumes. The composite vehicle has considerably more excess volume above that required for the design mission than the metal vehicle. The maximum fuel quantities for the composite and metal vehicles are 12,800 pounds (1969 gallons) and 8900 pounds (1369 gallons), respectively. All fuel is contained in integral tanks. The system plumbing and sealant weight was calculated at 0.3 pound/gallon. This unit weight does not include the inerting system for fire/explosion protection of the aerial refueling system.

	Composite D572-4B	Metal D572-5A
	Pounds	Pounds
Plumbing	590	410
Inerting System	60	60
Aerial Refueling	100	100
Total Fuel System	750	570

Cooling and Drain Engine Controls

The weight allocations of these systems were based on empirical data.

Engine Controls	40 pounds
Cooling and Drain	30 pounds

Equipment Subsystem

The following section describes the methods utilized in estimating the equipment subsystem weights. Also included are the assumptions and criteria used directly or indirectly in the weight buildup.

The ADCA subsystem weights reflect the state of the art advanced for the 1980's time period where applicable. Much of the equipment specified is current state of the art, e.g.; the advanced M-61 gun, reclining seat for higher acceleration tolerance for the pilot, etc.

Analytical and statistical methods are used to develop subsystem weights. System concepts are approximated; i.e., hydraulic, electrical groups and the weight estimates are based on these design concepts. The equipment subsystem weights for the composite and the metal configuration are the same except for flight control system. The larger size of tne metal configuration is reflected in the actuation system weight as shown in the flight control system discussion.

Instrument Group

The group includes the weight of four functional groups. These are the flight, engine, fuel quality, and the miscellaneous. Each group includes the

indicators, transmitters and amplifiers, and installation weights. The total system weights are listed as follows:

Item	Weights (lb)	
Flight Instruments		(42)
Indicators	22	
Transmitters and Amplifiers	10	
Installation	10	
Engine Instruments		(30)
Indicators	5	
Transmitters and Amplifiers	20	
Installation	5	
Fuel Quantity		(30)
Indicators	5	
Transmitters and Amplifiers	10	
Installation	15	
Miscellaneous		(18)
Indicators	4	
Transmitters and Amplifiers	6	
Installation	8	
Total Instrument Group		120.0

Emergency Power Unit

The emergency power system is sized to provide 10 minutes of continuous power to drive a hydraulic pump and an ac generator in the case of failure of the primary hydraulic or electrical system. The emergency system uses a mono-fuel (hydrazine) and requires less complex installation than a conventional APU. A total of 120 pounds was estimated, as detailed in the next paragraph.

EPU (30-shaft horsepower)	70
Controls	5
Generator Drive Pad	9
Hydrazine Tank and Plumbing	20
Equipment Support	16
Total EPU	120.0 lb

Fuel (hydrazine) required is 60 pounds based on fuel consumption rate of 6 pounds/min for 10 minutes. The hydrazine weight is included in useful load.

Hydraulic Group

Two completely independent, continuously operating, 4000 PSI systems are provided. Each system consists of two variable-delivery pressure-compensated pumps, one bootstrapped reservoir, filters on pressure and return side, valves, heat exchanger, and plumbing. Each pump is mounted on separate engine-driven gearboxes such that failure in either pump or an engine will not result in complete loss of that system. The pumps operate on master-slave concept, wherein the master pump supplies the normal demand and peak flow demand will activate the slave pump. An emergency system is provided. The emergency pump is driven by the monopropellant emergency power unit (MEPU) and is capable of delivering up to 10 gpm.

Each system is sized to provide 50 percent of the hydraulic loads. One of the systems (system No. 1) will provide hydraulic power to all functions. System No. 2 will provide power to all functions except for inflight refueling and nose gear extend/retract cylinder. The revolving M-61 gun is brought up to speed with two system-supplied hydraulic motor pumps driving through a differential gearbox. The peak hydraulic flows for the functions are listed.

Functions	Peak Flow (gpm)/Sys	No. of Sys
Inflight Refueling	1.0	1
Canard	2.0	1 & 2
Nose Gear	1.0	1
Gun Drive	14.0	1 & 2
Weapon Bay Door, Fwd	1.0	1 & 2
Weapon Bay Door, Aft	1.0	1 & 2
Main Gear	3.0	1 & 2
Leading Edge	5.0	1 & 2
Trailing Edge	3.0	1 & 2
Ailerons	5.0	1 & 2
Aft Weapons Bay Doors	1.0	1 & 2
Plug Nozzle Movable Flap	13.0	1 & 2
Plug Nozzle Thrust Vector	24.0	1 & 2
System Internal Leakage	3.0	1 & 2

The pumps are sized to 15 gpm each. The primary flight control system are duty cycled to a 2/3 peak flow value. Full flow on nozzle flaps and internal leakages was added to the primary flight control flow. Titanium lines are used with welded or brazed joints. The lines are sized for a flow velocity of 25 ft/sec (reference 12). Other components such as reservoirs, filters, and accumulators are sized according to methods shown in Reference 13. The pumps are in-line piston type. Fluid volume and weights are based on MIL-H-5606 fluids.

The two primary systems and the emergency system estimated weights are listed as follows:

Components	Weights (lb) System 1	System 2	Emerg
Pumps	18	18	5.5
Reservoirs	14	14	8
Filters	5.9	5.9	5.4
Accumulator	---	10.0	---
Heat Exchangers	7.0	7.0	---
Controls	8.0	8.0	4.0
Distribution Lines	37.0	40.0	15.0
Fittings	15.0	16.0	6.0
Supports	10.0	10.0	5.0
Fluids, Lines	30.0	32.0	14.0
Fluids, Heat Exchanger	7.0	7.0	---
Fluids, Accumulator	---	3.0	---
Fluids, Reservoir	9.0	9.0	3
Equipment Supports, Misc	9.1	10.1	4.1
Total System	170.0	190.0	70.0
Hydraulic Group Weight			430.0 lbs.

Electrical System

The electrical system consists of two 115/208 volts, 400 CPS ac systems. Each system will supply adequate power in case of failure of one of the generating system. An MEPU-driven generator system is provided to supply essential powers during complete loss of the two primary systems. A 5.7 AH battery is provided to supply electrical power when neither the main engines nor the MEPU is running.

The following is the estimated load for the ADCA.

Instruments	1000	
Hydraulics	500	
Furnishings	500	3000W
Env. Control	500	
Flight Controls	500	
Armament (dc)		
firing circuit	150	
clearing can	785	1000VA
bomb eject & misc	65	
Fuel System	2340W	
Load based on 1 boost and 1 transfer pump operating simultaneously		
Avionics		22,950VA
The load is based on 1600 lb of avionics. Current system weight is 1000 lb. The expected load reduction was not included at this time.		

The generator size is based on the following assumed factors:

Equipment power factor	0.8
Fuel pump power factor	0.6
System growth	2.0
Generator efficiency	0.85

$$\text{Generator size} - \left(\frac{3000}{0.8} + \frac{2340}{0.60} + 22{,}950 + 1000\right)$$

$$\frac{\times\ 2}{2 \times .85} = 37117\text{VA} \cong 40\ \text{KVA/GEN}$$

The total system weight is listed in the following paragraph. The generators are the integrated drive generator type.

Item	Weights (lb)
40 KVA IDG generators (2)	162
T/R Units	20
Battery (MA500H)	15
Generator Controls	8
Line Contractors	9
Emergency system generator	15
Emergency system gen. control & contractor	9
Distribution system	340
Lights and signal devices	60
Equipment supports	30
Miscellaneous & supports	12
Total	680

Avionics System

The system weight of 1000 pounds of equipment was specified by the customer. It is assumed that the equipment included are COMM/NAV system, computation, IFF, weapon release, store management, controls and displays, penetration aids, and missionized equipments. Acoustic and thermal protection provisions for the tail defense avionic bays are included.

The weights are summarized as follows:

Item	Weights (lb)
Equipment	1000.0
Installation	270.0
Acoustic provision	80.0
Total System	1350.0

Armament System

The armament group weight consists of M-61 ammunition storage and missile and bomb carriage. The provisions are hardpoint fitting assembly, wiring, wire bundle supports, and equipment supports. The M-61 gun installation weight includes gun-firing provisions, ammunition storage drum, the hydraulic drive system, gun gas purging system, and blast tubes and plates. The gun, ammunition, missiles and bombs will be listed under useful load. The weapon release and store management system weights are assumed to be in avionics weights.

M-61 storage and drive system

Item	Weights (lb)
Drums, single ended	140
Feed, chutes, and mechanism	85
Drum supports	17
Gun drive	28
Purging and blast protection	40
Total	310

Agile-type missile system

Hardpoint	10
Wiring & supports	10
Missile racks	40
Total	60

Guided Bombs

Hardpoints	20
Wiring and supports	15
Racks	70
Total	105 lbs
Conformal rack provision	65 lbs

The wiring and logic integration provision into the weapon management system is estimated at 20 pounds.

The armament weight is summarized as follows:

Item	Weights (lb)
M-61 gun system	310
Agile-type missile prov.	60
Guided Bombs	105
Additional hardpoints	65
Weapons Mgm't System prov.	20
Total	560

Furnishing Group

The furnishing group consists of personnel accommodation, miscellaneous equipment, furnishings, and emergency equipment. The weights are based on comparison to current aircraft and also to current in-house studies on high-acceleration cockpits. The system weights are summarized as follows:

Item	Weights (lb)	
Personnel Accommodation		(228)
Seat Structure	109	
Survival gear, parachute	57	
Non ejectable seat provisions	23	
Relief tube	2	
5 liter O_2 system with LOX	37	
Miscellaneous Equipment		(54)
Data case	1	
Rear view mirror	1	
Rain removal system	7	
Windshield wash	15	
Instrument panels	15	
Consoles	15	
Furnishing		(15)
Trim	5	
Acoustic & insulation	10	
Emergency equipment		(23)
Fire detection	9	
Fire suppression	14	
Total Furnishing Group		320

Environmental Control System

Two bootstrapped turbo-compressor units utilizing engine bleed air are provided for the heating and cooling requirements. The primary heat sink is ram air. Ram air scoops and valves are provided for emergency cooling and ventilation for the cockpit and equipment compartments.

The estimated weight is listed as follows:

Item	Weights (lb)	
Bleed-Air System		(179)
Pressure regulator & S.O. valves	48	
Check valve	6	
Bypass valve	5	
Primary heat exchanger	70	
Ducting and supports	50	
Refrigeration System		(280)
Refrigeration units (2)	65	
Water separators	15	
Valves	20	
Controllers, cockpit	5	
Controllers, Fwd Bay	5	
Controllers, Mid Bay	15	
Controllers, AFT	5	
Controllers, Wing	10	
Ducting	60	
Supports	15	
Cabin S.O. Valve	5	
Cabin pressure regulator	10	
Pressurization and sealing		(70)
Miscellaneous		(36)
Anti-Ice Provision		(15)
Total System		530

Flight Controls

A 3-channel fly-by-wire (FBW) flight control system with a 4000 PSI hydraulic system power supply is included. The electrical power supply consists of three transformer - rectifier (T/R) units and batteries each. Pilot controls consist of a side stick and rudder pedals.

The weight estimates for the cockpit (pilot's) control and the automatic flight control system are based on extensive Rockwell International's in-house studies; such as, Advanced Fighter Technology Integration (AFTI), and the Highly Maneuverable Technology (HiMAT) Programs.

The system weight is summarized as follows:

Item	Metal D572-5A	Composite D572-4B
Cockpit Controls	(45)	(45)
Side stick	14	14
Supports	6	6
Rudder pedals	12	12
Supports	8	8
Bungee	5	5
Automatic Flight Controls	(265)	(265)
Sensors	13	13
Rudder pedal transducers	3	3
Digital computer	19	19
Data adapter	22	22
CAS computer	35	35
Control & display panel	6	6
Supports	19	19
T/R Units	26	26
Batteries	62	62
Wiring	60	60
Actuation System	(695)	(520)
Aileron	200	175
Flaps, trailing edge	85	75
Flaps, leading edge	330	205
Canard	80	65
Total System	1005	830

Load and Handling Group

A weight allocation of 5 pounds was used for jacking and tiedown fittings.

MISSION AND DESIGN TRADE STUDIES

Sensitivities Studies

The sensitivity and trade studies performed on the composite airplane were based upon the D572-4B selected vehicle. The reference takeoff gross weight for the vehicle was 31,303 pounds.

The sensitivity and trade studies performed on the metallic airplane were based upon the D572-5A selected vehicle. The reference takeoff gross weight from sizing the vehicle to the design mission was computed to be 35,108 pounds.

Deadweight Sensitivity

The purpose of this sensitivity study was to establish the payload effects on the aircraft mission radius and takeoff gross weight. The appropriate metallic and composite selected vehicles served as the trade basepoints. The sensitivity study was first conducted with the takeoff gross weight held constant and the mission radius, the variable, and secondly, the vehicle was sized to the mission with takeoff gross weight being the fallout. Figure 39 shows the deadweight sensitivity for the composite and metallic aircraft. The fixed fuel decrement caused by a deadweight increment results in a substantially higher percentage of cruise fuel loss for the composite vehicle and, in turn, in a higher radius sensitivity. The metallic aircraft growth factor is 1.42.

Zero-Lift-Drag Sensitivity

The zero-lift-drag sensitivity study was conducted by adding a constant 10 and 20 counts of drag for all mach numbers to the selected basepoints. As in the previous trade, the performance was computed for a fixed takeoff gross weight with radius as the fallout and for a fixed mission radius with gross weight as the fallout. Figure 40 illustrates the zero-lift-drag sensitivity trades for the composite vehicle and for the metallic aircraft.

Considering the metallic aircraft, the addition of 20 counts of drag at a fixed gross weight results in a 40-nautical-mile decrease in the vehicle radius. For a fixed radius mission, 20 counts of drag causes the gross weight to grow by 910 pounds.

The effect of 20 counts of drag on the composite aircraft resulted in 40 nautical miles for constant weight and 510 pounds for fixed radius.

Thrust Sensitivity

The effect of varying the thrust multiplications factor for the composite and metallic aircraft is shown in Figure 41 for a fixed takeoff gross weight and a fixed mission radius. For the composite vehicle, the effect of a thrust multiplication factor of 0.95 upon the takeoff gross weight is 380 pounds for a fixed radius and the same factor on a fixed weight costs 20 nautical miles radius. A thrust multiplication factor of 0.95 causes the takeoff gross weight of the metallic airplane to grow by 570 pounds. The same factor applied to a fixed gross weight vehicle reduces the mission radius by 20 nautical miles.

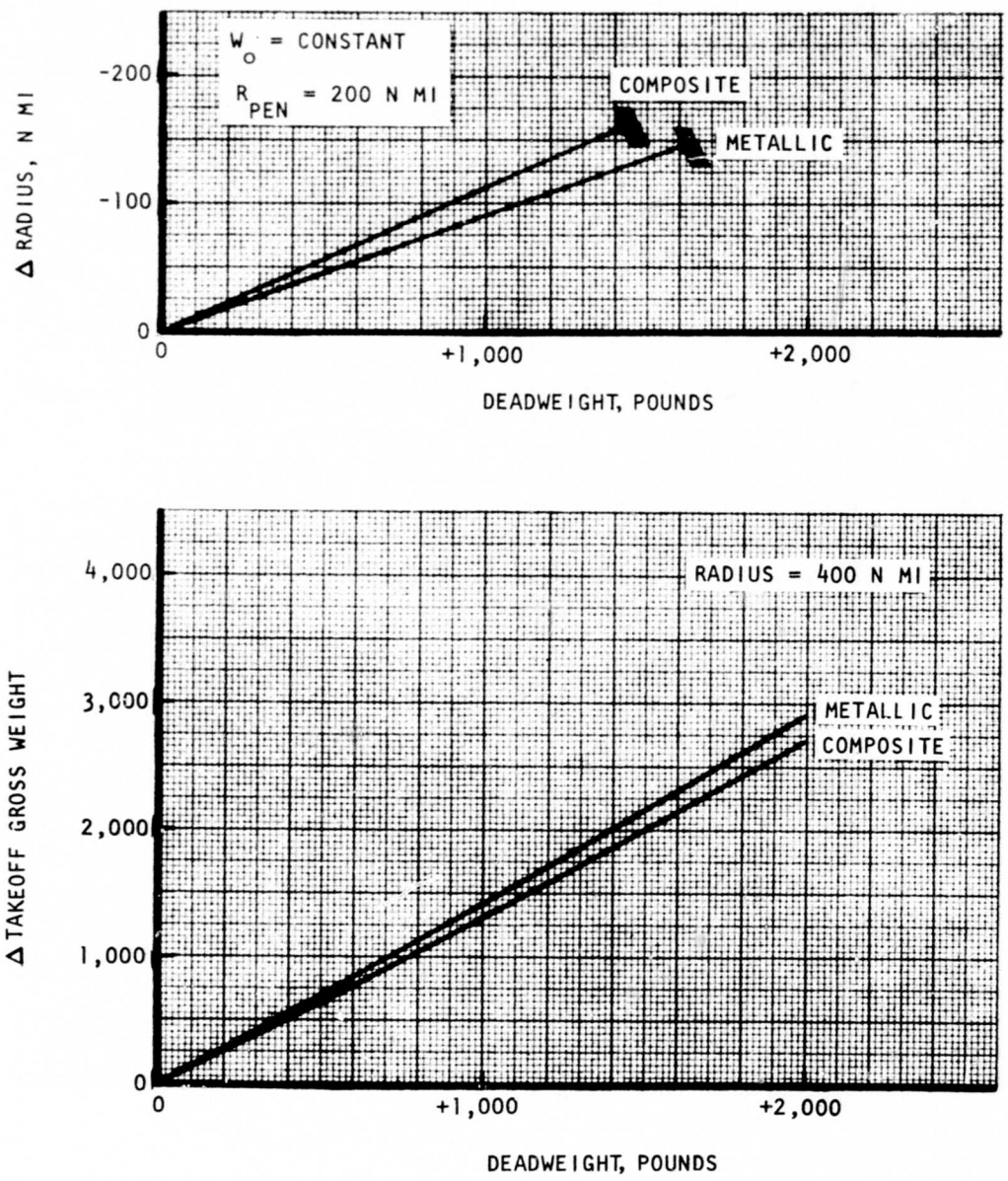

Figure 39. Deadweight trade.

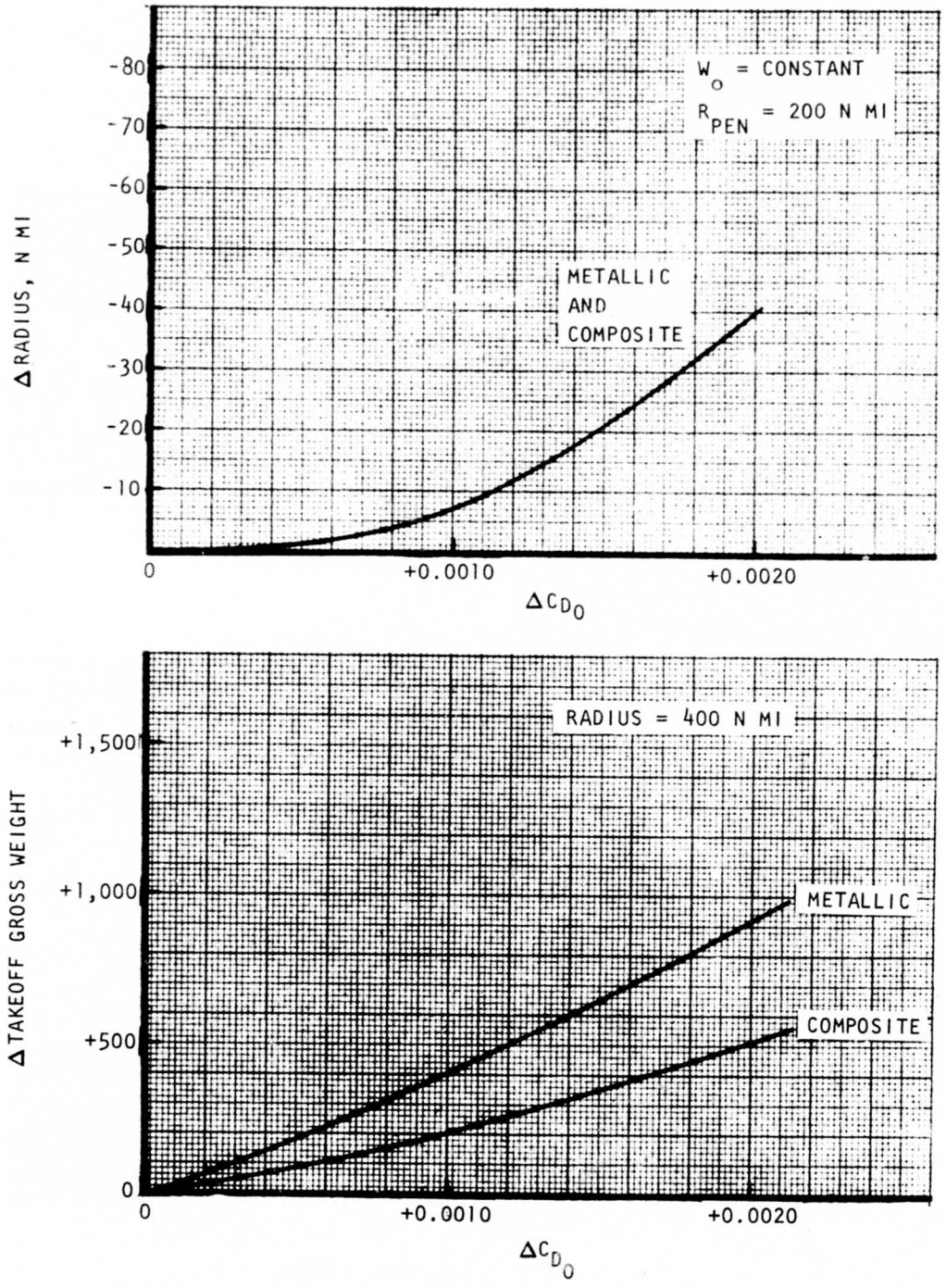

Figure 40. Drag sensitivity.

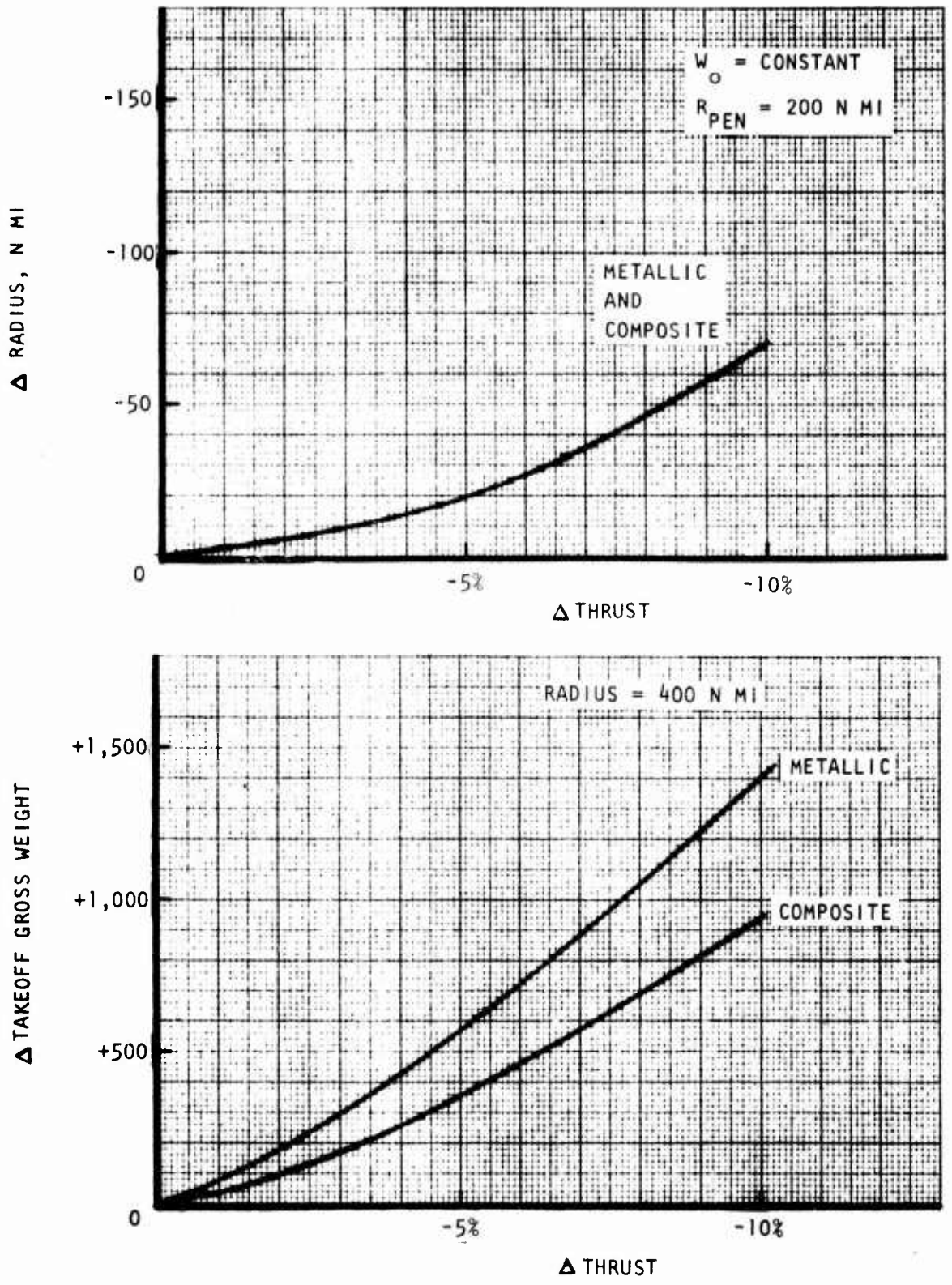

Figure 41. Thrust sensitivity.

Vehicle Geometry Trade Studies

Aspect ratio, sweep, and thickness trades were conducted on the selected basepoint vehicles, and the results of these trades were used to establish the next level of refinement in the design process.

The battlefield mission radius, ferry mission range, takeoff distance and selected P_S points were also tracked to aid in the selection process. The trade studies for the composite aircraft are shown in Figures 42, 43 and 44 and the trades for the metallic airplane are shown in Figures 45, 46 and 47.

Figures 48, 49, 50, and 51 present the alternate capability of the composite aircraft and Figures 52, 53, 54, and 55 are the metallic airplane alternate capability.

Summary

This section presents results and recommendations from the previously discussed mission and design trade studies, and defines the resulting aircraft to be used in task II studies. Additionally, recommendations relative to future fighter systems are made and discussed.

Mission trades made relative to total mission radius by varying both subsonic cruise distance and penetration/egress distance independently while holding the other leg constant showed that an increase in either distance is not a large driver in vehicle weight. Because of this, and to facilitate comparison with earlier vehicles, no change in design mission definition is recommended for the remainder of the ADCA contractual study. Useful data obtained from -4 and -4A vehicle studies is thus nearly directly comparable with the -4B and -4C studies. Additionally, the difference in growth factor between the two vehicles, metallic and composite, would merely show increases in the benefits of composites which are already demonstrated.

The recommendation for a future fighter vehicle would be to increase the potential of the aircraft as much as possible to provide maximum versatility on alternate mission radii and stores loadings. For this reason, the mission radius should be increased to 600 nautical miles total with 300 nautical miles of acceleration and supersonic cruise.

The penetration mach number trade exhibits the same trend as the radius trades and the same reasoning was applied; i.e., no change for the ADCA study with increases recommended for a future fighter system.

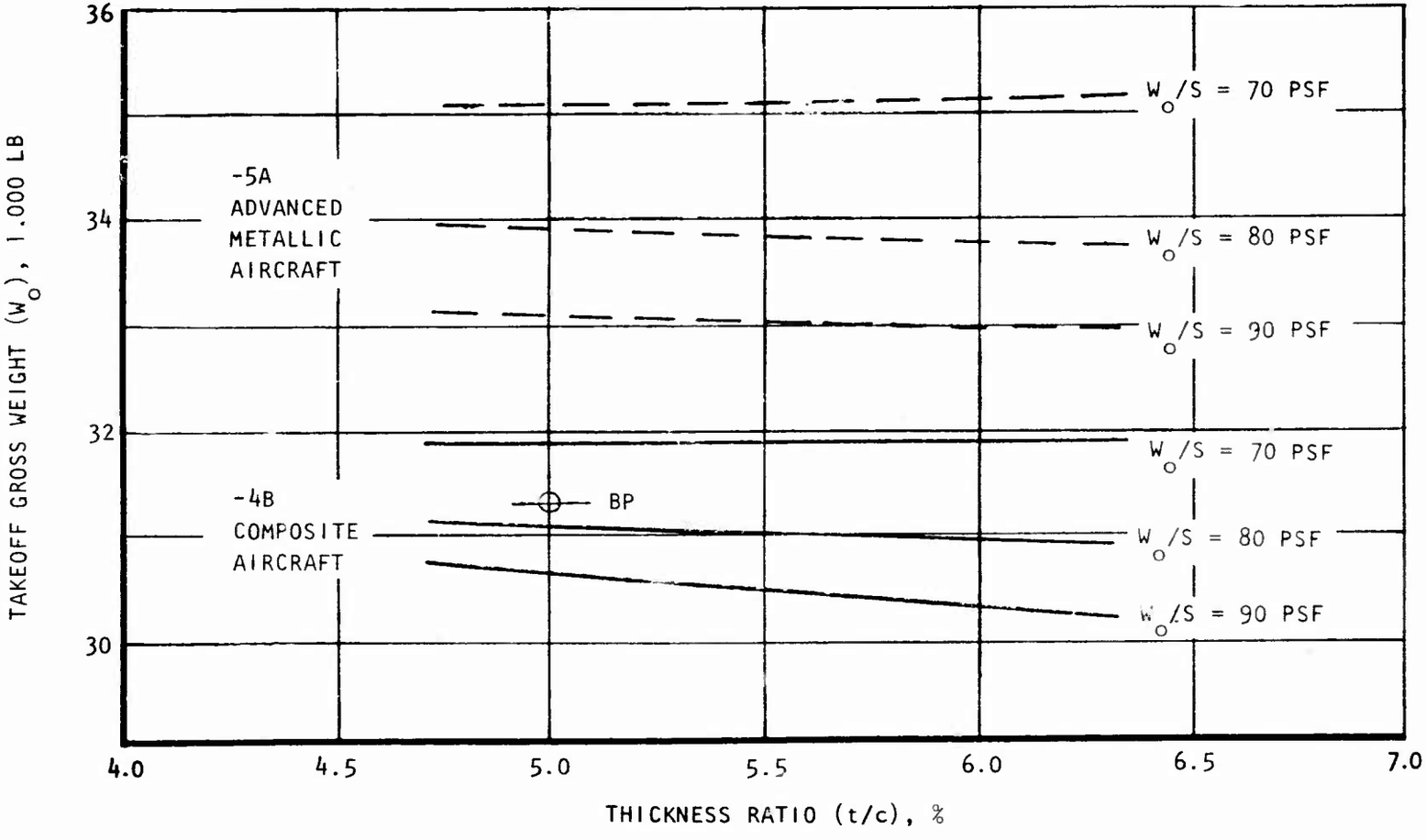

Figure 42. Thickness trade, composite aircraft.

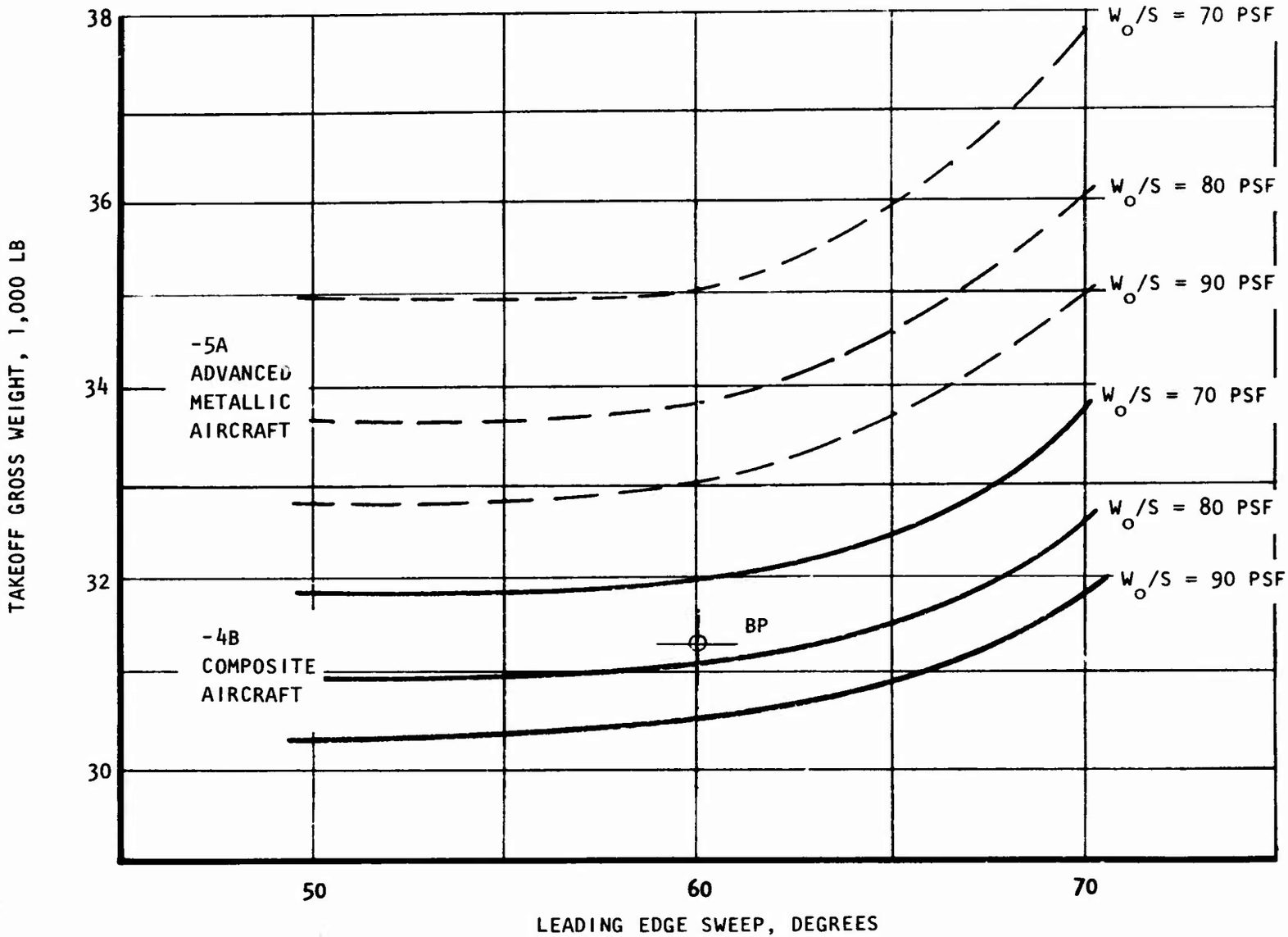

Figure 43. Sweep trade, composite aircraft.

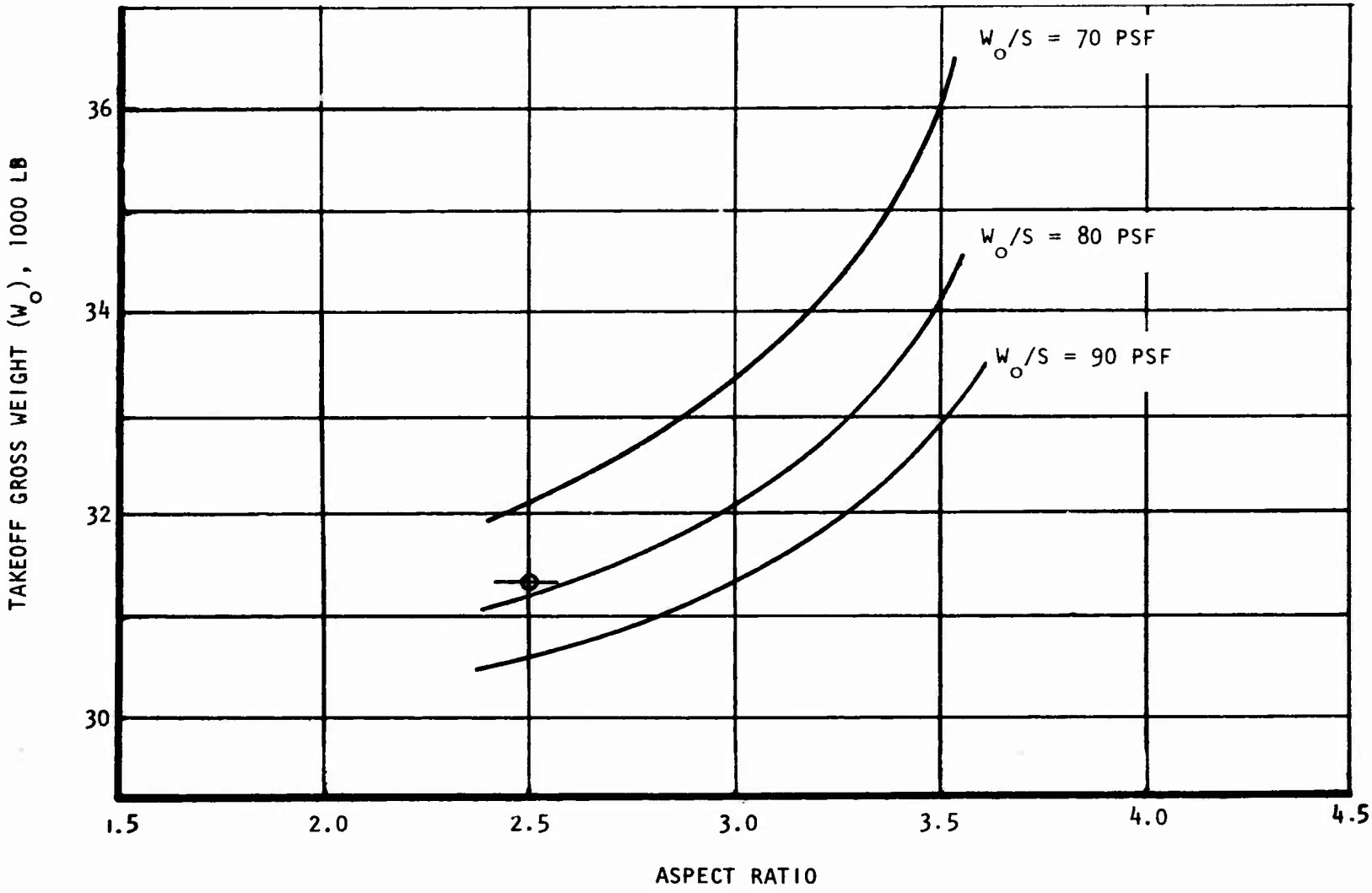

Figure 44. Aspect ratio trade, composite aircraft.

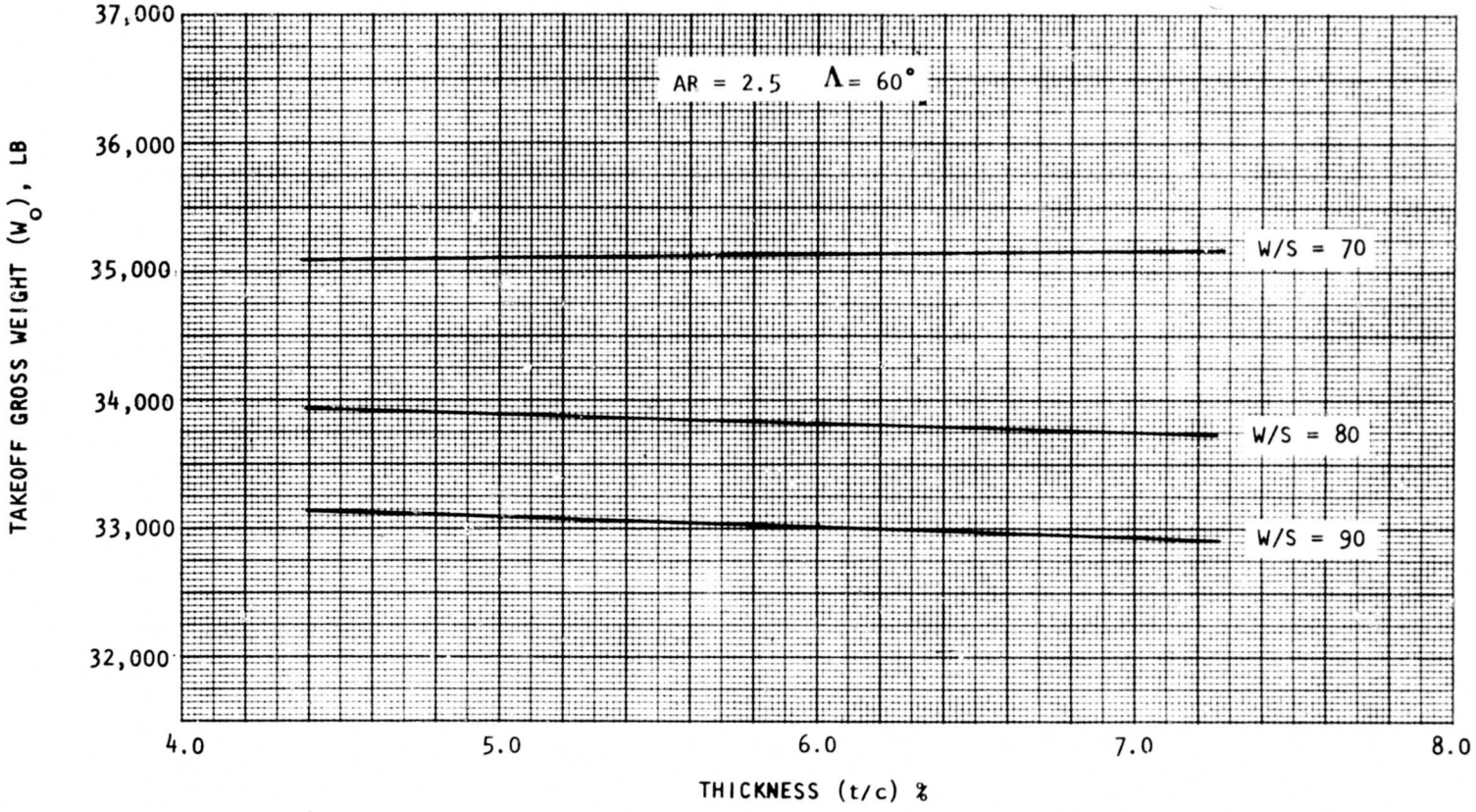

Figure 45. Thickness trade, metal airplane.

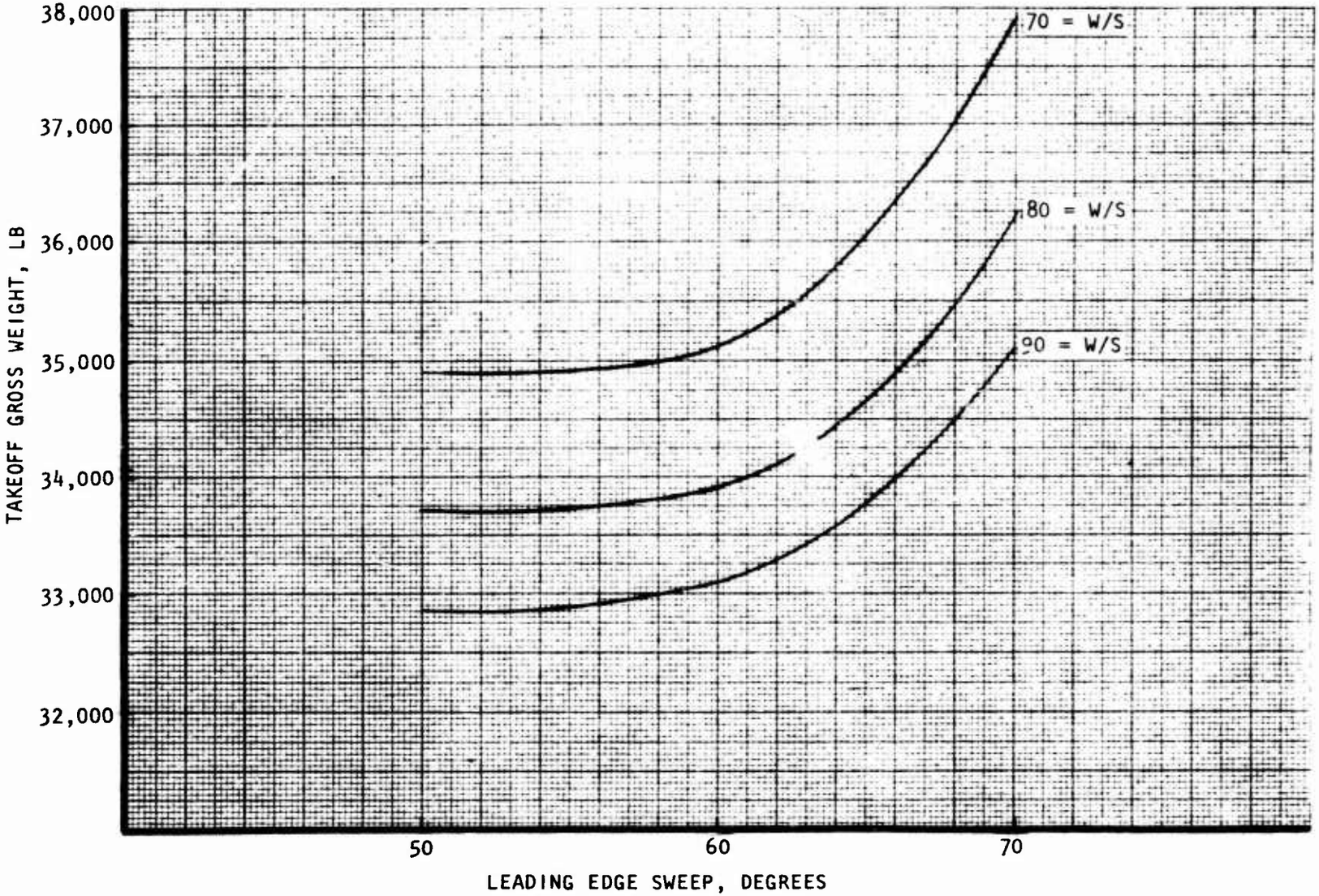

Figure 46. Sweep trade, metal airplane.

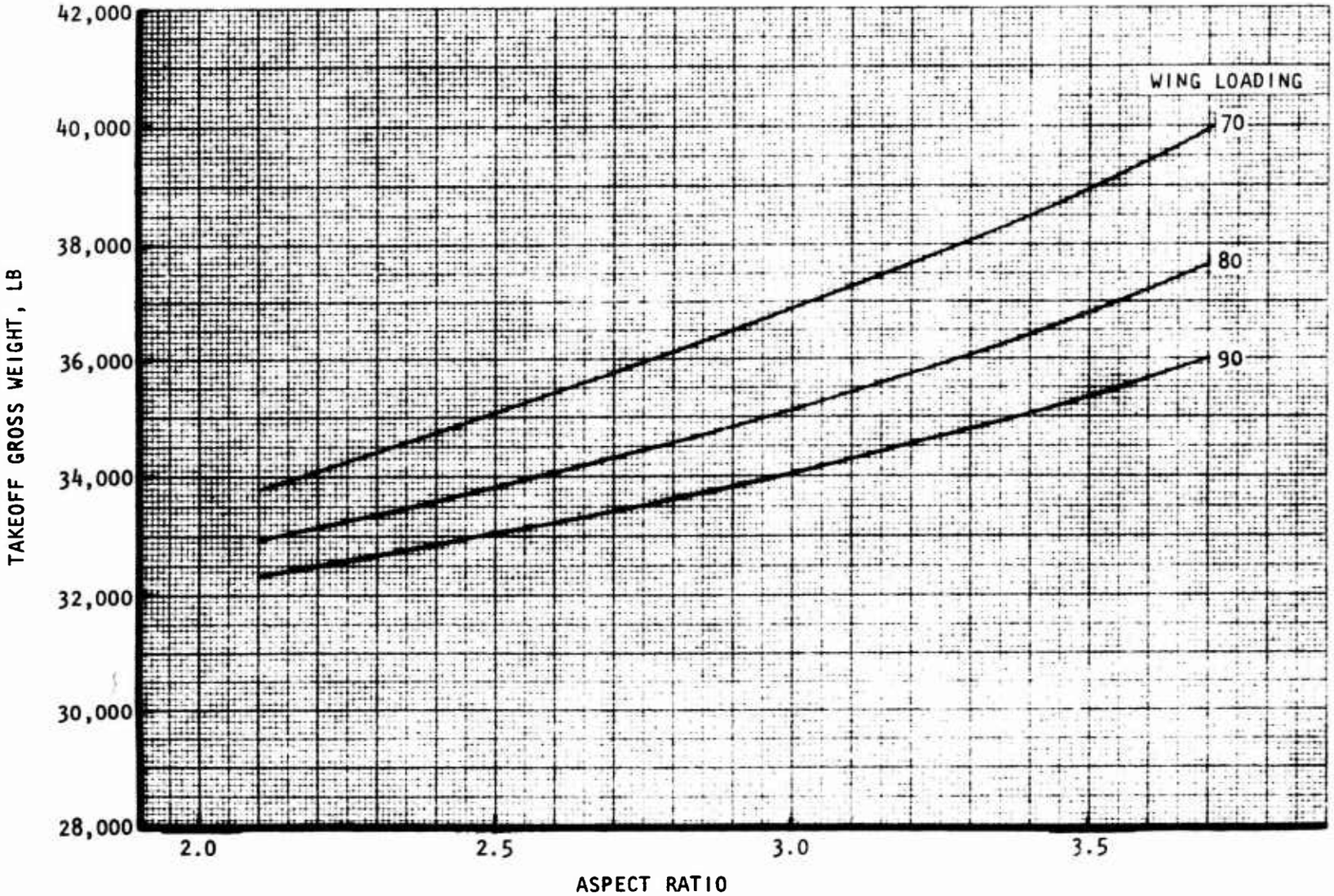

Figure 47. Aspect ratio trade, metal airplane.

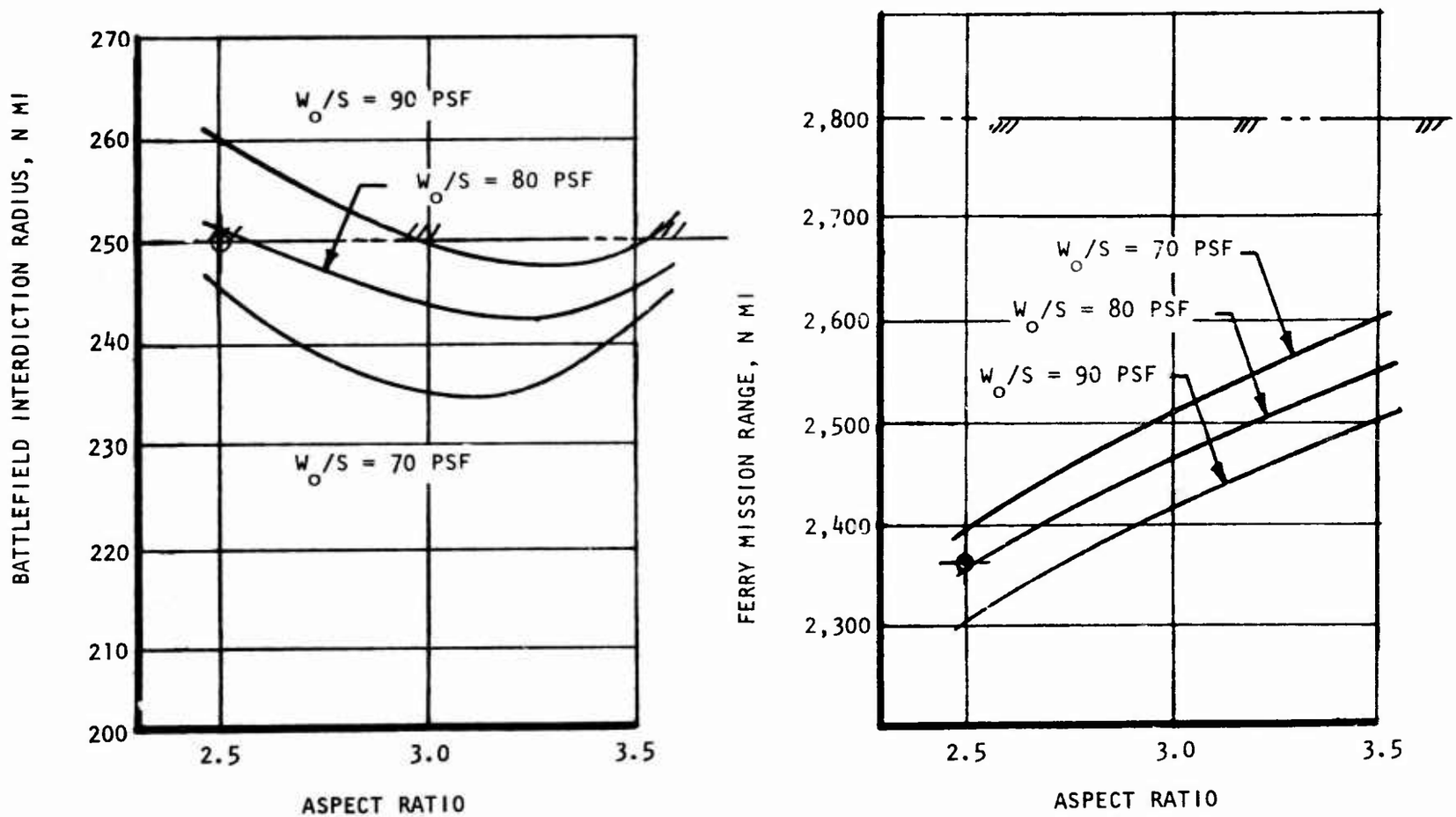

Figure 48. Alternate capability, composite aircraft.

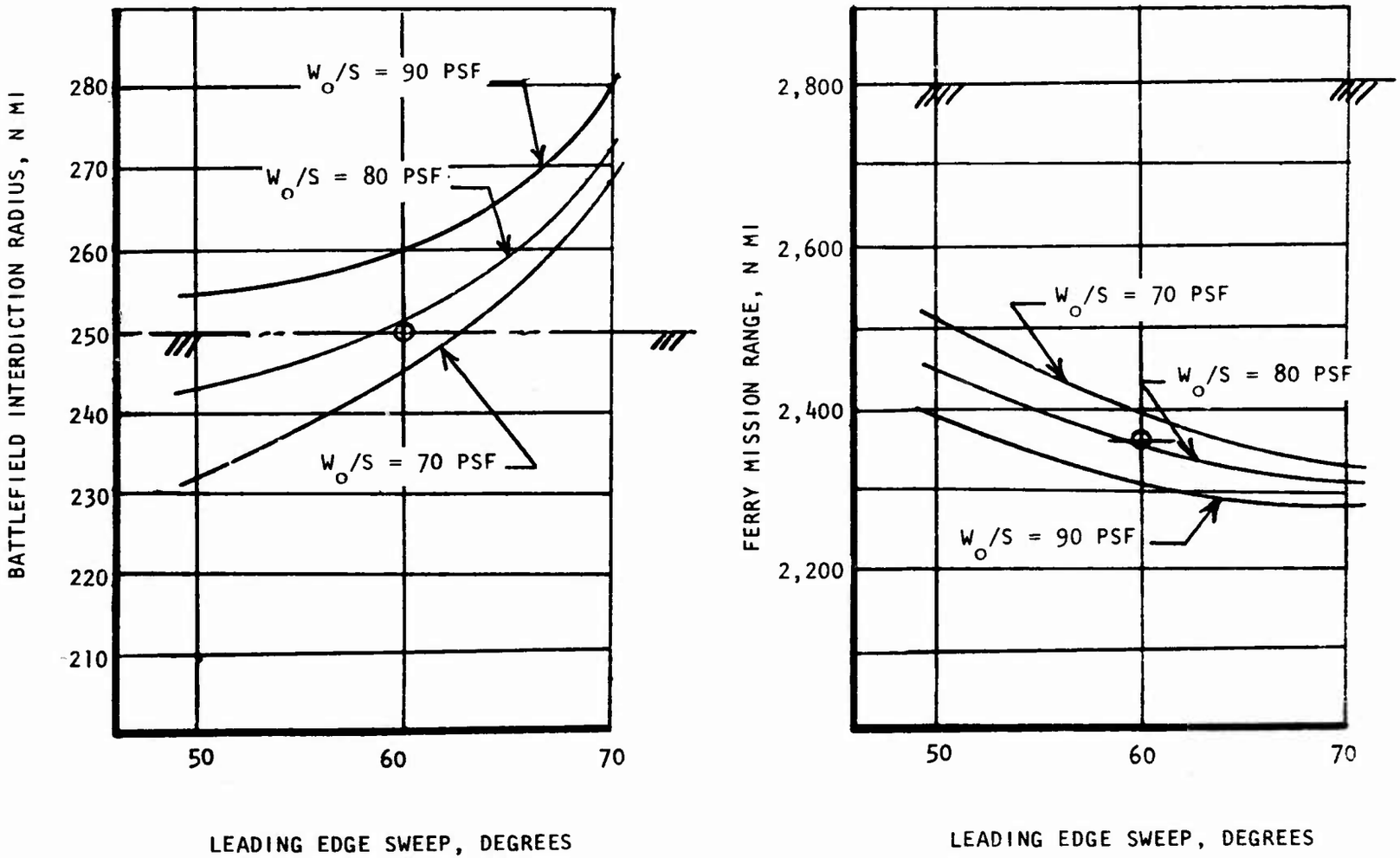

Figure 49. Alternate capability, composite aircraft.

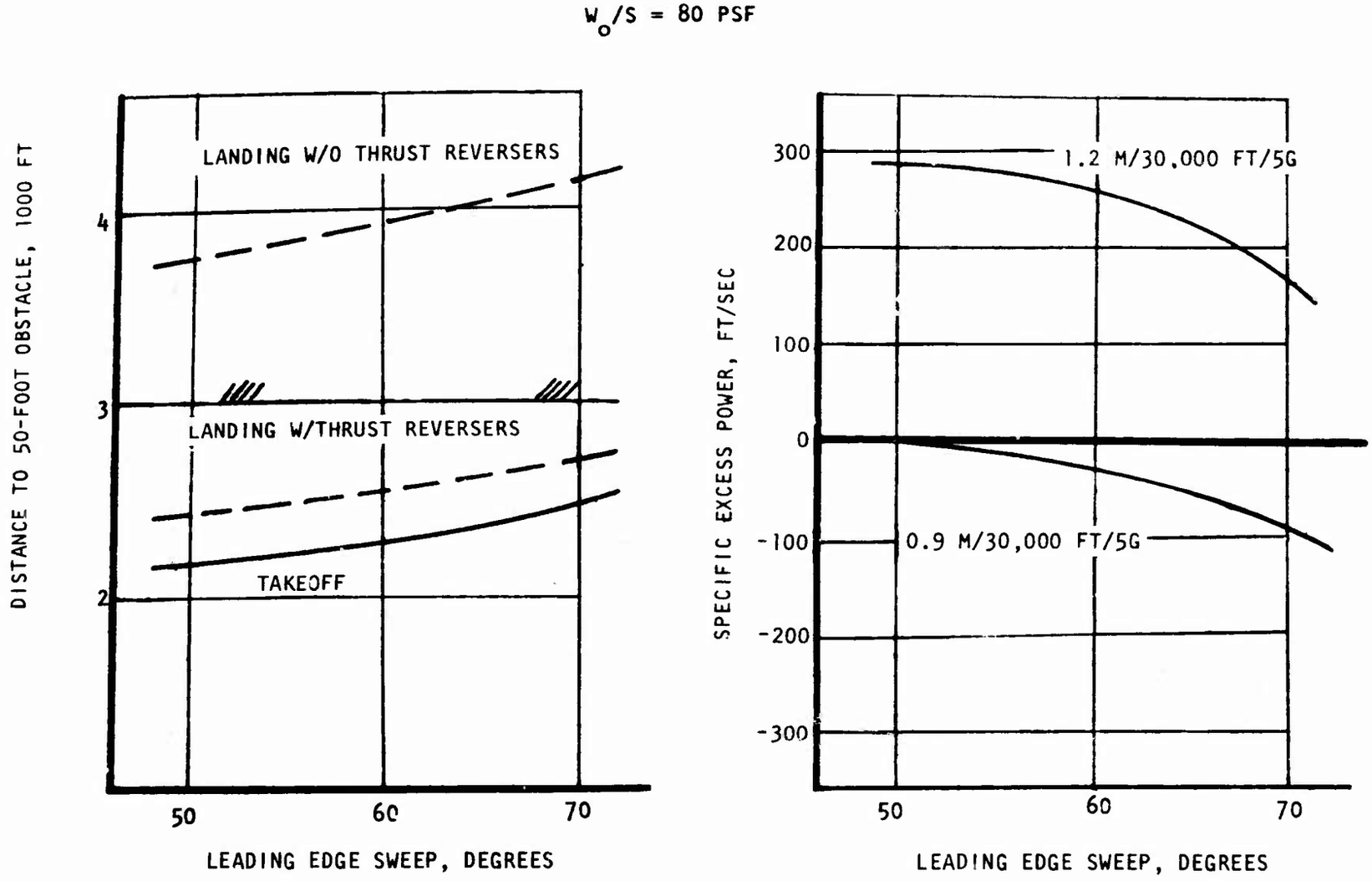

Figure 50. Alternate capability, composite aircraft.

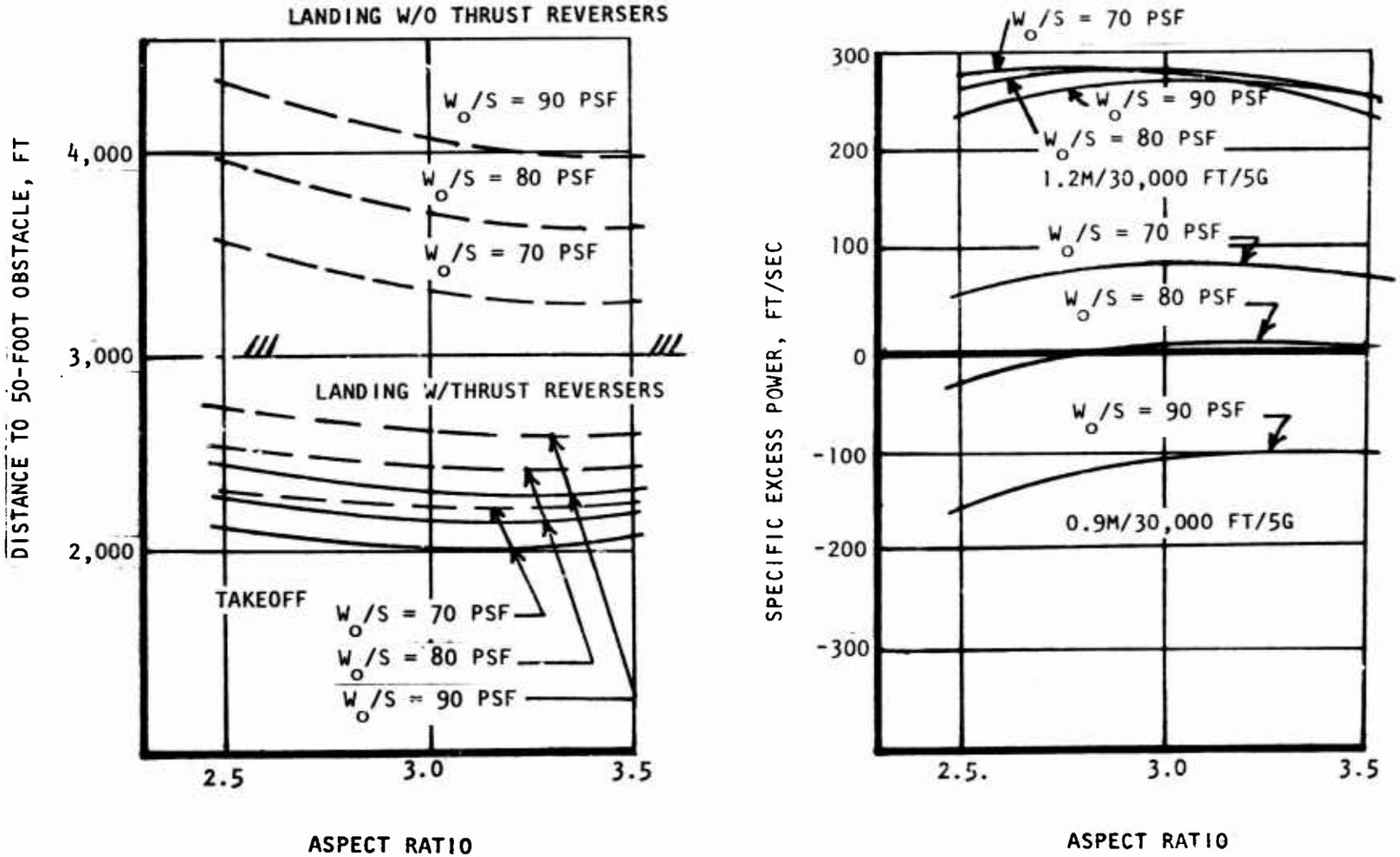

Figure 51. Alternate capability, composite aircraft.

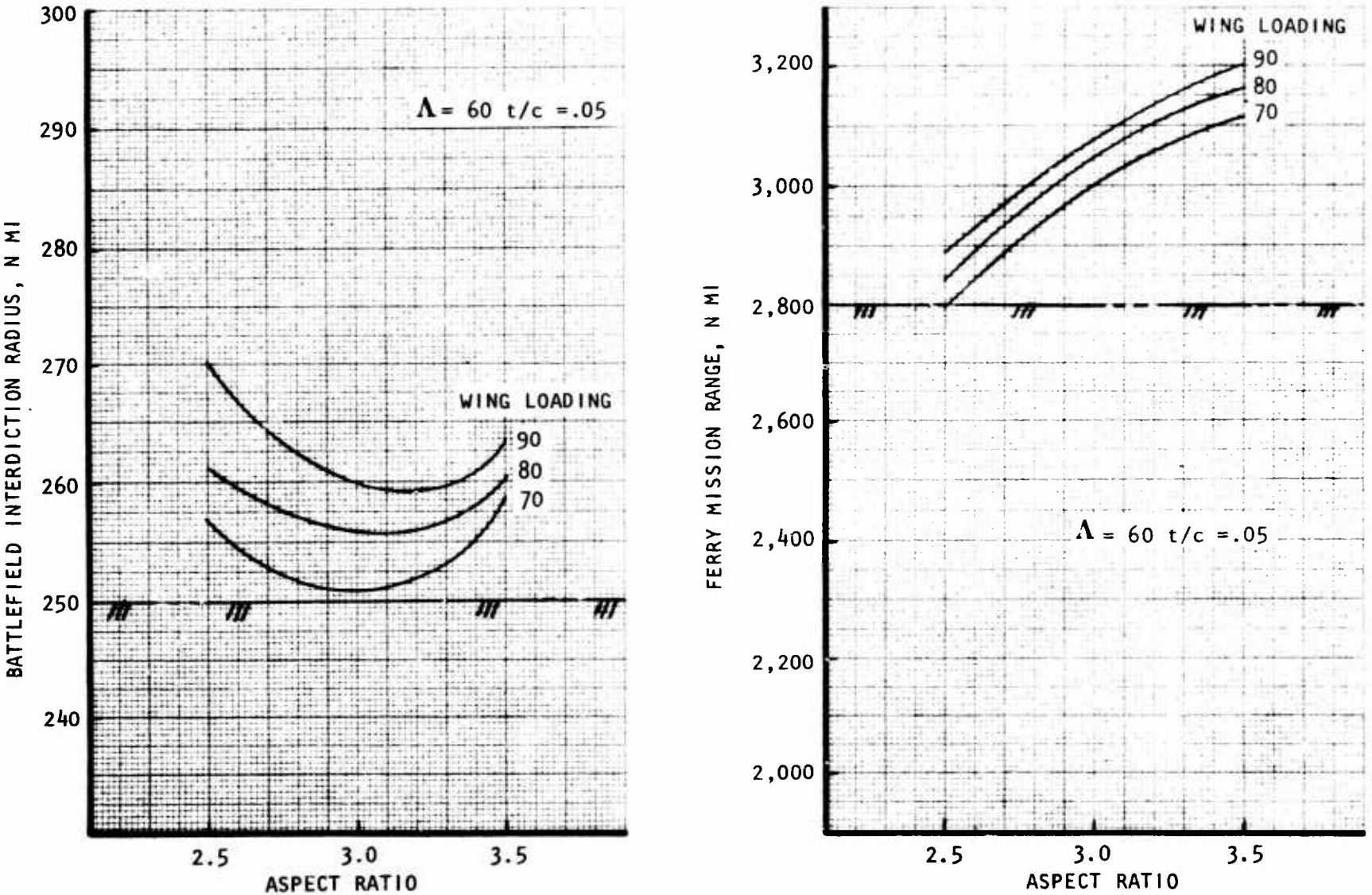

Figure 52. Alternate capability.

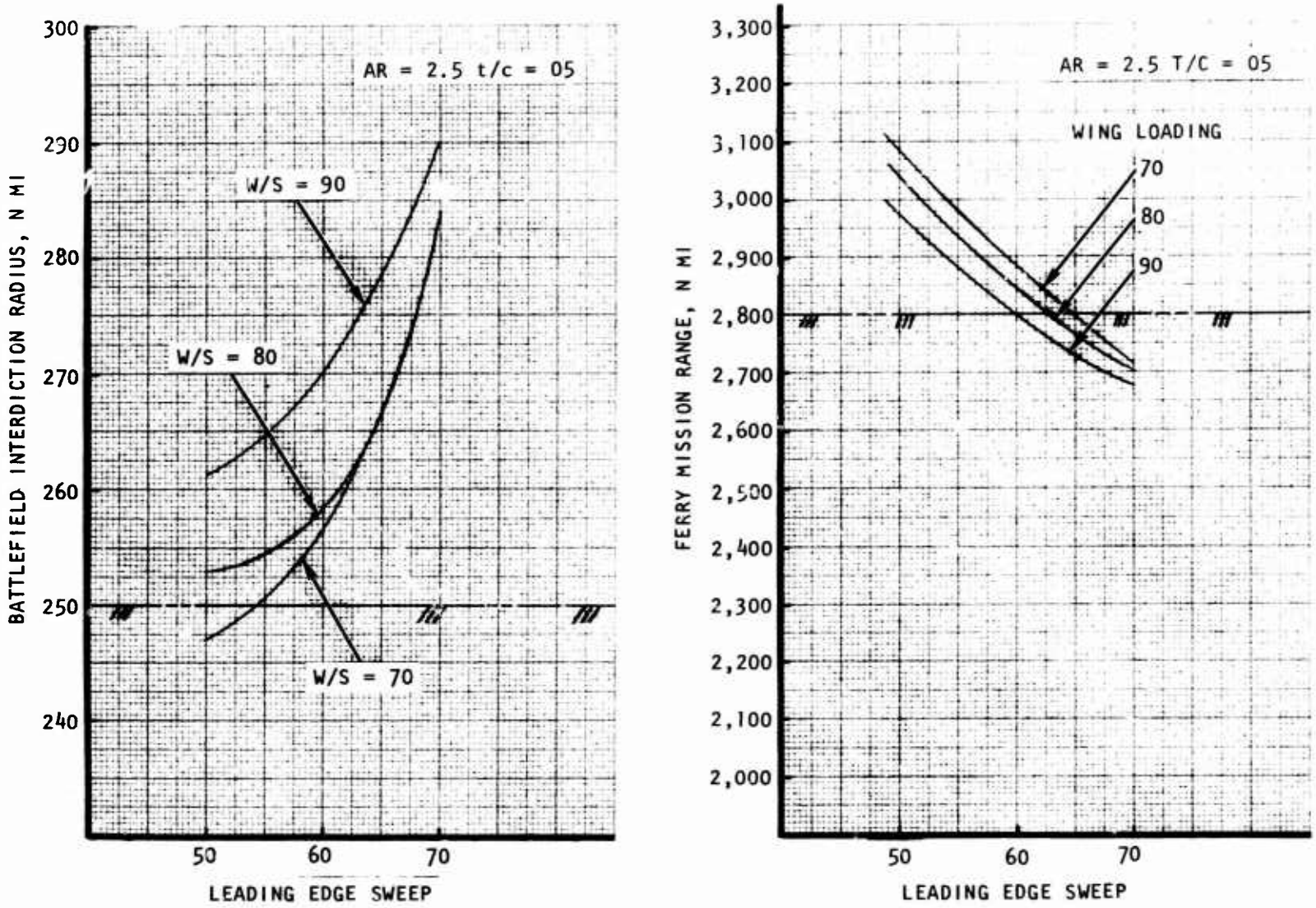

Figure 53. Alternate capability.

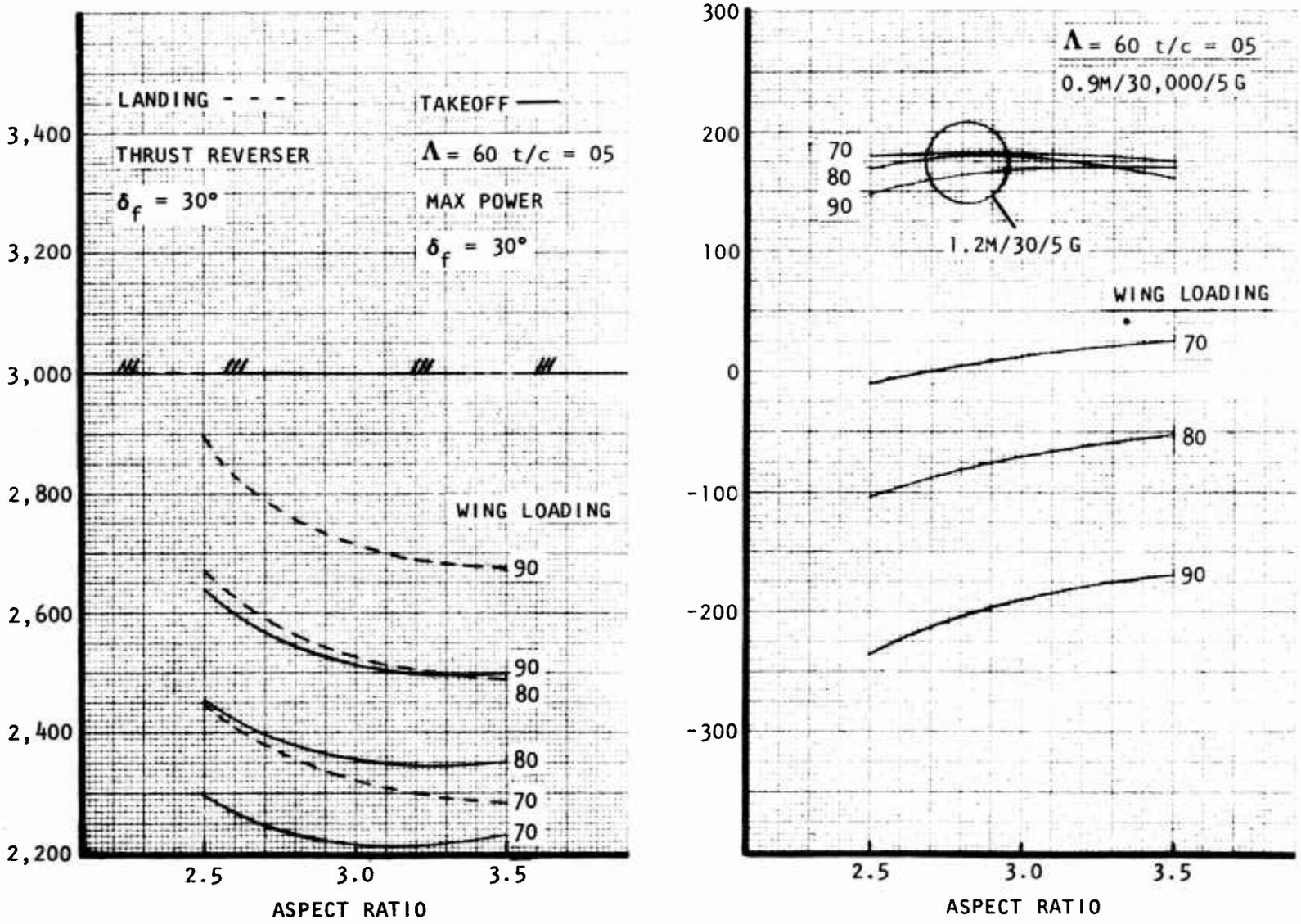

Figure 54. Alternate capability.

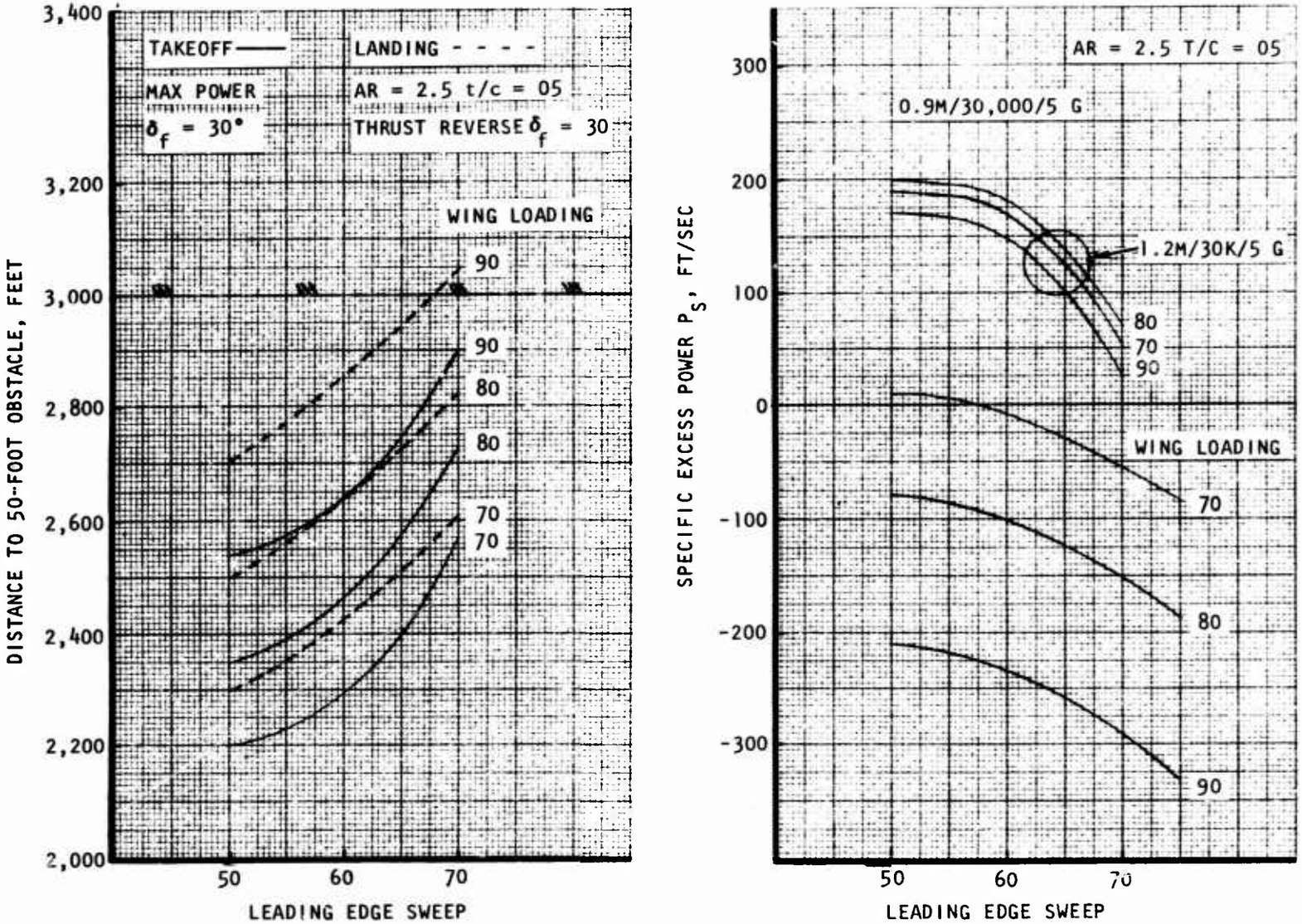

Figure 55. Alternate capability.

SELECTED VEHICLE

Composite Aircraft

The selection of the task II composite aircraft baseline D572-4C was made based upon the results of the trade studies. The primary driving factor in the selection of the -4C vehicle was takeoff gross weight. The premise being that the lighter aircraft costs less. The secondary factor in the selection process was the design and alternate mission requirements. The lighter airplanes favor the selection of higher wing loadings, lower sweeps, and lower aspect ratios. The alternate capability further constrains the selection indicating a preference of the 80 PSF wing loading and 60-degree sweep. The takeoff and landing and P_s are within the desired requirements. An aspect ratio of 3.0 was chosen since it favored the lower takeoff gross weight and more mission requirements could be attained. A thickness ratio of 5.0 percent was selected for the -4C aircraft. A 4-percent-thick wing was attainable at severe weight penalty and the 6-percent wing was determined to have a high wave drag decrement. The 5-percent wing represented the best compromise in the task II study composite aircraft.

Figure 56 illustrates the task II D572-4C composite aircraft baseline.

Metallic Aircraft

In a similar selection process as described for the composite aircraft, the task II baseline metallic aircraft D572-5B was chosen. However, the most important distinction in the method of selecting the metallic aircraft was that it was chosen such that its performance would be as nearly identical to that of the composite aircraft as practicable.

Figure 57 shows the metallic aircraft baseline.

- SUPERCRUISER CONCEPT
- TOGW 34,069
  - EMPTY WEIGHT 20,700
  - FUEL 6,962
  - WING AREA 400 FT^2
  - WING LOADING 85.2 PSF
- ENGINES (TWO)
  F404-GE-400 (F-18)
  THRUST-TO-WEIGHT (INST) 0.7012
- ARMAMENT
  TWO MK84 LGB 5,000 LB
  TWO SELF-DEFENSE MISSILE 600 LB
  ONE M61 GUN
  300 ROUNDS AMMO 170 LB
- AVIONICS 1,000 LB

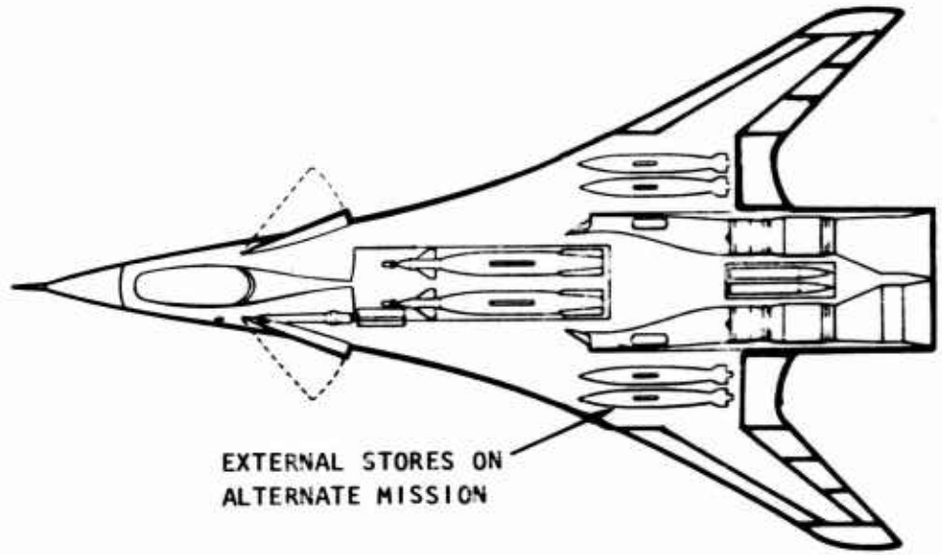

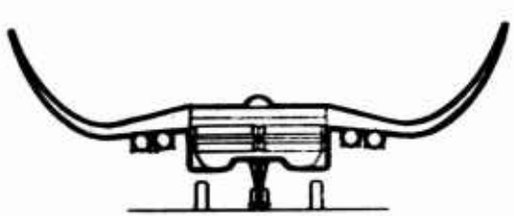

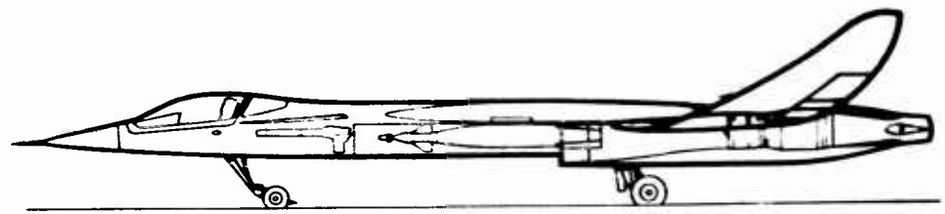

- NO WEIGHT FOR AEROELASTIC TAILORING

Figure 56. All-composite baseline configuration D572-4C.

- SUPERCRUISER CONCEPT
- TOGW 37,213 LB

EMPTY WEIGHT	22,996 LB
FUEL	7,865 LB
WING AREA	500 FT^2
WING LOADING	74.4 PSF

- ENGINES (TWO)
  - F404-GE-400 (F-18)
  - THRUST-TO-WT (INST) .6419
- ARMAMENT

TWO MK84 LGB	5,000 LB
TWO SELF-DEFENSE MISSILE	600 LB
ONE M61 GUN	
300 ROUNDS AMMO	170 LB

- AVIONICS 1,000 LB

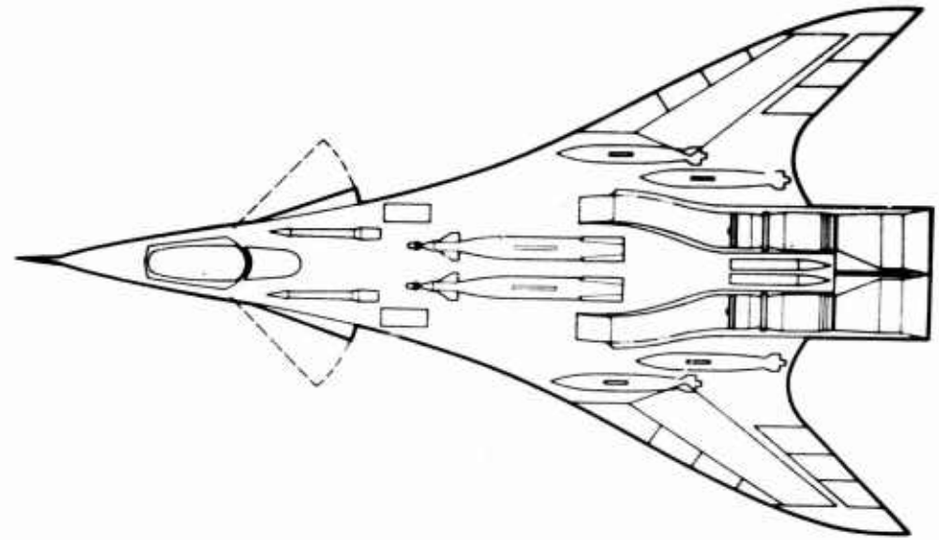

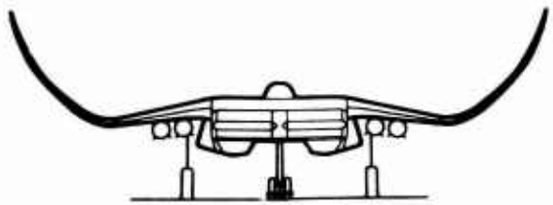

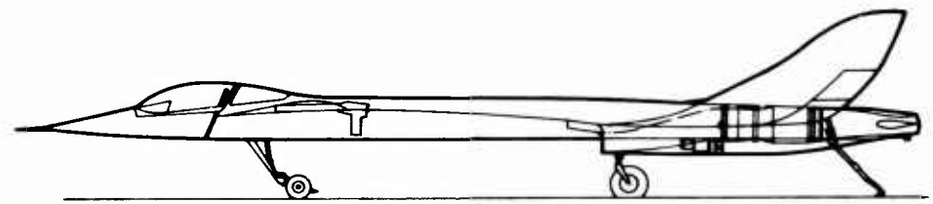

- NO WEIGHT FOR AEROELASTIC TAILORING

Figure 57. Advanced metallics baseline configuration 572-5B.

Section III

AERODYNAMICS

SUPERCRUISER CONCEPT DEFINITION

The aerodynamic goal that has led to a definition of the supercruiser concept is to reduce trimmed supersonic drag to a level which allows efficient (i.e., dry power) supersonic cruise while maintaining competitive levels of transonic/subsonic maneuverability. To achieve this goal, a configuration must be designed having low wave drag, low base drag, low skin friction drag, and low trim drag. The wave drag can be minimized by use of high fuselage fineness ratio, high wing sweep, and by blending these components together such that, at the supersonic cruise design mach number, the flow is subcritical over most of the vehicle except for a small region near the plane of symmetry. The base drag can be reduced by use of properly designed, two-dimensional nozzles. Skin friction drag can be minimized by deletion of conventional tail surfaces and of separate engine nacelles and pylons. Low skin friction drag results from deletion of high Reynolds number, short-chord horizontal and vertical tails from use of high fineness ratio components with low form factors, and, to a lesser extent, from reduced total wetted area. Low trim drag can be achieved by varying the longitudinal stability with a canard control system which retracts into the fuselage.

This concept definition has led to the configurations shown in Figures 4 and 5 in Section II. Curved-up wingtips provide lateral-directional stability. Trailing edge elevons provide longitudinal, lateral, and directional trim and control. Longitudinal control is augmented by a variable-stability canard and by vectorable two-dimensional jet nozzles. Lateral control is augmented by differentially vectorable two-dimensional nozzles. The sweep and curvature of the wing planform have been selected to maintain effective subsonic flow characteristics at the design supersonic cruise speed. This means that the transonic aerodynamic center shift is less than for conventional trapezoidal wings of lower sweep. However, the transonic aerodynamic center shift that does occur can be trimmed out by partial extension of the canard so that trim drag can be reduced to very low levels.

CHALLENGES OF SUPERCRUISER

During initial aerodynamic development of the supercruiser concept, several aerodynamic challenges have been identified as requiring careful attention to insure that the supercruiser will meet its aerodynamic goals: (1) achievement of low wave, base, skin-friction, and trim drags for efficient supersonic cruise, (2) effective use of vortex lift and jet vectoring for

subsonic/transonic maneuvering, with particular attention to trim and controllability, (3) achievement of satisfactory lateral-directional control during climbout after takeoff and during approach for landing, and (4) design of a variable-camber wing to achieve substantial leading edge suction at alternate cruise points.

BASEPOINT AERODYNAMIC DATA

Supersonic wave drag levels have been calculated for the all-composite (D572-4B) and advanced metallic (D572-5A) baseline configurations using available Rockwell/LAAD computer programs described in Reference 1. Subsonic drag rise for these two baseline configurations was estimated by application of NACA free-flight data and correlations available in References 2 and 3. The resulting curve of wave drag versus mach number is shown in Figure 58 for the -4B and in Figure 59 for the -5A configurations. The drag-due-to-lift curves presented in Figure 60 apply to both the -4B and -5A configurations and have been calculated using the FA475 computer program, which is an adaptation of the NASA Ames Woodward panel program and is described in Reference 4. These calculations assume that the wings can be twisted and cambered to achieve a leading-edge suction of 90 percent of that theoretically available. The takeoff and landing lift and drag curves shown in Figure 61 are based on low-speed wind-tunnel test data available in References 5 and 6. These takeoff and landing curves apply to both the -4B and -5A configurations.

The baseline stability and control data to be presented here have been worked up for the all-composite aircraft (-4B). Aerodynamic center and lift curve slope are shown in Figure 62 versus mach number for the rigid airframe. Comparable lateral and directional stability derivatives C_{n_β} and C_{l_β} are shown in Figure 63.

A tabulation of rigid stability derivatives for a six-degrees-of-freedom rigid airframe maneuver is included in Table 7. Flexible derivatives are shown in Figures 64 through 70; whereas, flexible-to-rigid ratios are shown in Figures 71 through 78. These preliminary flexible data are based on a simple stick model without twist, camber, thickness, or weight, but with sweep. Tabulation of flexible stability derivatives for six-degrees-of-freedom analyses are included in Tables 8, 9, and 10.

A review of the wind tunnel data and theoretical computation basis for these D572-4B baseline aerodynamic data is presented in Reference 8. Comparisons between the measured NASA supersonic test data of Reference 7 and LAAD theoretical computations are presented and discussed in Reference 9. Results of six-degrees-of-freedom dynamic studies are reviewed in Reference 10.

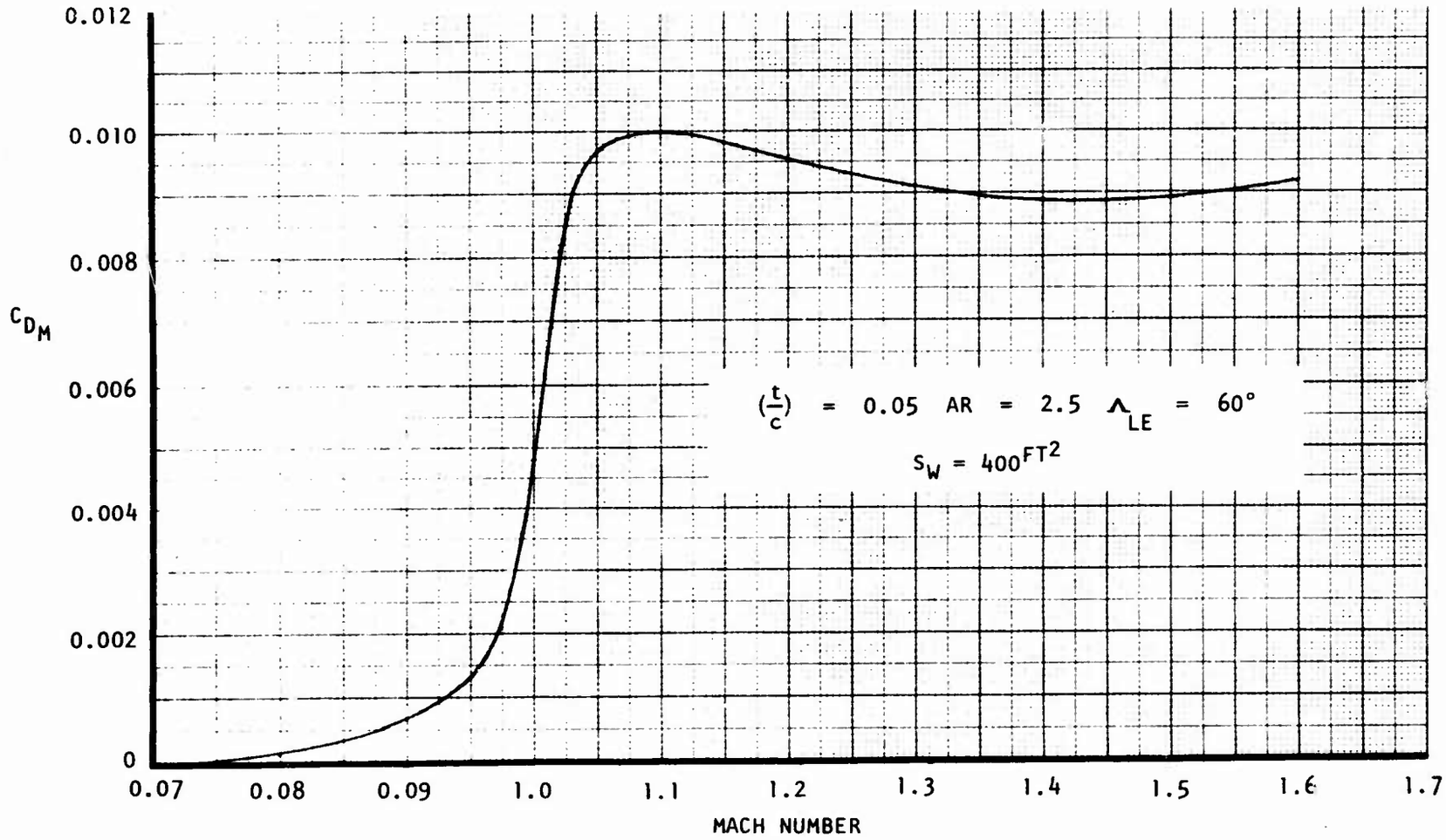

Figure 58. Advanced design composite aircraft - D572-4B (optimized at M = 1.4).

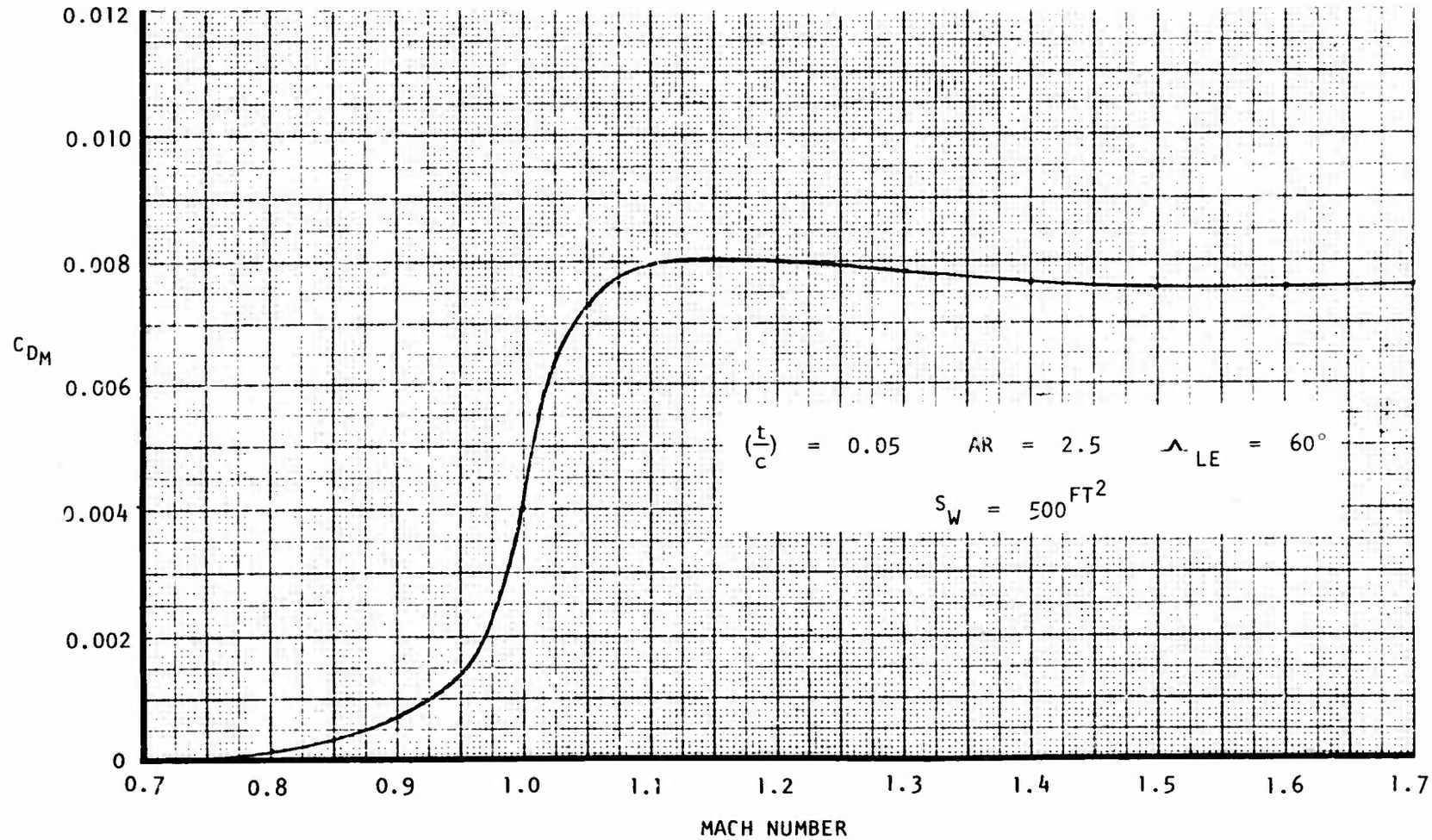

Figure 59. Advanced design all-metal aircraft - DS72-5A (as drawn)

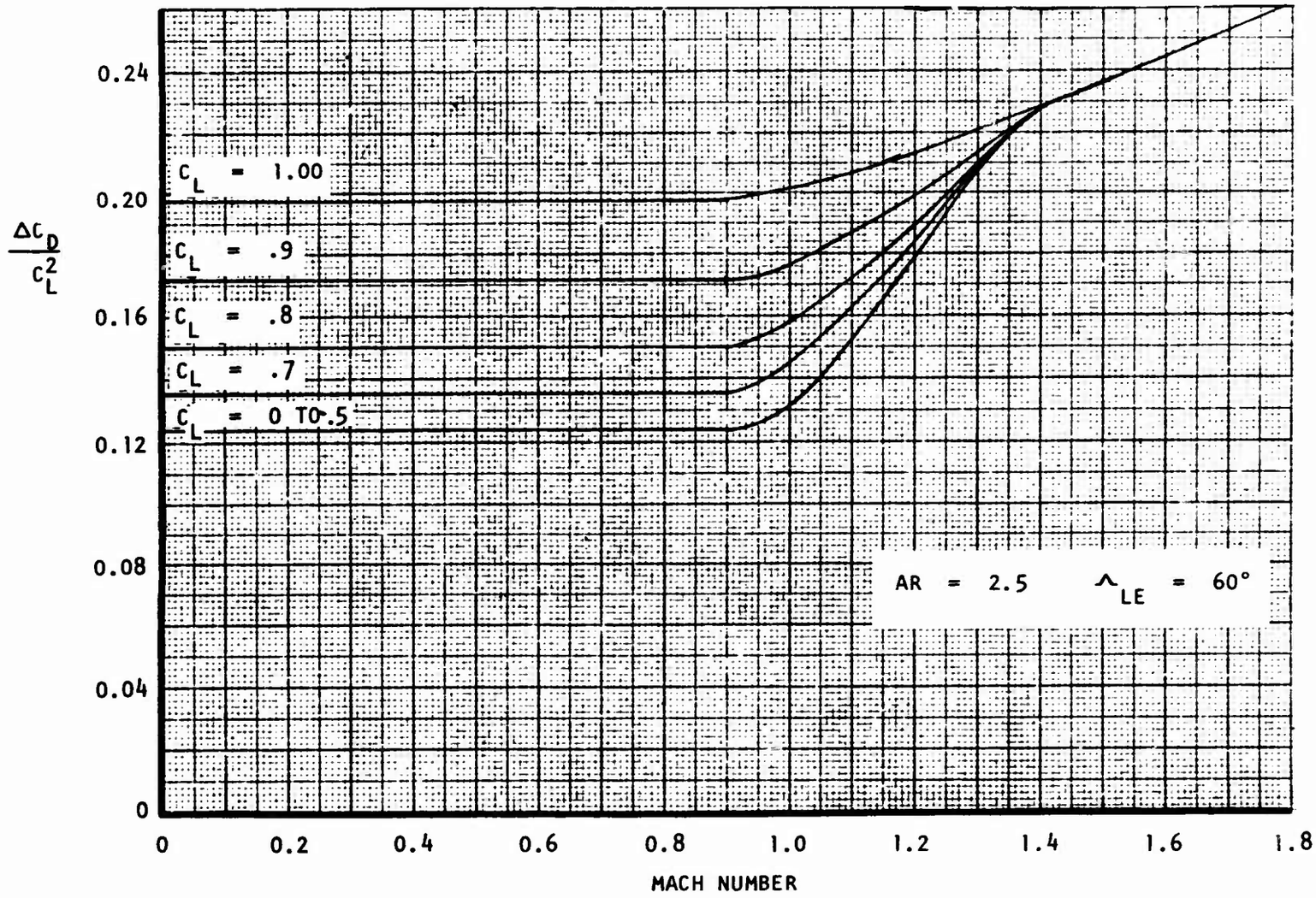

Figure 60. Advanced design composite and all-metal aircraft - D572-4B and -5A.

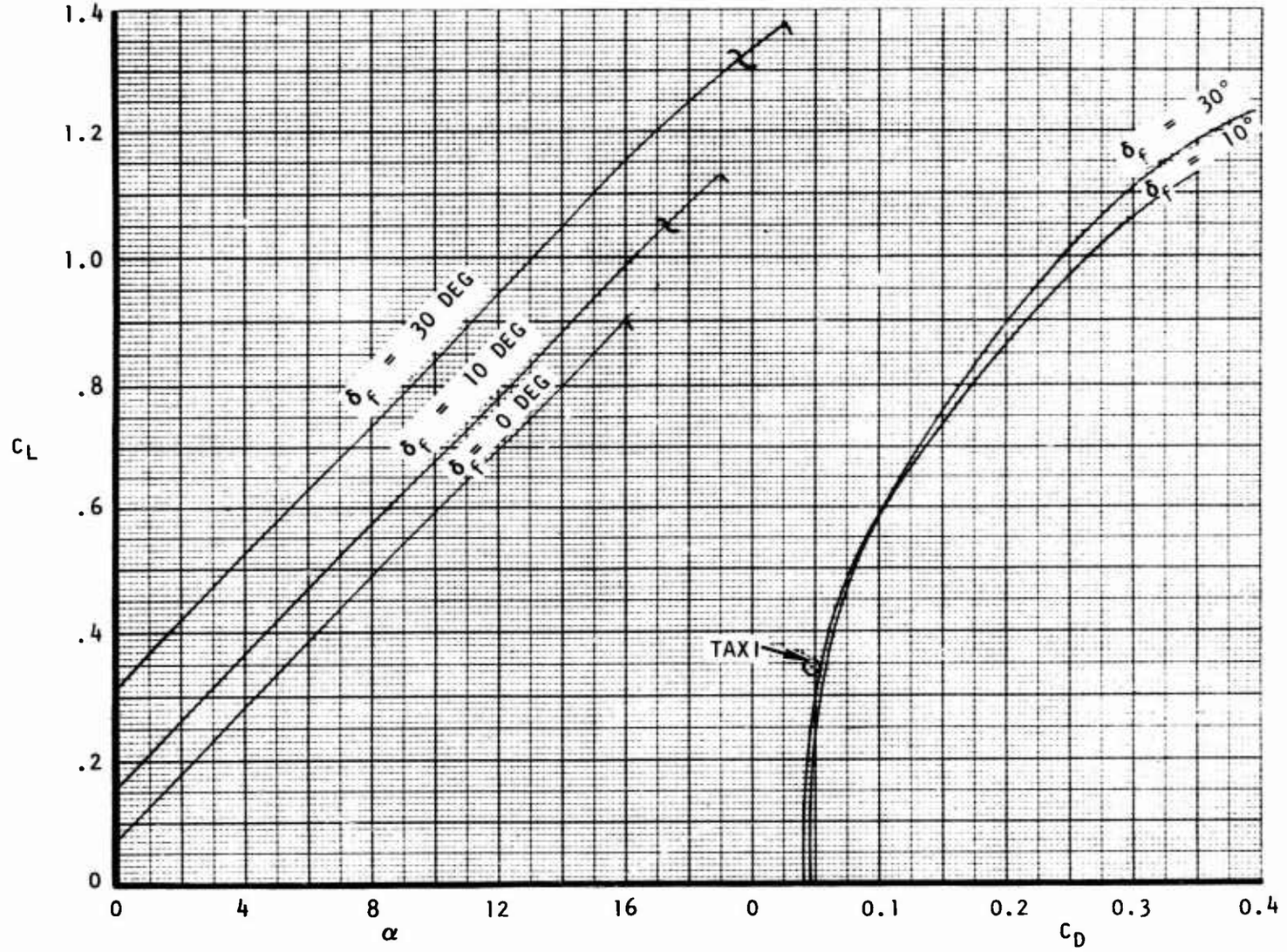

Figure 61. Takeoff and landing longitudinal characteristics - D572-4B and 5A.

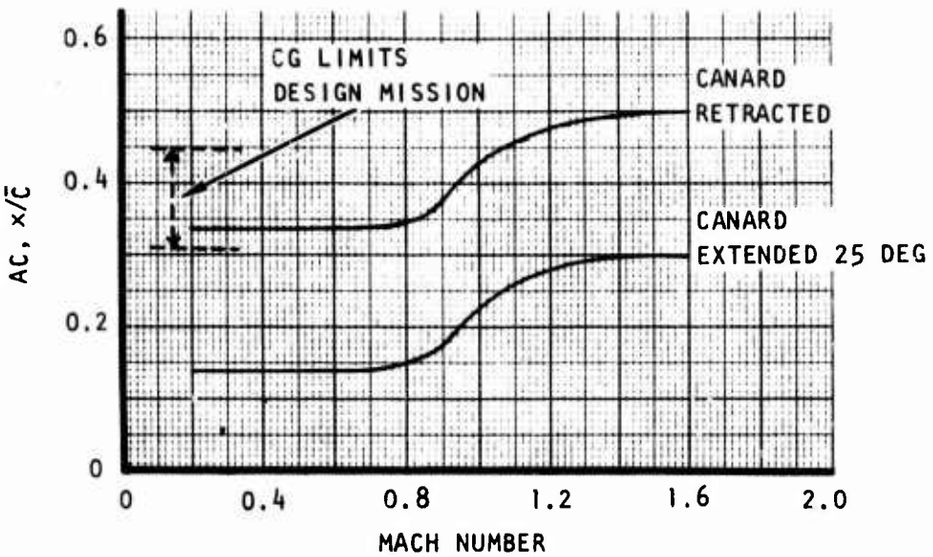

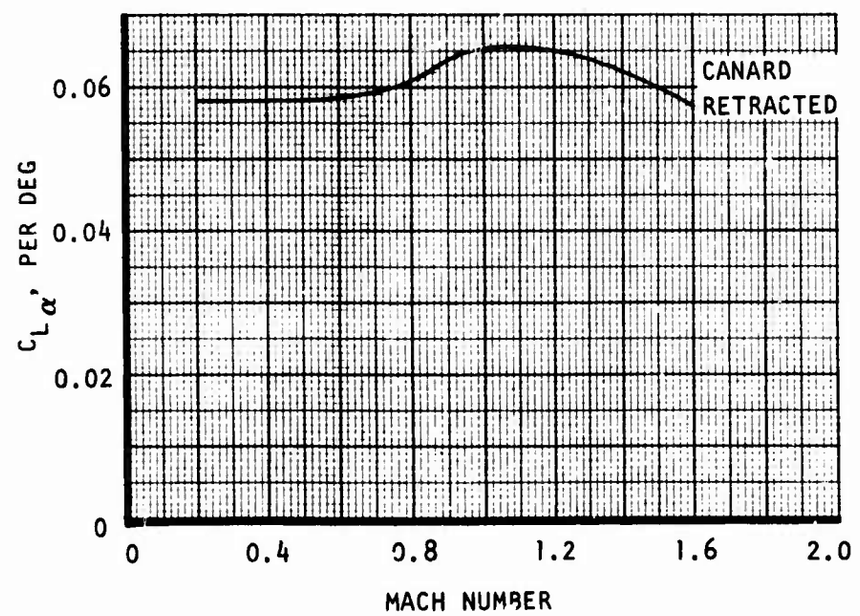

Figure 62. Variation of longitudinal characteristics with mach number - D572-4B rigid

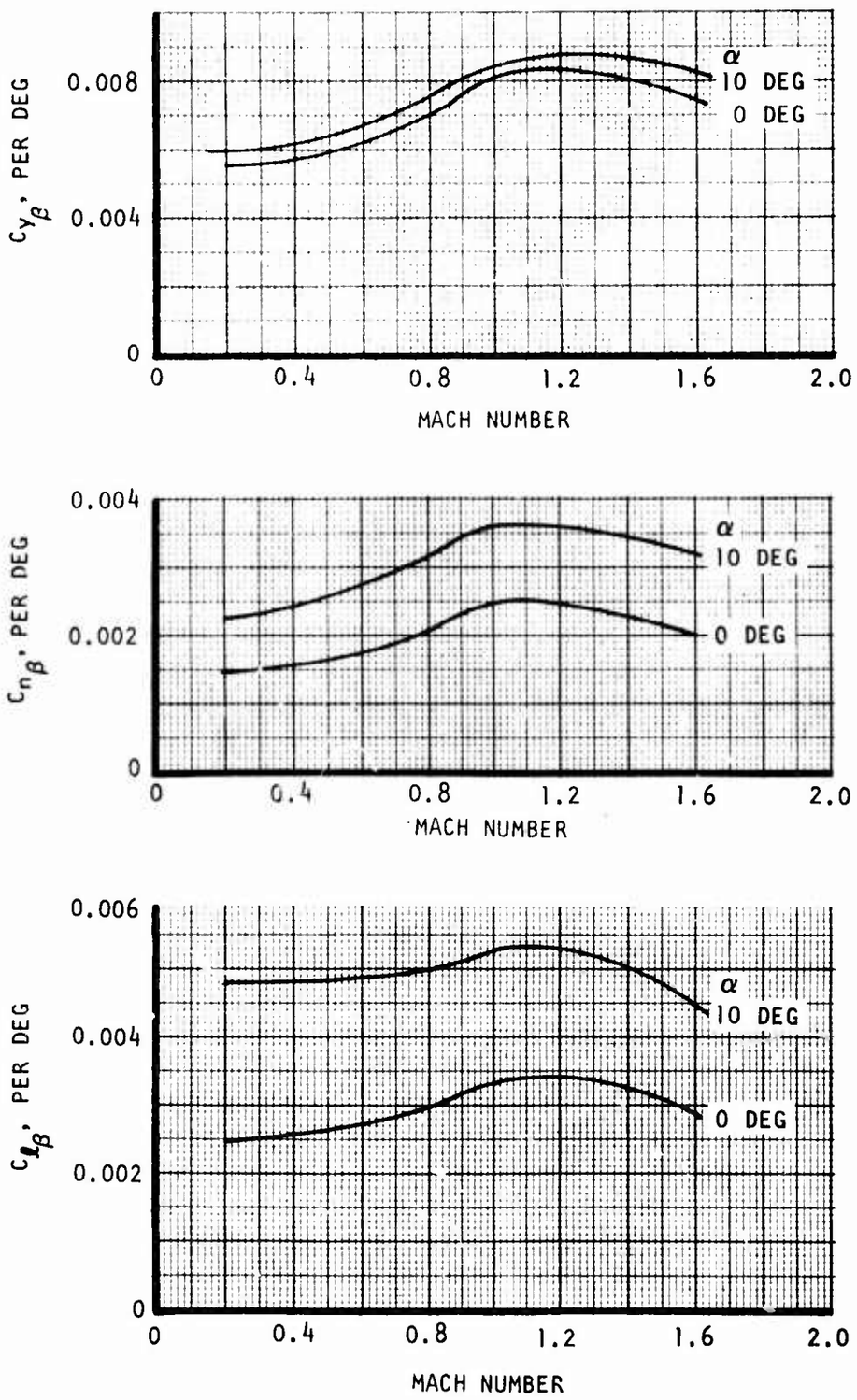

Figure 63. Variation of lateral-directional characteristics with mach number - D572-4B rigid.

TABLE 7. RIGID AERODYNAMIC DATA, M = 0.9

TITLE: D575-4B M: 0.90 q: 0.0

S_W: 400 ft^2 $\bar{C}$: 163.51 in. b: 425,976 in. Xc.g.: 501,86 in.

C_{L_α} = 0.0532
C_{m_α} = -0.0006
C_{Y_β} = -0.00780
C_{n_β} = 0.00230
C_{ℓ_β} = -0.00320

C_{M_q} = -4.162
C_{n_r} = -0.1575
C_{n_p} = 0.1576
C_{ℓ_r} = 0.1724
C_{ℓ_p} = -0.2884

C_{L_o}: 0.205 C_{D_o}: 0.0158 C_M : -0.0112 (α = 0°) $\frac{C_{di}}{C_L^2}$: 0.197

$C_{L_{\delta_f}}$ = 0.01914
$C_{m_{\delta_f}}$ = -0.01115

$C_{Y_{\delta_f}}$(dif) = 0.000486
$C_{n_{\delta_f}}$(dif) = -0.000210
$C_{\ell_{\delta_f}}$(dif) = +0.001335

$C_{L_{\alpha_c}}$ = 0.006368
$C_{m_{\alpha_c}}$ = 0.01841
$\Delta C_{L_{o_c}}$ = 0.009917

Full extension

Outboard wing flaps

$C_{Y_{\delta_r}}$ = 0.003062
$C_{n_{\delta_r}}$ = -0.001455
$C_{\ell_{\delta_r}}$ = 0.001124

$\delta_r = (-\delta_{f_{OTBD\ RIGHT}} + \delta_{f_{OTBD\ LEFT}}) / 2$

δ_f (dif) $= -\delta_{f_{INBD\ RIGHT}} + \delta_{f_{INBD\ LEFT}}$

δ_f: $\delta_{f_{INBD\ RIGHT}}$ Simultaneous with $\delta_{f_{INBD\ LEFT}}$

WITHOUT TWIST, CAMBER, THICKNESS, OR WEIGHT,
WITH SWEEP (STICK MODEL) STRUCTURAL INFLUENCE COEFFICIENT.

S_{REF} = 400 FT2 α_A = 1.0 DEG

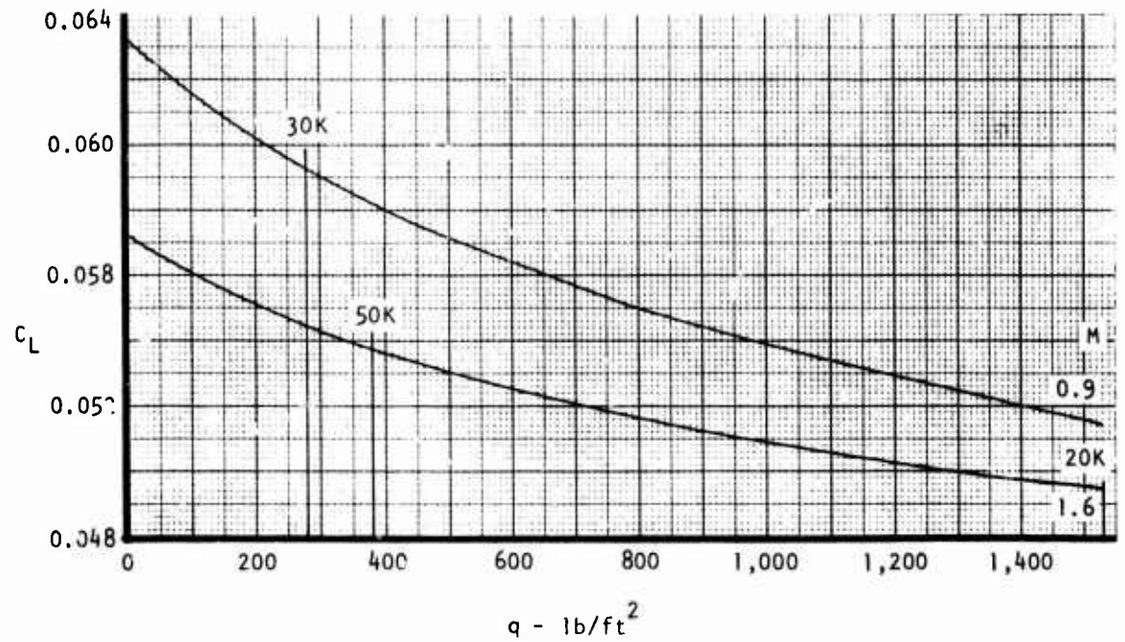

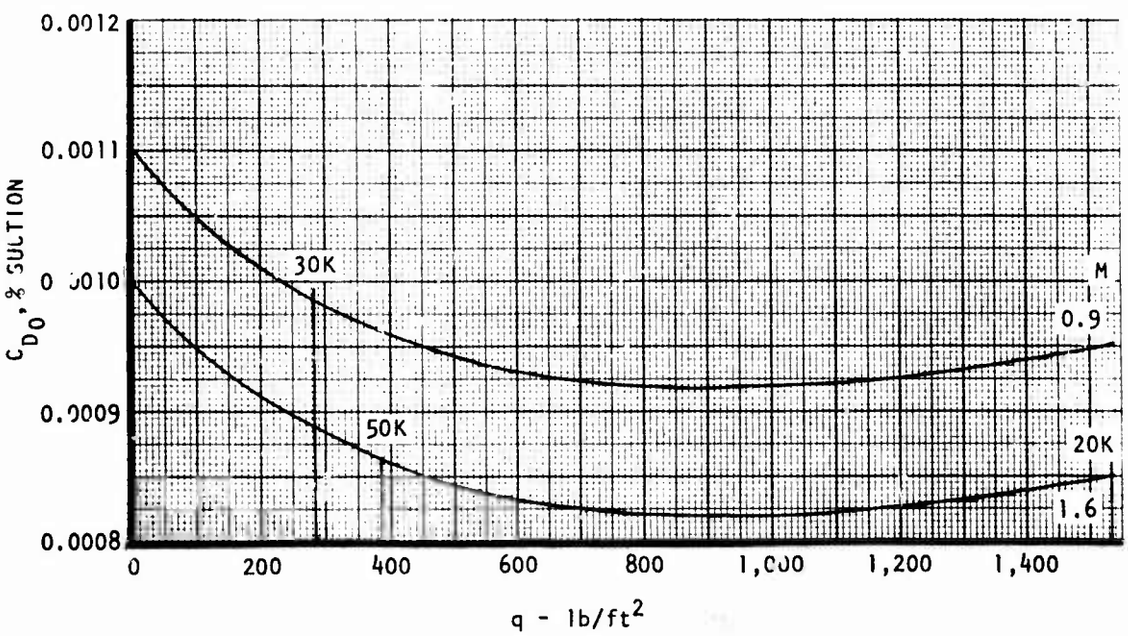

Figure 64. D572-4B lift and drag variation with q.

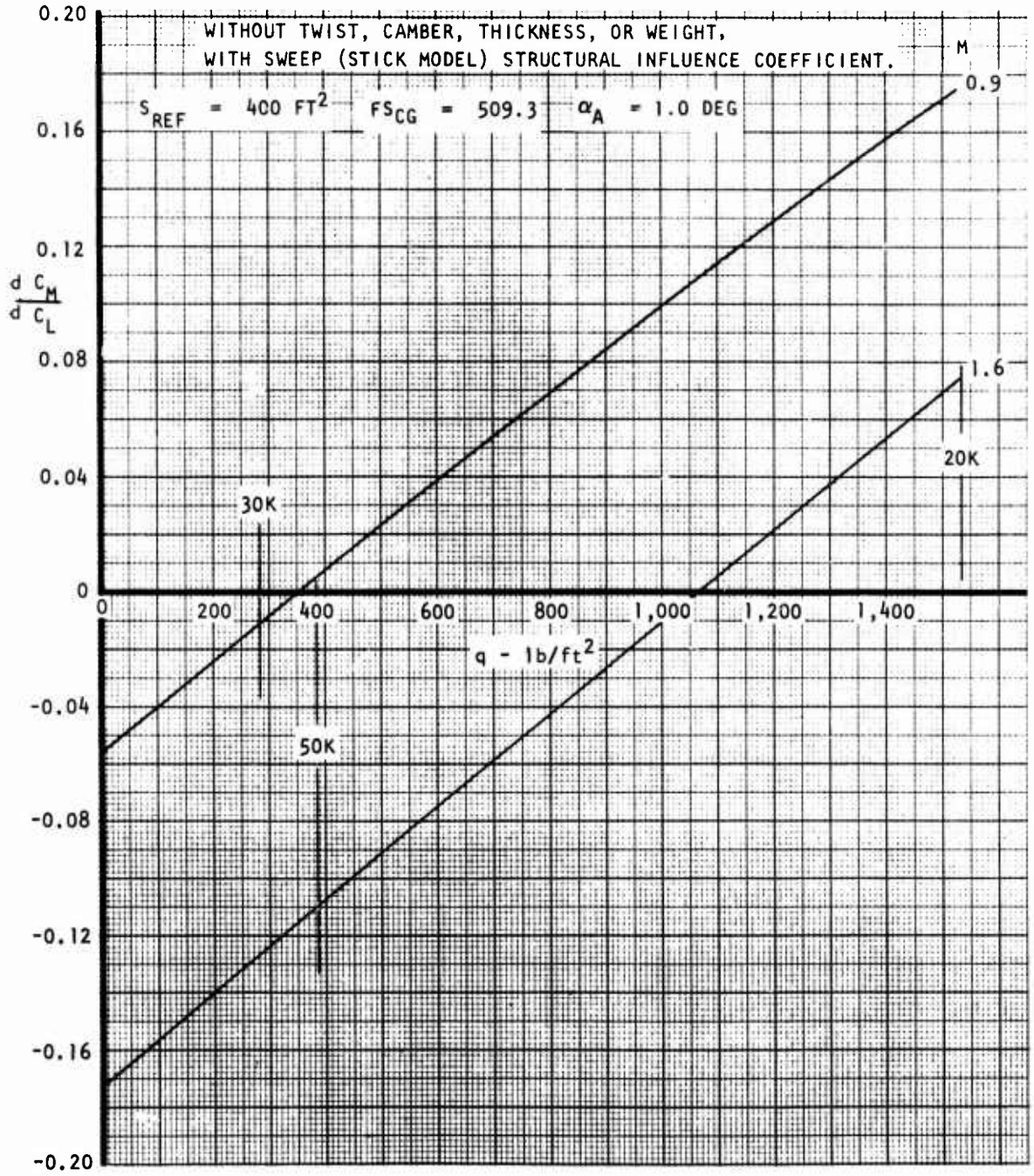

Figure 65. D572-4B longitudinal stability variation with q.

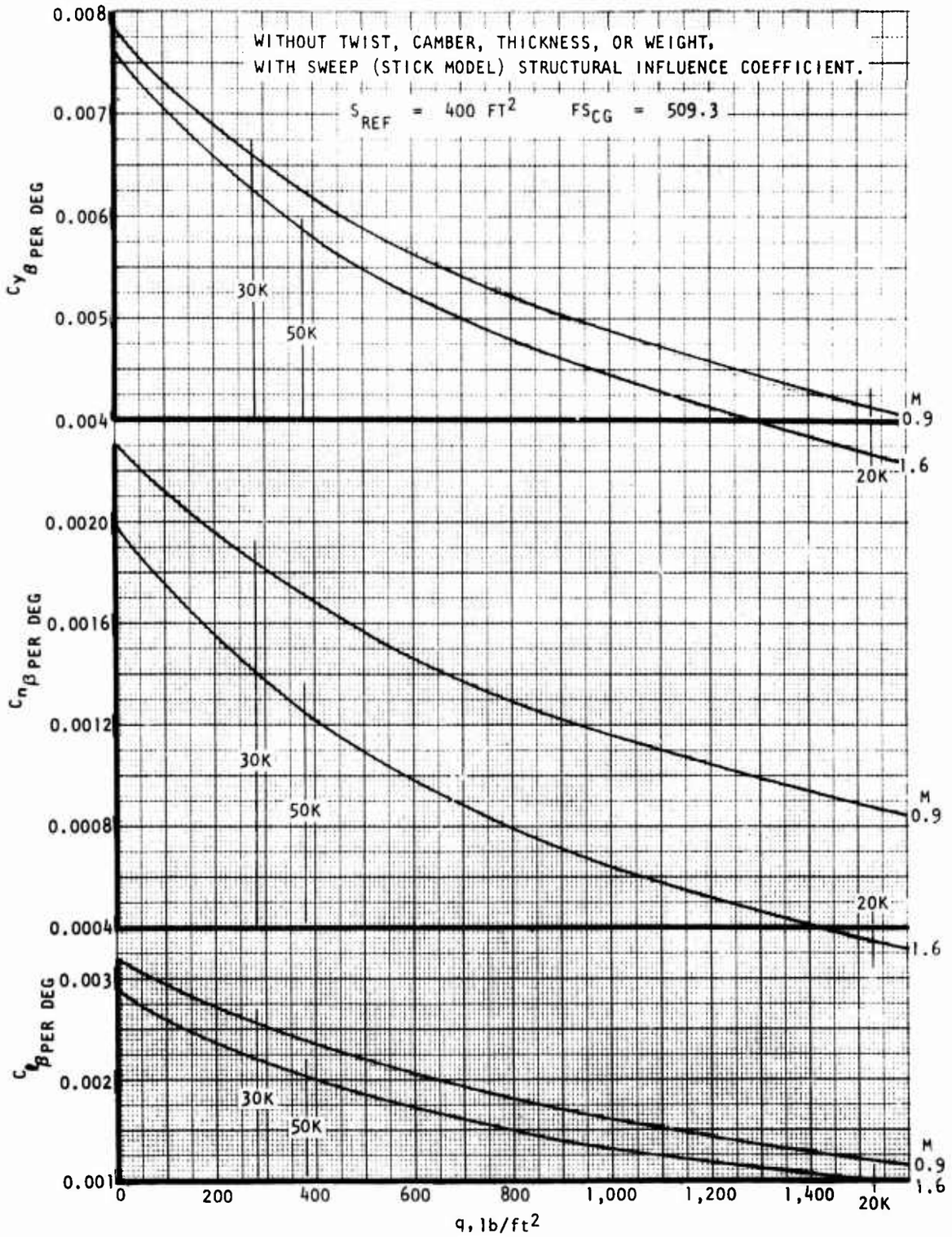

Figure 66. D572-4B lateral stability variation with q.

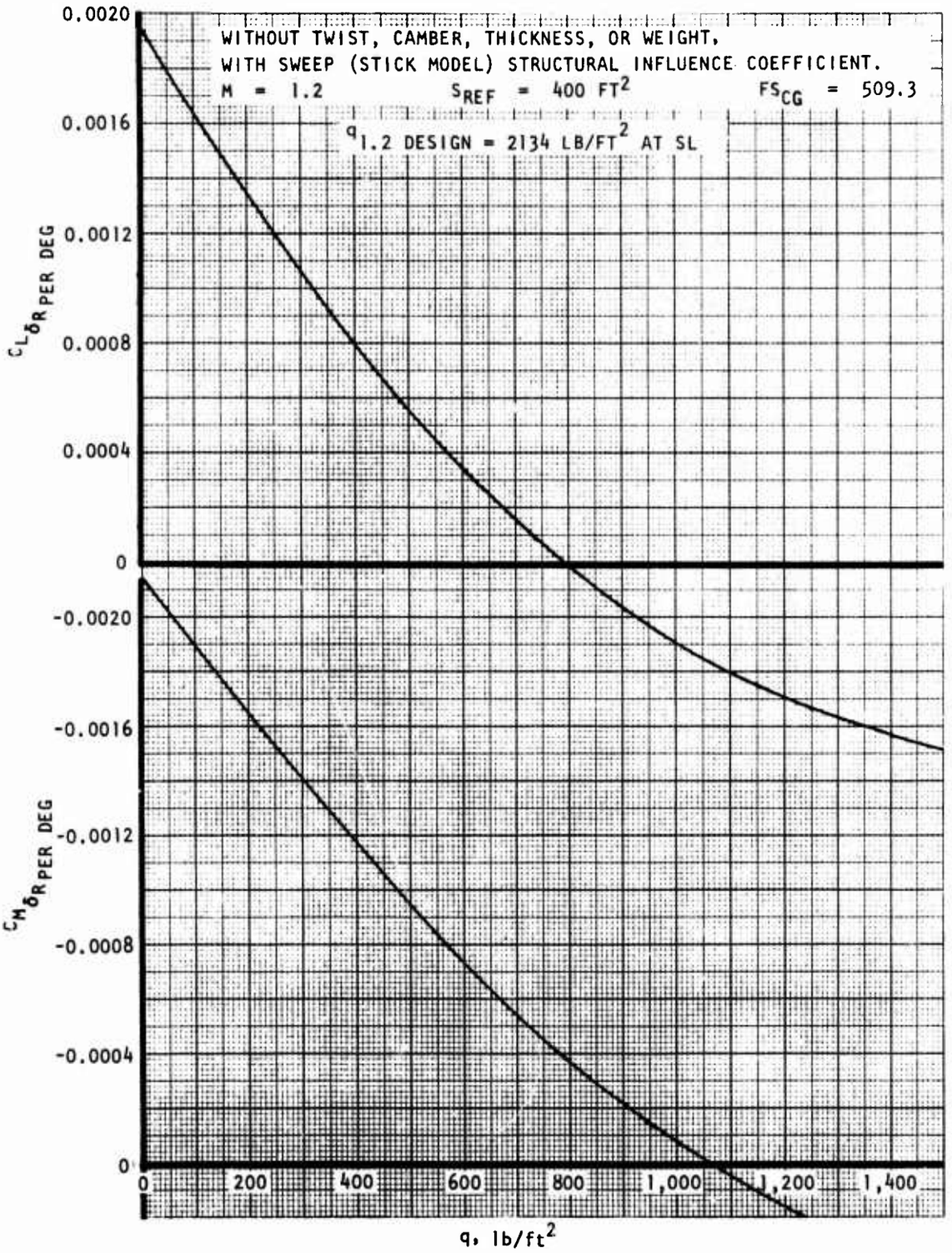

Figure 67. D572-4B longitudinal effect of rudder deflection variation with dynamic pressure.

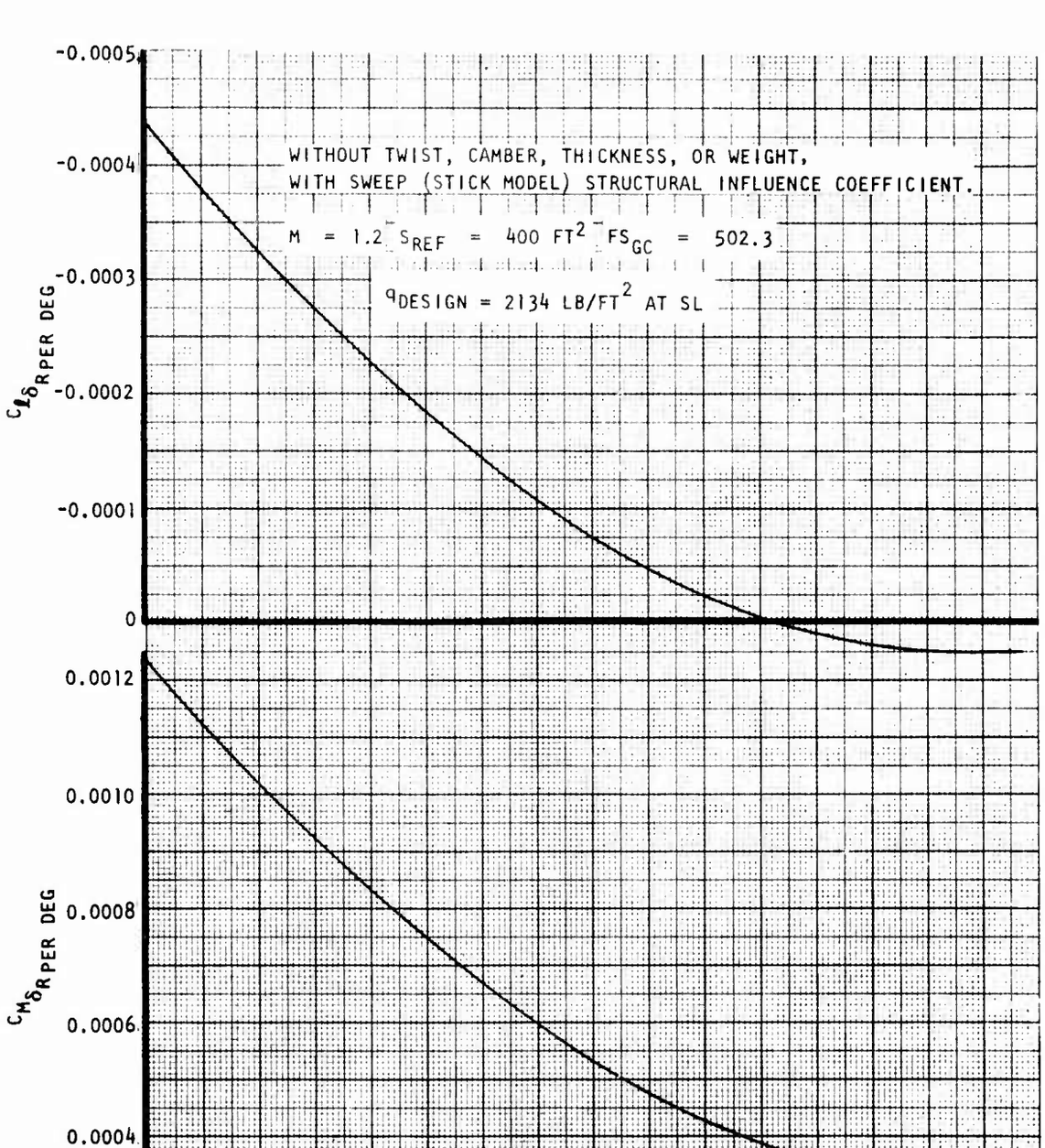

Figure 68. D572-4B lateral effect of rudder deflection variation with q.

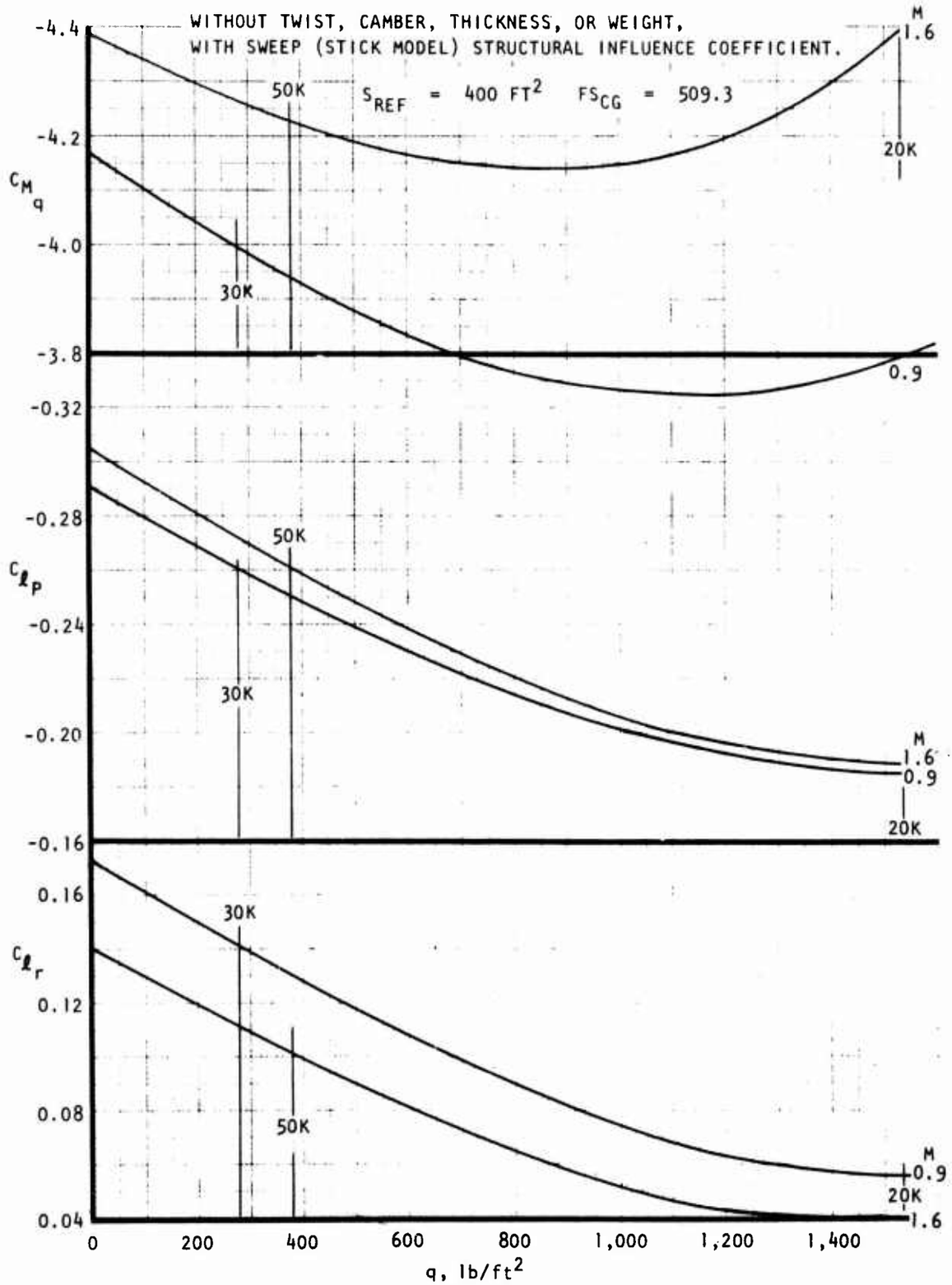

Figure 69. D572-4B pitch and roll rate variation with dynamic pressure.

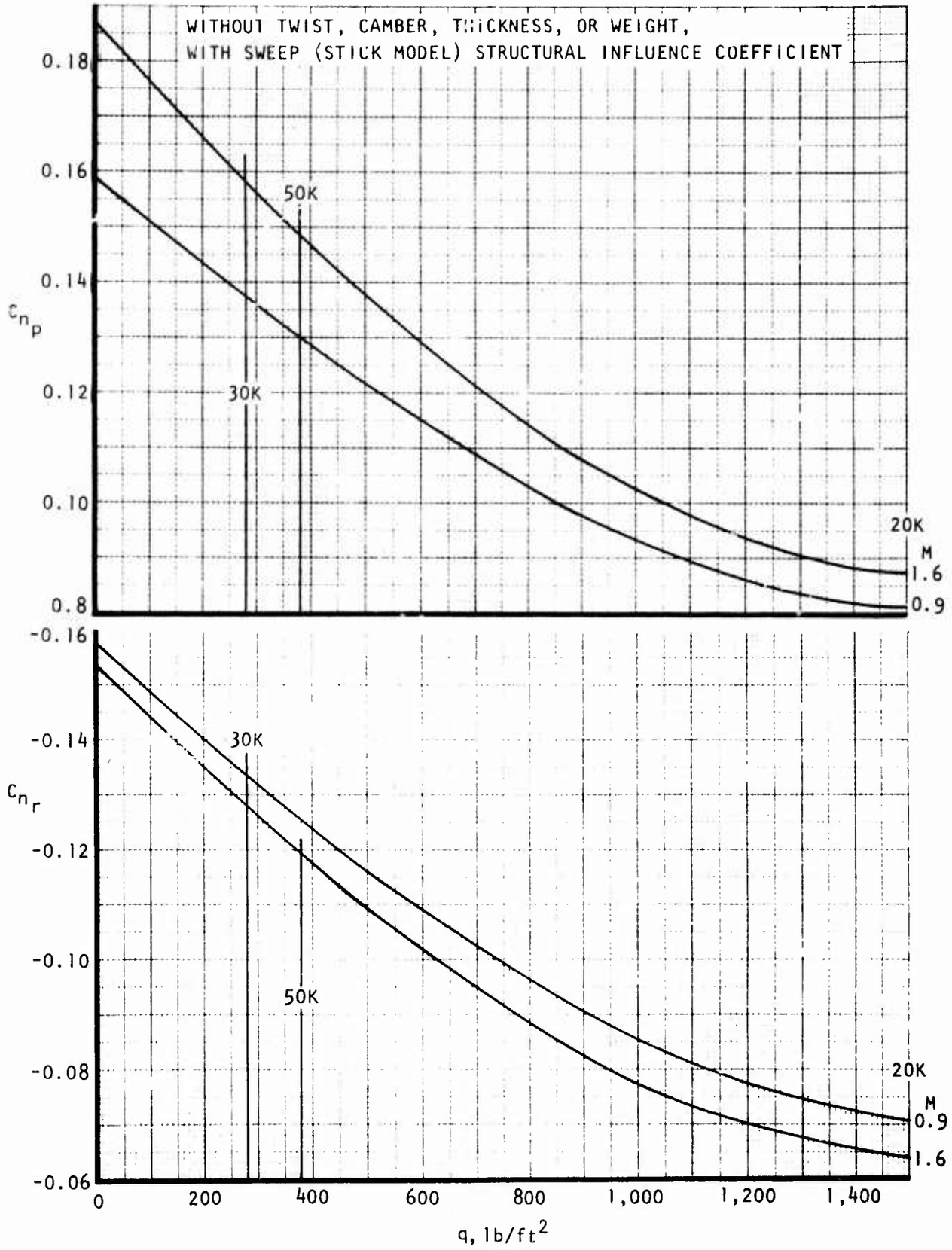

Figure 70. D572-4B yaw rate variation with dynamic pressure.

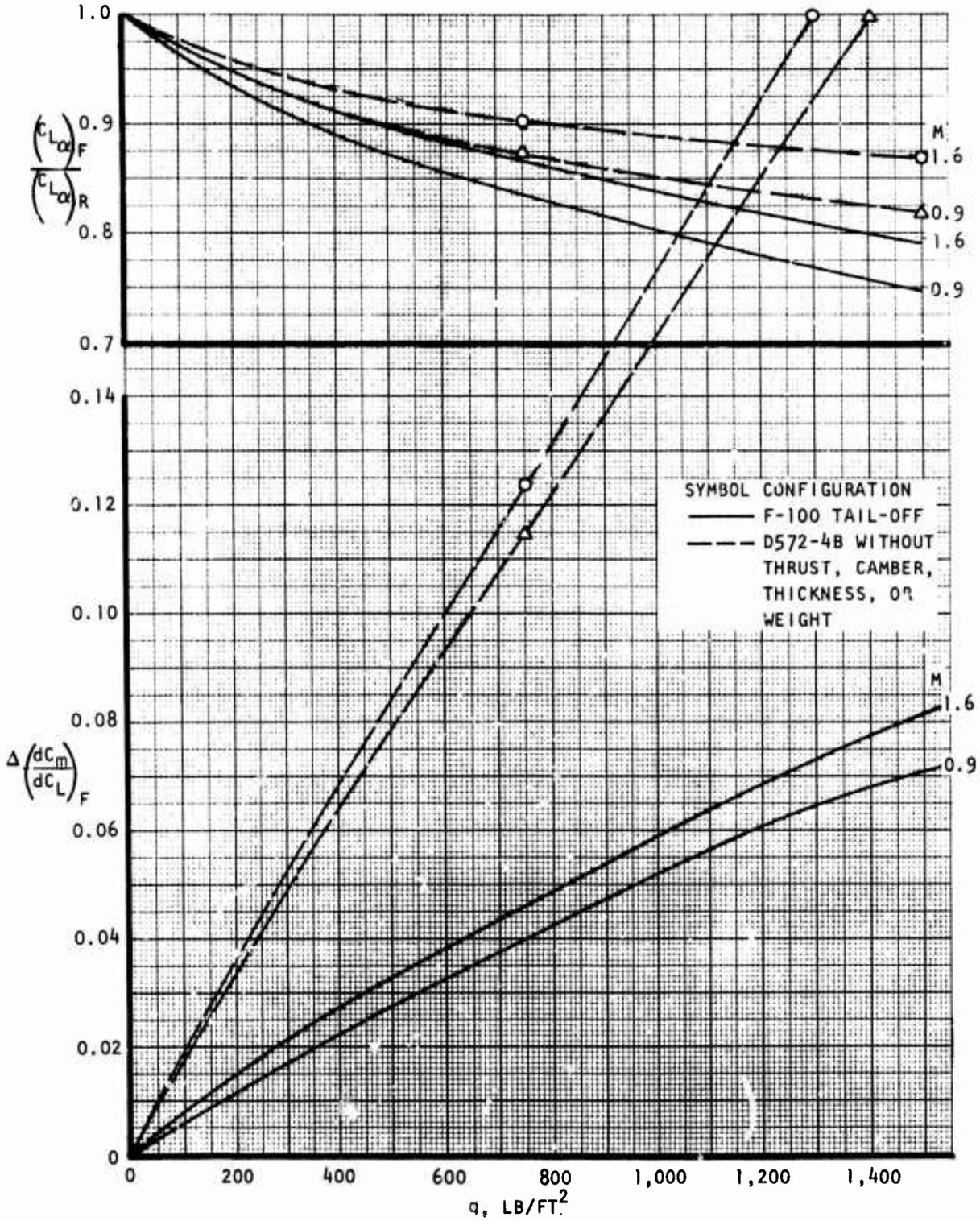

Figure 71. Ratio of flexible to rigid lift slope and effect of flexibility on longitudinal stability variation with dynamic pressure.

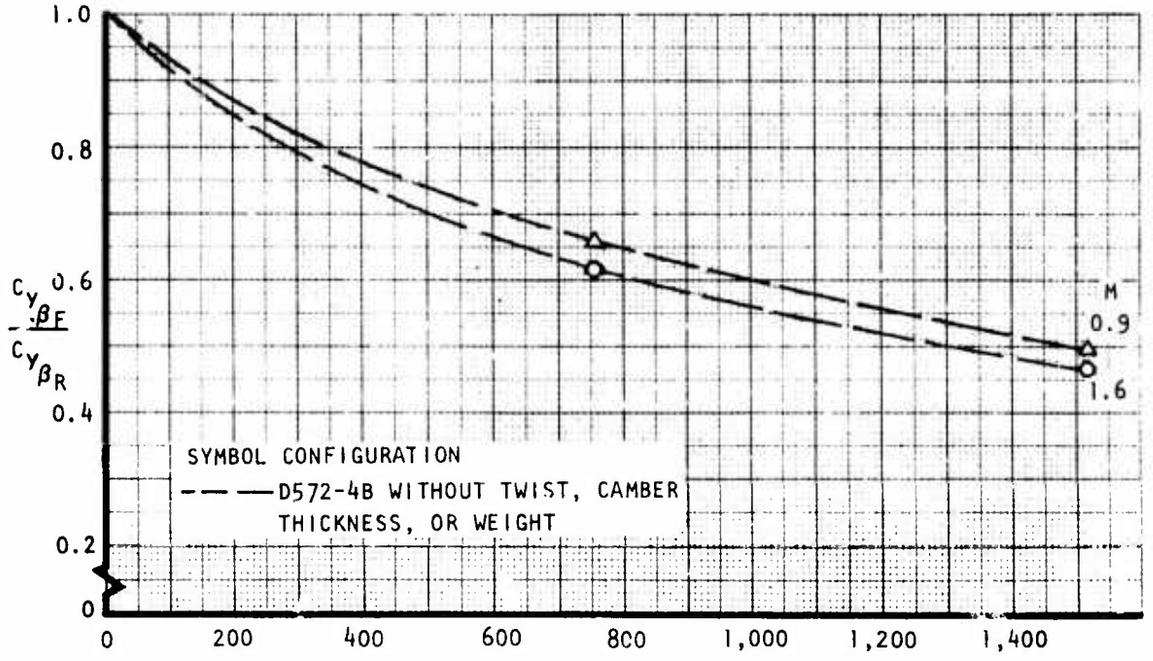

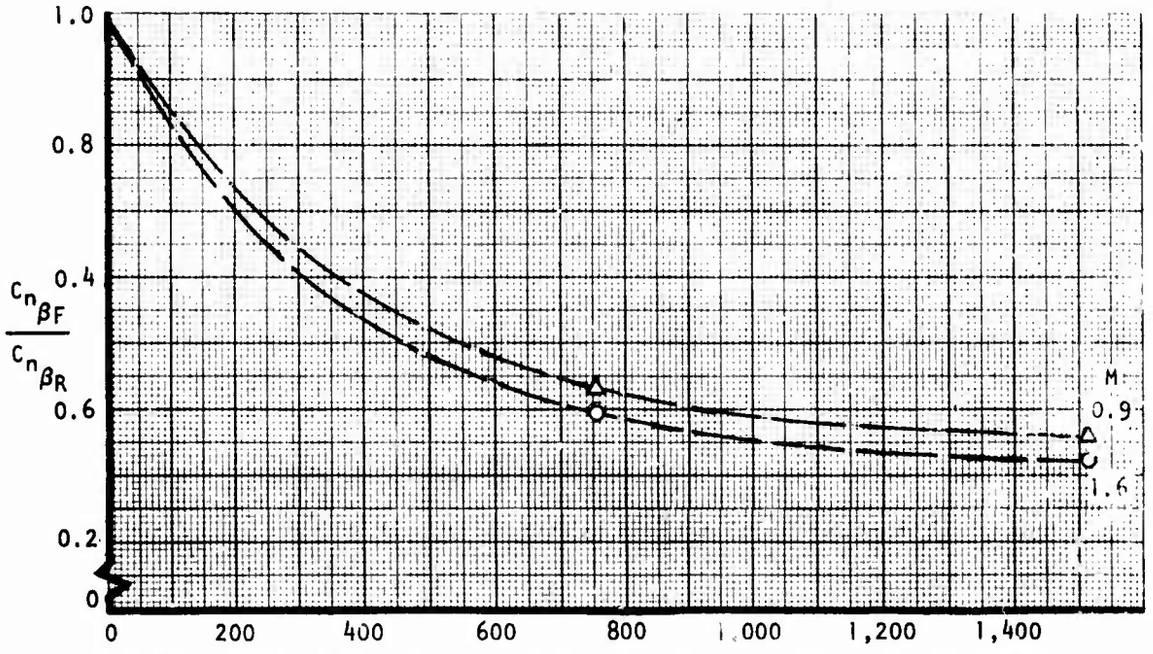

Figure 72. Ratio of flexible to rigid side force coefficient and yawing moment coefficient due to sideslip variation with dynamic pressure.

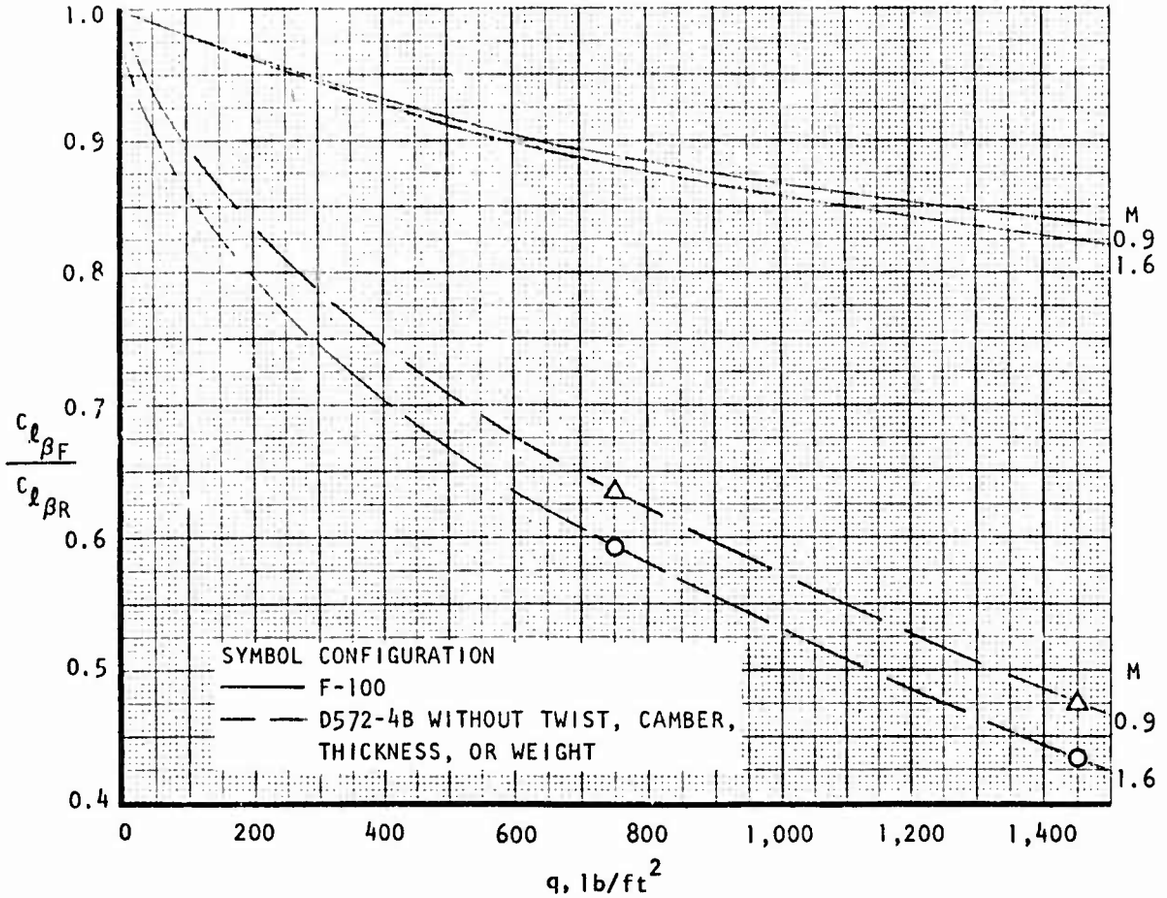

Figure 73. Ratio of flexible to rigid rolling moment coefficient due to sideslip variation with dynamic pressure.

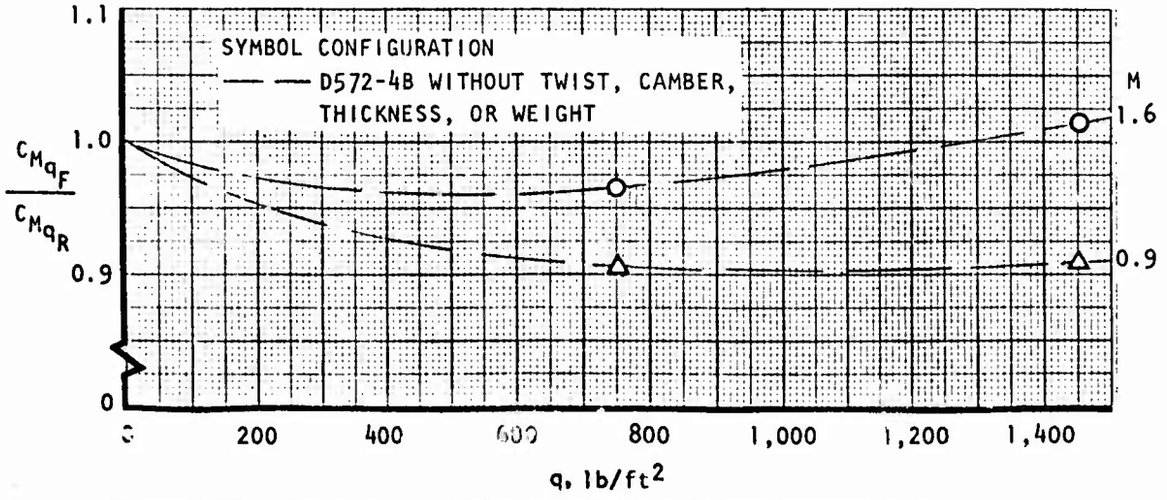

Figure 74. Ratio of flexible to rigid pitching moment coefficient due to pitch variation with dynamic pressure.

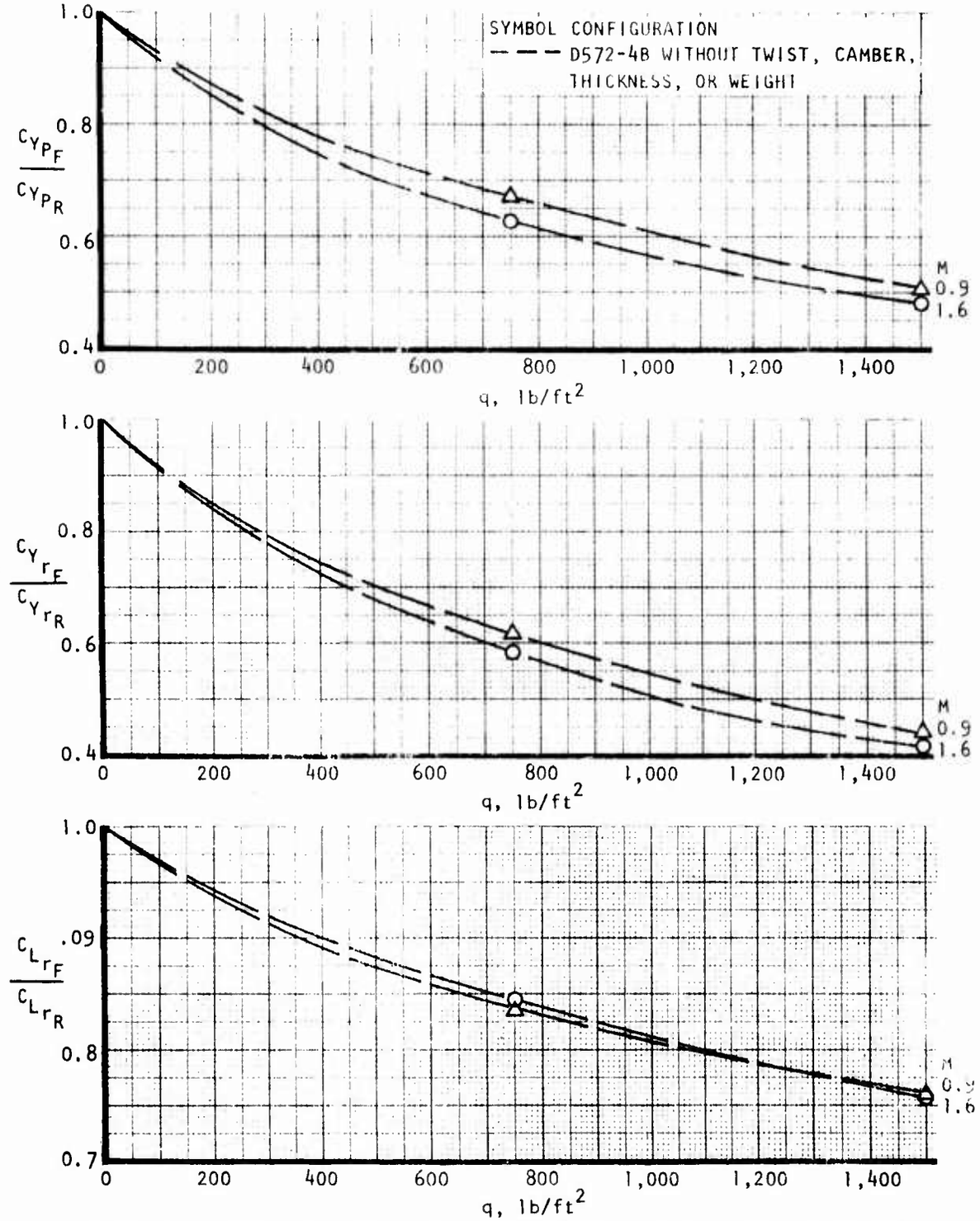

Figure 75. Ratio of flexible to rigid sideforce coefficient due to roll and yaw and lift coefficient due to yaw variation with dynamic pressure.

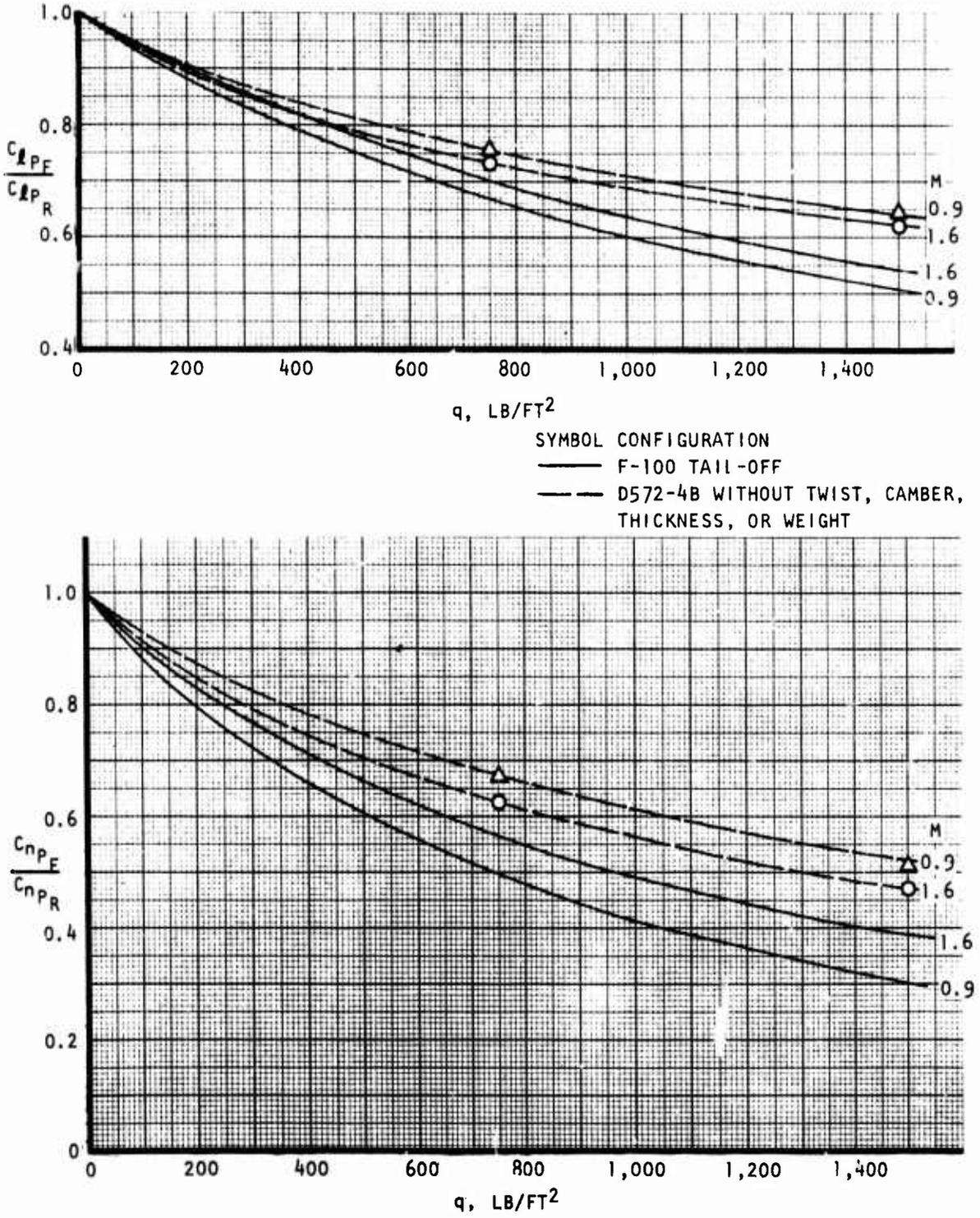

Figure 76. Ratio of flexible to rigid roll and yawing moment coefficient due to roll variation with dynamic pressure.

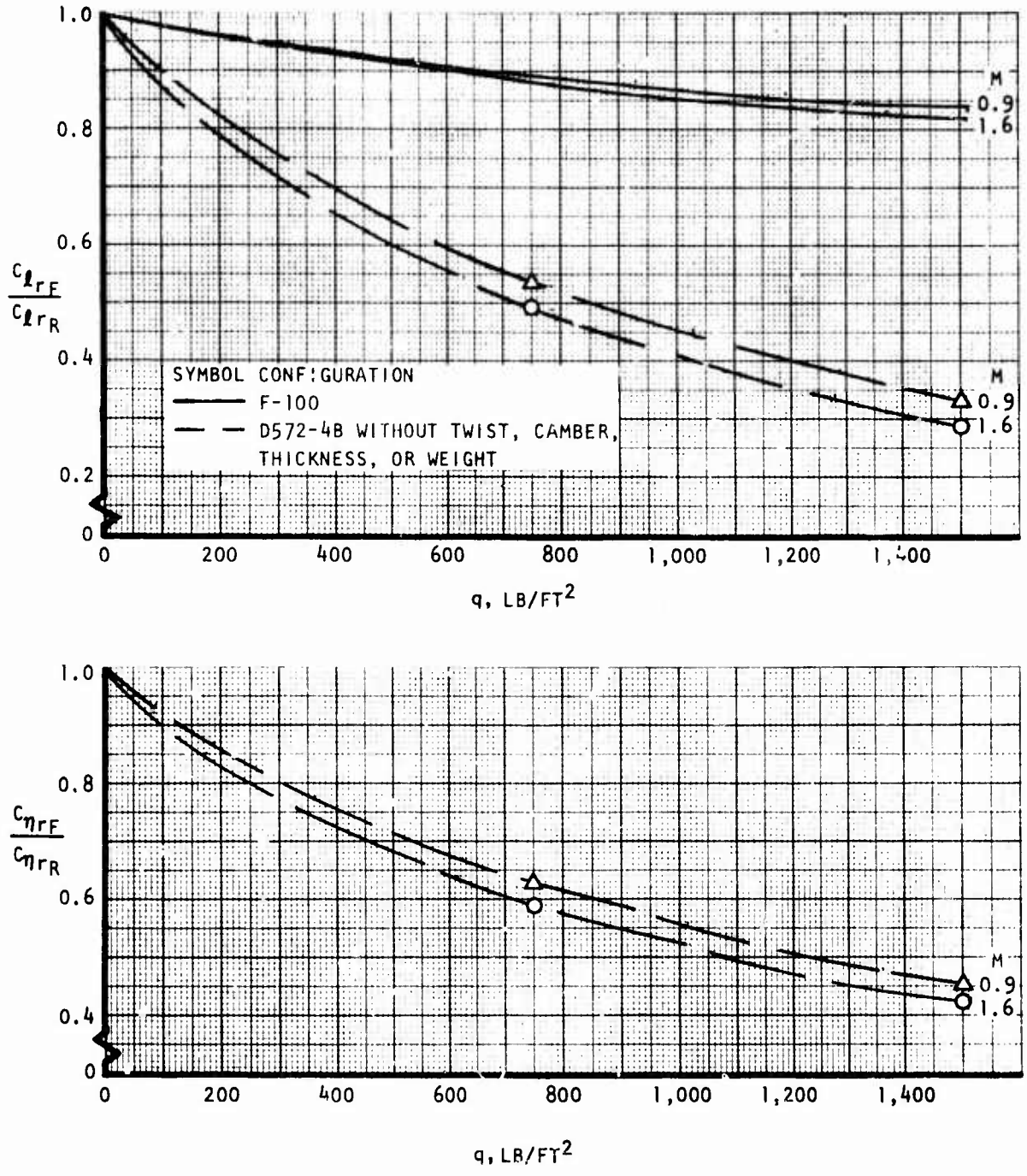

Figure 77. Ratio of flexible to rigid roll and yawing moment coefficient due to yaw variation with dynamic pressure.

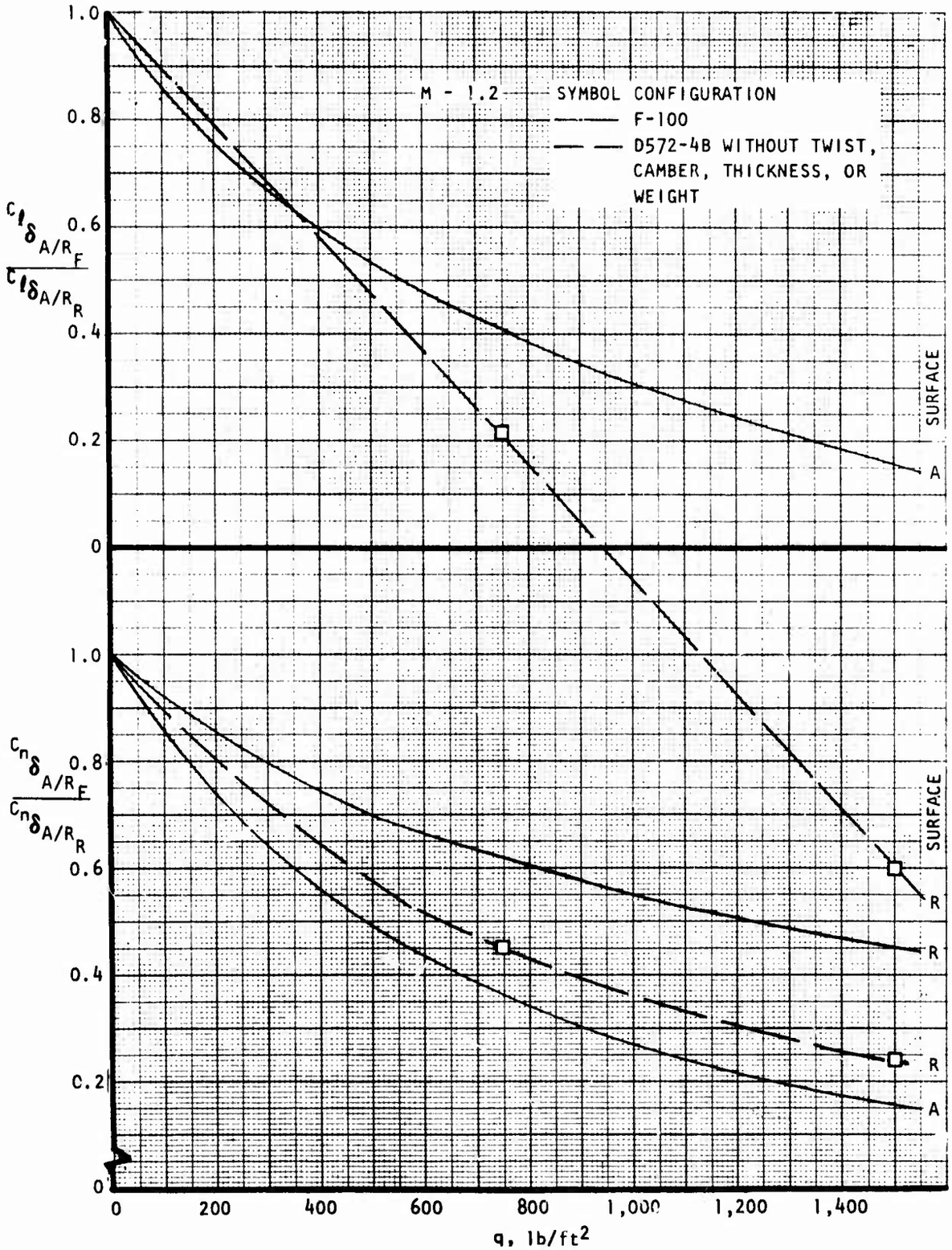

Figure 78. Ratio of flexible to rigid rolling and yawing moment coefficient due to deflected aileron/rudder variation with dynamic pressure.

TABLE 8. FLEXIBLE AERODYNAMIC DATA, SEA LEVEL, M = 0.2

TITLE: D575-4B M: 0.2 q: 58 lb/ft^2

S_W: 400 ft^2 $\bar{C}$: 163.512 in. b: 425.976 in. Xc.g.: 501.86 in.

C_{L_α} = 0.05228
C_{M_α} = 0.0
C_{Y_β} = -0.006105
C_{n_β} = 0.002217
C_{ℓ_β} = -0.00255

C_{M_q} = -3.0735
C_{n_r} = -0.1288
C_{n_p} = 0.1299
C_{ℓ_r} = 0.13898
C_{ℓ_p} = -0.2447

C_{L_o}: 0.15 C_{D_o}: 0.0121 C_M: 0.0 (α = 0°) $\frac{C_{di}}{C_L^2}$: 0.197

$C_{L_{\delta_f}}$ = 0.01374
$C_{m_{\delta_f}}$ = -0.00660

$C_{Y_{\delta_f}}$ (dif) = 0.00108
$C_{n_{\delta_f}}$ (dif) = -0.000145
$C_{\ell_{\delta_f}}$ (dif) = 0.001360

$C_{L_{\alpha_c}}$ = 0.01815 Full extension
$C_{m_{\alpha_c}}$ = 0.0485
$\Delta C_{L_{o_c}}$ = 0.005185

Outboard wing flaps

$C_{Y_{\delta_r}}$ = 0.00242
$C_{n_{\delta_r}}$ = -0.001137
$C_{\ell_{\delta_r}}$ = -0.000888

$\delta_r = (-\delta_{f_{\text{OTBD RIGHT}}} + \delta_{f_{\text{OTBD LEFT}}})/2$

$\delta_f(\text{dif}) = -\delta_{f_{\text{INBD RIGHT}}} + \delta_{f_{\text{INBD LEFT}}}$

δ_f: $\delta_{f_{\text{INBD RIGHT}}}$ SIMULTANEOUS WITH $\delta_{f_{\text{INBD LEFT}}}$

TABLE 9. FLEXIBLE AERODYNAMIC DATA, SEA LEVEL, M = 0.9

TITLE: D575-4B M: 0.9 q: 1245.6 lb/ft^2

S_W: 400 ft^2 $\bar{C}$: 163.51 in. b: 425.976 in. Xc.g.: 501.86 in.

C_{L_α}	= 0.0526	C_{M_q}	= -3.658
C_{M_α}	= +0.00479	C_{n_r}	= -0.0750
C_{Y_β}	= -0.00393	C_{n_p}	= 0.0855
C_{n_β}	= 0.00139	C_{ℓ_r}	= 0.0610
C_{ℓ_β}	= -0.00139	C_{ℓ_p}	= -0.1890

C_{L_o}: 0.205 C_{D_o}: 0.0158 C_M : -0.0108 (α = 0°) $\frac{C_{d_i}}{C_L^2}$: 0.197

$C_{L_{\delta f}}$	= 0.01515	$C_{Y_{\delta f}}$(dif)	= -0.000048
$C_{m_{\delta f}}$	= -0.009170	$C_{n_{\delta f}}$(dif)	= -0.000007
		$C_{\ell_{\delta f}}$(dif)	= 0.000889

Full extension

$C_{L_{\alpha_c}}$	= 0.00368	$C_{Y_{\delta r}}$	= 0.002853
$C_{m_{\alpha_c}}$	= 0.01841	$C_{n_{\delta r}}$	= -0.001386
$\Delta C_{L_{oc}}$	= 0.009917	$C_{\ell_{\delta r}}$	= -0.000719

Outboard wing flaps

$\delta_r = (-\delta f_{\text{OTBD RIGHT}} + \delta f_{\text{OTBD LEFT}}) / 2$

δ_f (dif) $= -\delta f_{\text{INBD RIGHT}} + \delta f_{\text{INBD LEFT}}$

δ_f: $\delta f_{\text{INBD RIGHT}}$ Simultaneous with $\delta f_{\text{INBD LEFT}}$

TABLE 10. FLEXIBLE AERODYNAMIC DATA, ALT. = 50,000 FT., M = 1.5

TITLE: D575-4B M: 1.50 q: 384.0 lb/ft^2

S_W: 400 ft^2 $\bar{C}$: 163.51 in. b: 425.976 in. Xc.g: 501.86 in.

C_{L_α}	= 0.0536	C_{M_q}	= -4.215
C_{M_α}	= -0.008388	C_{n_r}	= -0.1178
C_{Y_β}	= -0.00558	C_{n_p}	= 0.1470
C_{n_β}	= 0.00225	C_{ℓ_r}	= 0.0995
C_{ℓ_β}	= -0.00193	C_{ℓ_p}	= -0.2580

C_{L_o}: 0.198 C_{D_o}: 0.0187 C_M: -0.0118 (α = 0°) $\frac{C_{d_i}}{C_L^2}$: 0.244

$C_{L_{\delta f}}$	= 0.006954	$C_{Y_{\delta f}}$(dif)	= 0.00269
$C_{m_{\delta f}}$	= -0.006542	$C_{n_{\delta f}}$(dif)	= -0.0006948
		$C_{\ell_{\delta f}}$(dif)	= 0.0004783

$C_{L_{\alpha_c}}$	= 0.008175	Full	Outboard	$C_{Y_{\delta r}}$	= 0.001024
$C_{m_{\alpha_c}}$	= 0.01079	extension	wing	$C_{n_{\delta r}}$	= -0.000599
$\Delta C_{L_{o_c}}$	= 0.00		flaps	$C_{\ell_{\delta r}}$	= 0.000276

$$\delta_r = (-\delta_{f_{\text{OTBD RIGHT}}} + \delta_{f_{\text{OTBD LEFT}}}) / 2$$

$$\delta_{f\,(dif)} = -\delta_{f_{\text{INBD RIGHT}}} + \delta_{f_{\text{INBD LEFT}}}$$

δ_f: $\delta_{f_{\text{INBD RIGHT}}}$ Simultaneous with $\delta_{f_{\text{INBD LEFT}}}$

TRADE STUDY AERODYNAMIC DATA

Variations in supersonic wave drag levels with changes in wing area, aspect ratio, wing leading edge sweep, and wing thickness ratio have been calculated using available Rockwell/LAAD computer programs (Reference 1). Variations away from the all-composite baseline D572-4B are shown in Figures 79 through 85; whereas, variations away from the advanced metal baseline D572-5A are shown in Figures 86 through 92. Similar variations in drag-due-to-lift and lift curve slope are graphed in Figures 93 through 96 as given by the FA475 computer program (Reference 4). These aerodynamic data are used in the trade studies just described in Section II.

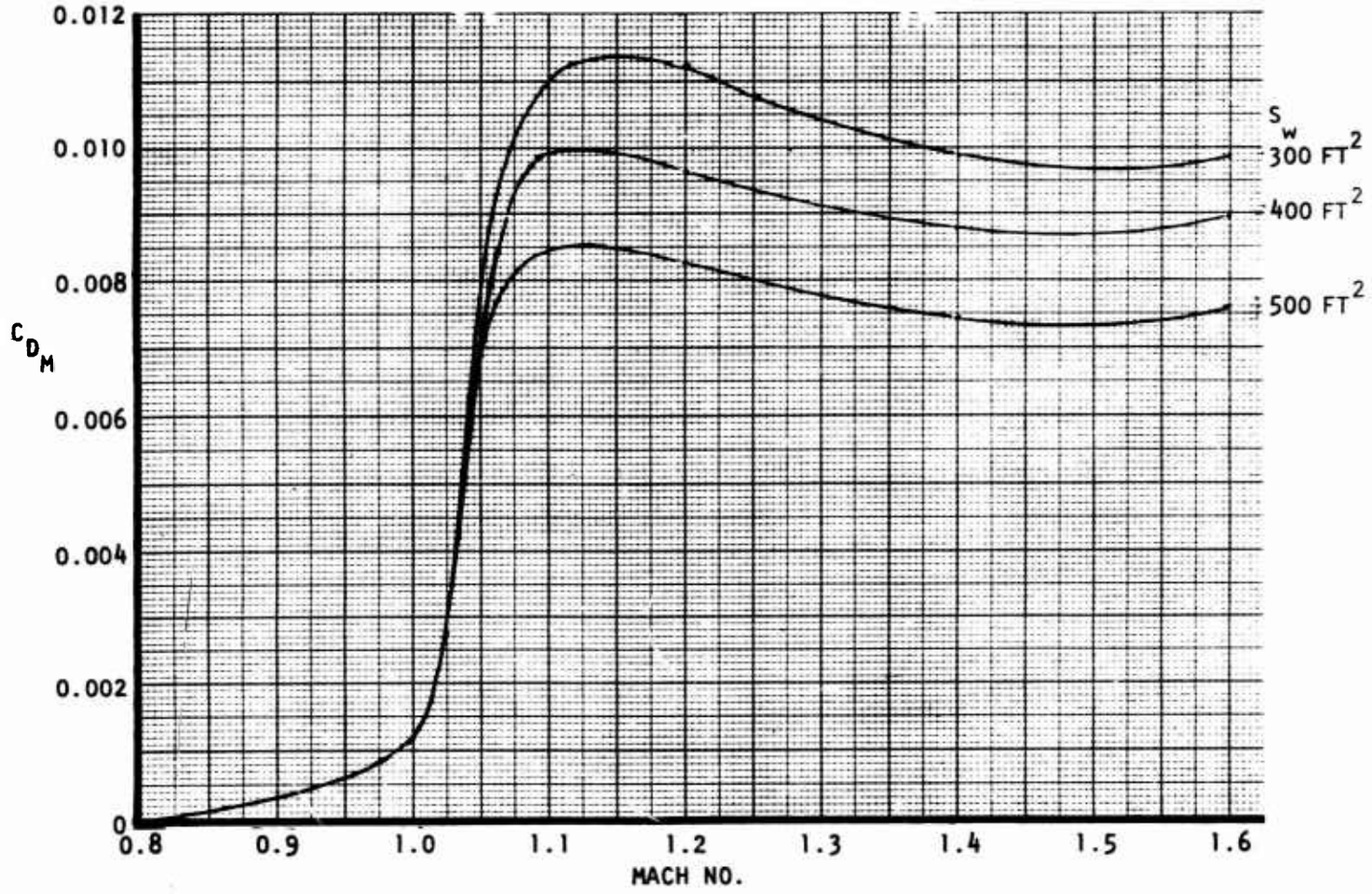

Figure 79. D572-4B configuration optimized at M=1.4 - t/c = 0.05, AR = 2.0, Λ_{LE} = 60°.

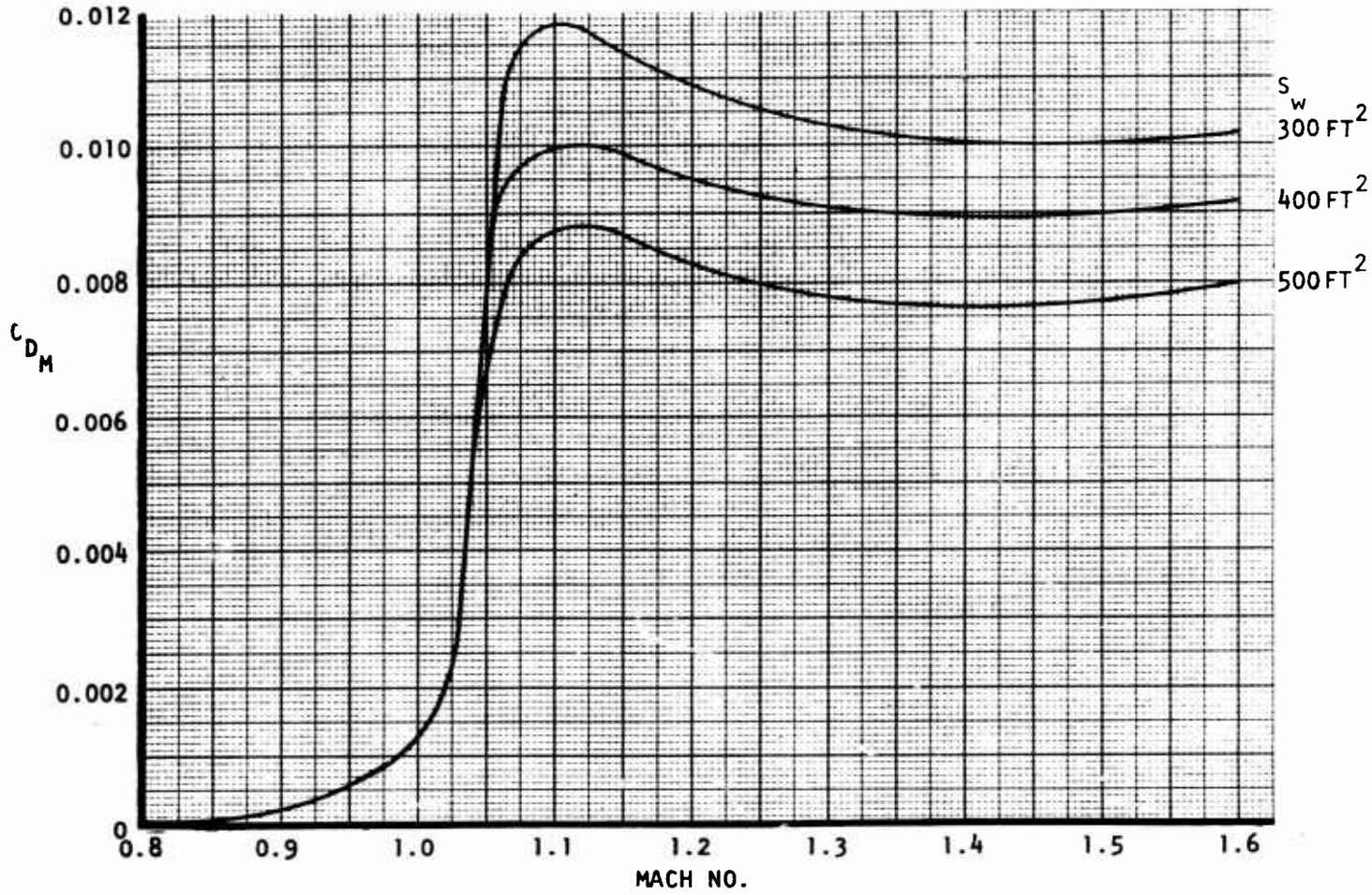

Figure 80. D572-4B configuration optimized at M=1.4 - t/c = 0.05, AR = 2.5, Λ_{LE} = 60°.

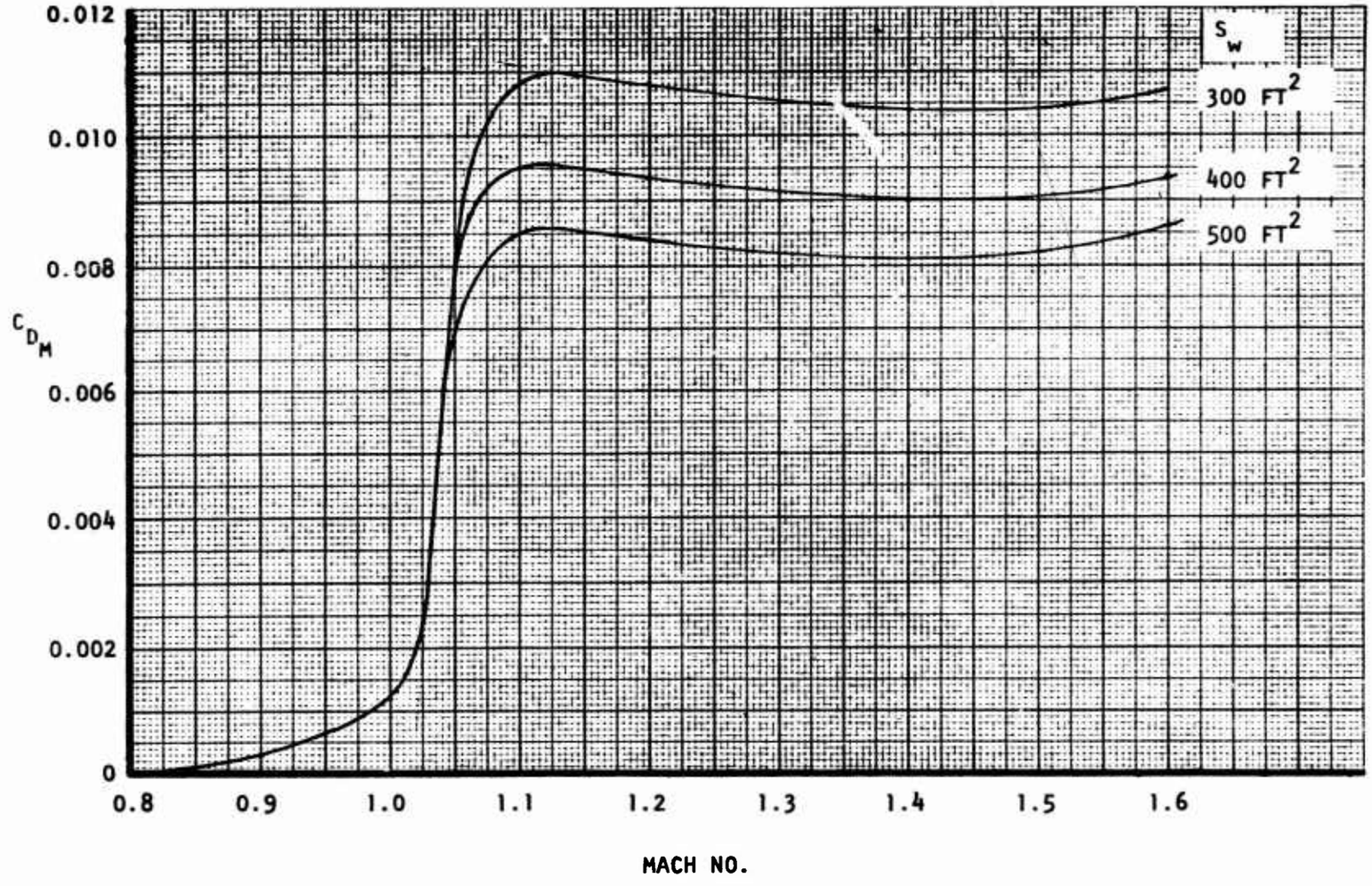

Figure 81. D572-4B configuration wave drag - t/c = 0.05, AR = 3.0, Λ_{LE} = 60°.

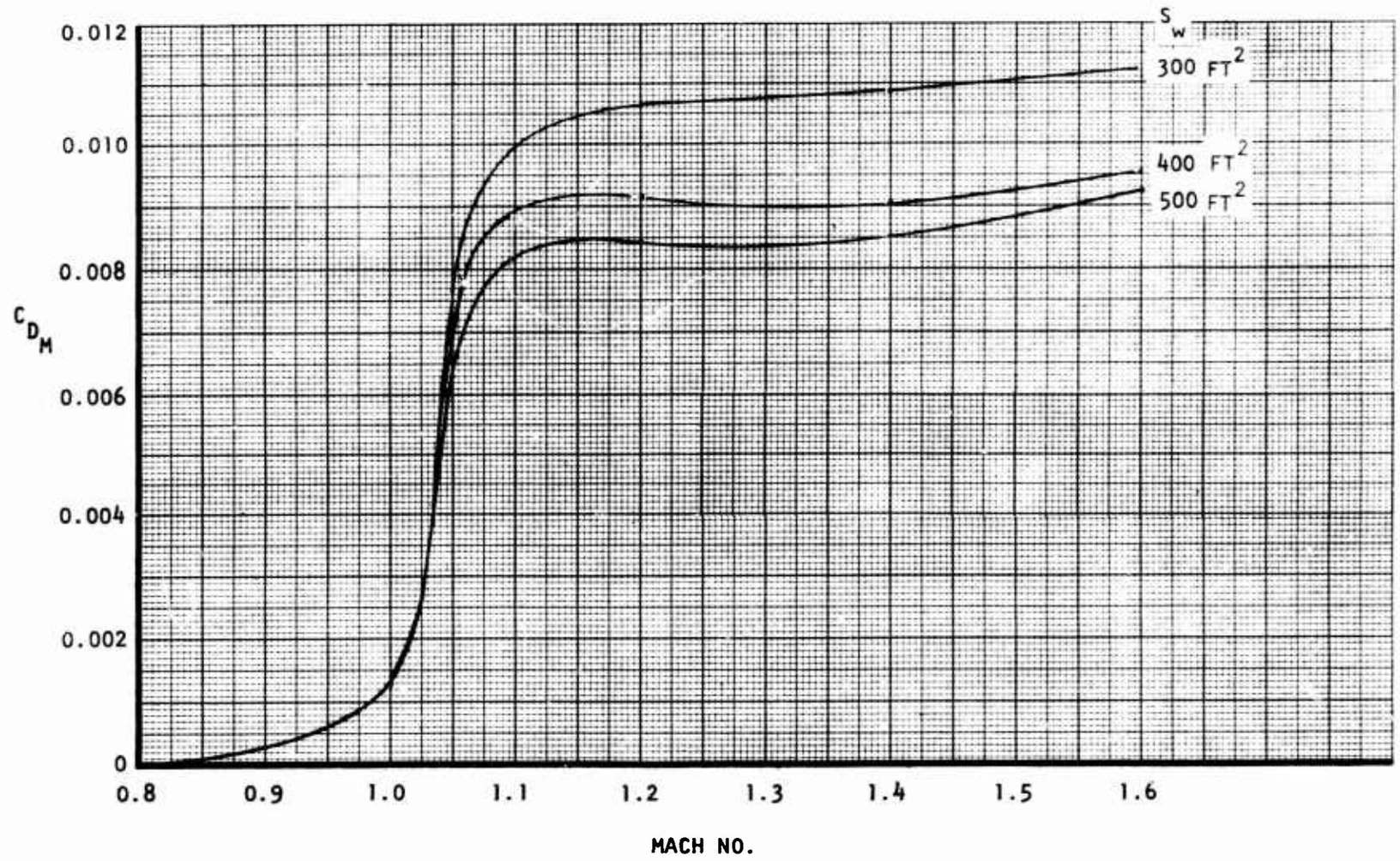

Figure 82. D572-4B configuration base optimized at M=1.4 - t/c = 0.06, AR = 3.5, Λ_{LE} = 60°.

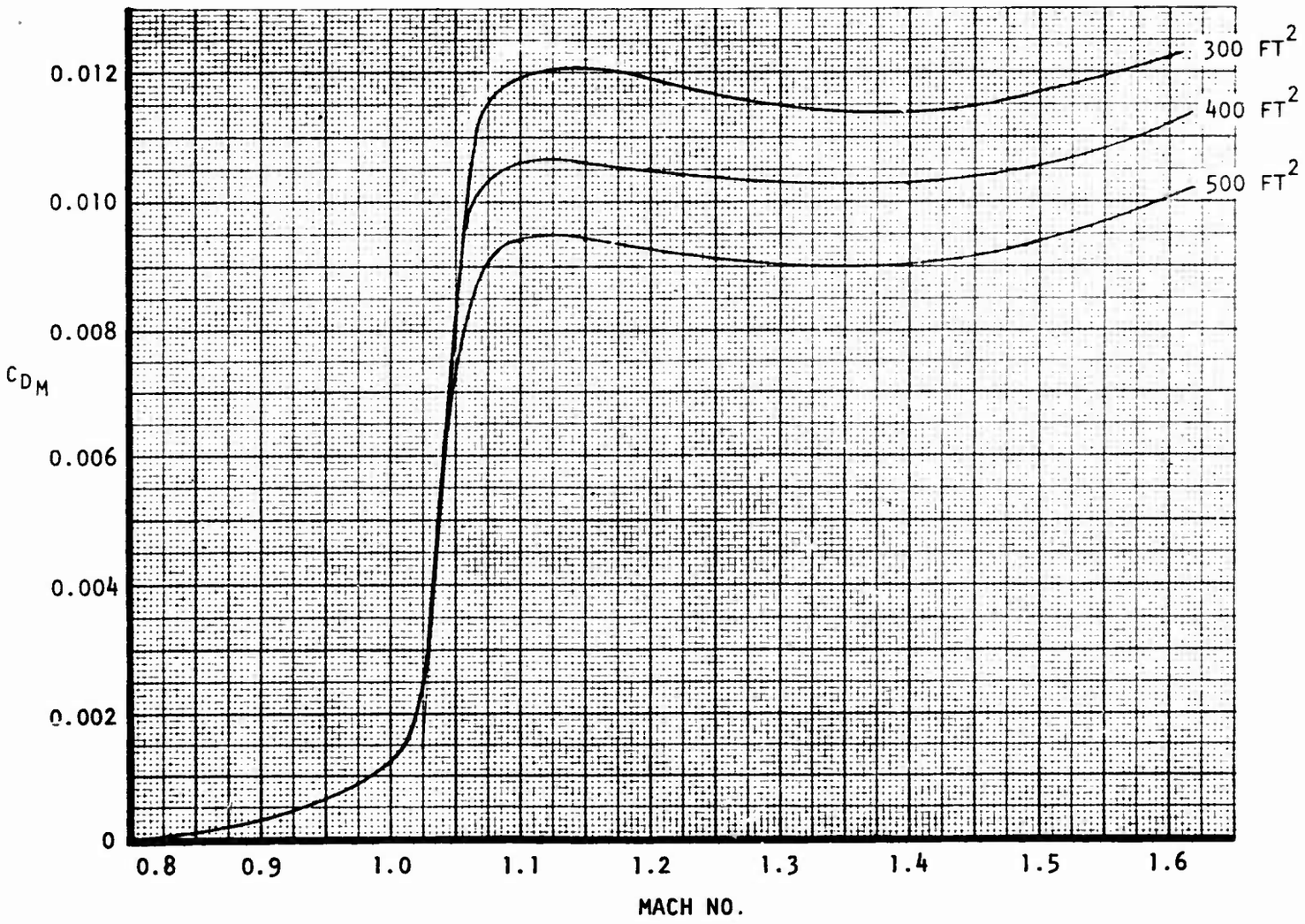

Figure 83. D572-4B configuration - t/c=0.05, AR=2.5, $\Lambda_{LE}=50^{o}$.

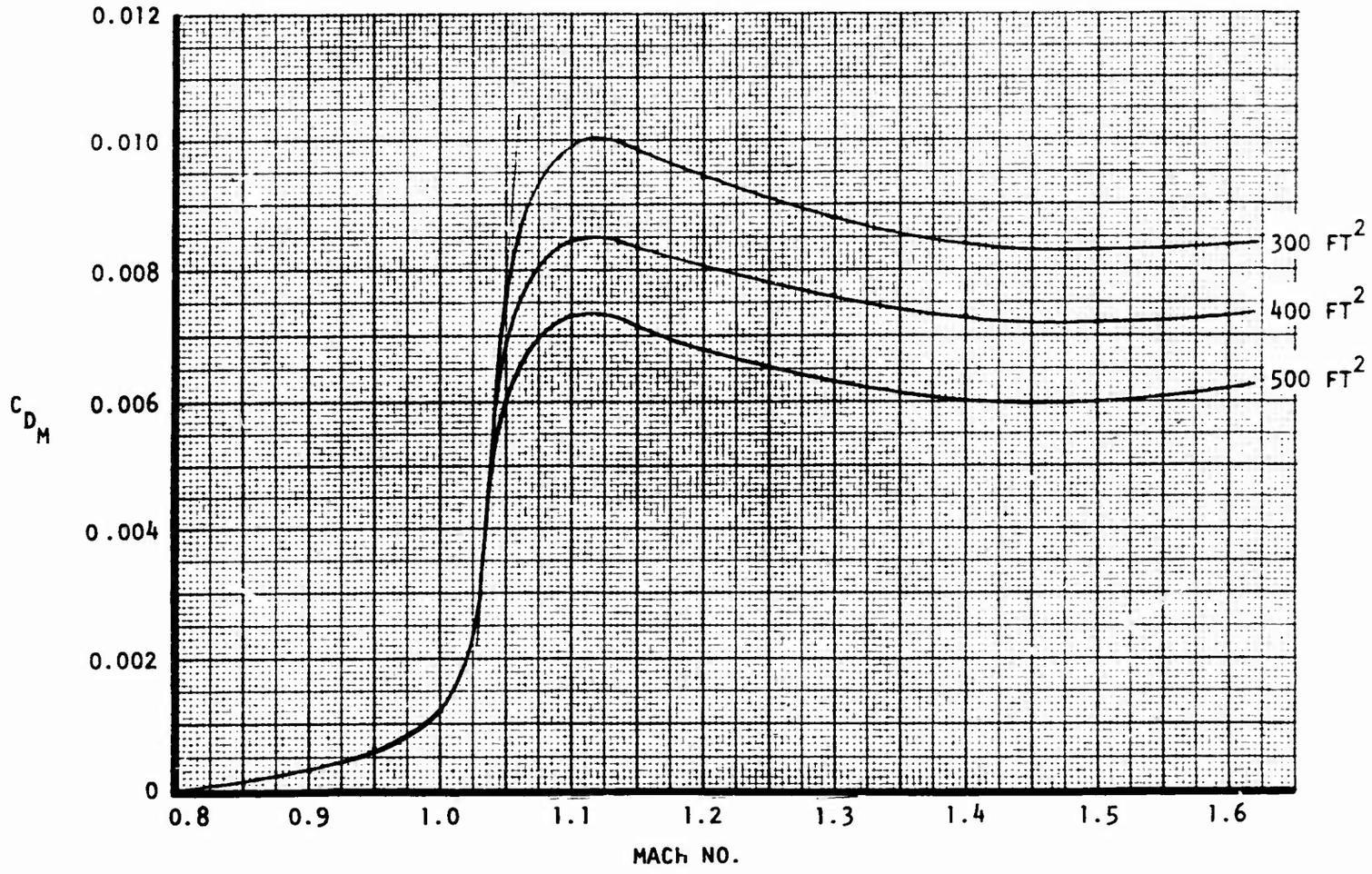

Figure 84. D572-4B configuration - t/c=0.05, AR=2.5, $\Lambda_{LE}=70^{o}$.

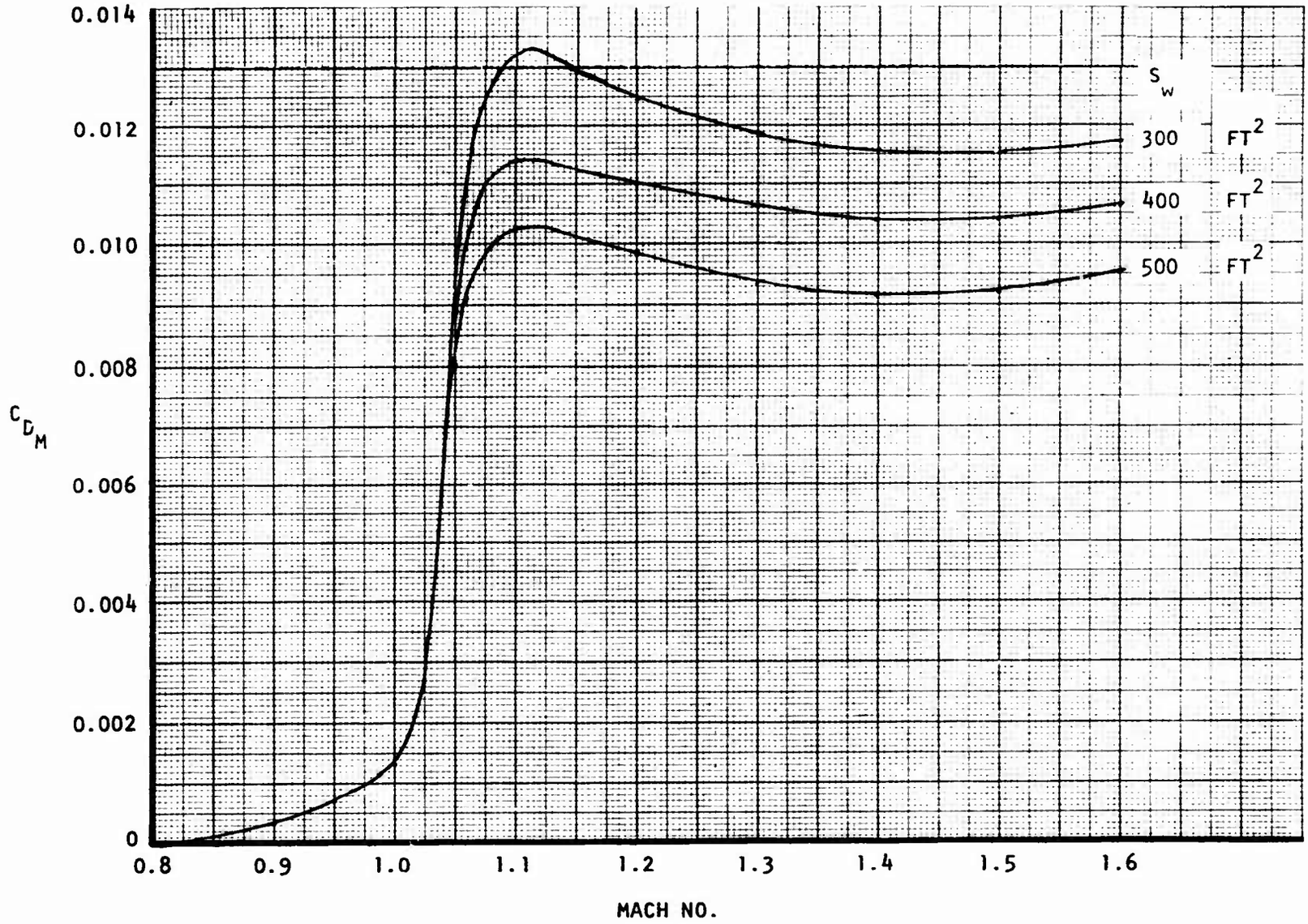

Figure 85. D572-4B configuration optimized at M=1.4 - t/c = 0.06, AR = 2.5, Λ_{LE} = 60°.

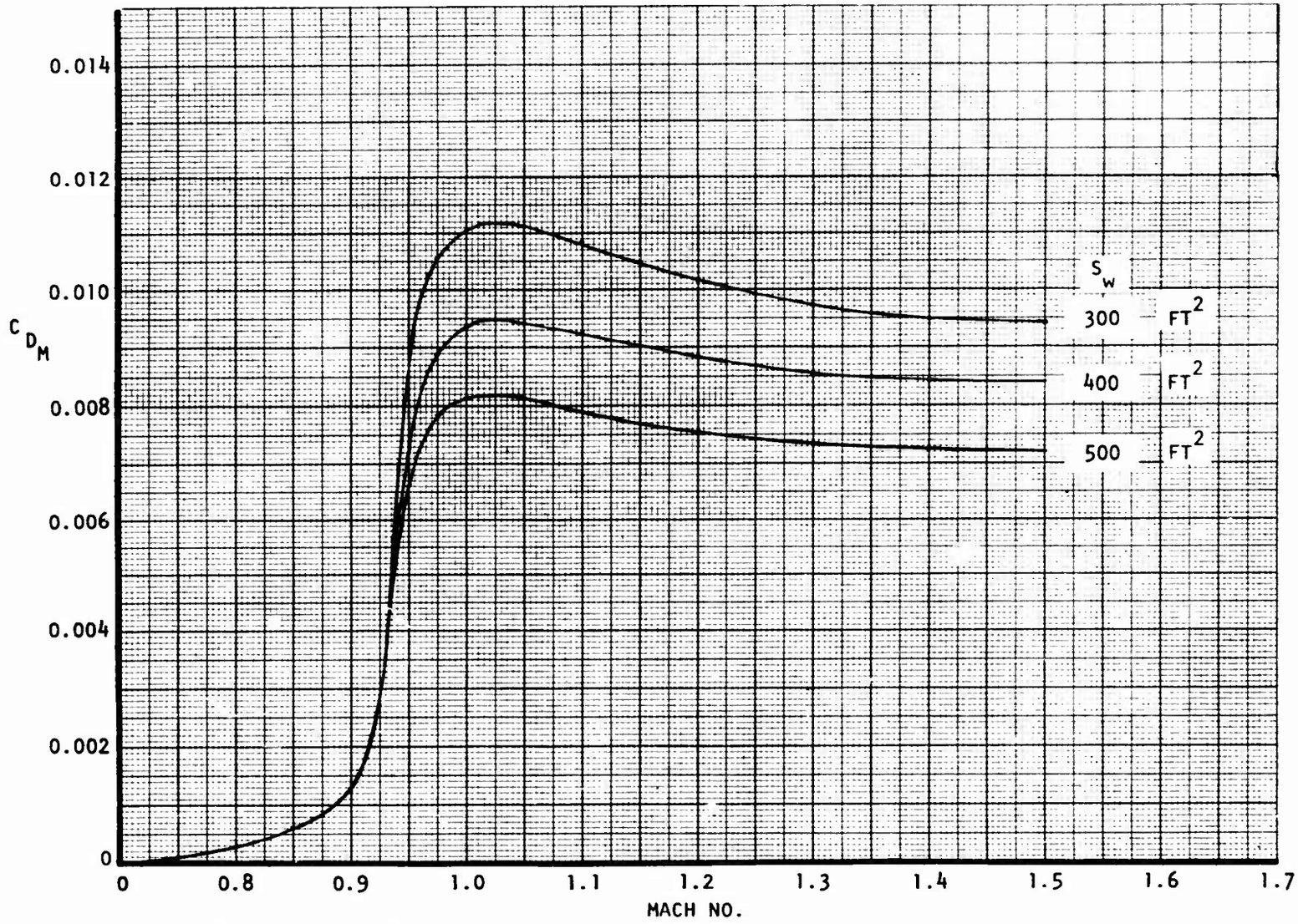

Figure 86. D572-5A metal configuration - t/c = 0.05, AR = 2.0, Λ_{LE} = 60°.

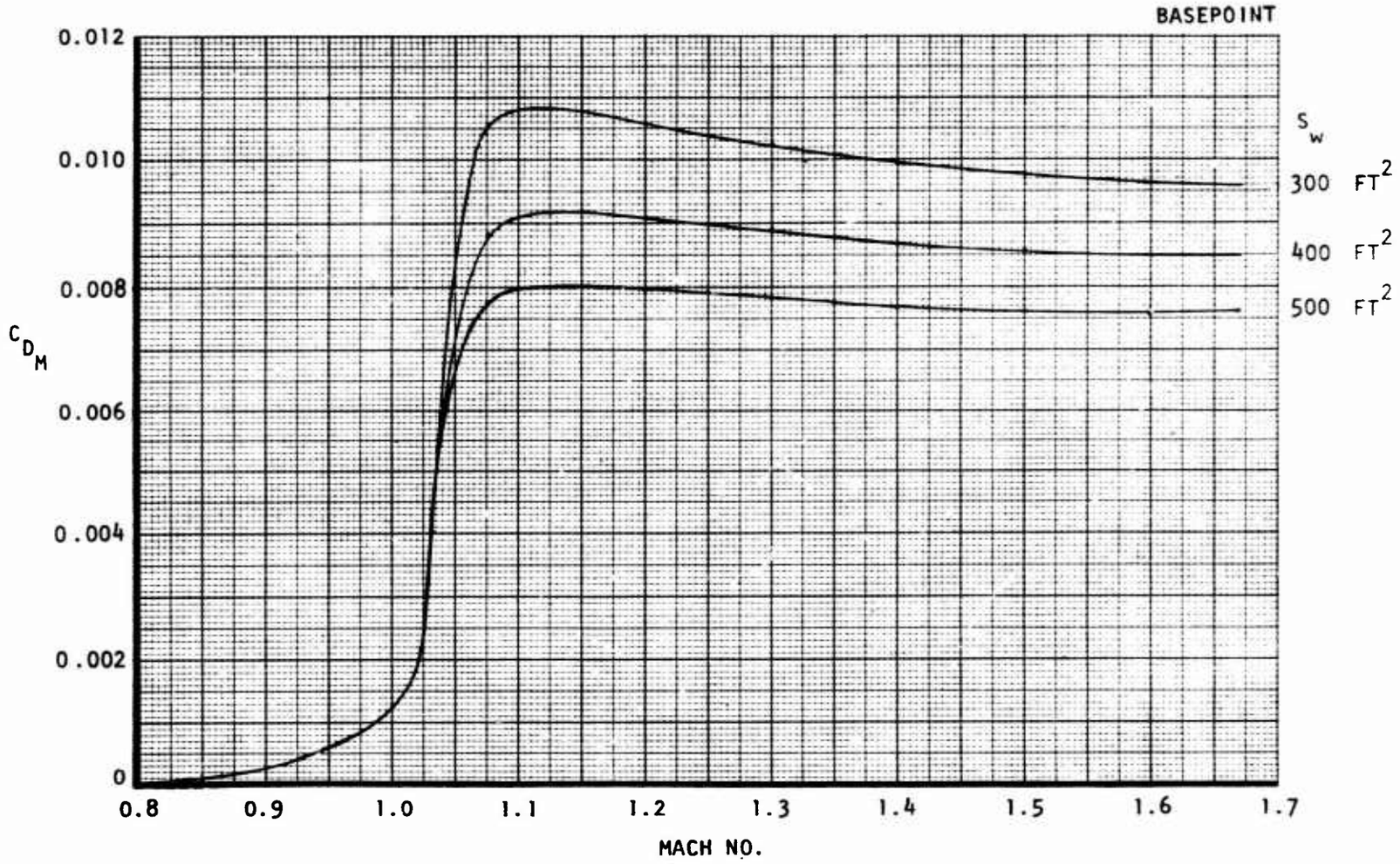

Figure 87. D572-5A metal configuration - t/c = 0.05, AR = 2.5, Λ_{LE} = 60°.

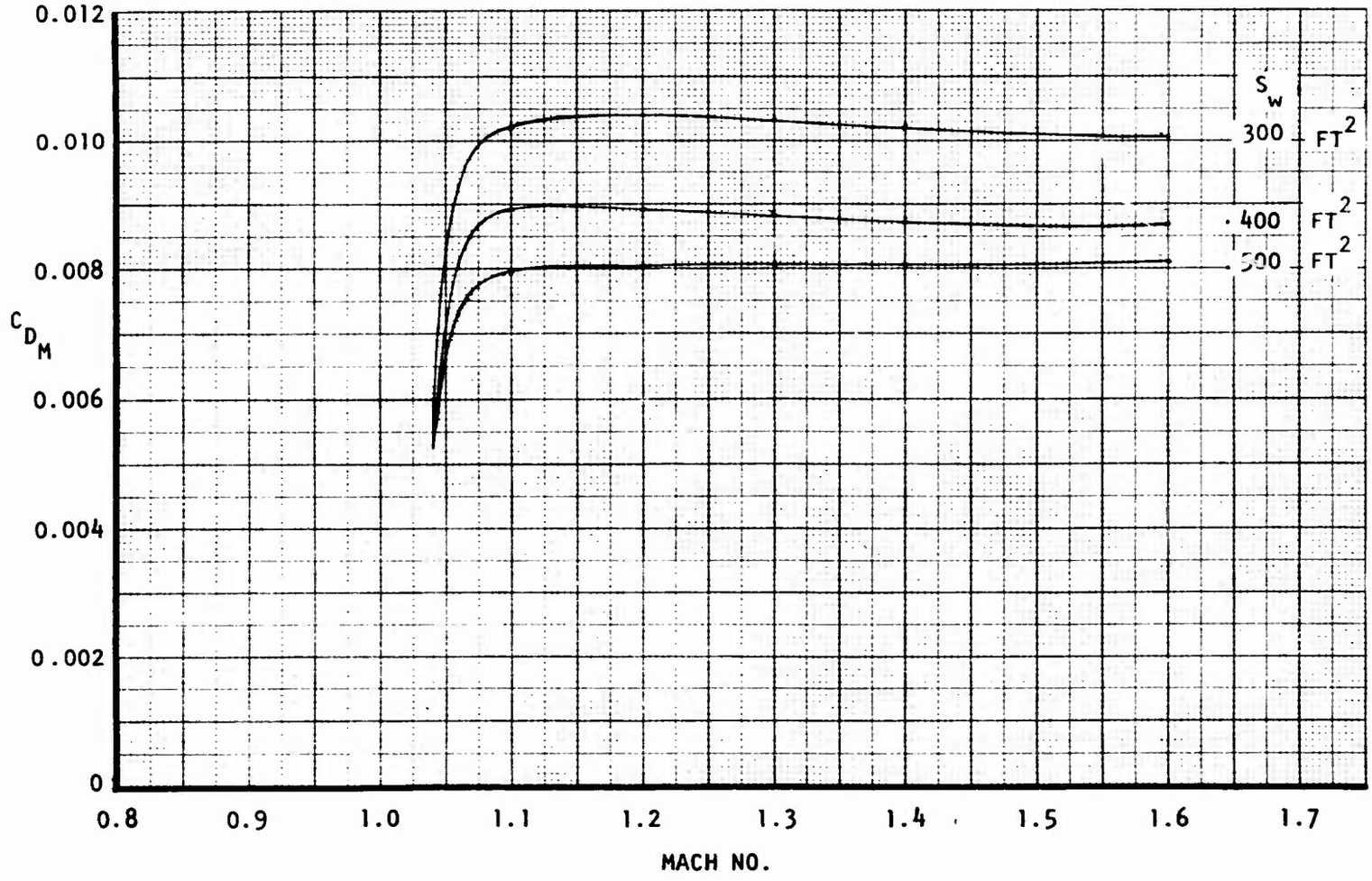

Figure 88. D572-5A metal configuration - t/c = 0.05, AR = 3.0 Λ_{LE} = 60°.

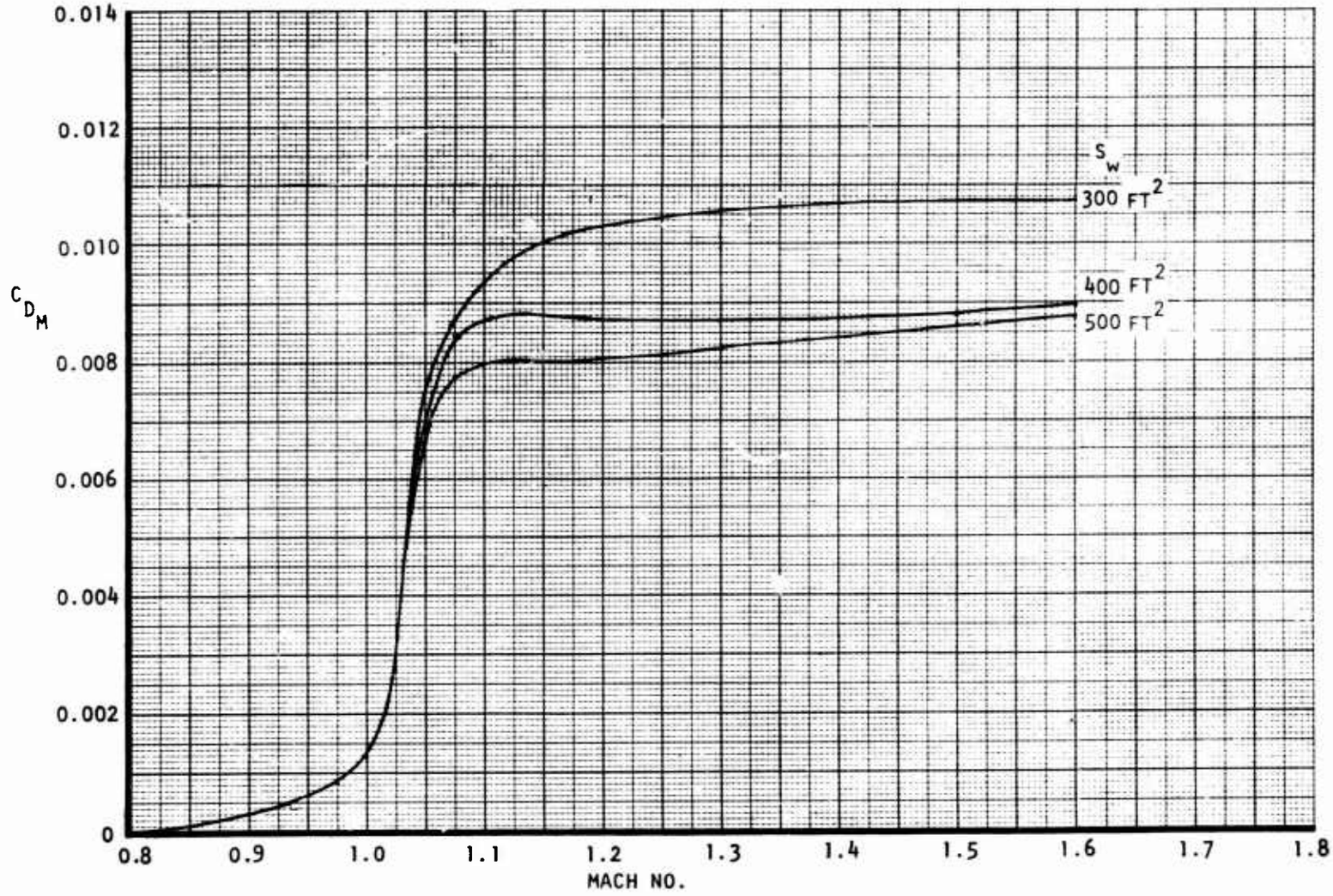

Figure 89. D572-5A metal configuration - t/c = 0.05, AR = 3.5 Λ_{LE} = 60°.

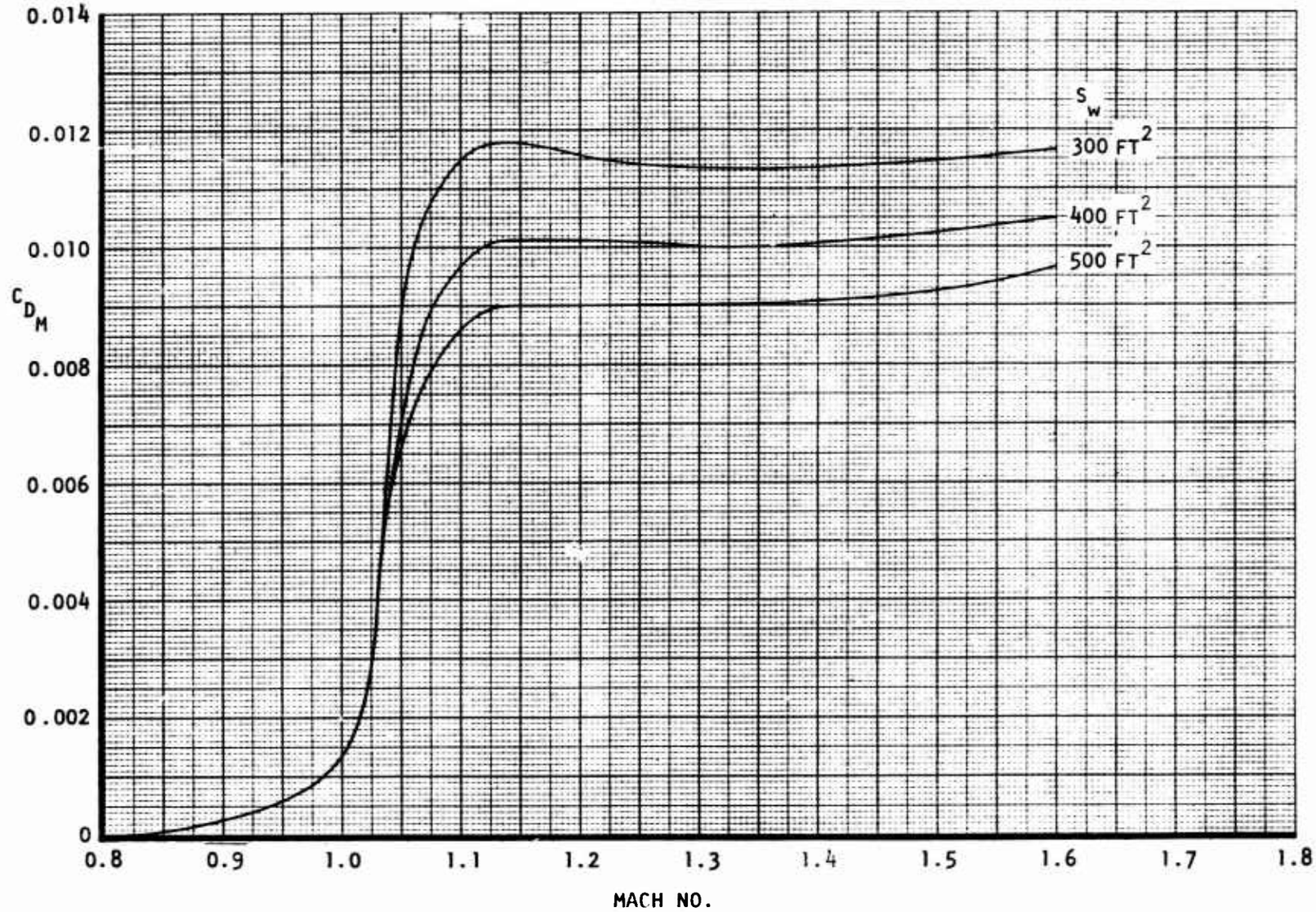

Figure 90. D572-5A metal configuration - t/c = 0.05, AR = 2.5, Λ_{LE} = 50°.

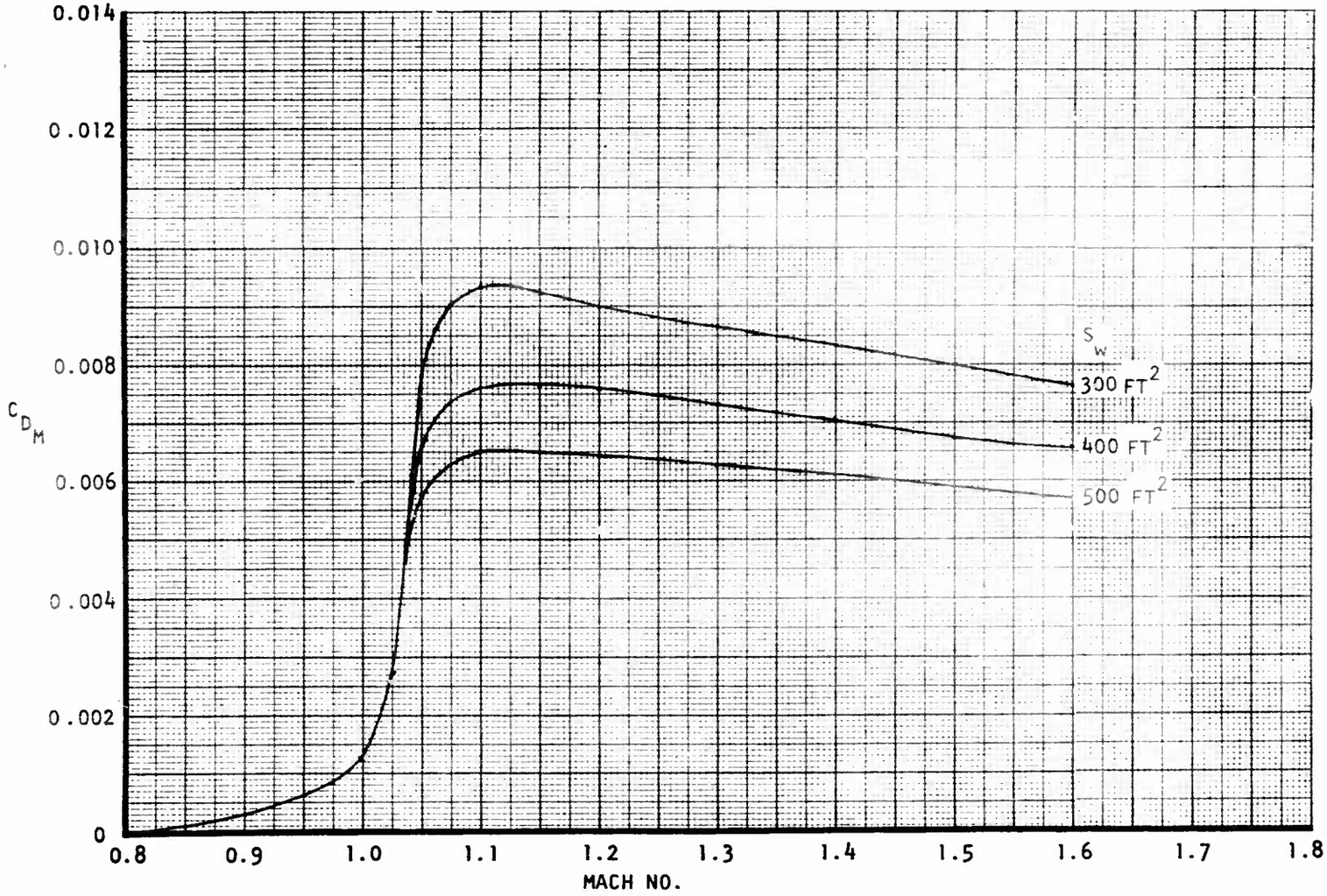

Figure 91. D572-5A metal configuration - t/c = 0.05, AR = 2.5, Λ_{LE} = 70°.

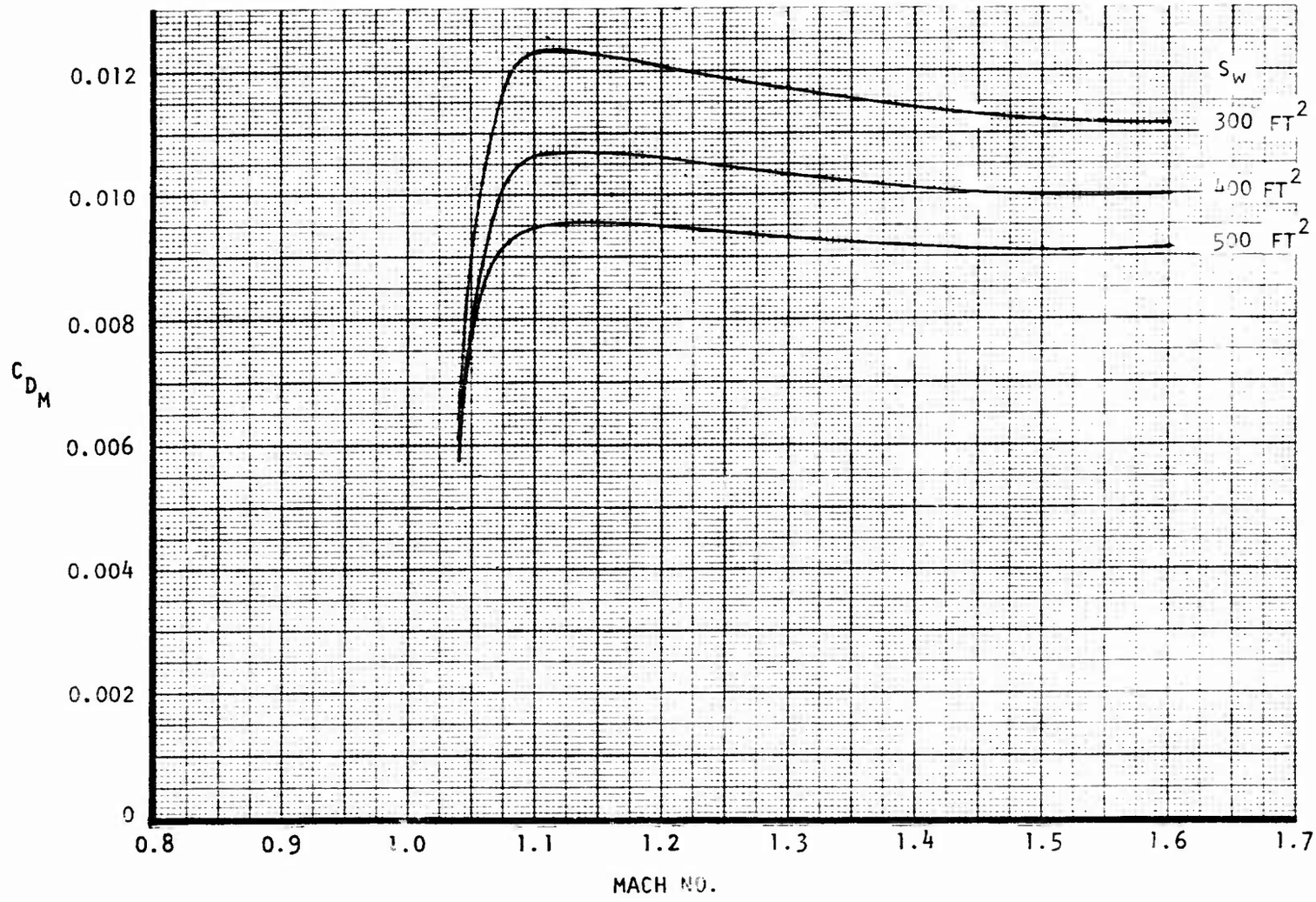

Figure 92. D572-5A metal configuration - t/c = 0.06, AR = 2.5, Λ_{LE} = 60°.

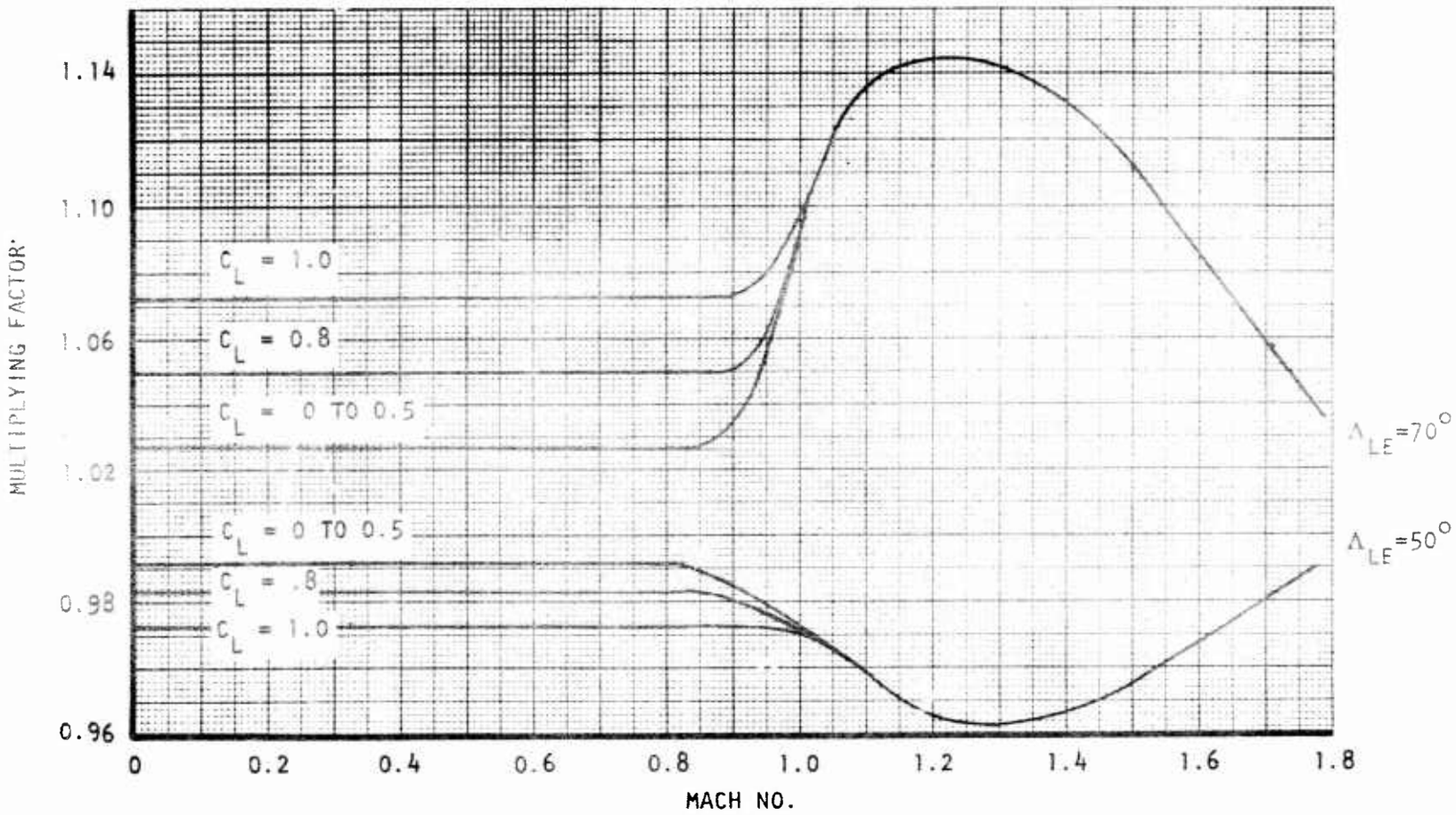

Figure 93. Multiplying factor for drag due to lift - AR=2.5.

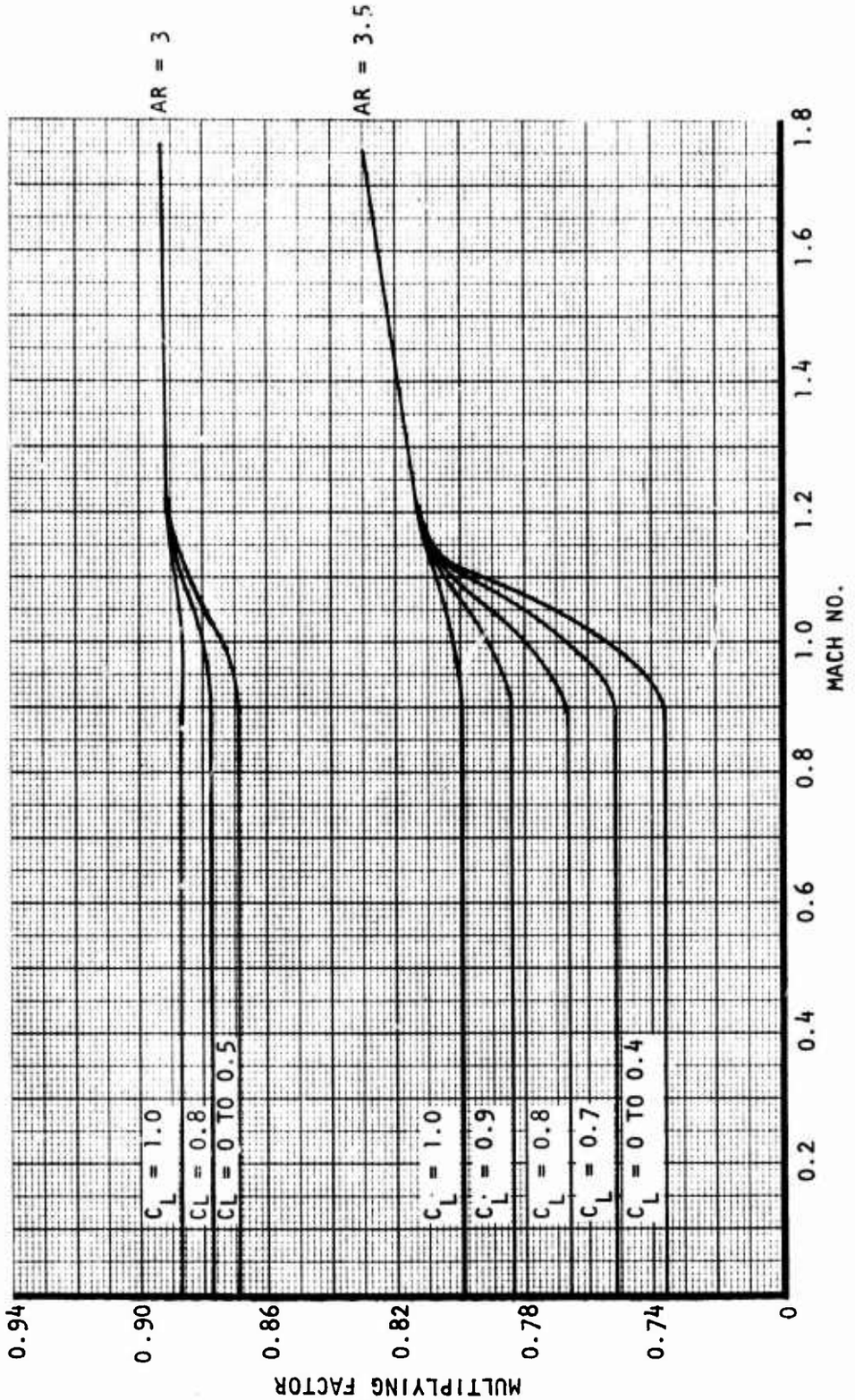

Figure 94. Multiplying factor for drag due to lift - $\Lambda_{LE}=60^{o}$.

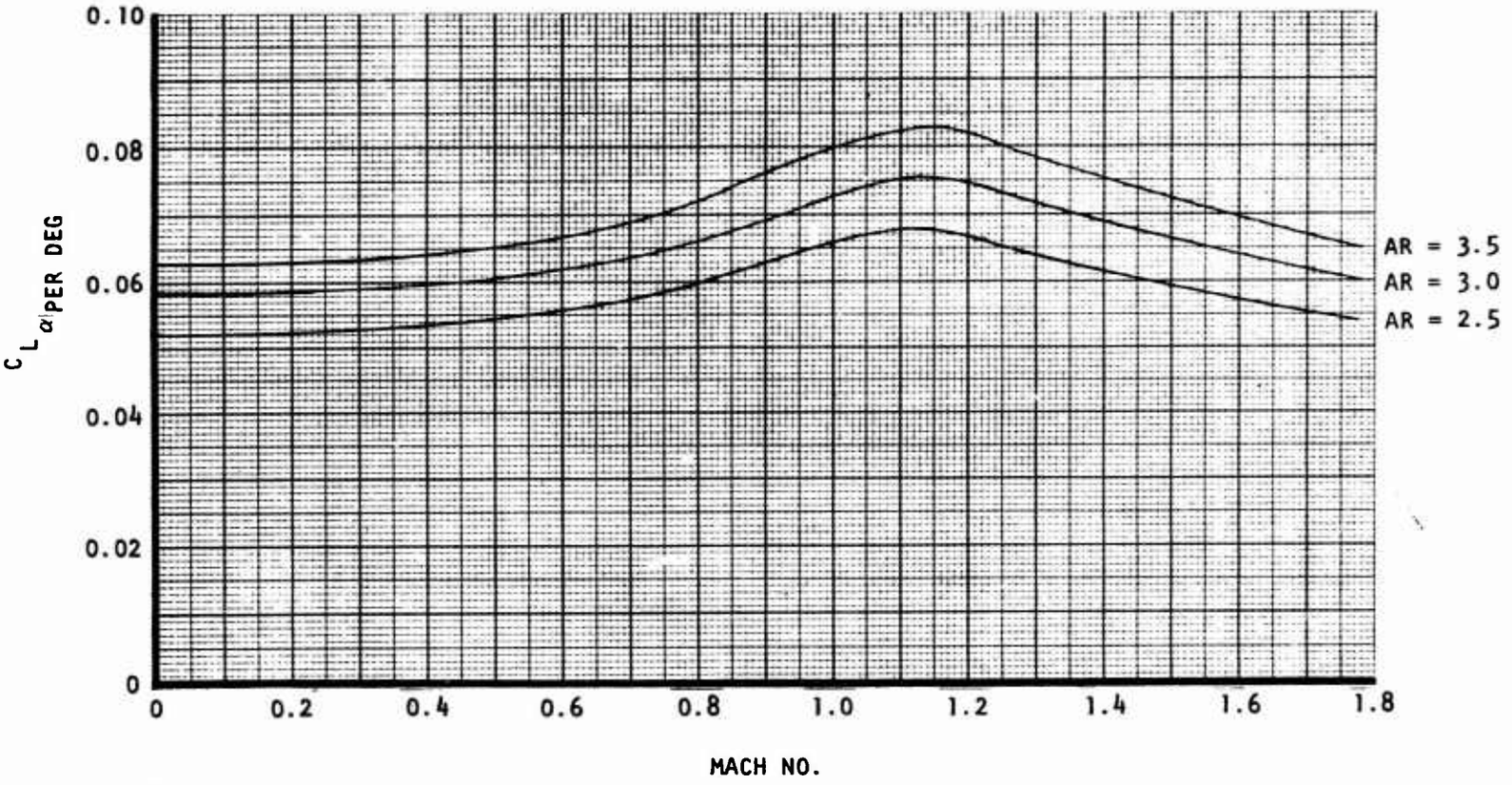

Figure 95. Variation of centerline with aspect ratio - $\Lambda_{LE}=60^{o}$.

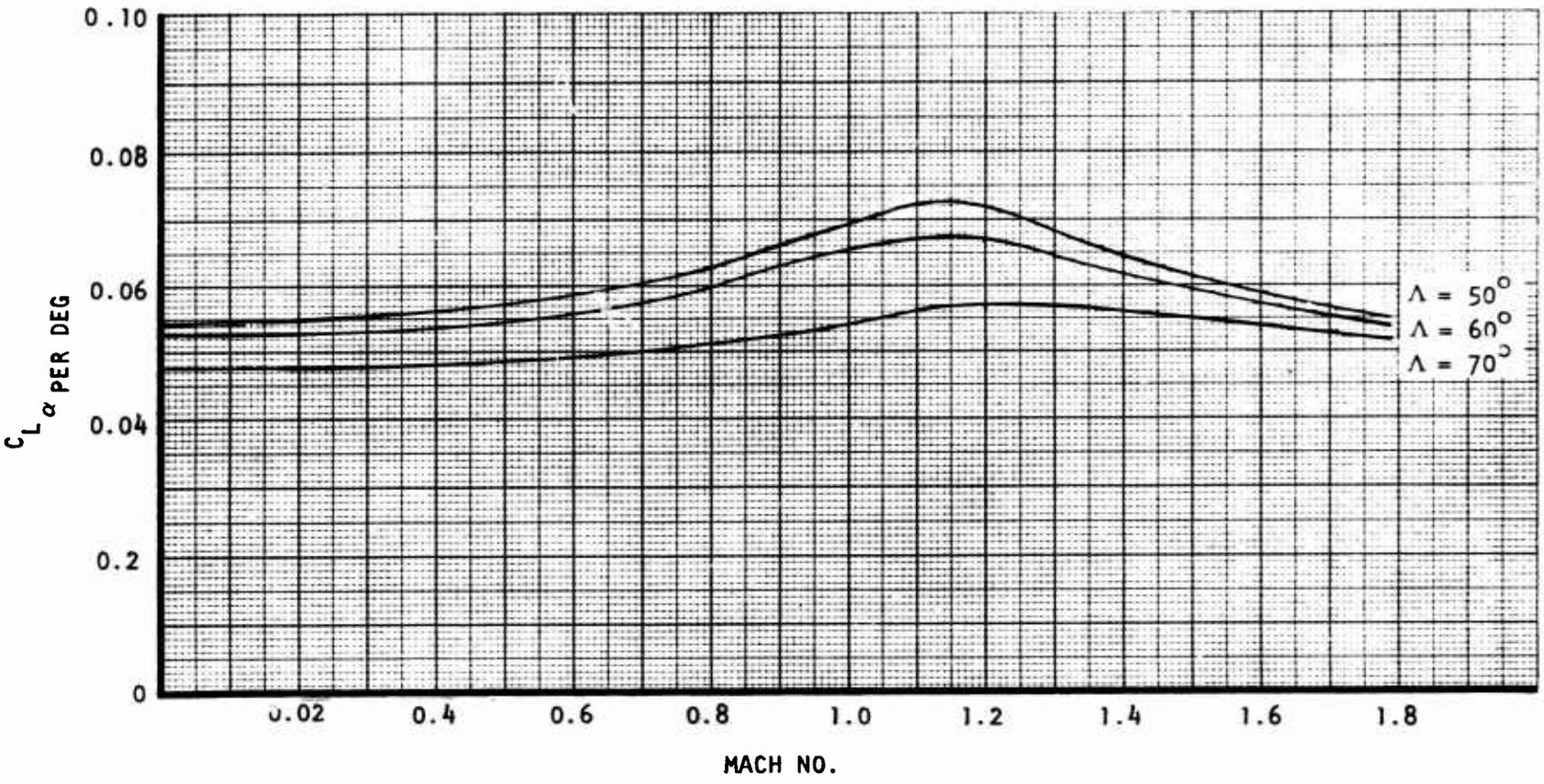

Figure 96. Variation of centerline with sweep angle - AR=2.5.

Section IV

STRUCTURE STUDIES

INTRODUCTION AND SUMMARY

The structures development for the ADCA conducted during the first task of this program consists of the following subtasks:

- Aircraft Structural Integrity Program (ASIP) Master Plan
- Design Criteria and Requirements
- Materials Selection
- Composite Application Trade Studies
- All-Composite Baseline Structure
- Advanced Metallic Baseline Structure

These tasks represent a logical sequence in the definition of the optimum structure for an all-composite fighter and in the determination of the cost-effectiveness of this fighter in relation to an advanced metallic fighter designed for the same mission. The ASIP Master Plan serves as the guide for the necessary steps in the airframe structural definition. The criteria and requirements define the conditions which are used for the establishment of the loads and environment of the airframe. From these conditions the candidate materials can be selected and trade studies on key structural areas conducted. The baseline composite airframe shown in Figure 97 is the result of the trade study results. Although cost trades were not conducted for the all-metal baseline structure, previous studies for the advanced tactical fighter and the B-1 strategic bomber have been used extensively for this structural arrangement.

DESIGN CRITERIA AND REQUIREMENTS

DESIGN WEIGHTS

Table 11 summarizes the design weights and centers of gravity data for each vehicle. The definition of flight design weight is basic mission takeoff weight less 20 percent of mission required fuel. The definition of landing design weight is basic mission takeoff weight less 60 percent of mission required fuel. Maximum design weight is defined as four MK-84 LGB (GBU-10C/B) (2 internally carried and 2 externally carried), full ammo, self-defense missiles and full internal fuel. The basic mission takeoff weight does not include ammo and self-defense missiles but the next configurations (D572-4C, D572-5B) which results from the vehicle sizing study include ammo and self-defense missiles. Section II contains the weight summary breakdown and center of gravity data for each vehicle.

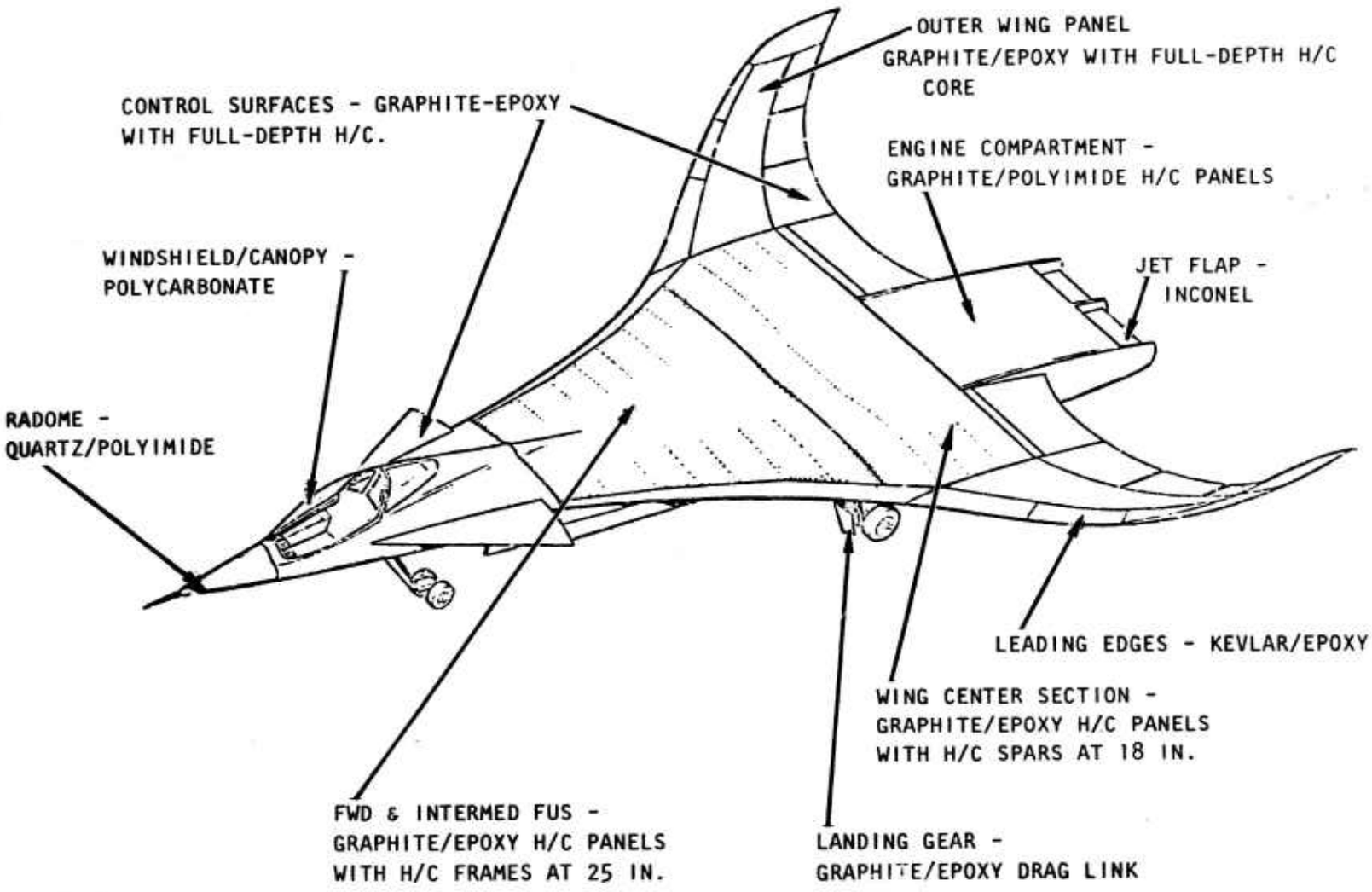

Figure 97. Advanced composite basepoint structure.

TABLE 11. VEHICLE DESIGN WEIGHTS AND CENTER OF GRAVITY

Composite Vehicle (D572-4B)		
Description	Weight (Pounds)	Center of Gravity (Fus. Sta.)
Flight Design	29,562	510.9
Landing Design	26,822	509.3
Maximum Design	41,772	502.5
Metal Vehicle (D572-5A)		
Flight Design	33,809	509.2
Landing Design	30,658	510.1
Maximum Design	41,297	512.6

LOADS

Four symmetrical flight conditions were selected to represent a sample of the ADCA load requirements. These conditions at flight design gross weights of the particular configuration are listed below.

Mach No.	Altitude	Vertical Load Factors	Canard Position	Condition Number
0.9	Sea Level	8.0	IN	3.0
1.2	Sea Level	8.0	IN	1.0
1.2	Sea Level	-3.0	IN	4.0
1.71	20,000 ft	6.5	IN	2.0

A taxi condition at maximum design weight was also included for fuselage loads and is referred to as condition five.

These conditions have been analyzed using programs newly developed under IR&D funds.

The new planar and non-planar load routines were created to supply SWEEP input loads in the conceptual and preliminary design phases of vehicle design.

A modified version of the Nonplanar Unified Distributed Panel Wing-Body Program which is used by the Rockwell/LAAD Aerodynamics group provides trimmed vehicle pressure distributions. This program computes subsonic and supersonic aerodynamic characteristics of wing-body configurations, surface pressures, load distributions, and total component and configuration loads. The programmed procedure is based on a constant source and vortex panel formulation for thin bodies and interference shells. A surface source representation is used on the slender body components. Pressure distribution is normalized to dynamic pressure and based on a trimmed lift coefficient of one for each mach number condition under investigation.

Three other new programs were developed to support this interface with the Aerodynamics group. The first is a unit inertia program which converts grid network mass distributions into unit shears, moments, and torques for the lifting surfaces of a configuration. The second (Load Influence Coefficient Program) converts the pressure distribution data into unit shears, moments, and torques for lifting surfaces and unit forebody, midbody and afterbody fuselage lift. The third (Design Loads Program) converts the unit data into limit loads for the required load factors, gross weight, altitude and dynamic pressure consistent with mach number conditions for the pressure data. These programs are structured to provide SWEEP with data required for the load analysis. SWEEP is then used to calculate net fuselage loads with the option to either calculate net lifting surface loads or accept input loads data.

Figures 98 and 99 show the assumed load reference axis used in the wing shear, moment, and torque calculations for the composite and metal configurations. The numbers of these figures represent the SWEEP structural analysis points. Figures 100 through 105 show net ultimate rigid loads for the composite wing outboard and inboard panels. Likewise, Figures 106 through 111 present the net rigid loads for the metal wing outboard and inboard panels. The shear loads in these figures are positive for load up and normal to the wing. The bending loads are positive for compression in the upper cover, while torque is positive for a leading edge up. These loads include the effects of vertical and side loads due to the nonplanar planform.

Figures 112 and 113 present net ultimate shear and bending moments for the composite fuselage while Tables 12 and 13 are a tabulation of these same loads. Figures 114 and 115 and Tables 14 and 15 present similar data for the metal fuselage. The main difference between the two sets of fuselage loads is the number of points assumed to react the external wing loads. Three points were assumed for the composite and only two for the metal.

Canard loads for the ADCA were estimated by using the airloads module of SWEEP with the planar wing model and trimming with the canard. This was done to expedite load analysis. This method gives conservative canard loads. The resulting exposed canard loads are listed in the following paragraphs.

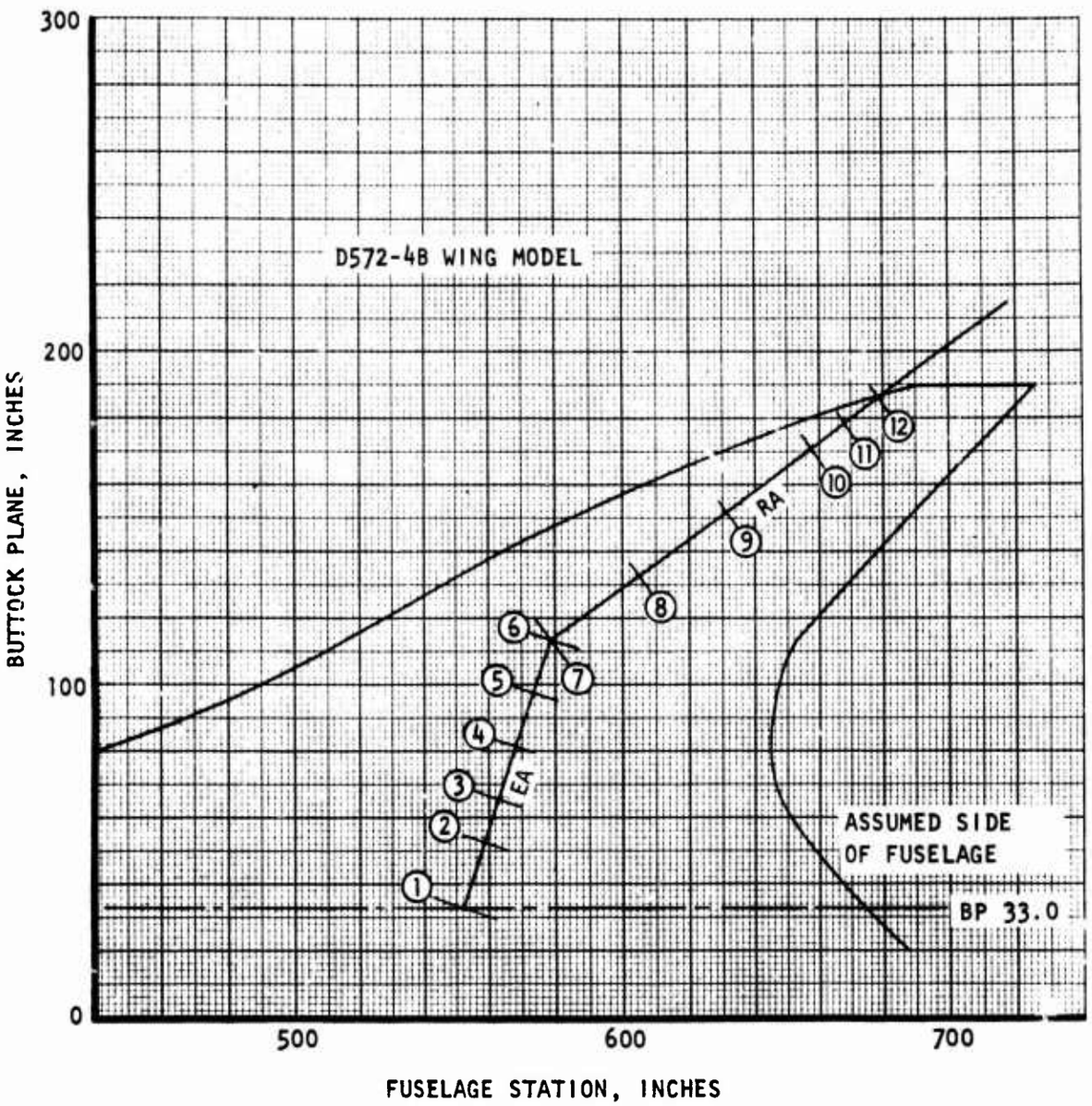

Figure 98. D572-4B load reference axis.

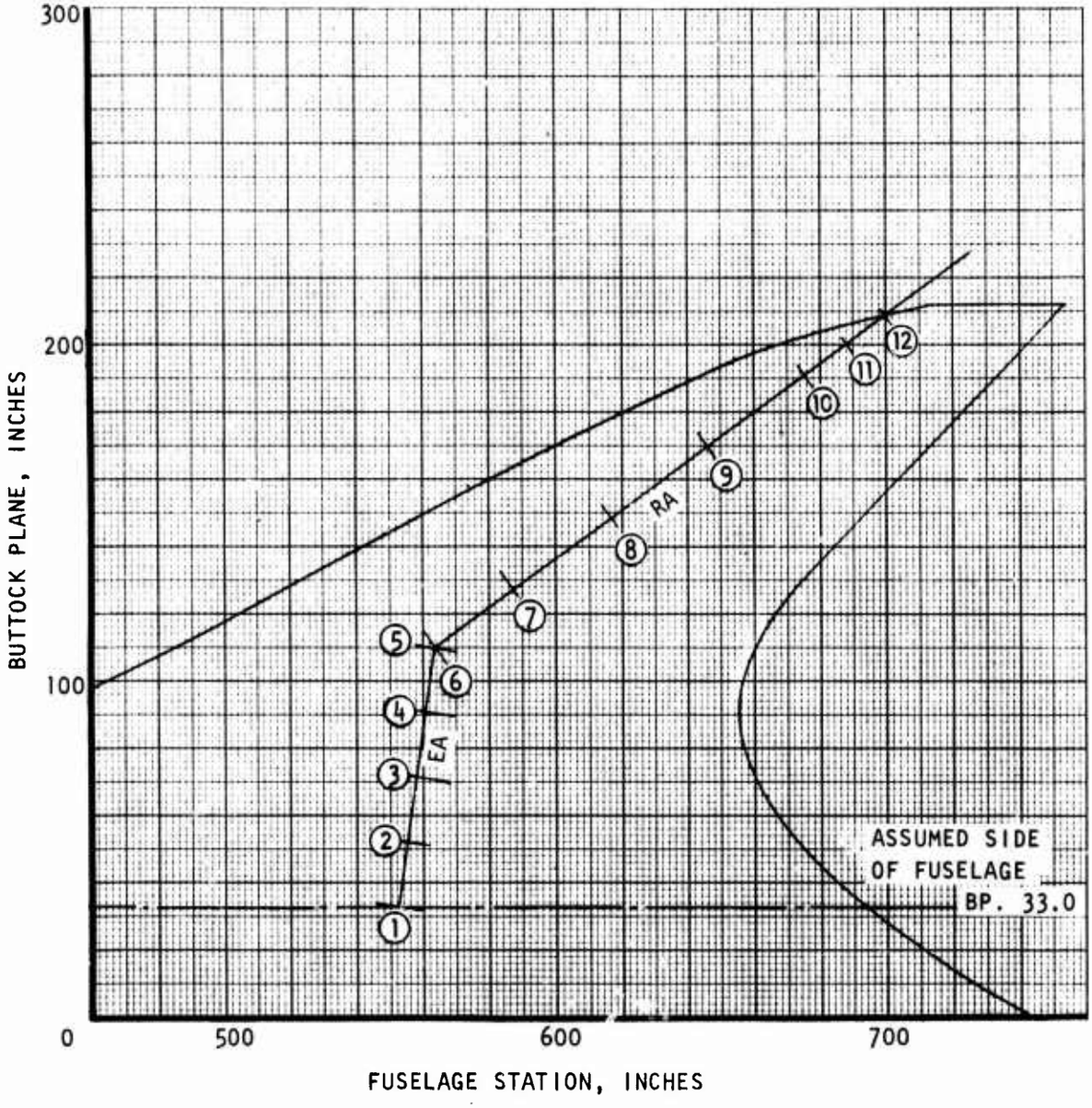

Figure 99. D572-5A load reference axis.

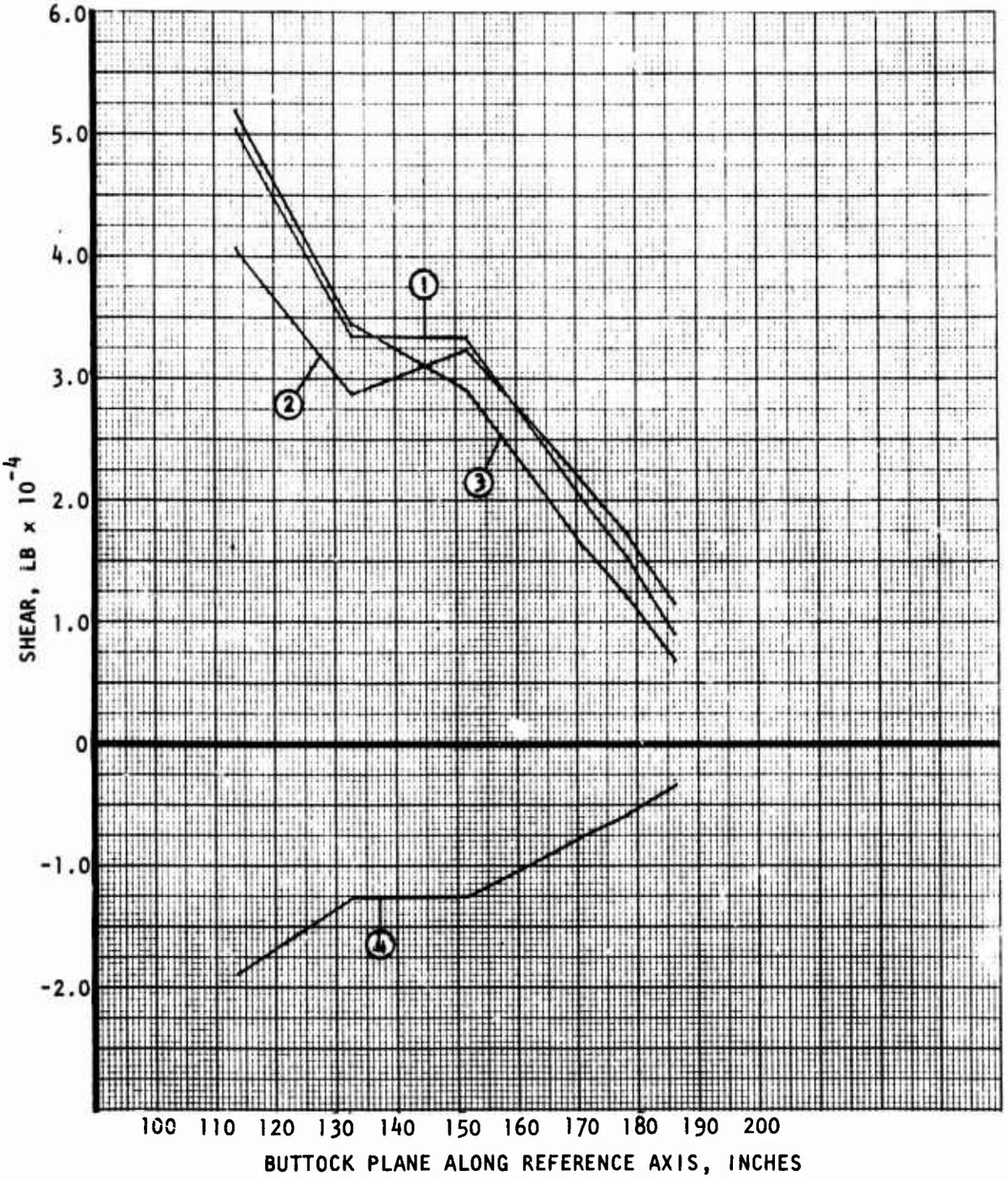

Figure 100. D572-4B outboard wing ultimate shear.

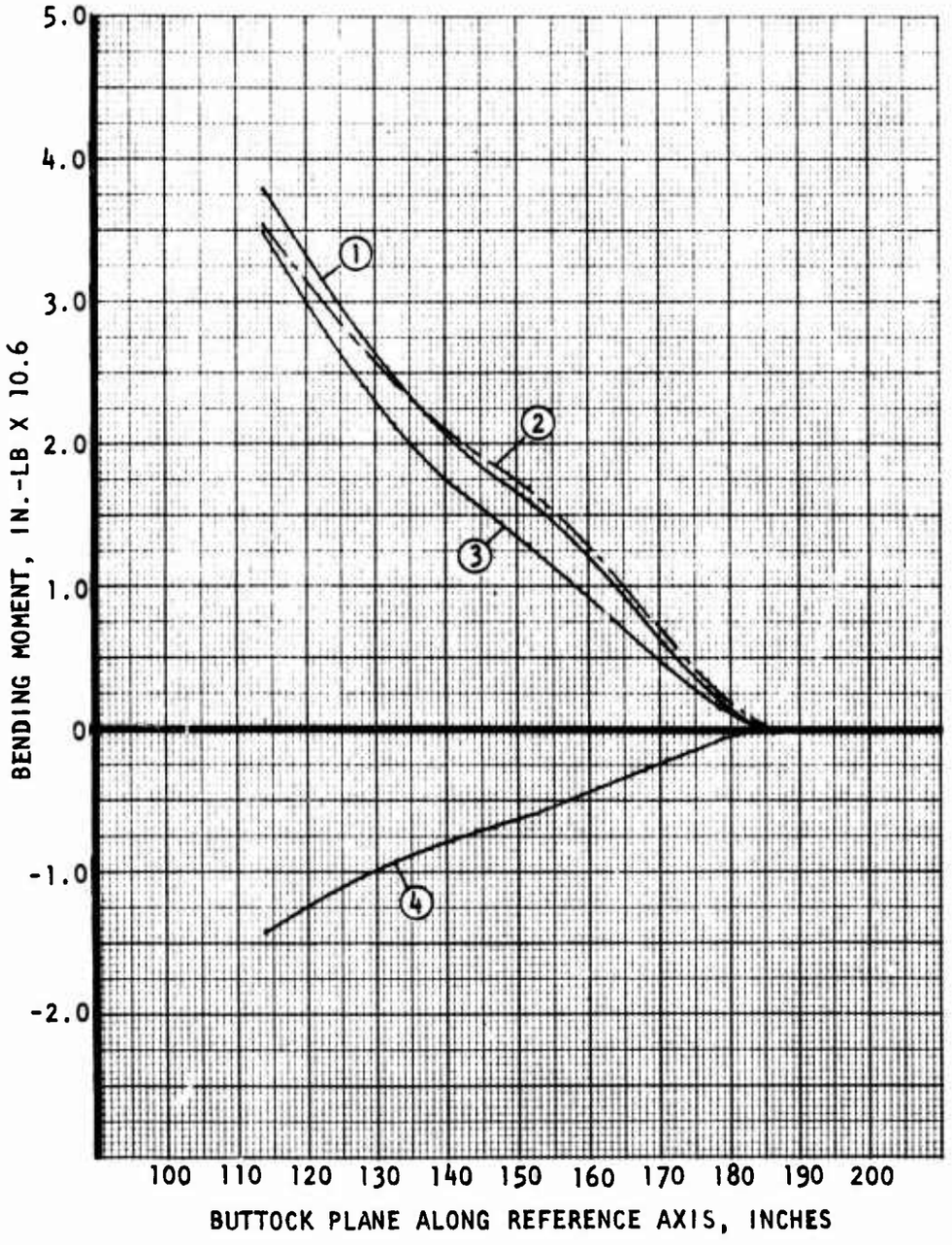

Figure 101. D572-4B outboard wing ultimate bending moment.

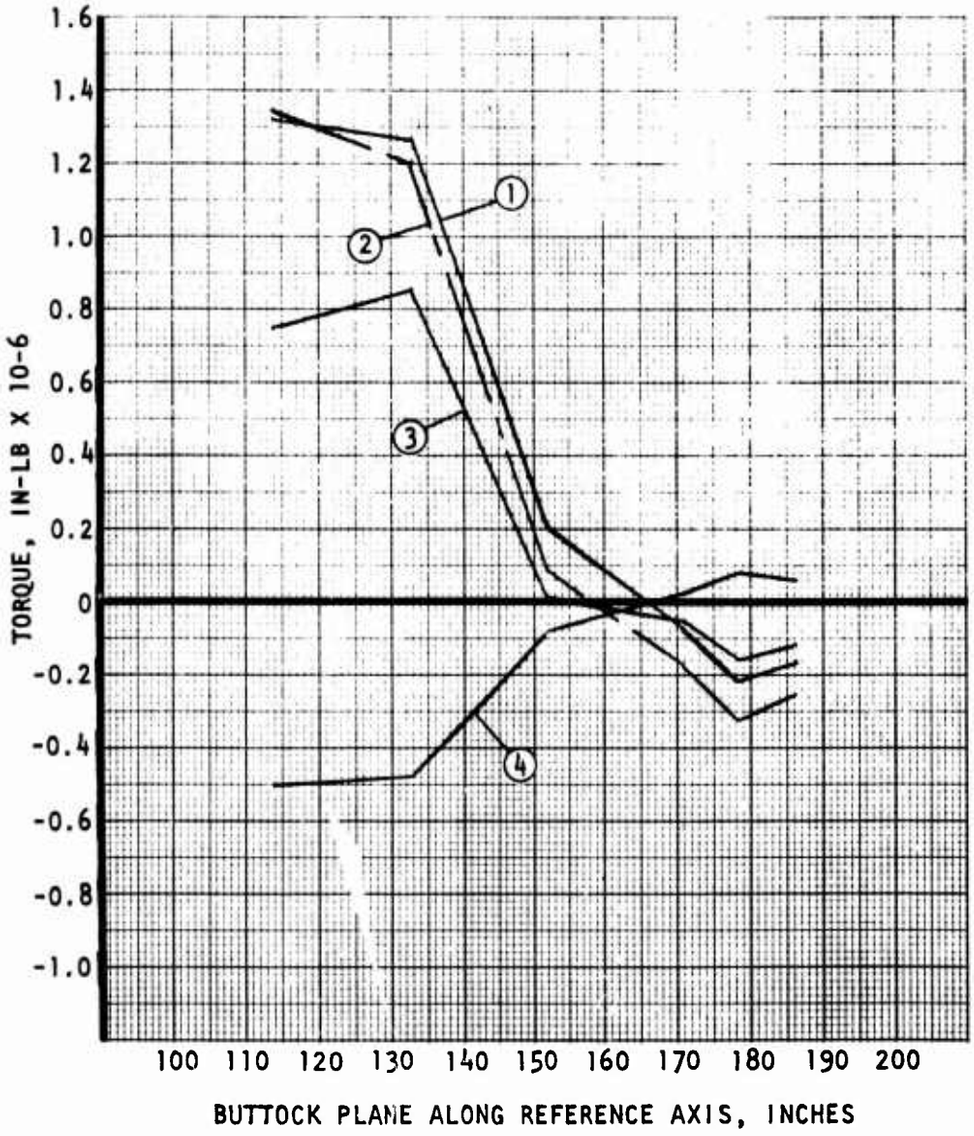

Figure 102. D572-4B outboard wing ultimate torque.

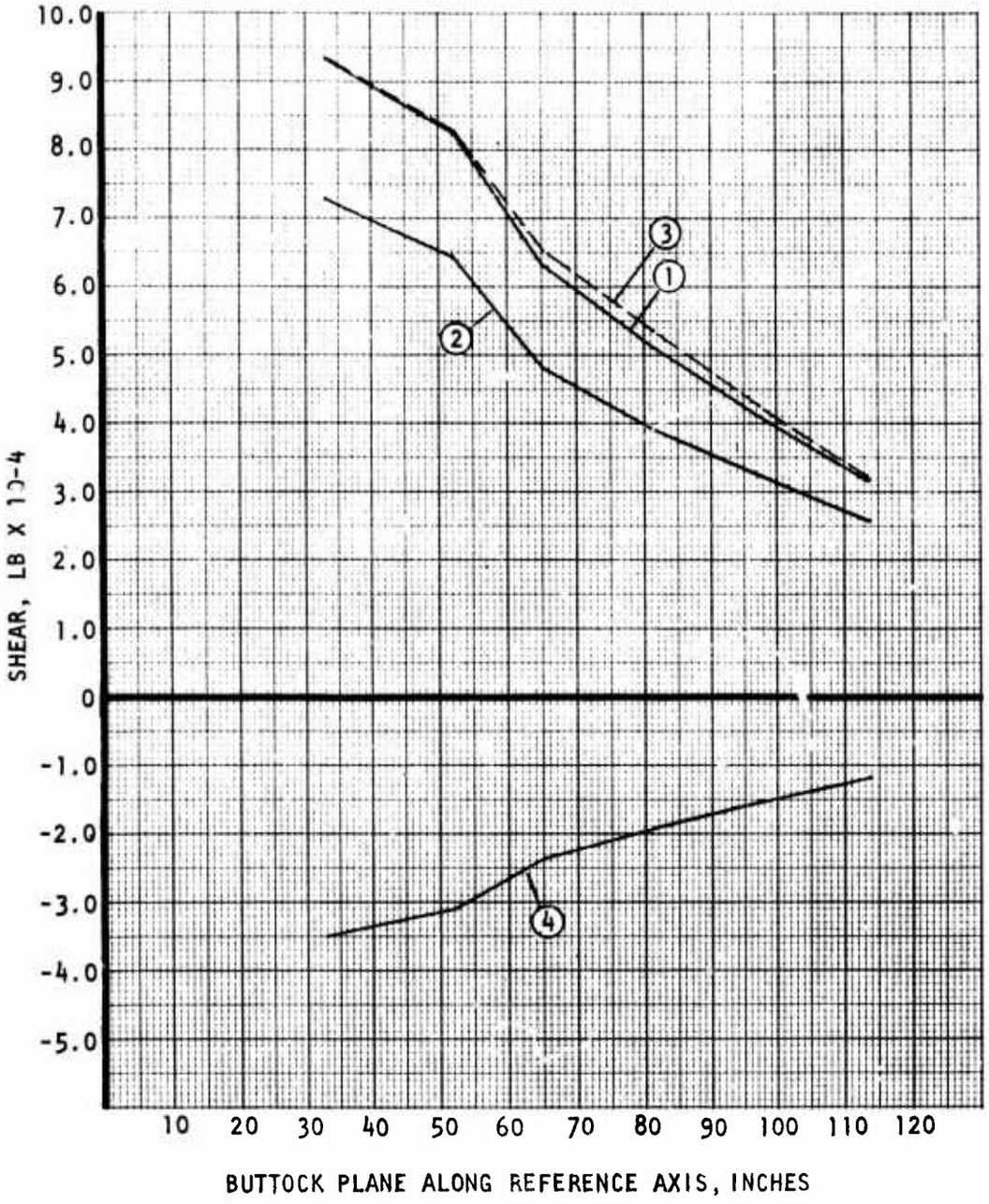

Figure 103. D572-4B inboard wing ultimate shear.

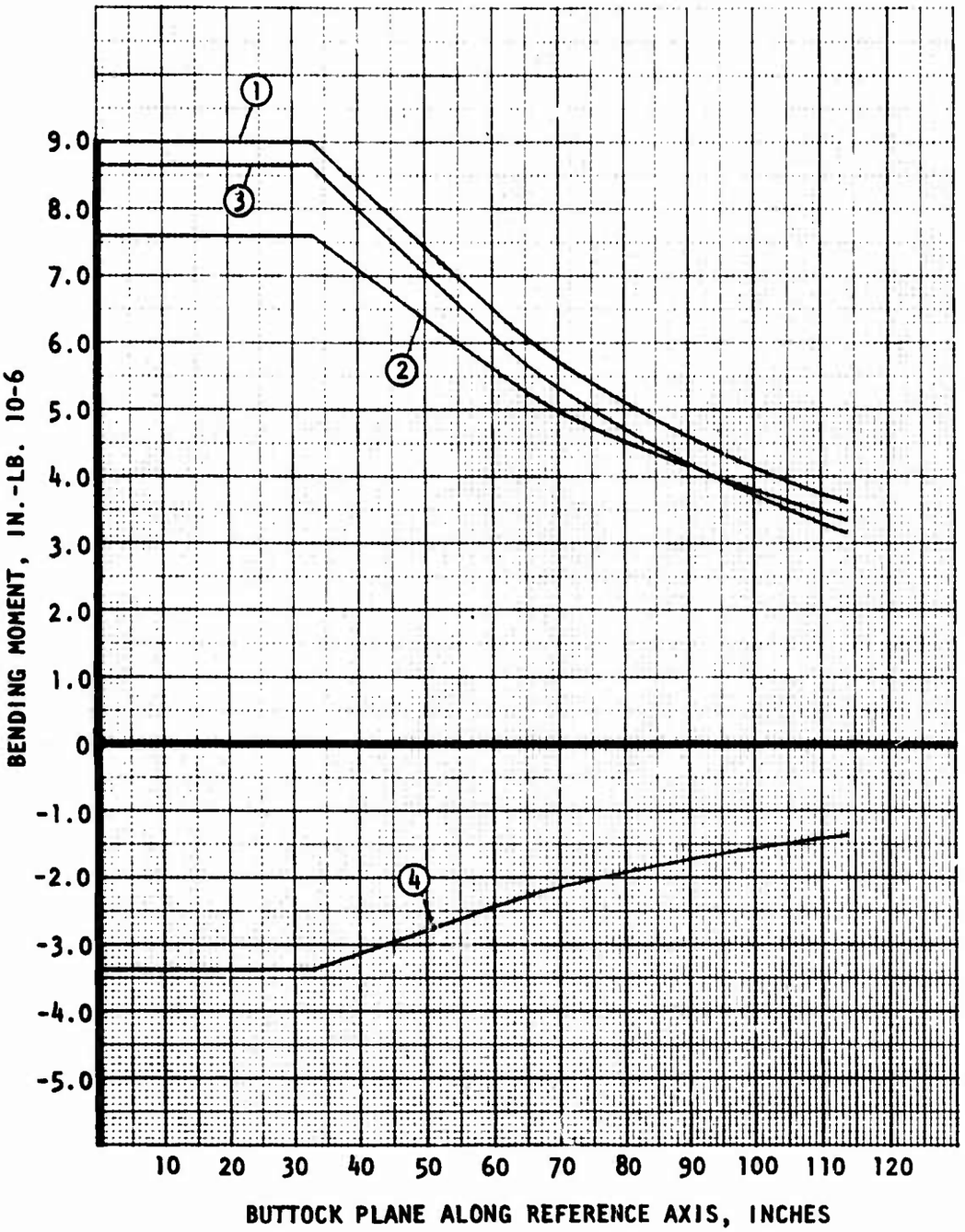

Figure 104. D572-4B inboard wing ultimate bending moment.

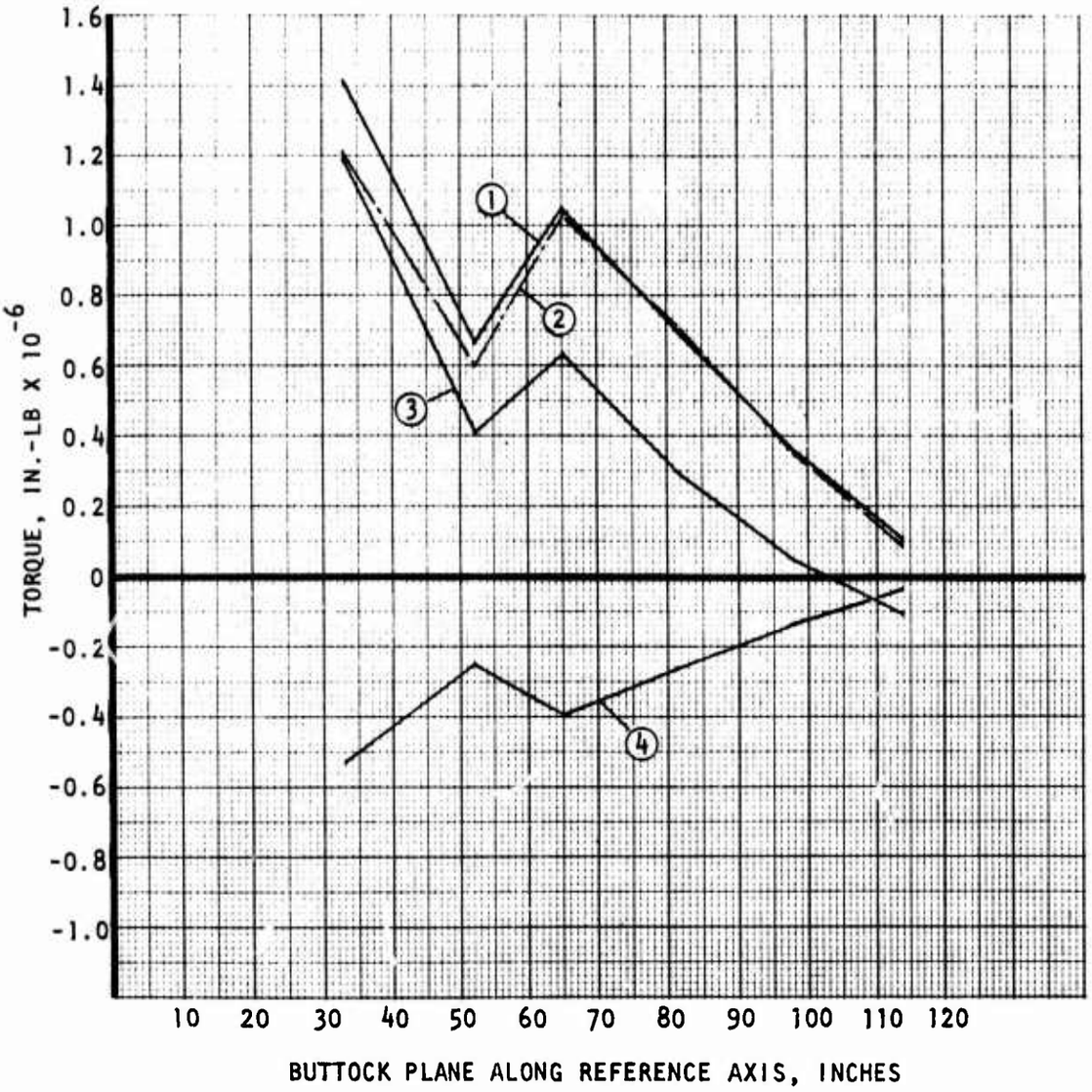

Figure 105. D572-4B inboard wing ultimate torque.

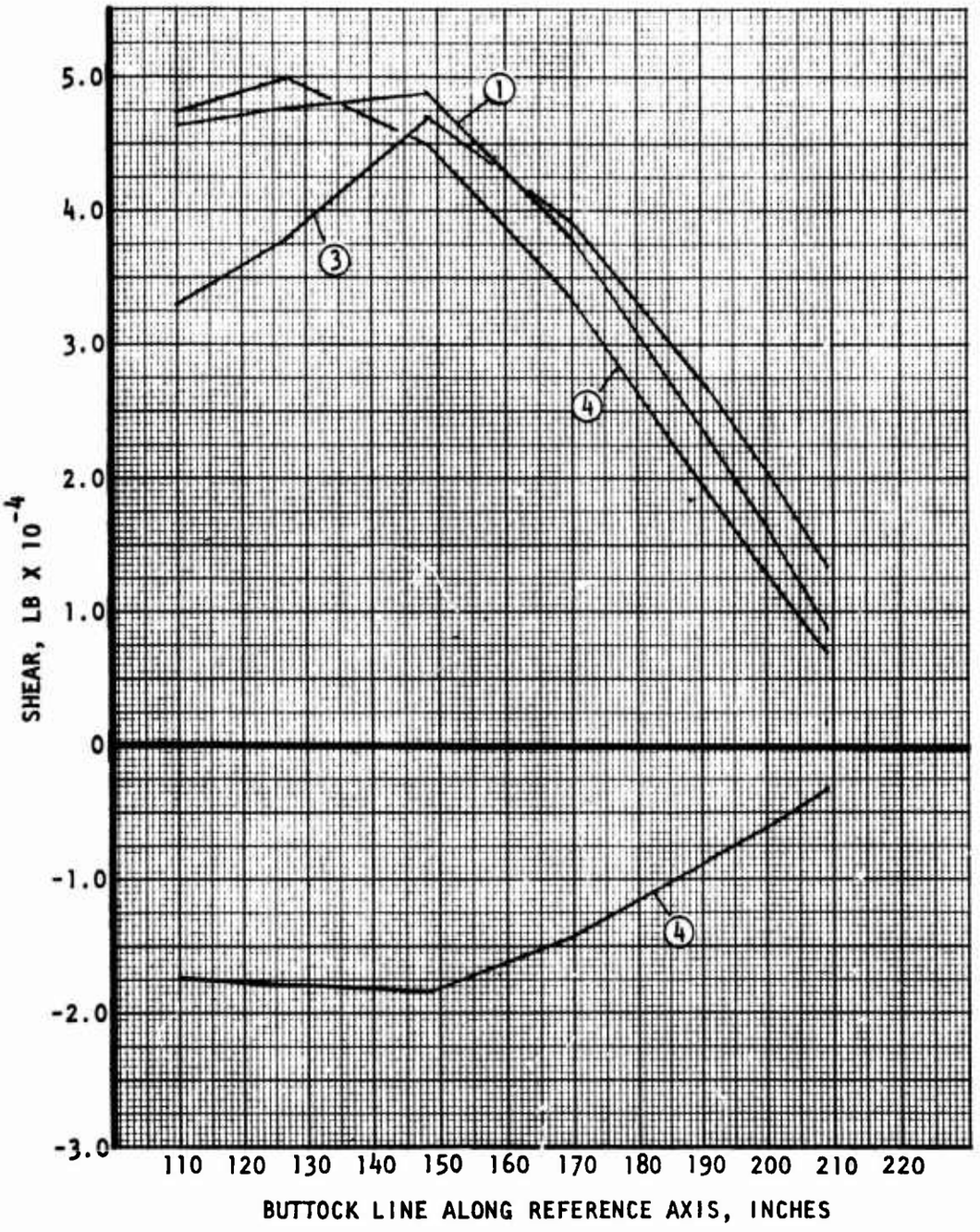

Figure 106. D572-5A outboard wing ultimate shear.

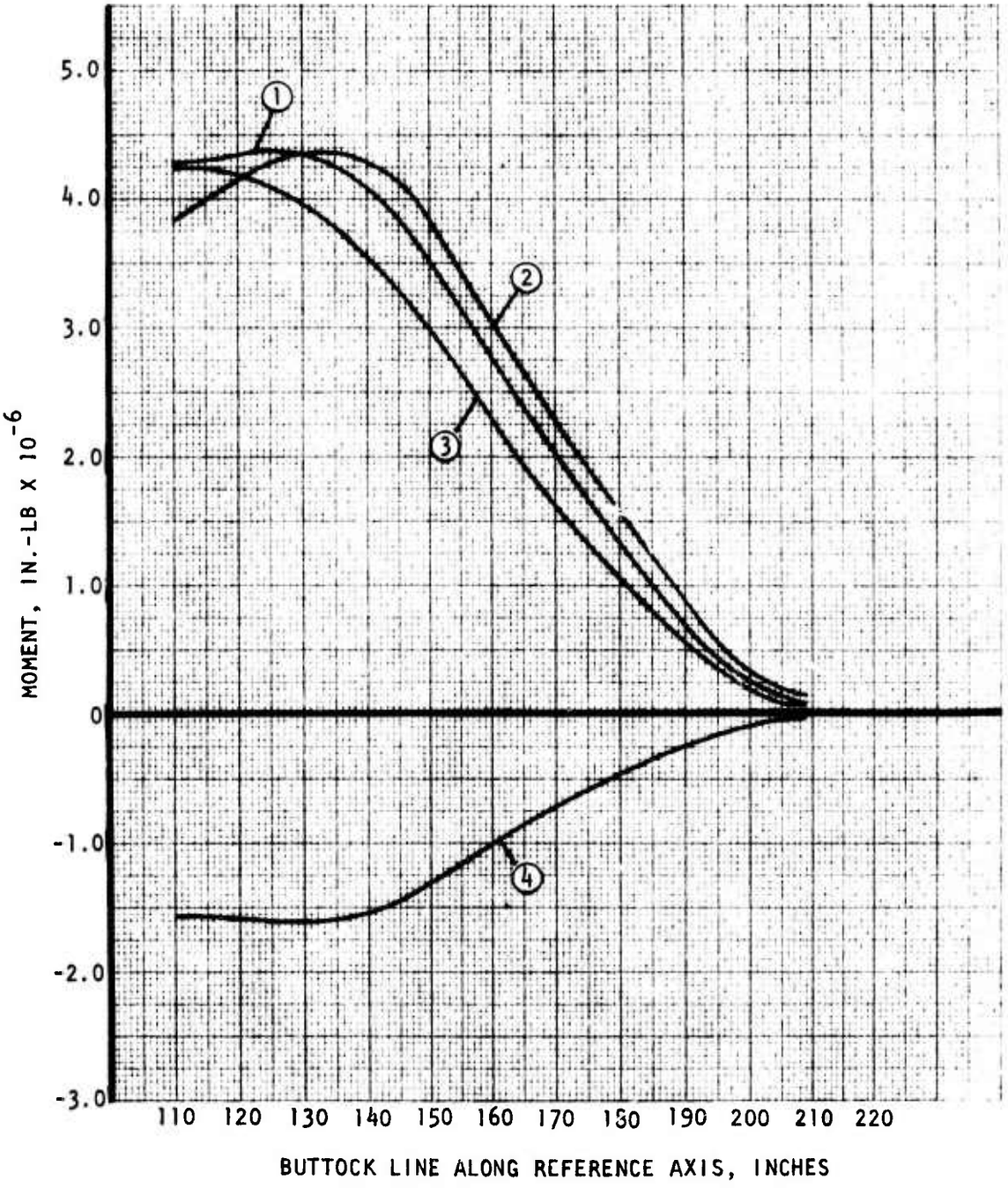

Figure 107. D572-5A outboard wing ultimate bending moment.

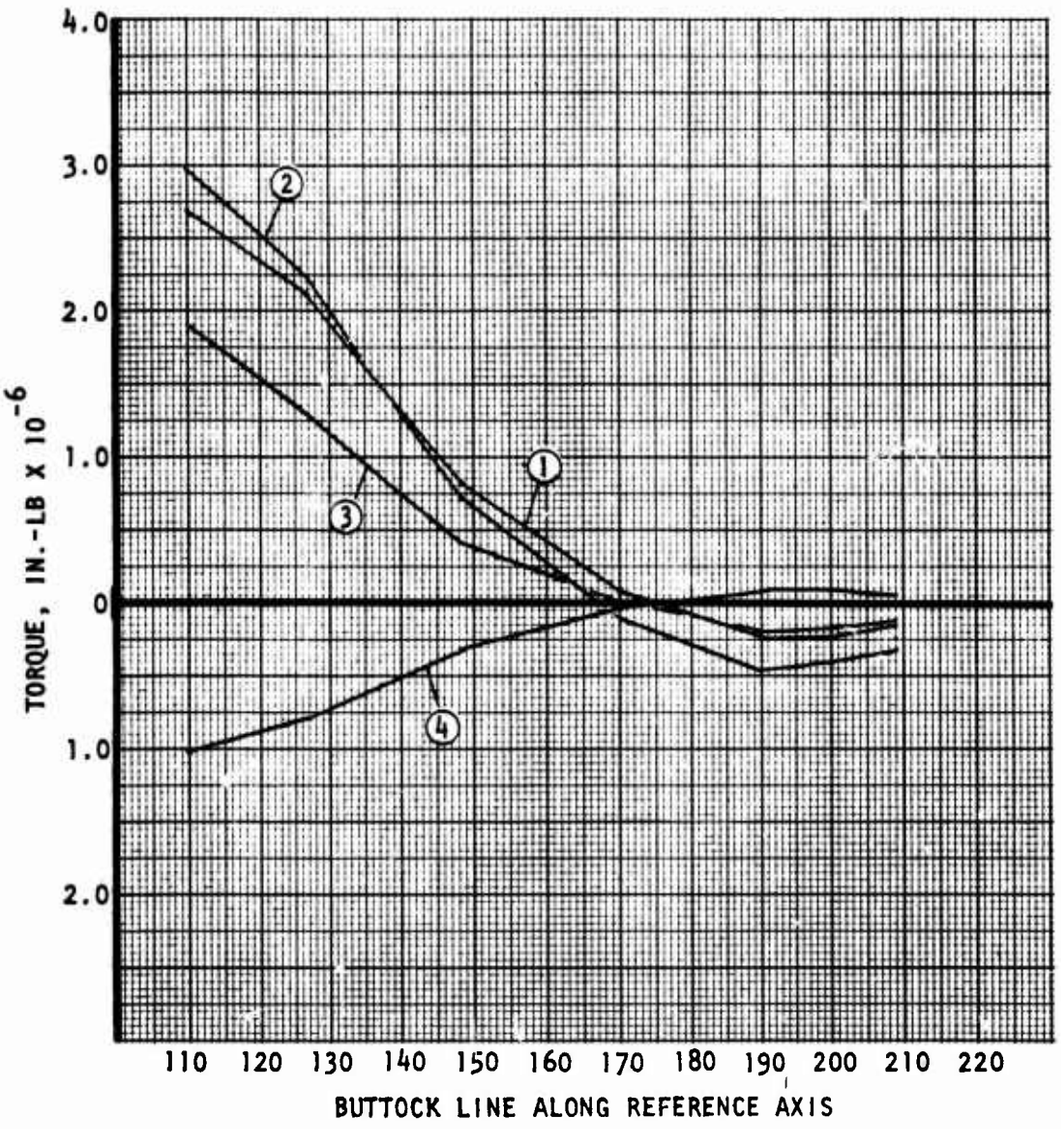

Figure 108. D572-5A outboard wing ultimate torque.

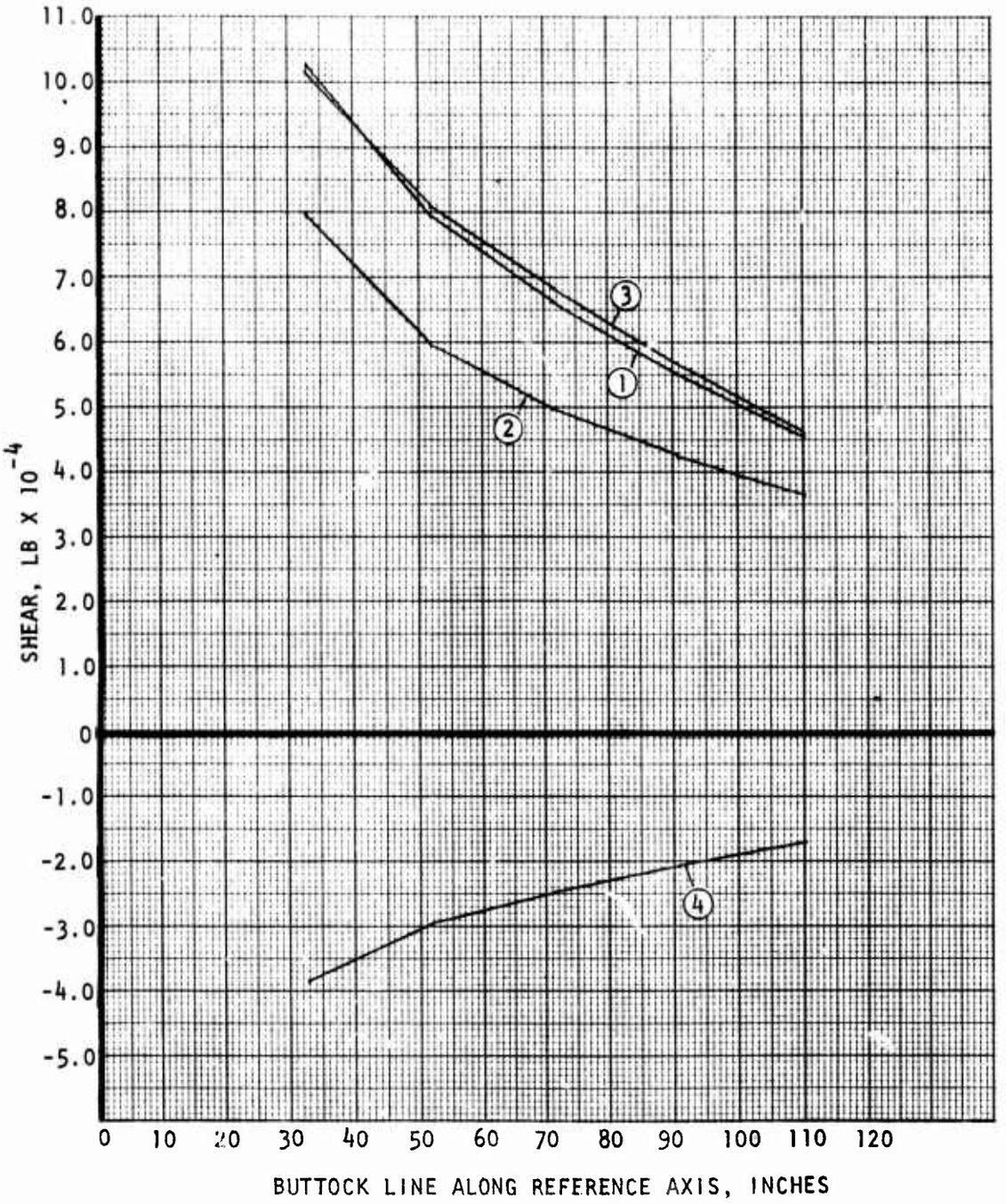

Figure 109. D572-5A inboard wing ultimate shear.

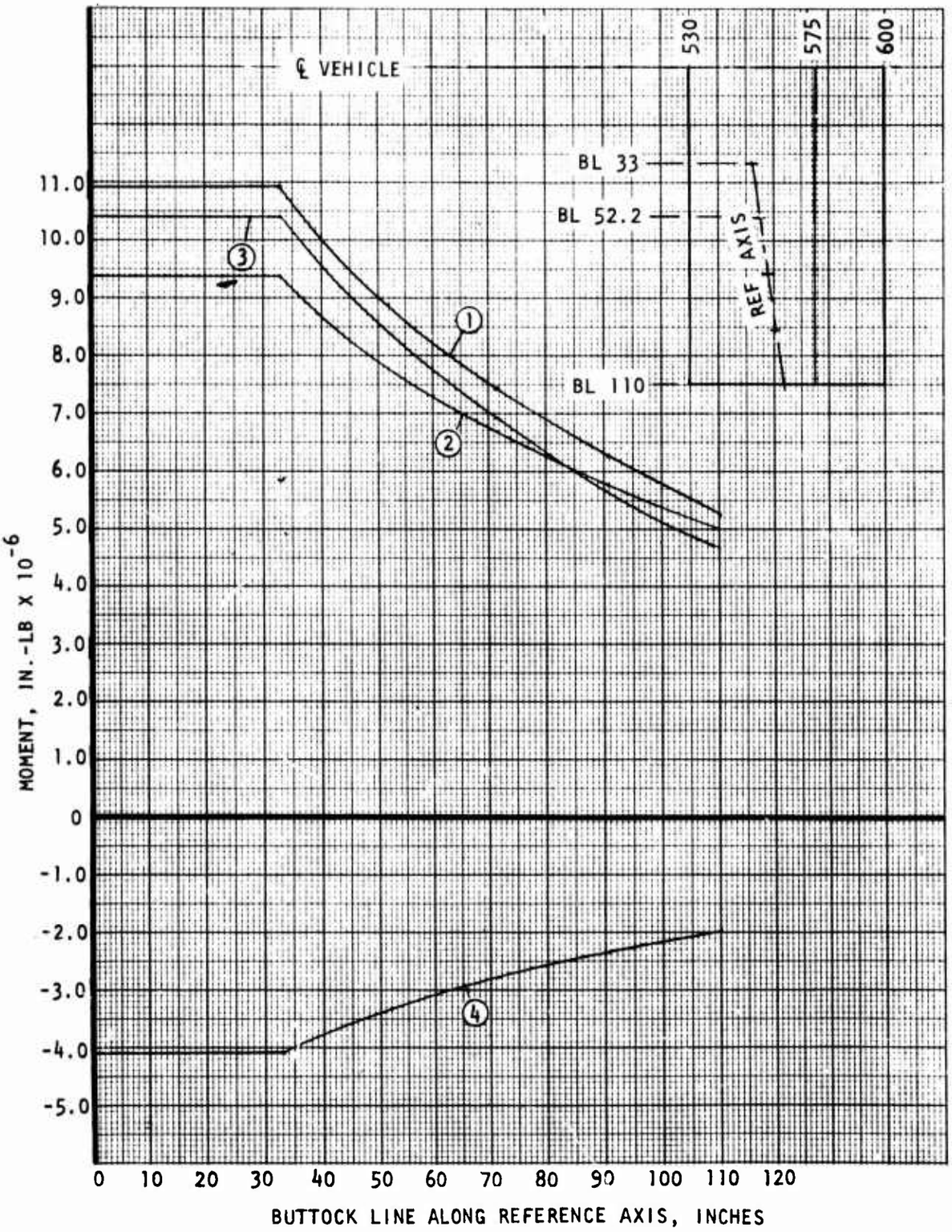

Figure 110. D572-5A inboard wing ultimate bending moment.

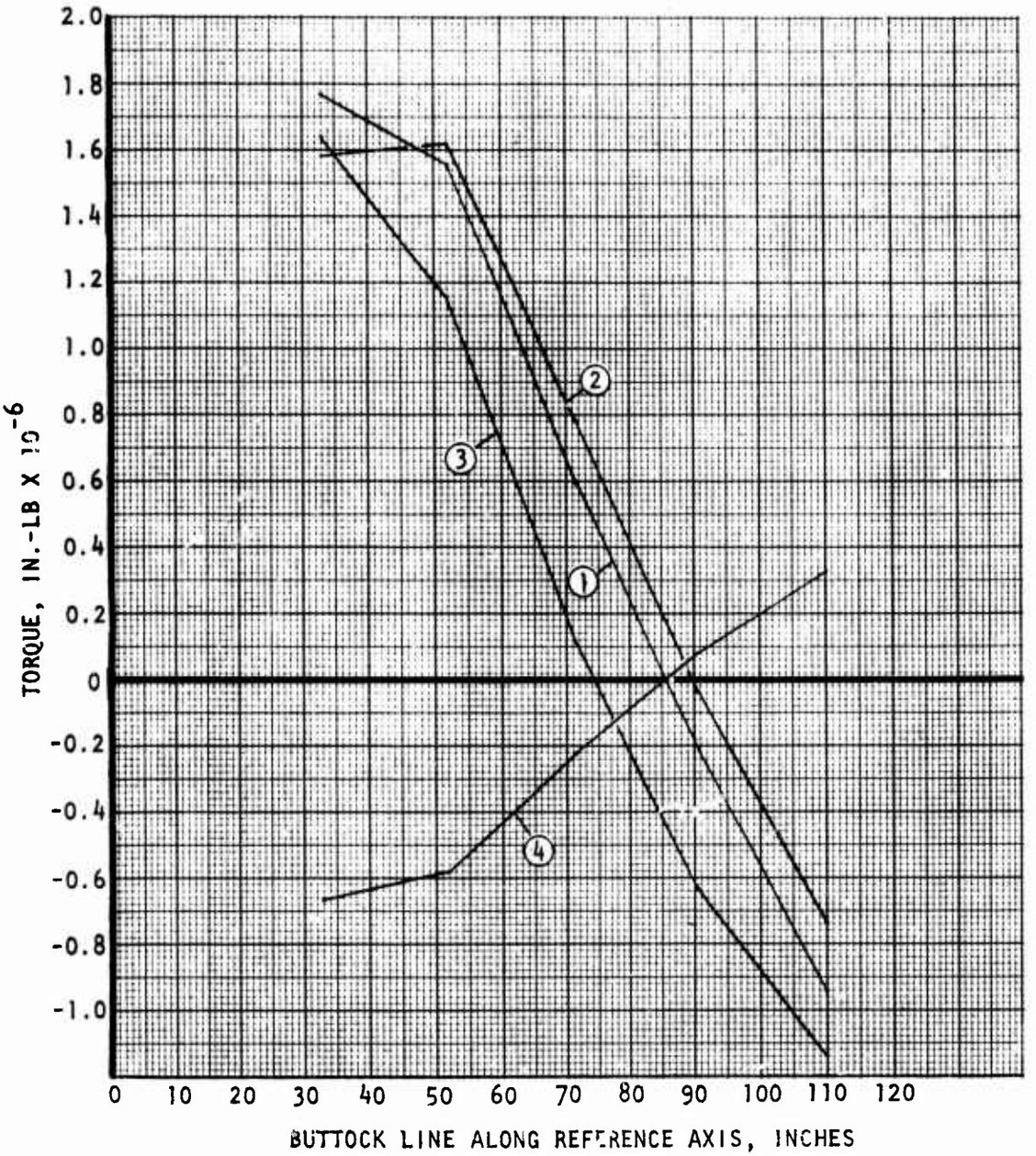

Figure 111. D572-5A inboard wing ultimate torque.

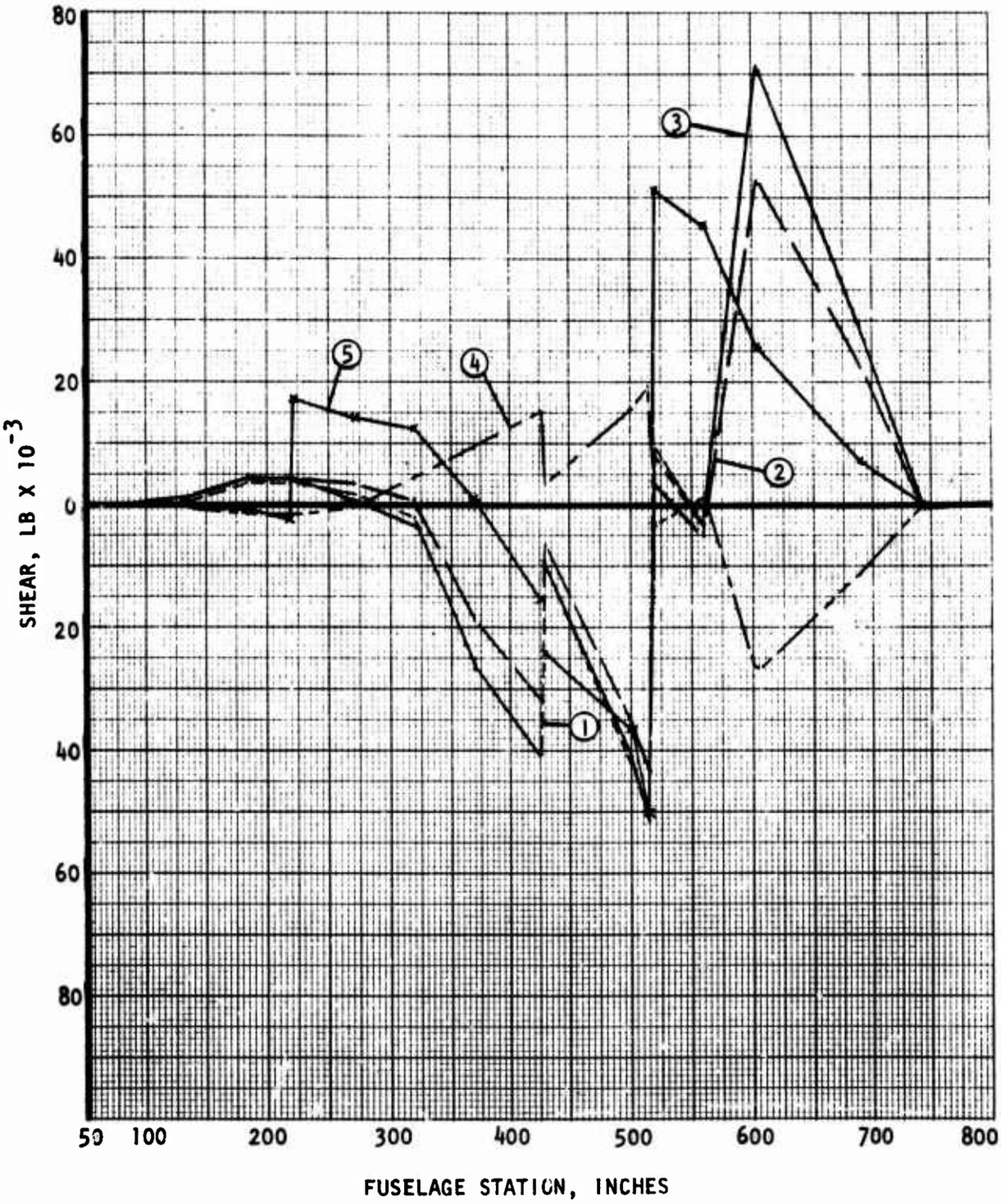

Figure 112. D572-4B fuselage ultimate shear diagram.

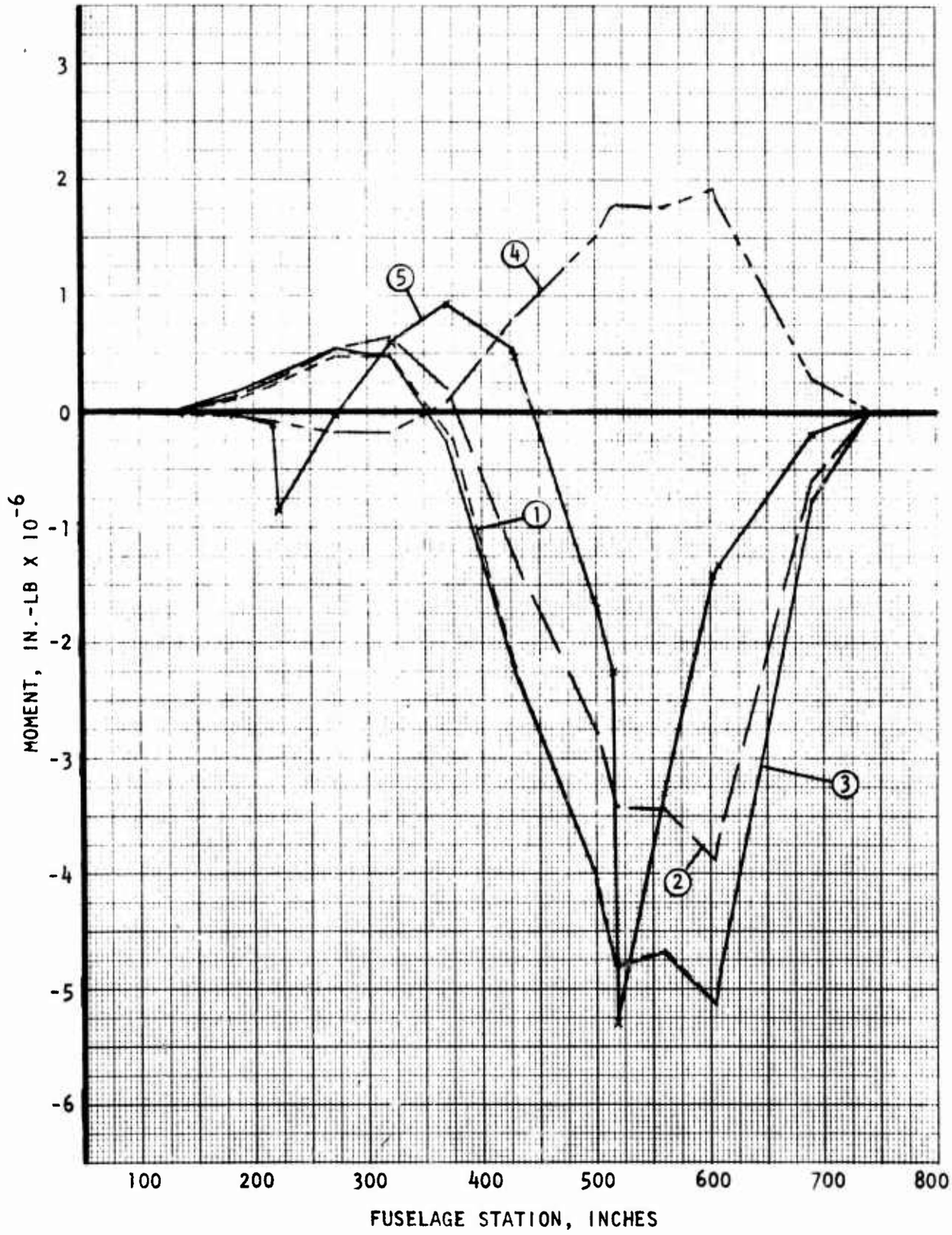

Figure 113. D572-4B fuselage ultimate bending moment diagram.

TABLE 12. D572-4B FUSELAGE ULTIMATE SHEAR AND BENDING MOMENTS

	CONDITION NO 1		CONDITION NO 2		CONDITION NO 3	
STATION	SHEAR-VZ	MOMENT-MY	SHEAR-VZ	MOMENT-MY	SHEAR-VZ	MOMENT-MY
138.0	754.1	12066.4	889.3	14228.7	1430.2	22883.0
184.0	3649.8	113357.6	3763.8	121250.6	4573.8	160975.6
218.0	3549.9	235752.9	4263.0	257706.6	4354.0	312749.6
222.0	3883.2	253619.0	4612.9	275458.4	4656.3	330770.2
272.0	1829.9	474590.1	3592.3	546519.7	701.1	545849.0
320.0	-2211.6	465428.4	660.1	648578.2	-3761.1	472409.9
370.0	-26013.7	-240205.3	-18773.9	195732.2	-26485.1	-283745.1
426.0	-40676.3	-2107524.0	-31613.7	-1215122.0	-40695.2	-2164794.0
430.0	-9712.9	-2209302.0	-6747.0	-1291842.0	-9232.0	-2264647.0
499.0	-41242.1	-3966248.0	-34627.7	-2719266.0	-40979.5	-3996942.0
501.0	-42179.7	-4049669.0	-35443.0	-2789336.0	-41946.7	-4079867.0
515.0	-51613.9	-4706223.0	-43185.8	-3339737.0	-51580.8	-4734559.0
519.0	8514.6	-4792421.0	3852.4	-3418403.0	9110.8	-4819498.0
560.0	-3207.9	-4683633.0	-5049.1	-3442934.0	-3109.5	-4696470.0
604.0	70878.4	-5117083.0	52768.2	-3876899.0	71295.2	-5134551.0
608.0	70055.1	-4835215.0	52231.1	-3666900.0	70441.4	-4851077.0
690.0	29184.7	-766383.0	22666.4	-596104.0	29184.7	-766405.0
741.0	588.9	-7156.8	478.4	-5912.4	568.9	-7178.8
743.0	535.4	-6032.5	434.9	-4999.1	535.4	-6054.5
764.0	0.0	0.0	0.0	0.0	0.0	0.0

TABLE 13. D572-4B FUSELAGE ULTIMATE SHEAR AND BENDING MOMENTS

	CONDITION NO 4		CONDITION NO 5	
STATION	SHEAR-VZ	MOMENT-MY	SHEAR-VZ	MOMENT-MY
138.0	-282.8	-4524.6	-409.4	-6549.8
184.0	-1368.6	-42506.9	-981.8	-38545.3
218.0	-1331.1	-88402.1	-2513.2	-97559.6
222.0	-1456.1	-93976.4	17249.1	-854019.3
272.0	-686.0	-177957.6	14239.2	-46526.6
320.0	829.6	-174511.1	12521.9	595738.1
370.0	9755.4	90113.4	1223.3	939365.6
426.0	15253.7	790367.7	-15303.9	545108.6
430.0	3642.4	828159.9	-24120.5	466259.8
499.0	15465.6	1487385.0	-36717.5	-1632649.0
501.0	15817.2	1518667.0	-37112.2	-1706477.0
515.0	19355.0	1764871.0	-40544.4	-2250072.0
519.0	-3193.0	1797194.0	51302.8	-5291215.0
560.0	1202.8	1756393.0	45785.0	-3330914.0
604.0	-26579.2	1918925.0	20741.9	-1407545.0
608.0	-26270.5	1813225.0	20358.8	-1325343.0
690.0	-10944.2	287421.4	7296.0	-191496.7
741.0	-220.8	2714.7	147.0	-1698.8
743.0	-200.7	2293.2	133.7	-1418.1
764.0	0.0	0.0	0.0	0.0

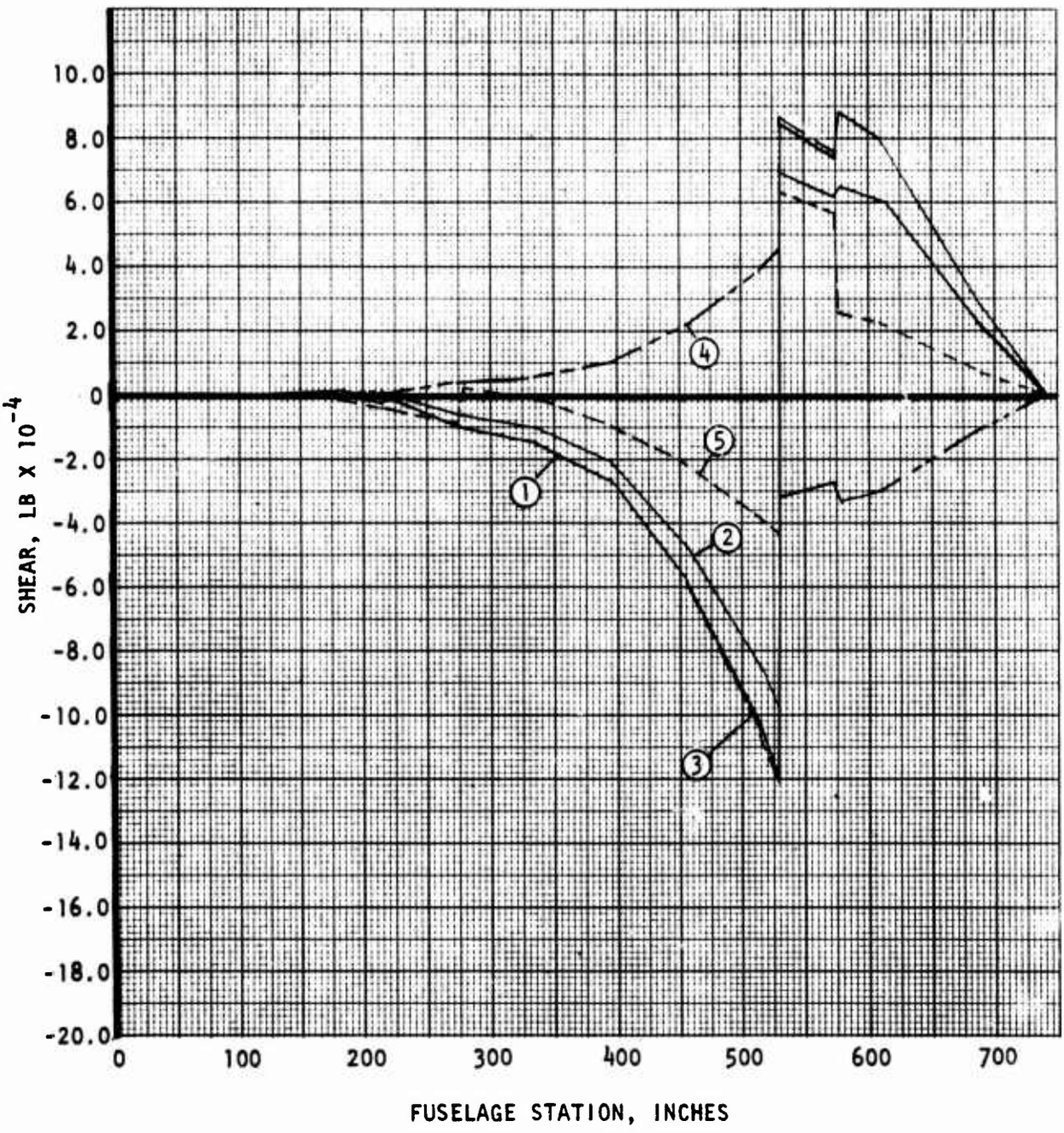

Figure 114. D572-5A fuselage ultimate shear diagram.

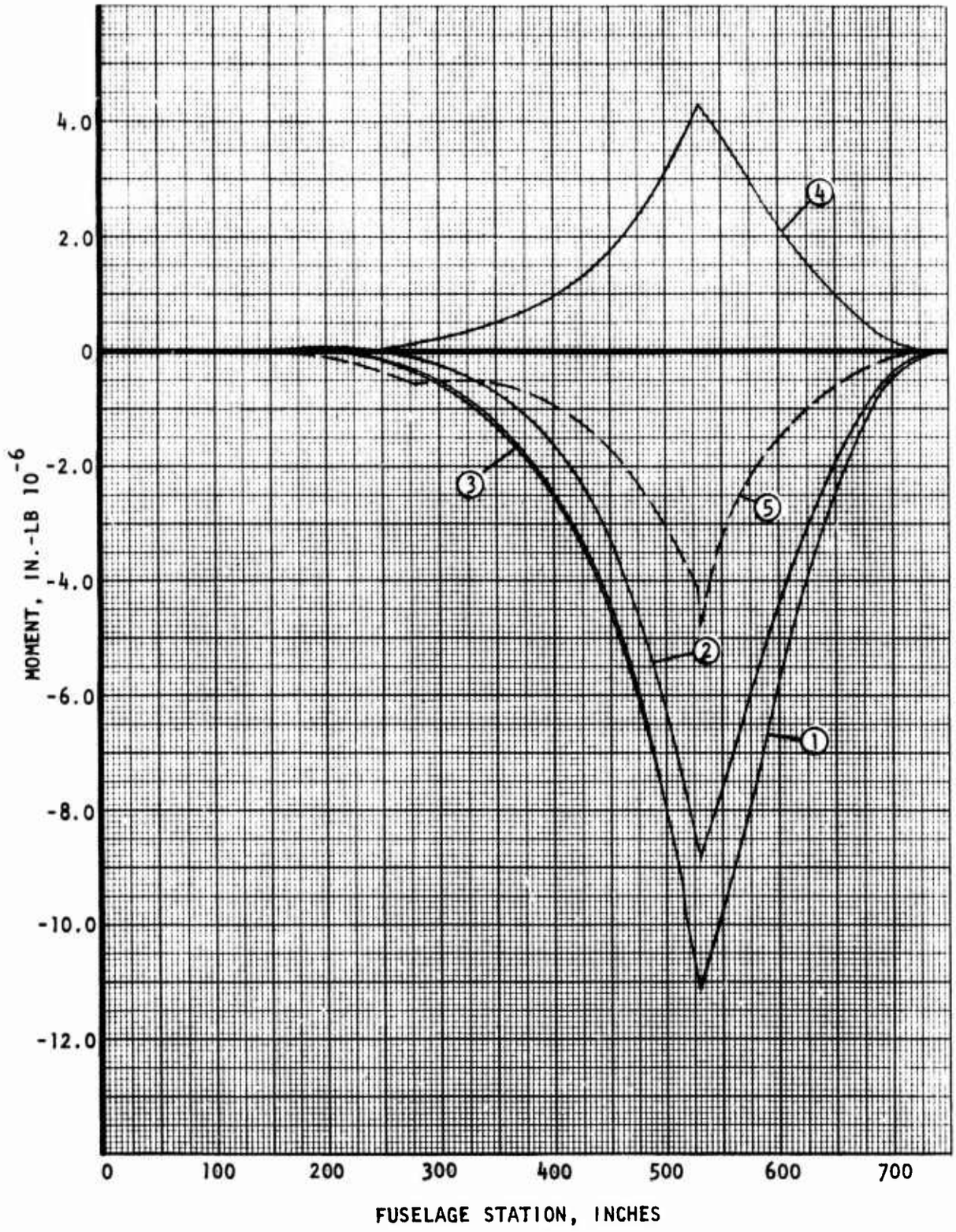

Figure 115. D572-5A fuselage ultimate bending moment diagram.

TABLE 14. D572-5A FUSELAGE ULTIMATE SHEARS AND BENDING MOMENTS

	CONDITION NO. 1		CONDITION NO 2		CONDITION NO 3	
STATION	SHEAR-VZ	MOMENT-MY	SHEAR-VZ	MOMENT-MY	SHEAR-VZ	MOMENT-MY
138.0	497.2	5611.6	769.8	14682.0	457.7	8849.5
184.0	173.7	25042.3	1032.3	56329.7	155.5	22954.3
214.0	-3140.9	-19464.3	-1180.5	54106.7	-3114.6	-21431.5
218.0	-1211.2	-28168.5	459.6	52664.8	-1177.2	-30615.0
274.0	-10116.3	-319791.4	-6130.7	-85370.6	-9511.9	-305760.9
278.0	-9699.6	-359823.2	-5919.2	-109469.7	-9261.3	-341307.2
335.0	-15135.0	-1073309.0	-10073.9	-565271.3	-14660.7	-1021374.7
395.0	-27307.4	-2346581.0	-20654.1	-1487111.0	-27225.7	-2276167.0
455.0	-58557.0	-4922516.0	-47292.3	-3525502.0	-59280.7	-4671357.0
514.0	-103305.6	-9697466.0	-85228.2	-7434855.0	-104800.0	-9711737.0
516.0	-105094.3	-9905865.0	-86624.6	-7606707.0	-106551.8	-9923088.0
528.0	-119273.5	-11252071.0	-97794.0	-8713219.0	-120515.2	-11285489.0
532.0	84659.2	-11321695.0	69414.9	-8769977.0	86637.6	-11353243.0
573.0	73904.3	-8670744.0	62043.9	-6075071.0	76541.2	-8008075.0
577.0	87965.5	-7747003.0	65167.5	-5820647.0	86726.4	-7681539.0
608.5	80033.6	-5101015.0	59942.4	-3850167.0	79220.7	-5067671.0
690.0	27411.9	-722609.0	20956.0	-553558.0	27411.9	-722590.0
741.0	650.4	-7018.6	528.5	-5703.1	650.4	-7000.6
743.0	584.6	-5783.6	475.0	-4699.6	584.6	-5765.6
764.0	0.0	0.0	0.0	0.0	0.0	0.0

TABLE 15. D572-5A FUSELAGE ULTIMATE SHEARS AND BENDING MOMENTS

	CONDITION NO. 4		CONDITION NO. 5	
STATION	SHEAR-VZ	MOMENT-MY	SHEAR-VZ	MOMENT-MY
138.0	-186.5	-3605.0	-629.5	-12169.7
184.0	-65.2	-5594.3	-1951.4	-71529.2
214.0	1177.7	7292.3	-3966.0	-160289.9
218.0	454.1	11555.7	-3604.2	-175550.2
274.0	3793.3	119902.7	-6952.1	-520740.0
278.0	3712.1	134913.4	2290.7	-534062.9
335.0	5675.3	402452.5	-1542.0	-512725.1
395.0	10239.9	879906.2	-9402.0	-841043.7
455.0	21958.4	1845855.0	-21957.5	-1781627.0
514.0	38739.1	3636433.0	-38320.7	-3560031.0
516.0	39409.9	3714581.0	-38930.4	-3637281.0
528.0	44727.1	4219402.0	-43510.5	-4131926.0
532.0	-31744.6	4245366.0	62742.4	-4772902.0
573.0	-27711.6	3026514.0	57277.4	-2313316.0
577.0	-32986.9	2905116.6	26014.1	-2146732.0
608.5	-30012.5	1912876.0	22604.1	-1380995.0
690.0	-10279.3	270985.5	6852.8	-180626.8
741.0	-243.8	2645.9	162.4	-1740.7
743.0	-219.1	2183.0	145.9	-1432.4
764.0	0.0	0.0	0.0	0.0

Composite Vehicle (D572-4B)

Mach No.	Altitude	Load Factor	Load per Side (pounds)
1.2	Sea Level	8	6820
1.2	Sea Level	-3	-2558

Metal Vehicle (D572-5A)

1.2	Sea Level	8	8104
1.2	Sea Level	-3	-3039

Landing gear limit loads are presented in Tables 16 and 17 for the composite and metal configuration. These loads were calculated by the landing gear module of SWEEP. They are referenced as paralleled and normal to the gear structure.

DAMAGE TOLERANCE

The damage tolerance criteria established in MIL-STD-1530 is proposed for ADCA. The criteria presented in "Durability and Damage Tolerance Certification Criteria for Advanced Composite Structures," reproduced in NA-75-604, is used as a guide.

SERVICE LIFE

The ADCA will be designed for a service life of 10,000 hours.

MATERIAL ALLOWABLES

The material properties for use in the structural design of ADCA have been documented in TFD-75-766, "Materials Properties Data for Preliminary Structural Design/Analysis of Advanced Design Composite Aircraft." The data have been selected from sources including MIL-HDBK-5B, AFML TR 72-232, and the Advanced Composites Design Guide. Cross-ply properties have been developed using Rockwell's AC-50 computer program.

STRUCTURAL TEMPERATURES

A preliminary definition of the temperatures that the ADCA structure will experience is presented to identify the structural areas where potential thermal problems may occur. Two points in the flight envelope were examined. The resulting steady-state temperatures are shown in the following paragraph.

TABLE 16. D572-4B LANDING GEAR LOADS

** LGEAR - IP(60) **

	WEIGHT	LOAD FACTOR	LANDING SPEED (FT/SEC)	SINKING SPEED (FT/SEC)
TAKE-OFF	41772.0	1.629	299.7	6.00
LANDING	26822.0	2.748	241.0	10.00

LANDING GEAR LOADS

		MAIN LANDING GEAR		NOSE LANDING GEAR	
		TAKE-OFF	LANDING	TAKE-OFF	LANDING
TWO POINT	AXIAL	18859.	33888.	4478.	6825.
	NORMAL	7660.	13764.	4643.	7077.
SPIN UP	AXIAL	21326.	35586.	3460.	5176.
	NORMAL	6873.	11469.	8671.	12971.
SPRING BACK	AXIAL	16273.	29241.	5308.	8089.
	NORMAL	-4328.	-6564.	4425.	6526.
BRAKED ROLL	AXIAL	39003.	30277.		
	NORMAL	9647.	7488.		
DRIFT LANDING	AXIAL	9819.	17645.		
	NORMAL	7029.	12630.		
UNSYS. BRAKING	AXIAL	29871.	19876.	10757.	6173.
	NORMAL	7388.	4916.	11395.	6967.
TOWING	AXIAL	27659.		472.	
	NORMAL	7681.		18008.	
TURNING	AXIAL	50125.		8432.	
	NORMAL	29939.		7244.	

TABLE 17. D572-5A LANDING GEAR LOADS

** LGEAR - IP(6C) **

	WEIGHT	LOAD FACTOR	LANDING SPEED (FT/SEC)	SINKING SPEED (FT/SEC)
TAKE-OFF	41297.0	1.629	284.0	6.00
LANDING	30658.0	2.748	249.1	10.00

LANDING GEAR LOADS

		MAIN LANDING GEAR		NOSE LANDING GEAR	
		TAKE-OFF	LANDING	TAKE-OFF	LANDING
TWO POINT	AXIAL	18461.	38097.	3436.	8869.
	NORMAL	8041.	16593.	859.	2222.
SPIN UP	AXIAL	16676.	30968.	2764.	8805.
	NORMAL	10447.	34253.	2200.	6779.
SPRING BACK	AXIAL	19267.	39761.	3436.	8869.
	NORMAL	13247.	23929.	1969.	6053.
BRAKED ROLL	AXIAL	26513.	23636.		
	NORMAL	29611.	26396.		
DRIFT LANDING	AXIAL	9104.	18787.		
	NORMAL	7540.	15560.		
UNSYS. BRAKING	AXIAL	21960.	15916.	11184.	9233.
	NORMAL	24527.	17776.	7760.	5624.
TOWING	AXIAL	26000.		5460.	
	NORMAL	15741.		14964.	
TURNING	AXIAL	42072.		5460.	
	NORMAL	22438.		2730.	

Altitude (ft)	Mach	Temperature T_{TOTAL} (°F)	Temperature T_{SKIN} (°F)
20,000	1.5	185	170
20,000	1.7	250	220

The total temperature is the temperature that will occur in inlet ducts and on leading edges. The skin temperature will be experienced over the external surfaces with very little variations. For metal surfaces small gradients of the temperature through the skins will occur. For relatively thick low thermal conductivity, composite materials, larger thermal gradients will exist at the onset of heating. A transient temperature analysis is required to obtain these gradients.

The temperature of the engine case is shown in Figure 116.

MATERIALS SELECTION

GUIDELINES

The materials selected as potential candidates for the structural concepts used in this study were only those considered to be mature by 1980. This implies that the material must not only be in production but that physical properties and producibility data will be available by 1980.

COMPOSITES

Twenty-two combinations of fiber and matrix material have been considered for application to ADCA. These materials are based on a survey of the potential materials which are presently in use or in development. As shown in Figure 117, the composites which are judged to meet the guidelines described above are indicated by a check (✓) mark in the matrix. Other combinations which are not expected to be available by 1980 or which offer no advantages which would justify their development are shown as a blank. For the Task I study, the advanced composites which are shaded in Figure 118 have been selected for ADCA applications. These are graphite (PAN)/epoxy, graphite (PAN)/polyimide, Kevlar/epoxy, fiberglass/epoxy, and quartz-polyimide.

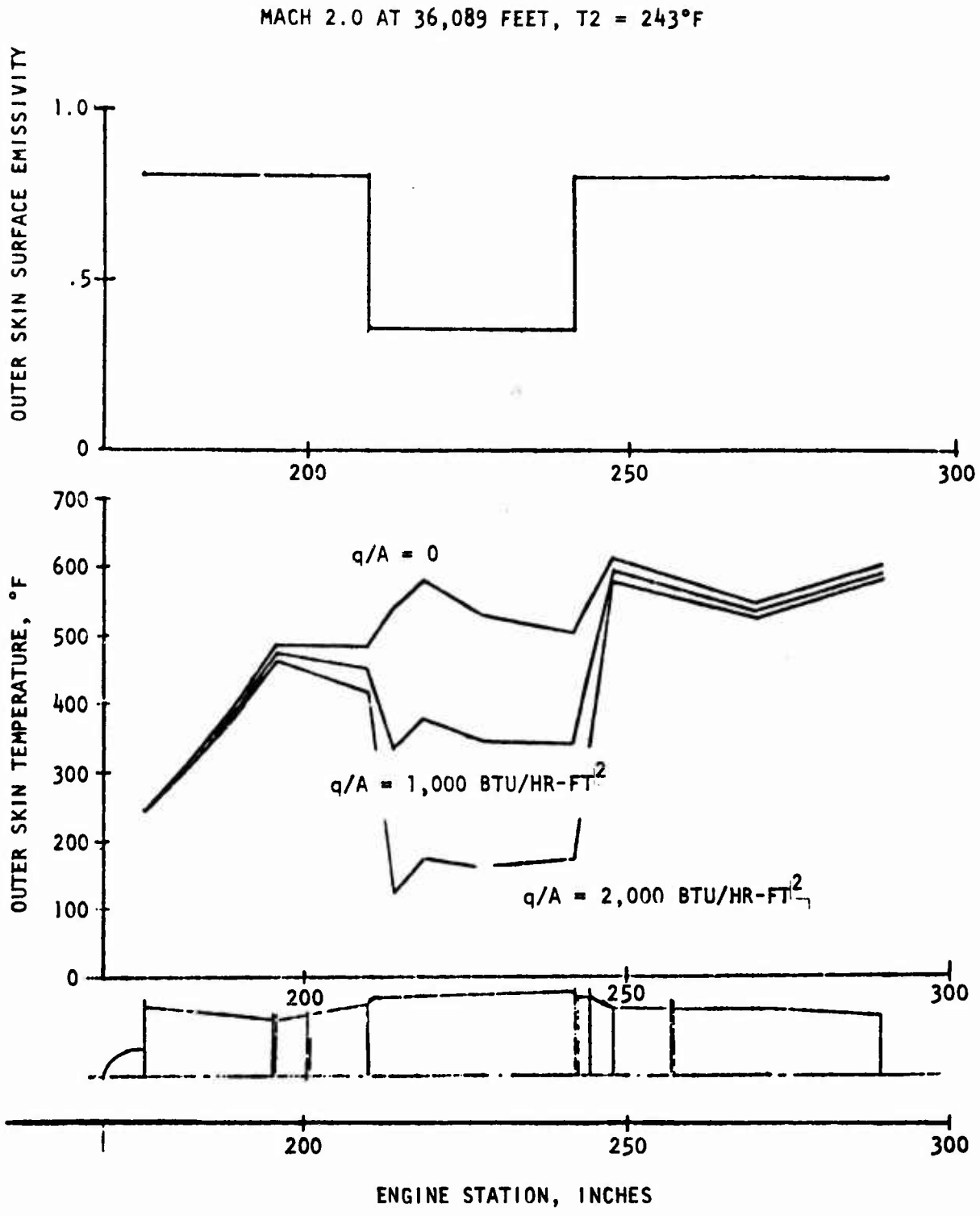

Figure 116. Engine heat rejection YJ101.

MATRIX \ REINFORCEMENT	GRAPHITE-PAN	GRAPHITE-PITCH	BORON/W	BORON/C	KEVLAR	FIBERGLASS	QUARTZ
EPOXY	✓	✓	✓	✓	✓	✓	✓
POLYIMIDE	✓	✓	✓	✓	✓	✓	✓
POLYSULPHONE	✓	✓			✓	✓	
ALUMINUM			✓	✓			
TITANIUM			✓	✓			

Figure 117. Composite material candidates.

METALLICS

The following new aluminum alloys have been reviewed:

2024-T81	Sheet and Plate
2048-T851	Sheet and Plate
7005-T63	Sheet and Plate
7049-T73	Die Forging
7050-T736	Die Forging
7050-T73651	Plate
7175-T736	Die Forging
7475-T76	Sheet

The selection of aluminum alloys for use on the ADCA metal baseline aircraft was based primarily on a few key properties. For fuselage skins and lower wing skins where the primary loads are shear or tension, high fracture toughness and good tensile yield were dominating properties, resulting in the choice of 2048-T851 for these applications. This alloy has the same toughness as the 2024 series but a 20 percent higher yield. For upper wing skins or fuselage longerons where high strength and good fracture toughness is required, 7475-T76 was selected. This material exhibits slower crack growth than 7175 and 7075 with a slightly lower yield strength. For die forgings, 7049, 7050, or 7175 will be used depending on thickness.

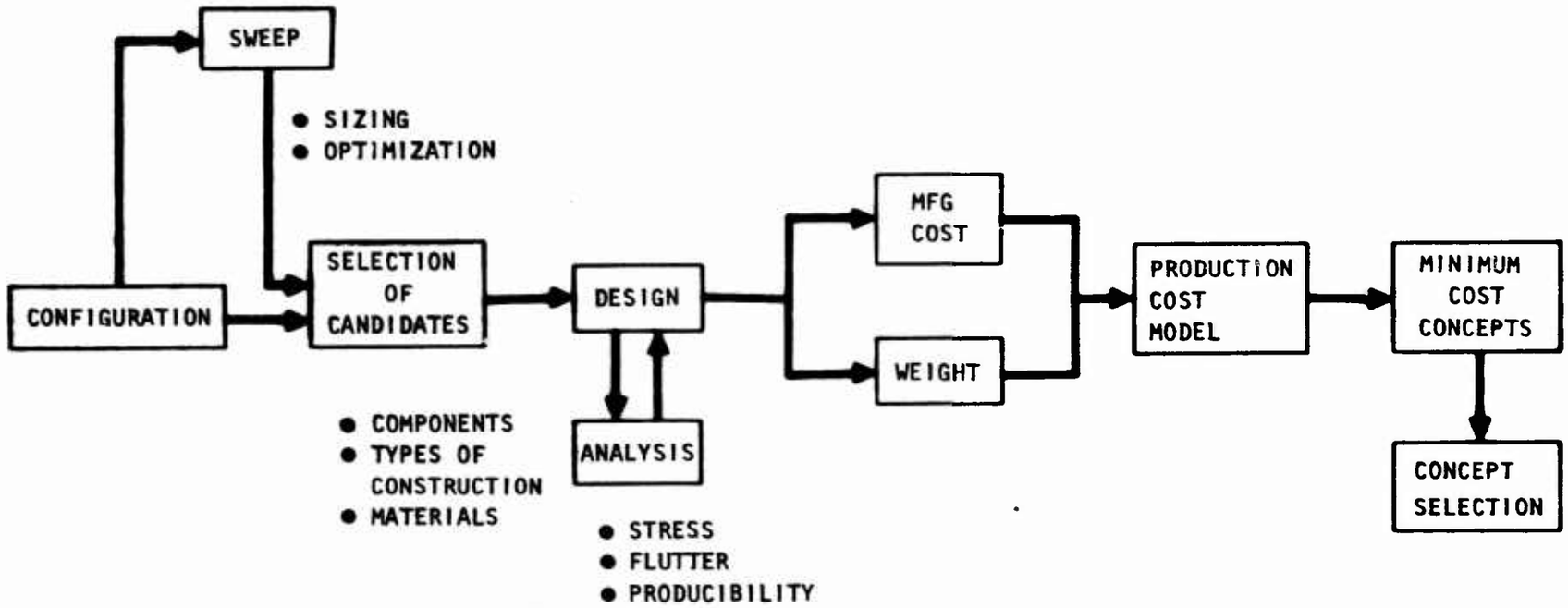

Figure 118. Trade study flow diagram.

Among the titanium alloys considered are:

10V-2Fe-3Al
3Al-8V-6Cr-4Mo-4Zr
6Al-2Mo-2Cr-2Sn-2Zr-.25Si
6Al-4V

Although the first three of these alloys have distinct advantages for special applications, 6-4 is the titanium alloy which has most successfully demonstrated superplasticity in Rockwell's superplastic forming process development. Since the majority of the titanium applications for the all-metal baseline airplane employ this unique process, 6-4 alloy has been selected. The alloy also offers the promise of higher strength properties with improved, low-distortion heat treatment processes now being developed.

HONEYCOMB CORE

Honeycomb core materials which were evaluated for ADCA applications include both metallics and composites. These are:

5052 Aluminum Alloy
5056 Aluminum Alloy
2024 Aluminum Alloy
Aluminum Alloy ACG (commercial grade)
Nomex
HRP Fiberglass/Phenolic
HRH Fiberglass/Polyimide
Graphite/epoxy
Graphite/Polyimide

Because of the corrosion problems experienced with aluminum core, its use has been limited to a few applications on the all-metal airplane. The alloy selected is 5056, which represents the best compromise between cost, weight, and corrosion resistance. For temperatures up to 350° F, HRP fiberglass is used where stiffness is not critical. Graphite/epoxy core is the choice for areas where a high shear modulus is required. In higher temperature applications, HRH fiberglass/polyimide or graphite/polyimide core will be used.

COMPOSITE APPLICATION TRADE STUDY

To assure that the all-composite airplane has exploited the most cost-effective structural arrangement, trade studies on areas of the aircraft have

been conducted. The methodology used for the trade studies is shown in Figure 118. Starting with the -4B configuration, three structural areas were identified for detail study. For each of these areas, candidate types of construction were selected, resulting in the following design concepts.

Wing Outer Panel

- Full-depth honeycomb
- Multi-spar, plate skins

Wing Center Section

- Honeycomb panel
- Multi-spar, plate skins
- Plate stiffener

Fuselage Section

- Honeycomb panel
- Skin stiffener

After the concepts were identified, detail designs of each one were prepared. Simultaneously, the optimization module of the SWEEP was used to optimize the spar spacing, skin thickness, and other variables for minimum weight. The SWEEP data were then used for the designs. Analysis of the designs for strength, flutter, and producibility was then conducted and resulting changes iterated through the design loop. The manufacturing cost and the weight of the final designs was determined and the results (in terms of dollars per pound) were inputted into the Production Cost Model (PCM) computer program. The program calculates the flyaway cost of the airframe structure for each of the different designs. Using these costs, in conjunction with an assessment of relative reliability, technical risk, maintainability, repairability, and compatibility with the rest of the structure, the optimum design for each area was selected.

WING OUTER PANEL

The main structural box from Xp114 to Xp171, between the front and rear spars, was investigated for this study. The spars, the root joint, and tip splice were not considered part of the trade. Figure 119 shows the full-depth honeycomb concept. Graphite/epoxy skins with 0°, ±45° and 90° plies are cocured to graphite/epoxy honeycomb core. The skins vary from .27 inch thick at the root to .11 inch at the tip. The core density varies from 6.5 pounds per cubic foot (pcf) to 4 pcf. The wing has been sized to meet both strength and flutter requirements.

The inboard skin panel and honeycomb core (X_F114 to X_F133) are sized by crushing loads resulting from the small radius of curvature. Outboard of X_F133 where the radius of curvature is greatly increased, thus reducing crushing loads, flutter requirements determine the ±45° skin plies, while bending loads establish the 0° ply requirements. The structural analysis of this design is shown on Figure 120.

The aircraft weight, using the full-depth honeycomb outer wing panel, is shown in Table 18. These data are part of the input to the PCM which was used to determine the cost of the aircraft using this type of construction. Table 19 shows the cost breakdown based on a 300-ship contract. The cost is flyaway cost in 1975 dollars and does not include engineering, research, test, spares, or maintenance.

An alternate design for the wing outer panel, employing a multi-spar concept, is shown on Figure 121. The number of spars was determined using a weight study on SWEEP in which a one-spar wing was compared to a two-spar arrangement. As shown in Table 20, the two-spar concept is over 100 pounds lighter so it was used for the design. As shown in Figure 121, the cover thickness varies from .60 inch at the root to .25 at X_F171. The 0° and 90° ply requirements in the inboard bay are determined by crushing loads as shown in the analysis in Figure 122. Outboard of X_F133, ±45° plies are established by GJ for flutter, while 0° and 90° ply thickness are designed by bending. The intermediate spars are sine wave beams fabricated from graphite/epoxy and secondary-bonded to the skins.

Table 21 shows the weight breakdown using the multi-spar construction. The cost of the aircraft is shown in Table 22.

A summary of the cost and weight of the outer wing concepts is shown in the next paragraph.

Concept	AMPR Weight (lb)	Cost Per Aircraft
Full-Depth Honeycomb	13,211	$2,769,000
Multi-Spar/Plate	13,265	$2,801,000

An assessment of the relative risk and comparison of the "illities" does not reveal any basic differences between the two concepts. Since both weight and cost of the full-depth honeycomb outer wing panel is lower than the alternate, the honeycomb wing has been selected.

WING CENTER SECTION

The wing center section extends from its junction with the outer panel at X_F114 to the centerline of the aircraft and from Y_F515 to Y_F606. Wing loads are transferred in the wing box across the top of the fuselage. The fuselage structure in this area is independent of the wing except for vertical shear and drag attachments. Three concepts for the structure in this area were investigated: honeycomb panels, plate skins with multi-spar, and plate skins with stringers.

TYP SPAR LAY-UP

SCHEMATIC ONLY ~ DO NOT SCALE

REF STRUCTURE

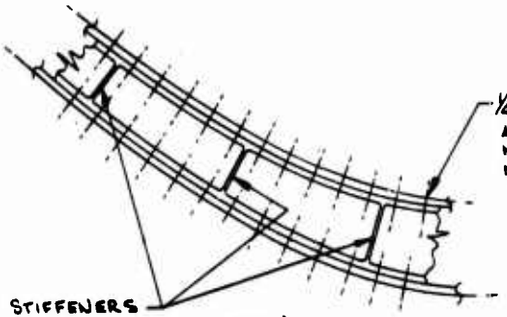

SECTION F-F

SCALE 1/4

UP

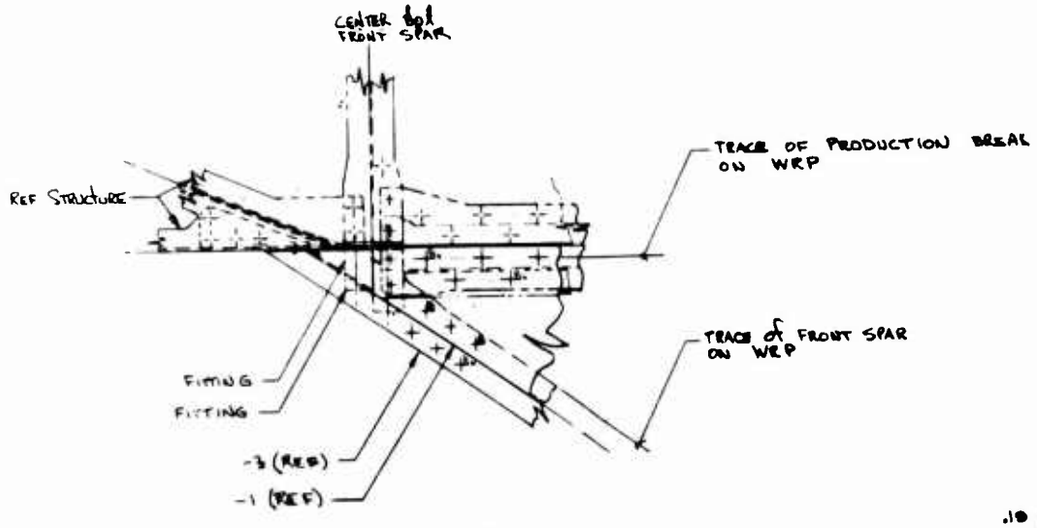

DETAIL E
PLAN VIEW
SCALE 1/4

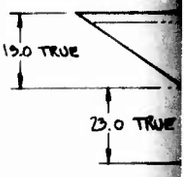

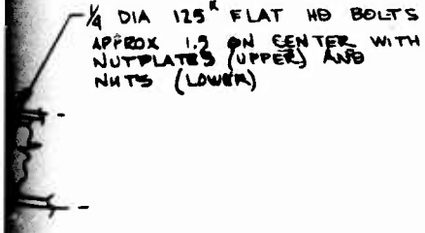

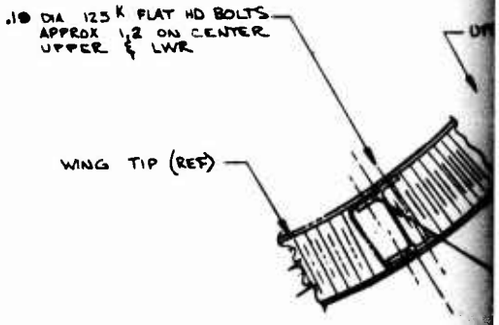

DETAIL C
SCALE 1/4
UP

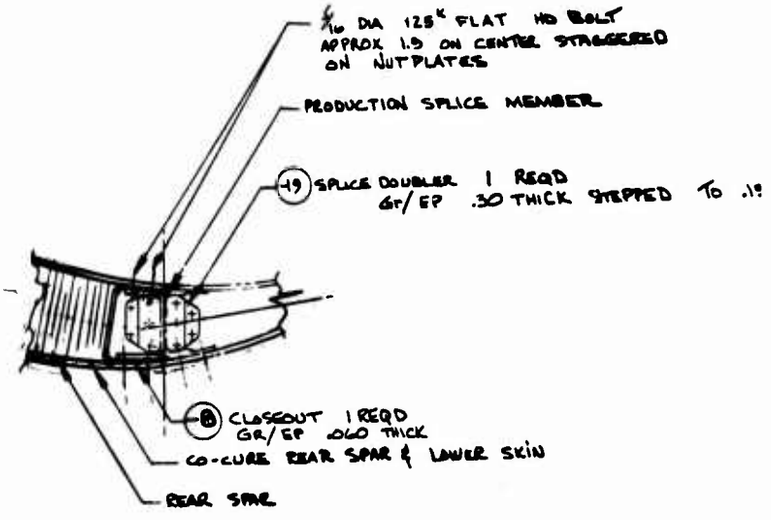

DETAIL D
SCALE 1/4

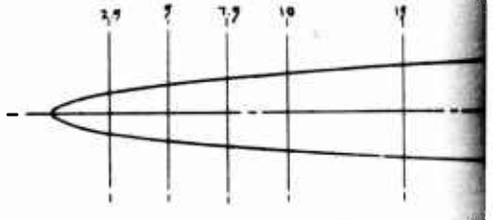

-3 FRONT SPAR
GR/EP
CAPS T. .
TO T. .
WEB T. .
STIFFENERS
(FWD SIDE
-2 LOWER
GR/

2

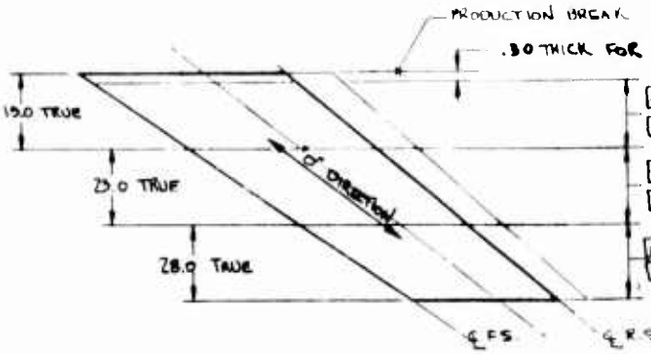

$[9_{16}/\pm 45_7/90_2]_s$ UPPER SKIN CONSTANT
$[9_{12}/\pm 45_9/90_1]_s$ LOWER SKIN CONSTANT
$[9_{11}/\pm 45_8/90_1]_s$ TAPERING TO $[0_7/\pm 45_6/90_1]_s$ UPPER SKIN
$[9_9/\pm 45_{11}/90_1]_s$ TAPERING TO $[0_6/\pm 45_6/90_1]_s$ LOWER SKIN
$[9_7/\pm 45_8/90_1]_s$ TAPERING TO $[0_2/\pm 45_6/90_1]_s$ UPPER SKIN
$[9_8/\pm 45_7/90_1]_s$ TAPERING TO $[0_4/\pm 45_6/90_1]_s$ LOWER SKIN

SKIN GAUGE SKETCH

NO SCALE
TYP UPPER & LWR

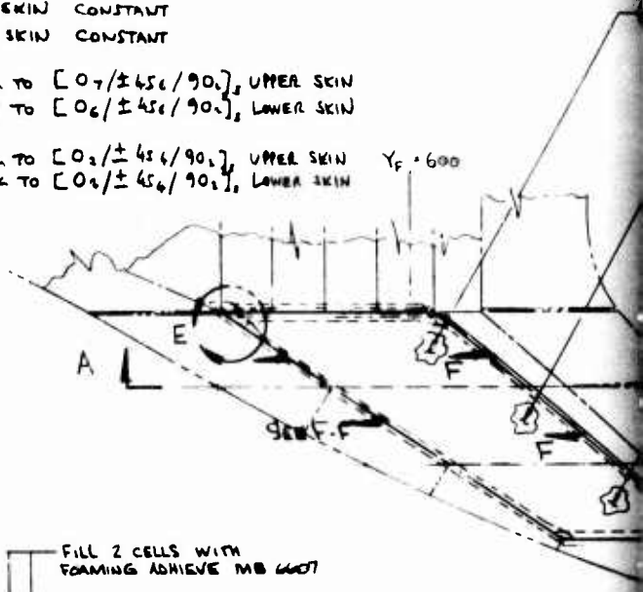

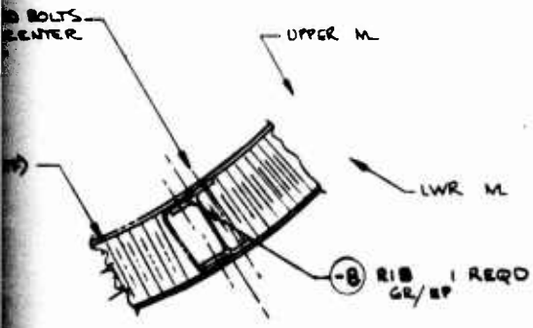

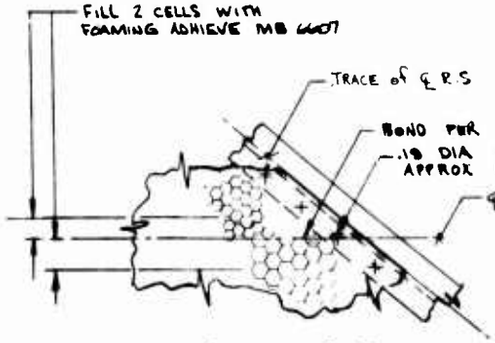

DETAIL C

SCALE 1/4
UP

SECTION B-B

SCALE 1/4

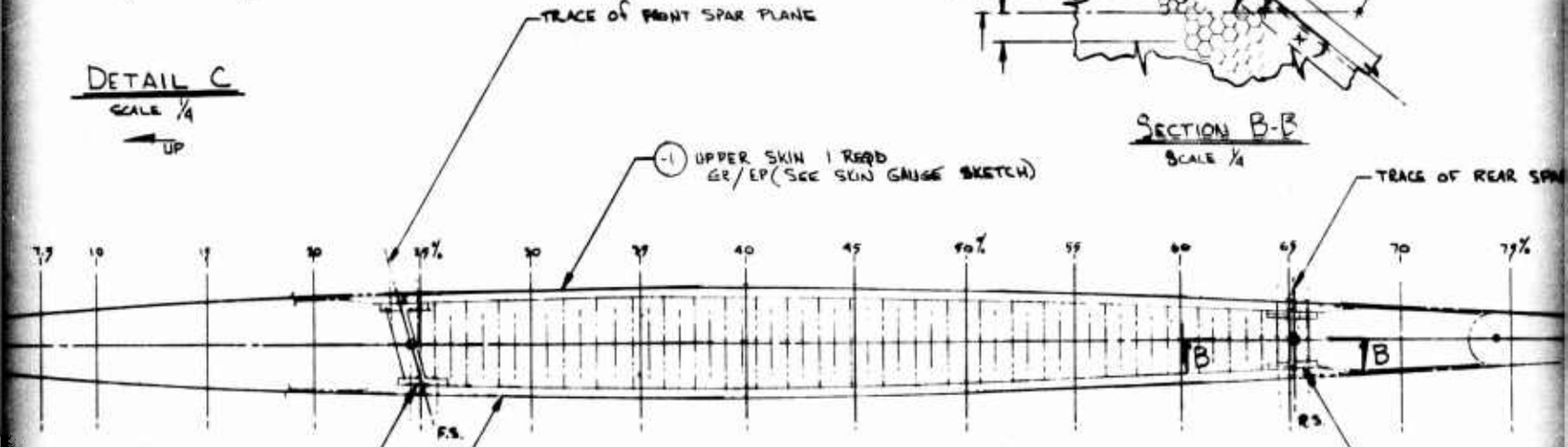

-3 FRONT SPAR 1 REQD
GR/EP
CAPS T = .80 INBD END TAPERS TO T = .20 OUTBD END
WEB T = .12
STIFFENERS .090 THICK 8.0 O.C. (FWD SIDE ONLY)

-2 LOWER SKIN 1 REQD
GR/EP (SEE SKIN GAUGE SKETCH)

-4 REAR SPAR 1 REQD
GR/EP
CAPS T = .80
TO T = .20
WEB T = .12
STIFFENERS .090

SECTION A-A

ROTATED NORMAL TO RIB CHORD
SCALE 1/4

BOND PER LB0120-032

NOTES:

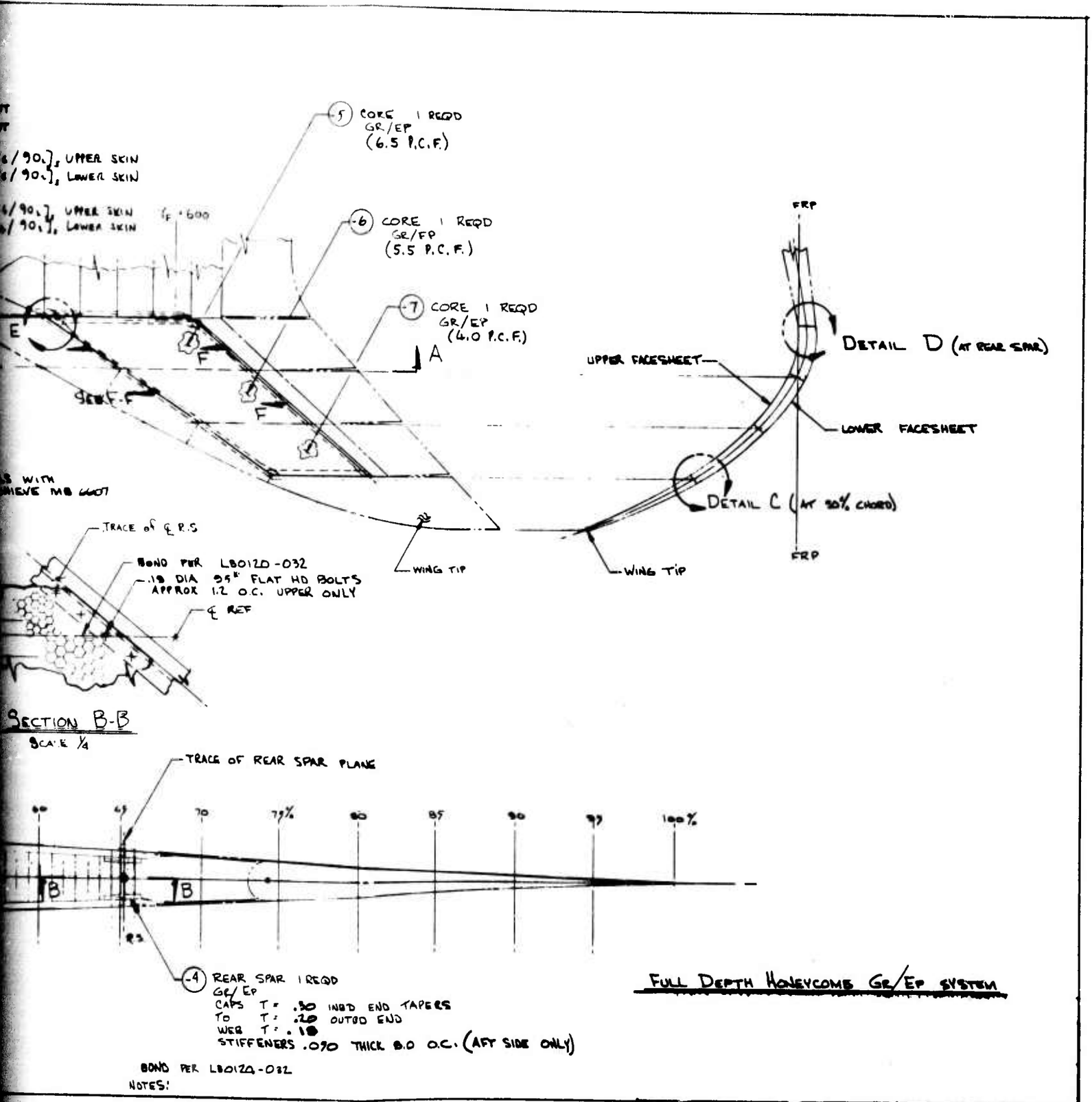

Figure 119. Full-depth honeycomb - wing outer panel.

4

ALL COMPOSITE AIRCRAFT

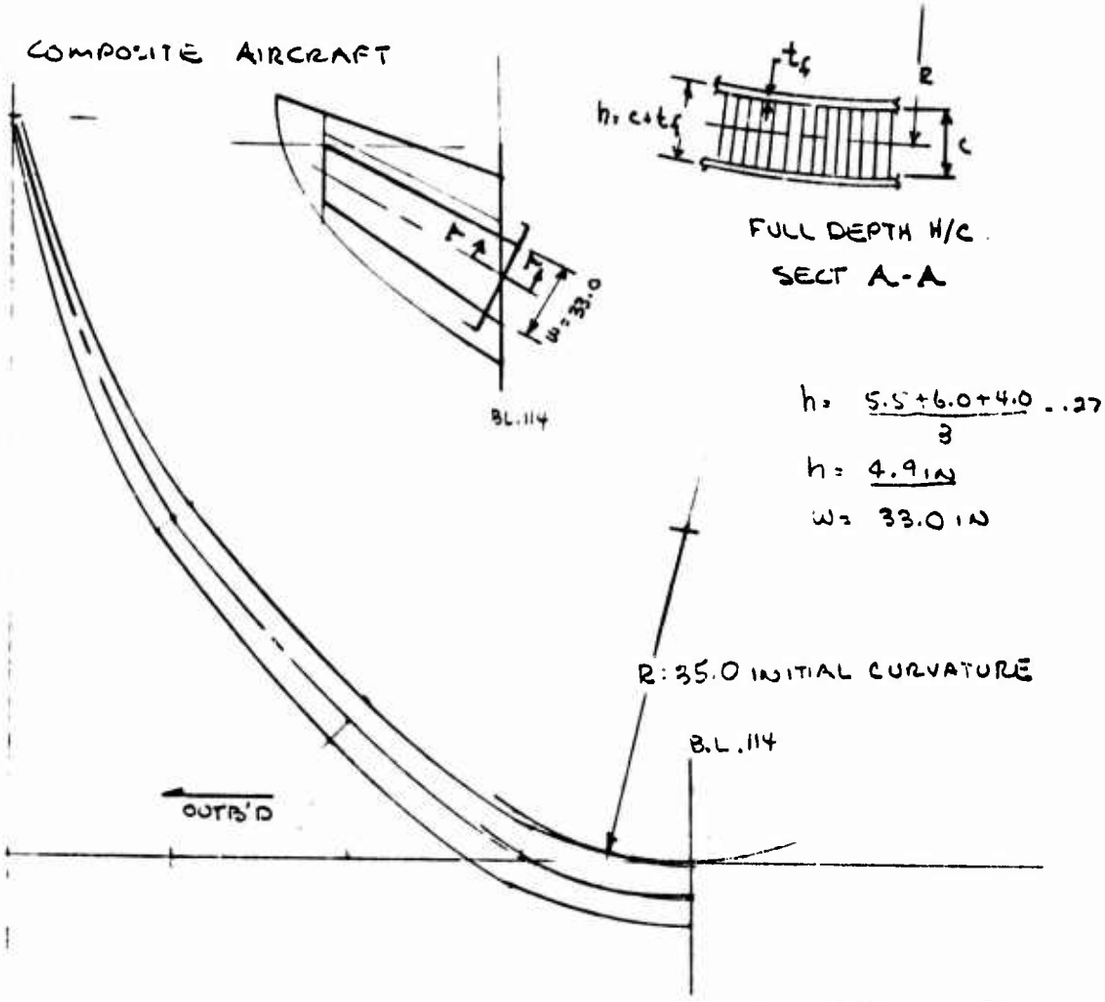

$h = \frac{5.5 + 6.0 + 4.0}{3} = .27$

$h = 4.9$ IN

$w = 33.0$ IN

FACESHEET MAT'L - GRAPHITE EPOXY HTS $[0_{11}^{40\%} / \pm 45_{9}^{50\%} / 90_{2}^{10\%}]_{S}$ · 54 PLIES

$h = 4.9$ IN $\quad t_f = .27$ IN

CORE MAT'L - GRAPHITE FABRIC (USE HRP PROPERTIES)

$Mom_{max} = 3.781 \times 10^6$ IN-LBS (ULT) UPLOADING

$N_Z = 8.0$
M_N 1.2 @ S.L
TEMP: 250 °F

$$f_b = \frac{M}{t_f h (w)} = \frac{3.781 \times 10^6}{(.27)(4.90)(33.0)} =$$

$$= \underline{36,606 \text{ PSI}} \quad (\text{HIGH})$$

$$N_x = \frac{M}{h w} = \frac{3.781 \times 10^6}{4.90 \times 33.0} = \underline{23,383} \text{ LB/IN}$$

Figure 120. Full-depth honeycomb - wing outer panel analysis.

REVISE 't' AND CROSSPLY PERCENT

$$[0_{14} / \pm 45_{7} / 90_{2}]_S = 60 \text{ PLIES}$$

47 % 47 % 6 %

$t_f = .30$ IN

$h = 5.17 - .30 = 4.87$ IN

REVISED MAT'L

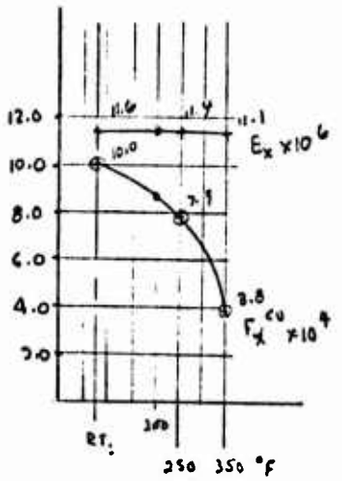

$E_x = 11.5 \times 10^6$

$F_x^{cu} = 88,000$

AT TEMP = 200°F

MOM = 3.781×10^6 IN-LBS (ULT)

$$f_b = \frac{3.781 \times 10^6}{(.30)(4.87)(33.0)} = 78,420 \text{ PSI}$$

$$N_x = \frac{3.781 \times 10^6}{4.87 \times 33.0} = 23,530 \text{ LB/IN CHORD}$$

R = 35.0 IN (INITIAL CURVATURE)

$$P_{N_{CRUSH}} \text{ (CORE)} = \frac{2 t_f (f_b)^2}{h E_s} + \frac{N_x}{R}$$

$$= \frac{2(.30)(78,420)^2}{4.87(11.5 \times 10^6)} + \frac{23530}{35.0}$$

$$= 65.9 + 672.3$$

$$= 738 \text{ PSI (ULT)}$$

USE 6.5 PCF CORE TEMP REDUCT. = .85

COMP. ALLOW = 900 (.85) = 765 PSI

$$M.S. = \frac{765}{738} - 1 = + .037$$

Figure 120. Full-depth honeycomb - wing outer panel analysis (cont).

CORE SHEAR CRIMPING

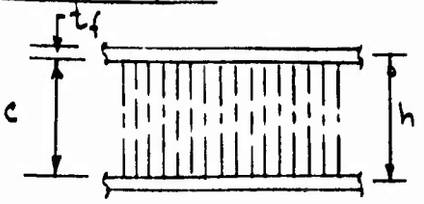

$t_f = .30$ in
$c = 4.57$ in

CORE: 5.5 PCF

$G_c' = 8{,}500$ PSI

$$F_{cs_{MAX}} = \frac{G_c'(c+2t_f)}{2t_f}, \quad \frac{8500(4.57+.60)}{2(.30} = 73{,}241 \text{ PSI}$$

INCREASE CORE -

CORE: 6.5 PCF $\quad G_c' = 11{,}000$ PSI

$F_{cs_{MAX}} = 94{,}782$ PSI $\qquad$ USE $F_n^{cu} = 88{,}000$ PSI

$$M.S. = \frac{88{,}000}{78{,}420} - 1 = + .12$$

Figure 120. Full-depth honeycomb - wing outer panel analysis (concl).

TABLE 18. D572-4B COMPOSITE ADCA BASELINE WEIGHTS

AIRCRAFT: C572-4 COMPOSITE ACCA BASELINE

AIRCRAFT WEIGHTS - IN POUNDS

	AL	TI	SI	BE	GR	EG	SA	TOTAL
FUSELAGE	78.	171.	69.	C.	2886.	27.	0.	3236.
FRAME/LONG	C.	171.	69.	C.	695.	0.	0.	935.
SKIN-STRGR	78.	C.	C.	C.	C.	C.	0.	78.
BOND HONEY	C.	0.	C.	C.	1391.	27.	0.	1418.
BRAZE HONEY		0.	C.				0.	0.
DIFF BOND		C.					0.	0.
MISC								805.
WING	125.	25.	0.	C.	2923.	0.	0.	3224.
SKIN-STRGR	C.	0.	C.	C.	C.	0.	0.	0.
MULTI-SPAR	C.	25.	C.	C.	515.	0.	0.	540.
BOND HONEY	125.	0.	C.	C.	2408.	0.	0.	2533.
BRAZE HONEY		0.	C.				0.	0.
DIFF BOND		0.					0.	0.
MISC								151.
CANARDS	C.	16.	2.	C.	117.	0.	0.	145.
SKIN-STRGR	C.	0.	C.	C.	C.	0.	0.	0.
MULTI-SPAR	C.	0.	C.	C.	C.	0.	0.	0.
BOND HONEY	C.	16.	2.	C.	117.	0.	0.	135.
BRAZE HONEY		0.	C.				0.	0.
DIFF BOND		C.					0.	0.
MISC								10.
NACELLE	C.	C.	C.	C.	C.	0.	0.	C.
FRAME/LONG	C.	C.	C.	C.	C.	0.	0.	0.
SKIN-STRGR	C.	0.	0.	C.	C.	0.	0.	0.
BOND HONEY	0.	0.	C.	C.	C.	0.	0.	0.
BRAZE HONEY		0.	C.				0.	0.
DIFF BOND		C.					0.	0.
MISC								0.

WEIGHT DATA - IN POUNDS	
AMPR WEIGHT	13211.
STRUCTURE WT	7885.
STRUCTURAL HOWE WT	133.
SYSTEM HOWE WT	133.
LANDING GEAR WT	1280.
FUEL SYSTEM WT	750.
ELECTRICAL SYSTEM WT	680.
HYDRAULIC SYSTEM WT	430.
AUX POWER SYSTEM WT	310.
ECS WT	530.
CREW ACCOM WT	320.
CONTROL & DISPLAY WT	120.
FLIGHT CONTROL WT	950.
ARMAMENT WT	500.
AICS MECHANISM WT	300.
EQUIPMENT WT	80.
ENGINE WT	5375.
EMPTY WT	19265.
FUEL WT	7060.
TOGW	30932.
DESIGN VARIABLES	
WING AREA-SQ FT	400.
CANARDS AREA-SQ FT	35.
WETTED AREA-SQ FT	1772.
WING + HORIZ AREA	435.
WING SPAN-FT	31.6
HORIZ SPAN-FT	10.0
OVERALL LENGTH-FT	57.0
ASPECT RATIO	2.50
DYNAMIC PRESSURE	2133.

TABLE 19. D572-4B COST BREAKDOWN FOR 300 UNITS

AIRCRAFT: D572-4 COMPOSITE ACCA BASELINE
ALL COSTS IN MILLIONS AND IN 1975 DOLLARS

PRODUCTION COST FOR 300 UNITS
UNIT AVG. FLYAWAY COST 2.769

WORK BREAKDOWN STRUCTURE	LABOR COST					MATERIAL COST		TOTAL
	MFG.	TOOL.	PLNG.	ENGR.	Q&A	MFG.	TOOL.	COST
TOTAL PROGRAM COST INCLUDING FEE	387.62	71.22	34.20	40.52	52.26	235.66	9.01	830.82
TOTAL PROGRAM COST INCLUDING G&A	352.38	64.74	31.09	36.84	47.51	214.24	8.19	755.32
TOTAL PROGRAM COST LESS G&A	320.84	58.95	28.31	33.54	43.26	195.06	7.46	687.75
AIR VEHICLE	320.84	58.95	28.31	33.54	43.26	195.06	7.46	687.75
AIRFRAME	164.22	52.33	17.11	33.54	24.63	188.89	6.62	487.33
BASIC STRUCTURE	96.89	52.33	10.73	8.11	16.93	58.96	6.62	250.58
FUSELAGE	37.54	33.60	5.17	4.85	8.05	24.31	4.25	117.78
WING	33.22	12.50	3.30	2.53	5.20	32.11	1.58	90.44
CANARDS	1.49	5.19	0.50	0.73	0.75	1.56	0.66	10.89
NACELLES	0.0	0.0	0.0	0.0	0.0	0.0	0.0	0.0
BASIC STRUCTURE ASSEMBLY	24.64	1.04	1.76	0.0	2.93	0.97	0.13	31.47
LANDING GEAR	0.0	0.0	0.0	0.60	0.0	13.48	0.0	14.07
FUEL SYSTEM	6.40	0.0	0.56	1.72	0.73	4.61	0.0	14.01
FLIGHT VEHICLE POWER	31.07	0.0	2.55	6.00	3.55	58.12	0.0	101.29
ENVIRONMENTAL CONTROL	0.0	0.0	0.0	2.09	0.0	25.90	0.0	27.99
CREW ACCOMMODATIONS	6.75	0.0	0.52	0.80	0.77	0.0	0.0	8.84
CONTROLS AND DISPLAYS	0.0	0.0	0.0	0.0	0.0	8.56	0.0	8.56
FLIGHT CONTROLS	20.72	0.0	1.42	0.0	2.37	0.0	0.0	24.50
ARMAMENT	0.0	0.0	0.0	0.30	0.0	19.26	0.0	19.55
AIR INDUCTION CONTROL SYSTEM	2.39	0.0	0.21	0.66	0.27	0.0	0.0	3.53
AIRFRAME INTEGRATION & CHECK	0.0	0.0	0.0	16.92	0.0	0.0	0.0	16.92
ENGINEERING TECHNOLOGIES	0.0	0.0	0.0	12.28	0.0	0.0	0.0	12.28
DESIGN SUPPORT TECHNOLOGIES	0.0	0.0	0.0	1.74	0.0	0.0	0.0	1.74
AIRFRAME INSTALL & CHECKOUT	0.0	0.0	0.0	2.89	0.0	0.0	0.0	2.89
PROPULSION (GFE)	0.0	0.0	0.0	0.0	0.0	0.0	0.0	0.33
AVIONICS (GFE)	0.0	0.0	0.0	0.0	0.0	0.0	0.0	0.0
A/V INTEGRATION, ASSY, INSTALL	156.62	6.62	11.20	0.0	18.63	6.17	0.84	200.08

TABLE 20. OUTBOARD WING PANEL COVER THICKNESSES

HONEYCOMB PANELS
DATA DITTO-T
8/29/75 2P

D572-4R WITH CURRENT FLUTTER DATA
OUTER EQUIVALENCE TORQUE BOX

STA NO	LOAD AXIS FUS STATION	LOAD AXIS BUTT PLANE	TOTAL THICKNESS UPPER	TOTAL THICKNESS LOWER	UPPER COVER 0	UPPER COVER +45°	UPPER COVER -45°	UPPER COVER 90°	LOWER COVER 0°	LOWER COVER +45°	LOWER COVER -45°	LOWER COVER 90°
					FULL DEPTH HONEYCOMB TORQUE BOX WT = 614 LBS/AC							
6	578.9	113.8	.25	.25	22	12	12	4	20	14	14	2
7	605.2	132.8	.29	.29	20	18	18	2	16	20	20	2
8	631.5	151.8	.23	.23	20	12	12	2	16	14	14	2
9	657.8	170.8	.17	.16	12	10	10	2	10	10	10	2
10	668.5	178.5	.12	.11	6	8	8	2	4	8	8	2
11	679.2	186.3	.08	.08	2	6	6	2	2	6	6	2
					MULTI-SPAR-PLATE-SKINS - 2 INTERM. SPARS TORQUE BOX WT. = 634 LBS/AC							
6			.41	.31	22	28	28	4	20	20	20	2
7			.31	.28	20	26	26	2	18	18	18	2
8			.34	.25	18	24	24	2	16	16	16	2
9			.25	.18	12	18	18	2	10	12	12	2
10			.20	.17	6	16	16	2	4	14	14	2
11			.14	.16	2	12	12	2	2	14	14	2
					MULTI-SPAR-PLATE-SKINS - 1 INTERM. SPAR TORQUE BOX WT. = 742 LBS/AC							
6			.53	.39	22	40	40	4	20	28	28	2
7			.49	.36	20	38	38	2	18	26	26	2
8			.41	.31	20	32	32	2	16	22	22	2
9			.33	.24	12	26	26	2	10	18	18	2
10			.26	.21	6	22	22	2	4	18	18	2
11			.25	.20	2	18	18	2	2	18	18	2

ALL WEIGHTS QUOTED ARE PER AIRCRAFT

TYP SPAR LAY-UP

TYP SINE WAVE LAY-UP

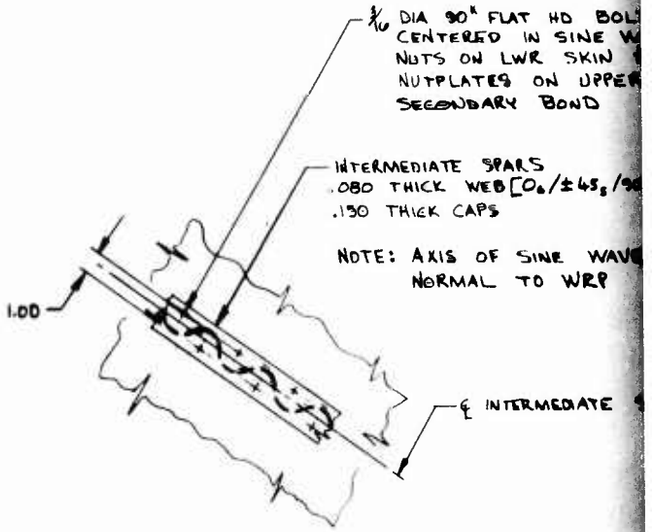

DETAIL D

SCALE 1/4

TYP INTERMEDIATE SPARS

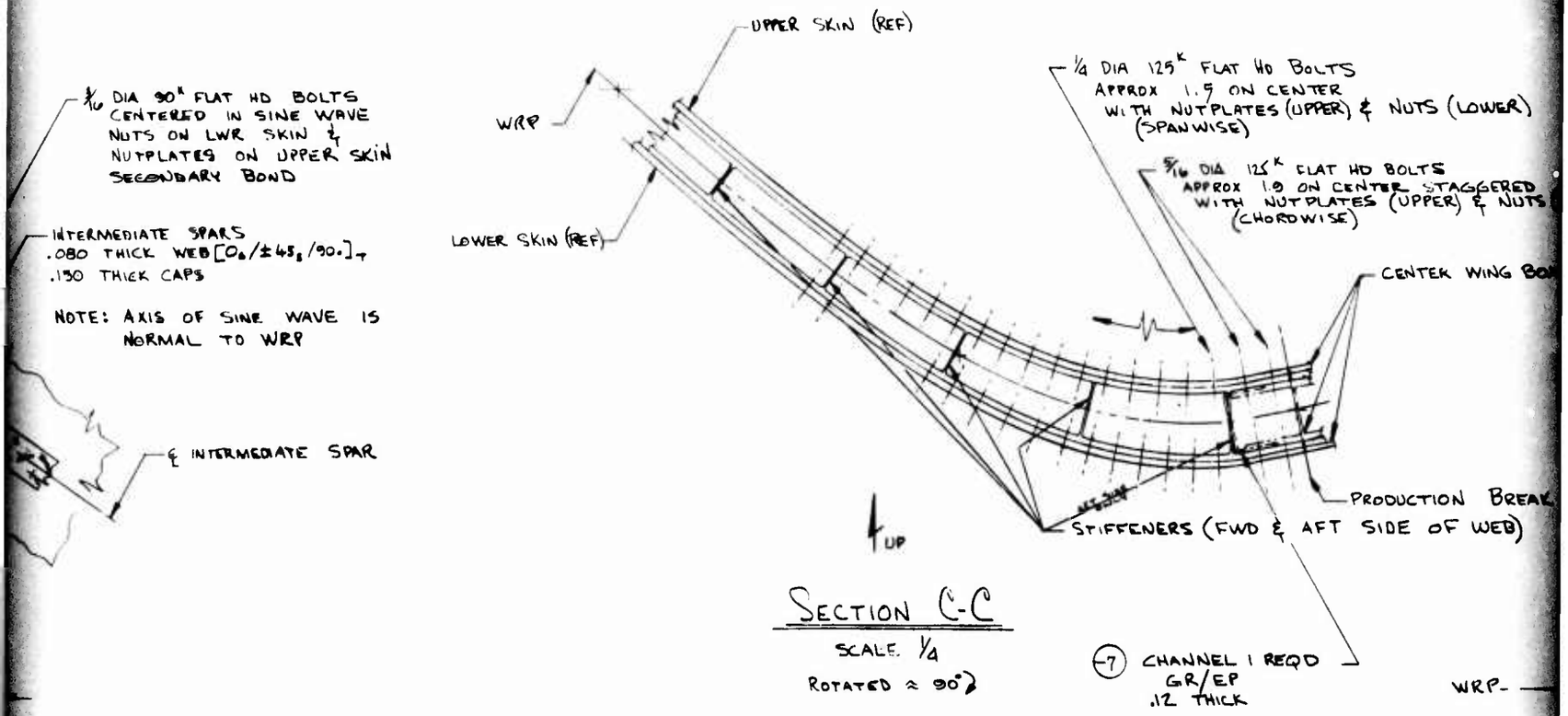

SECTION C-C

SCALE 1/4

ROTATED ≈ 90°

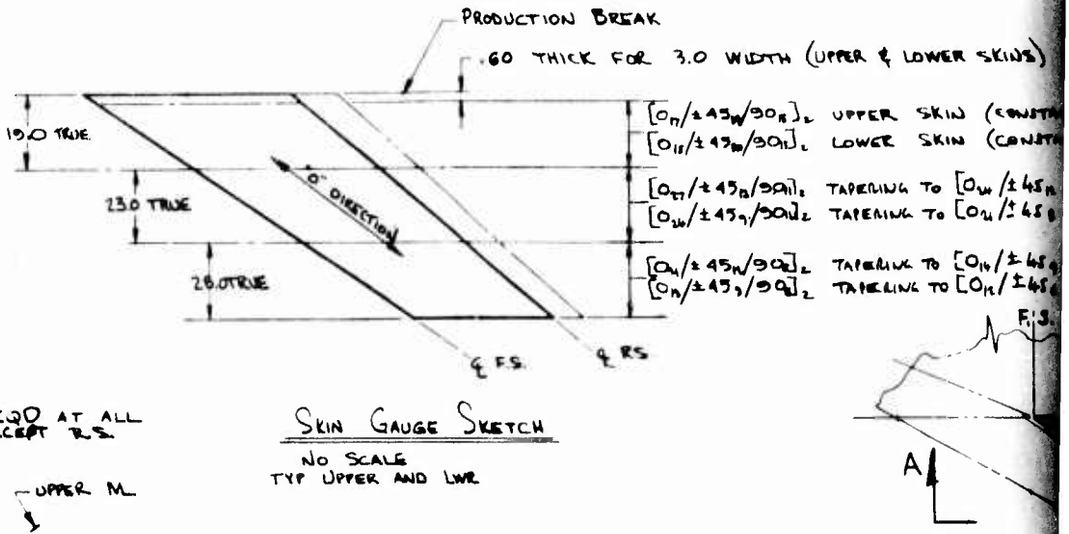

SKIN GAUGE SKETCH

NO SCALE
TYP UPPER AND LWR

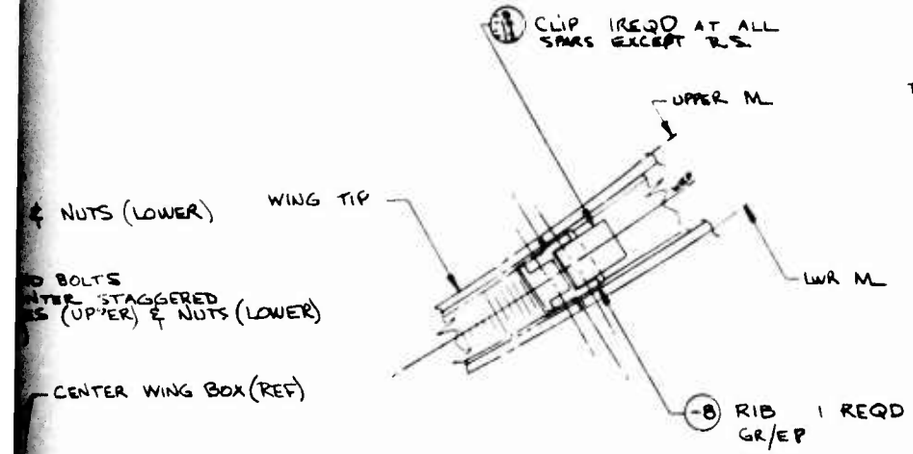

DETAIL B
SCALE 1/4
UP

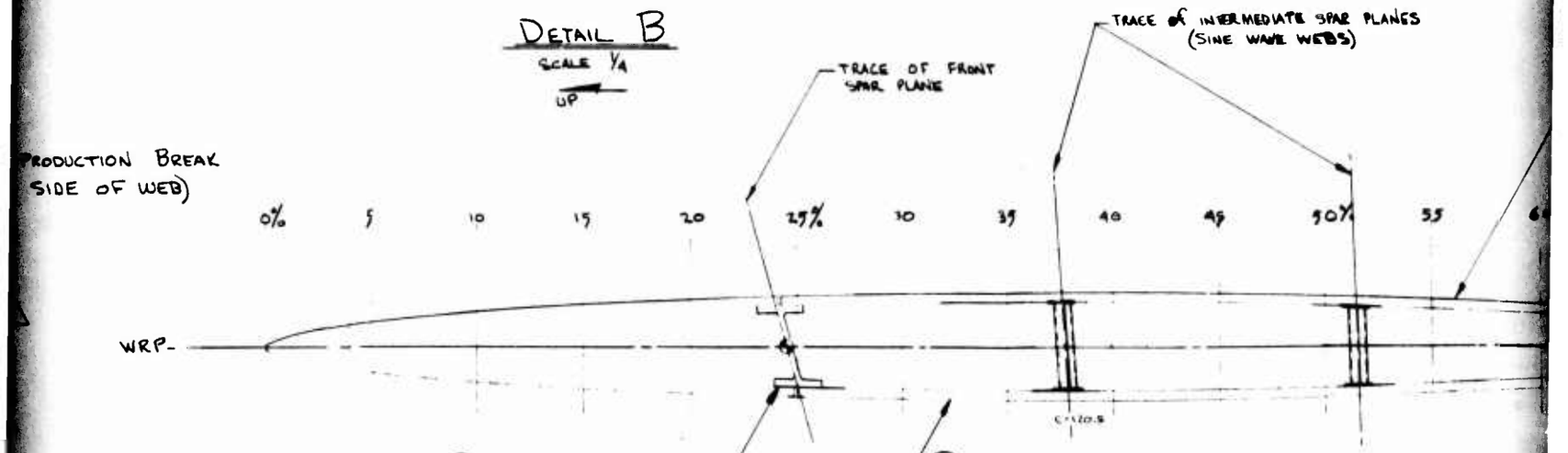

CAPS: T = .30 INBD END TAPERS TO
T = .20 OUTBD END.
WEB: T = .20 INBD END TAPERS TO
T = .10 OUTBD END.
STIFFENERS: .050 THICK AT 8.0 O.C.

SECTION A-A
ROTATED NORMAL TO RIB CHORD
SCALE 1/4

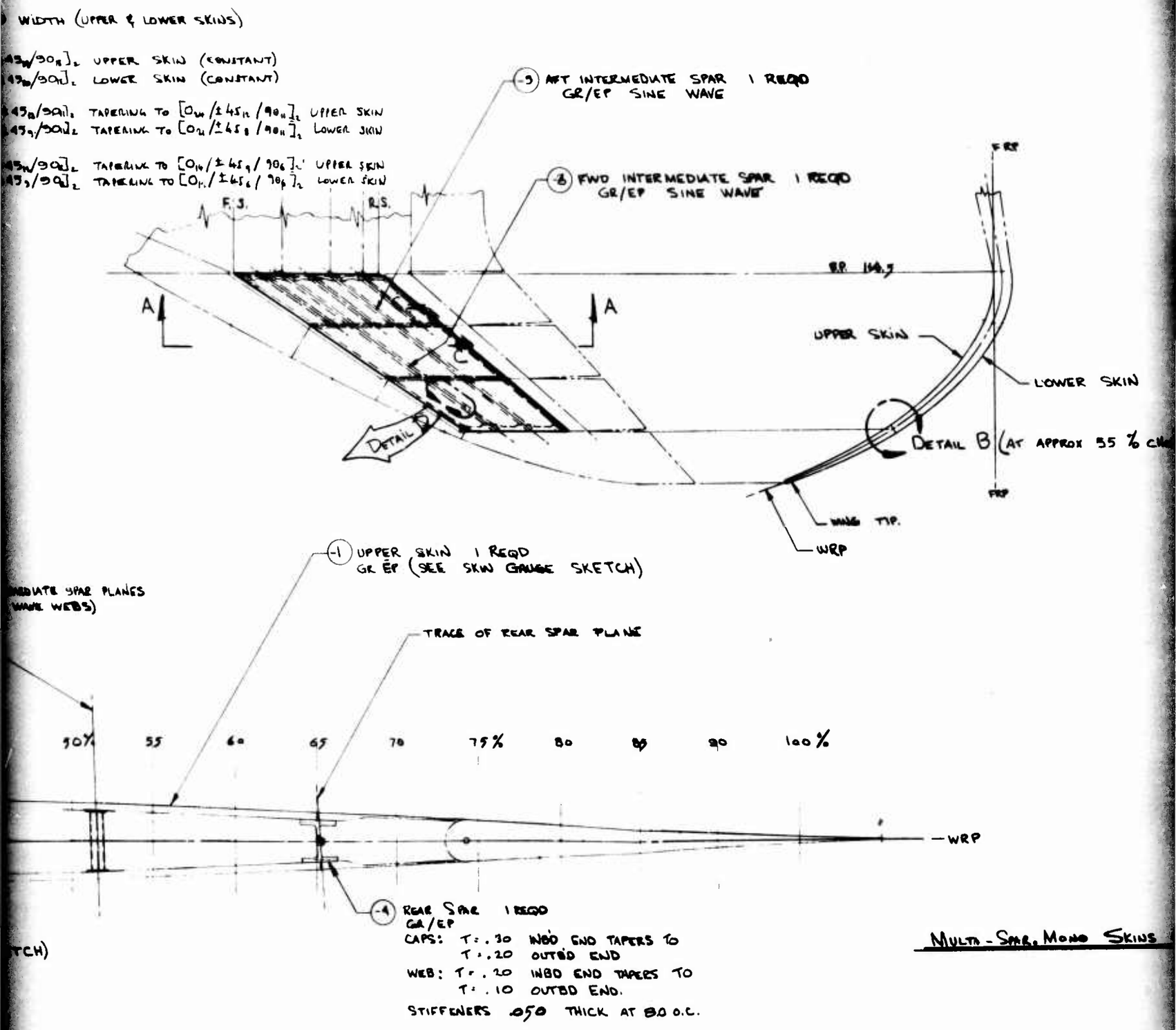

Figure 121. Multispar trade study -

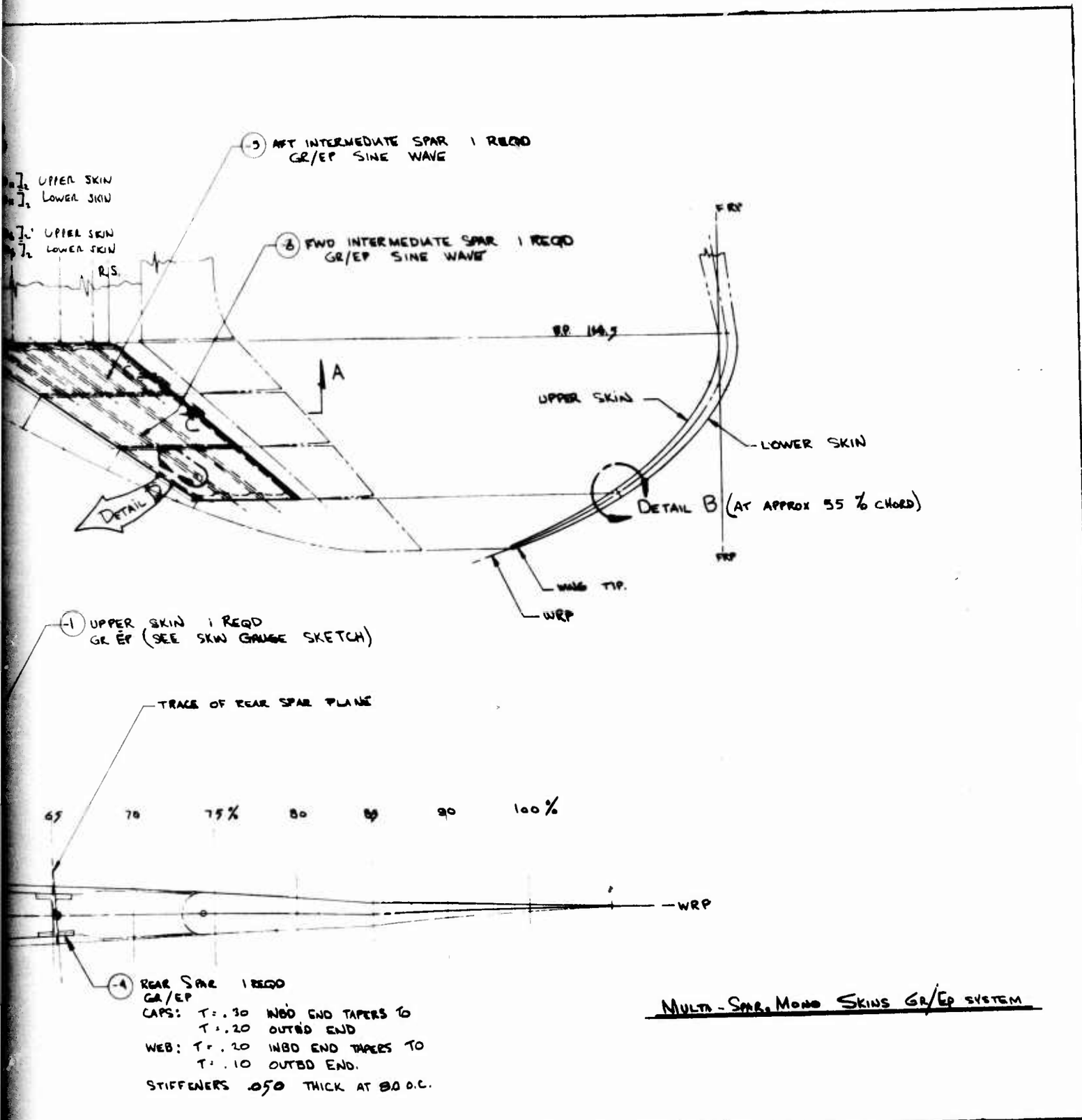

Figure 121. Multispar trade study - wing outer panel.

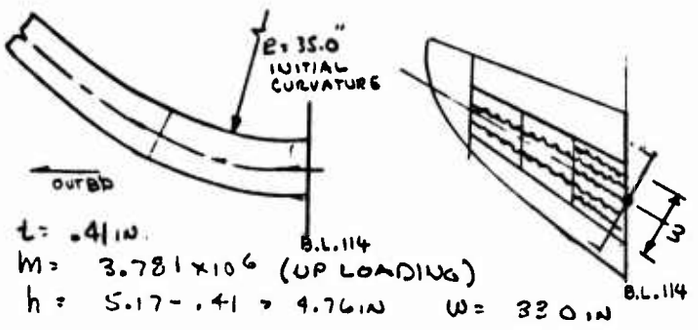

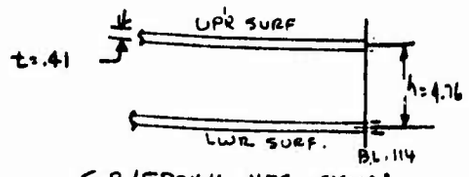

GR/EPOXY HTS SKINS

$t_f = 2[41 \times .005] = .41$ IN

$t = .41$ IN.

$M = 3.781 \times 10^6$ (UP LOADING)

$h = 5.17 - .41 = 4.76$ IN $\quad W = 330$ IN

$$N_x = \frac{M}{h\,W} = \frac{3.781 \times 10^6}{4.76 \times 33.0} = \underline{24070\ \text{lb/in (ULT)}}$$

$[E^{0}_{11} / \pm 45_{14} / 90_{2}]_s$ (27% / 68% / 5%)

(SWEEP RESULTS)

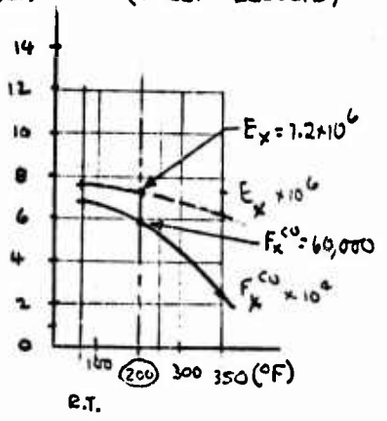

$$f_b = \frac{N_x}{t_f} = \frac{24{,}070}{.41} = \underline{58710\ \text{PSI (ULT)}}$$

SPAR SPACING = $W/3 = 33.0/6 = 5.5$ IN

$$P_{CRUSH} = 5.5\left[\frac{2t}{h}\frac{f_b}{E_s} + \frac{N_x}{R}\right]$$

$$P_{CRUSH} = 5.5\left[\left[\frac{2(.41)(58{,}710)^2}{4.76 \times 7.2 \times 10^6}\right] + \left[\frac{24{,}070}{35.0}\right]\right]$$

$$5.5\left[82.5 + 687\right]$$

WING PANELS (SKINS)

E_x 7.2×10^6

$F_x^{cu} = 60{,}000$

TEMP = 200 °F

$P_{CRUSH} = \underline{4232\ \text{lb/in (ULT)}}$ / SPAR

P_{CRUSH} NORMAL UNIFORM LOAD ON PANEL = $\underline{769.5\ \text{PSI (ULT)}}$

Figure 122. Multispar trade study - wing outer panel.

MULTI SPAR / V END-SKIN OUTER WING PANEL
CHECK OF SKIN COVER FOR STRENGTH
LOADING - UP-BENDING M = 3.781×10⁷ IN-lbs (ULT)

UPPER SKIN PANEL

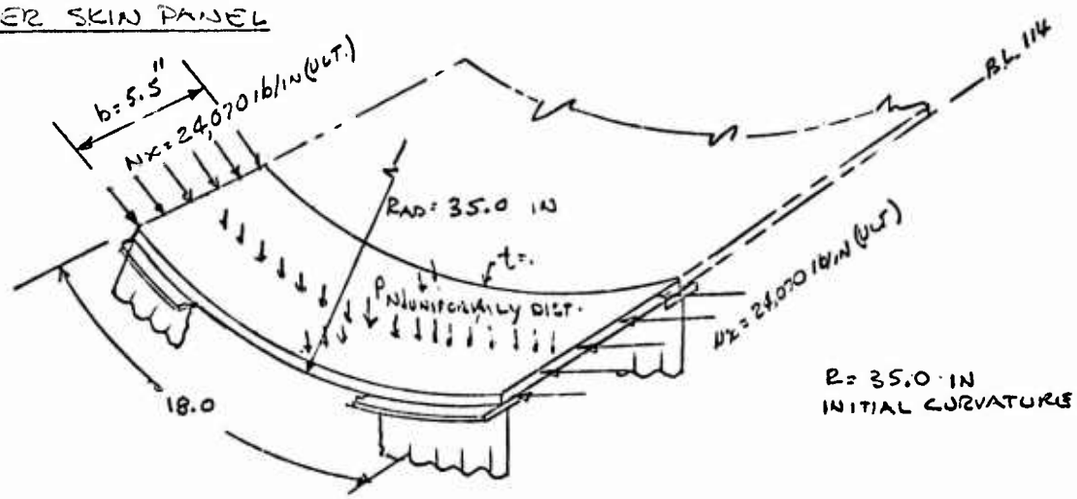

MAT'L = GRAPHITE/EPOXY (HTS)

$[0_{11} / \pm 45_{16} / 90_2]_{.2}$ (SWEEP)

TEMP = 200°F

N_x = 24,070 lb/in

P_N = CRUSHING LOAD UNIFORMLY DISTRIBUTED (DOWN LOAD) PSI
= 769.5 PSI

SINCE THE COVER SHEET DOES NOT HAVE CONTINUOUS SUPPORT TO REACT THE CRUSHING LOADS AS DOES A FULL DEPTH H/C CONCEPT, THESE LOADS MUST BE TRANSFERRED TO THE SPARS AS PLATE BENDING. THIS INDUCES ADDITIONAL STRESS TO BE CONSIDERED FOR STRENGTH.
THE INITIAL "t" WAS ADEQUATE FOR FLUTTER, THEREFORE THE ADDITIONAL "t" WILL BE FOR STRENGTH ONLY.

ADD ADDITIONAL (3) SPARS TO DECREASE WIDTH OF THE NON SUPPORTED PANEL.

Figure 122. Multispar trade study - wing outer panel (cont).

INITIAL CHECK FOR STRENGTH

ASSUME FLAT PLATE WITH N_x + P_N (UNIFORM NORMAL LOADING DUE TO CURVATURE)

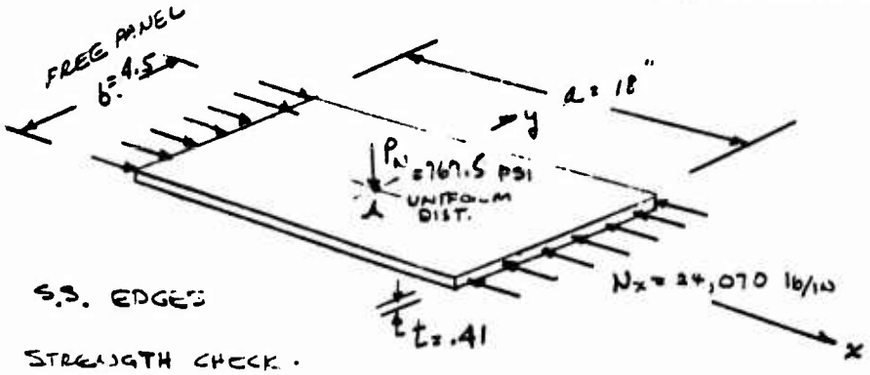

STRENGTH CHECK.

$a/b = 18/4.5 = 4.0$ $t = .41$

$M_x = K_{m_{x_{P_1}}} \cdot p b^2$ $K_{m_{x_{P_1}}} = .043$

$= .043\ (769.5)(4.5)^2 = 670.0$ IN-lbs (ULT.)

$f_{b_x} = \frac{6M}{t^2} = \frac{6(670)}{(.41)^2} = 23\,914$ PSI

$f_{TOTAL} = f_b + \frac{N_x}{t} = 23\,914 + 58,710$

$= 82\,624$ PSI $>$ $F_x^{cu} = 60,000$

M.S. $= \frac{60000}{82,624} - 1 =$ **0.27**

$M_y = K_{m_{y_{PD}}} \cdot p(b)^2$ $K_{m_{y_{PD}}} = .125$

$= .125\ (769.5)(4.5)^2$

$= 1948$ IN-LBS.

$f_{b_y} = \frac{6(1948)}{(.41)^2} = 69,530$ PSI

THE ABOVE CALCULATIONS INDICATE THAT ADDITIONAL "t" IS REQUIRED TO REDUCE THE APPLIED STRESS. ADDITIONAL [0] [90] PLIES ARE REQUIRED TO INCREASE THE ALLOWABLES IN THOSE ORIENTATION AXIS.

Figure 122. Multispar trade study - wing outer panel (cont).

REVISED THICKNESS t AND CROSSPLY PERCENT

TO $t = .60$ $[0_{17}/\pm 45_{14}/90_{15}]_s$

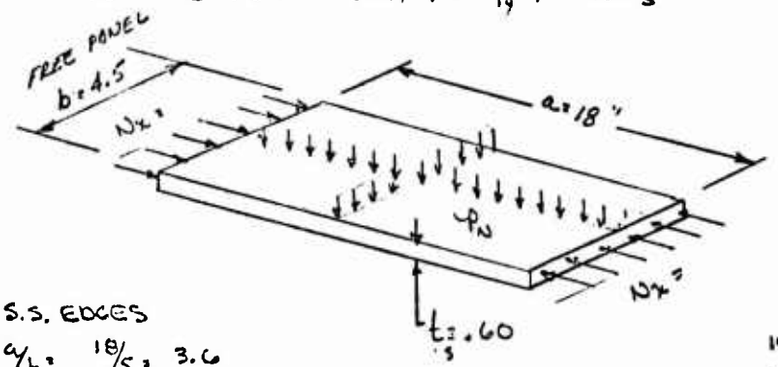

(REVISED)
GR/EPOXY HTS
28% 47% 25%
$[0_{17}/\pm 45_{14}/90_{15}]_s$
$t_s = 2(60)(.005) = .60$ IN.

S.S. EDGES

$a/b = 18/5 = 3.6$

$h = 5.17 - t = 5.17 - .60 = 4.57$ IN

$N_x = \frac{m}{hw} = \frac{3.781 \times 10^6}{4.57(33.0)} = 25{,}070$ lb/IN ULT.

$f_b = \frac{N_x}{t} = \frac{25070}{.60} = 41{,}783$ PSI

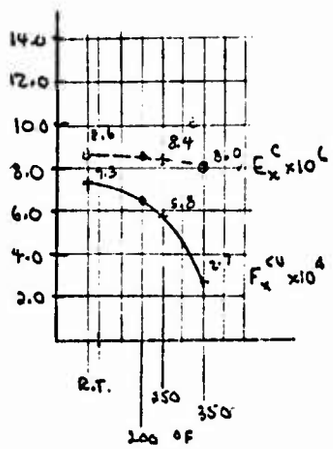

WING PANEL SKINS

$E_x = 8.5 \times 10^6$

$F_x^{cu} = 65 \times 10^4$

TEMP = 200°F

FOR SPAR SPACING = W/ = 33.0/6 = 5.5 IN

$$p_{N_{CRUSHING}} = 5.5\left[\frac{2t f_b}{h E_s} + \frac{N_x}{R}\right]$$

$$= 5.5\left[\frac{2(.60)(41{,}783)^2}{(4.57)(8.5\times10^6} + \frac{25{,}070}{55.0}\right]$$

$$P_{N_{CRUSHING}} = 5.5\,[53.93 + 716] = \underline{4236}\ \text{lb/IN/SPAR}.$$

$P_{N_{UNIFORM\ ON\ PLATE}} = \underline{770\ \text{PSI (ULT)}}$

Figure 122. Multispar trade study - wing outer panel (cont).

REVISED THICKNESS t AND CROSS PLIES (CONT)

STRENGTH CHECK FOR

$P_{BUCKLING} = 770$ PSI (ULT)

$N_x = 25{,}070$ lbs/in (ULT)

FOR $a/b = 4.0$ $\quad K_{m_{x_{PO}}} = .043$ $\quad K_{m_{y_{PO}}} = .125$

$$M_x = K_{m_{x_{PO}}}(\psi)(b^2)$$

$$= .043(769.5)(4.5)^2 = 670.0 \text{ in-lbs}$$

$$f_{b_x} = \frac{6M}{t^2} = \frac{6(670.0)}{(.60)^2} = 11{,}167 \text{ PSI}$$

$$f_{TOTAL} = f_{b_x} + \frac{N_x}{t}$$

$$= 11{,}167 + 41{,}783 = 52{,}950 \text{ PSI}$$

$$M.S. = \frac{65\,000}{52{,}950} - 1 = \underline{+.23}$$

$$M_y = .125(769.5)(4.5)^2 = 1948 \text{ in-lbs}$$

$$f_{b_y} = \frac{6(1948)}{(.60)^2} = 32{,}466$$

Figure 122. Multispar trade study - wing outer panel (cont).

SPAR CRUSHING

(6) SPAR CONFIG.

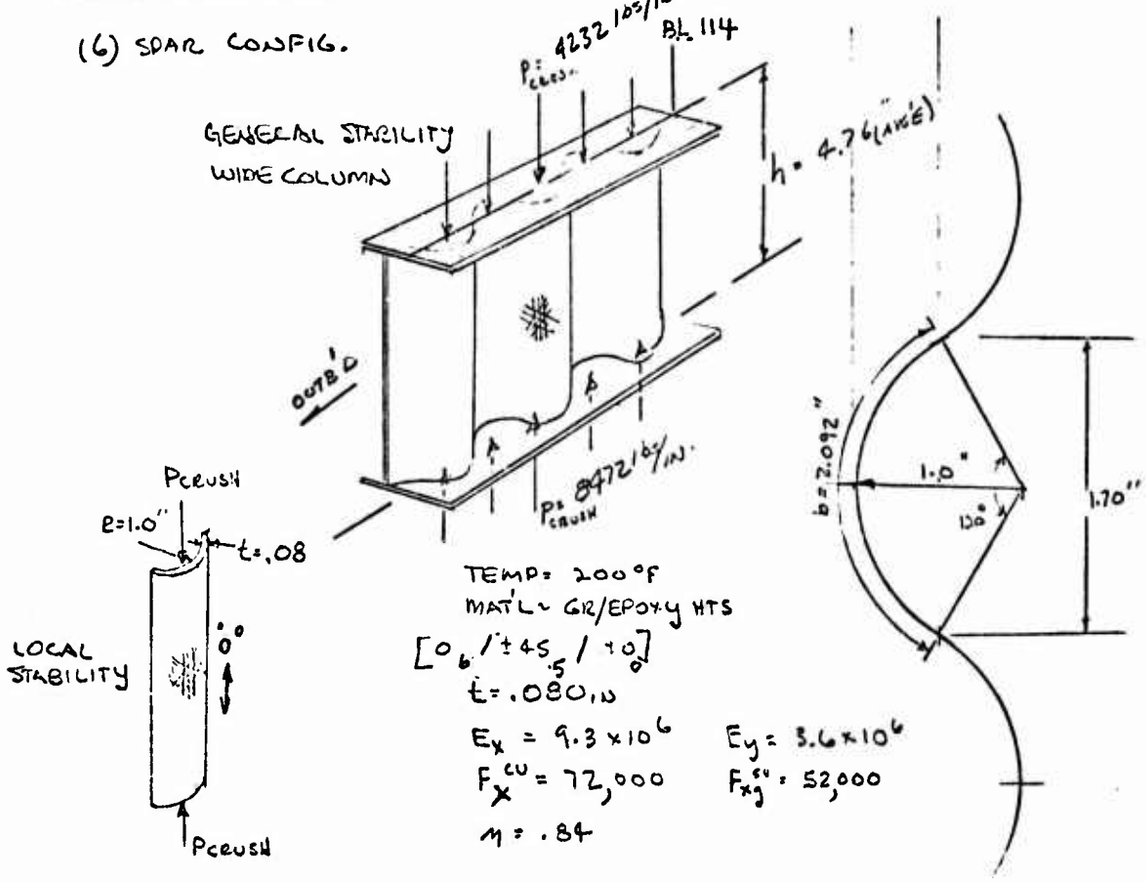

ASSUME SPAR IS A WIDE COLUMN

RUNNING LOAD = P_{CRUSH} = 5,901 lbs/in ULT

LOCAL STABILITY (ASSUME ISOTROPIC FOR FIRST CUT)

R = 1.0 b = 2.092 in, t = .080 in a/b = 4.76/2.092 = 2.28 > .5

b = π D 120/360 = π 2.0 (.333) = 2.092 in.

$$Z = \frac{b^2}{Rt}\sqrt{1-\mu^2}$$

$$= \frac{(2.092)^2}{(1.0)(.08)}\sqrt{1-(.84)^2} = 29.7$$

R/t = 1.0/.08 = 12.5

K_c = 11.0 REF NA-72-1 PGE 11-242

Figure 122. Multispar trade study - wing outer panel (cont).

$[0_6 / \pm 45_5 / 90]_T$ GR/EPOXY HTS AT 200°F

CHECK FOR LOCAL STABILITY (COMPOSITE MATERIAL) COMPRESSION

$$\sigma_{cr_L} = 0.327 (G_{xy})^{1/2} (E_x E_y)^{1/4} \left[\frac{1 + \nu_{xy}\nu_{yx}}{1 - \nu_{xy}\nu_{yx}}\right]^{1/2} \frac{t}{R}$$ REF. GRUMMAN

$$= 0.327 \left(3.6 \times 10^6\right)^{1/2} \left[(9.3 \times 10^6)(3.6 \times 10^6)\right]^{1/4} \left[\frac{1 + .74 \times .29}{1 - .74 \times .29}\right]^{1/2} \frac{.08}{1.0}$$

$$(.327)\ (1.897 \times 10^3)\quad (2.406 \times 10^3)\quad (1.24357)\ (.08)$$

$$\sigma_{cr_L} = .14848 \times 10^6 = 148{,}480 \text{ PSI}$$

USE $F_x^{cu} = 72{,}000$ PSI (CUT OFF)

CHECK FOR LOCAL STABILITY (COMPOSITE MATERIAL) SHEAR.

SHEAR LOAD q: $\frac{V_3}{4(h)} = \frac{32{,}000}{4(4.76)} = 1681$ lb/in

APPLIED STRESS = $\frac{q}{t} = \frac{1681}{.08} = 21{,}008$ PSI

$$\tau_{xy_{cr_{LOCAL}}} = \frac{1.55 (E_x E_y^3)^{1/4}}{(1 - \nu_{xy}\nu_{yx})^{1/4}} \left(\frac{t}{2R}\right)^{3/2}$$

$[0_6 / \pm 45_5 / 90]_T$

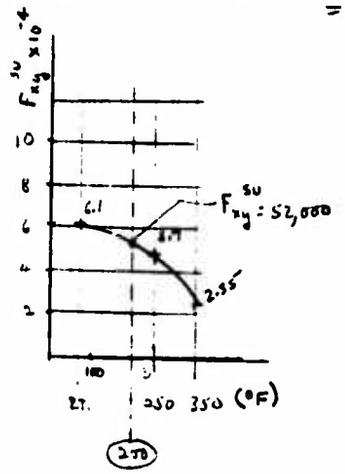

$$= 1.55 \frac{\left[(9.3 \times 10^6)(3.6 \times 10^6)^3\right]^{1/4}}{\left[1 - (.74)(.29)\right]^{1/4}} \left[\frac{.08}{2(1.0)}\right]^{3/2}$$

$$1.55 \left[\frac{433.9 \times 10^{24}}{.94140}\right]^{1/4} \left[.04\right]^{1.5}$$

$$= 1.55 \left(4.6334 \times 10^6\right)(.008)$$

$$= .057450 \times 10^6 = 57{,}450 \text{ PSI}$$

USE $F_{xy}^{su} = 52000$ PSI (CUT OFF).

Figure 122. Multispar trade study - wing outer panel (cont).

LOCAL STABILITY ($t = .08$) = 16 PLIES

$$\sigma_{cr} = K_c \frac{\pi^2 E}{12(1-\mu^2)}\left[\frac{t}{b}\right]^2$$

$$= \frac{11.0(\pi^2)(7.0\times10^6)}{6.5}\left[\frac{.08}{2.092}\right]^2$$

(116.9×10^6, 1460×10^{-6})

$\sigma_{cr} = 170,674$ PSI $> F_L^{cu} = 50,000$

USE F_L^{cu} ALLOWABLES

APPLIED STRESS -

$$\frac{4232.(1.7)}{(2.092)(.08)} = 42290 \text{ PSI (ULT)}$$

$42,990 < F_x^{cu} = 50,000$

$$M.S. = \frac{50000}{42,990} - 1 = +.16$$

GR/EPOXY HTS

$[0_4 / \pm45_6 / 90_0]_T$

25% 75% 0%

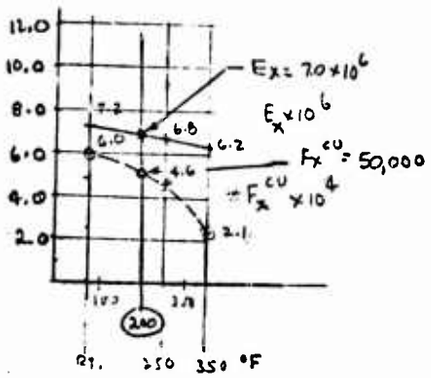

SPAR WEBS $t = .080$ = 16 PLIES

$E_x = 7.0\times10^6$

$F_x^{cu} = 50,000$

TEMP = 200°F

$t = .08$ APPLIED STRESS = 42,290 PSI

REVISE LAMINATE ORIENTATION

$$\sigma_{cr} = \frac{11.0(\pi^2)(9.3\times10^6)}{6.5}\left[\frac{.08}{2.092}\right]^2 = 226,752$$

$226,752 > 72,000$ PSI

USE $t = .08$

$[0_6 / \pm45_5 / 90_0]$

37.5% 62.5% 0

GR/EPOXY (HTS)

$[0_6 / \pm45_5 / 90_0]_T$

37.5% 62.5% 0%

$t = .08 = 16$ PLIES

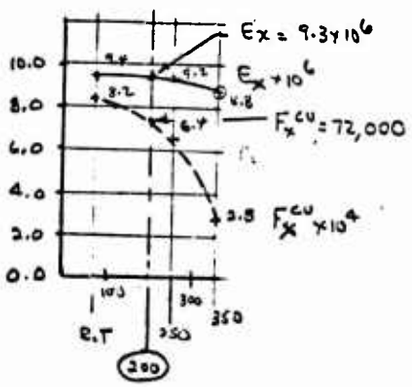

$M.S. = \frac{72,000}{42,290} - 1 = +.70$

$E_x = 9.3\times10^6$ $E_y =$

$F_x^{cu} = 72,000$ $G_{xy} =$

TEMP = 200°F

$t = .08$ APPLIED STRESS: 42,290

Figure 122. Multispar trade study - wing outer panel (cont).

$$R_c + R_s^2 \geq 1.0$$

$$\frac{42290}{72,000} + \left(\frac{21008}{52,000}\right)^2$$

$$.5874 + .1632 = .7506 \geq 1.0$$

Figure 122. Multispar trade study - wing outer panel (concl).

TABLE 21. WING OUTER PANEL - MULTISPAR PLATE WEIGHTS

AIRCRAFT: WNG OUTER PANEL MULTI-SPAR PLATE

AIRCRAFT WEIGHTS - IN POUNDS	AL	TI	SI	BC	GB	EG	SA	TOTAL
FUSELAGE	78.	171.	69.	C.	2088.	27.	0.	3236.
FRAME/LONG	C.	171.	69.	C.	695.	0.	0.	935.
SKIN-STRGR	78.	0.	0.	C.	0.	0.	0.	78.
BOND HONEY	C.	0.	C.	C.	1391.	27.	0.	1418.
BRAZE HONEY		0.	0.				0.	0.
DIFF BOND		0.					0.	0.
MISC								805.
WING	126.	25.	C.	C.	2971.	0.	0.	3275.
SKIN-STRGR	C.	0.	0.	C.	0.	0.	0.	0.
MULTI-SPAR	C.	25.	0.	C.	523.	0.	0.	548.
BOND HONEY	126.	0.	0.	C.	2448.	0.	0.	2574.
BRAZE HONEY		0.	C.				0.	0.
DIFF BOND		0.					0.	0.
MISC								153.
CANARDS	C.	16.	2.	C.	117.	0.	0.	145.
SKIN-STRGR	C.	0.	C.	C.	0.	0.	0.	0.
MULTI-SPAR	C.	0.	0.	C.	0.	0.	0.	0.
BOND HONEY	C.	16.	2.	C.	117.	0.	0.	135.
BRAZE HONEY		0.	C.				0.	0.
DIFF BOND		0.					0.	0.
MISC								10.
NACELLE	C.	0.	0.	C.	C.	0.	0.	0.
FRAME/LONG	C.	0.	C.	C.	0.	0.	0.	0.
SKIN-STRGR	C.	0.	0.	C.	0.	0.	0.	0.
BOND HONEY	C.	0.	0.	C.	C.	0.	0.	0.
BRAZE HONEY		0.	C.				0.	0.
DIFF BOND		0.					0.	0.
MISC								0.

WEIGHT DATA - IN POUNDS	
AMPR WEIGHT	13265.
STRUCTURE WT	7939.
STRUCTURAL HOWE WT	133.
SYSTEM HOWE WT	133.
LANDING GEAR WT	1280.
FUEL SYSTEM WT	750.
ELECTRICAL SYSTEM WT	680.
HYDRAULIC SYSTEM WT	430.
AUX POWER SYSTEM WT	310.
ECS WT	530.
CREW ACCOM WT	320.
CONTROL & DISPLAY WT	120.
FLIGHT CONTRCL WT	950.
ARMAMENT WT	560.
AICS MECHANISM WT	300.
EQUIPMENT WT	80.
ENGINE WT	5375.
EMPTY WT	19319.
FUEL WT	7060.
TOGW	30986.

DESIGN VARIABLES	
WING AREA-SQ FT	400.
CANARDS AREA-SQ FT	35.
WETTED AREA-SQ FT	1772.
WING + HORIZ AREA	435.
WING SPAN-FT	31.6
HORIZ SPAN-FT	10.0
OVERALL LENGTH-FT	57.0
ASPECT RATIO	2.50
DYNAMIC PRESSURE	2133.

TABLE 22. WING OUTER PANEL - MULTISPAR PLATE COSTS

AIRCRAFT: WNG OUTER PANEL MULTI-SPAR PLATE
ALL COSTS IN MILLIONS AND IN 1975 DOLLARS

PRODUCTION COST FOR 300 UNITS
UNIT AVG. FLYAWAY COST 2.801

WORK BREAKDOWN STRUCTURE	LABOR COST					MATERIAL COST		TOTAL
	MFG.	TOOL.	PLNG.	ENGR.	G&A	MFG.	TOOL.	COST
TOTAL PROGRAM COST INCLUDING FEE	394.73	71.50	34.71	40.62	53.11	236.28	9.04	840.34
TOTAL PROGRAM COST INCLUDING G&A	358.85	65.00	31.56	36.93	48.28	214.80	8.22	763.97
TOTAL PROGRAM COST LESS G&A	326.73	59.18	28.73	33.63	43.96	195.58	7.49	695.62
AIR VEHICLE	326.73	59.18	28.73	33.63	43.96	195.58	7.49	695.62
AIRFRAME	167.12	52.52	17.33	33.63	24.98	189.39	6.64	491.61
BASIC STRUCTURE	59.80	52.52	10.95	8.14	17.29	59.46	6.64	254.80
FUSELAGE	37.50	33.73	5.18	4.88	8.07	24.31	4.27	117.94
WING	35.92	12.55	3.49	2.53	5.51	32.63	1.59	94.21
CANARDS	1.59	5.21	0.51	0.73	0.77	1.56	0.66	11.03
NACELLES	C.0	C.0	0.0	0.0	0.0	0.0	0.0	0.0
BASIC STRUCTURE ASSEMBLY	24.78	1.03	1.77	0.0	2.95	0.96	0.13	31.62
LANDING GEAR	0.0	C.0	0.0	0.60	0.0	13.48	0.0	14.07
FUEL SYSTEM	6.40	C.0	0.56	1.72	0.73	4.61	0.0	14.01
FLIGHT VEHICLE POWER	31.07	0.0	2.55	6.01	3.55	58.12	0.0	101.30
ENVIRONMENTAL CONTROL	C.0	C.0	0.0	2.09	0.0	25.90	0.0	27.98
CREW ACCOMMODATIONS	6.75	C.0	0.52	0.80	0.77	0.0	0.0	8.84
CONTROLS AND DISPLAYS	0.0	C.0	0.0	0.0	0.0	8.56	0.0	8.56
FLIGHT CONTROLS	20.72	C.0	1.42	0.0	2.37	0.0	0.0	24.50
ARMAMENT	C.0	C.0	0.0	0.30	0.0	19.26	0.0	19.55
AIR INDUCTION CONTROL SYSTEM	2.39	0.0	0.21	0.67	0.27	0.0	0.0	3.54
AIRFRAME INTEGRATION & CHECK	C.0	C.0	0.0	16.95	0.0	0.0	0.0	16.95
ENGINEERING TECHNOLOGIES	C.0	C.0	0.0	12.30	0.0	0.0	0.0	12.30
DESIGN SUPPORT TECHNOLOGIES	C.0	C.0	0.0	1.75	0.0	0.0	0.0	1.75
AIRFRAME INSTALL & CHECKOUT	C.0	C.0	0.0	2.90	0.0	0.0	0.0	2.90
PROPULSION (GFE)	C.C	C.0	0.0	0.0	0.0	0.0	0.0	0.33
AVIONICS (GFE)	C.0	C.0	0.0	0.0	0.0	0.0	0.0	0.0
A/V INTEGRATION, ASSY, INSTALL	159.61	6.66	11.40	0.0	18.98	6.18	0.84	203.68

The geometry for the honeycomb panel concept was established using SWEEP analysis of different spar spacing and panel thicknesses. As shown in Table 23, the 18-inch spar spacing produces the minimum weight, so this spacing was selected for the design. Also shown in the table is the linear variation of weight with honeycomb panel thickness, with .5 inch being the lowest weight. However, since SWEEP does not include the effects of fuel pressure, .75 inch was selected for the honeycomb to provide for this loading. Figure 123 shows the concept. Honeycomb panels are used for wing covers, spars, and ribs. Potted-in inserts allow the upper cover to be removed for resealing, repair, or maintenance. Four pcf graphite/epoxy core is used throughout except in local areas where spars or ribs are bonded to covers. In these areas, six pcf core is specified to transfer fuel pressure loads into the panels. Cover panel thicknesses are sized to meet flutter, fuel pressure, wing bending and fuselage bending loads. Figure 124 shows stress analysis of this concept.

The weight distribution of the aircraft with this structural concept is shown in Table 18. Costs appear in Table 19.

The multi-spar/plate concept was developed using the optimum spar spacing calculated on SWEEP, as shown on Table 23. The 10-inch spar spacing, which is minimum weight, was used on the design shown on Figure 125. Honeycomb panels with graphite epoxy facesheets and core, .5-inch thick, are used for both spars and ribs. The covers are graphite/epoxy plate sized by fuel pressure, flutter, and bending loads. Figure 126 shows the analysis of this concept for fuel pressure. SWEEP sizing was used for other loading conditions as shown in Table 24.

Weights of the aircraft components with this structural concept employed on the wing center section are shown in Table 25 and costs in Table 26.

Figure 127 shows a third concept for the wing carry-through section. Skins, with stiffeners running inboard and outboard, are employed in this design. Preliminary sizing using SWEEP (shown on Tables 27 and 28) was conducted to compare T-stiffeners with hat sections. A 13-pound weight savings was responsible for hat sections being used for the design. As shown in Figure 127, .090 graphite/epoxy hats spaced 5-1/2 inches on center are bonded to graphite/epoxy skins. Ribs spaced at 16 inches are graphite/epoxy channels with angle stiffeners. Spars at Y_F551.5 and Y_F515 are .5-inch graphite/epoxy honeycomb panels while the rear spar is a built-up graphite/epoxy beam. The spars, ribs, and lower skin are bonded together and the upper skin and its stiffeners are attached to the box with mechanical fasteners. Fuel pressure check appears on Figure 128.

Table 29 shows the weight breakdown of the ADCA with this concept. Costs are shown on Table 30.

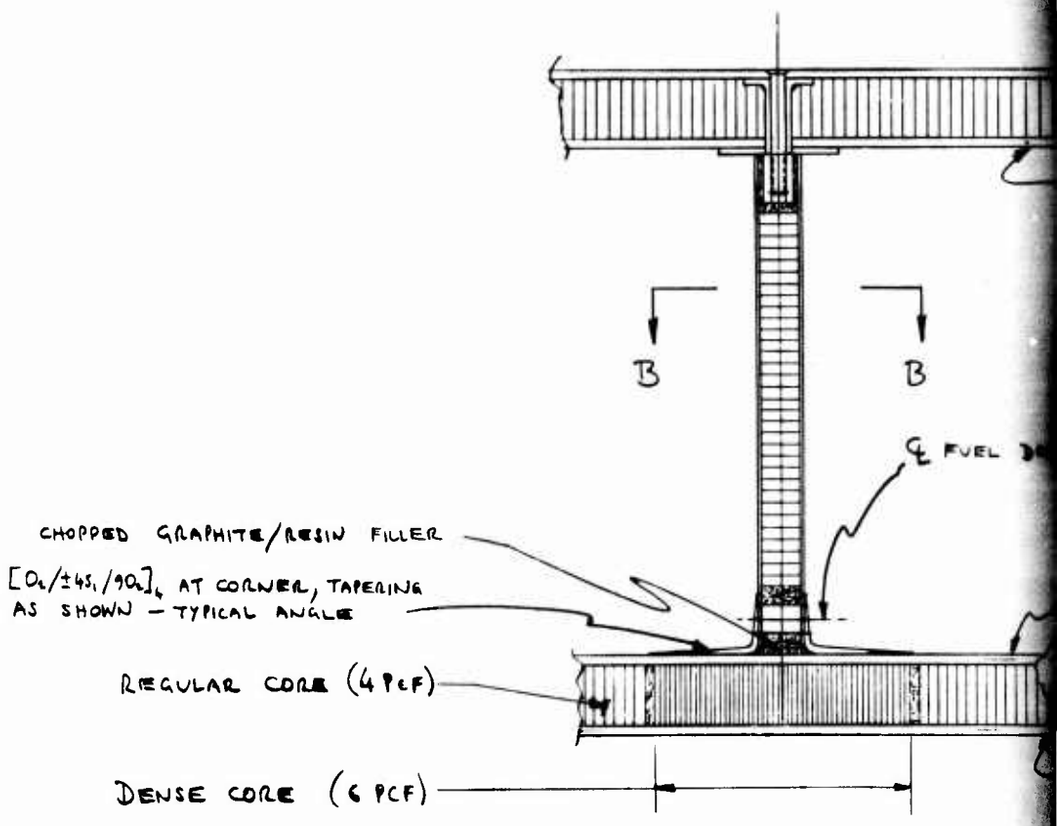

SECTION A-A
(FULL SIZE)

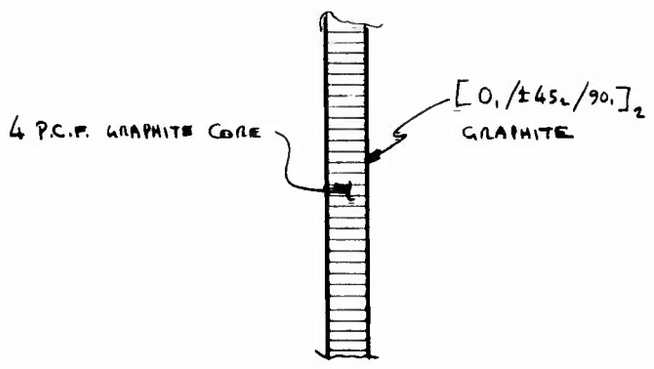

SECTION B-B
FULL SIZE

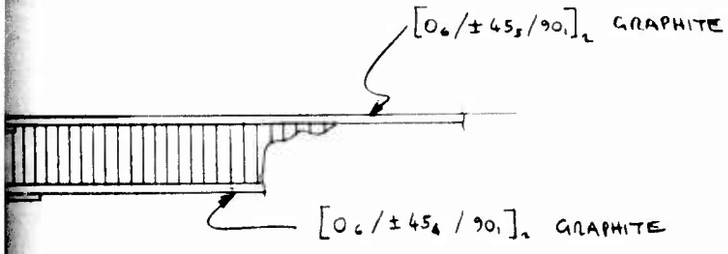

B

℄ FUEL DRAINAGE ORIFICES

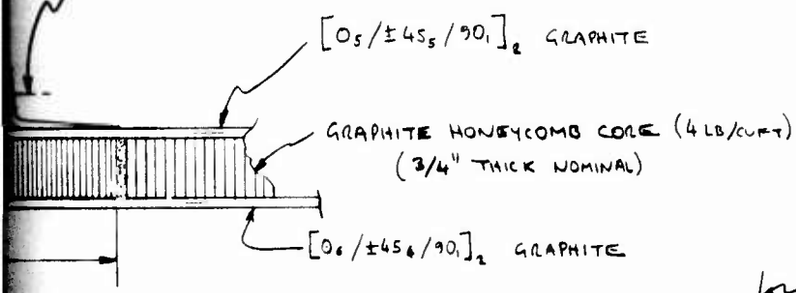

A-A
SIZE)

$]_2$

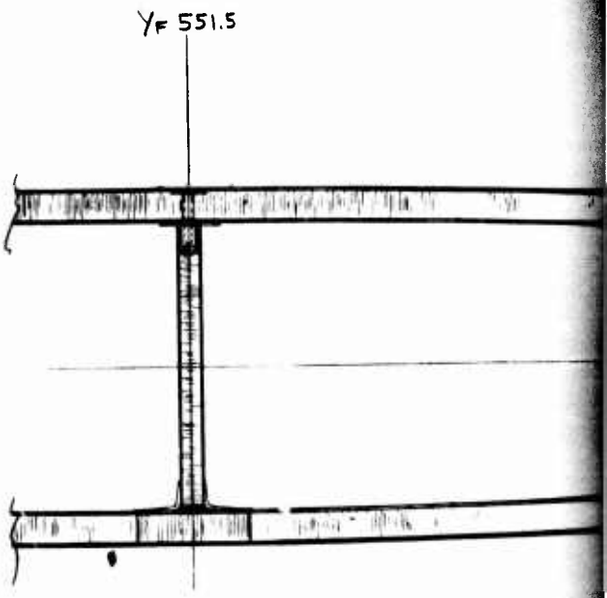

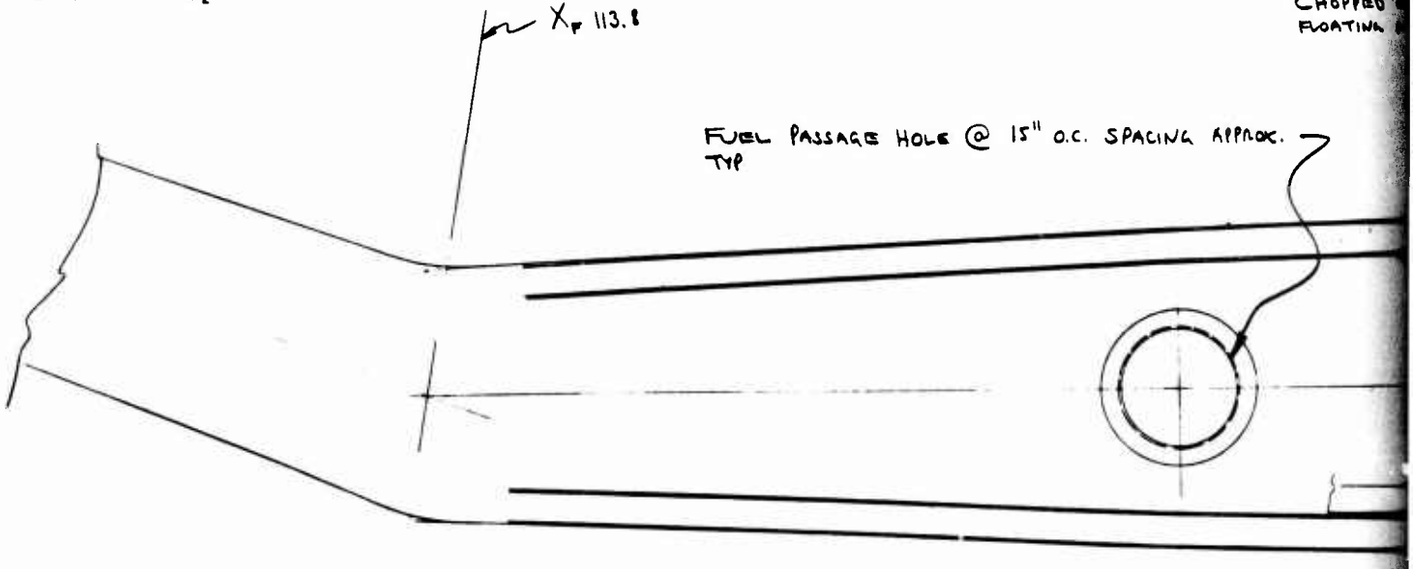

CHOPPED
FLOATING

SECTION D-D

2

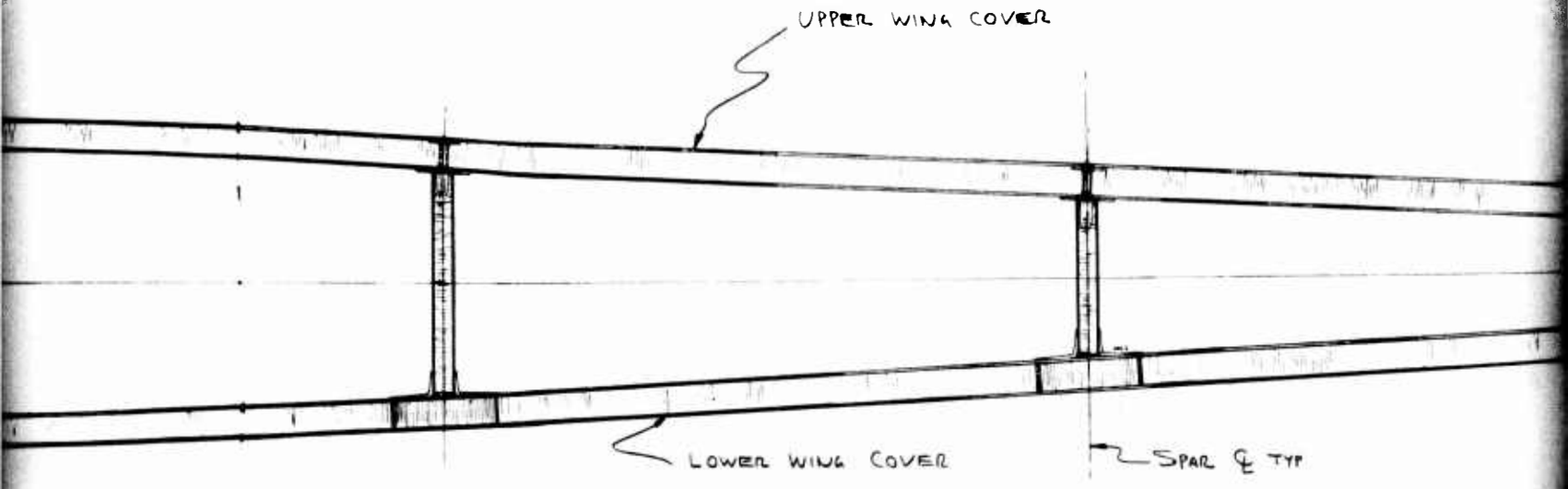

SECTION C-C
VIEW LOOKING INBD.
(1/2 SIZE)

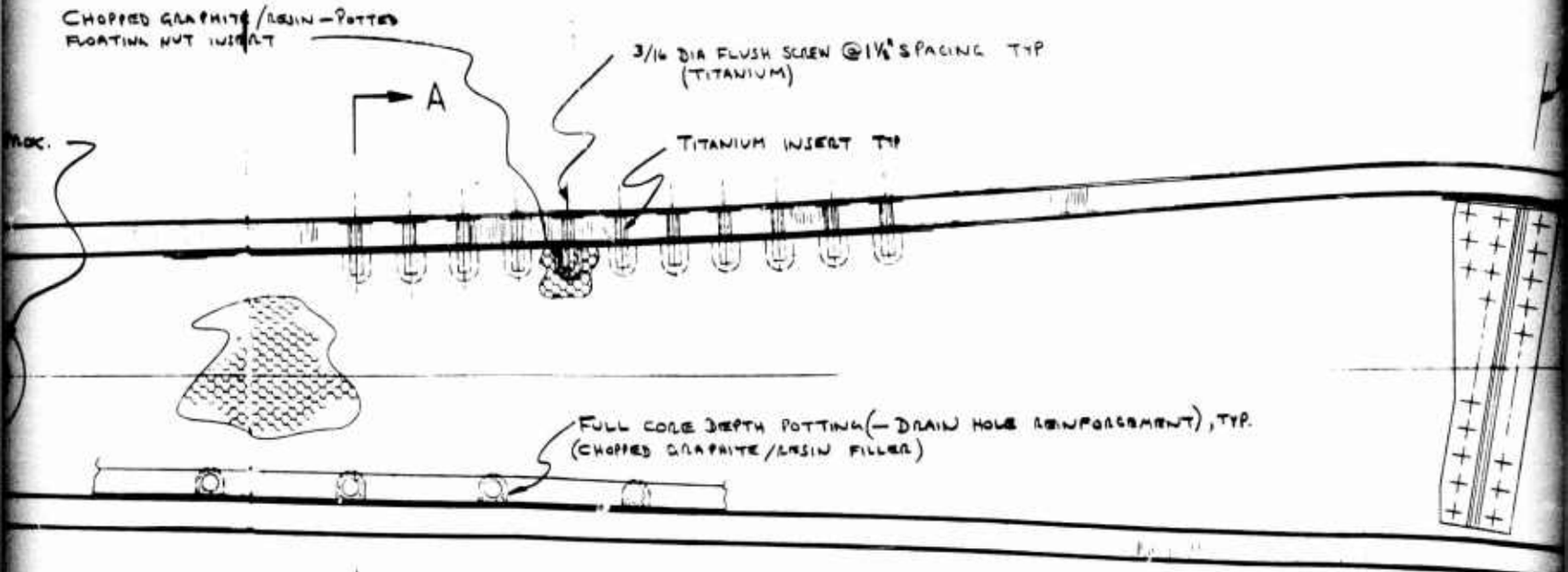

ION D-D

A

SECTION @ YF 551.5
LOOKING FWD
(1/2 SIZE)

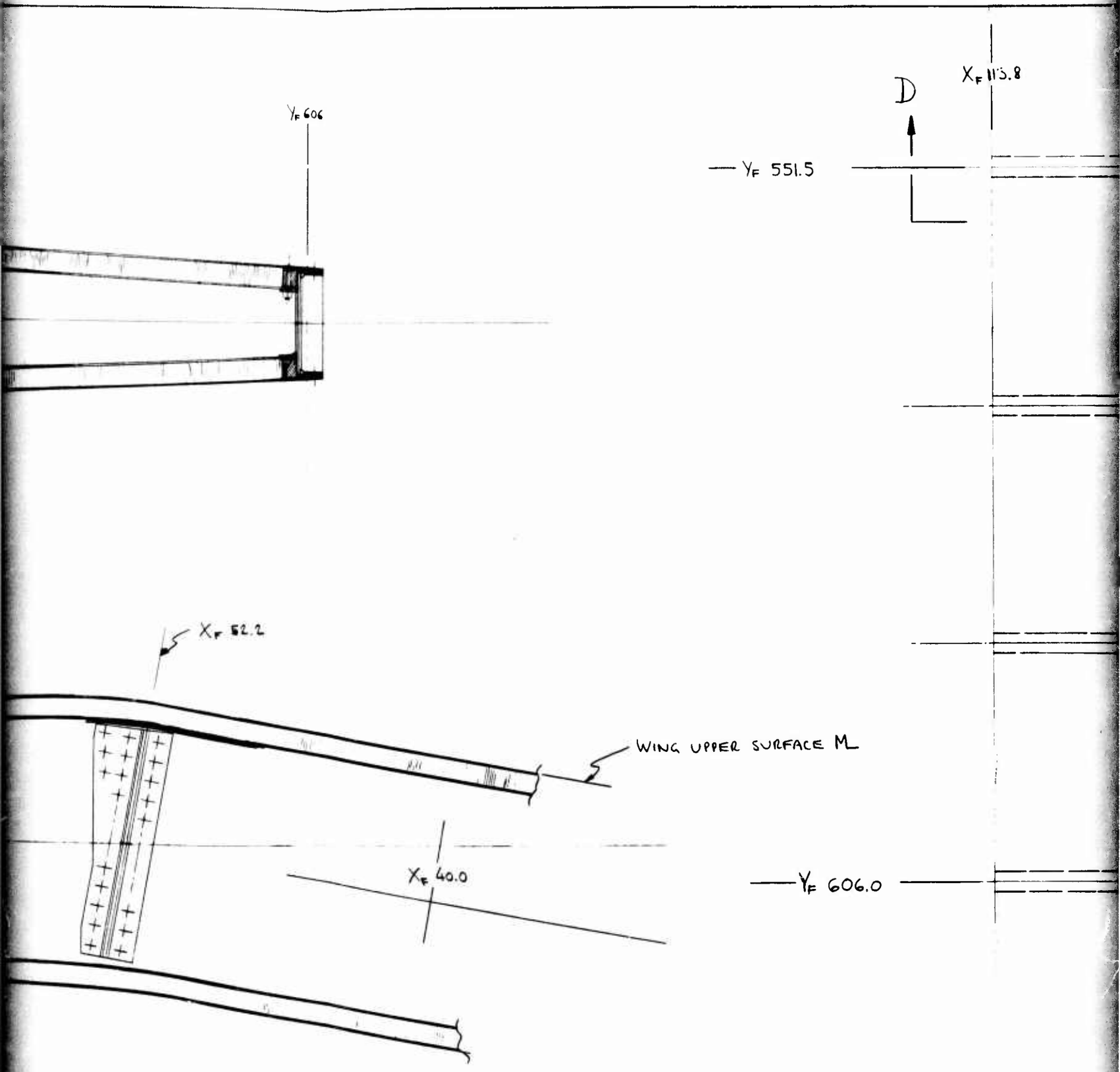
X_F 115.8
D
Y_F 606
Y_F 551.5
X_F 52.2
WING UPPER SURFACE ML
X_F 40.0
Y_F 606.0

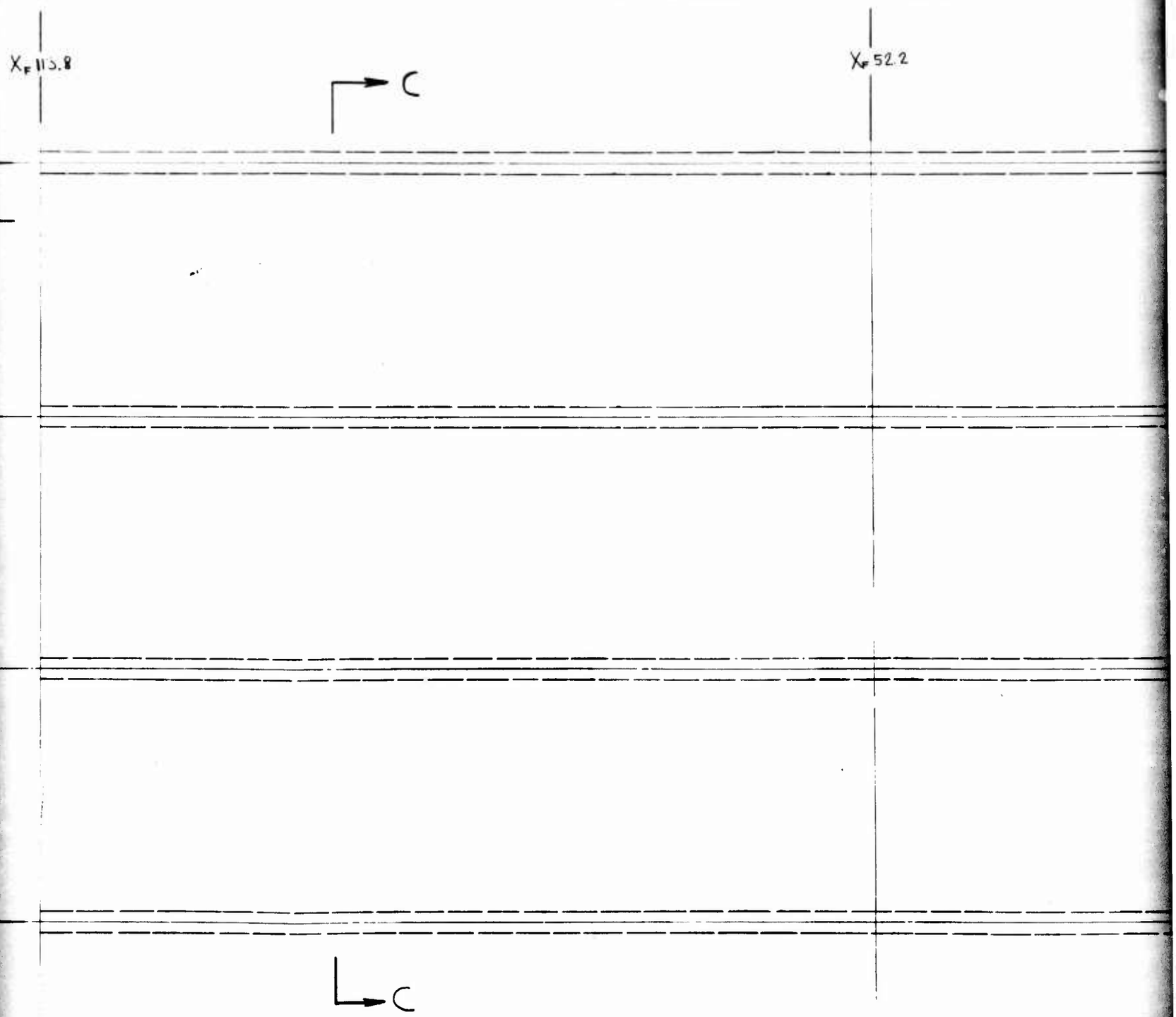
X_F 113.8
C
X_F 52.2
C

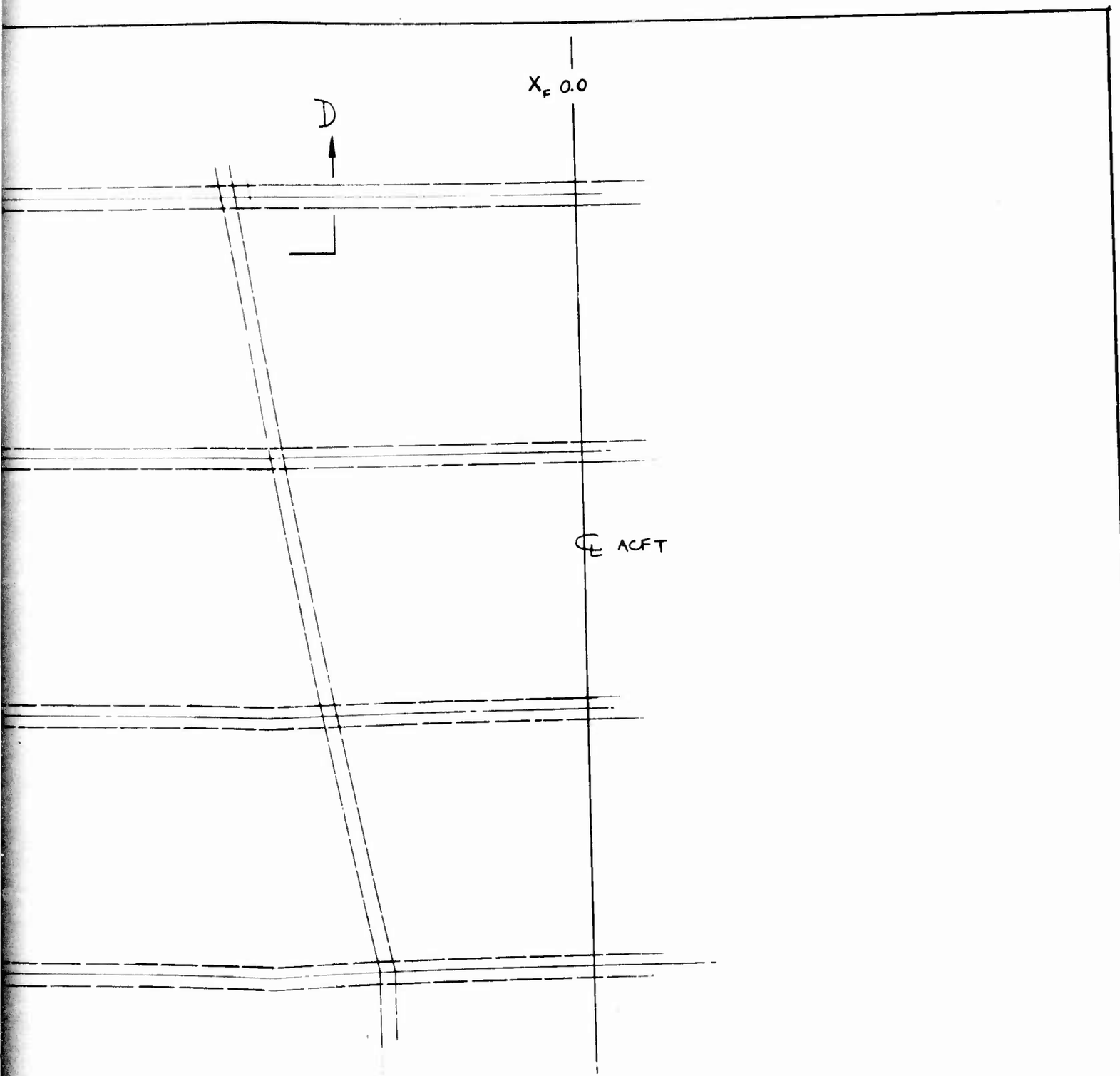

Figure 123. Wing carry-through structure - honeycomb panels.

TABLE 23. WING CENTER SECTION - MULTISPAR PLATE COVER THICKNESSES

MULTI-SPAR - PLATES
DATA SHEET D512-4R WITH CURRENT FLUTTER DATA
8/28/75 SP — INBD EQUIVALENCE TORQUE BOX

STA NO.	LOAD MIG STATION FUS. STA.	B. PLANE	TOTAL THICKNESS UPPER	LWR	UPPER COVER 0°	+45°	-45°	90°	LOWER COVER 0°	+45°	-45°	90°	
			MULTI-SPAR PLATE-SKINS										
			18" SPAR SPACING TORQUE BOX WT. = 1757 LBS/AC										
1	552	33	.45	.32	12	38	38	2	10	26	26	2	
2	558.3	52.2	.44	.32	10	38	38	2	10	26	26	2	
3	562.8	65.3	.43	.32	12	36	36	2	10	26	26	2	
4	568.1	81.5	.45	.33	12	38	38	2	12	26	26	2	
5	573.5	97.7	.48	.35	14	40	40	2	12	28	28	2	
6	578.9	113.8	.49	.36	16	40	40	2	14	28	28	2	
			MULTI-SPAR PLATE-SKINS										
			14" SPAR SPACING TORQUE BOX WT. = 1614 LBS/AC										
1			.39	.28	12	32	32	2	10	22	22	2	
2			.36	.28	10	30	30	2	10	22	22	2	
3			.37	.28	12	30	30	2	10	22	22	2	
4			.39	.29	12	32	32	2	12	22	22	2	
5			.40	.29	14	32	32	2	12	22	22	2	
6			.43	.32	16	34	34	2	14	24	24	2	
			MULTI-SPAR PLATE-SKINS										
			10" SPAR SPACING TORQUE BOX WT. = 1437 LBS/AC										
1			.31	.22	12	24	24	2	10	16	16	2	
2			.30	.22	10	24	24	2	10	16	16	2	
3			.31	.22	12	24	24	2	10	16	16	2	
4			.31	.23	12	24	24	2	12	16	16	2	
5			.32	.25	14	24	24	2	12	18	18	2	
6			.35	.26	16	26	26	2	14	18	18	2	

ALL WEIGHTS QUOTED ARE PER AIRCRAFT

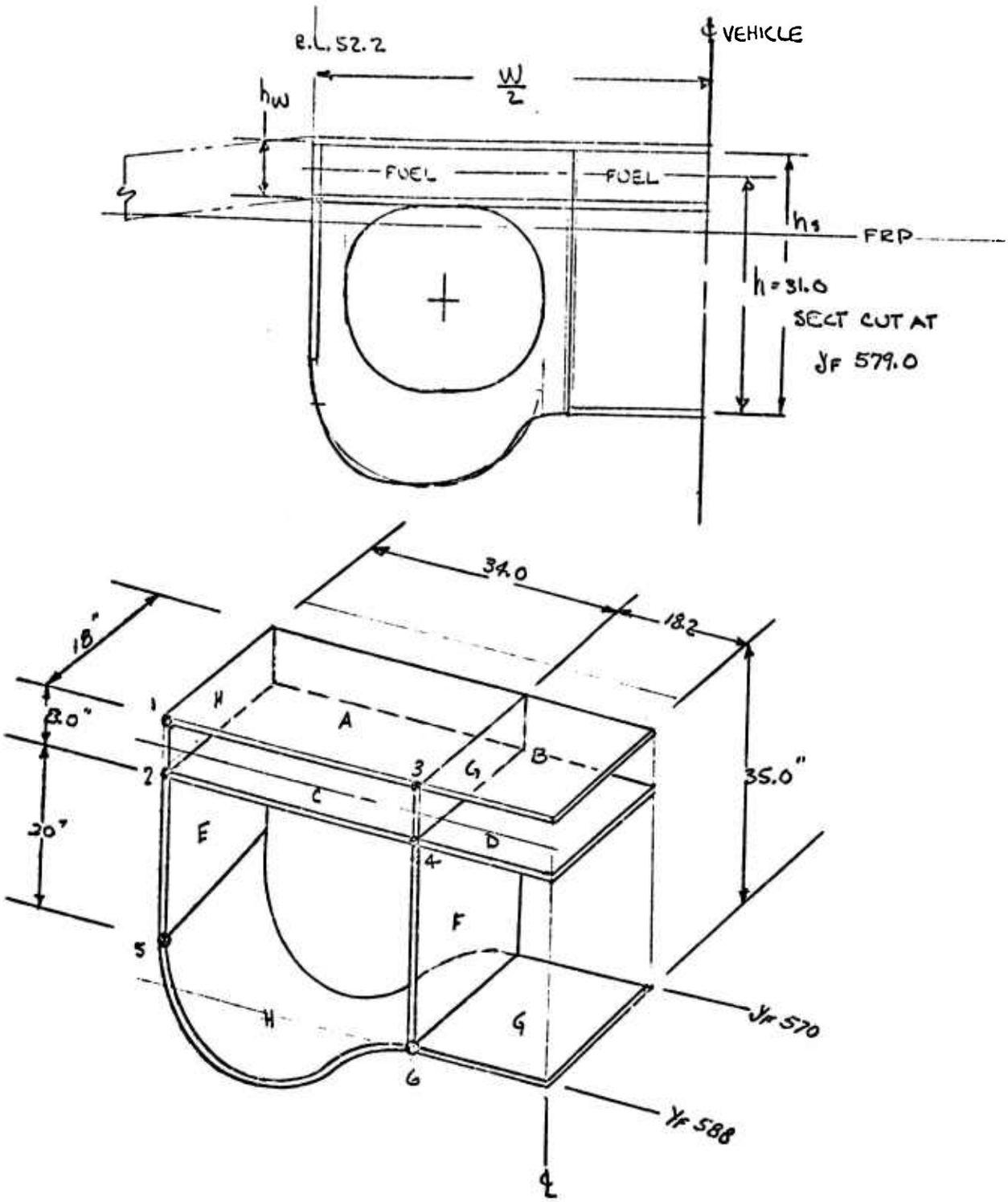

Figure 124. Wing center section honeycomb panel analysis.

ADCA MATERIAL PROPERTIES AND ALLOWABLES
HTS GR/EP
$[0_L/\pm 45_M/90_N]_s$; L = 40%, M = 20% N = 40%

MATERIAL PROPERTIES

ELASTIC PROPERTY	VALUE AT TEMP		
	RT	250°F	350°F
E_x	10.25	10.07	9.80
E_y	10.25	10.07	9.80
G_{xy}	1.62	1.48	1.33
ν_{xy}	.128	.126	.120

DESIGN ALLOWABLE

ALLOWABLE	VALUE AT TEMPERATURE		
	RT	250°F	350°F
F_x^{tu}	74.1	79.6	69.2
F_x^{cu}	87.7	69.0	32.6
F_y^{tu}	74.1	79.6	69.2
F_y^{cu}	87.7	69.0	32.6
F_{xy}^{su}	27.5	20.1	8.9

Figure 124. Wing center section honeycomb panel analysis (cont).

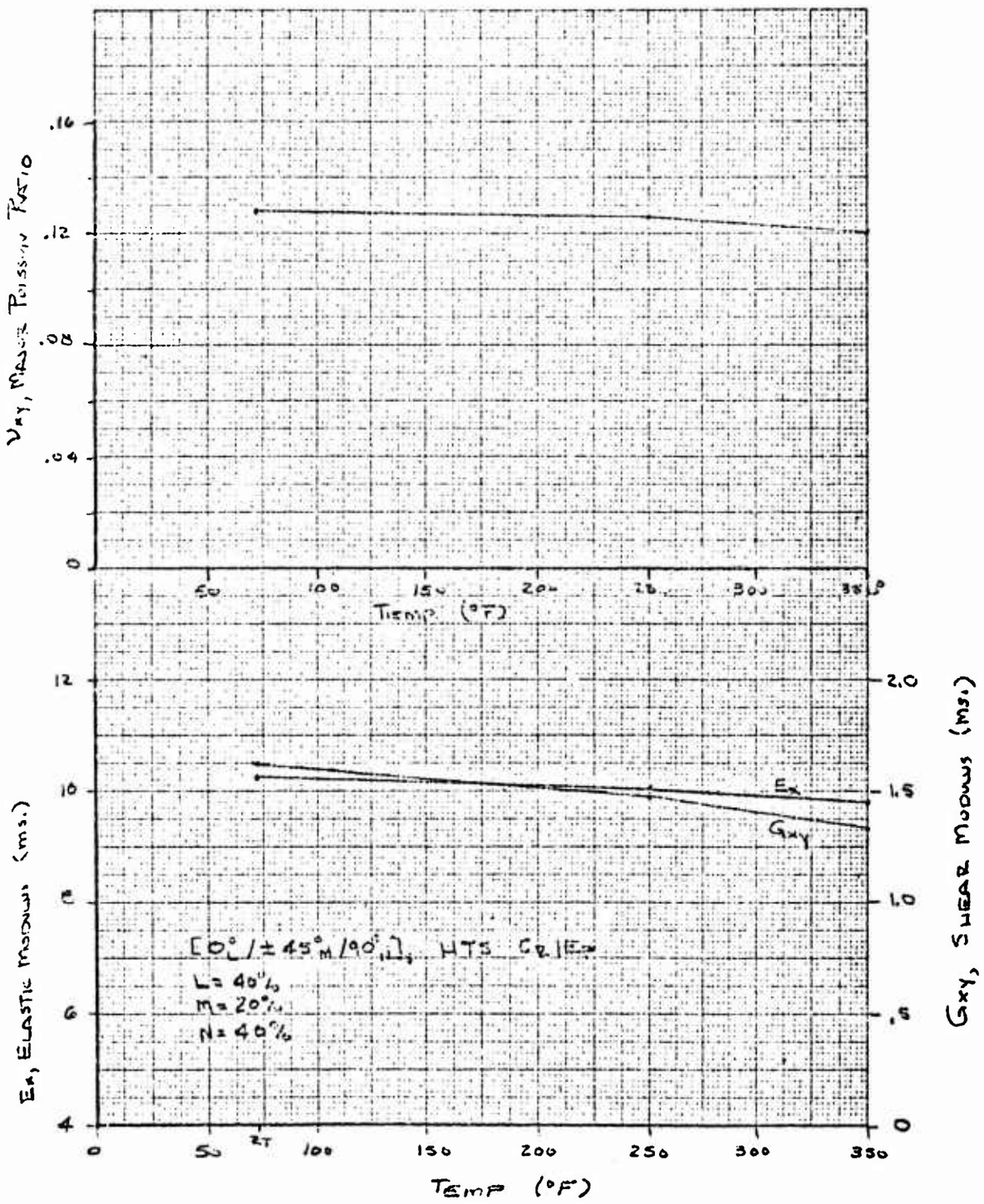

Figure 124. Wing center section honeycomb panel analysis (cont).

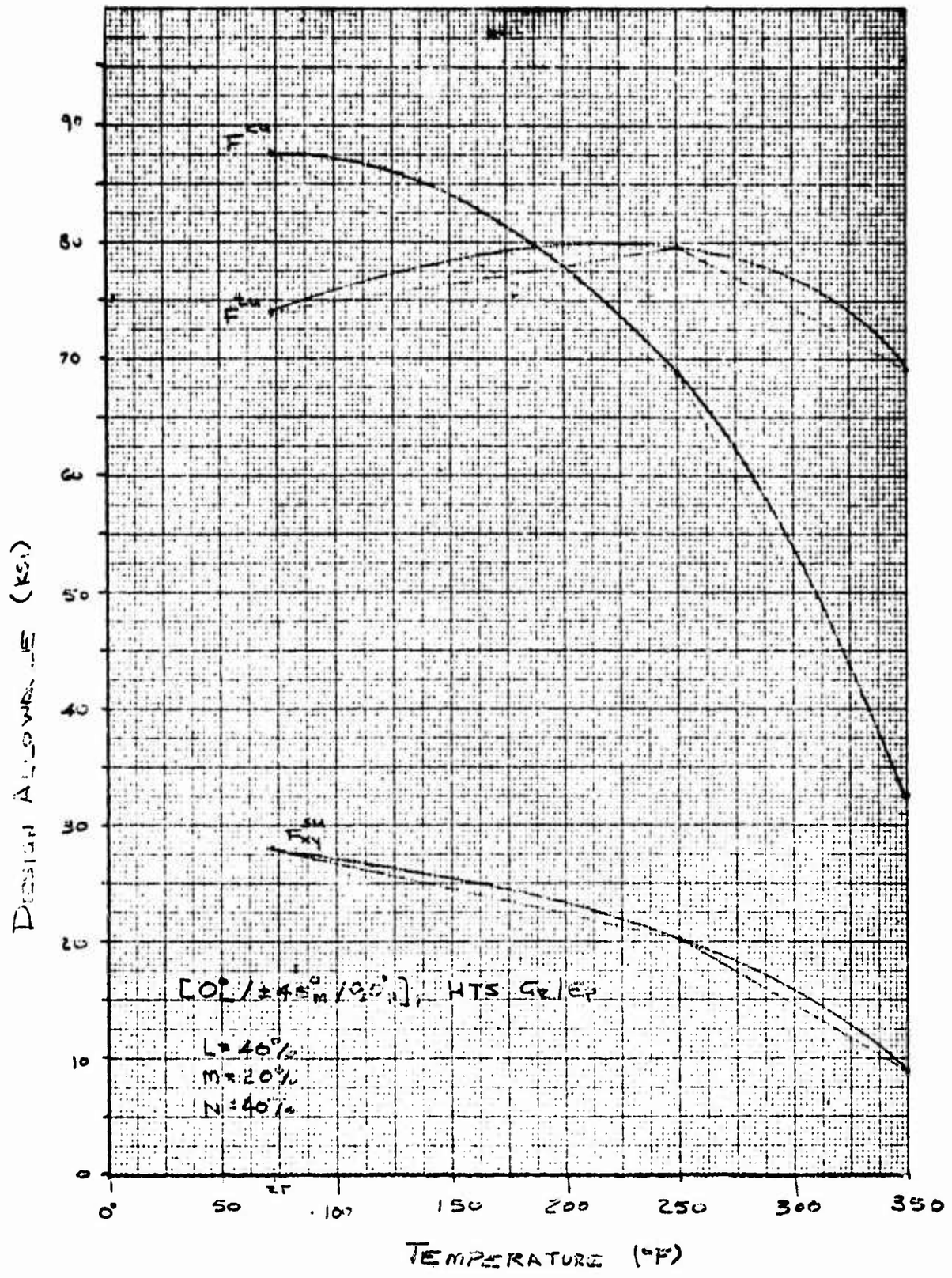

Figure 124. Wing center section honeycomb panel analysis (cont).

AVGE LOADING FOR FUSELAGE SECTION LOCATED BETWEEN y_F 570 TO 588.

DOWN BENDING COND
$-M = 5.0 \times 10^6$ IN-lbs (ULT)

UP BENDING
$+M = 1.85 \times 10^6$ IN-lbs (ULT)

VERT. SHEAR (MAX)
$+V = 50 \times 10^3$ lbs (ULT)

FUEL LOADS

15.0 PSI LIMIT. SURGE
1(g) IN FLIGHT REFUEL

3.0 + HEAD $\times N_z$ (LIMIT)
FOR MANEUVER
F.S. = 1.5

LONGERONS ARE LOCATED AT 1, 2, 3, 4, 5, 6
HONEYCOMB PANELS LOCATED AT A, B, C, D, E, F, G, H

LONGERONS
MATERIAL - GRAPHITE/EPOXY HTS [0 / ±45]

HONEYCOMB PANELS
SHEAR PANELS E F G H
MATERIAL
FACESHEETS GRAPHITE/EPOXY(HTS)[0/±45/90]
t_f = IN.
CORE ~ GRAPHITE FABRIC h = 1.0 IN

Figure 124. Wing center section honeycomb panel analysis (cont).

LOADS -

ASSUME FUSELAGE STRUCTURE EXTENDS FROM BL 0 TO BL ± 52.2 INCLUSIVE OF WING CARRY THROUGH (y_p 515 TO 606) AND DUCT STRUCTURE.

THE UPPER WING CARRY THROUGH STRUCTURE PANELS WILL ACT AS COMPRESSION MEMBERS FOR FUSELAGE UP BENDING PLUS WING CARRY THROUGH BENDING MEMBERS. THESE LOADS WILL COMBINE TO BI AXIALLY LOAD THE PANELS IN COMBINATIONS OF COMPRESSION AND TENSION. (N_{x_T}, N_{x_C})

THE LOWER PANELS WILL BE ANALYZED FOR FUSELAGE DOWN BENDING ONLY. (N_{x_C})

THE LONGERON AREA DISTRIBUTION WILL BE ASSUMED AS EQUALLY DISTRIBUTED BETWEEN UPPER AND LOWER LONGERONS.

FOR PRELIMINARY ANALYSIS PURPOSES THE HONEYCOMB PANELS WILL BE ASSUMED NOT TO BUCKLE AT ULTIMATE LOADS THEREFORE, THE STRAINS OF THE LONGERONS AND PANELS WILL BE ASSUMED IDENTICAL.

AN AREA DISTRIBUTION OF 20% LONGERON 80% H/C PANEL WILL BE ASSUMED.

THE BENDING STRUCTURAL DEPTH FOR FUSELAGE STRUCTURE IS 31.0 IN.

Figure 124. Wing center section honeycomb panel analysis (cont).

FUSELAGE LOADS

FUS. DOWN BENDING (COND 1)

$$\pm N_{y_{PANELS}} = .80\left[\frac{M}{h(W)}\right] = .80\left[\frac{5.0\times10^6}{31\times104.4}\right] = \pm 1236 \text{ lb/in ULT.}$$

$$\text{TOTAL } \pm P_{LONGERONS} = .20\left[\frac{M}{h}\right] = .20\left[\frac{5.0\times10^6}{31}\right] = \pm 32,258 \text{ lbs ULT}$$

16,124/LOWER LG

FUS. UP BENDING (COND 4)

$$\pm N_{x_{PANELS}} = .80\left[\frac{1.85\times10^6}{31\times104.4}\right] = \pm 457.30 \text{ lb/in ULT}$$

$$\text{TOTAL } \pm P_{LONGERONS} = .20\left[\frac{1.85\times10^6}{31}\right] = \pm 11,936 \text{ lbs ULT}$$

11,936/4 = UPPER

11,936/2 = LOWER

FUS. VERTICAL SHEAR (COND 7)

$$q = \frac{V}{h_s} = \frac{50\times10^3}{33.0} = 1515 \text{ lb/in (ULT)}$$

4 PANELS. q_f = 378 lb/in/EACH

WING CARRYTHROUGH LOADS

WING DOWN BENDING (COND 1)

$$\pm N_{x_{PANELS}} = .80\left[\frac{M}{h_w(91.0)}\right] = .80\left[\frac{9.0\times10^6}{7.0(91.0)}\right] = \pm 11,302 \text{ lb/in (ULT)}$$

$$\text{TOTAL } \pm P_{SPAR\ CAPS} = .20\left[\frac{M}{h_w}\right] = .20\left[\frac{9.0\times10^6}{7.0}\right] = \pm 228885 \text{ lbs (ULT)}$$

228,885/4 = UPPR

228,885/2 = LWR

WING UP BENDING (COND 4)

$$\pm N_{x_{PANELS}} = .80\left[\frac{3.4\times10^6}{7.0(91.0)}\right] = \pm 4,269 \text{ lbs/in (ULT)}$$

$$\text{TOTAL } \pm P_{SPAR\ CAPS} = .20\left[\frac{3.4\times10^6}{7.0}\right] = \pm 66,468 \text{ lbs (ULT)}$$

FUEL LOADS

IN FLIGHT 1(g) REFUEL PRESS = 15.0 PSI (1.5) = 22.5 PSI (ULT) at RT

MANEUVER LOADS = (3.0 PSI + HEAD)(N_2)(1.5)

Figure 124. Wing center section honeycomb panel analysis (cont).

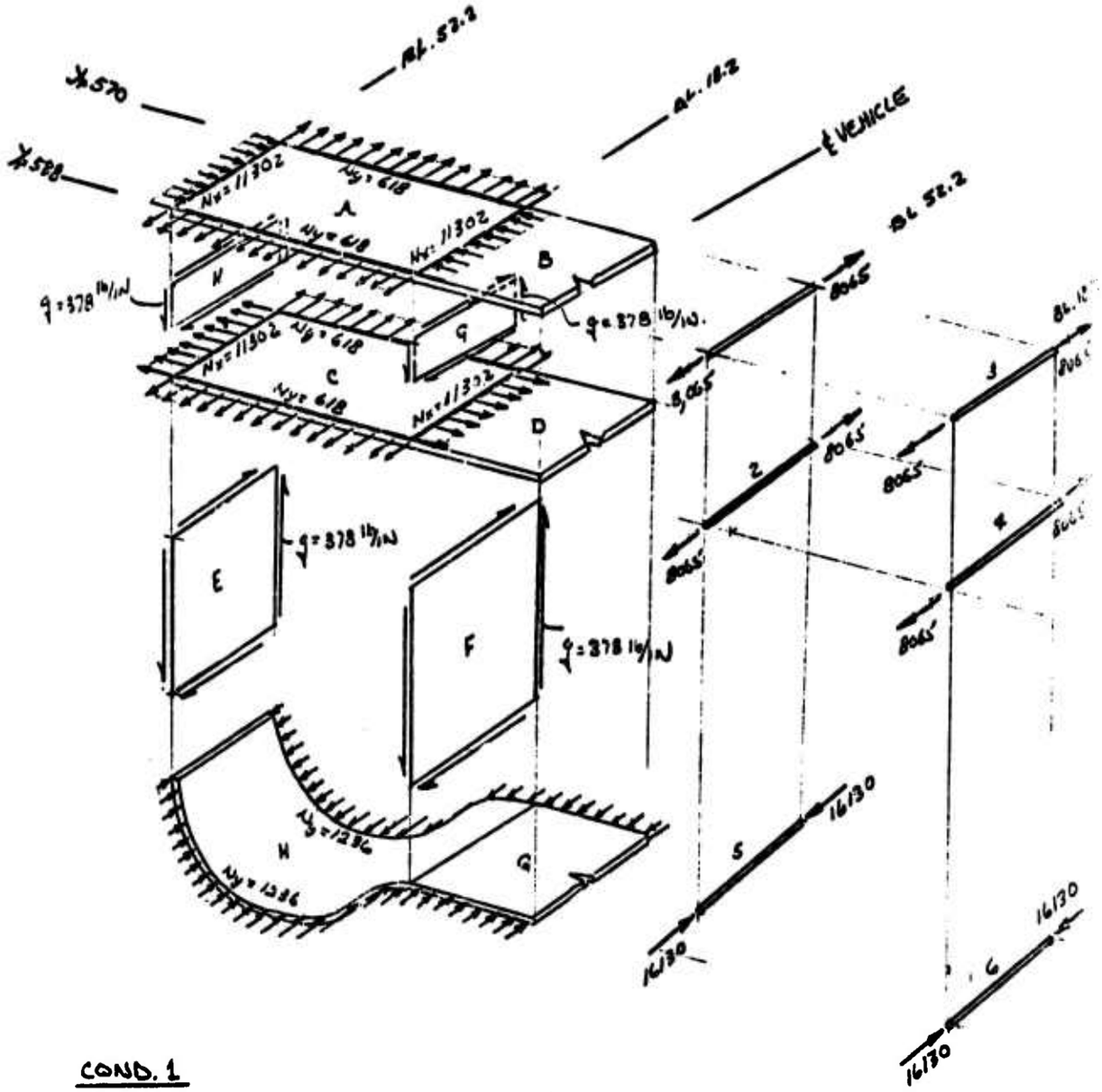

Fiugre 124. Wing center section honeycomb panel analysis (cont).

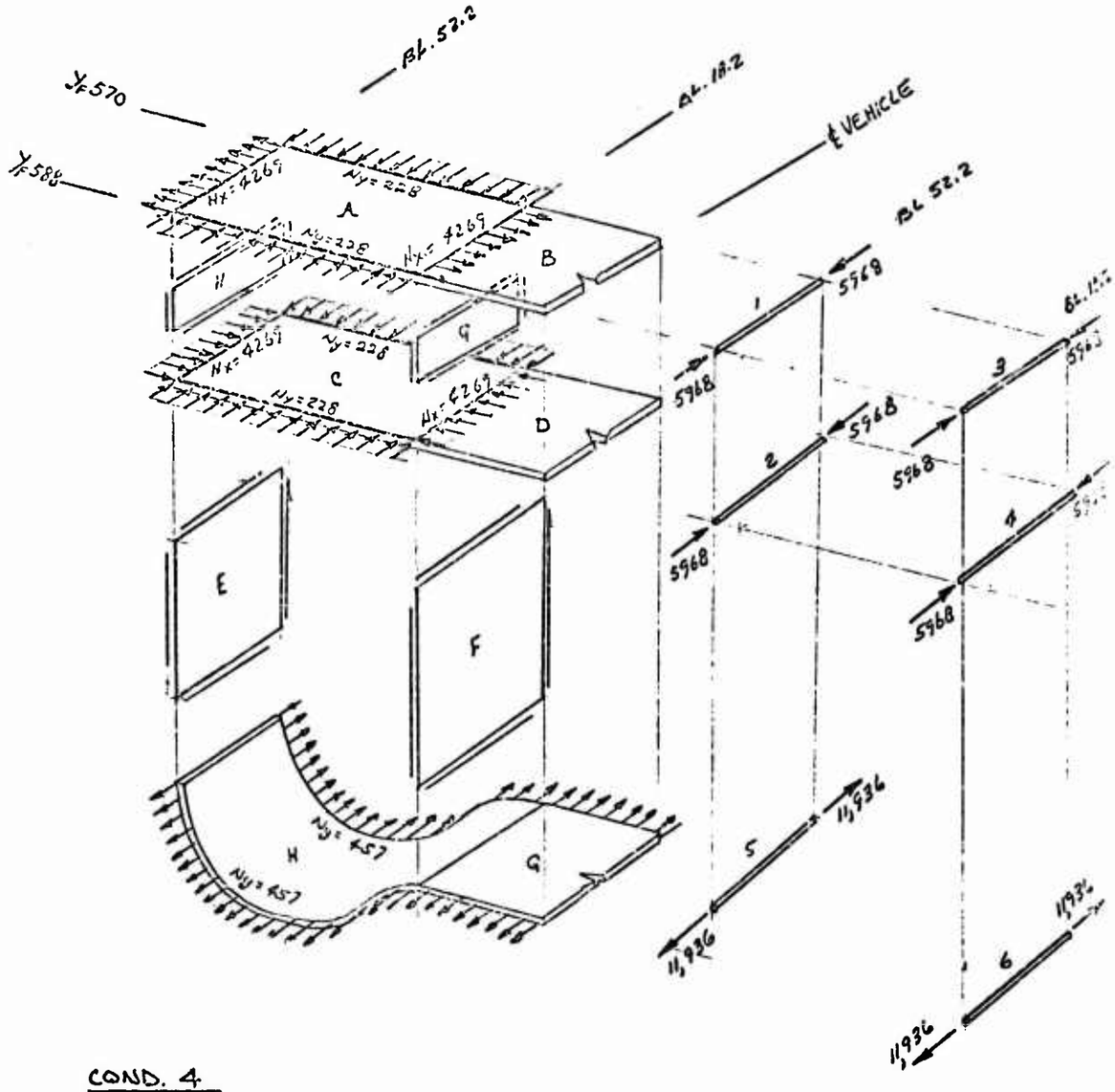

Figure 124. Wing center section honeycomb panel analysis (cont).

PANEL A & B

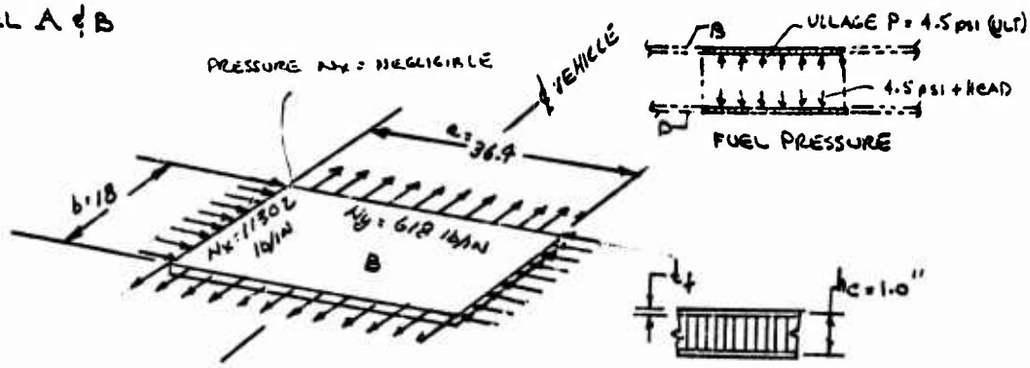

MAT'L ~

FACESHEETS - GRAPHITE/EPOXY (HTS)

$[0_4/\pm 45_1/90_4]_s$

CORE - GRAPHITE FABRIC
(USE MRP VALUES)

CHECK FOR FUEL PRESSURE OF 4.5 PSI (ULT) (NO HEAD DUE TO - N_z)
FOR PANEL NORMAL LOAD BENDING

$a/b = 36.4/18 = 2.02$

$Mom_{MAX} = M_y = K_{myPo}(P)(b)^2$ $\qquad K_{myPo} = .110$

$= .110(4.5)(324) = 160.4$ in-lbs/in (ULT)

For $h_c = 1.0"$ $N_{y\,PRESS} = \frac{160.4}{1.0} = \pm 160.4$ lbs/in/in (ULT)

$M_x = K_{MxPo}(P)(b)^2$ $\qquad K_{MxPo} = .0465$

$= .0465(4.5)(324) = 67.8$ in-lbs/in (ULT)

For $h_c = 1.0"$ $N_{x\,PRESS} = \frac{67.8}{1.0} = \pm 67.8$ lbs/in/in ULT

USE $[0_4^{40}]\,[\pm 45_1^{20}]\,[90_4^{40}]_s$

Assume $t_f = .10$ in (BASED ON WING BENDING COND 1 AT 200°F)

$f_y = 160.4/.10 = 1600$ psi ULT (LOW)

Figure 124. Wing center section honeycomb panel analysis (cont).

PANEL A & B

FUEL PRESSURE CHECK FOR

1 (g) INFLIGHT REFUEL AT RT.

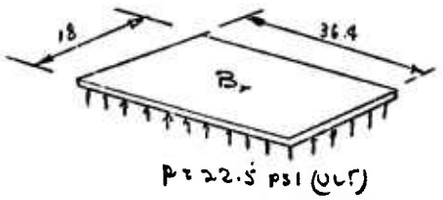

φ = 15.0 PSI LIMIT = 22.50 PSI ULT

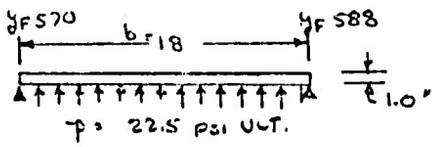

a/b = 2.02

MAX → $mom_{max} = K_{m_y p_o}(p)(b)^2 = .110(22.5)(18)^2 = 8,015.$ IN-lbs/IN (LIMIT)
12 03 IN-lbs/IN (ULT)

$mom_{MAX} \quad K_{m_x p_o}(p)(b)^2 = .0465(22.5)(324) =$ 339.0 IN-lbs/IN (LIMIT)
509. IN-lbs/IN (ULT)

MAX → $q = K_{q_y p_o}(p)(b) = .47(22.5)(18) =$ 190.4 lbs (LIMIT)
285.5 lbs (ULT)

$K_{q_x p_o}(p)(b) = .37(22.5)(18) =$ 149.9 lbs (LIMIT)
224.8 lbs (ULT)

FOR h_c = 1.0 IN. t_f .010 TEMP = R.T.

$N_y = \frac{1203}{1.0} =$ 12 03 lbs/IN/IN (ULT) $\quad f_y = \frac{1203}{.10} =$ 12,030 psi (ULT

$N_x = \frac{5085}{1.0} =$ 509 lbs/IN/IN (ULT) $\quad f_{mx} = \frac{509}{.10} =$ 5,090 psi (ULT

USING $[0_4 / \pm 45_4 / 90_4]_s$ GRAPHITE/EPOXY AT RT. FOR 1 (g) LOAD

(40% 0° / 40% ±45° / 20% 90°)

$f_y^{TU} =$ 74000 PSI AT RT.

$$m.s = \frac{74000}{12,030} - 1 = 5.15 \text{ HIGH}$$

Figure 124. Wing center section honeycomb panel analysis (cont).

PANEL A & B

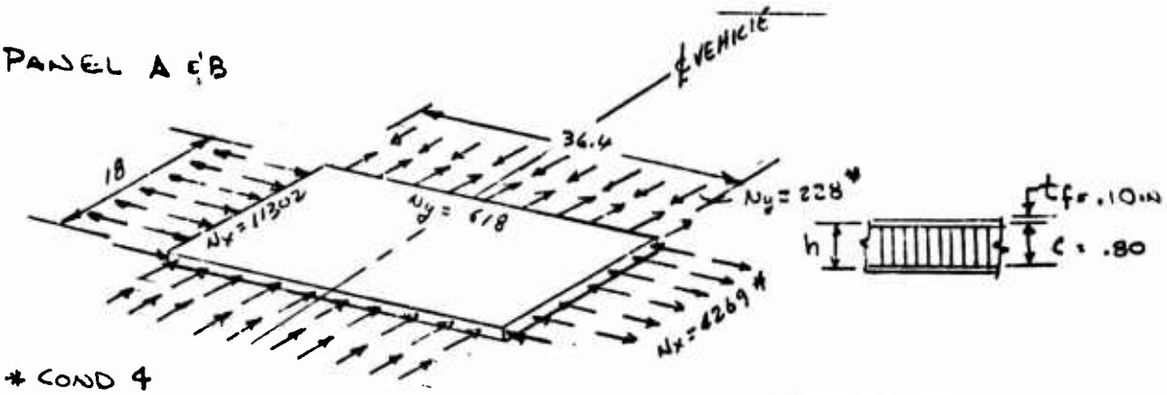

* COND 4

CRITICAL LOADING CONDITION

COND 1

N_x/N_y = 11302/618 = 18.3

CHECK FOR UNIDIRECTIONAL LOAD N_x ONLY

INITIAL THICKNESS FOR STRENGTH (COMP)

$$t_f = \frac{N_x}{2(F_x^{cu})} = \frac{11302}{2(78000)} = .073$$

USE t_f = .10 (FOR LAYUP)

CHECK FOR PANEL STABILITY (COND. 1)

N_x = 11302 lb/in. UNIDIRECTIONAL (COMP)

S.S. EDGES

h = 1.0 IN

a/b = 36.4/18 = 2.02

FACESHEET PROPERTIES

t_f = .10

$$\alpha = \sqrt{E_x/E_y} = \sqrt{10.1\times10^6/10.1\times10^6} = 1.0$$

$$\psi = \sqrt{E_x E_y}/(1-N_{xy}\nu_{yx}) = 10.1\times10^6/1-(.123\times.123) = \frac{1.0}{.98} = 10.3\times10^6$$

CORE PROPERTIES

c = .80 in (4.5 PCF. 5052 AL.)

(G'_{cy}/G'_{cx}) = 1.00

G'_{cx} = 31,000 (TEMP RED.)

= 31000 (.85) = 26,000 PSI

FACESHEETS
GRAPHITE/EPOXY (HTS)

$[0_4 / \pm 45_4 / 90_4]_s$
40% 20% 40%

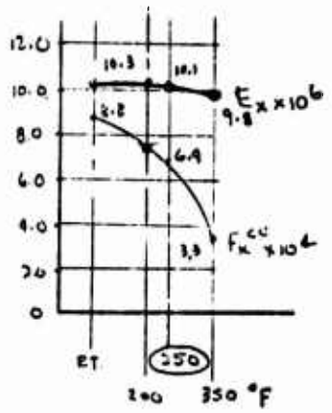

E_x = 10.1 x 10^6

F_x^{co} = 78,000

AT 200°F

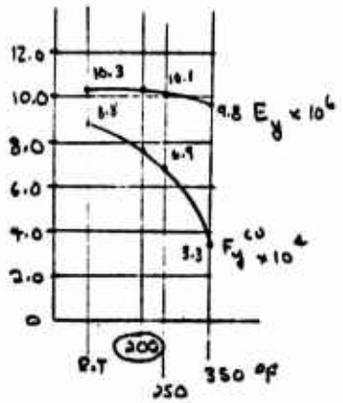

E_y = 10.1

F_y^{co} = 78,000

AT 200 °F

Figure 124. Wing center section honeycomb panel analysis (cont).

$b/c = 18/.80 = 22.5$

$t_f/c = .10/.8 = .125$

FROM FIG. 1

$V G'_{cx}/\psi = 0.0014$

$$V = \frac{(0.0014)(10.3\times10^{6})}{2,6.0\times10^{3}} = \frac{1.4\times10.3}{26} = .55$$

FROM FIG. 2

$b/a \quad 18/36.4 = .49$

$V = .55,$

$\psi = 10.3\times10^{6}$

$K_x \cong 1.75$

$$(N_x)_{CR} = \frac{K_x \pi^2 \psi t_f c(c+t_f)}{2b^2}$$

$$= \frac{(1.75)(\pi^2)(10.3\times10^{6})(.10)(.80)(.80+.10)}{2(18)^2}$$

(.08) (.90)

C48

$N_{x_{CR}} = 1.75(11300) = 19775 \text{ lb/in}$

$$M.S. = \frac{19775}{11,302} - 1 = \underline{+.75}$$

REDUCE CORE DEPTH TO $c = .55 \quad h = .75$

Figure 124. Wing center section honeycomb panel analysis (cont).

CHECK FOR

$c = .55$ IN.

$b/c = 18/.55 = 32.73$

$t_f/c = .10/.55 = .182$

FROM FIG. 1

$V G'_{cx}/\psi = .008$

$$V = \frac{(0.0008 \times 10.3 \times 10^6)}{26.0 \times 10^3} = .32$$

FROM FIG. 2

$b/a = 18/36.4 = .49$

$V = .32$

$\psi = 10.3 \times 10^6$

$K_x \cong 2.75$

$$N_{x_{cr}} = \frac{2.75(\pi^2)(10.3 \times 10^6)(.10)(.55)(.55 + .10)}{2(18)^2}$$

$= 15{,}420$ lbs/in.

$$m.s. = \frac{15{,}420}{11302} - 1 = \underline{+ .36}$$

FACESHEETS $t_f = .10$ $[0_4 / \pm 45_2 / 90_4]_s$

CORE 4.5 PCF. $G = 26{,}000$

CORE SHEAR CRIMPING

$$F_{cs} = G'_c \frac{(c + 2t_f)}{2t_f} = \frac{26\,000(.55 + 2(.10)}{2(.1)}$$

$= 97500$ PSI USE $F_x^{cu} = 78\,000$

$$m.s = \frac{78000}{56\,520} - 1 = \underline{+ .38}$$

Figure 124. Wing center section honeycomb panel analysis (cont).

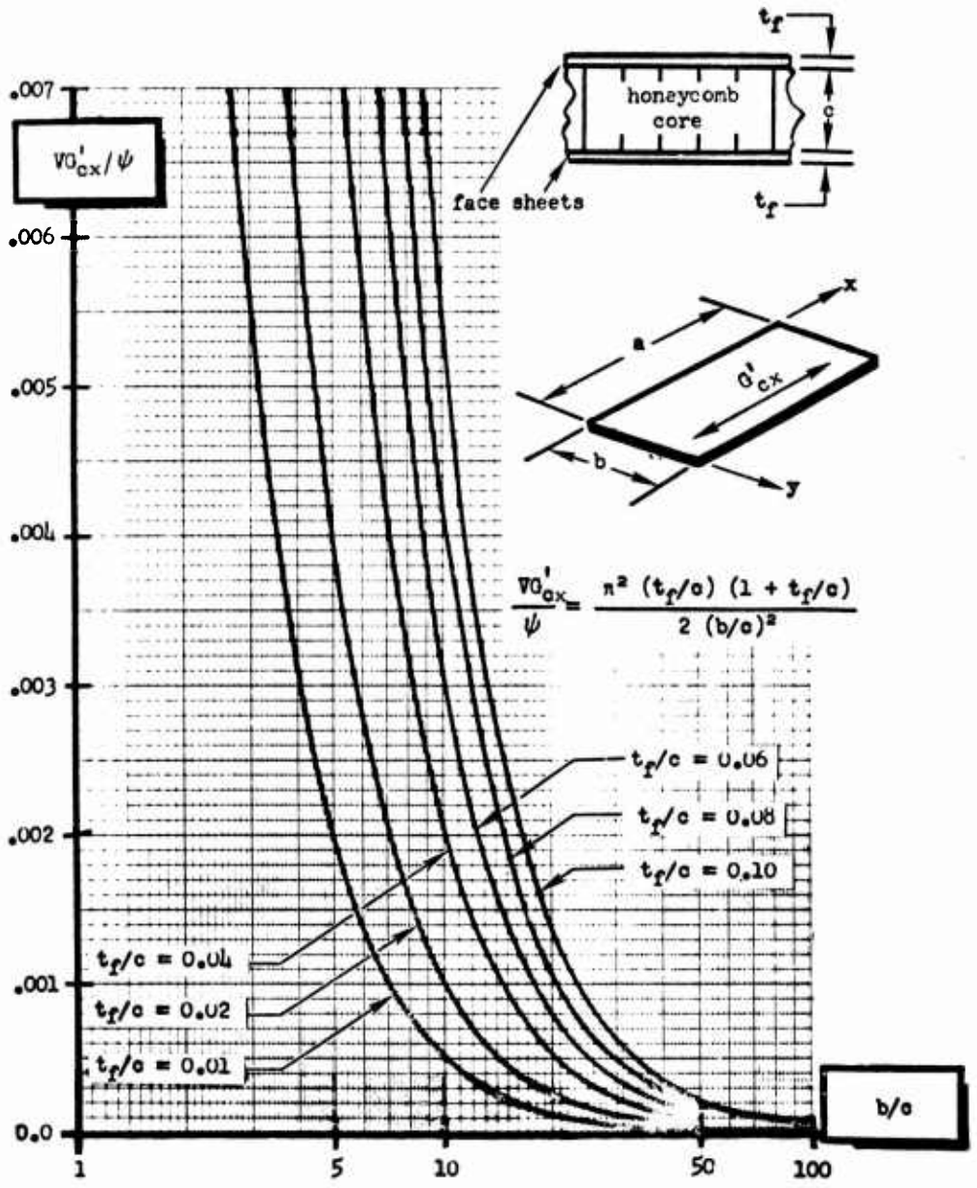

SHEAR STIFFNESS PARAMETER V VERSUS GEOMETRY
FOR HONEYCOMB SANDWICH PANELS

Figure 124. Wing center section honeycomb panel analysis (cont).

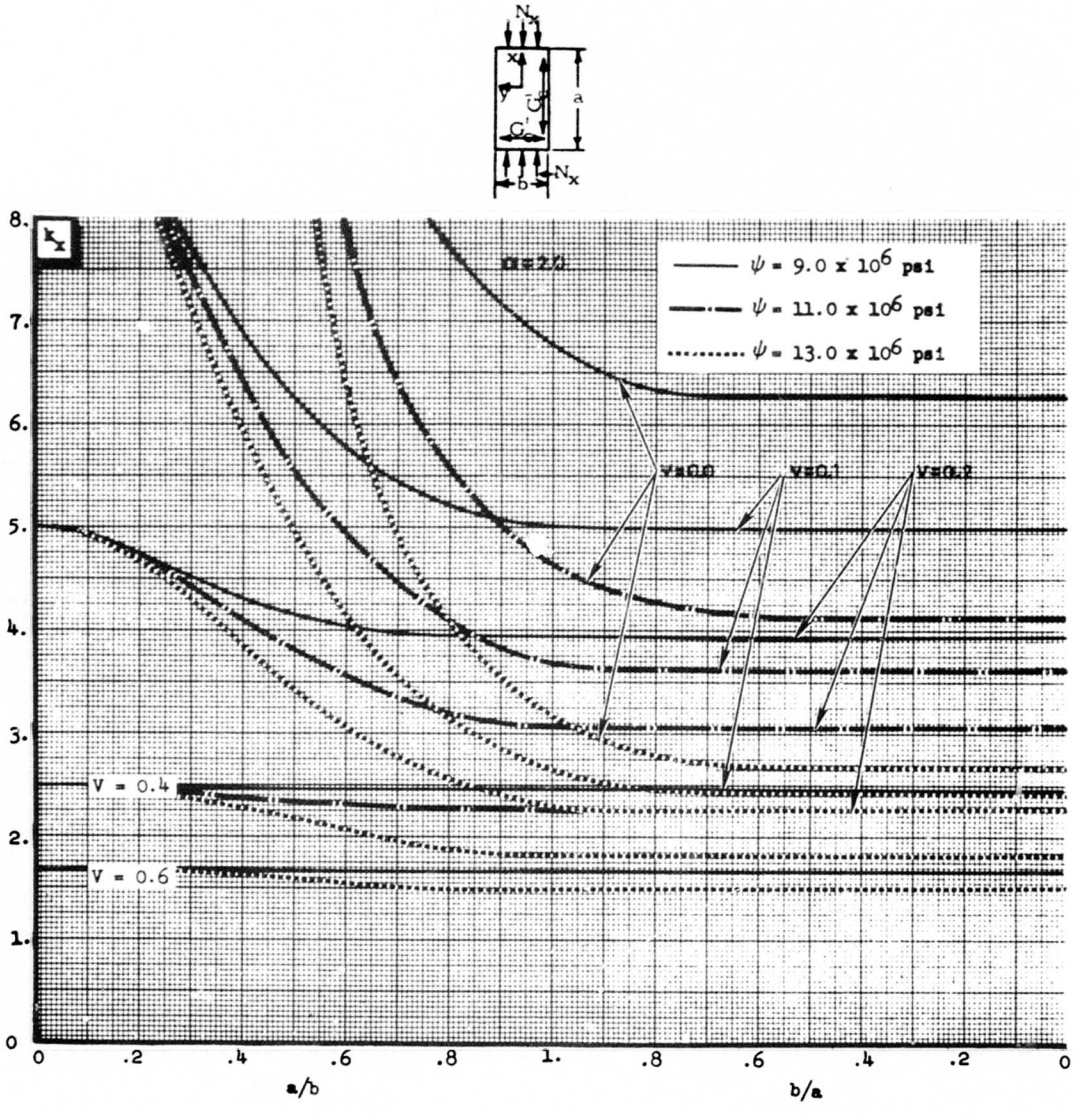

BUCKLING COEFFICIENT FOR SIMPLY SUPPORTED FLAT SANDWICH PANELS, α = 1.0, $G'_{cy} = G'_{cx}$

Figure 124. Wing center section honeycomb panel analysis (cont).

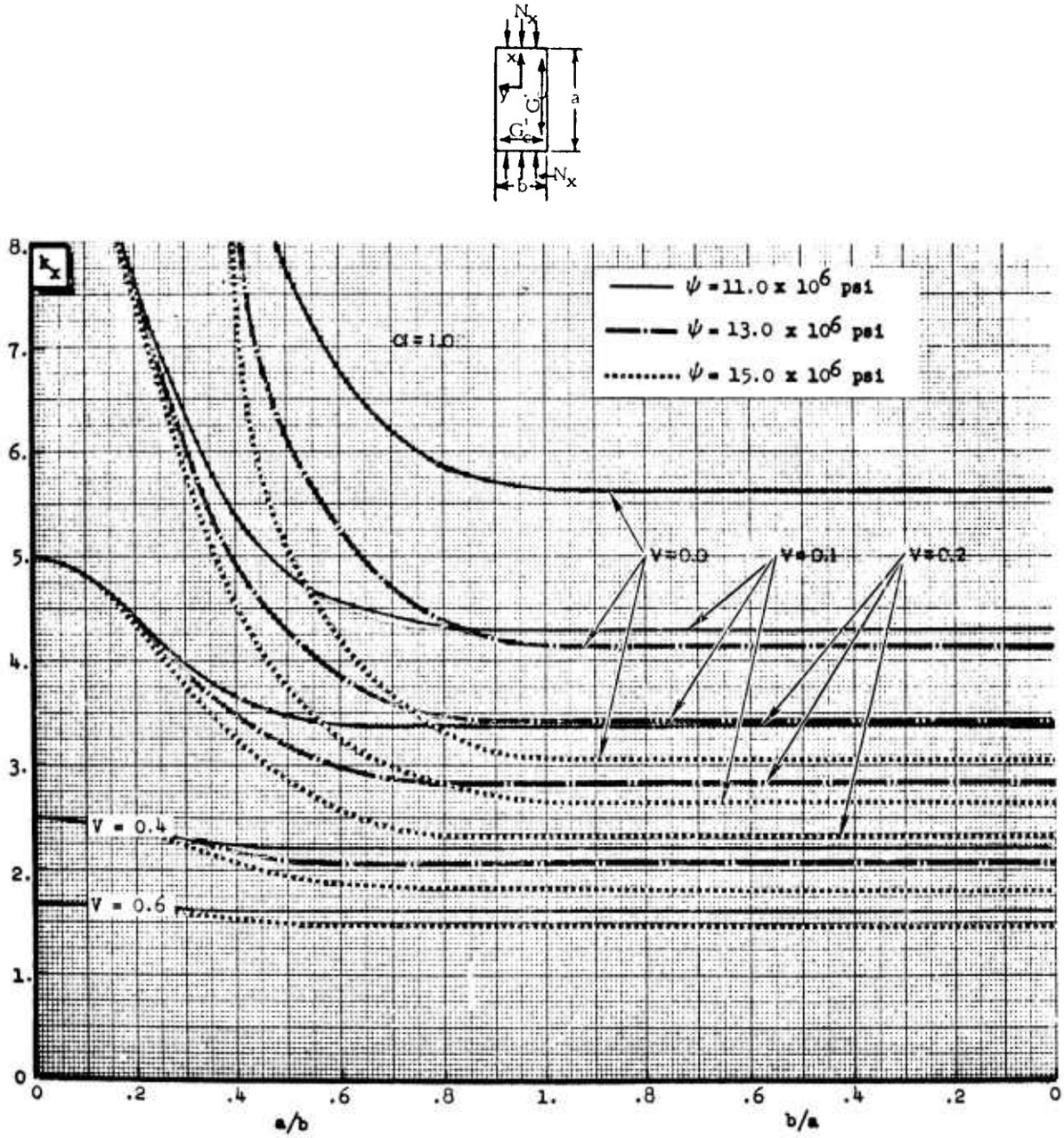

BUCKLING COEFFICIENT FOR SIMPLY SUPPORTED FLAT SANDWICH PANELS, α = 2.0, G'_{cx}

Figure 124. Wing center section honeycomb panel analysis (cont).

PANEL "C" & D

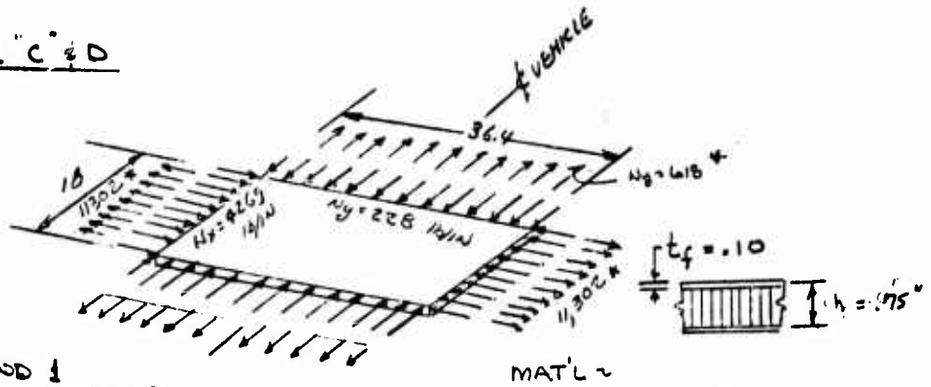

* COND 1
CRITICAL LOADING
COND. 4 N_x = 4269 lb/in (comp)
$N_x/N_y = \frac{4269}{228} = 18.72$
CHECK FOR UNIDIRECTIONAL LOAD N_x only
h_c = 1.0 in.

MAT'L ~
FACESHEETS ~ GRAPHITE/EPOXY (HTS)
$[0_4 / \pm 45_1 / 90]_s$
CORE ~ GRAPHITE FABRIC
(USE HMP VALUES)

STRENGTH CHECK FOR CRITICAL TENSION LOADING. COND 1
*COND 1 N_x = 11,302 lb/in. (TENS) INITIAL

$$t_{f_{REQ'D}} = \frac{N_x}{2(F_x^{tu})} = \frac{11,302}{2(79,000)} = .072 \text{ in.}$$

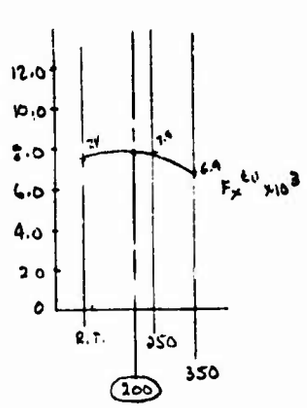

F_x^{tu} = 79,000 psi
AT 200°F

CHECK FOR PANEL STABILITY (COND 4)
N_x = 4269 lb/in (UNIDIRECTIONAL COMP)
S.S EDGES
h = .75 t_f = 1.0
a/b = 36.4/18 = 2.02

M.S. BASED ON PANEL A & B STABILITY

$$M.S. = \frac{15,420}{4269} - 1 = \underline{+ 2.6}$$

$$M.S._{TENSION} \quad \frac{15800}{11302} - 1 = \underline{+ .39}$$

Figure 124. Wing center section honeycomb panel analysis (cont).

PANELS G & H

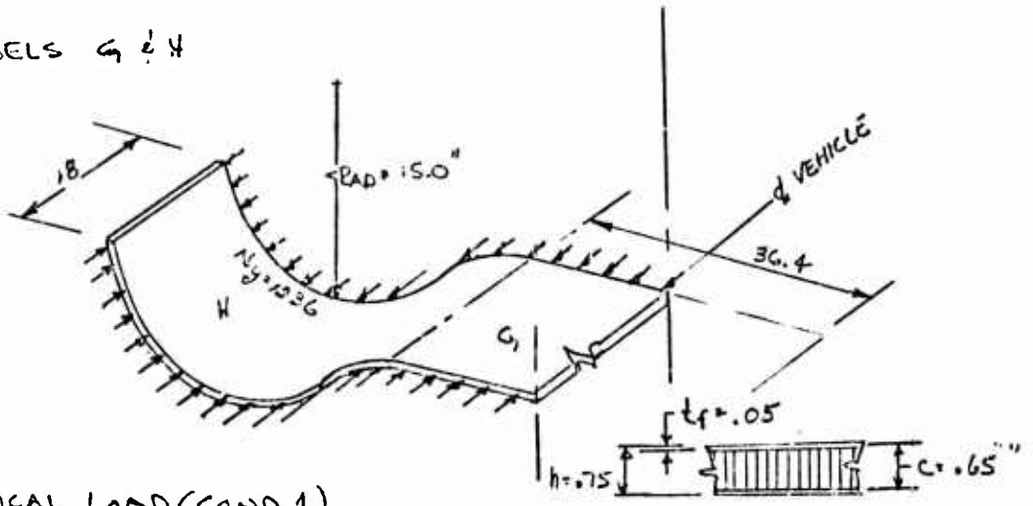

CRITICAL LOAD (COND 1)

N_x = .1236 lb/in (ULT)

MAT'L -

FACESHEETS - GRAPHITE/EPOXY (HTS)

$[0_2 / \pm 45_3 / 90_2]_S$

40% +45% 20%

CHECK PANEL "G" FOR STABILITY

t_f = .12(.005) = .05

FLAT PANEL, SS. EDGES

N_x = 1236 lb/in (ULT) COMP.-UNIDIRECTIONAL

a/b = 36.4/18 = 2.02

h = .75

CORE - GRAPHITE FABRIC (USE ALUM. VAL.) 4.5 PCF.

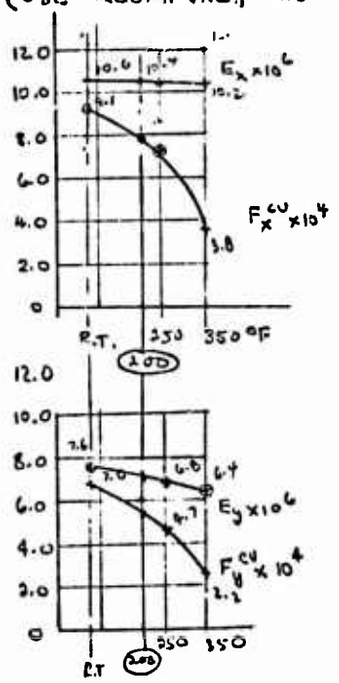

FACESHEET PROPERTIES

t_f = .05

$\psi = \sqrt{E_x E_y} / (1 - \nu_{xy}\nu_{yx}) = \sqrt{10.5 \times 10^6 \times 7 \times 10^6} / (1 - .314 \times .062) = 8.5 \times 10^6 / .938 = \underline{9.06 \times 10^6}$

$\alpha = \sqrt{E_x / E_y}$, 1.225

CORE PROPERTIES

$c = h - 2t_f = .75 - .10 = .65$

4.5 PCF (5052 AL PROPERTIES)

$G'_{cy} / G'_{cx} = 1.0$

$G'_{cx} = 31.0 \times 10^3 (.85) = 26000$ PSI

Figure 124. Wing center section honeycomb panel analysis (cont).

$b/c = 18/.65 = 27.7$

$t_f/c = .077$

FROM FIG. 1

$$\gamma G'_{tx}/\psi = .0005$$

$$\gamma = \frac{(0.0005)(9.06\times10^6)}{26.0\times10^3} = .174$$

FROM FIG. 3

FOR $b/c = 18/36.4 = .49$

$\gamma = .174$

$\psi = 9.06\times10^6$

$K_x = 3.9$ (CONSERV.)

$$N_{x_{CR}} = \frac{K_x \pi^2 \psi t_f e (c + t_f)}{2b^2}$$

$$= \frac{3.9(\pi^2)(9.06\times10^6)(.05)(.65)(.65+.05)}{2(18)^2}$$

$$= 12{,}233 \text{ lb/in}$$

$$M.S. = \frac{12{,}233}{1236} - 1 = +8.90 \quad \underline{\text{HIGH}}$$

REDUCE t_f to .025 $\quad [0_2/\pm45_1/90_1]_T$

Figure 124. Wing center section honeycomb panel analysis (cont).

REDUCE t_f TO .025 $[0_2 / \pm 45_1 / 90_1]_T$
h TO .50

$b/c = 18/.45 = 40.0$

$t_f/c = .025/.45 = .056$

FROM FIG. 1

$V G'_{cx} / \psi = .00015$

$V = \frac{(.00015)(9.06 \times 10^6)}{26.0 \times 10^3} = .053$

FROM FIG. 3

FOR $b/c = .49$

$V = .053$

$\psi = 9.06$

$K_x = 5.25$ (CONSERV.)

$$N_{x_{CR}} = \frac{5.25(\pi^2)(9.06 \times 10^6)(.025)(.45)(.45+.025)}{648}$$

$= 3770$ lb/in

$$M.S. = \frac{3770}{1236} - 1 = + 2.05$$

CORE SHEAR CRIMPING.

$$F_{cs} = \frac{G'_c (c + 2t_f)}{2 t_f}$$

$$= \frac{26000 (.45 + 2(.025)}{2(.025)} = 260{,}000 \text{ PSI}$$

CUT OFF AT $F_x^{cu} = 78000$

$$M.S. = \frac{78000}{49{,}440} - 1 = + .58$$

Figure 124. Wing center section honeycomb panel analysis (cont).

PANEL H

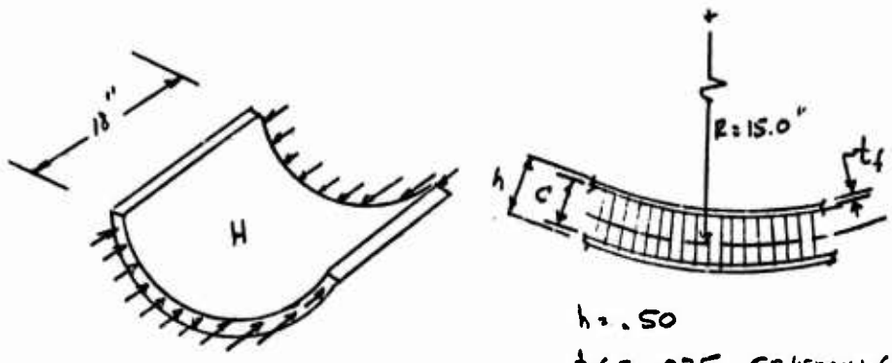

h = .50

t_f = .025 GR/EPOXY (HTS)

$[0_2/\pm 45_1/0_1]_T$

CORE =

C = 4.5 4.5 PCF (ALUM EQIV.)

$$\sigma_{cr\,rc} = h/R\left[E_x E_y / (1 - \mu_{xy}\nu_{yx})\right]^{1/2}$$

$$= \frac{.50}{15}\left[(10.5\times10^6)(7.0\times10^6) / (1 - .32\times.2)\right]^{1/2}$$

$$= .033\left[78.36\times10^{12}\right]^{1/2}$$

$$= .033\,(8.85\times10^6) = 292{,}120 \text{ PSI.}$$

CUT OFF AT $F_x^{cu} = 78{,}000$

$$M.S. = \frac{78000}{49{,}440} - 1 = \underline{+ .58}$$

Figure 124. Wing center section honeycomb panel analysis (concl).

TABLE 24. WING CENTER SECTION HONEYCOMB PANEL COVER t

STA No.	LOAD AXIS STATION FUS. STA.	B. PLANE	TRIAL THICKNESS UPPER	LWR	UPPER COVER 0°	+45°	-45°	90°	LOWER COVER 0°	+45°	-45°	90°	CORE THICKNESS
			MULTI-SPAR H/C PANELS										
			18" SPAR SPACING TORQUE BOX WT= 1372 LBS/AC										
1	552	33	.13	.13	12	6	6	2	12	6	6	2	1.0
2	558.3	52.2	.13	.12	12	6	6	2	10	6	6	2	
3	562.8	65.3	.15	.15	12	8	8	2	12	8	8	2	
4	568.1	81.5	.18	.17	14	10	10	2	12	10	10	2	
5	573.5	97.7	.19	.18	16	10	10	2	14	10	10	2	
6	578.9	113.8	.18	.17	18	8	8	2	16	8	8	2	
NOTE ALL WEIGHTS QUOTED ARE PER AIRCRAFT													
			MULTI-SPAR H/C PANELS										
			18" SPAR SPACING TORQUE BOX WT= 1239 LBS./AC										
1			.13	.13	12	6	6	2	12	6	6	2	0.75
2			.13	.12	12	6	6	2	10	6	6	2	
3			.15	.14	12	8	8	2	10	8	8	2	
4			.16	.15	16	8	8	2	12	8	8	2	
5			.19	.18	16	10	10	2	14	10	10	2	
6			.17	.17	16	8	8	2	16	8	8	2	
			MULTI-SPAR H/C PANELS										
			18" SPAR SPACING TORQUE BOX WT= 1117 LBS/AC										
1			.13	.11	12	6	6	2	12	4	4	2	0.50
2			.13	.10	12	6	6	2	10	4	4	2	
3			.13	.12	12	6	6	2	10	6	6	2	
4			.16	.15	14	8	8	2	12	8	8	2	
5			.18	.18	14	10	10	2	14	10	10	2	
6			.17	.14	16	8	8	2	14	16	6	2	
			MULTI-SPAR H/C PANELS										
			13" SPAR SPACING TORQUE BOX WT= 1175 LBS/AC										
1			.13	.12	12	6	6	2	10	6	6	2	0.50
2			.13	.12	12	6	6	2	10	6	6	2	
3			.13	.12	12	6	6	2	10	6	6	2	
4			.15	.15	12	8	8	2	12	8	8	2	
5			.18	.18	14	10	10	2	14	10	10	2	
6			.17	.16	16	8	8	2	14	8	8	2	

REV. 12-64

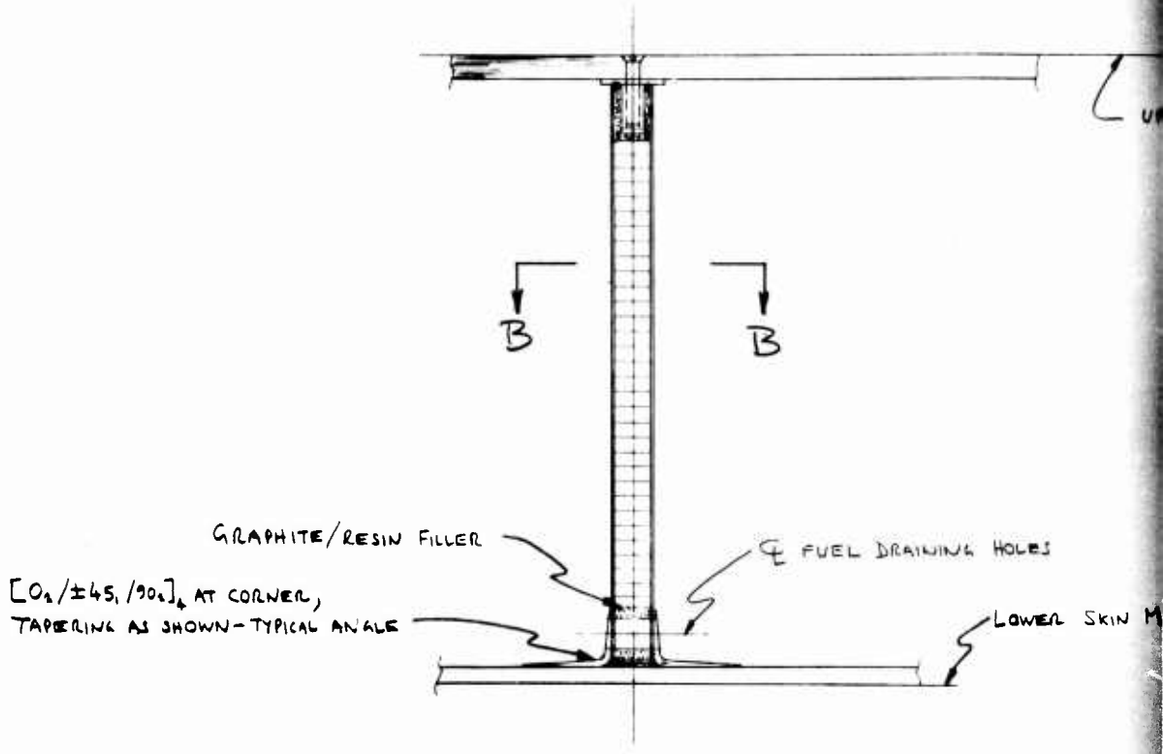

SECTION A-A
(FULL SIZE)

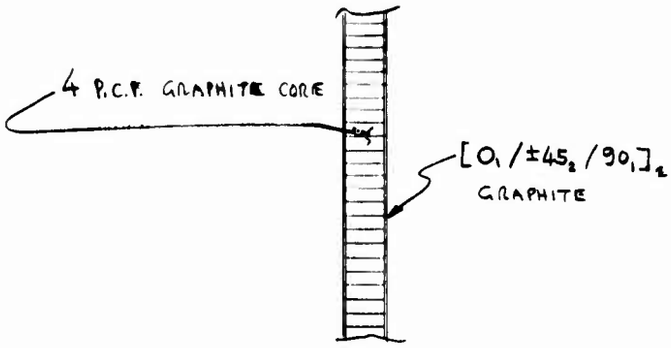

SECTION B-B
FULL SIZE

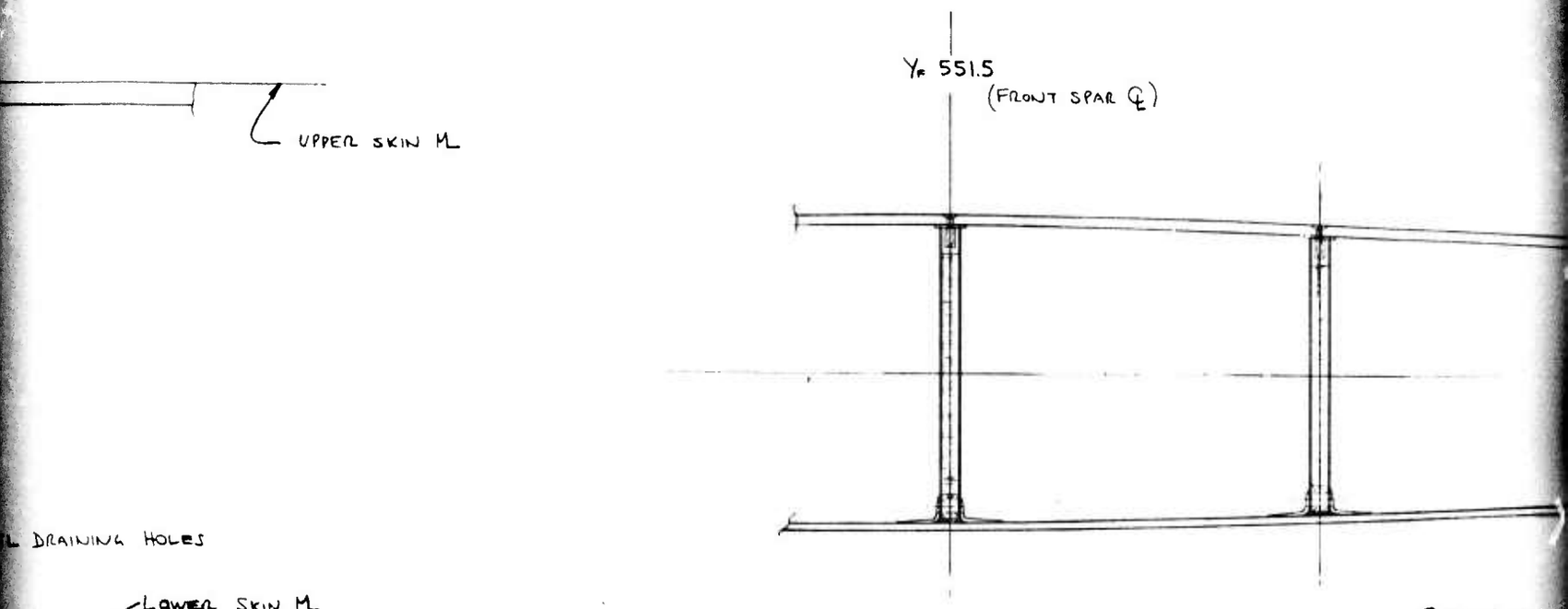

SECTION
VIEW LOOKIN
(1/2 SI

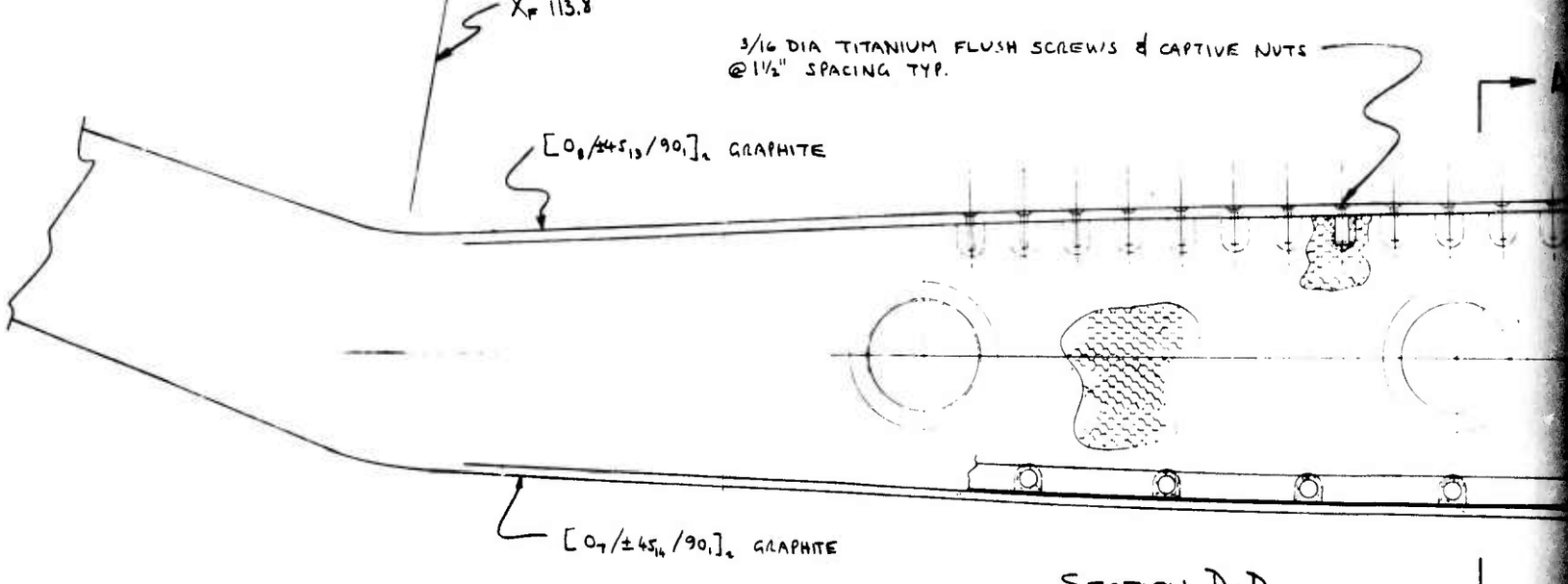

SECTION D-D

A

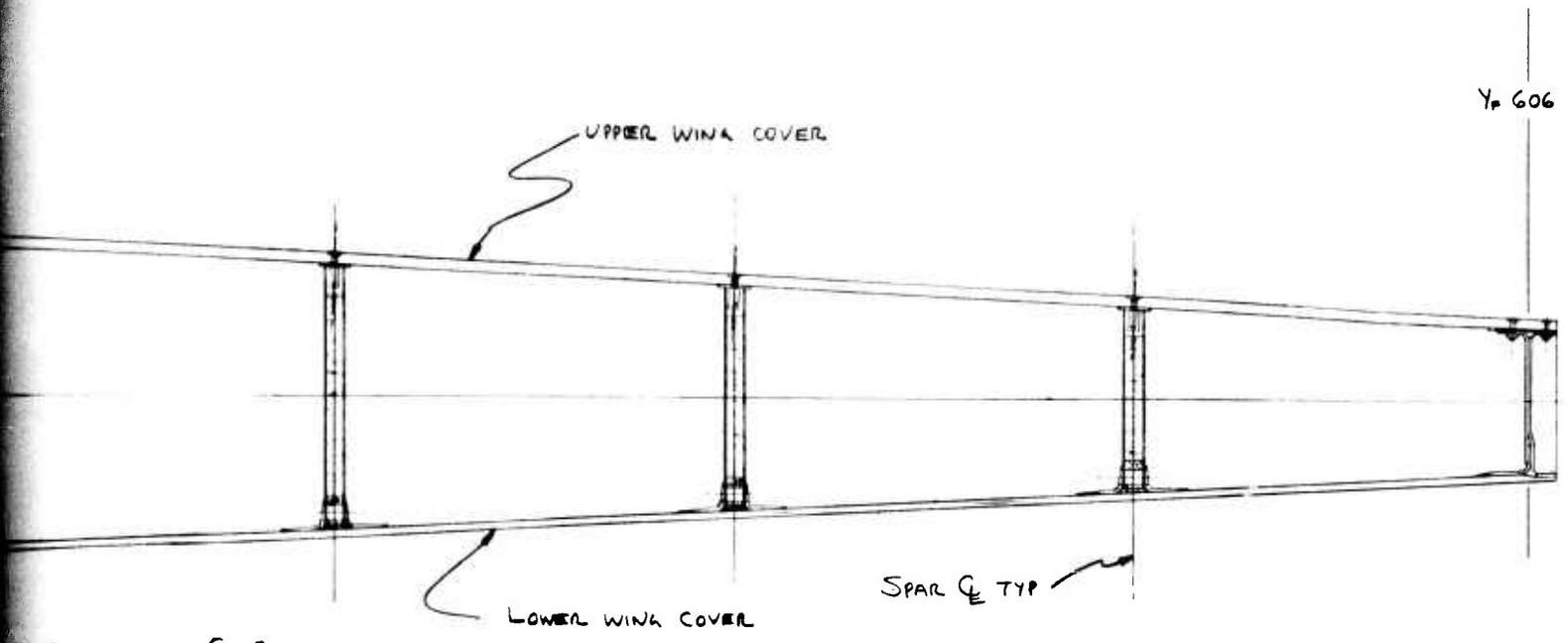

SECTION C-C
EW LOOKING INBD.
(1/2 SIZE)

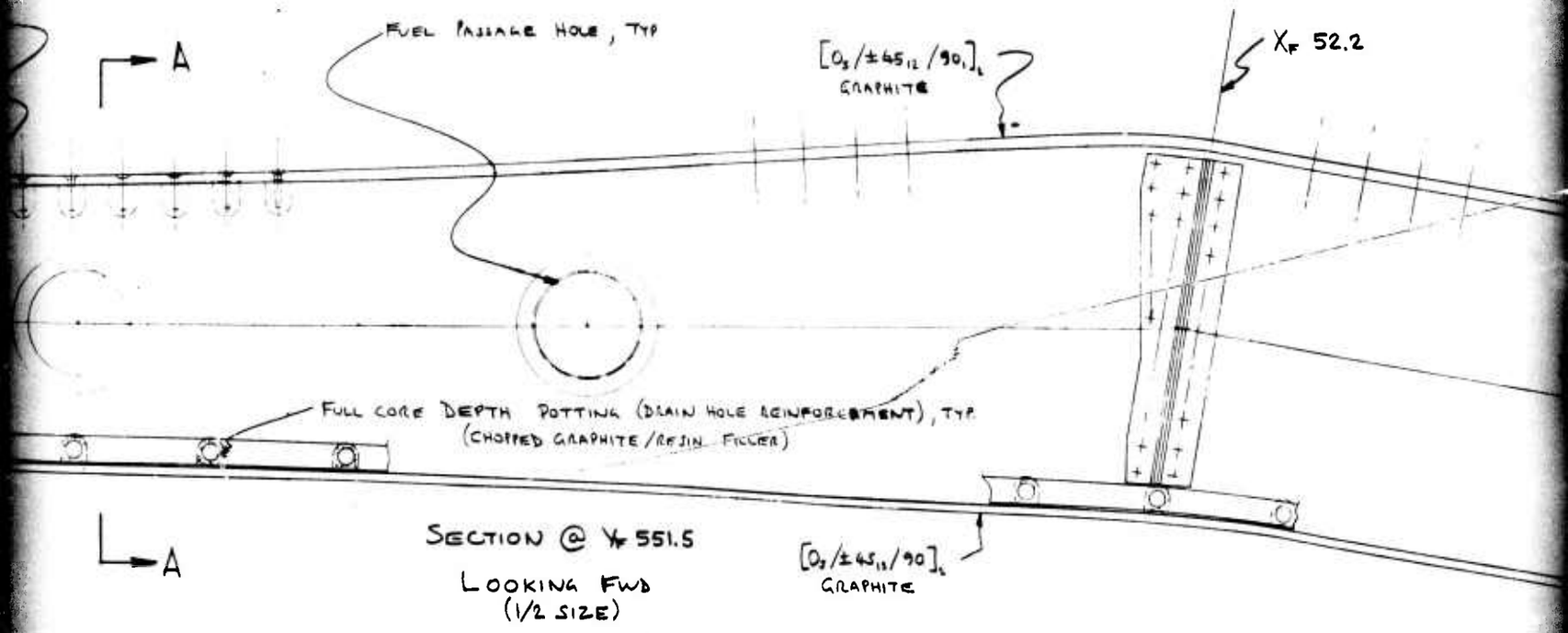

SECTION @ Y_F 551.5
LOOKING FWD
(1/2 SIZE)

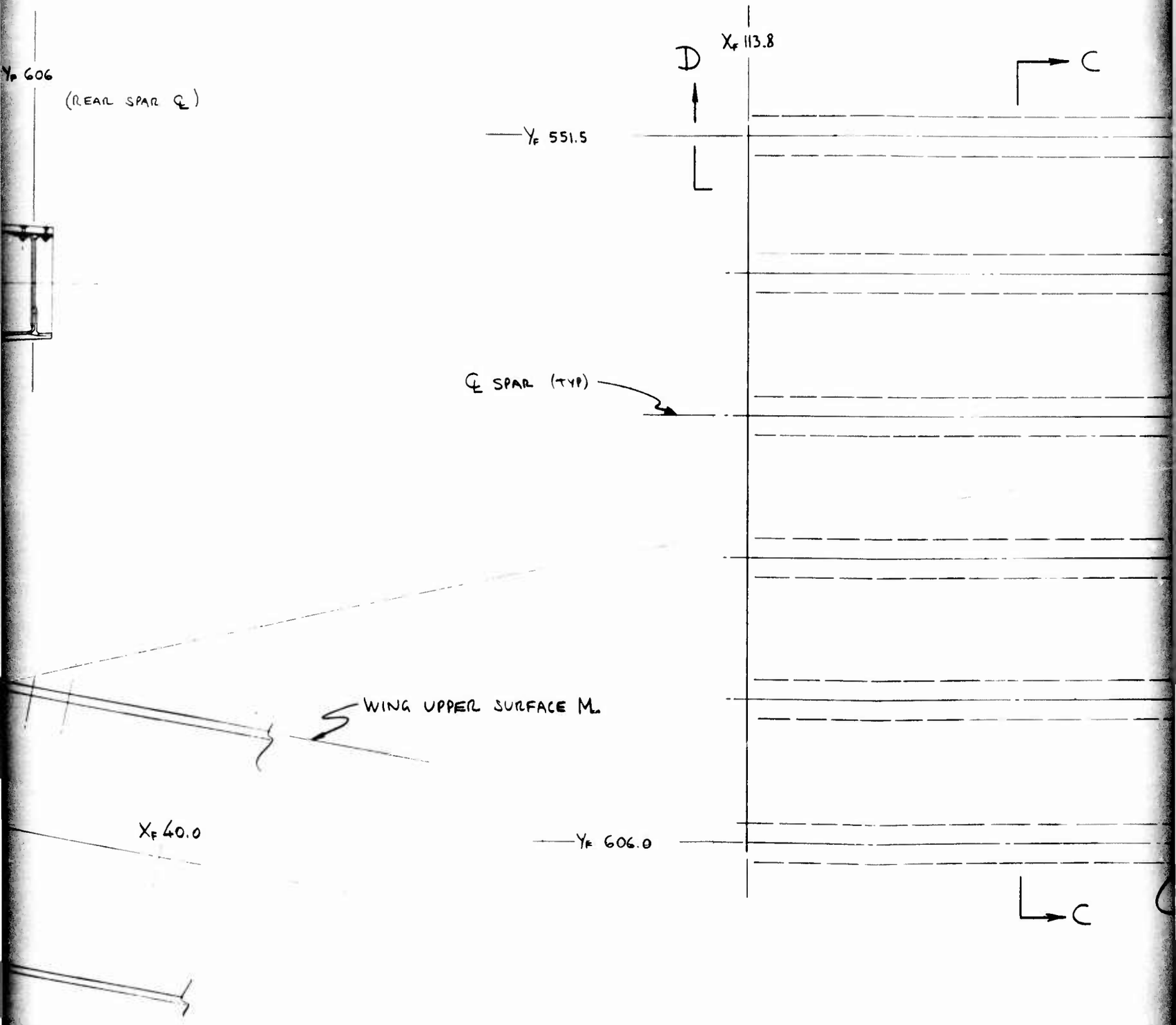
Y_F 606
(REAR SPAR ℄)
X_F 113.8
D
C
Y_F 551.5
L
℄ SPAR (TYP)
WING UPPER SURFACE ML
X_F 40.0
Y_F 606.0
C

4

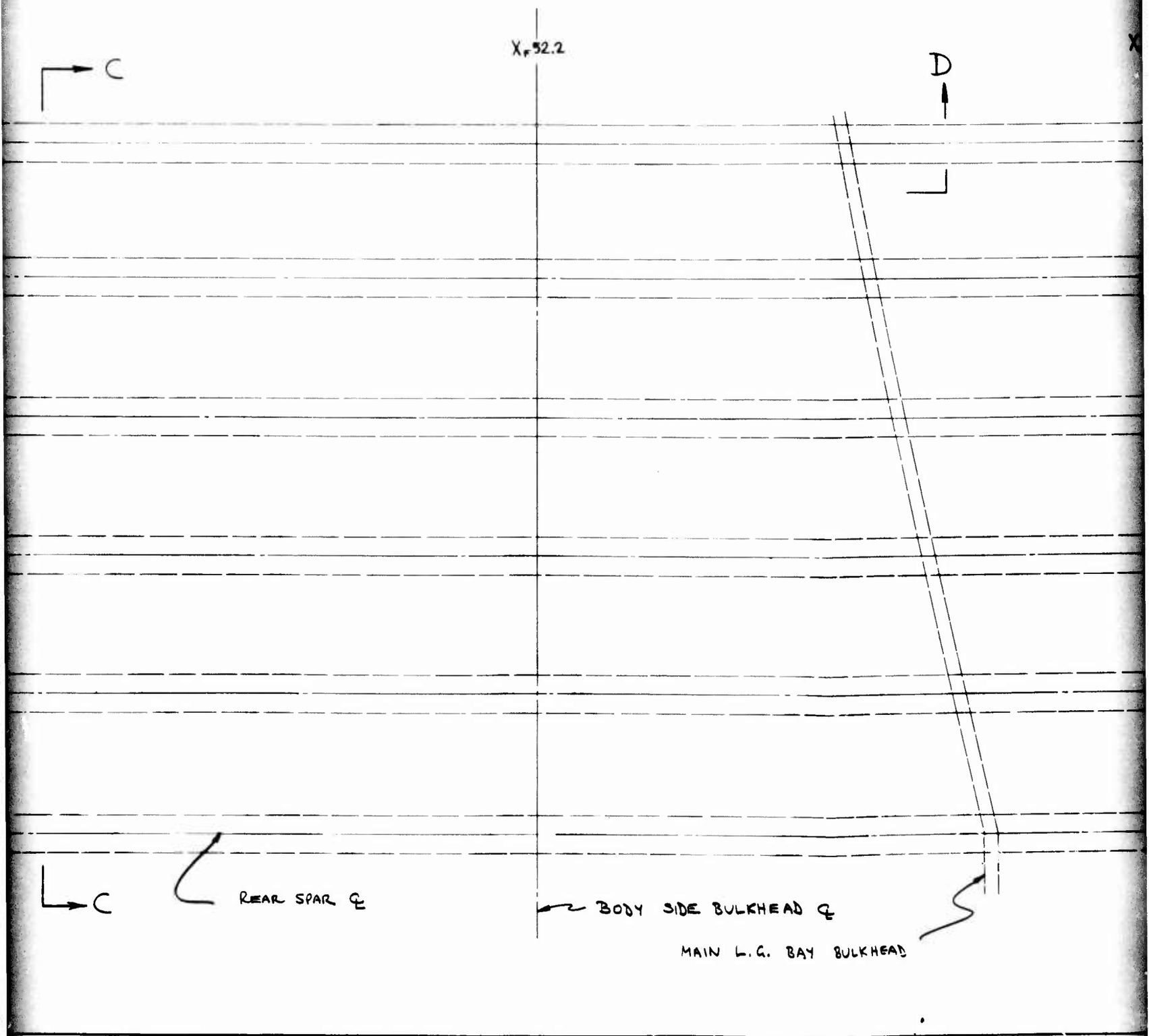

Fig

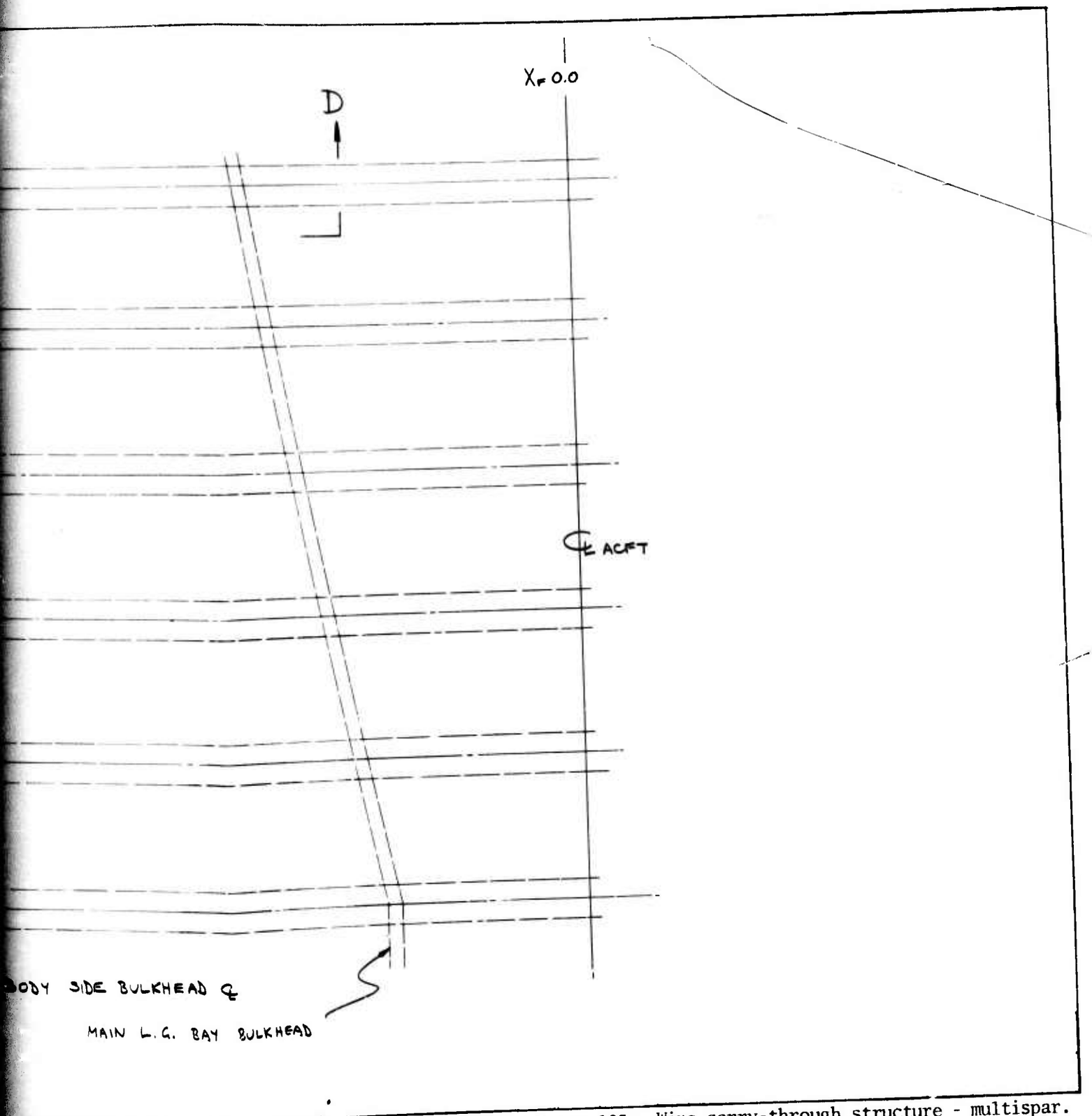

Figure 125. Wing carry-through structure - multispar.

6

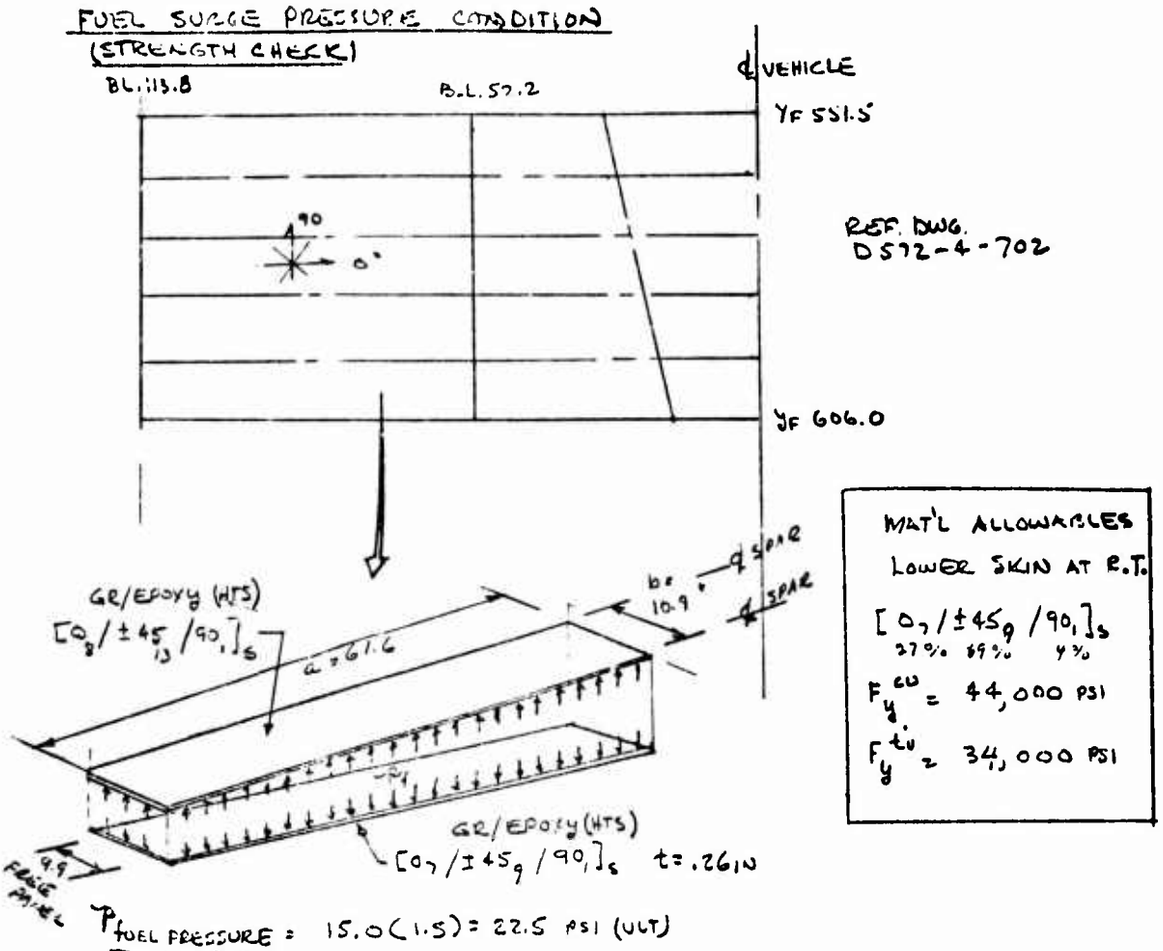

$P_{\text{FUEL PRESSURE}} = 15.0(1.5) = 22.5$ PSI (ULT)

TEMP = R.T.

CHECK LOWER SKIN PANEL FOR SURGE PRESS.

$a/b = 61.6/9.9 = 6.2$ (S.S. EDGES)

$t_1 = 52(.005) = .26$ IN

$$Mom_{MAX} = K_{myp_o} P(b)^2$$

$$= .125(22.5)(9.9)^2 = 275 \text{ IN-lbs}$$

USING PLATE BENDING

$$f_{b_y} = \frac{6m}{t^2} = \frac{6(275)}{(.26)^2} = 24{,}408 \text{ PSI}$$

$$M.S = \frac{34{,}000}{24{,}408} - 1 = \underline{+.39}$$

Figure 126. Multispar wing carry-through analysis.

TABLE 25. WING CARRY-THROUGH MULTISPAR PLATE SKINS WEIGHTS

AIRCRAFT; WNG CARRY-THRU MLLTI-SPAR FLATE SKINS

AIRCRAFT WEIGHTS - IN POUNDS

	AL	TI	SI	BC	GR	EG	SA	TOTAL
FUSELAGE	78.	171.	69.	C.	2086.	27.	0.	3236.
FRAME/LONG	C.	171.	69.	C.	695.	0.	0.	935.
SKIN-STRGR	78.	0.	0.	C.	C.	0.	0.	78.
BOND HONEY	C.	0.	C.	C.	1391.	27.	0.	1418.
BRAZE HONEY		C.	0.				0.	0.
DIFF BOND		C.					C.	0.
MISC								805.
WING	130.	27.	C.	C.	3105.	C.	0.	3422.
SKIN-STRGR	C.	0.	C.	C.	0.	0.	0.	0.
MULTI-SPAR	C.	27.	C.	C.	547.	0.	0.	574.
BOND HONEY	130.	0.	C.	C.	2558.	0.	0.	2688.
BRAZE HONEY		0.	C.				0.	0.
DIFF BOND		C.					0.	0.
MISC								160.
CANARDS	C.	16.	2.	C.	117.	0.	0.	145.
SKIN-STRGR	C.	0.	C.	C.	C.	0.	0.	0.
MULTI-SPAR	C.	0.	0.	C.	0.	C.	0.	0.
BOND HONEY	.	16.	2.	C.	117.	0.	0.	135.
BRAZE HONEY		0.	C.				0.	0.
DIFF BOND		0.					0.	0.
MISC								10.
NACELLE	C.	0.	C.	C.	C.	0.	0.	0.
FRAME/LONG	C.	0.	C.	C.	0.	0.	0.	0.
SKIN-STRGR	C.	0.	C.	C.	0.	0.	0.	0.
BOND HONEY	C.	0.	C.	C.	C.	0.	C.	0.
BRAZE HONEY		0.	C.				0.	0.
DIFF BOND		0.					0.	0.
MISC								0.

WEIGHT DATA - IN POUNDS	
AMPR WEIGHT	13411.
STRUCTURE WT	8C85.
STRUCTURAL HOWE WT	133.
SYSTEM HOWE WT	133.
LANDING GEAR WT	1280.
FUEL SYSTEM WT	750.
ELECTRICAL SYSTEM WT	680.
HYDRAULIC SYSTEM WT	430.
AUX POWER SYSTEM WT	310.
ECS WT	530.
CREW ACCOM WT	320.
CONTROL & DISPLAY WT	120.
FLIGHT CONTRCL WT	950.
ARMAMENT WT	560.
AICS MECHANISM WT	300.
EQUIPMENT WT	80.
ENGINE WT	5375.
EMPTY WT	19465.
FUEL WT	7C60.
TOGW	31132.

DESIGN VARIABLES	
WING AREA-SQ FT	400.
CANARDS AREA-SQ FT	35.
WETTED AREA-SQ FT	1772.
WING + HORIZ AREA	435.
WING SPAN-FT	31.6
HORIZ SPAN-FT	10.0
OVERALL LENGTH-FT	57.0
ASPECT RATIO	2.50
DYNAMIC PRESSURE	2133.

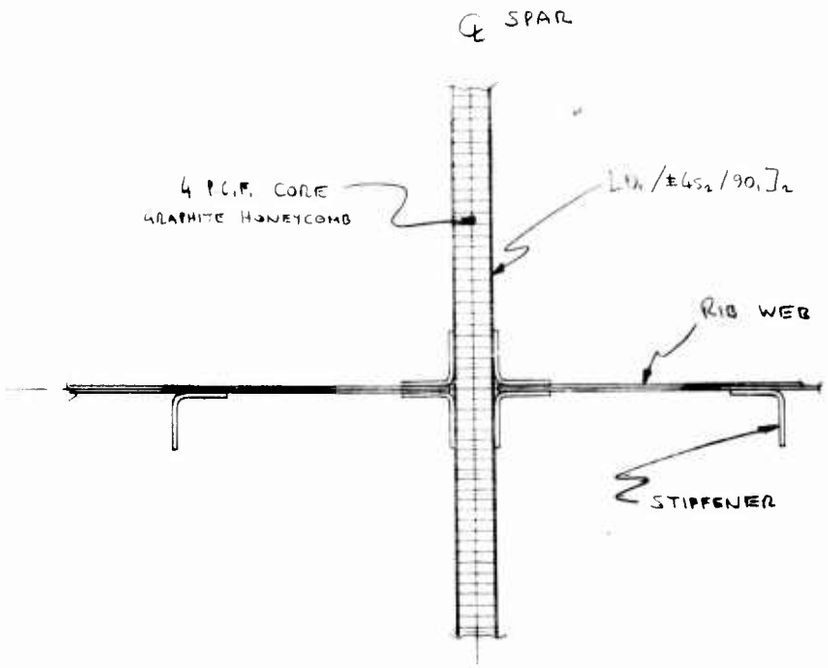

SECTION B-B
FULL SIZE

TYPICAL RIB WEB
3/4 x 3/4 ANGLE

B

SKIN

STIFFEN
TY
FULL

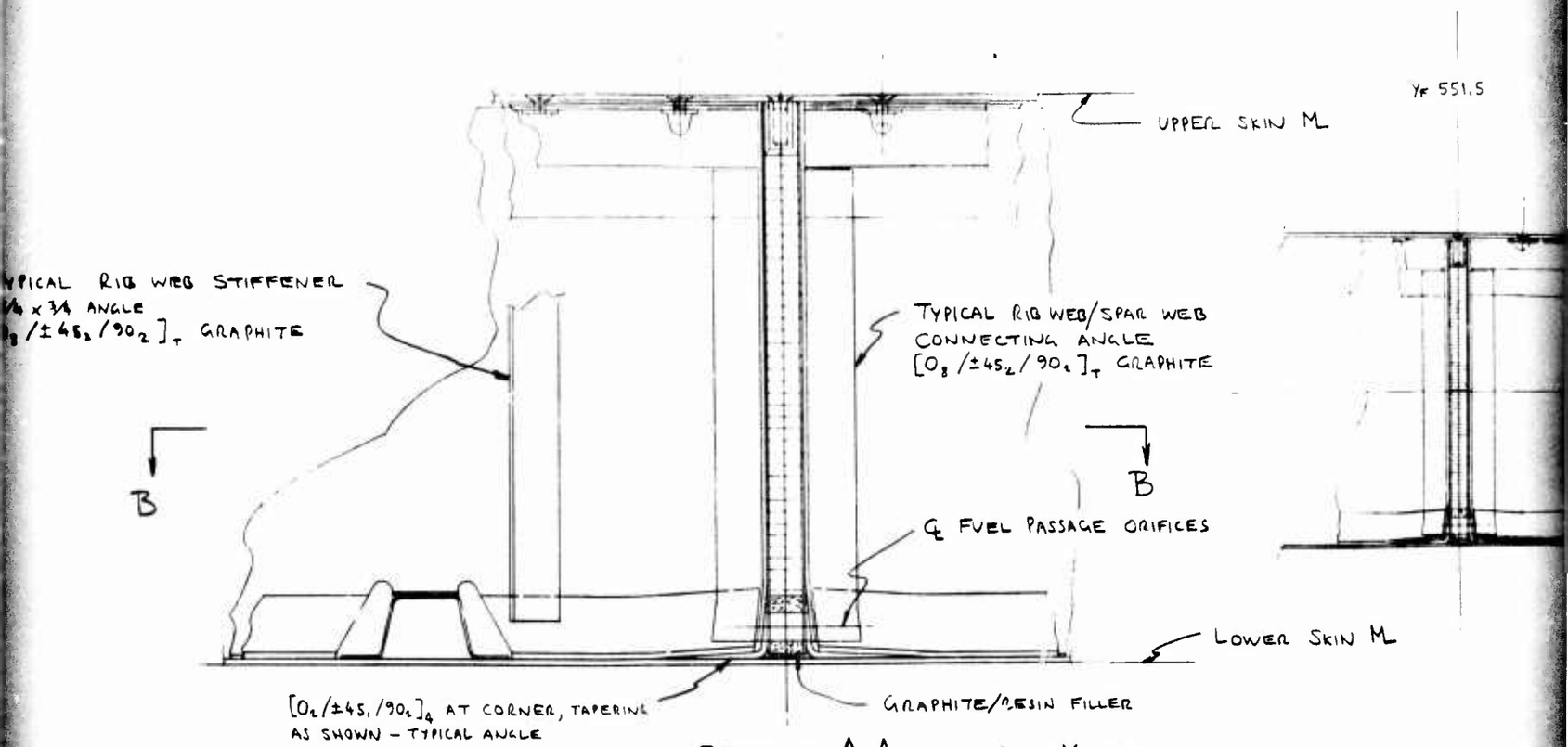

SECTION A-A
FULL SIZE

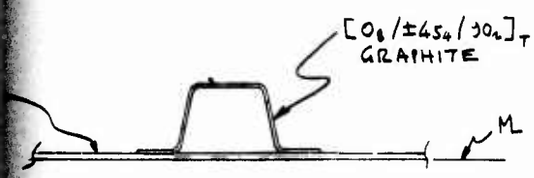

STIFFENER SECTION
TYPICAL
FULL SIZE

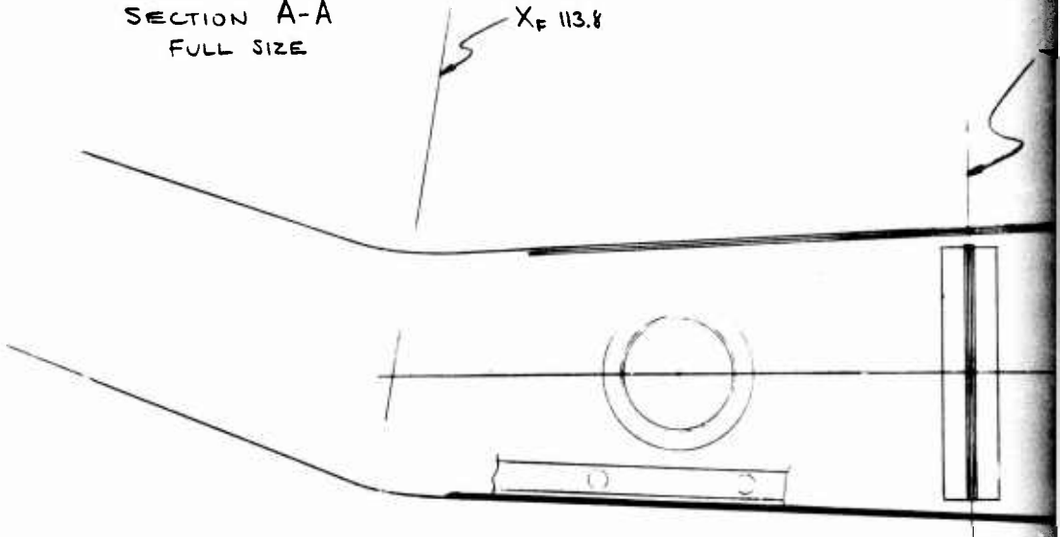

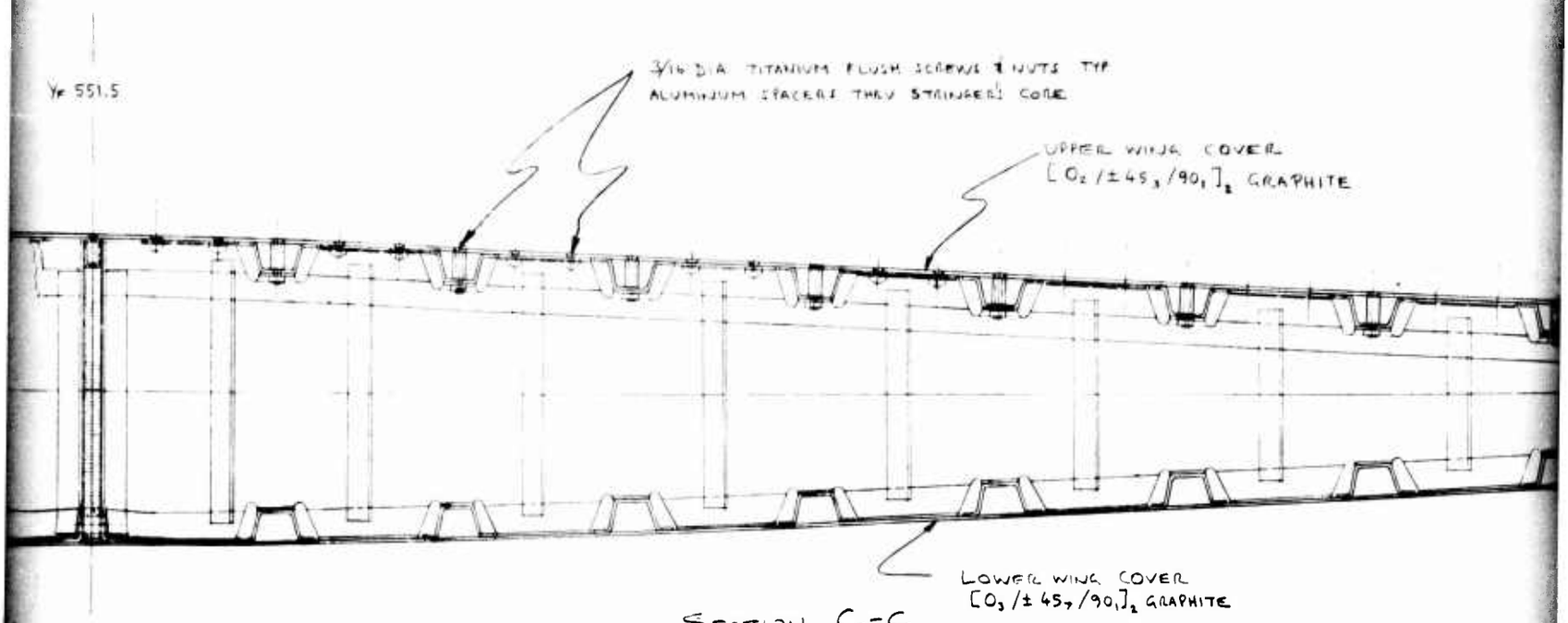

SECTION C-C
VIEW LOOKING INBD.
(1/2 SIZE)

TYPICAL RIB —

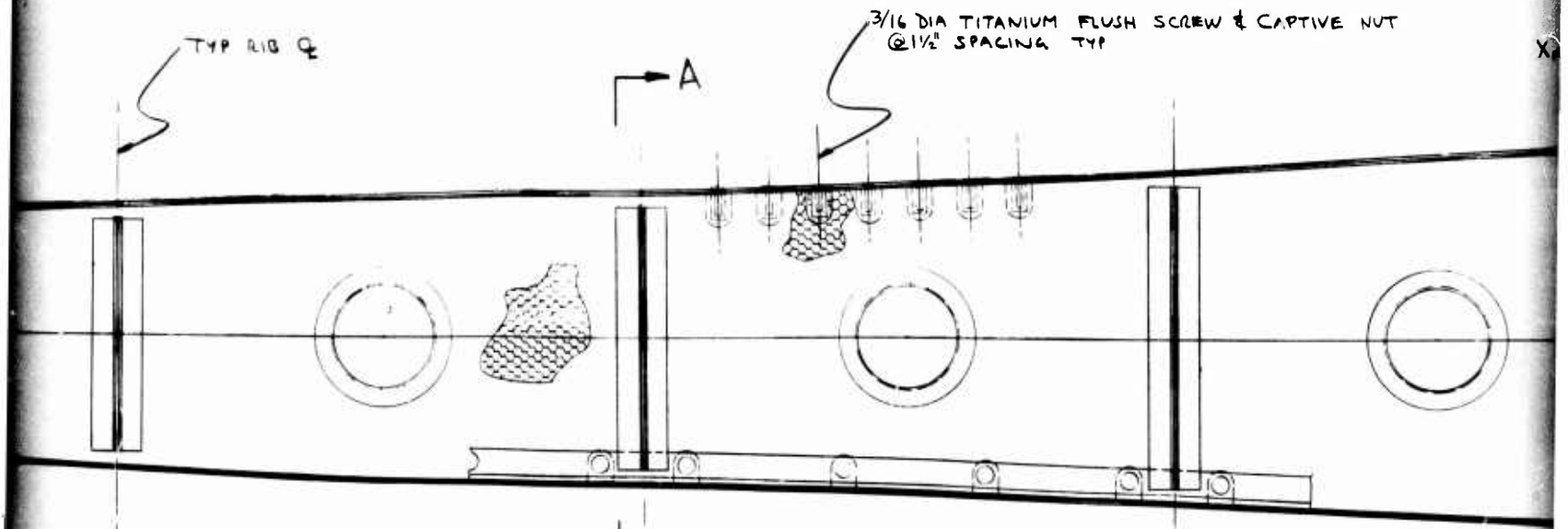

SECTION D-D

SECTION @ Yₑ 551.5
LOOKING FWD.
(1/2 SIZE)

PHITE

Y_F 606.0

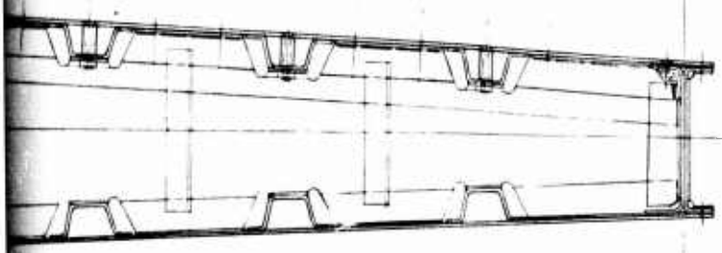

X_F 112.

D

Y_F 551.5

VE NUT

X_F 52.2

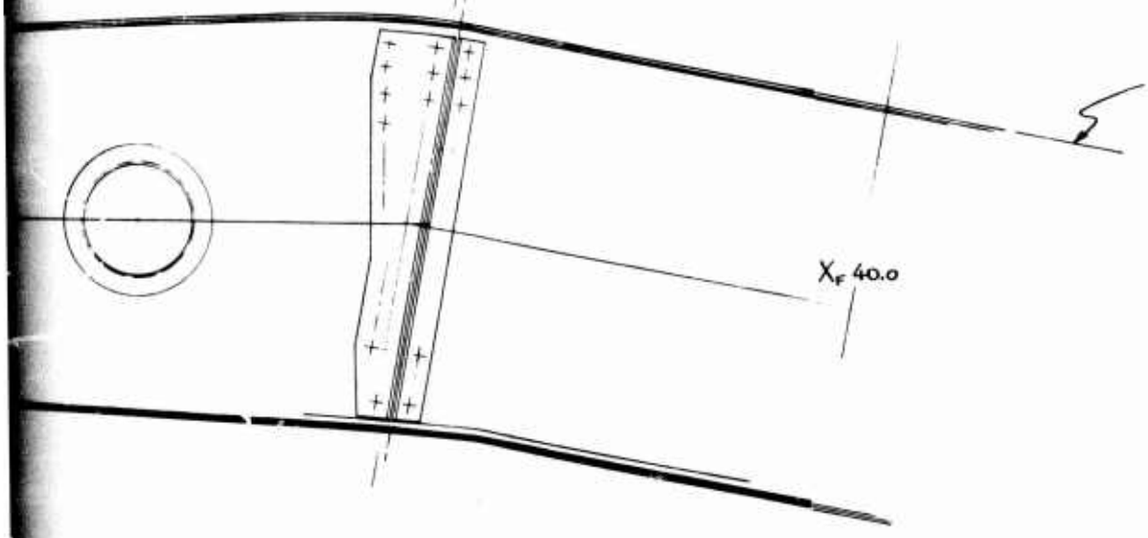

Y_F 606.0

4

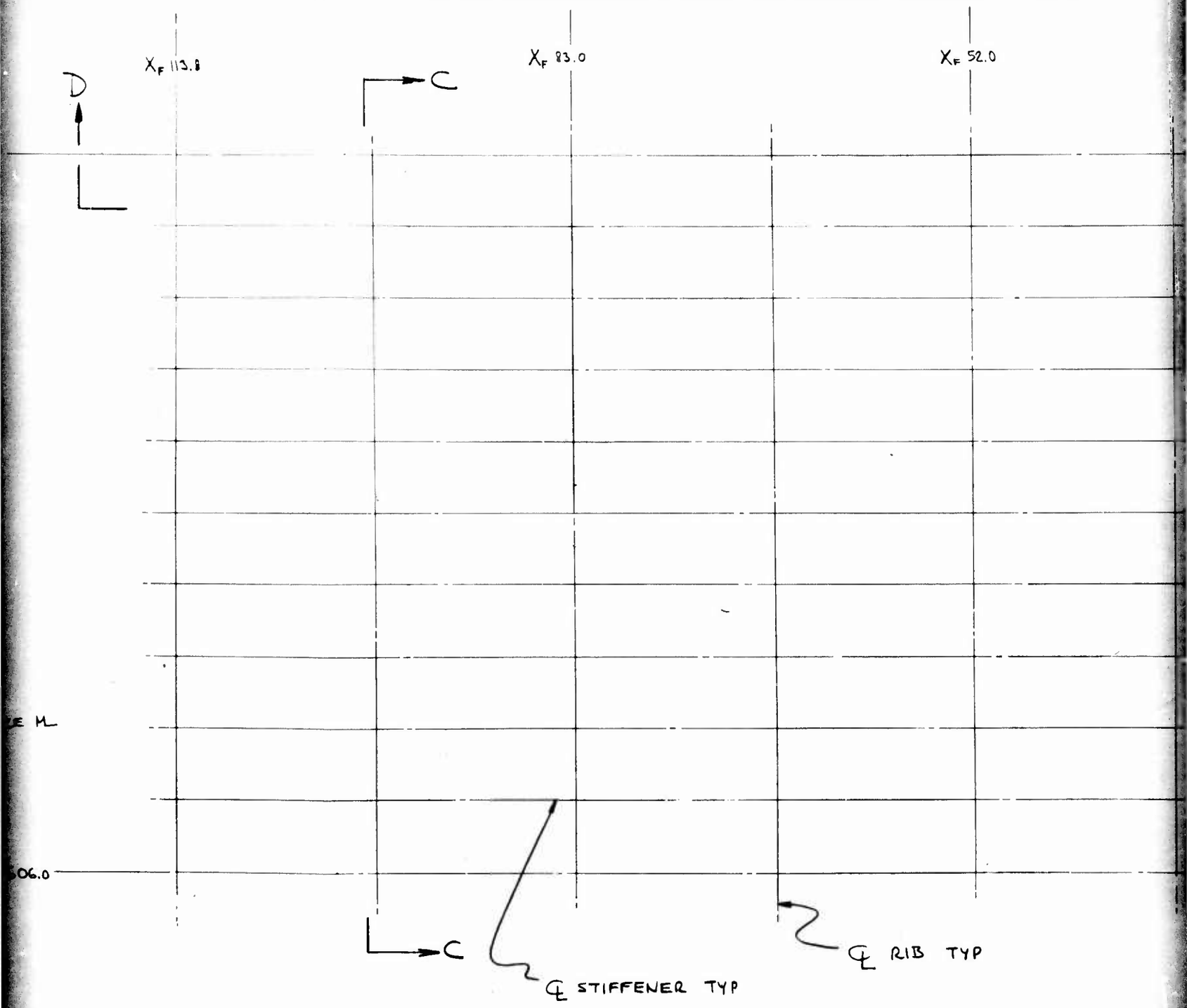

5

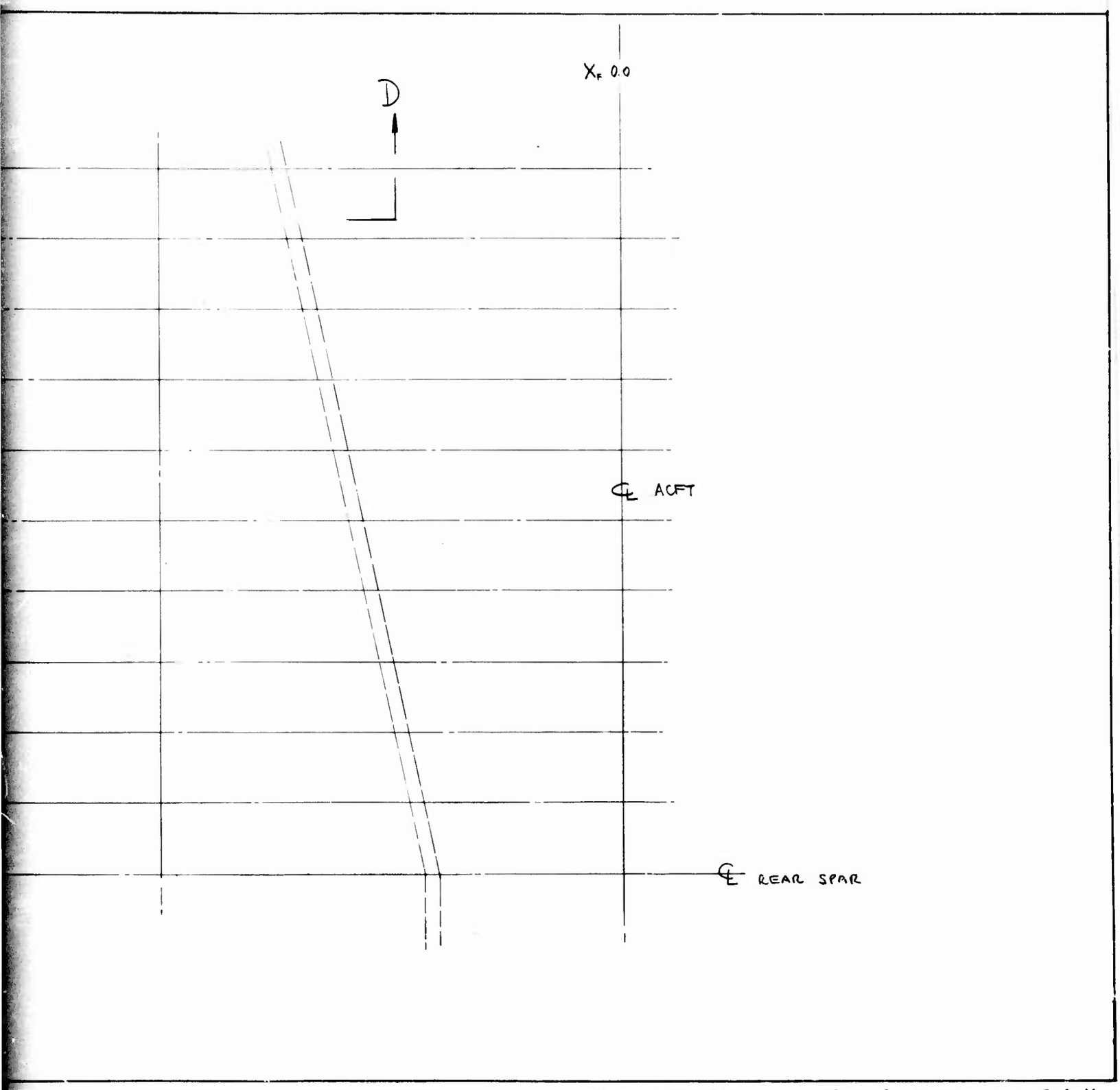

Figure 127. Wing carry-through structure - multirib.

6

TABLE 26. WING CARRY-THROUGH MULTISPAR PLATE SKINS COSTS

AIRCRAFT: WNG CARRY-THRU MULTI-SPAR PLATE SKINS
ALL COSTS IN MILLIONS AND IN 1975 DOLLARS

PRODUCTION COST FOR 300 UNITS
UNIT AVG. FLYAWAY COST 2.836

WORK BREAKDOWN STRUCTURE	LABOR COST					MATERIAL COST		TOTAL
	MFG.	TOOL.	PLNG.	ENGR.	G&A	MFG.	TOOL.	COST
TOTAL PROGRAM COST INCLUDING FEE	400.99	72.27	35.21	40.89	53.91	238.06	9.14	850.81
TOTAL PROGRAM COST INCLUDING G&A	364.54	65.70	32.01	37.18	49.01	216.42	8.31	773.49
TOTAL PROGRAM COST LESS G&A	331.91	59.82	29.15	33.85	44.62	197.05	7.57	704.29
AIR VEHICLE	331.91	59.82	29.15	33.85	44.62	197.05	7.57	704.29
AIRFRAME	170.89	53.09	17.64	33.85	25.47	190.87	6.72	498.53
BASIC STRUCTURE	103.56	53.09	11.25	8.22	17.78	60.94	6.72	261.56
FUSELAGE	37.40	34.10	5.21	4.95	8.09	24.31	4.31	118.38
WING	39.32	12.68	3.73	2.53	5.91	34.10	1.60	99.88
CANARDS	1.67	5.26	0.52	0.73	0.78	1.56	0.67	11.19
NACELLES	0.0	0.0	0.0	0.0	0.0	0.0	0.0	0.0
BASIC STRUCTURE ASSEMBLY	25.17	1.05	1.80	0.0	2.99	0.97	0.13	32.11
LANDING GEAR	0.0	0.0	0.0	0.60	0.0	13.48	0.0	14.07
FUEL SYSTEM	6.40	0.0	0.56	1.72	0.73	4.61	0.0	14.01
FLIGHT VEHICLE POWER	31.07	0.0	2.55	6.03	3.55	58.12	0.0	101.32
ENVIRONMENTAL CONTROL	0.0	0.0	0.0	2.09	0.0	25.90	0.0	27.99
CREW ACCOMMODATIONS	6.75	0.0	0.52	0.80	0.77	0.0	0.0	8.84
CONTROLS AND DISPLAYS	0.0	0.0	0.0	0.0	0.0	8.56	0.0	8.56
FLIGHT CONTROLS	20.72	0.0	1.42	0.0	2.37	0.0	0.0	24.50
ARMAMENT	0.0	0.0	0.0	0.30	0.0	19.26	0.0	19.55
AIR INDUCTION CONTROL SYSTEM	2.39	0.0	0.21	0.70	0.27	0.0	0.0	3.57
AIRFRAME INTEGRATION & CHECK	0.0	0.0	0.0	17.05	0.0	0.0	0.0	17.05
ENGINEERING TECHNOLOGIES	0.0	0.0	0.0	12.36	0.0	0.0	0.0	12.36
DESIGN SUPPORT TECHNOLOGIES	0.0	0.0	0.0	1.77	0.0	0.0	0.0	1.77
AIRFRAME INSTALL & CHECKOUT	0.0	0.0	0.0	2.93	0.0	0.0	0.0	2.93
PROPULSION (GFE)	0.0	0.0	0.0	0.0	0.0	0.0	0.0	0.33
AVIONICS (GFE)	0.0	0.0	0.0	0.0	0.0	0.0	0.0	0.0
A/V INTEGRATION, ASSY, INSTALL	161.02	6.73	11.50	0.0	19.15	6.18	0.85	205.43

TABLE 27. MULTIRIB TEE STRINGERS

MULTI-RIB 'T' STRINGERS DS72-4B WITH CURRENT FLUTTER DATA

DATA SHEET

8/28/17 INBD EQUIVALENCE TORQUE BOX

STA No.	LOAD AXIS STATION FUS. STA.	LOAD AXIS STATION B. PLANE	SKIN THICKNESS UPPER	SKIN THICKNESS LWR.	UPPER SKIN 0°	UPPER SKIN +45°	UPPER SKIN -45°	UPPER SKIN 90°	LWR. SKIN 0°	LWR. SKIN +45°	LWR. SKIN -45°	LWR. SKIN 90°	STRINGER SPACING
			MULTI- RIB 'T' STRINGERS										
			30" RIB SPACING TORQUE BOX WT. = 11.05 LBS/A										
1	552	33	.13	.09	4	10	10	2	4	6	6	2	4.0
2	558.3	52.2	.13	.09	4	10	10	2	4	6	6	2	4.0
3	562.8	65.3	.13	.09	4	10	10	2	4	6	6	2	4.0
4	568.1	81.5	.13	.09	4	10	10	2	4	6	6	2	4.0
5	573.5	97.7	.14	.09	6	10	10	2	4	6	6	2	4.0
6	578.9	113.8	.14	.09	6	10	10	2	4	6	6	2	4.0

	UPPER STRINGERS t_{BAR}	UPPER STRINGERS t	UPPER STRINGERS No. at 0°	LWR STRINGERS t_{BAR}	LWR STRINGERS t	LWR STRINGERS No. at 0°
1	.086	.175	35	.060	.125	25
2	.078	.160	32	.053	.110	22
3	.081	.165	33	.055	.115	23
4	.100	.200	40	.073	.150	30
5	.103	.205	41	.089	.180	36
6	.120	.235	47	.106	.210	42

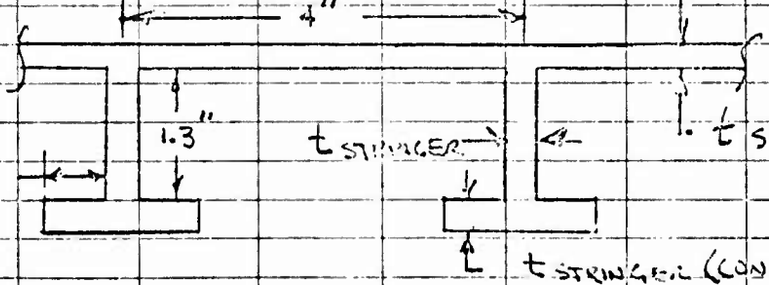

ALL WEIGHTS QUOTED ARE PER AIRCRAFT

TABLE 28. MULTIRIB HAT STRINGERS

MULTI-RIB HAT STRINGERS DS72-48 WITH CURRENT FLUTTER DATA

DATA SHEET 8/20/75

INBD EQUIVALENCE TORQUE BOX

STA NO.	LOAD. ANL FUS STA.	STATIONS B. PLANE	SKIN THICKNES UPPER	SKIN THICKNES LWR	UPPER SKINS 0°	UPPER SKINS +45°	UPPER SKINS -45°	UPPER SKINS 90°	LWR SKINS 0°	LWR SKINS +45°	LWR SKINS -45°	LWR SKINS 90°	STRINGER SPACING
			MULTI - RIB HAT STRINGERS										
			30" RIB SPACING TORQUE BOX WT = 1093 LBS/AC										
1	552	33	.09	.07	4	6	6	2	4	2	2	2	4.0
2	558.3	52.2	.09	.07	4	6	6	2	4	2	2	2	4.0
3	562.8	65.3	.09	.09	4	6	6	2	4	4	4	2	4.0
4	568.1	81.5	.12	.12	6	8	8	2	6	7	7	2	4.0
5	573.5	97.7	.13	.12	8	8	8	2	6	7	7	2	4.0
6	578.9	113.8	.12	.11	10	6	6	2	8	6	6	2	4.0

	UPPER STRINGERS t_{BAR}	UPPER STRINGERS t	UPPER STRINGERS No. OF 0°	LOWER STRINGERS t_{BAR}	LOWER STRINGERS t	LOWER STRINGERS No. OF 0°
1	.125	.130	26	.070	.075	15
2	.105	.120	24	.075	.080	16
3	.120	.125	25	.070	.075	15
4	.125	.130	26	.070	.075	15
5	.136	.140	28	.080	.085	17
6	.146	.150	30	.075	.080	16

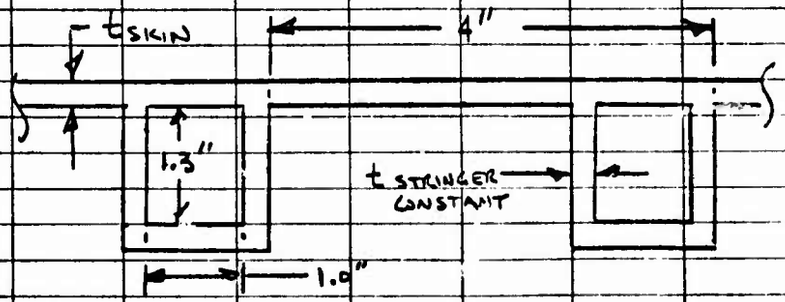

ALL WEIGHTS QUOTED ARE PER AIRCRAFT

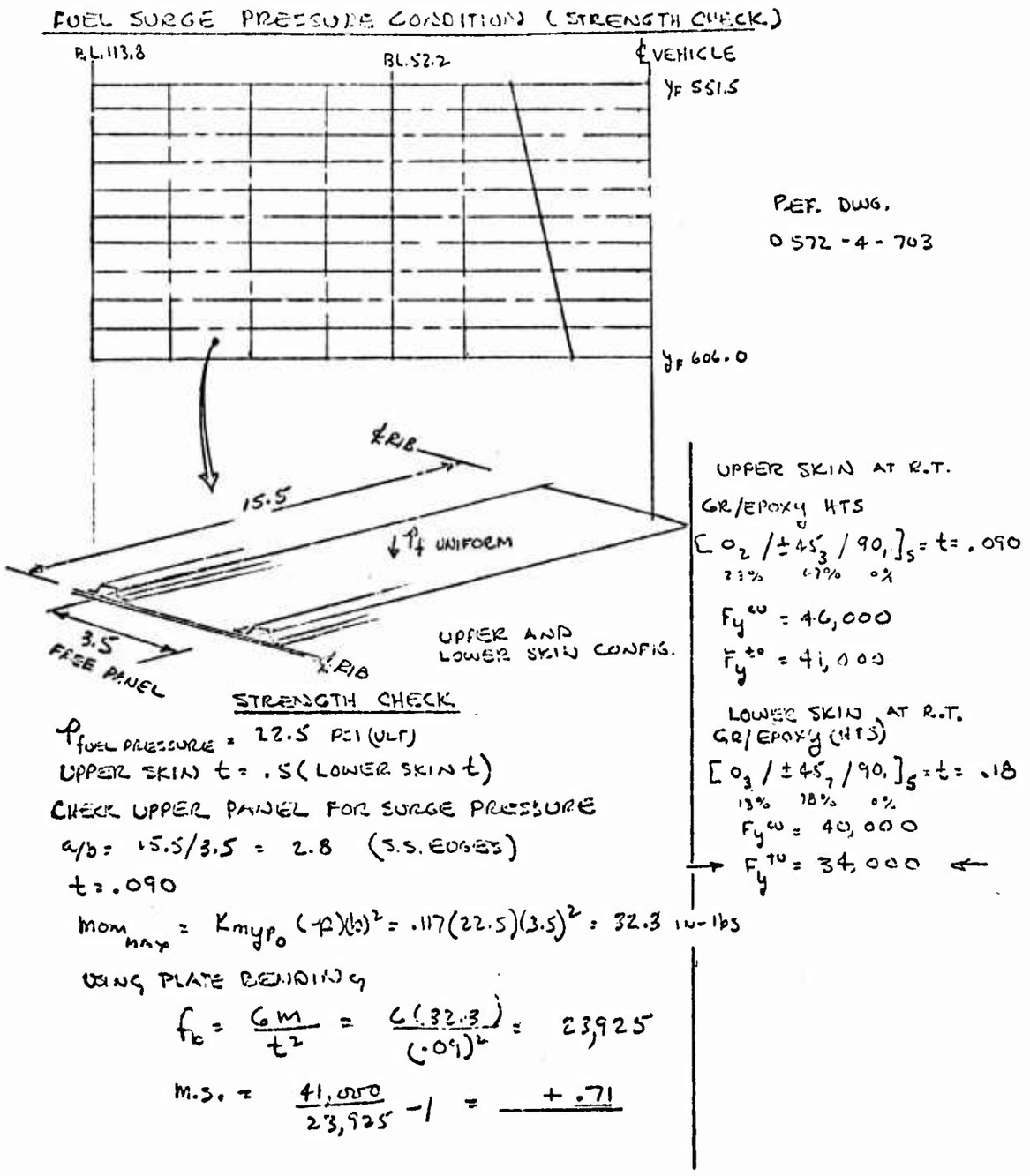

Figure 128. Multirib wing carry-through analysis.

FUEL SURGE PRESSURE CONDITION

PANEL STIFFENER STRENGTH CHECK

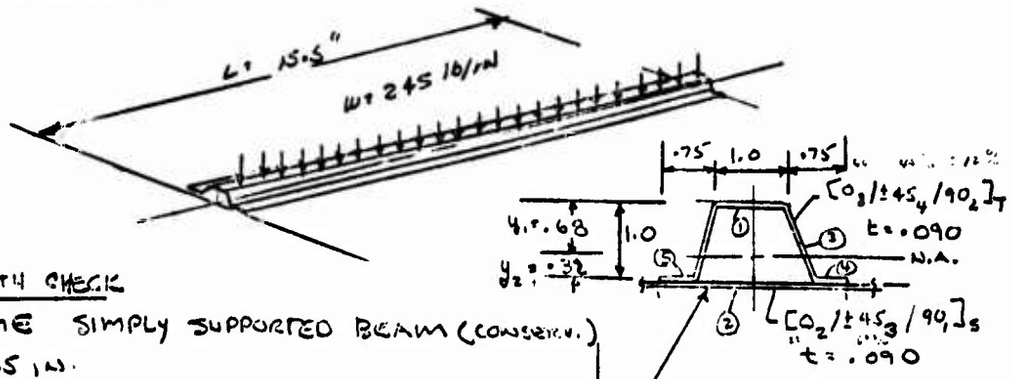

STRENGTH CHECK

ASSUME SIMPLY SUPPORTED BEAM (CONSERV.)

L = 15.5 IN.

w = 10.9 (22.5) = 245. lbs/IN (ULT)

BENDING

$M = \frac{wL^2}{8} =$

$\frac{245(15.5)^2}{8} = 7358$ IN-lbs

① $f_b = \frac{Mc}{I} = \frac{7358(.68)}{.096} = 52{,}119$ PSI (COMP)

$M.S._{①} = \frac{84000}{52{,}119} - 1 = \underline{+.61}$

② $f_b = \frac{Mc}{I} = \frac{7358(.32)}{.096} = 24526$ (TENS)

$M.S._{②} = \frac{58000}{24526} - 1 = \underline{+1.36}$

SHEAR WEBS.

③ $V_{s_{MAX}} = \frac{WL}{2(2)} = \frac{245(15)}{4} = 919$ lbs/WEB

$q_{③} = 919/1.0 = 919$ lb/in

$f_s = 919/.090 = 10{,}211$ PSI

$M.S._{③} = \frac{46{,}200}{10{,}211} - 1 = \underline{+3.5}$

ORIGINAL CROSS SECTION

$I_{CAPS} = A_{①} y_{①}^2 + A_{(2+4+5)} y_{③}^2$

$= .09(.68)^2 + .315(.32)^2$

$= .042 + .033$

$I_{CAPS} = .075$ IN^4

I_{WEBS} $bd^3/3$

$2\left[\frac{.090(.68)^3}{3} + \frac{.090(.32)^3}{3}\right]$

$= 2[.00094 + .000018]$

$I_{WEBS} = .021$

$I_{TOTAL} = .075 + .021 = \underline{.096}$ IN^4

MATL ALLOWABLES AT R.T.

STIFFENER $[0_8/\pm45_4/90_2]_T$ t = .090

$F_x^{TU} = 86{,}000$ PSI

$F_x^{CO} = 84{,}000$ PSI

$F_{xy} = 46{,}000$ PSI

SKIN $[0_2/\pm45_3/90_1]_S$ L = .090

$F_x^{TU} = 58{,}000$ PSI

$F_x^{CO} = 64{,}000$ PSI

Figure 128. Multirib wing carry-through analysis (concl).

TABLE 29. WING CARRY-THROUGH MULTIRIB HAT STRINGERS WEIGHTS

AIRCRAFT: WNG CARRY-THRU MULTI-RIB HAT STRINGERS

AIRCRAFT WEIGHTS - IN POUNDS

	AL	TI	SI	BE	GR	EG	SA	TOTAL
FUSELAGE	76.	171.	69.	C.	2086.	27.	0.	3236.
FRAME/LONG	C.	171.	69.	C.	695.	0.	0.	935.
SKIN-STRGR	76.	0.	0.	C.	0.	0.	0.	78.
BOND HONEY	C.	0.	C.	C.	1391.	27.	0.	1418.
BRAZE HONEY		0.	0.				0.	0.
DIFF BOND		0.					0.	0.
MISC								805.
WING	127.	24.	0.	C.	2793.	0.	0.	3088.
SKIN-STRGR	C.	0.	0.	C.	0.	0.	0.	0.
MULTI-SPAR	C.	24.	0.	C.	491.	0.	0.	515.
BOND HONEY	127.	0.	0.	C.	2302.	0.	0.	2429.
BRAZE HONEY		0.	C.				0.	0.
DIFF BOND		0.					0.	0.
MISC								144.
CANARDS	C.	16.	2.	C.	117.	0.	0.	145.
SKIN-STRGR	C.	0.	C.	C.	C.	0.	0.	0.
MULTI-SPAR	C.	0.	0.	C.	C.	0.	0.	0.
BOND HONEY	C.	16.	2.	C.	117.	0.	0.	135.
BRAZE HONEY		0.	0.				0.	0.
DIFF BOND		0.					0.	0.
MISC								10.
NACELLE	C.	0.	0.	C.	C.	0.	0.	0.
FRAME/LONG	C.	0.	0.	C.	0.	0.	0.	0.
SKIN-STRGR	C.	0.	0.	C.	0.	0.	0.	0.
BOND HONEY	0.	0.	0.	C.	0.	0.	0.	0.
BRAZE HONEY		0.	C.				0.	0.
DIFF BOND		0.					0.	0.
MISC								0.

WEIGHT DATA - IN POUNDS	
AMPR WEIGHT	13071.
STRUCTURE WT	7745.
STRUCTURAL HDWE WT	133.
SYSTEM HDWE WT	133.
LANDING GEAR WT	1280.
FUEL SYSTEM WT	750.
ELECTRICAL SYSTEM WT	680.
HYDRAULIC SYSTEM WT	430.
AUX POWER SYSTEM WT	310.
ECS WT	530.
CREW ACCOM WT	320.
CONTROL & DISPLAY WT	120.
FLIGHT CONTROL WT	950.
ARMAMENT WT	560.
AICS MECHANISM WT	300.
EQUIPMENT WT	80.
ENGINE WT	5375.
EMPTY WT	19125.
FUEL WT	7060.
TOGW	30792.
DESIGN VARIABLES	
WING AREA-SQ FT	400.
CANARDS AREA-SQ FT	35.
WETTED AREA-SQ FT	1772.
WING + HORIZ AREA	435.
WING SPAN-FT	31.6
HORIZ SPAN-FT	10.0
OVERALL LENGTH-FT	57.0
ASPECT RATIO	2.50
DYNAMIC PRESSURE	2133.

TABLE 30. WING CARRY-THROUGH MULTIRIB HAT STRINGERS COSTS

AIRCRAFT: WNG CARRY-THRU MULTI-RIB HAT STRINGERS
ALL COSTS IN MILLIONS AND IN 1975 DOLLARS

PRODUCTION COST FOR 300 UNITS
UNIT AVG. FLYAWAY COST 2.806

WORK BREAKDOWN STRUCTURE	LABOR COST					MATERIAL COST		TOTAL
	MFG.	TOOL.	PLNG.	ENGR.	Q&A	MFG.	TOOL.	COST
TOTAL PROGRAM COST INCLUDING FEE	355.39	70.49	34.94	40.26	53.53	233.98	8.92	841.83
TOTAL PROGRAM COST INCLUDING G&A	363.08	64.08	31.76	36.60	48.66	212.71	8.10	765.33
TOTAL PROGRAM COST LESS G&A	330.58	58.34	28.92	33.33	44.30	193.67	7.38	696.86
AIR VEHICLE	330.58	58.34	28.92	33.33	44.30	193.67	7.38	696.86
AIRFRAME	166.20	51.73	17.19	33.33	24.79	187.45	6.54	487.23
BASIC STRUCTURE	98.87	51.73	10.83	8.04	17.09	57.51	6.54	250.63
FUSELAGE	37.63	33.26	5.15	4.77	8.03	24.31	4.21	117.36
WING	35.32	12.37	3.43	2.54	5.42	30.72	1.56	91.37
CANARDS	1.66	5.13	0.51	0.73	0.77	1.56	0.65	11.01
NACELLES	0.0	0.0	0.0	0.0	0.0	0.0	0.0	0.0
BASIC STRUCTURE ASSEMBLY	24.26	0.98	1.73	0.0	2.88	0.92	0.12	30.89
LANDING GEAR	0.0	0.0	0.0	0.60	0.0	13.48	0.0	14.08
FUEL SYSTEM	6.40	0.0	0.56	1.72	0.73	4.61	0.0	14.01
FLIGHT VEHICLE POWER	31.07	0.0	2.55	5.98	3.55	58.12	0.0	101.27
ENVIRONMENTAL CONTROL	0.0	0.0	0.0	2.09	0.0	25.90	0.0	27.99
CREW ACCOMMODATIONS	6.75	0.0	0.52	0.80	0.77	0.0	0.0	8.84
CONTROLS AND DISPLAYS	0.0	0.0	0.0	0.0	0.0	8.56	0.0	8.56
FLIGHT CONTROLS	20.72	0.0	1.42	0.0	2.37	0.0	0.0	24.50
ARMAMENT	0.0	0.0	0.0	0.30	0.0	19.26	0.0	19.55
AIR INDUCTION CONTROL SYSTEM	2.39	0.0	0.21	0.63	0.27	0.0	0.0	3.50
AIRFRAME INTEGRATION & CHECK	0.0	0.0	0.0	16.82	0.0	0.0	0.0	16.82
ENGINEERING TECHNOLOGIES	0.0	0.0	0.0	12.22	0.0	0.0	0.0	12.22
DESIGN SUPPORT TECHNOLOGIES	0.0	0.0	0.0	1.73	0.0	0.0	0.0	1.73
AIRFRAME INSTALL & CHECKOUT	0.0	0.0	0.0	2.87	0.0	0.0	0.0	2.87
PROPULSION (GFE)	0.0	0.0	0.0	0.0	0.0	0.0	0.0	0.33
AVIONICS (GFE)	0.0	0.0	0.0	0.0	0.0	0.0	0.0	0.0
A/V INTEGRATION, ASSY, INSTALL	164.38	6.61	11.73	0.0	19.52	6.23	0.84	209.30

A summary of the cost and weight of the three concepts investigated for the Wing Center Section Trade Study is shown below.

Concept	AMPR Weight (lb)	Cost in Dollars/Ship
Honeycomb Panel	13211	2,767,000
Multi-Spar/Plate	13411	2,836,000
Plate/Stringer	13071	2,806,000

The honeycomb panel concept has been assessed as being the most compatible with the full-depth honeycomb wing outer panel, and as presenting lower technical and manufacturing risk than the skin-stringer concept. Since this concept also exhibits the lowest cost, it has been selected for the baseline.

FUSELAGE SECTION

A section of the fuselage at Yp400 has been selected as being representative of both the cockpit section (which is designed by cockpit pressurization loads) and of the intermediate fuselage and wing section forward of the wing carry-through section (which is designed by fuel pressure). Figure 129 shows the honeycomb panel concept for this application. All mold line surfaces are 3/4-inch honeycomb panels with graphite/epoxy skins and graphite/epoxy core. Frames and bulkheads are 1/2-inch thick. Composite pultrusions are used to form attachments of intersecting panels.

The structural integrity of the design has been confirmed as shown in Figure 130.

The weight breakdown of the aircraft with the honeycomb panel structure is shown in Table 18 (basepoint).

The itemized cost of this structural arrangement is shown in Table 19.

An alternate concept for fuselage structure is shown in Figure 131. In this design, woven graphite/epoxy skins are stiffened by longitudinal hat section stringers. The stringers are stabilized by honeycomb core and are tapered to flat sections where they are crossed by frames. Reinforced graphite/epoxy frames are bonded to the skins except for the upper fuel tank skin which is attached with mechanical fasteners. Longitudinal beams in the tank area are fabricated from graphite/epoxy honeycomb panels.

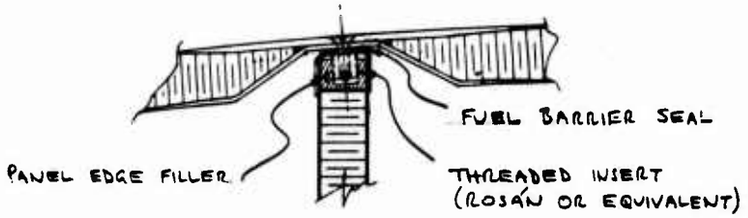

SECTION D-D
SCALE 1/1

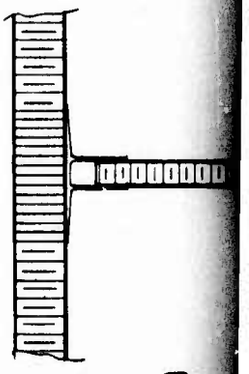

SEC

OUTER M

1

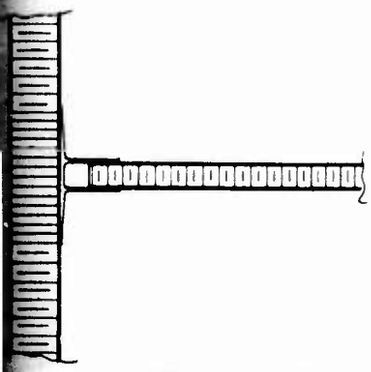

SECTION B-B
SCALE 1/1

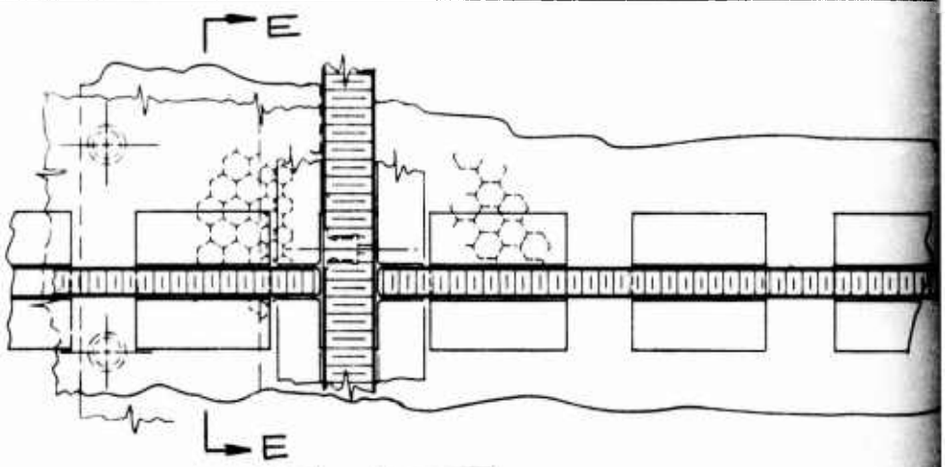

SECTION E-E
SCALE 1/1

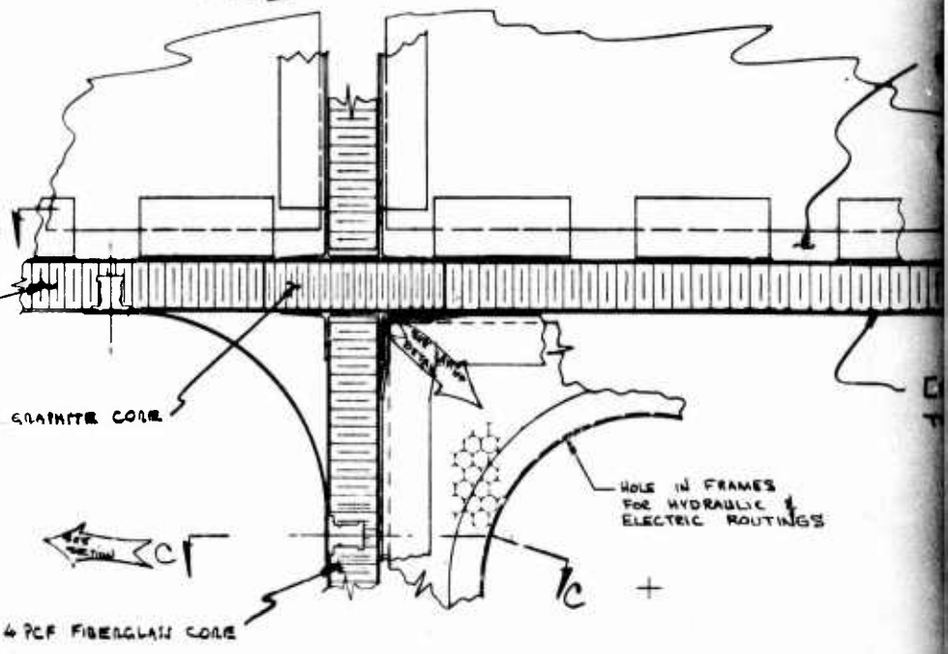

DETAIL A-A
SCALE 1/1

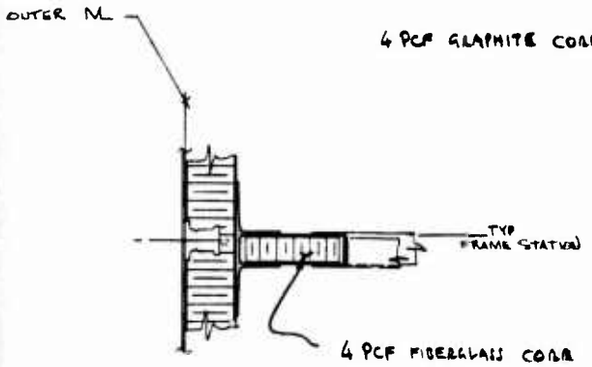

SECTION C-C
SCALE 1/1

TYP Pultrusion
No Scale

2

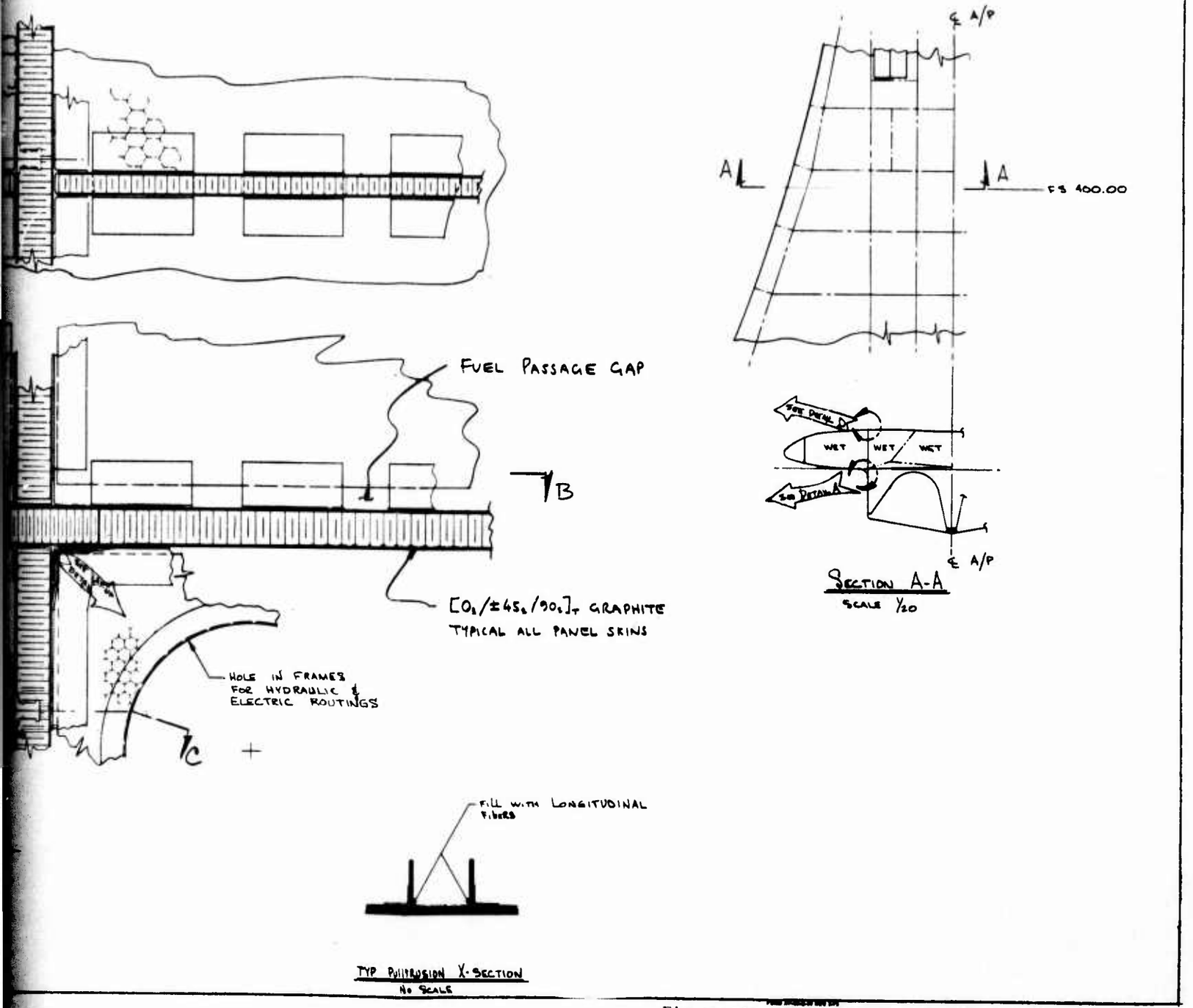

Figure 129. Honeycomb panel - fuselage trade study.

3

HONEYCOMB PANELS - FUSELAGE TRADE STUDY

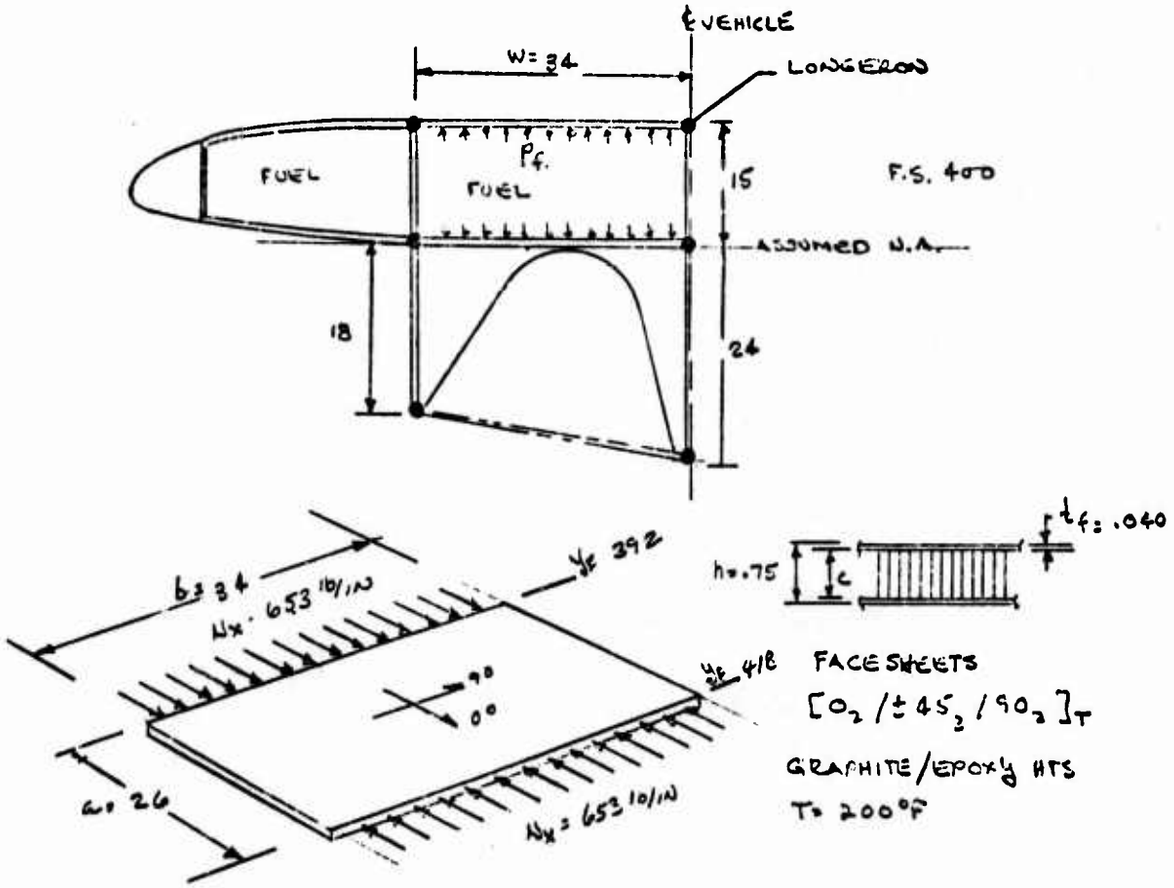

DESIGN LOADS. COND 1 N_z = 8.0 (LIMIT)

ASSUME LONGERONS CARRY 20% FUS. BEND.

$M_x = +2.6 \times 10^6$ IN-lbs

$V = -4.2 \times 10^4$ lbs

$P_f = [3.0 + 8.0(.028) \times 15]\,1.5 = 9.54$ PSI ULT.

$N_x'' = \frac{M}{W'H'} = \frac{2.0 \times 10^6}{2(34)(15 + \frac{18+24}{2})} = 817$ lb/in

$N_{x_{N.C}} = .8(817) = 653$ lb/in (ULT)

$P/\text{LONG}_{\text{UPPER}} = .2(2.0 \times 10^6)/21 \times 3 = 6350$ lbs/LONG.

$P/\text{LONG. LWR} = .2(2.0 \times 10^6)(21 \times 3 = 6350$ lb/LONG.

Figure 130. Fuselage trade study - skin stringer analysis.

CHECK FOR SURGE REFUELLING PRESSURE (NO FUS. BENDING)

p_f = 15.0 × 1.5 = 22.5 psi ULT AT R.T.

a/b = 34/26 = 1.3

η = .75 c = .75 − 2(t_f) = .75 − .08 = .67 IN

t_f = .040 CORE = 4.0 PCF (ALUM EQIV. ALLOWABLES)

$M_{max} = K_{myp_o}(p)(b^2)$

$= .066(22.5)(26)^2 = 1004$ IN-LB/IN

$K_{Mxp_o} = .05$

$K_{myp_o} = .066$

$K_{qxp_o} = .355$

$K_{qyp_o} = .40$

$f_{x_{MAX}} = \frac{M_{max}}{t_f c} = \frac{1004}{.04(.67)} = \pm 55914$ psi

$M.S._{\%} = \frac{62000}{55914} - 1 = \underline{+.109}$

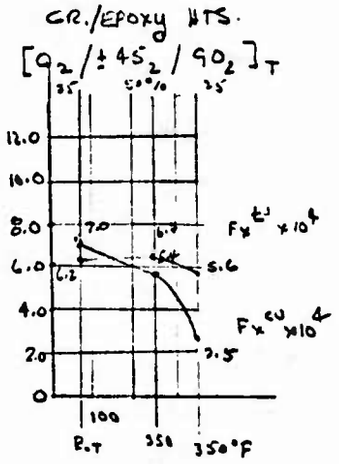

$Q_{MAX} = K_{qyp_o}(p)(b)$

$= .40(22.5)(26) = 234$ LB/IN

$f_{s_{MAX}} = \frac{Q_{MAX}}{c + t_f} = \frac{234}{(.67+.04)} = 329.6$ psi

FOR 3.8 PCF $M.S. = \frac{215}{329.6} - 1 = \underline{-.348}$

INCREASE CORE TO 5.3 PCF.

$M.S. = \frac{370}{329.6} - 1 = \underline{+.123}$

Figure 130. Fuselage trade study - skin stringer analysis (cont).

CHECK FOR MAX FUSELAGE BENDING

N_y = 653 lb/in (ULT)

GR/EPOXY HTS

$[0_2 / \pm 45_2 / 90_2]_T$

35% 50% 15%

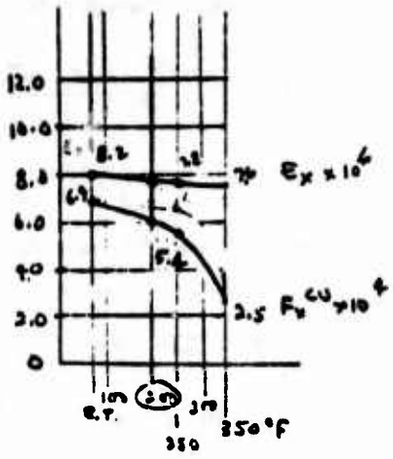

FACESHEET PROPERTIES

t_f = .040

$n = \sqrt{E_x/E_y} = \sqrt{8.0\times10^6/8.0\times10^6} = 1.0$

$\psi = \sqrt{E_x E_y}/(1 - \underset{.154}{\nu_{xy}}\,\underset{.130}{\nu_{yx}}) = 8.0\times10^6/.884 = 9.05\times10^6$ (.1156)

CORE PROPERTIES

C = .67 in (5.3 PCF) 5052 AL EQUIV.

$G'_{cy}/G'_{cx} = 1.0$

G'_{cx} = 36,000 PSI (.85)

= 30,000 PSI @ 200°F.

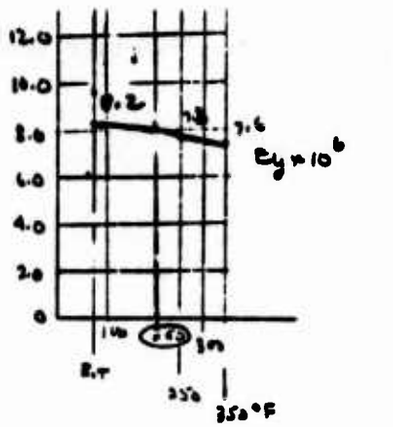

b/c = 34/.67 = 50.7

t_f/c = .040/.67 = .060

From Fig. —

$V G'_{cx}/\psi$ = .0001

$V = \dfrac{(0.0001)(9.05\times10^6)}{30{,}000} = .302$

From Fig. 2

a/b = 26/34 = .765

V = .302

$\psi = 9.05\times10^6$

INTERPOLATING —

$K_y \doteq 3.0$

$(N_y)_{cr} = K_y \pi^2 \psi t_f c (c + t_f)/2 b^2$

$= 3.0(\pi^2)\, 9.05\times10^6 (.040)(.67)(.67 + .040)/2(34)^2$ (.71; 2312)

= 2,210 lbs/in

M.S. = $\dfrac{2210}{653} - 1 = 2.34$ HIGH

Figure 130. Fuselage trade study - skin stringer analysis (cont).

CHECK FOR CORE SHEAR CRIMPING

$$F_{cs} = \frac{G_c' (c + 2t_f)}{2 t_f} = \frac{30{,}000\,(.675 + 2(.040))}{2\,(.040)}$$

$$= 281{,}250 \text{ PSI}$$

USE $F_{cx}^{cu} = 60{,}000$

APPLIED STRESS: $653/.080 = 8162$ PSI

$$M.S. = \frac{60{,}000}{8162} - 1 = \underline{+ 6.35} \quad \text{HIGH}$$

Figure 130. Fuselage trade study - skin stringer analysis (concl).

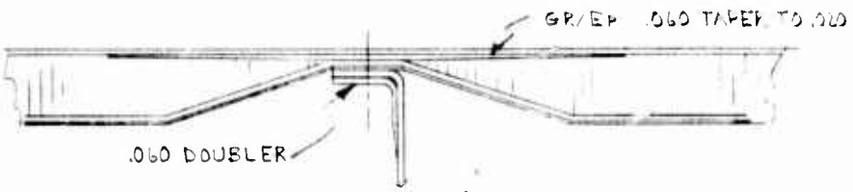

SECTION GG

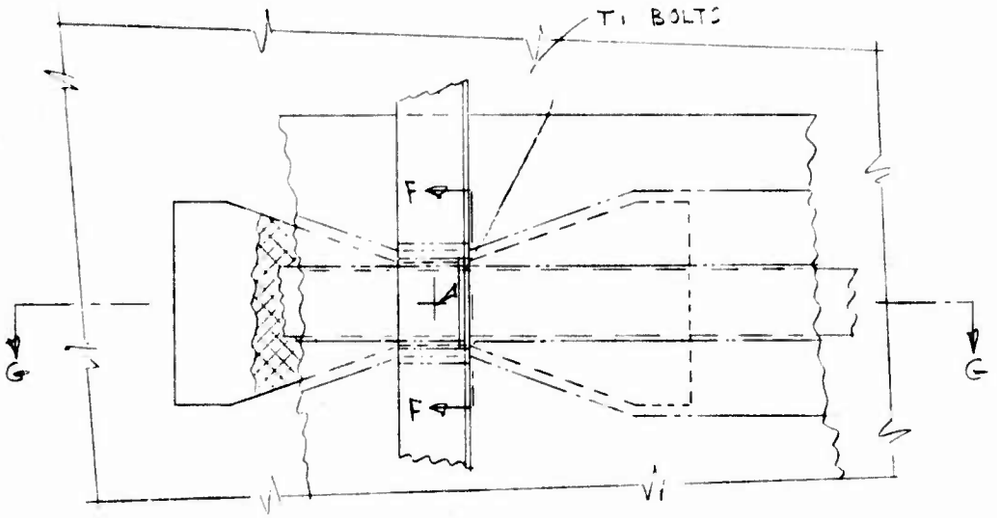

SECTION EE

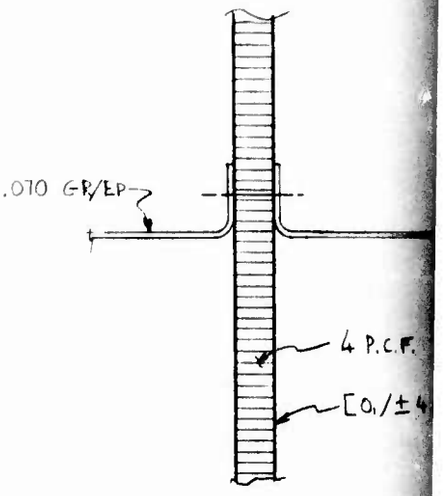

SECTION CC

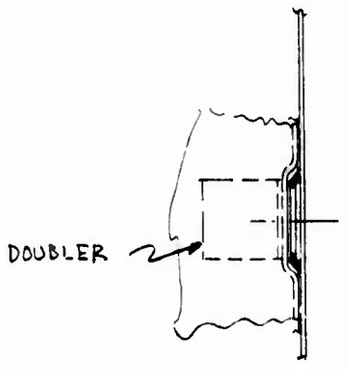

SECTION FF

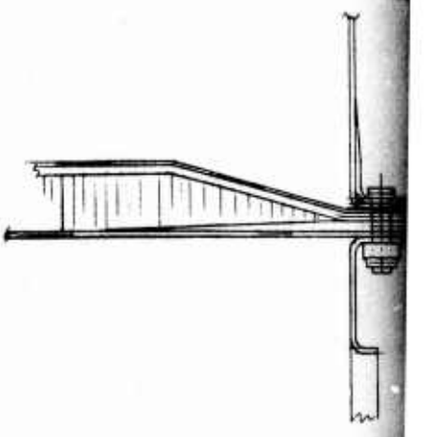

SECTION
TYP. FUL

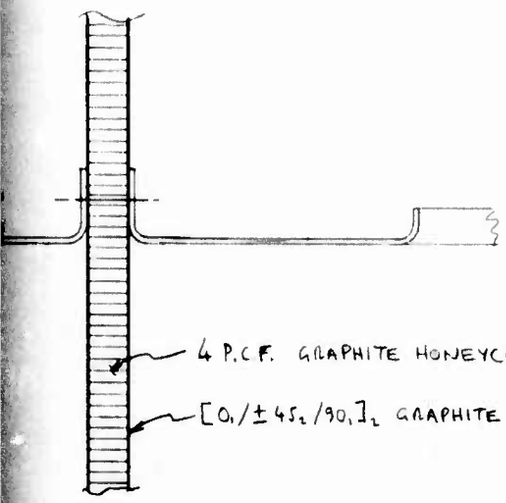

SECTION CC

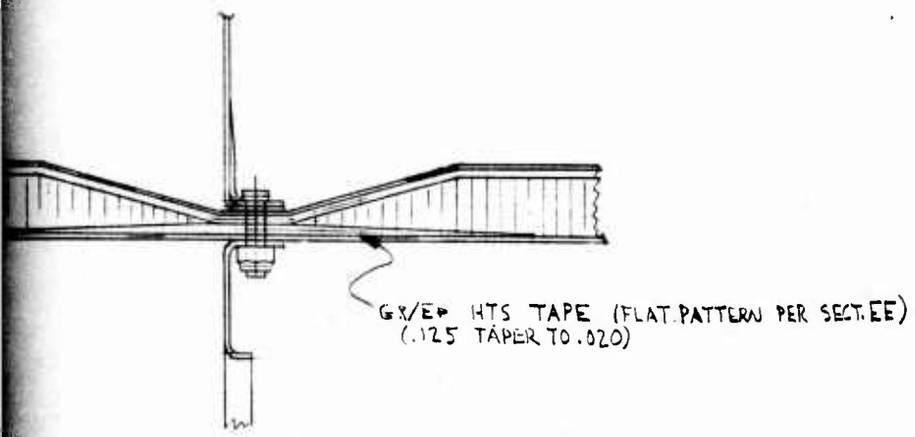

SECTION DD
TYP. FULL BAY STIFFENER

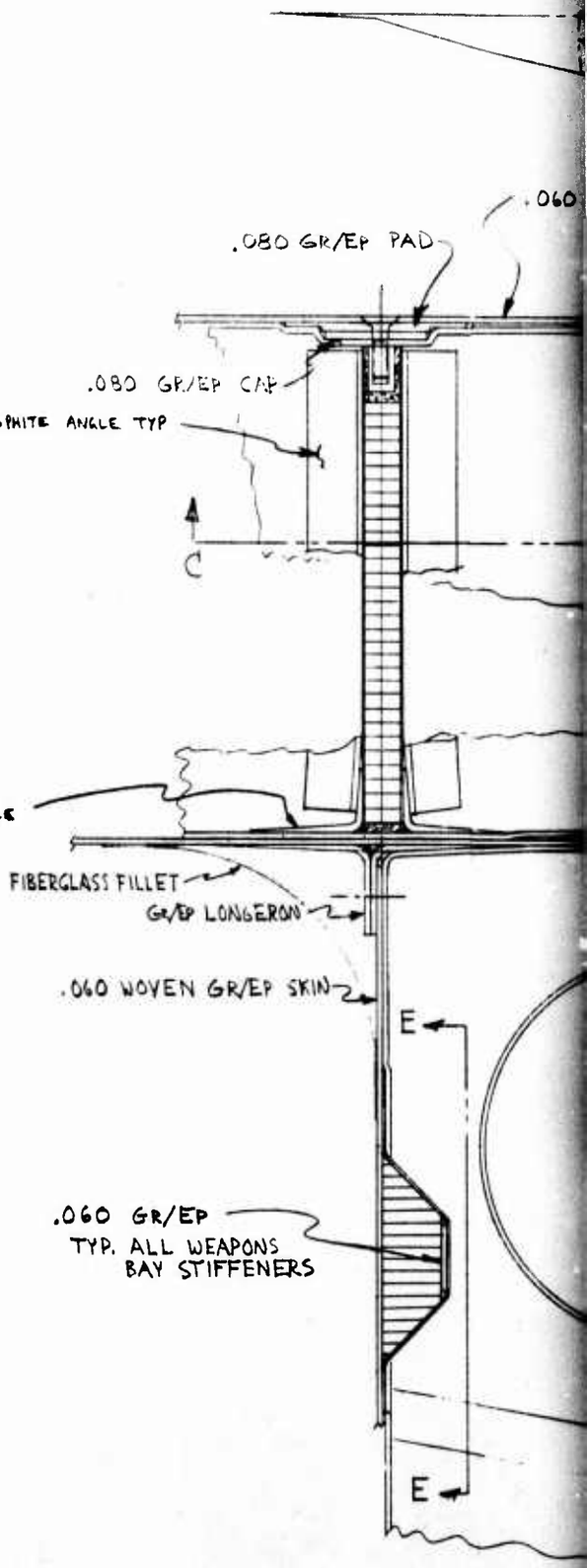

2

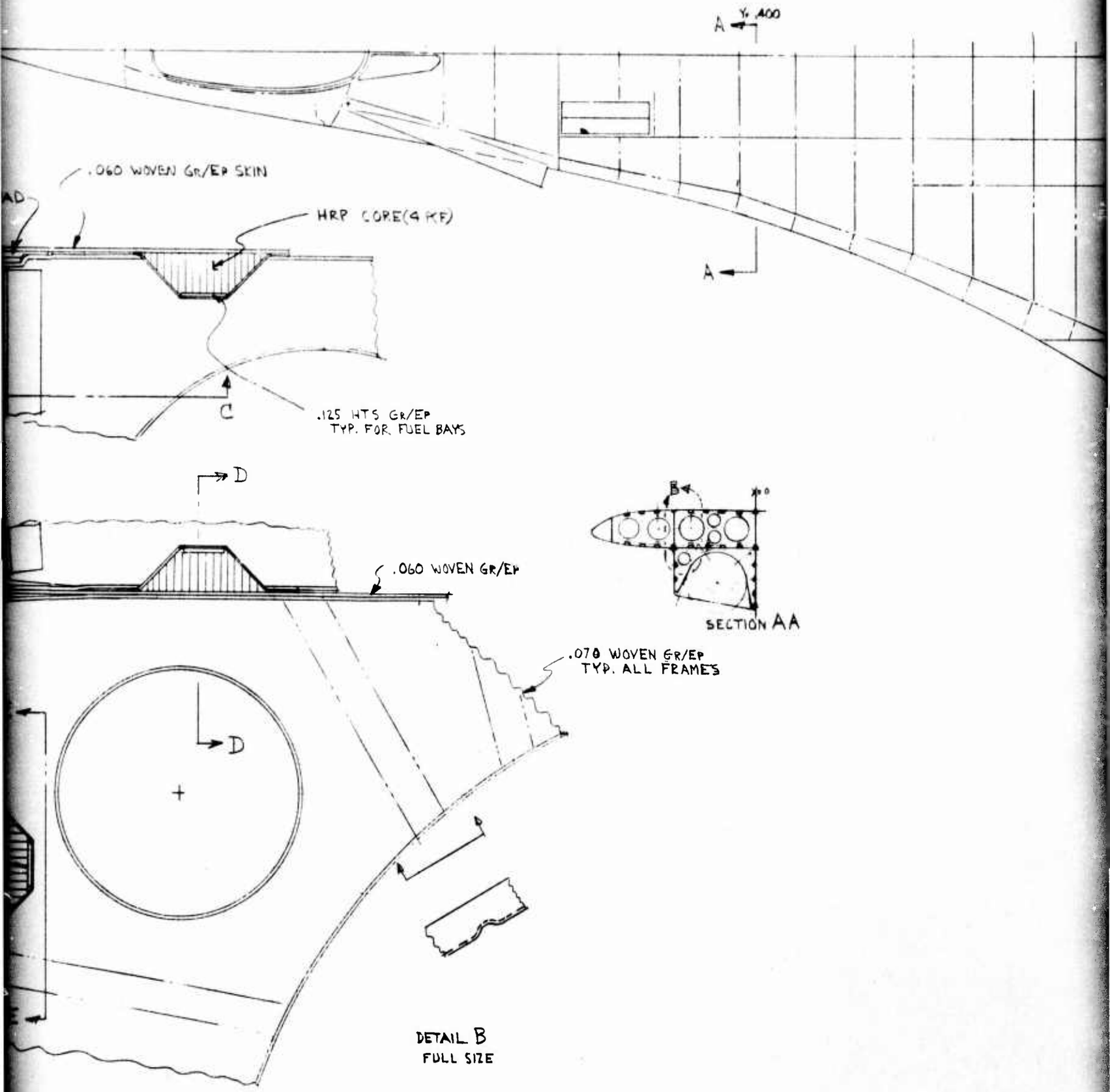
A
Y= 400
.060 WOVEN GR/EP SKIN
AD
HRP CORE(4 PF)
A
C
.125 HTS GR/EP
TYP. FOR FUEL BAYS
D
.060 WOVEN GR/EP
B
Y=0
SECTION AA
.070 WOVEN GR/EP
TYP. ALL FRAMES
D
DETAIL B
FULL SIZE

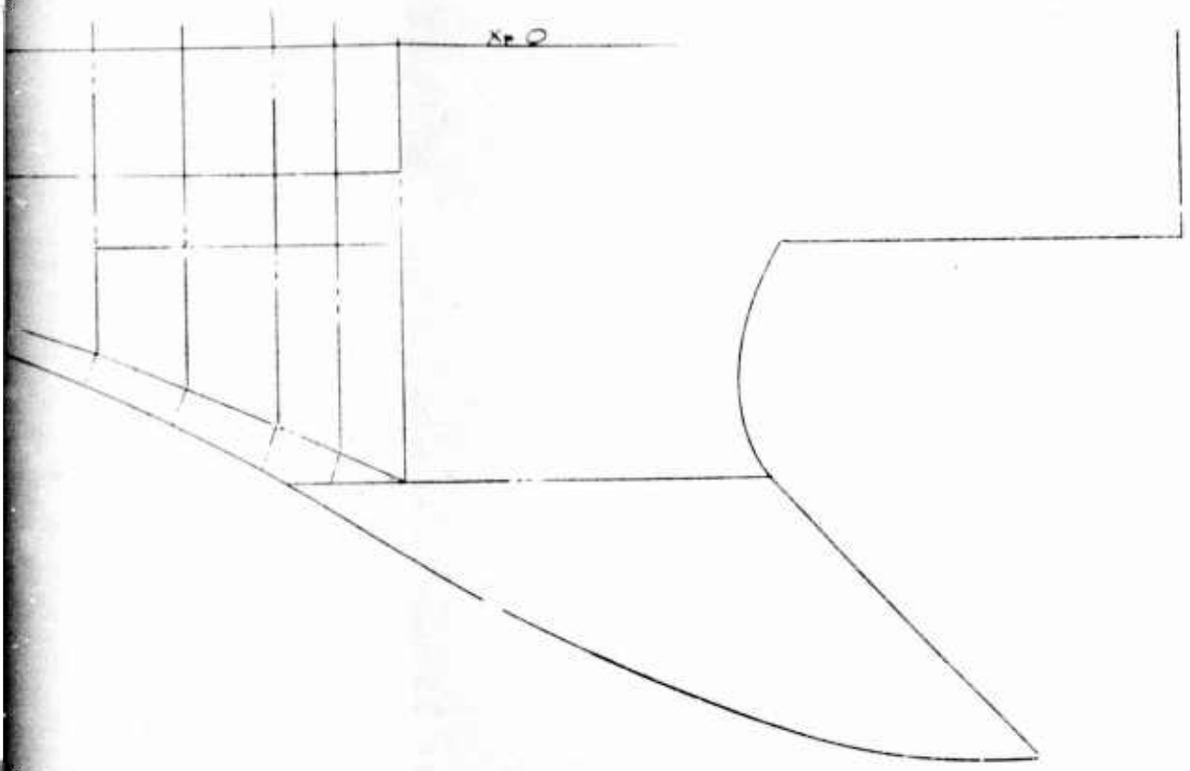

Figure 131. Skin-stringer fuselage trade study.

Figure 132 shows the structural analysis of this concept. The weight breakdown of the aircraft with this structure is shown on Table 31. Costs are shown in Table 32.

Comparing the costs of the two concepts of fuselage construction shows the honeycomb panel concept to be $15,000 per aircraft lower than the stringer design as shown in the following paragraphs.

Type of Construction	AMPR Weight (lb)	Flyaway Cost ($)
Honeycomb Panel	13,211	2,769,000
Skin-Stringer	13,104	2,784,000

Since the honeycomb panel design is lower in weight, presents a lower technical risk, and is more compatible with the similar type of construction selected for the wing carry-through structure, it has also been selected for the fuselage.

ALL-COMPOSITE BASELINE STRUCTURE

STRUCTURAL DESCRIPTION

The general structural arrangement for the -4B all-composite aircraft is shown in Figure 133. The structure is semimonocoque with skins, frames, and longerons. As a result of the trade studies, the majority of the fuselage and wing center section employ honeycomb panel covers. Eighty percent of the fuselage bending and axial loads are reacted by these panels while the longerons take the remaining 20 percent. Because of the stability of the sandwich panels, frame spacing up to 25 inches has been used. This large spacing results in a minimum number of frames, which tends to produce a low-cost structure. High-strength graphite/epoxy is the primary material selected, based on its superior producibility features and projected low cost in the 1980 time period. The selection is predicted on the assumption that an improved version of epoxy will be available by 1980, with capabilities up to 300° F. In the aft fuselage, where temperatures may approach 500° F, a graphite/polyimide system has been selected to meet the high-temperature environment.

As shown in Figure 133, the nose radome is constructed from filament-wound quartz-polyimide. Tests on comparative materials, have shown this composite to offer the optimum radar transmission characteristics. The cockpit structure, immediately aft of the radome, is fabricated from graphite/epoxy honeycomb panels with frames spaced at 25 inches. The windshield and canopy are fabricated as a single unit from polycarbonate. This construction not only provides unrestricted forward and side vision, but offers reduced cost and maximum birdproofing as well.

FOR A TRADE STUDY OF FUSELAGE FROM STATION $Y_F = 320$ TO $Y_F = 515$, CONSIDER SECTION $Y_F = 392 - 418$ AS TYPICAL.

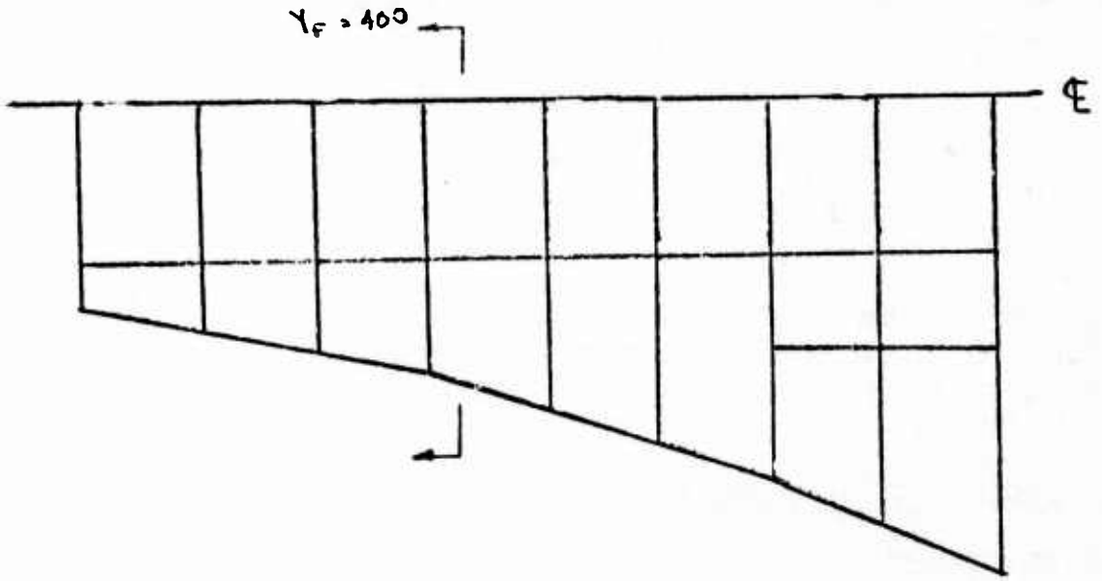

STATION $Y_F = 400$.

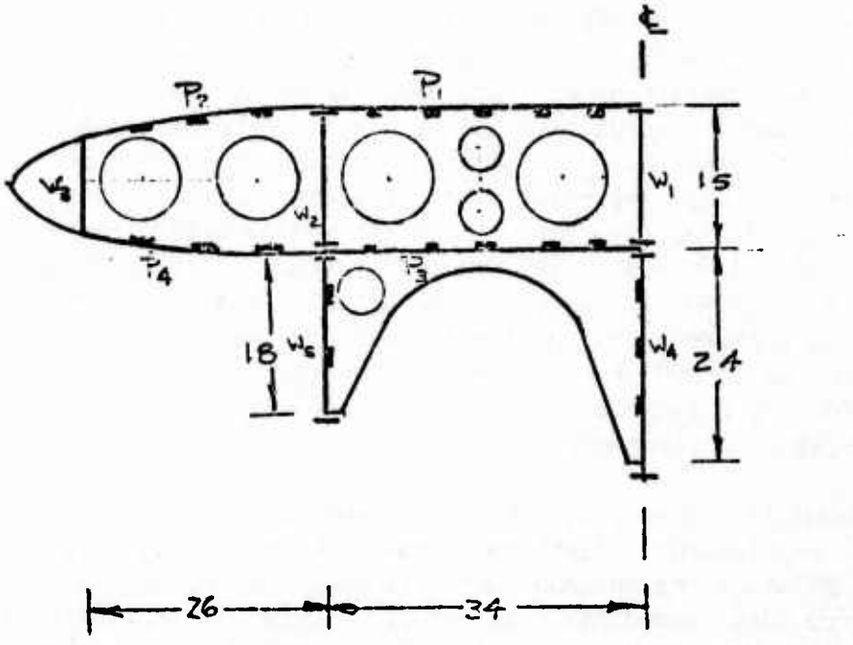

Figure 132. Fuselage trade study - skin stringer analysis.

ASSUMPTIONS

1. N.A. LIES IN PLANE OF PANELS P_3, P_4
2. TEMPERATURE = 200°F
3. PANELS W_4, W_5 DO NOT CARRY ANY FUSELAGE BENDING LOAD
4. UPPER LONGERONS CARRY 20% OF BENDING LOAD, N_x^4

CONSIDER

1. PANEL P_1 AS TYPICAL OF PANELS P_2, P_3, P_4
2. WEB W_2 AS TYPICAL OF WEBS W_1, W_3

DESIGN LOADS

CONDITION 1

$M = 2.0 \times 10^6$ in-lb

$V = -4.2 \times 10^4$ lb

$N_z = 8.0$ LIMIT

$$P_f = [3.0 + N_z \rho_f H] \text{ psi} \times 1.5$$

$$= [3.0 + 8.0 \times .028 \times 15] \times 1.5$$

$$= 9.54 \text{ psi}$$

$$N_x^4 = \frac{M}{WH} = \frac{M}{[2 \times W_{P_1}][H_{W_1} + \frac{H_{W_3} + H_{W_4}}{2}]}$$

$$= \frac{2.0 \times 10^6}{2(34)[15 + \frac{18+24}{2}]}$$

$$= 817 \text{ lb/in}$$

$$N_x^{4S} = .8 \times N_x^4$$

$$= 654 \text{ lb/in}$$

Figure 132. Fuselage trade study - skin stringer analysis (cont).

CONDITION 2

FUEL PRESSURE ONLY

$P_f = 1.5 \times 15.0$ psi

$= 22.5$ psi

ASSUME SKINS $-[0/\pm 45_2/90]_s$ GR/EP HTS

PROPERTY	VALUE AT TEMPERATURE		
	RT	250°F	200°F
E_x (msi)	6.8	6.4	6.51
E_y (msi)	6.8	6.4	6.51
G_{xy} (msi)	3.8	3.8	3.8
A_{11} (msi)	8.5	8.0	8.14
A_{12} (msi)	3.6	3.6	3.6
A_{22} (msi)	8.5	8.0	8.14
A_{66} (msi)	3.8	3.8	3.8
F_x^{tn} (ksi)	51	53	53
F_x^{cn} (ksi)	57	44	48
F_y^{tn} (ksi)	51	53	53
F_y^{cn} (ksi)	57	44	48
F_{xy}^{sn} (ksi)	64	53	56

Figure 132. Fuselage trade study - skin stringer analysis (cont).

STRINGER CAPS - $[0_{20}/\pm 45_2]_T$ HTS GR/EP

PROPERTY	VALUE AT TEMPERATURE		
	RT	250 F	206°F
E_x (msi)	18.1	18.0	18.0
A_{11} (msi)	18.6	18.6	18.6
F_x^{cu} (ksi)	156	124	133
F_x^{tu} (ksi)	156	156	156

STRINGER WEBS - $[\pm 45]_S$ HTS GR/EP

PROPERTY	VALUE AT TEMPERATURE		
	RT	250° F	206°F
E_x (msi)	2.4	1.8	1.97
G_{xy} (msi)	5.5	5.45	5.45
A_{11} (msi)	6.6	6.2	6.3
A_{12} (msi)	5.2	5.3	5.3
A_{66} (msi)	5.5	5.45	5.45
F_x^{tu} (ksi)	23	22	22
F_x^{cu} (ksi)	24	22	22
F_{xy}^{su} (ksi)	90	76	80

Figure 132. Fuselage trade study - skin stringer analysis (cont).

PANEL P_1

SPACING OF STRINGERS IS 6" ℄ TO ℄

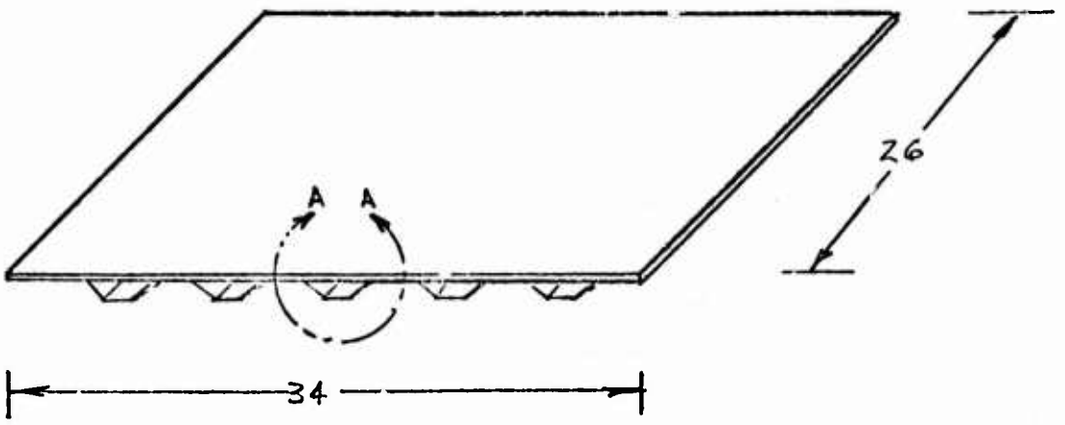

SECTION A-A

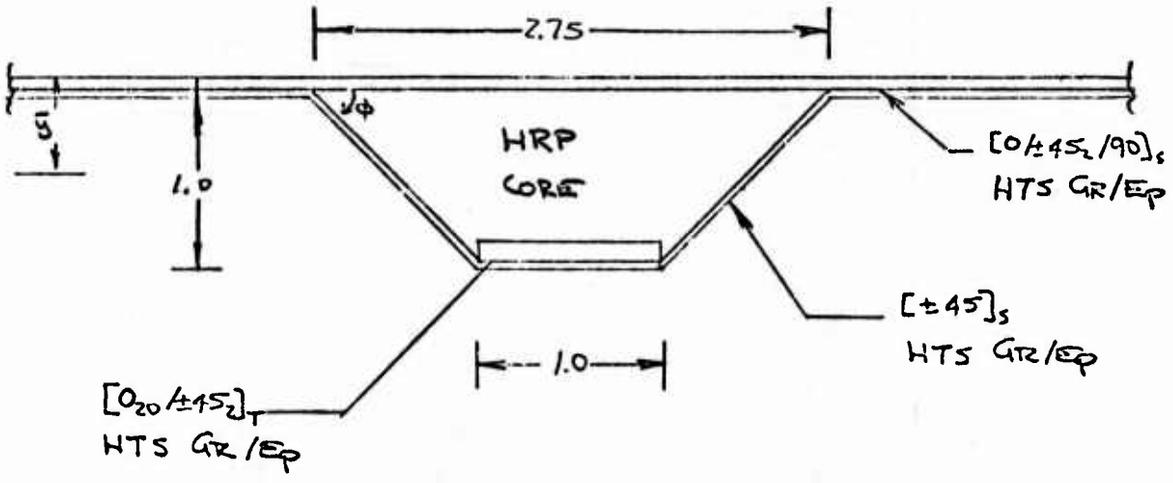

Figure 132. Fuselage trade study - skin stringer analysis (cont).

PANEL FLUTTER REQUIREMENT

ASSUME THERE IS NO FUEL PRESSURE IN TANK TO STABILIZE SKIN PANEL.

FLUTTER REQUIREMENT IS AT $M = 1.2$ AT S.L. WHERE $q = 2133\ lb/ft^2$

UNSUPPORTED SKIN PANEL WIDTH $= 6 - 2.75$
$= 3.25$ IN.

THEN

$$\frac{L}{w} = \frac{26}{3.25}$$
$$= 8.0$$

$$\beta = \sqrt{M^2 - 1}$$
$$= \sqrt{1.2^2 - 1}$$
$$= .663$$

$$\left[\frac{\beta E}{q}\right]^{\frac{1}{3}} \frac{t}{L} = \left[\frac{\beta A_{11sk}}{q}\right]^{\frac{1}{3}} \frac{t}{L} = \left[\frac{.663 \times 8.14 \times 10^6 \times 144}{2133}\right]^{\frac{1}{3}} \frac{.06}{26}$$
$$= [364.3]^{\frac{1}{3}} \frac{.6}{26}$$
$$= .165$$

FROM FIGURE PAGE 7 (REF SDL-66-26)

IT CAN BE SEEN THAT $b_s = 6.0$" SATISFIES FLUTTER REQUIREMENT.

Figure 132. Fuselage trade study - skin stringer analysis (cont).

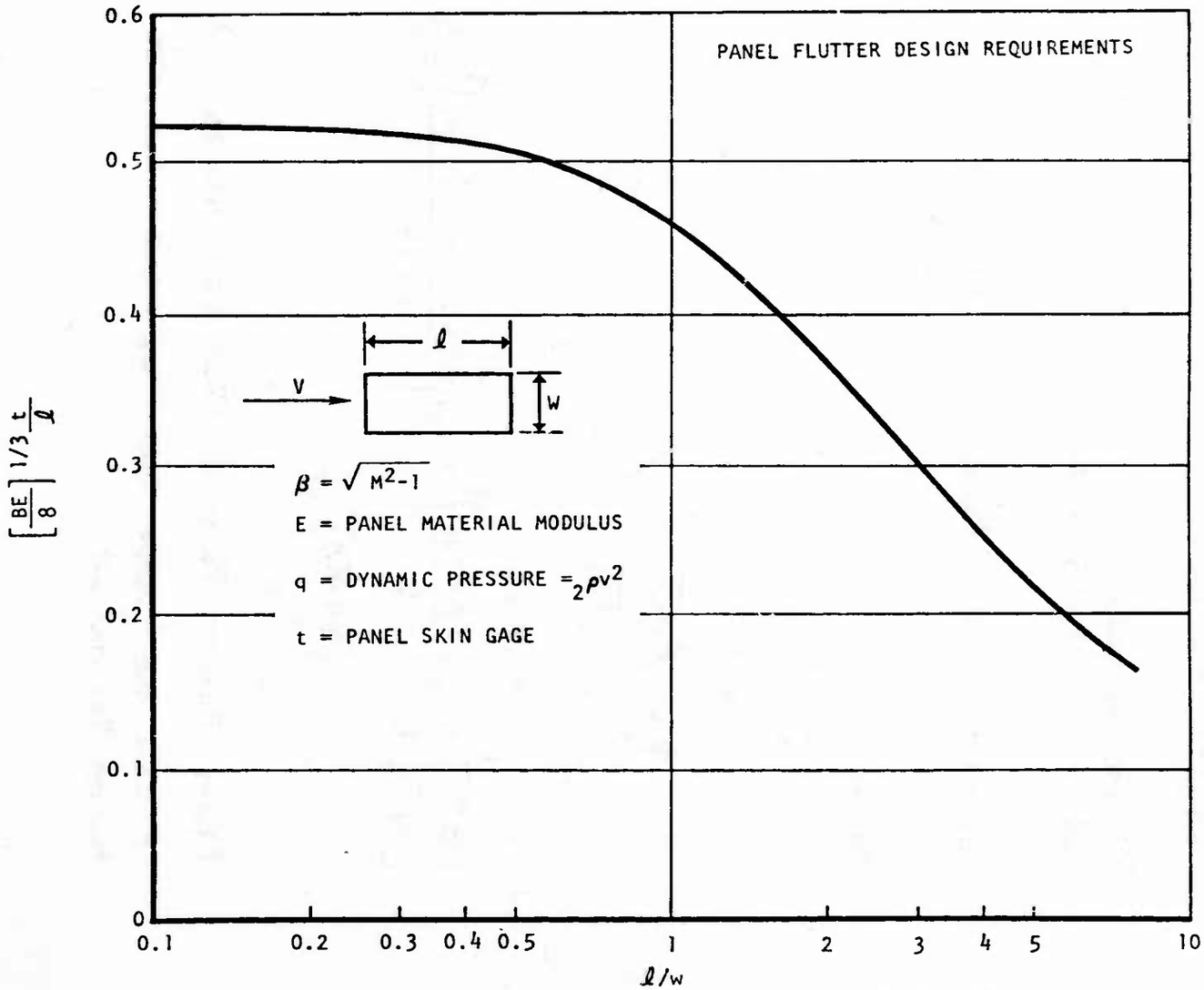

Figure 132. Fuselage trade study - skin stringer analysis (cont).

BENDING STIFFNESS CALCULATION (R.T.)

$(EI)_x$

SKIN

$$(EI)_{sk} = \frac{1}{3} A_{11sk}\, b_s\, t_{sk}^3 + \cancel{(EI)_\omega} + (b_s - b_b)\, t_w \left(t_{sk} + \frac{t_w}{2}\right)^2 A_{11w}$$

$\cancel{(EI)_\omega} \approx 0$

$$= \frac{1}{3} \times 8.5 \times 10^6 \times 6 \times (.06)^3 + 3.25 \times .02 \times (.07)^2 \times 6.6 \times 10^6$$

$$= 5774.1 \text{ lb-in}^2$$

WEB

$$(EI)_\omega = \frac{1}{3} t_w\, b_w^3\, E_{xw} \cos^2\phi$$

$$= \frac{1}{3} \times .02 \times (1.329)^3 \times 2.4 \times 10^6 \times \left(\frac{.875}{1.329}\right)^2$$

$$= 16280.0 \text{ lb-in}^2$$

CAP

$$(EI)_c = \cancel{(EI_0)_c} + t_c W_c E_{xc} \left(H - t_w - \frac{t_c}{2}\right)^2 + E_w t_w W_c \left(H - \frac{t_c}{2}\right)^2$$

$\cancel{(EI_0)_c} \approx 0$

$$= .125 \times 1 \times 18.1 \times 10^6 (1 - .02 - .0625)^2 + 2.4 \times 10^6 \times .02 \times 1 \times (1 - .01)^2$$

$$= 195163.0 \text{ lb-in}^2$$

$$(EI)_x = (EI)_{sk} + 2(EI)_\omega + (EI)_c$$

$$= 5774 + 16280 \times 2 + 195163$$

$$= 1.990 \times 10^6 \text{ lb-in}^2$$

(EA_y)

SKIN

$$(EA_y)_{sk} = \frac{1}{2} t_{sk}^2\, b_s\, A_{11sk} + t_w (b_s - b_b)\left(t_{sk} + \frac{t_w}{2}\right) A_{11w}$$

$$= \frac{1}{2} \times (.06)^2 \times 6 \times 8.5 \times 10^6 + .02 \times 3.25 \times .07 \times 6.6 \times 10^6$$

$$= 121880.0 \text{ lb-in}$$

Figure 132. Fuselage trade study - skin stringer analysis (cont).

WEB

$$(EAy)_w = \frac{1}{2} t_w b_w H E_w$$

$$= \frac{1}{2} \times .02 \times 1.329 \times 1 \times 2.4 \times 10^6$$

$$= 31896.0 \text{ lb-in}$$

CAP

$$(EAy)_c = t_c b_c (H - t_w - \frac{t_c}{2}) E_c + t_w b_c (H - \frac{t_w}{2}) E_w$$

$$= .125 \times 1 \times (1 - .02 - .0625) \times 18.1 \times 10^6 + .02 \times 1 \times (1 - .01) \times 2.4 \times 10^6$$

$$= 2123373.0 \text{ lb-in}$$

$$\Sigma(EAy) = (EAy)_{sk} + 2(EAy)_w + (EAy)_c$$

$$= 121830 + 2 \times 31896 + 2123373$$

$$= 2.309 \times 10^6 \text{ lb-in}$$

(EA)

SKIN

$$(EA)_{sk} = t_{sk} b_s A_{11sk} + t_w (b_s - b) A_{11w}$$

$$= .06 \times 6 \times 8.5 \times 10^6 + .02 \times 3.25 \times 6.6 \times 10^6$$

$$= 3489000. \text{ lb}$$

WEB

$$(EA)_w = t_w b_w E_w$$

$$= .02 \times 1.329 \times 2.4 \times 10^6$$

$$= 63792.0 \text{ lb}$$

CAP

$$(EA)_c = t_w b_c E_w + t_c b_c E_c$$

$$= .02 \times 1 \times 2.4 \times 10^6 + .125 \times 1 \times 18.1 \times 10^6$$

$$= 2310500. \text{ lb}$$

Figure 132. Fuselage trade study - skin stringer analysis (cont).

$$\Sigma(EA) = (EA)_{sk} + 2\times(EA)_{\omega} + (EA)_{c}$$
$$= 3489000 + 2\times 63792 + 2310500$$
$$= 5.927 \times 10^{6} \text{ lb.}$$

Distance from skin outer surface to N.A. is

$$\bar{y} = \frac{\Sigma(EAy)}{\Sigma(EA)}$$
$$= \frac{2.309 \times 10^{6}}{5.927 \times 10^{6}}$$
$$= .390 \text{ in}$$

Bending stiffness about N.A. is

$$(EI)_{b} = (EI)_{x} - \frac{[\Sigma(EAy)]^{2}}{\Sigma(EA)}$$
$$= 1.990 \times 10^{6} - \frac{[2.309 \times 10^{6}]^{2}}{5.927 \times 10^{6}}$$
$$= 1.090 \times 10^{6} \text{ lb-in}^{2}$$

Then

$$D_{11} = \frac{(EI)_{b}}{b_{s}}$$
$$= \frac{1.090 \times 10^{6}}{6}$$
$$= 0.1817 \times 10^{6} \text{ lb-in}^{2}$$

Also

$$D_{22} = \frac{t_{sk}^{3}}{12} A_{22_{sk}}$$
$$= \frac{(.06)^{3}}{12} \times 8.14 \times 10^{6}$$
$$= 146.5 \text{ lb-in}^{2}$$

Figure 132. Fuselage trade study - skin stringer analysis (cont).

SINCE $D_{11} >> D_{22}$, PANEL P_1 CAN BE CONSIDERED TO BEHAVE AS A SIMPLY SUPPORTED BEAM RATHER THAN AS A SIMPLY SUPPORTED PLATE.

CROSS-SECTIONAL AREA IS

$$A_T = b_s t_{sk} + t_w [(b_s - b_b) + 2xb_w + b_c] + t_c b_c$$

$$= 6 \times .06 + .02 [3.25 + 2 \times 1.329 + 1.0] + .125 \times 1.0$$

$$= .6232 \text{ IN}^2$$

THEN EQUIVALENT MODULUS IS

$$\bar{E}_x = \frac{\Sigma(EA)}{A_T}$$

$$= \frac{5.927 \times 10^6}{6232}$$

$$= 9.511 \times 10^6 \text{ PSI}$$

MOMENT OF INERTIA OF CROSS-SECTION IS

$$\bar{I}_o = \frac{(EI)_o}{\bar{E}_x}$$

$$= \frac{1.090 \times 10^6}{9.511 \times 10^6}$$

$$= .11461 \text{ IN}^4$$

DEFINE

$$n_{sk} = \frac{A_{11sk}}{\bar{E}_x}$$

$$= \frac{8.5 \times 10^6}{9.511 \times 10^6}$$

$$= 894$$

Figure 132. Fuselage trade study - skin stringer analysis (cont).

$$n_{w_2} = \frac{E_w}{E_x} = \frac{2.4 \times 10^6}{9.511 \times 10^6} = .252 \qquad n_{w_1} = \frac{A_{HW}}{E_x} = \frac{6.6 \times 10^6}{9.511 \times 10^6} = .694$$

$$n_c = \frac{E_c}{E_x} = \frac{18.1 \times 10^6}{9.511 \times 10^6} = 1.903$$

FUEL PRESSURE ONLY CONDITION (R.T.)

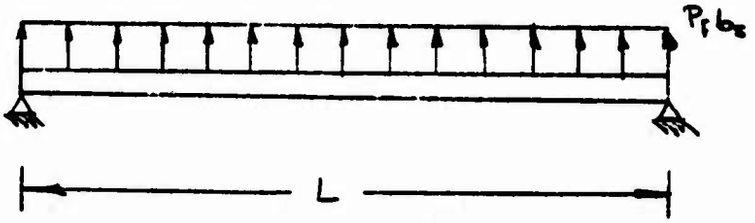

MAXIMUM MOMENT IS

$$M_{max} = \frac{1}{8} P_f b_s L^2 = \frac{1}{8} \times 22.5 \times 6 \times (26)^2 = 11407.5 \text{ lb-in}$$

BENDING STRESS ON SKIN IS

$$\sigma^F_{SK} = \frac{M_{max} C_{SK} n_{GK}}{I_o} = \frac{11407.5 \times .390 \times .894}{11461} = 34.70 \text{ ksi (TENSILE)} < F^{tu}_{x_{SK}} \quad \text{OK}$$

Figure 132. Fuselage trade study - skin stringer analysis (cont).

MAX. SHEAR ON STRINGER IS

$$V_{MAX} = \frac{P_f b_s L}{2}$$

$$= \frac{27.5 \times 6 \times 26}{2}$$

$$= 1755 \text{ lb.}$$

CONSIDER CORE TO BE HRP ($\frac{1}{4}$" CELL ; 3.5 lb /ft^3)

THE SHEAR STRAIN OF THE GRIEP WEBS IS

$$\gamma_w = \gamma_{CORE} \sin\phi$$

OR

$$\frac{\tau_w}{G_w} = \frac{\tau_{CORE}}{G_{CORE}} \sin\phi$$

$$\tau_w = \tau_{CORE} \sin\phi \frac{G_w}{G'_{CORE}}$$

ALSO $V = V_{CORE} + V_w$

$$= \tau_{CORE} A_c + 2\tau_w t_w b_w$$

$$= \tau_{CORE} \left[A_c + 2 t_w b_w \sin\phi \frac{G_w}{G'_{CORE}} \right]$$

ASSUME ONLY 1" x 1" CROSS-SECTION OF H/C CARRIES ANY SHEAR LOAD.

THEN

$$\tau_{CORE} = \frac{V_{max}}{A_c + 2 t_w b_w \sin\phi \frac{G_w}{G'_c}}$$

$$= \frac{1755}{1 \times 1 + 2 \times .02 \times 1.329 \times \frac{1}{1.329} \times \frac{55 \times 10^6}{9 \times 10^3}}$$

$$= 69.0 \text{ psi}$$

Figure 132. Fuselage trade study - skin stringer analysis (cont).

BENDING STRESS ON CAP IS

$$\sigma_c^f = \frac{M_{MAX} C_c n_c}{I_o}$$

$$= \frac{11407.5 \times (.61 - .02)\, 1.903}{.11461}$$

$$= 111.8 \text{ ksi (COMPRESSION)} < F_{x_c}^{cu} \quad \text{OK}$$

BENDING STRESS ON WEB

TENSILE

$$\sigma_w^f = \frac{M_{MAX}\, C_w^t\, n_{w_1}}{I_o}$$

$$= \frac{11407.5\ (.300 - .06) \times .694}{.11461}$$

$$= 22.8 \text{ ksi} \quad < F_{x_w}^{tu} \quad \text{OK}$$

< CLOSE

COMPRESSION

$$\sigma_w^f = \frac{M_{MAX}\, C_w^c\, n_{w_2}}{I_o}$$

$$= \frac{11407.5 \times .61 \times .252}{.11461}$$

$$= 15.3 \text{ ksi} \quad < F_{x_w}^{cu} \quad \text{OK}$$

Figure 132. Fuselage trade study - skin stringer analysis (cont).

ALLOWABLE SHEAR STRESS FOR HRP IS

F'_{su} = HEIGHT REDUCTION FACTOR × F_{su}

= .87 × 230 psi

= 200 psi

(REF. TFD-75-766, I-CHC)

THEN $\tau_{CORE} < F'_{su}$ OK

FOR GR/EP WEBS

$$\tau_w = \tau_{CORE} \sin\phi \frac{G_w}{G'_c}$$

$$= 69.0 \times \frac{1}{1.389} \frac{5.5 \times 10^6}{9 \times 10^{+3}}$$

$$= 31.7 \text{ ksi} < F^{su}_{xy} \quad \text{OK}$$

Figure 132. Fuselage trade study - skin stringer analysis (cont).

WEB

$$(EA_y)_w = \frac{1}{2} t_w b_w H E_w$$

$$= \frac{1}{2} \times .02 \times 1.329 \times 1 \times 1.97 \times 10^6$$

$$= 26181 \text{ lb-in.}$$

CAP

$$(EA_y)_c = t_c b_c (H - t_w - \frac{t_c}{2}) E_{x_c} + t_w b_c (H - \frac{t_w}{2}) E_{x_w}$$

$$= .125 \times 1 \times (1 - .02 - .0625) \times 18.0 \times 10^6 + .02 \times 1 \times .99 \times 1.97 \times 10^6$$

$$= 2103390 \text{ lb-in}$$

$$\Sigma(EA_y) = (EA_y)_{SK} + 2 \times (EA_y)_w + (EA_y)_c$$

$$= 116577 + 2 \times 26181 + 2103390$$

$$= 2.272 \times 10^6 \text{ lb-in.}$$

(EA)

SKIN

$$(EA)_{SK} = t_{SK} b_s A_{11_{SK}} + t_w (b_s - b_b) A_{11_w}$$

$$= .06 \times 6 \times 8.14 \times 10^6 + .02 (6 - 2.75) \times 6.3 \times 10^6$$

$$= 3339900 \text{ lb}$$

WEB

$$(EA)_w = t_w b_w E_{x_w}$$

$$= .02 \times 1.329 \times 1.97 \times 10^6$$

$$= 52363 \text{ lb.}$$

CAP

$$(EA)_c = t_w b_c E_{x_w} + t_c b_c E_{x_c}$$

$$= .02 \times 1 \times 1.97 \times 10^6 + .125 \times 1 \times 18.0 \times 10^6$$

$$= 2289400 \text{ lb}$$

Figure 132. Fuselage trade study - skin stringer analysis (cont).

$$\Sigma(EA) = (EA)_{SC} + 2\times(EA)_w + (EA)_c$$

$$= 3339900 + 2\times 52363 + 2289400$$

$$= 5.734\times10^6 \text{ lb}$$

DISTANCE FROM SKIN OUTER SURFACE TO N.A. IS

$$\bar{y} = \frac{\Sigma(EAy)}{\Sigma(EA)}$$

$$= \frac{2.272\times10^6}{5.734\times10^6}$$

$$= .396 \text{ IN}$$

BENDING STIFFNESS ABOUT N.A. IS

$$(EI)_o = (EI)_x - \frac{[\Sigma(EAy)]^2}{\Sigma(EA)}$$

$$= 1.965\times10^6 - \frac{[2.272]^2}{5.734}\times10^6$$

$$= 1.065\times10^6 \text{ lb-in}^2$$

CROSS-SECTIONAL AREA IS

$$A_T = .6232 \text{ in}^2 \quad \text{(REF PG. 11)}$$

EQUIVALENT MODULUS IS

$$\bar{E}_x = \frac{\Sigma(EA)}{A_T}$$

$$= \frac{5.734\times10^6}{.6232}$$

$$= 9.201\times10^6 \text{ psi}$$

Figure 132. Fuselage trade study - skin stringer analysis (cont).

MOMENT OF INERTIA OF CROSS-SECTION IS

$$\bar{I}_0 = \frac{(EI)_0}{\bar{E}_x}$$

$$= \frac{1.065 \times 10^6}{9.201 \times 10^6}$$

$$= .11575 \text{ IN}^4$$

DEFINE

$$n_{SK} = \frac{A_{11SK}}{\bar{E}_x}$$

$$= \frac{8.14 \times 10^6}{9.201 \times 10^6}$$

$$= .885$$

$$n_{\omega_1} = \frac{A_{11\omega}}{\bar{E}_x}$$

$$= \frac{6.3 \times 10^6}{9.201 \times 10^6}$$

$$\approx .685$$

$$n_{\omega_2} = \frac{E_{x\omega}}{\bar{E}_x}$$

$$= \frac{1.97 \times 10^6}{9.201 \times 10^6}$$

$$= .214$$

$$n_c = \frac{E_{xc}}{\bar{E}_x}$$

$$= \frac{18.0 \times 10^6}{9.201 \times 10^6}$$

$$= 1.956$$

Figure 132. Fuselage trade study - skin stringer analysis (cont).

CONDITION 1 (200°F)

FUEL PRESSURE LOAD

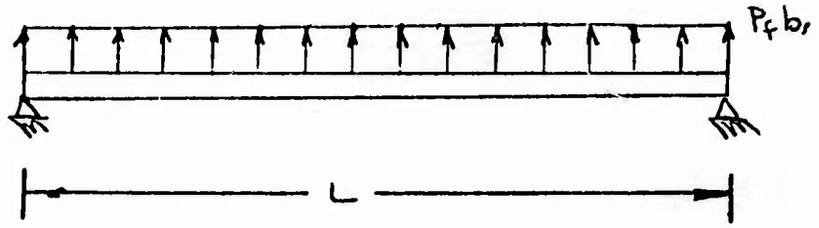

MAXIMUM MOMENT IS

$$M_{max} = \frac{P_f b_s L^2}{8}$$

$$= \frac{1}{8} \times 9.54 \times 6 \times (26)^2$$

$$= 4837 \text{ IN-LB}$$

BENDING STRESS ON SKIN IS

$$\sigma_{SK}^f = \frac{M_{max} C_{SK} n_{SK}}{\bar{I}_o}$$

$$= \frac{4837 \times .396 \times .885}{.11575}$$

$$= 14.7 \text{ KSI} \quad \text{(TENSILE)}$$

BENDING STRESS ON CAP IS

$$\sigma_C^f = \frac{M_{max} C_c n_c}{\bar{I}_o}$$

$$= \frac{4837 \times (.604 - .02) 1.956}{.11575}$$

$$= 47.7 \text{ KSI} \quad \text{(COMPRESSION)}$$

Figure 132. Fuselage trade study - skin stringer analysis (cont).

BENDING STRESSES ON WEB

TENSILE

$$\sigma_{w_1}^f = \frac{M_{max}\, C_w^t\, n_{w_1}}{\bar{I}_o}$$

$$= \frac{4837 \times (.396 - .06) \times .685}{.11575}$$

$$= 9.6 \text{ KSI}$$

COMPRESSION

$$\sigma_{w_2}^f = \frac{M_{max}\, C_w^c\, n_{w_2}}{\bar{I}_o}$$

$$= \frac{4837 \times .604 \times .214}{.11575}$$

$$= 5.4 \text{ KSI}$$

LOAD ON CROSS-SECTION DUE TO FUSELAGE BENDING IS

$$P_T = N_x^{us} b_s$$

$$= 654 \times 6$$

$$= 3924 \text{ lb. (COMPRESSION)}$$

HOWEVER

$$P_T = P_{SK} + P_{w_1} + P_{w_2} + P_c$$

$$= \sigma_{SK} A_{SK} + \sigma_{w_1} A_{w_1} + \sigma_{w_2} A_{w_2} + \sigma_c A_c$$

$$= \sigma_{SK}\, t_{SK}\, b_s + \sigma_{w_1}\, t_w (b_s - b_c) + \sigma_{w_2}\, t_w [2b_w + b_c]$$

$$+ \sigma_c\, t_c b_c$$

Figure 132. Fuselage trade study - skin stringer analysis (cont).

FROM STRAIN COMPATIBILITY

$$\varepsilon_{sk} = \varepsilon_{w_1} = \varepsilon_{w_2} = \varepsilon_c$$

OR

$$\frac{\sigma_{sk}}{A_{11sk}} = \frac{\sigma_{w_1}}{A_{11w}} = \frac{\sigma_{w_2}}{E_{xw}} = \frac{\sigma_c}{E_{xc}}$$

OR

$$\sigma_{sk} = \sigma_c \frac{A_{11sk}}{E_{xc}}$$

$$\sigma_{w_1} = \sigma_c \frac{A_{11w}}{E_{xc}}$$

$$\sigma_{w_2} = \sigma_c \frac{E_{xw}}{E_{xc}}$$

THEN

$$P_T = \sigma_c \left[\frac{A_{11sk}}{E_{xc}} t_{sk} b_s + \frac{A_{11w}}{E_{xc}} t_w (b_s - b_b) + \frac{E_{xw}}{E_{xc}} t_w (2b_w + b_c) + t_c b_c \right]$$

$$P_T = \sigma_c \left[\frac{8.14 \times 10^6}{18.0 \times 10^6} \times .06 \times 6 + \frac{6.3 \times 10^6}{18.0 \times 10^6} \times .02 \times (6 - 2.75) + \frac{1.97 \times 10^6}{18.0 \times 10^6} \times .02 \times (2 \times 1.329 + 1.0) + .125 \times 1 \right].$$

$$= \sigma_c \times .3186$$

THEN

$$\sigma_c = P_T / .3186$$

$$= 3924 / .3186$$

$$= 12.3 \text{ ksi} \quad \text{(COMPRESSION)}$$

$$\sigma_{sk} = \sigma_c \frac{A_{11sk}}{E_{xc}}$$

$$= 12.3 \times \frac{8.14 \times 10^6}{18.0 \times 10^6} \text{ ksi}$$

Figure 132. Fuselage trade study - skin stringer analysis (cont).

$$\sigma_{sk} = 5.6 \text{ ksi} \quad \text{(COMPRESSION)}$$

$$\sigma_{w_1} = \frac{A_{11w}}{E_{xc}} \sigma_c$$

$$= \frac{6.3 \times 10^6}{18.0 \times 10^6} 12.3 \text{ ksi}$$

$$= 4.3 \text{ ksi} \quad \text{(COMPRESSION)}$$

$$\sigma_{w_2} = \frac{E_{xw}}{E_{xc}} \sigma_c$$

$$= \frac{1.97 \times 10^6}{18 \times 10^6} 12.3 \text{ ksi}$$

$$= 1.3 \text{ ksi} \quad \text{COMPRESSION}$$

THEN

$$f_{sk} = \sigma^f_{sk} + \sigma_{sk}$$

$$= 14.7 - 5.6$$

$$= 9.1 \text{ ksi} \quad \text{(TENSION)} \quad \text{OK}$$

$$f_{w_1} = \sigma^f_{w_1} + \sigma_{w_1}$$

$$= 9.6 - 4.3$$

$$= 5.3 \text{ ksi} \quad \text{(TENSION)} \quad \text{OK}$$

$$f_{w_2} = \sigma^f_{w_2} + \sigma_{w_2}$$

$$= -5.4 - 1.3$$

$$= -6.7 \text{ ksi} \quad \text{(COMPRESSION)} \quad \text{OK}$$

$$f_c = \sigma^f_c + \sigma_c$$

$$= -47.7 - 12.3$$

$$= -60.0 \text{ ksi} \quad \text{(COMPRESSION)} \quad \text{OK}$$

Figure 132. Fuselage trade study - skin stringer analysis (cont).

CHECK COLUMN BUCKLING

$$P_{CR} = \frac{\pi^2 (EI)_b}{L^2}$$

$$= \frac{(3.14159)^2 [1.065 \times 10^6]}{(26)^2}$$

$$= 15{,}549 \text{ lbs} \quad > P_T = 3924 \text{ lb} \quad \text{OK}$$

CHECK SKIN STABILITY

$$N_x^{SK} = \bar{\sigma}_{SK} t_{SK}$$

$$= 5.6 \times .06$$

$$= 336 \text{ lb/in.}$$

$$\frac{a}{b} = \frac{26}{3.25} = 8.0 \approx \infty$$

THEN BUCKLING EQ. IS

$$N_{xCR} = \frac{2\pi^2}{b^2} \left[\sqrt{D_{11} D_{22}} + D_{12} + 2D_{66} \right]$$

USE $D_{ij} = \frac{A_{ij} t_{SK}^3}{12}$

THEN $D_{11} = D_{22} = 8.14 \times \frac{(.06)^3}{12} \times 10^6$

$$= 146.5 \text{ lb-in}$$

$$D_{12} = 3.6 \times \frac{(.06)^3}{12} \times 10^6$$

$$= 64.8 \text{ lb-in}$$

Figure 132. Fuselage trade study - skin stringer analysis (cont).

$$D_{66} = 3.8 \times \frac{(.06)^3}{12} \times 10^6$$

$$= 68.4 \text{ lb-in}$$

Then $$N_{xcr} = \frac{2\pi^2}{(3.25)^2}\left[\sqrt{(146.5)^2} + 64.8 + 2 \times 68.4\right]$$

$$= 651 \text{ lb/in} \quad > N_x^{sk} = 386 \text{ lb/in} \quad \text{OK}$$

Figure 132. Fuselage trade study - skin stringer analysis (concl).

TABLE 31. FUSELAGE SECTION STRINGER DESIGN WEIGHTS

AIRCRAFT: FUSELAGE SECTION STRINGER DESIGN

AIRCRAFT WEIGHTS - IN POUNDS

	AL	II	SI	BE	GB	EG	SA	ICIAL
FUSELAGE	76.	171.	69.	0.	2058.	27.	0.	3208.
FRAME/LONG	0.	171.	69.	0.	695.	0.	0.	935.
SKIN-STRGR	76.	0.	0.	0.	0.	0.	0.	78.
BOND HONEY	0.	0.	0.	0.	1363.	27.	0.	1390.
BRAZE HONEY		0.	0.				0.	0.
DIFF BOND		0.					0.	0.
MISC								805.
WING	125.	25.	0.	0.	2852.	0.	0.	3155.
SKIN-STRGR	0.	0.	0.	0.	0.	0.	0.	0.
MULTI-SPAR	0.	25.	0.	0.	523.	0.	0.	548.
BOND HONEY	125.	0.	0.	0.	2329.	0.	0.	2454.
BRAZE HONEY		0.	0.				0.	0.
DIFF BOND		0.					0.	0.
MISC								153.
CANARDS	0.	16.	2.	0.	117.	0.	0.	145.
SKIN-STRGR	0.	0.	0.	0.	0.	0.	0.	0.
MULTI-SPAR	0.	0.	0.	0.	0.	0.	0.	0.
BOND HONEY	0.	16.	2.	0.	117.	0.	0.	135.
BRAZE HONEY		0.	0.				0.	0.
DIFF BOND		0.					0.	0.
MISC								10.
NACELLE	0.	0.	0.	0.	0.	0.	0.	0.
FRAME/LONG	0.	0.	0.	0.	0.	0.	0.	0.
SKIN-STRGR	0.	0.	0.	0.	0.	0.	0.	0.
BOND HONEY	0.	0.	0.	0.	0.	0.	0.	0.
BRAZE HONEY		0.	0.				0.	0.
DIFF BOND		0.					0.	0.
MISC								0.

WEIGHT DATA - IN POUNDS	
AMPR WEIGHT	13104.
STRUCTURE WT	7778.
STRUCTURAL HDWE WT	133.
SYSTEM HDWE WT	133.
LANDING GEAR WT	1280.
FUEL SYSTEM WT	750.
ELECTRICAL SYSTEM WT	680.
HYDRAULIC SYSTEM WT	430.
AUX POWER SYSTEM WT	310.
ECS WT	530.
CREW ACCOM WT	320.
CONTROL & DISPLAY WT	120.
FLIGHT CONTROL WT	950.
ARMAMENT WT	560.
AICS MECHANISM WT	300.
EQUIPMENT WT	80.
ENGINE WT	5375.
EMPTY WT	19158.
FUEL WT	7060.
TOGW	30825.

DESIGN VARIABLES	
WING AREA-SQ FT	400.
CANARDS AREA-SQ FT	35.
WETTED AREA-SQ FT	1772.
WING + HORIZ AREA	435.
WING SPAN-FT	31.6
HORIZ SPAN-FT	10.0
OVERALL LENGTH-FT	57.0
ASPECT RATIO	2.50
DYNAMIC PRESSURE	2133.

TABLE 32. FUSELAGE SECTION STRINGER DESIGN COSTS

AIRCRAFT: FUSELAGE SECTION STRINGER DESIGN
ALL COSTS IN MILLIONS AND IN 1975 DOLLARS

PRODUCTION COST FOR 300 UNITS
UNIT AVG. FLYAWAY COST 2.784

WORK BREAKDOWN STRUCTURE	LABOR COST					MATERIAL COST		TOTAL
	MFG.	TOOL.	PLNG.	ENGR.	Q&RA	MFG.	TOOL.	COST
TOTAL PROGRAM COST INCLUDING FEE	393.06	70.66	34.52	40.33	52.82	234.44	8.94	835.11
TOTAL PROGRAM COST INCLUDING G&A	357.33	64.24	31.38	36.66	48.02	213.13	8.12	759.22
TOTAL PROGRAM COST LESS G&A	325.35	58.49	28.58	33.38	43.72	194.06	7.40	691.30
AIR VEHICLE	325.35	58.49	28.58	33.38	43.72	194.06	7.40	691.30
AIRFRAME	164.64	51.89	17.10	33.38	24.62	187.85	6.56	486.04
BASIC STRUCTURE	97.31	51.89	10.73	8.06	16.93	57.92	6.56	249.40
FUSELAGE	37.88	33.34	5.18	4.79	8.06	24.02	4.22	117.49
WING	33.54	12.40	3.31	2.54	5.22	31.39	1.57	89.98
CANARDS	1.54	5.15	0.50	0.73	0.75	1.56	0.65	10.89
NACELLES	0.0	0.0	0.0	0.0	0.0	0.0	0.0	0.0
BASIC STRUCTURE ASSEMBLY	24.35	1.00	1.74	0.0	2.89	0.94	0.13	31.05
LANDING GEAR	0.0	0.0	0.0	0.60	0.0	13.48	0.0	14.07
FUEL SYSTEM	6.40	0.0	0.56	1.72	0.73	4.61	0.0	14.01
FLIGHT VEHICLE POWER	31.07	0.0	2.55	5.98	3.55	58.12	0.0	101.27
ENVIRONMENTAL CONTROL	0.0	0.0	0.0	2.09	0.0	25.90	0.0	27.99
CREW ACCOMMODATIONS	6.75	0.0	0.52	0.80	0.77	0.0	0.0	8.84
CONTROLS AND DISPLAYS	0.0	0.0	0.0	0.0	0.0	8.56	0.0	8.56
FLIGHT CONTROLS	20.72	0.0	1.42	0.0	2.37	0.0	0.0	24.50
ARMAMENT	0.0	0.0	0.0	0.30	0.0	19.26	0.0	19.55
AIR INDUCTION CONTROL SYSTEM	2.39	0.0	0.21	0.64	0.27	0.0	0.0	3.50
AIRFRAME INTEGRATION & CHECK	0.0	0.0	0.0	16.84	0.0	0.0	0.0	16.84
ENGINEERING TECHNOLOGIES	0.0	0.0	0.0	12.24	0.0	0.0	0.0	12.24
DESIGN SUPPORT TECHNOLOGIES	0.0	0.0	0.0	1.73	0.0	0.0	0.0	1.73
AIRFRAME INSTALL & CHECKOUT	0.0	0.0	0.0	2.88	0.0	0.0	0.0	2.88
PROPULSION (GFE)	0.0	0.0	0.0	0.0	0.0	0.0	0.0	0.33
AVIONICS (GFE)	0.0	0.0	0.0	0.0	0.0	0.0	0.0	0.0
A/V INTEGRATION, ASSY, INSTALL	160.71	6.60	11.47	0.0	19.10	6.20	0.84	204.93

The forward fuselage construction is continued throughout the equipment compartment, the forward wing stub, the wing carry-through section, and the missile bay. Honeycomb panels are also used for the engine inlet duct with graphite/epoxy skins except at the leading edges. Here, Kevlar skins are specified because of its high impact and abrasion resistance.

The aft fuselage section also employs honeycomb panels but with graphite/polyimide skins and HRH (fiberglass/polyimide) core. The temperature of the structure in this compartment, with cooling air flow, is not expected to exceed 450° F which is well within the capabilities of polyimide. The jet flap structure will employ inconel to meet the high engine exhaust temperatures.

The outboard wing panel will be constructed of graphite/epoxy skins with full-depth graphite/epoxy honeycomb core. This selection is based on the trade study described previously, which showed this type of construction to be lower in both cost and weight than a multi-spar wing. Full-depth honeycomb is also used for the flaps and elevons with graphite/epoxy and for the wing tip with fiberglass core. The leading edge devices employ graphite/epoxy skins with a nose cap of full-depth honeycomb with Kevlar skins, which are used on all leading edges because of their impact resistance capabilities.

Advanced composites are also used on the landing gear. As shown in Figure 133, the nose gear drag structure will be fabricated from graphite/epoxy laminate, with filaments wrapped around the hinge points to provide a maximum efficiency joint. Trade studies on this concept for other landing gear drag struts have shown weight reductions up to 58 percent and cost reductions of 60 percent over metal components.

FLUTTER ANALYSIS

Structural optimization flutter analyses of the ADCA D572 wing were conducted to obtain minimum weight structure to meet the required flutter speed, which was considered to be 15 percent above 1.2M at sea level. The program used to achieve the required composite structure (COP) is a modified version of the optimization program for metallic structures (STROP). COP allows for independent variation in the torsional and bending strain energy densities in the flutter mode, whereas STROP maintains the same local energy density. The initial data for the flutter optimization studies were strength-designed structures derived from the SWEEP program. STROP and COP both permit rapid turnaround time to impact on the design.

The -4A configuration was the first to be analyzed. Aerodynamic data at .9M, as defined by $2\pi \cos\lambda$ for the lift curve slope and the aerodynamic center at the quarter chord, was used initially. Figures 134 and 135 show the strength and flutter stiffness requirements for bending and torsion.

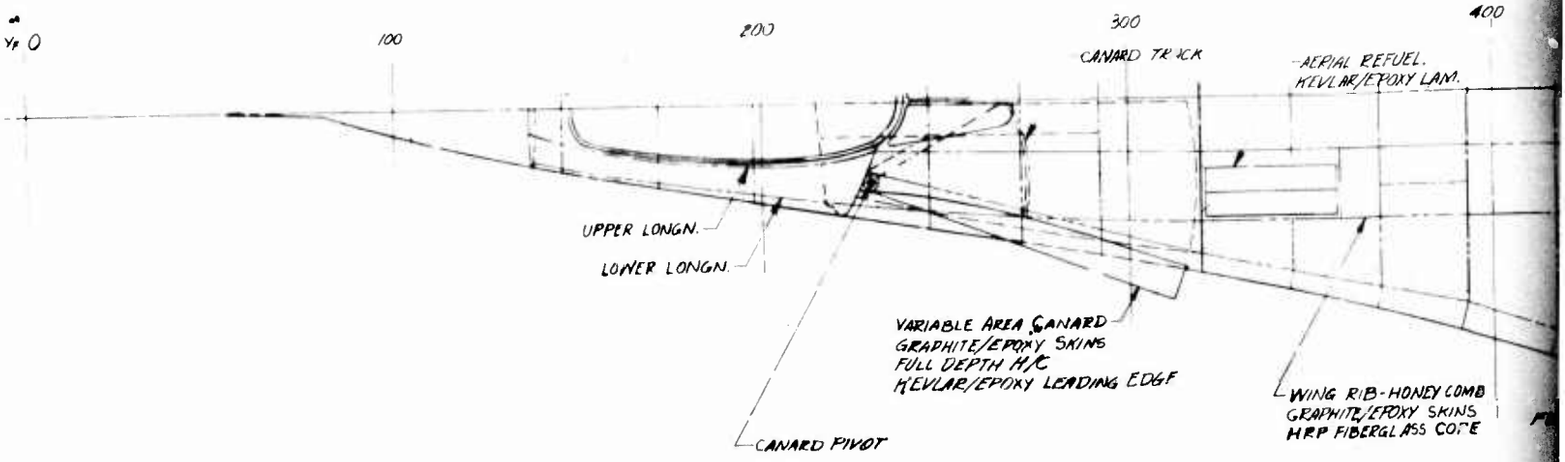

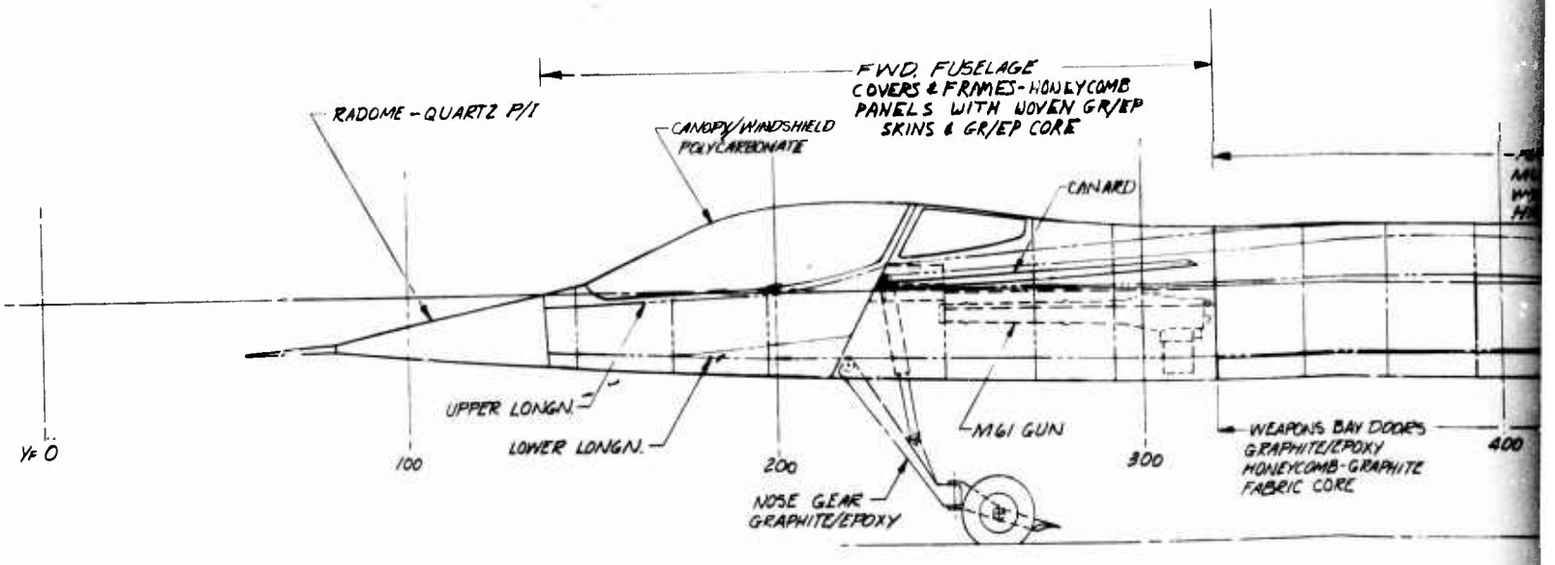

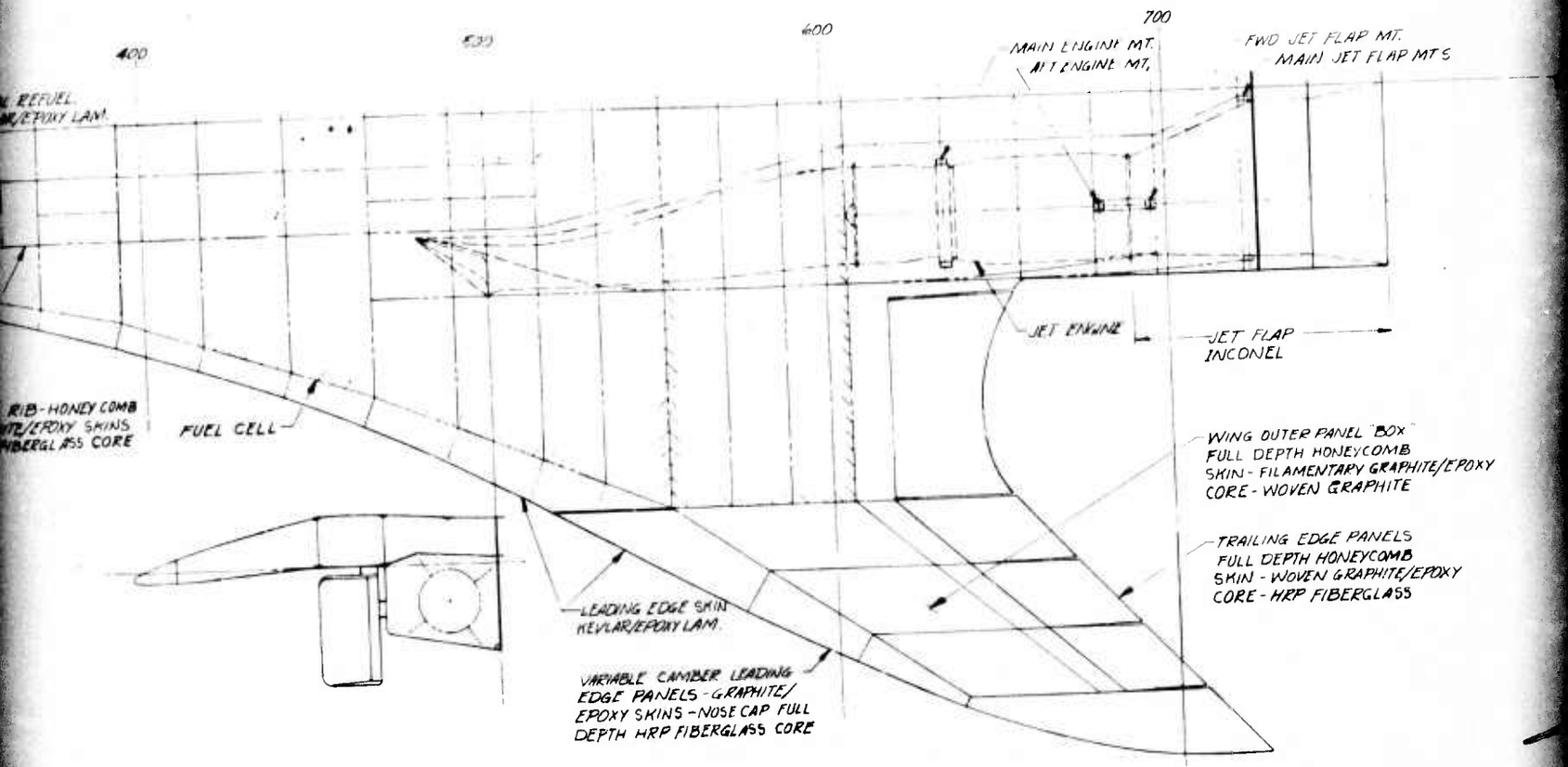
400
500
600
700
MAIN ENGINE MT.
AFT ENGINE MT.
FWD JET FLAP MT.
MAIN JET FLAP MTS
REFUEL
JET ENGINE
JET FLAP
INCONEL
RIB - HONEY COMB
FUEL CELL
WING OUTER PANEL "BOX"
FULL DEPTH HONEYCOMB
SKIN - FILAMENTARY GRAPHITE/EPOXY
CORE - WOVEN GRAPHITE
TRAILING EDGE PANELS
FULL DEPTH HONEYCOMB
SKIN - WOVEN GRAPHITE/EPOXY
CORE - HRP FIBERGLASS
LEADING EDGE SKIN
KEVLAR/EPOXY LAM.
VARIABLE CAMBER LEADING
EDGE PANELS - GRAPHITE/
EPOXY SKINS - NOSE CAP FULL
DEPTH HRP FIBERGLASS CORE

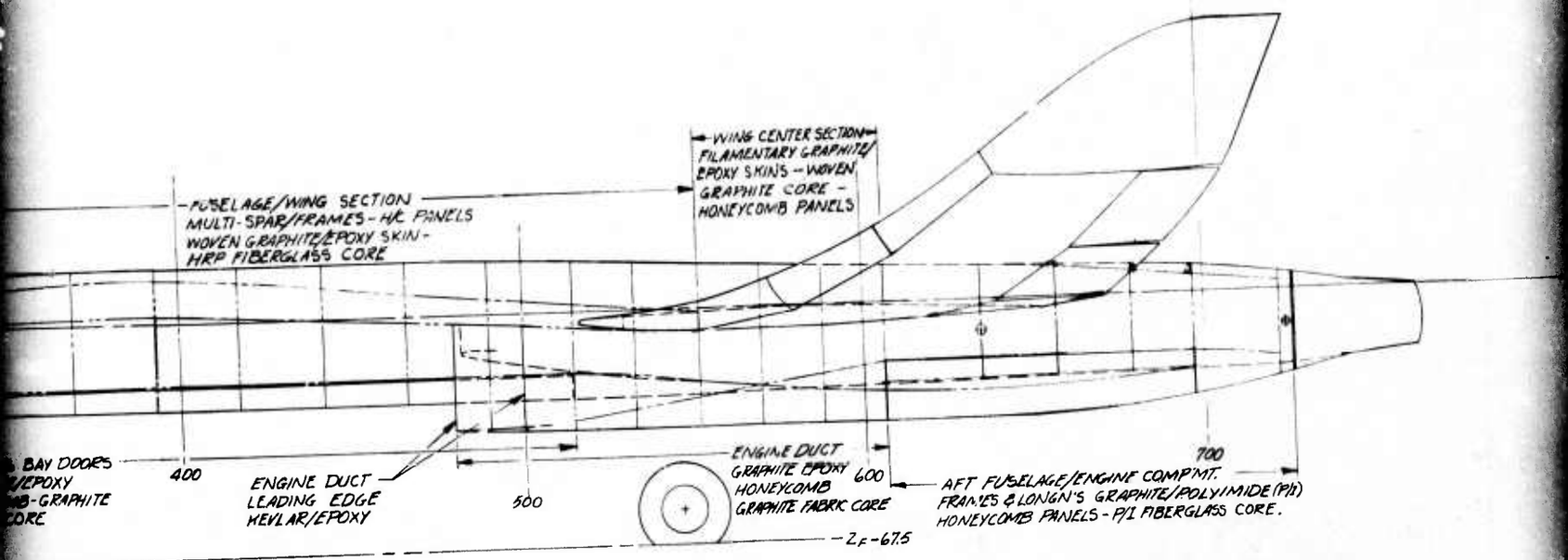
WING CENTER SECTION
FILAMENTARY GRAPHITE/
EPOXY SKINS - WOVEN
GRAPHITE CORE -
HONEYCOMB PANELS
FUSELAGE/WING SECTION
MULTI-SPAR/FRAMES - HR PANELS
WOVEN GRAPHITE/EPOXY SKIN -
HRP FIBERGLASS CORE
BAY DOORS
400
ENGINE DUCT
LEADING EDGE
KEVLAR/EPOXY
500
ENGINE DUCT
GRAPHITE EPOXY
HONEYCOMB
GRAPHITE FABRIC CORE
600
700
AFT FUSELAGE/ENGINE COMP MT.
FRAMES & LONGN'S GRAPHITE/POLYIMIDE (P/I)
HONEYCOMB PANELS - P/I FIBERGLASS CORE.
Z_F - 67.5

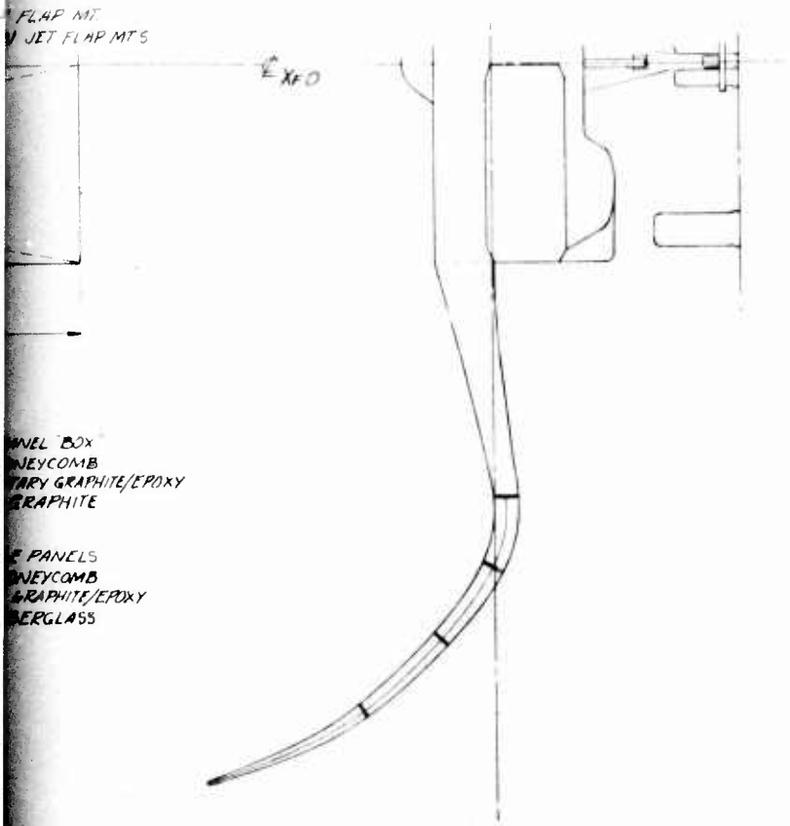

5. CONTROL SURFACES - FULL DEPTH HONEYCOMB CONSTRUCTION - WOVEN GRAPHITE/EPOXY SKINS.
4. WING OUTER PANEL "BOX" - FULL DEPTH HONEYCOMB CONSTRUCTION - FILAMENTARY GRAPHITE/EPOXY SKINS.
3. WING CENTER SECTION - MULTI-SPAR & HONEY COMB PANELS - FILAMENTARY GRAPHITE/EPOXY FACE SHEETS.
2. FUSELAGE/WING SECTION - MULTI-FRAME/SPAR & HONEYCOMB PANELS - WOVEN GRAPHITE/EPOXY FACE SHEETS.
1. FUSELAGE - LONGERONS, FRAMES & SKIN CONSTRUCTION - GRAPHITE/EPOXY.

NOTES: UNLESS OTHERWISE NOTED.

Figure 133. Structural arrangement - advanced design composite aircraft.

3

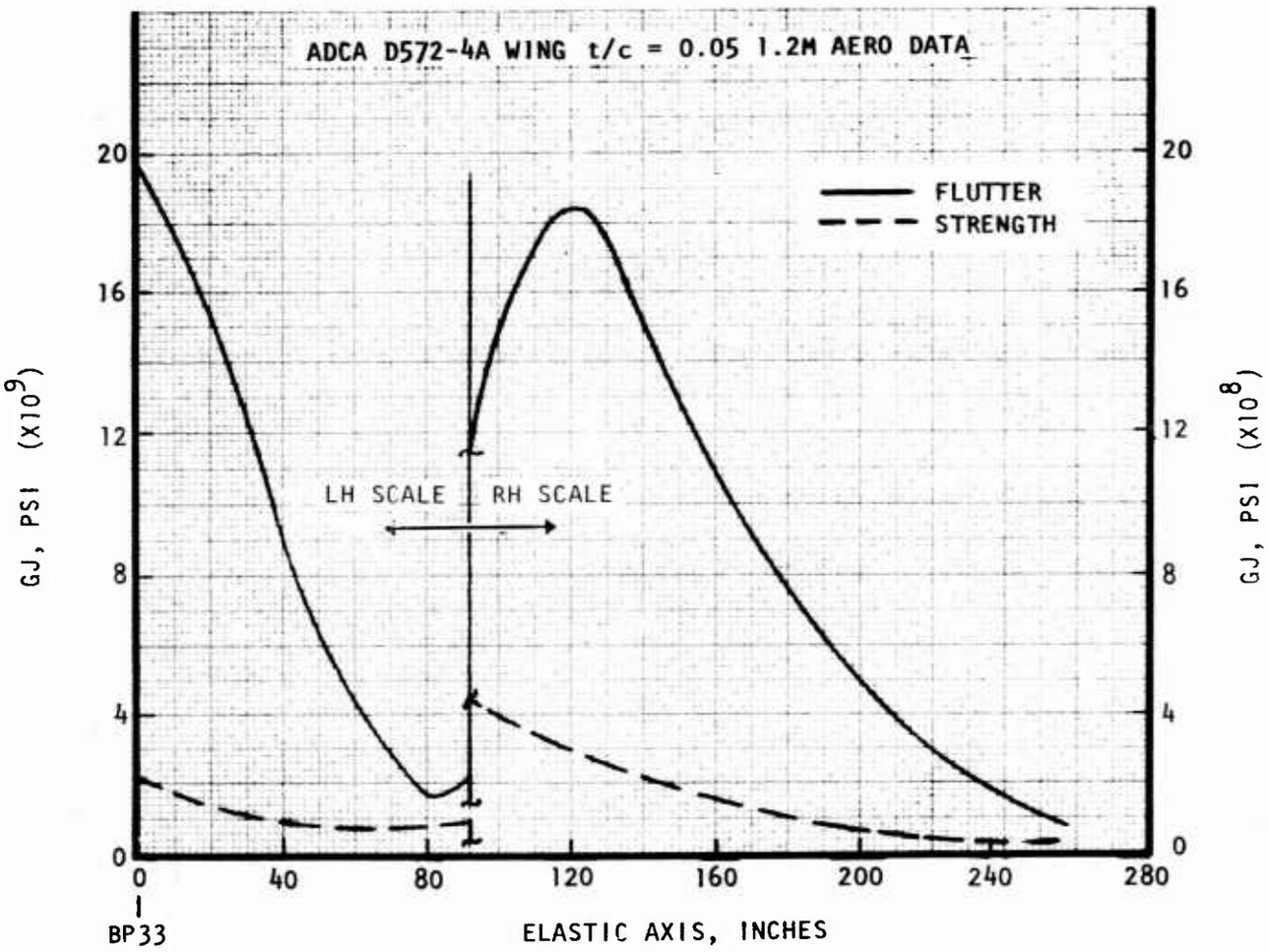

Figure 134. Required torsional stiffness, D572-4A.

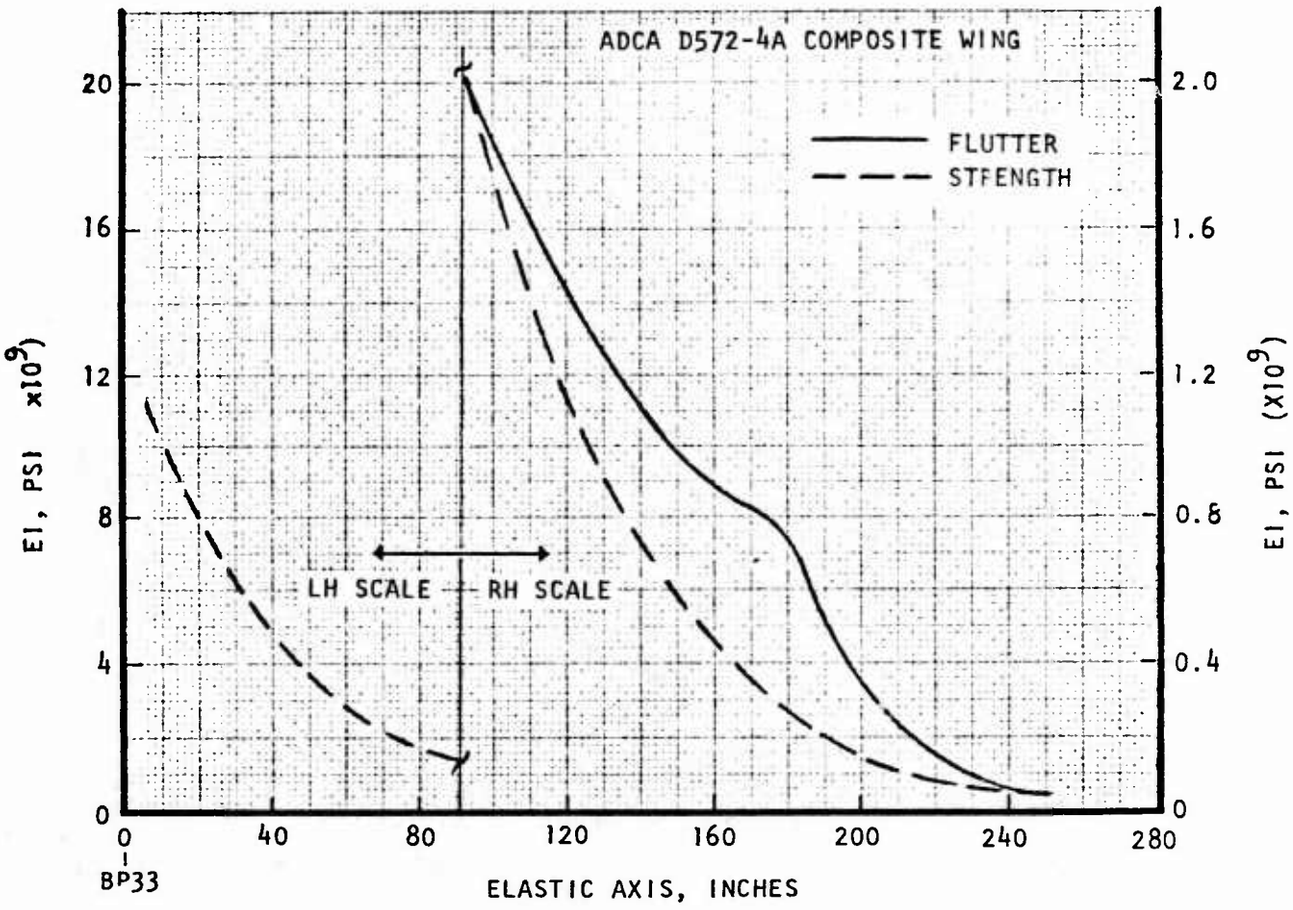

Figure 135. Required bending stiffness, D572-4A.

The large torsional stiffness increase required near the root caused an increase in the t/c ratio such that t/c became a constant spanwise value of 0.05. Another run was made using the new strength requirement and a more realistic description of the lift curve slopes and aerodynamic centers. The required stiffnesses for bending and torsion under these circumstances are shown in Figures 136 and 137, indicating significant reduction in requirements from the previous configuration. The mathematical model of these analyses assumed the wing to a planar, as imposed by the COP program.

An analysis was performed to determine the effect on flutter speed of the outer wing panel dihedral using a basic flutter analysis program. The required stiffness and associated mass distributions as determined by COP were used as input data to the mathematical model. The resulting flutter speed, frequency, and mode were almost identical to the planar results. This comparison gave credence to the validity of assuming a planar wing for the flutter of this configuration.

The -4B configuration was next optimized for flutter using COP. The flutter and strength required stiffnesses are shown on Figures 138 and 139, indicating small increases in bending stiffness on the outboard wing and large increases in torsional stiffness over most of the wing.

AEROELASTIC TAILORING

One of the unique features of advanced composite structure is the capability of being tailored to match strength and stiffness requirements in several different directions. This anisotropic property is particularly useful in meeting three structural dynamics requirements:

1. Flutter, where torsional stiffness and bending stiffness requirements require different moduli.

2. Controlled twist, in which the twist introduced by the bending deflection of a swept wing with isotropic skins may not be ideal for optimum performance.

3. Controlled camber, in which bending deflection may be used to modify the wing camber.

The designs for the wing trade studies have been tailored to some extent. Composite plies were added (in addition to those required for strength) only in the direction required for stiffness to meet flutter requirements. A preliminary run on the TSO composite wing optimization program indicates that the wing skins can be further optimized by changing the ply orientation. This program has been recently modified to accommodate nonplanar wings and will be used in Task II to improve the wing design.

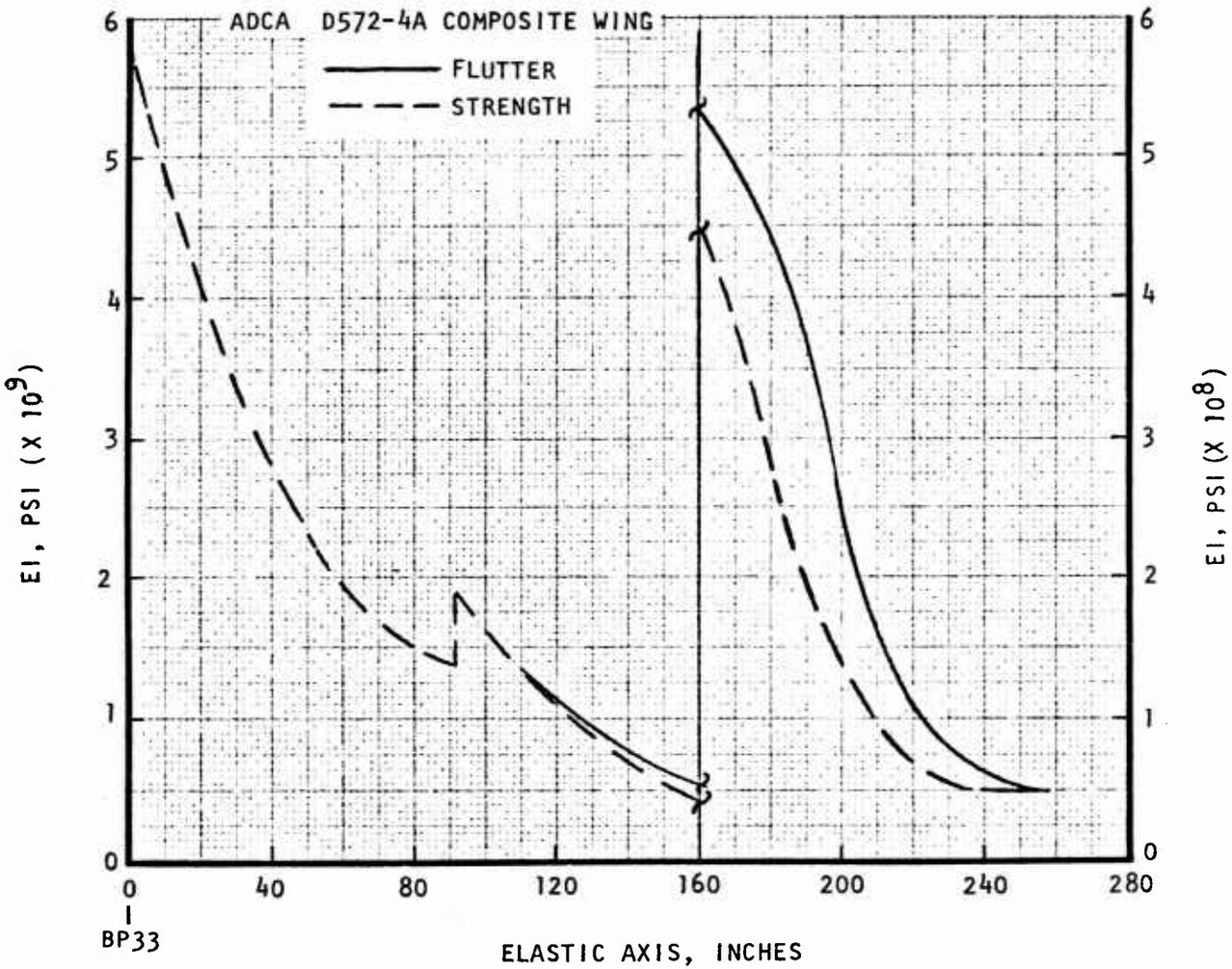

Figure 136. Required bending stiffness revised D572-4A.

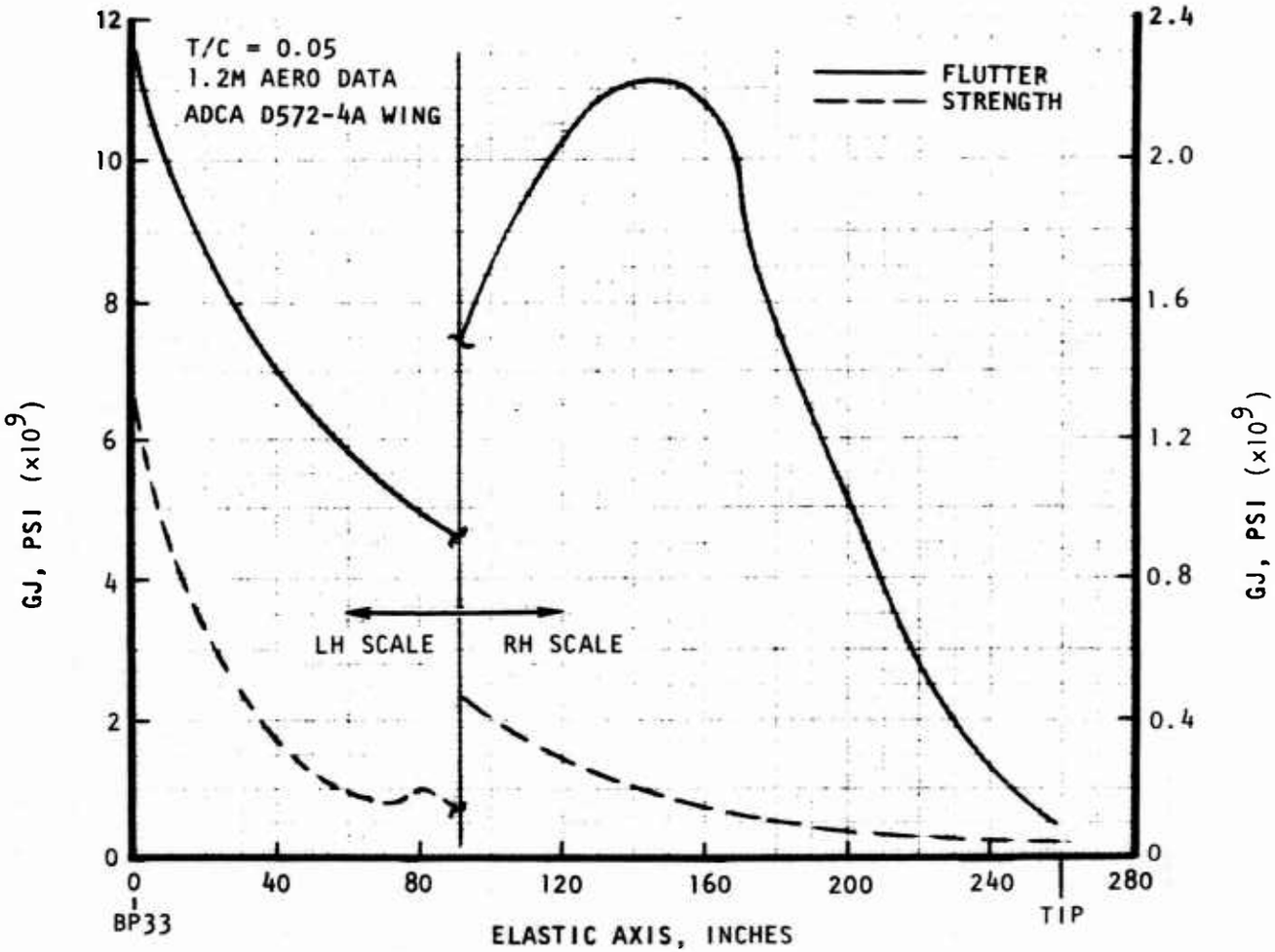

Figure 137. Required torsional stiffness, D572-4B.

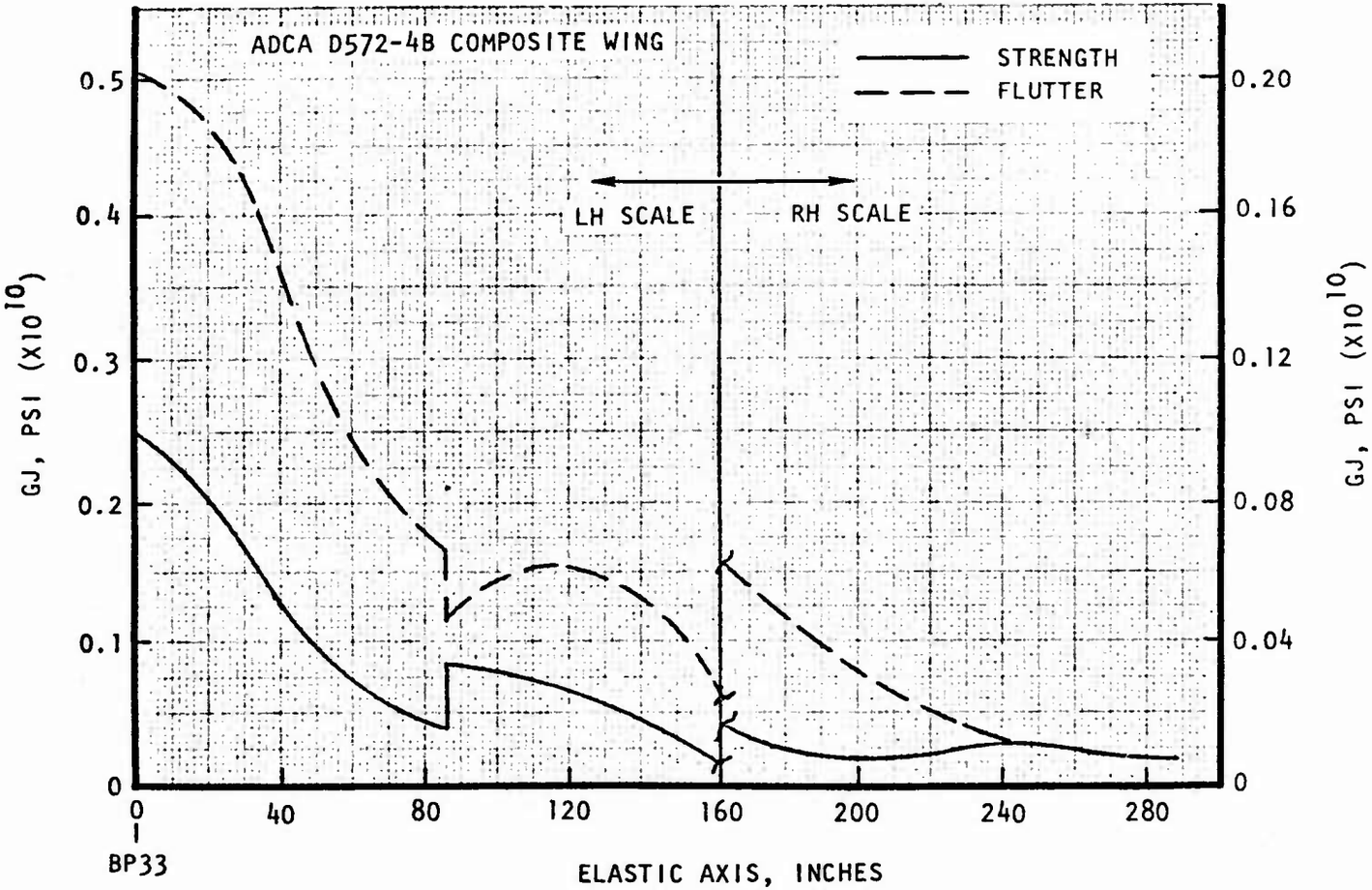

Figure 138. Required torsion stiffness, D572-4B.

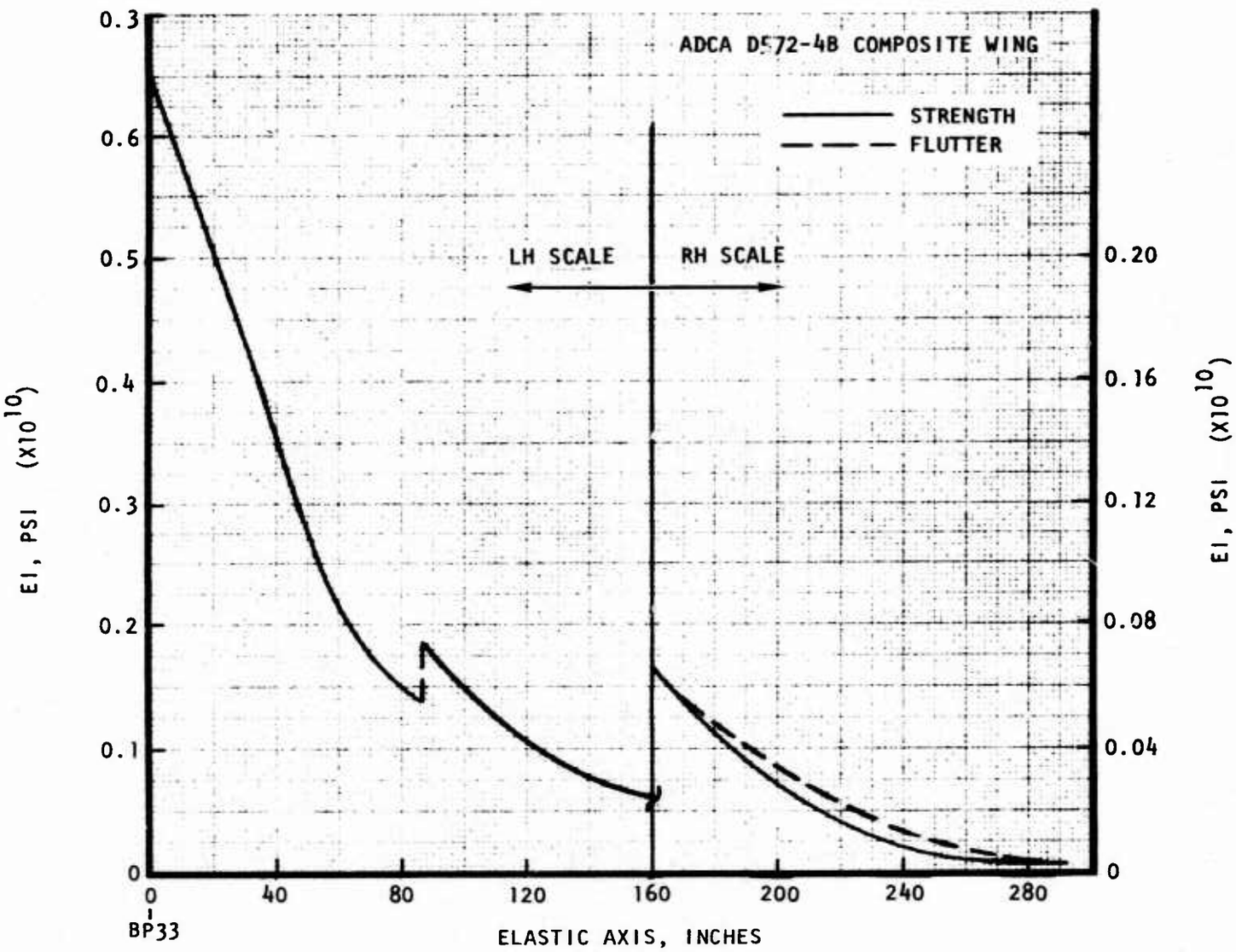

Figure 139. Required bending stiffness, D572-4B.

Aerodynamic requirements for controlled twist for two critical points in the ADCA envelope have been determined. These are expressed in terms of both twist and camber. Figure 140 shows the twist requirements for the two conditions, M .2 and M 1.5. Additional requirements for two critical stability and control points will also be determined and the final wing behavior will be tailored to match the more critical condition.

The aeroelastic tailoring process used at Rockwell is a combination of a number of programs, including TSO. The process uses TSO (which operates on the wing only) for a preliminary sizing and ply orientation, then conducts a more refined, finite-element analysis using flutter, aerodynamic, loads, weights, and structural programs. The complete tailoring process was planned to be conducted during Task II.

ADVANCED METALLIC BASELINE STRUCTURE

STRUCTURE DESCRIPTION

The all-metal baseline aircraft structure is an advanced version of a semi-monocoque skin-frame-longeron airframe. Improved alloys and newly emerging fabrication techniques have been combined to produce a 1980 technology design.

The primary aluminum alloy to be used is 2048-851. This alloy is used in applications where 2024 would be used in todays airframe. It exhibits the same degree of toughness but higher tensile properties. The cost increase is minimal. The alloy 7475-T76 has been selected to replace 7075, since it has higher toughness and virtually the same strength properties. For many of the frames and spars in this airframe, welded sine wave structures are proposed using 7005 aluminum alloy. This alloy will enable Rockwell's low-cost "Red-eye" welding process to be used for fabrication without greatly sacrificing high strength properties.

The titanium alloy selected for ADCA is 6Al-4V alloy. The primary applications of titanium use the superplastic forming process, with concurrent diffusion bonding.

The structural arrangement is shown in Figure 141. The radome is the same as the all-composite aircraft radome, employing quartz-polyimide filament wound. The cockpit structure, equipment bay, weapons bay, including the forward wing stub use skin-frame-longeron construction. All skins are 2048-851 aluminum alloy. Frames spaced at 10 inches are welded sine wave construction. Bulkheads are 7475-T6 aluminum built-up sections with weld-bonded caps and stiffeners.

The wing outer panel and center section are multi-spar designs with superplastically formed titanium sine wave intermediate spars and aluminum front and rear spars machined from 7475 alloy, which is also used for the

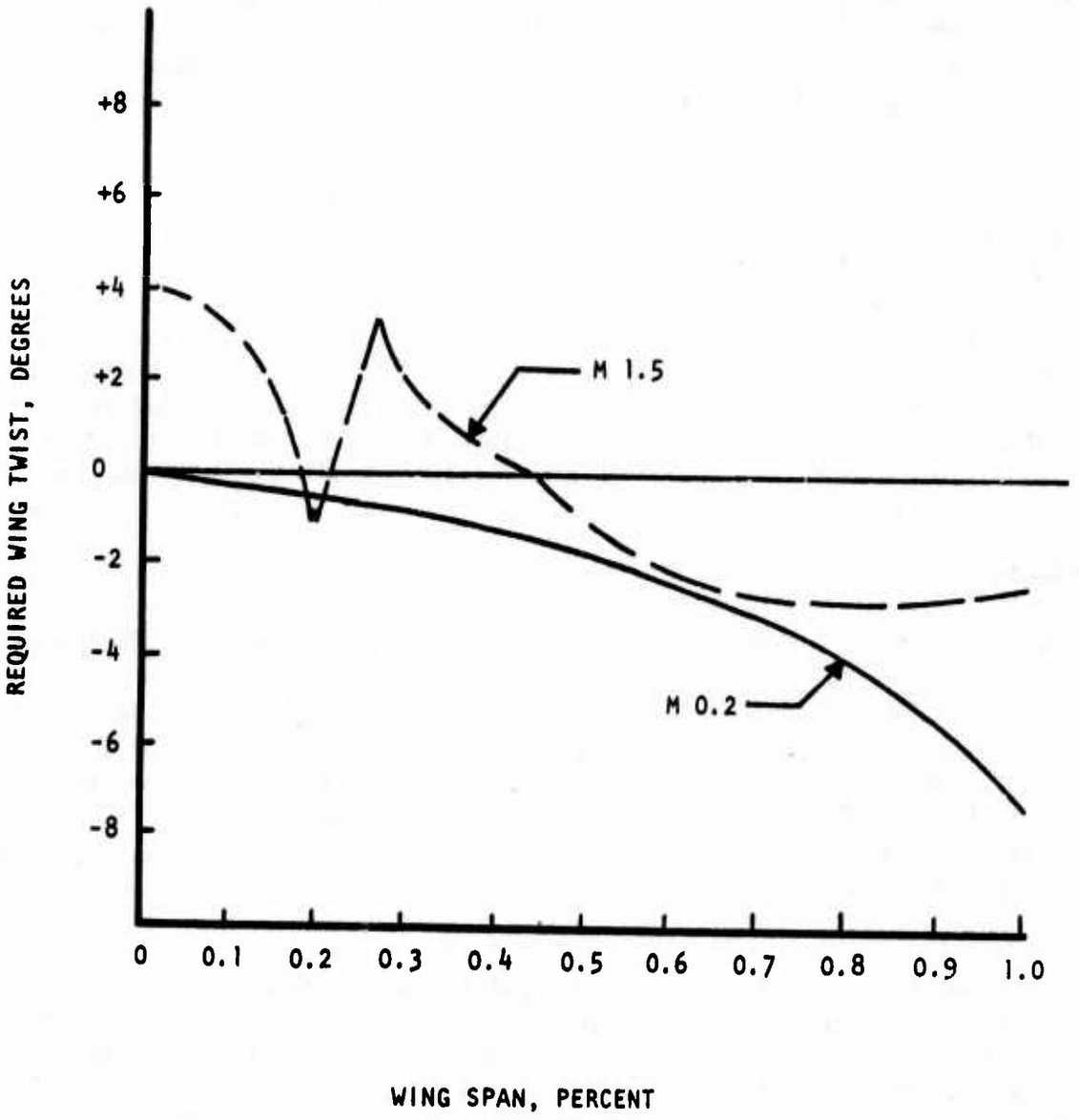

Figure 140. Aeroelastic wing twist requirements.

skins. The leading and trailing edge devices and the weapons bay doors are constructed from graphite/epoxy with full-depth honeycomb, to take advantage of the high stiffness-to-weight ratio of the material.

The engine compartment will be 6-4 titanium alloy. The fixed, primary structure will be fabricated from an external skin with an inner skin concurrently formed and diffusion bonded to it, to form integral frames and longerons. The engine doors will be superplastically formed and bonded truss core sandwich. This advanced metallic structural concept has been evaluated for similar applications, showing cost savings up to 50 percent and weight savings up to 30 percent compared to current fabrication methods.

FLUTTER ANALYSIS

The comparable metal wing versions to the composite wings were analyzed for their flutter requirements using the metal flutter optimization program, STROP. The -5 configuration, the metal version comparable to the -4A composite configuration, was optimized for flutter, and the resulting stiffness requirements are shown on Figures 142 and 143. The -5A configuration, comparable to the -4B composite configuration, was also optimized for flutter and the resulting stiffness requirements are shown on Figure 144. Nominal stiffness increases were required for both bending and torsion in the outboard wing.

STRUCTURAL SIZING

The metal vehicle (D572-5A) structural sizing and weight were derived with SWEEP. The wing torque box sizing was based on multi-spar plate skin construction. Table 33 gives the outboard wing panel applied loading, stresses, and cover sizes, while Table 34 gives similar data for the inboard wing panel. The fuselage skin gages are presented in Table 35. The last column of this figure is minimum gage required for panel flutter. If any of the upper, side, or lower skin panel gages equal the last column, it has been sized by panel flutter. The longeron sizes are presented in Table 36.

SWEEP was also used to optimize the outer wing panel construction. A comparison between full-depth honeycomb, multi-spar construction and integrally stiffened plate construction was made. As shown in Figure 145, the multi-spar design is the lowest weight. The integral stiffener design weight is the minimum obtained when SWEEP searched stringer spacings from 4 to 6 inches. The actual spar spacing selected was five intermediate spars in the two inboard bays where the wing is strength-critical and two intermediate spars in the outboard bays where flutter is critical.

Spar spacing for the wing center section was also optimized in SWEEP. As shown in Figure 146, the wing weight decreases with spar spacing. However, because of geometric constraints, the spacing was limited to a minimum 10 inches

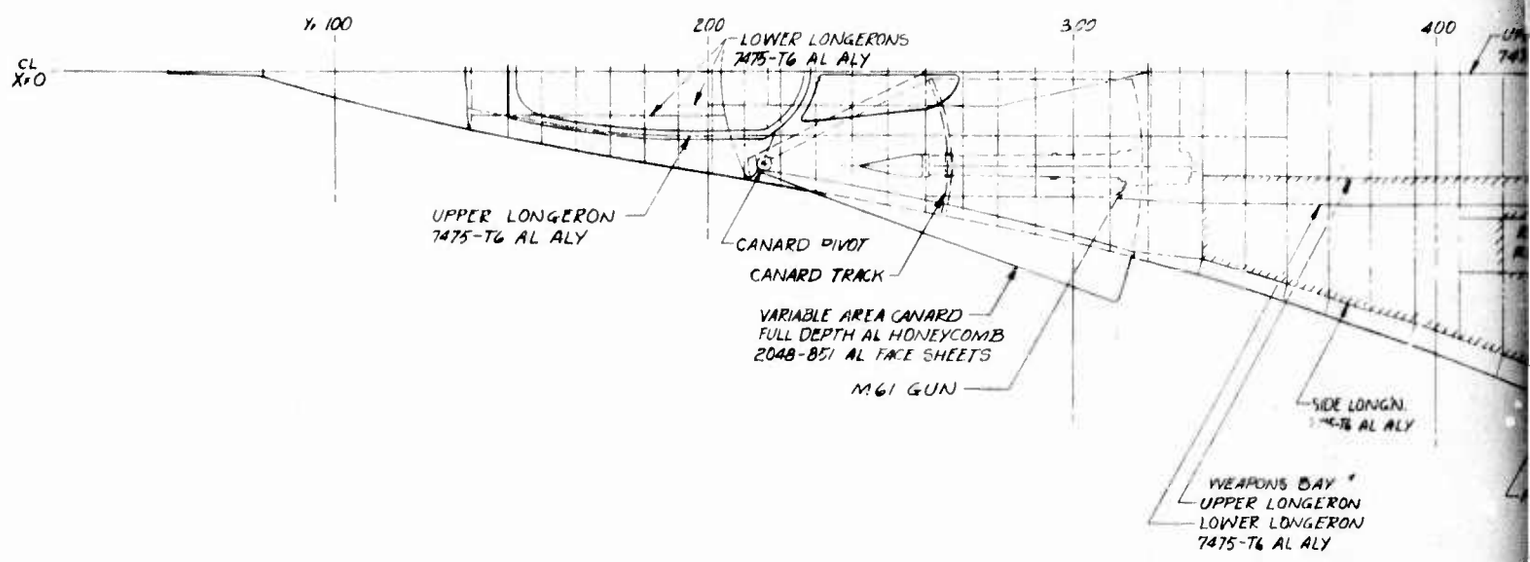
Y, 100
200
300
400
CL
X=0
LOWER LONGERONS
7475-T6 AL ALY
UPPER LONGERON
7475-T6 AL ALY
CANARD PIVOT
CANARD TRACK
VARIABLE AREA CANARD
FULL DEPTH AL HONEYCOMB
2048-851 AL FACE SHEETS
M.61 GUN
SIDE LONGN.
WEAPONS BAY
UPPER LONGERON
LOWER LONGERON
7475-T6 AL ALY

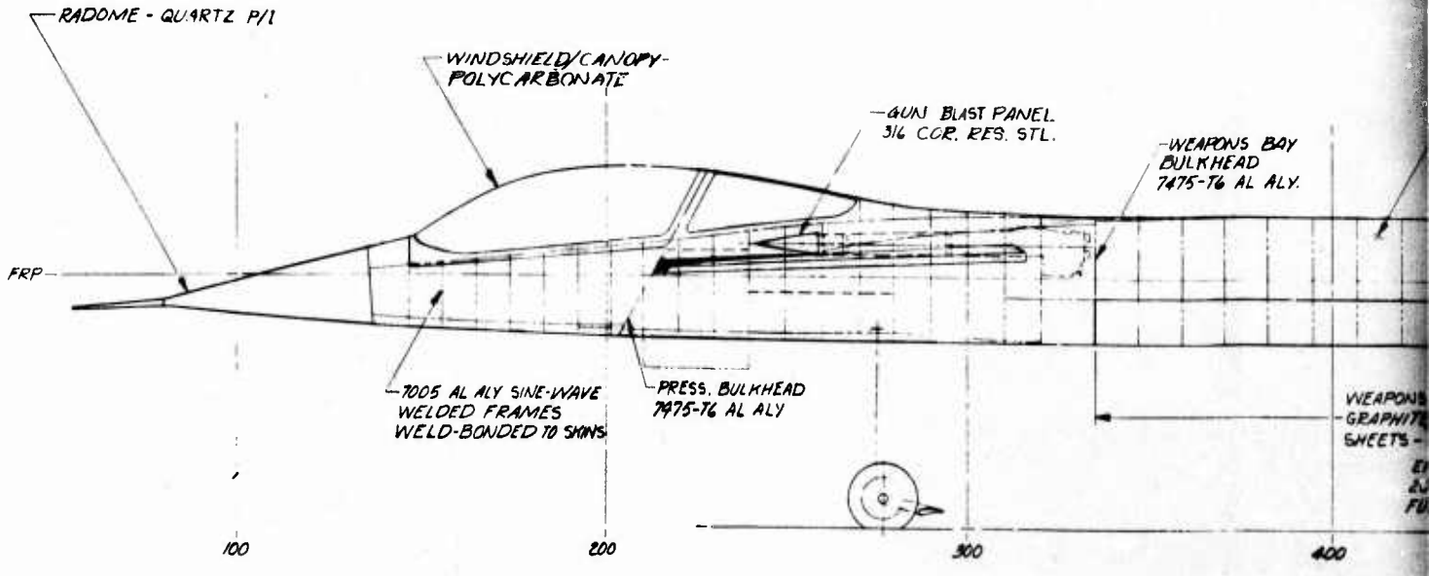
RADOME - QUARTZ P/L
WINDSHIELD/CANOPY-
POLYCARBONATE
GUN BLAST PANEL
316 CCR. RES. STL.
WEAPONS BAY
BULKHEAD
7475-T6 AL ALY.
FRP
7005 AL ALY SINE-WAVE
WELDED FRAMES
WELD-BONDED TO SKINS
PRESS. BULKHEAD
7475-T6 AL ALY
100
200
300
400

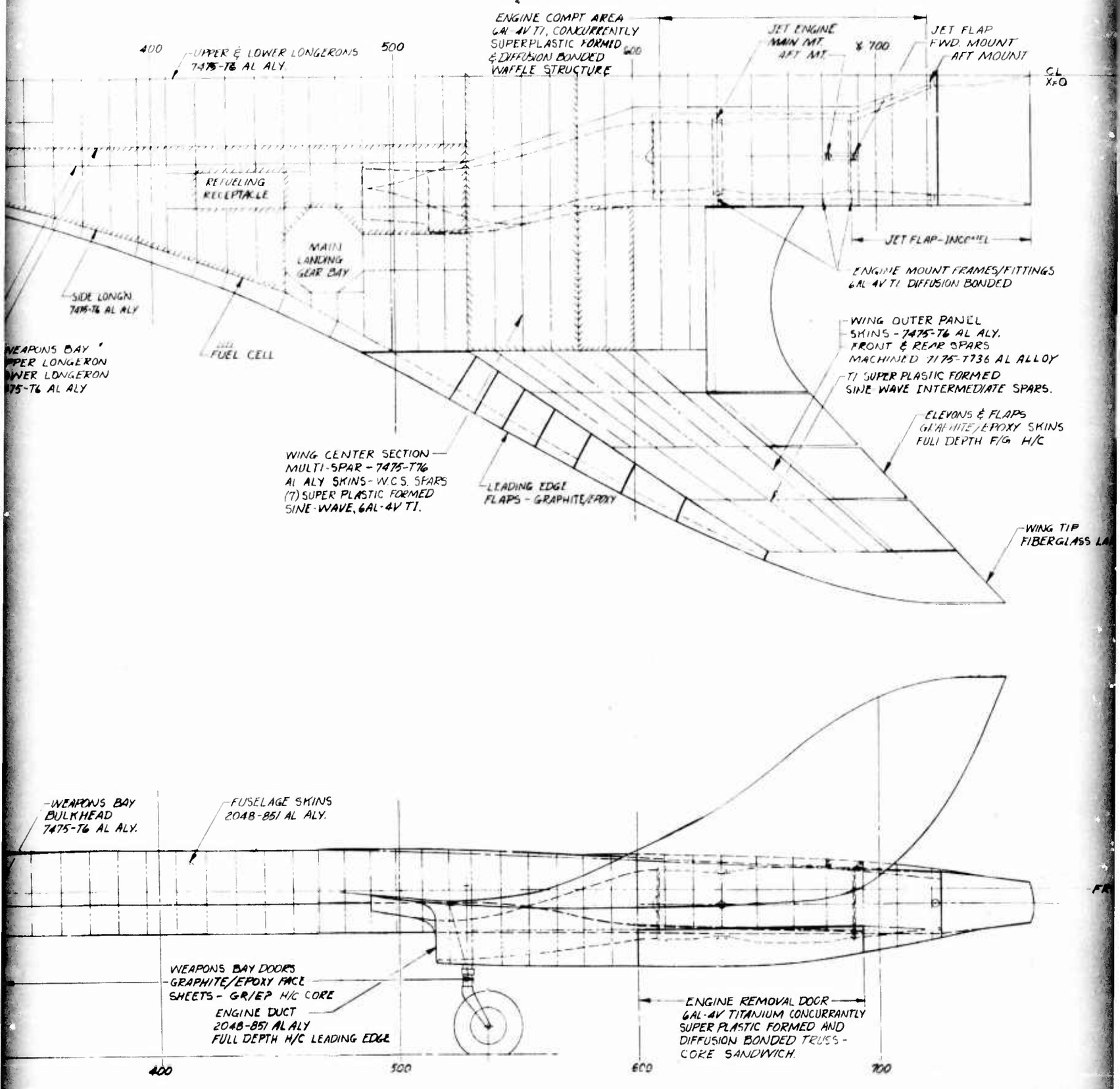
400
UPPER & LOWER LONGERONS
7475-T6 AL ALY.
500
ENGINE COMPT AREA
6AL 4V TI, CONCURRENTLY
SUPERPLASTIC FORMED
& DIFFUSION BONDED
WAFFLE STRUCTURE
600
JET ENGINE
MAIN MT.
AFT MT.
& 700
JET FLAP
FWD. MOUNT
AFT MOUNT
CL
XFO
REFUELING
RECEPTACLE
MAIN
LANDING
GEAR BAY
JET FLAP - INCONEL
ENGINE MOUNT FRAMES/FITTINGS
6AL 4V TI DIFFUSION BONDED
SIDE LONGN.
7475-T6 AL ALY
WEAPONS BAY
UPPER LONGERON
LOWER LONGERON
7475-T6 AL ALY
FUEL CELL
WING OUTER PANEL
SKINS - 7475-T6 AL ALY.
FRONT & REAR SPARS
MACHINED 7175-T736 AL ALLOY
TI SUPER PLASTIC FORMED
SINE WAVE INTERMEDIATE SPARS.
ELEVONS & FLAPS
GRAPHITE/EPOXY SKINS
FULL DEPTH F/G H/C
WING CENTER SECTION —
MULTI-SPAR - 7475-T76
AL ALY SKINS - W.C.S. SPARS
(7) SUPER PLASTIC FORMED
SINE-WAVE, 6AL-4V TI.
LEADING EDGE
FLAPS - GRAPHITE/EPOXY
WING TIP
FIBERGLASS LA

WEAPONS BAY
BULKHEAD
7475-T6 AL ALY.
FUSELAGE SKINS
2048-851 AL ALY.
WEAPONS BAY DOORS
GRAPHITE/EPOXY FACE
SHEETS - GR/EP H/C CORE
ENGINE DUCT
2048-851 AL ALY
FULL DEPTH H/C LEADING EDGE
ENGINE REMOVAL DOOR
6AL-4V TITANIUM CONCURRANTLY
SUPER PLASTIC FORMED AND
DIFFUSION BONDED TRUSS-
CORE SANDWICH.
400
500
600
700

2

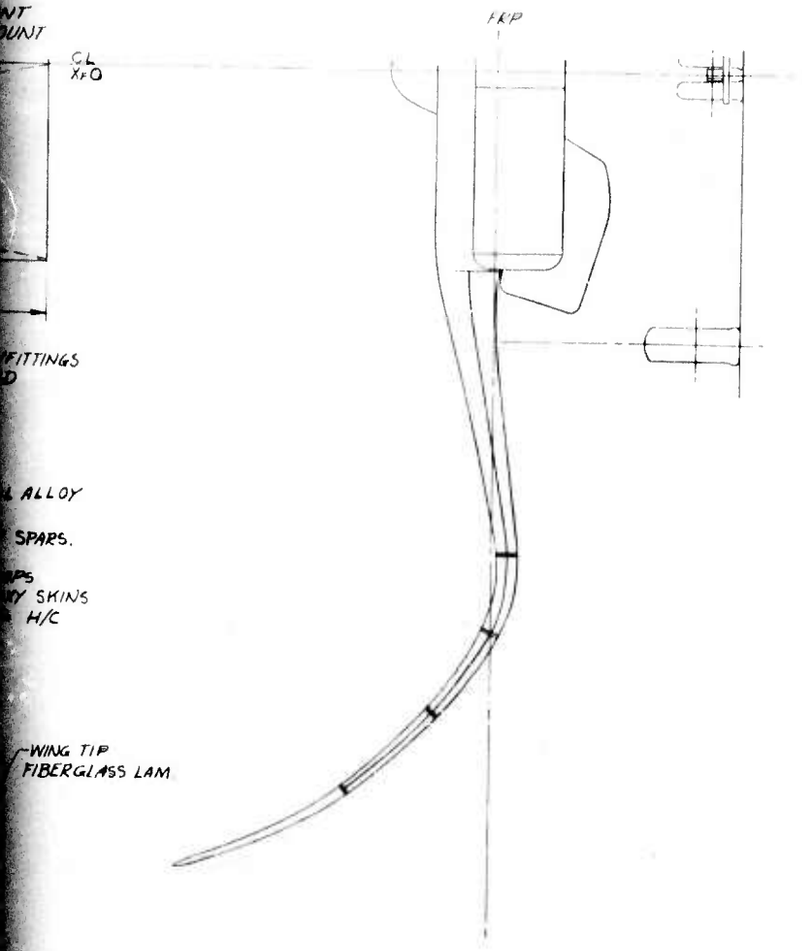

3. CONTROL SURFACES - FULL DEPTH HONEYCOMB - GRAPHITE/EPOXY SKINS, F/G CORE.
2. WING - MULTI-SPAR CONSTRUCTION - AL ALY 7475-T6 SKINS, 6AL-4V TI SPARS INBD & AL ALY & TI SPARS OUTBD. WING BOX.
1. FUSELAGE - LONGERONS FRAMES & SKIN CONSTRUCTION - AL ALY, 2048-851 SKINS, 7005 FRAMES & 7475 LONGNS.

NOTES: UNLESS OTHERWISE NOTED

Figure 141. Structural arrangement - all-metal baseline.

3

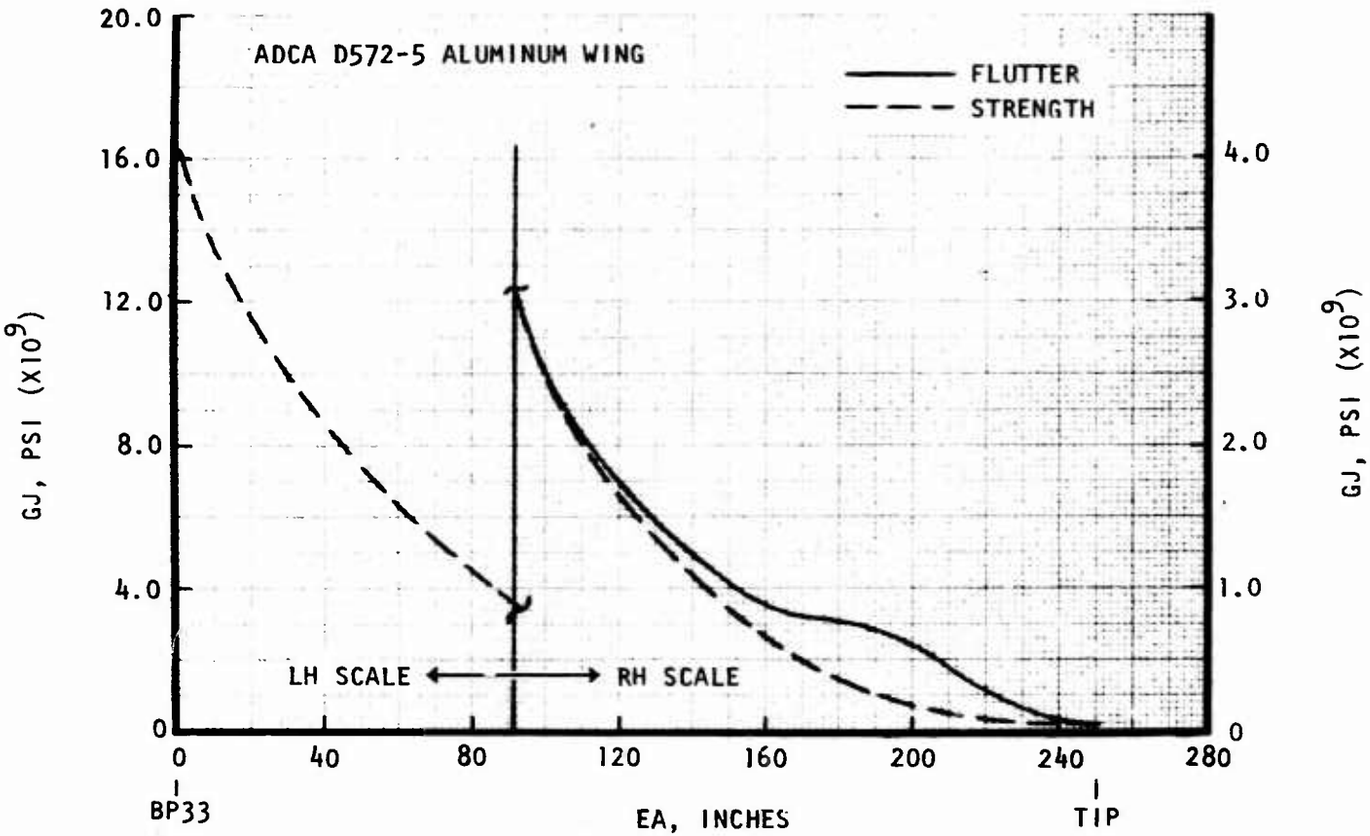

Figure 142. Required torsional stiffness, D472-5.

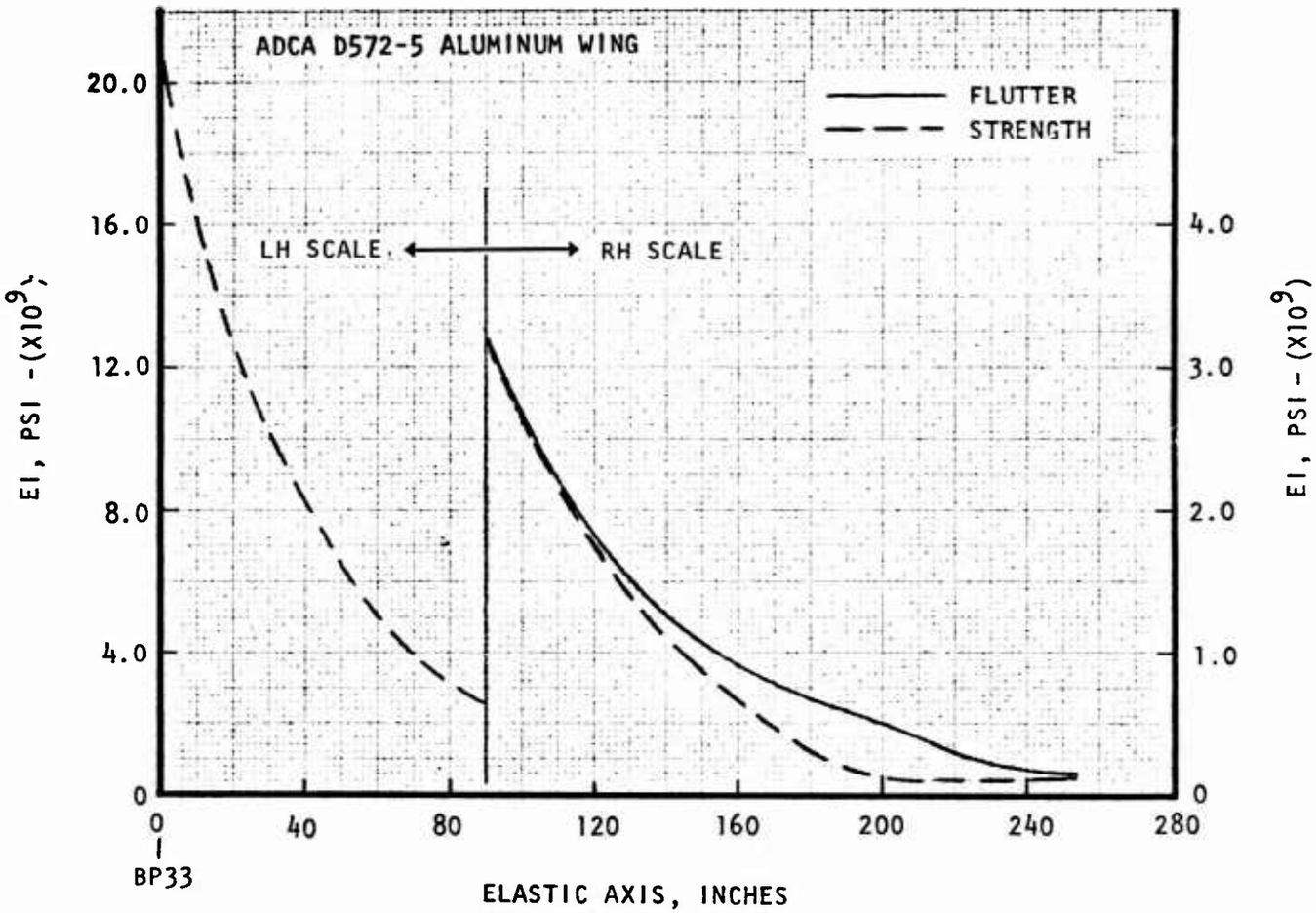

Figure 143. Required bending stiffness, D472-5.

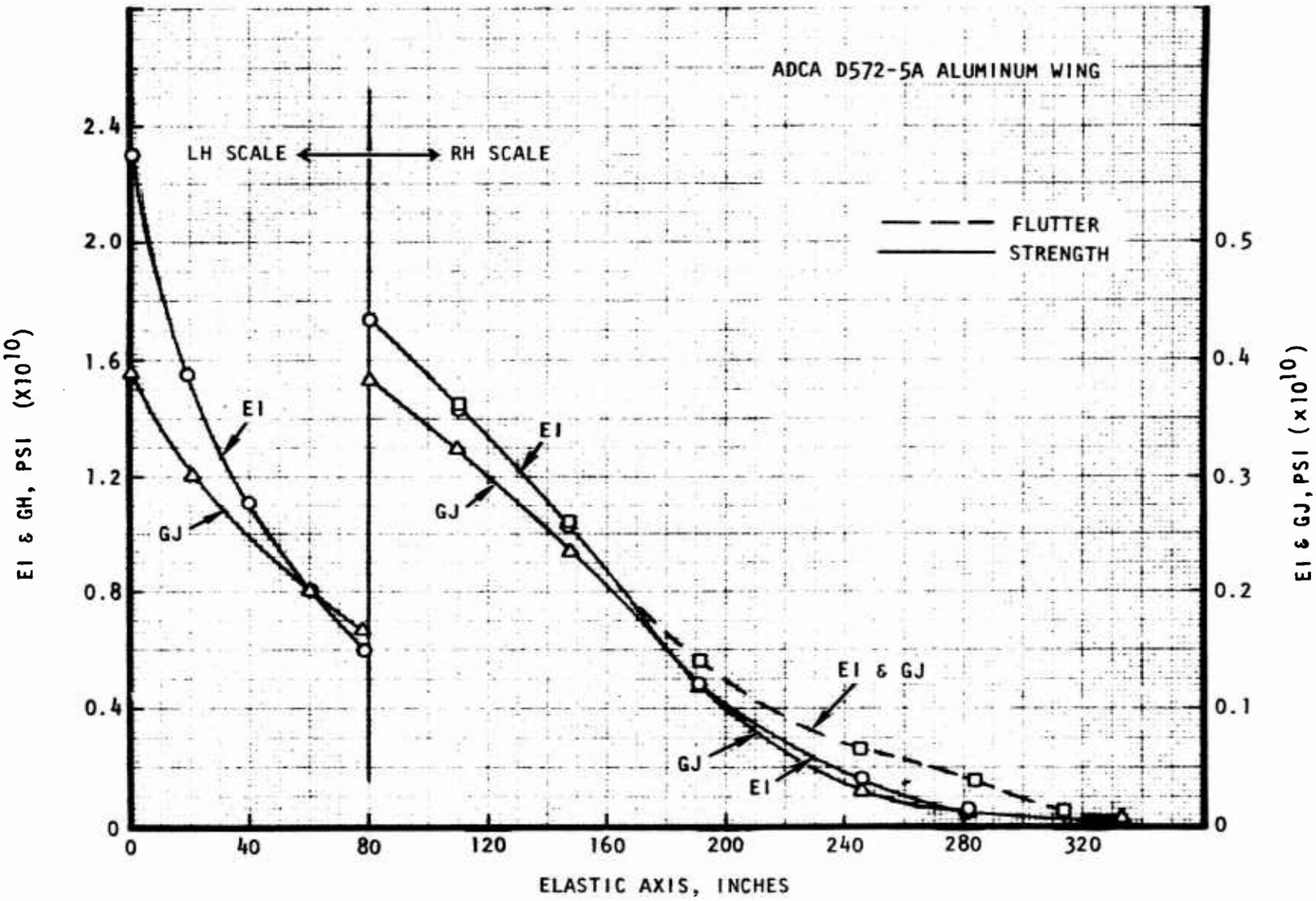

Figure 144. Required bending and torsion stiffness, D472-5.

TABLE 33. D572-5A OUTBOARD WING SIZING

BUTTOCK PLANE	-**-SECTION DATA - +NX	-NX	STIFF. REQMTS. FCU	FCL	- ST. REQMTS. FTU	FTL	BSTR	NOS
110.00	13.06	4.45	33.14	16.13	11.62	48.68	13.073	2.0
127.27	16.06	5.68	40.66	17.74	14.29	53.63	12.208	2.0
148.48	17.63	6.08	44.82	17.70	15.79	53.63	11.146	2.0
169.69	12.81	4.37	39.35	17.63	13.91	53.63	9.838	2.0
190.90	6.45	2.20	23.05	8.33	8.19	25.47	8.275	2.0
199.87	2.66	0.91	12.05	4.32	4.31	13.27	7.208	2.0
208.83	1.60	0.55	12.12	6.31	4.72	19.51	6.143	2.0

BUTTOCK PLANE	TSKU	TSKL	T-U	T-L	TSTR
110.00	0.391	0.273	0.394	0.276	0.040
127.27	0.406	0.316	0.410	0.320	0.040
148.48	0.394	0.339	0.398	0.343	0.040
169.69	0.353	0.268	0.326	0.248	0.040
190.90	0.275	0.275	0.280	0.264	0.040
199.87	0.215	0.215	0.221	0.210	0.040
208.83	0.116	0.080	0.122	0.087	0.040

NX=KIPS, FC,FT=KSI-**-

TABLE 34. D572-5A INBOARD WING SIZING

BUTTOCK PLANE	-**-SECTION DATA - ST. REQMTS. +NX	-NX	FCU	FCL	FTU	FTL	BSTR	NOS
33.00	16.17	5.51	47.59	17.65	16.81	53.63	9.000	3.9
52.20	14.70	5.01	45.17	17.66	15.94	53.63	9.000	4.5
71.65	13.09	4.46	42.07	17.67	14.84	53.63	9.000	5.1
90.82	11.57	3.94	38.83	17.68	13.69	53.63	9.000	5.7
110.00	10.39	3.54	36.17	17.54	12.75	53.19	9.000	6.3

BUTTOCK PLANE	TSKU	TSKL	T-U	T-L	TSTR
33.00	0.334	0.306	0.340	0.312	0.040
52.20	0.319	0.278	0.326	0.284	0.040
71.65	0.305	0.246	0.311	0.253	0.040
90.82	0.292	0.217	0.298	0.223	0.040
110.00	0.281	0.196	0.287	0.202	0.040

NX=KIPS, FC,FT=KSI-**-

TABLE 35. D572-5A FUSELAGE SKIN GAGES

STATION	FRAME SPACING	BASIC THICKNESS UPPER	SIDE	LOWER	LAND REQUIREMENTS UPPER	SIDE	LOWER	BASIC FLUTTER
138.0	8.00	0.0346	0.0346	0.0346	0.0500	0.0500	0.0500	0.0346
184.0	8.00	0.0366	0.0366	0.0366	0.0500	0.0500	0.0500	0.0366
214.0	8.00	0.0371	0.0371	0.0371	0.0500	0.0500	0.0500	0.0371
218.0	8.00	0.0372	0.0372	0.0372	0.0500	0.0500	0.0500	0.0372
274.0	8.00	0.0379	0.0379	0.0379	0.0500	0.0500	0.0500	0.0379
278.0	8.00	0.0379	0.0379	0.0379	0.0500	0.0500	0.0500	0.0379
335.0	8.00	0.0383	0.0383	0.0383	0.0500	0.0500	0.0500	0.0383
395.0	8.00	0.0383	0.0383	0.0383	0.0500	0.0500	0.0500	0.0383
455.0	8.00	0.0383	0.0383	0.0383	0.0500	0.0500	0.0500	0.0383
514.0	8.00	0.0383	0.0534	0.0383	0.0500	0.0698	0.0500	0.0383
516.0	8.00	0.0398	0.0481	0.0398	0.0500	0.0624	0.0500	0.0398
528.0	8.00	0.0347	0.0559	0.0347	0.0500	0.0681	0.0500	0.0347
532.0	8.00	0.0397	0.0409	0.0397	0.0500	0.0500	0.0500	0.0397
573.0	8.00	0.0397	0.0397	0.0397	0.0500	0.0500	0.0500	0.0397
577.0	8.00	0.0397	0.0451	0.0397	0.0500	0.0528	0.0500	0.0397
606.5	8.00	0.0396	0.0471	0.0396	0.0537	0.0564	0.0500	0.0396
640.0	8.00	0.0384	0.0384	0.0384	0.0500	0.0500	0.0500	0.0384
741.0	8.00	0.0368	0.0368	0.0368	0.0500	0.0500	0.0500	0.0368
743.0	8.00	0.0371	0.0371	0.0371	0.0500	0.0500	0.0500	0.0371

TABLE 36. D572-5A FUSELAGE LONGERON AREAS

STATION	LONG./STRING. DEPTH/SPACE	NUMBER	AREA - LONGERON/STRINGER UPPER	LOWER	LONG STIFF	AREA - LONG C/O UPPER	LOWER
138.0	0.70	4.0	0.145	0.145	0.145	0.145	0.0
184.0	0.70	4.0	0.145	0.145	0.145	0.145	0.0
214.0	0.70	4.0	0.145	0.145	0.145	0.145	0.0
218.0	0.70	4.0	0.145	0.145	0.145	0.145	0.0
274.0	0.90	4.0	0.145	0.155	0.145	0.145	0.0
278.0	0.90	4.0	0.145	0.158	0.145	0.0	0.145
335.0	0.90	4.0	0.145	0.379	0.145	0.0	0.145
395.0	0.90	4.0	0.324	0.937	0.145	0.0	0.145
455.0	0.90	4.0	0.679	2.089	0.145	0.0	0.145
514.0	0.90	4.0	2.822	4.271	0.145	0.0	0.145
516.0	0.72	4.0	1.660	4.503	0.145	0.0	0.145
528.0	0.71	4.0	1.967	5.320	0.145	0.0	0.145
532.0	0.71	4.0	1.985	5.369	0.145	0.0	0.145
573.0	0.69	4.0	1.537	4.174	0.145	0.0	0.145
577.0	0.69	4.0	1.479	4.018	0.145	0.0	0.145
608.5	0.62	4.0	1.240	3.381	0.145	0.0	0.145
690.0	0.78	4.0	0.145	0.378	0.145	0.0	0.145
741.0	0.90	4.0	0.145	0.145	0.145	0.0	0.145
743.0	0.90	4.0	0.145	0.145	0.145	0.0	0.145

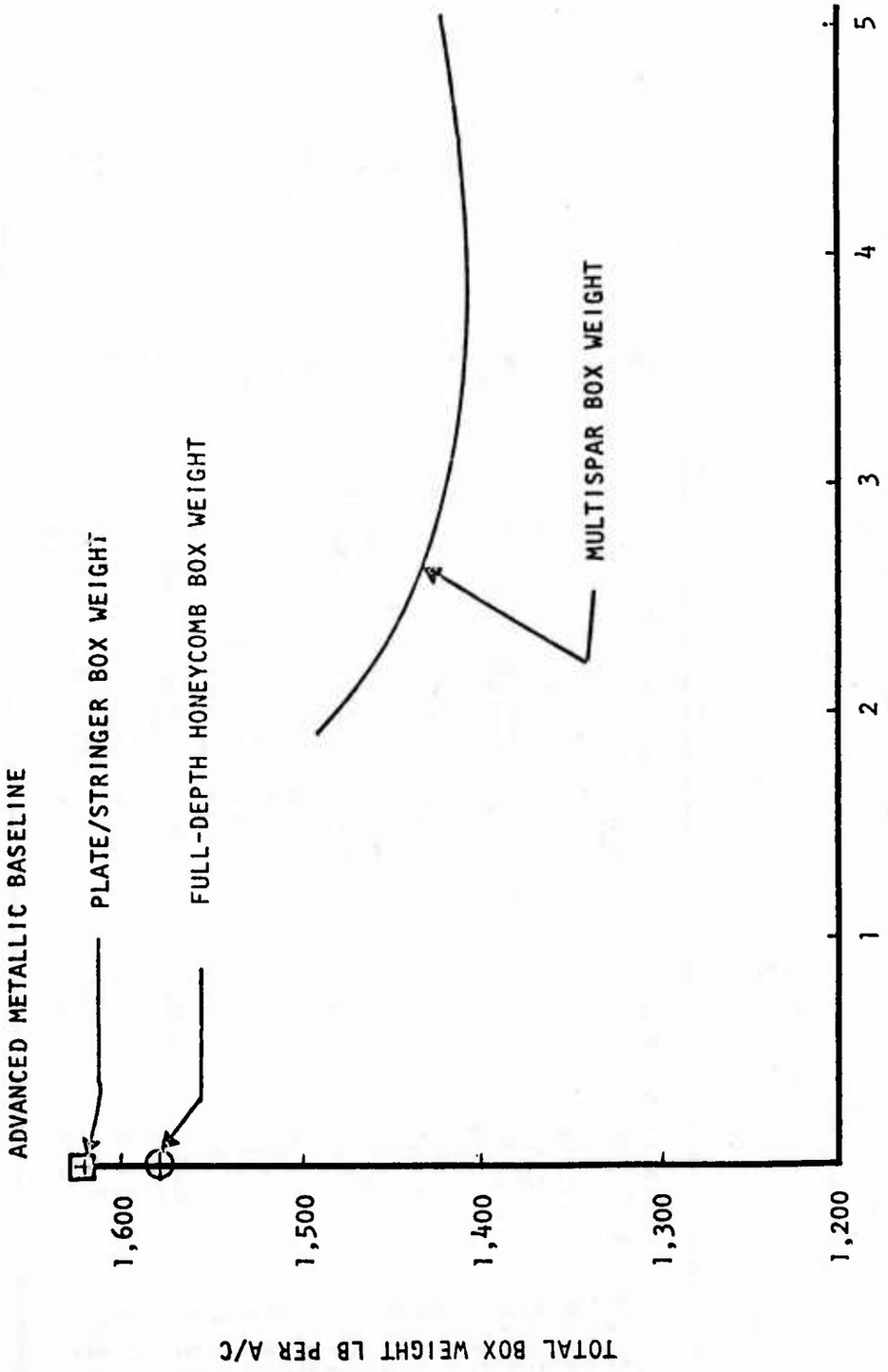

Figure 145. Outer wing panel trade study.

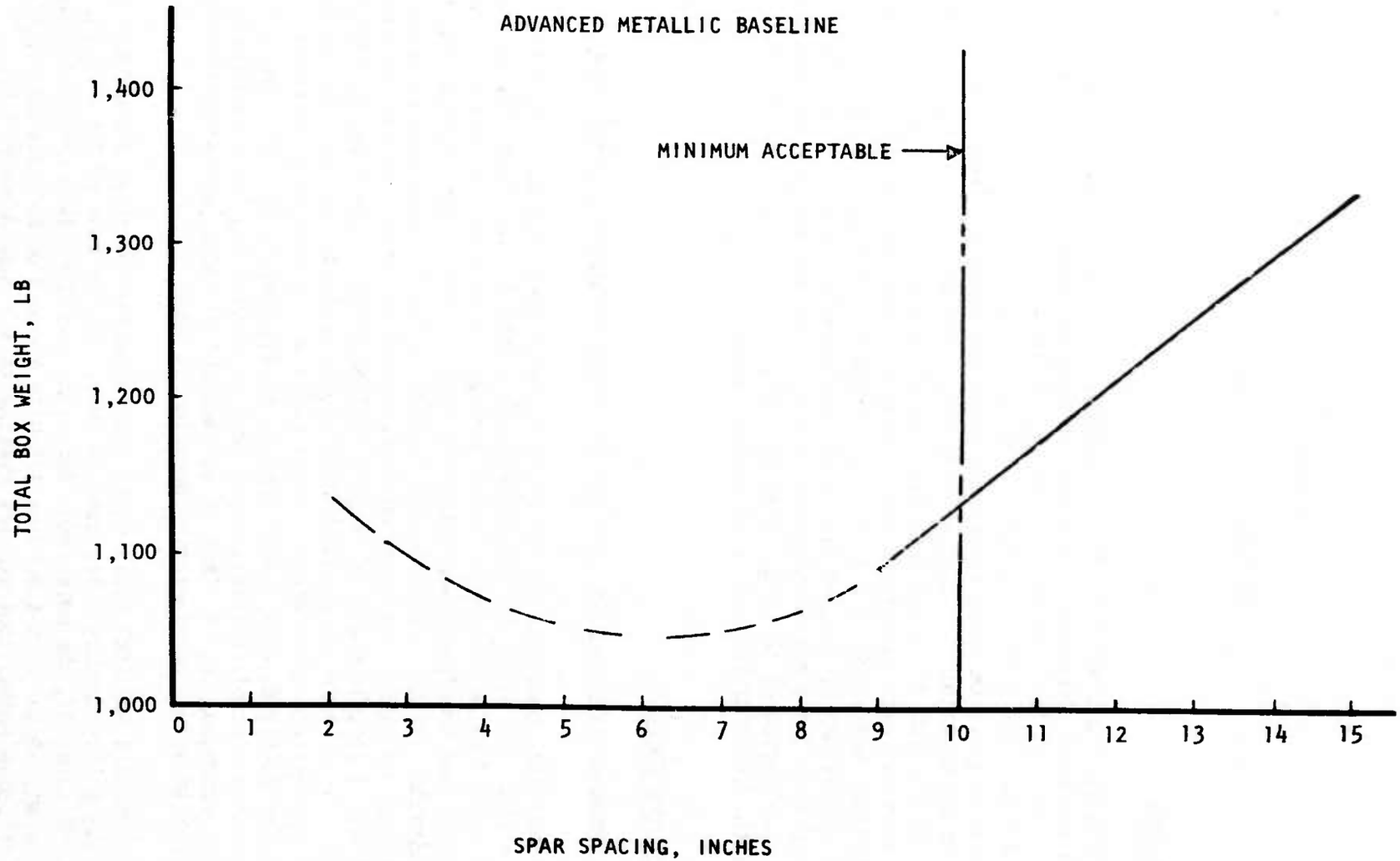

Figure 146. Wing center section trade study.

Section V

MANUFACTURING STUDIES

INTRODUCTION

Manufacturing studies in this reporting period were primarily concerned with the advanced composites structures components identified as baseline (refer to Section IV). These concepts were evolved by a close design/manufacturing interface and reflect aggressive materials and process approaches. Widespread use of graphite fiber reinforced honeycomb core is planned; polyimide and pultruded materials are used. Processing features entertained include co-cure fabrication of larger and more complex integrated substructure/cover modules than hitherto attempted, use of trapped elastromer as pressure application medium, wet processing of holes, automated trimming, and tape laying of multi-ply blanks by machine for subsequent pattern cutout. The risk associated with the proposed measures is considered low for the assumed production time period of the ADCA (1980 to 1985) since in each case feasibility proof of the basic technology is already on hand.

MANUFACTURING CONCEPTS

FORWARD, FORWARD INTERMEDIATE, AND AFT INTERMEDIATE FUSELAGE STRUCTURES

The baseline configuration of these structures is typically depicted in Figure 133. The lower skins are honeycomb sandwich structures, employing graphite/epoxy (Gr/Ep) facings. These facings, as well as the bulkheads and upper skins, are developed from automatic tape-laid or vendor purchased multiply broadgoods. In the manufacturing concept presently considered optimum and costed as baseline, the upper and lower sandwich skins, sandwich bulkheads, and pultrusion longerons are fabricated independently. Substructure members are bonded to the lower skins and bonded and/or mechanically fastened to each other by appropriate tie members. Upper skins are mechanically fastened. Patterns for facing details - this applies to all components - will be cut by electronically controlled laser, water jet, or oscillating knife machinery, the choice depending on the state of development of these automated methods at the time an actual manufacturing decision is made.

An alternate approach still under consideration for these structures is employment of large module integrated co-cure. In the case of the forward fuselage, Figure 147, the bulkheads, longeron, and lower skin details would be laid up and co-cured in a bonding jig with the aid of an inflatable rubber bag and silicone rubber tool members similar to the ones developed for Rockwell/LADD's Vertical Stabilizer Program. (See Figure 148.) If detail

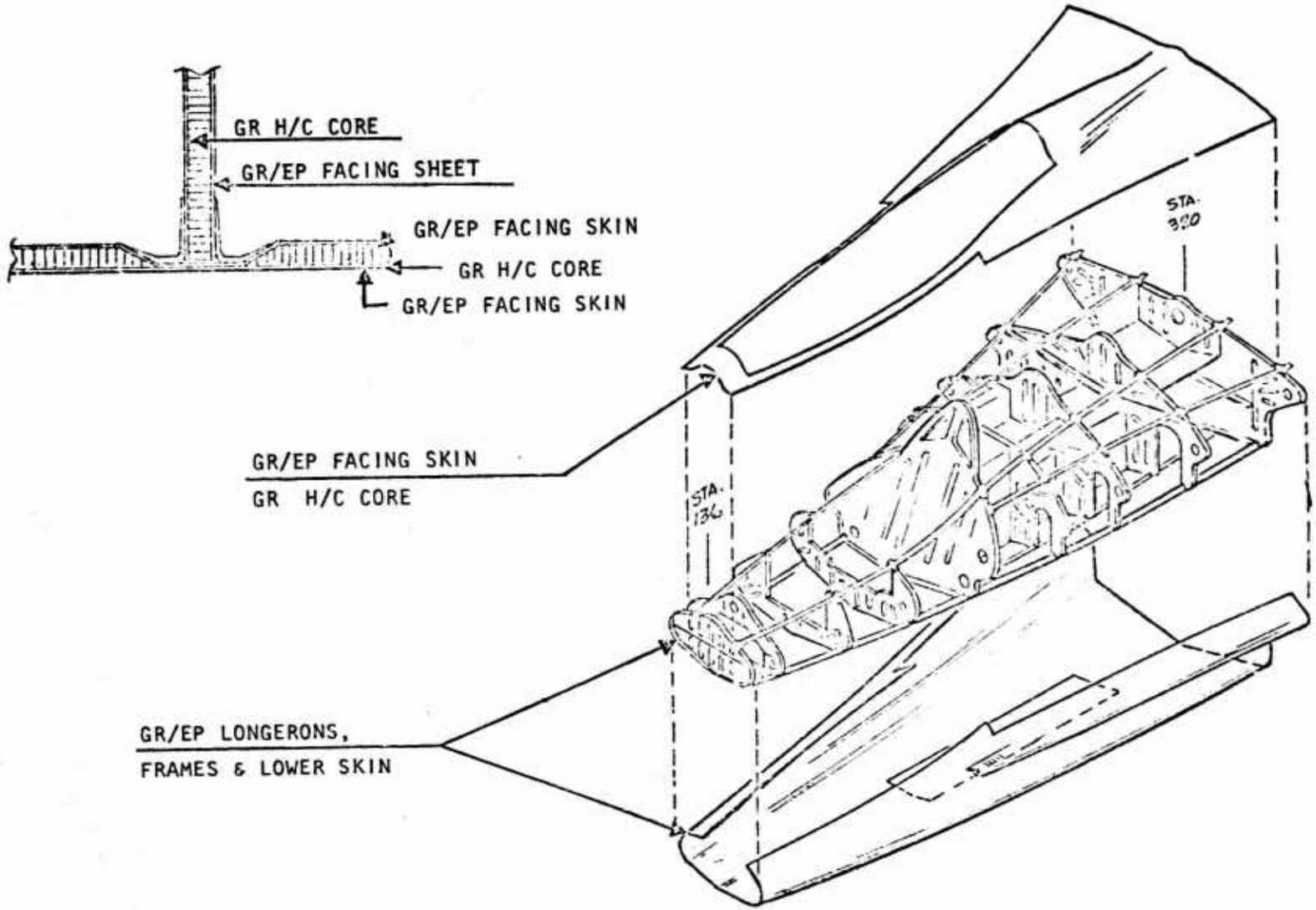

Figure 147. ADCA-forward fuselage structure.

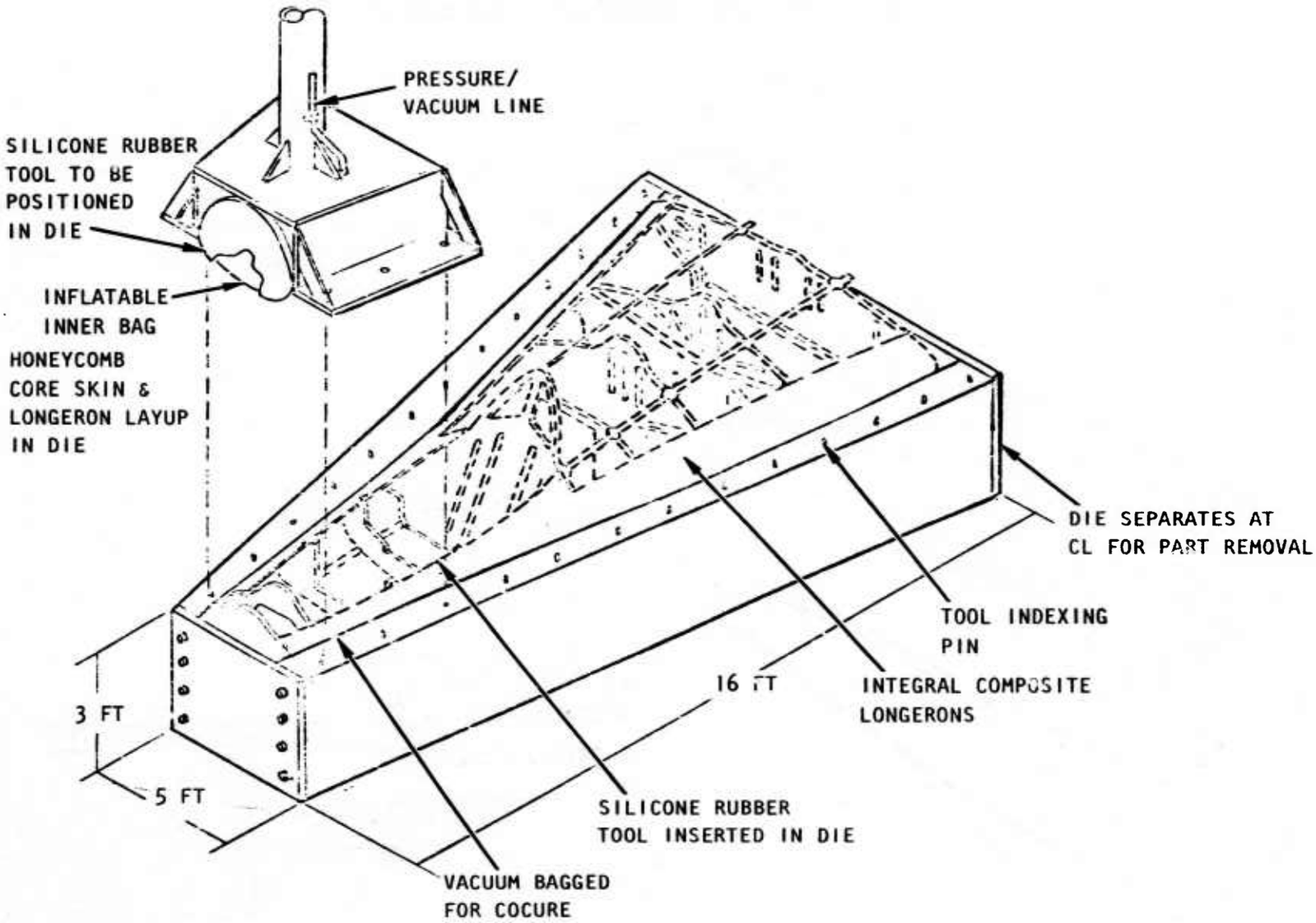

Figure 148. ADCA forward fuselage integral (alternate) fabrication concept.

design considerations should indicate that tighter dimensional control of the substructure member depth is required than possible with the approach discussed, ceramic tool inserts will be provided to control this parameter as well as contour.

WING CARRY-THROUGH CENTER SECTION

The clean baseline design of this wet cell structure, figure 123, maintains uniform thickness in the major structural cover and spar web members, thus suggesting the manufacturing approach depicted in Figure 149. The honeycomb core covers and spar webs are fabricated by conventional co-cure procedures, with facings developed from multi-ply blanks. Several spar webs may be cured in a simultaneous operation with a common caul. Closeout fill is provided by placement of core filling compound or foaming tape into proper core locations in layup. After trimming to size, spar webs and prefabricated attach angles and clips are bonded to each other and the lower cover. The upper cover and lower cover/substructure subassembly are fitted up and hole locations matching the spar attach insert patterns of the upper cover established. The upper edge core fill of the substructure members is provided with inserts matching these patterns. After application of sealing compound to interior surfaces, the upper cover is attached to the lower cover substructure subassembly by mechanical fasteners. Conventional groove sealing is employed for peripheral sealing.

The manufacturing concept envisioned for the hat stringer stiffened cover/multi-rib design considered in the trade studies, Figure 127, employs an ambitious approach in which all of the major curing and bonding operations are carried out simultaneously. As shown in the sketch of Figure 148 and the manufacturing sequence for this concept (Figure 150 thru 153), all of the lower cover skin, hat section stiffeners, and ribs are laid up on collapsible or retractable tooling members. After assembly of these members and placement of a release film at the upper cover faying surfaces, the upper cover details are added to the layup. Teflon plug inserts which can later be withdrawn are provided at prepunched (wet processed) hole locations. Caul sheets are added, defining the outer mold line of the upper cover. The total assembly is secured and cured in fixturing designed to limit pressure exerted by the expanding rubber tooling to a controlled maximum. Air bags or sets of springs or hydraulic cylinders may be used for this purpose.

Final assembly operations for this wing carry-through concept are similar to that discussed for the baseline one; i.e., fitup, insert installation into substructure webs, application of sealing compound to interior surfaces, attachment of upper cover by mechanical fasteners, and peripheral groove sealing.

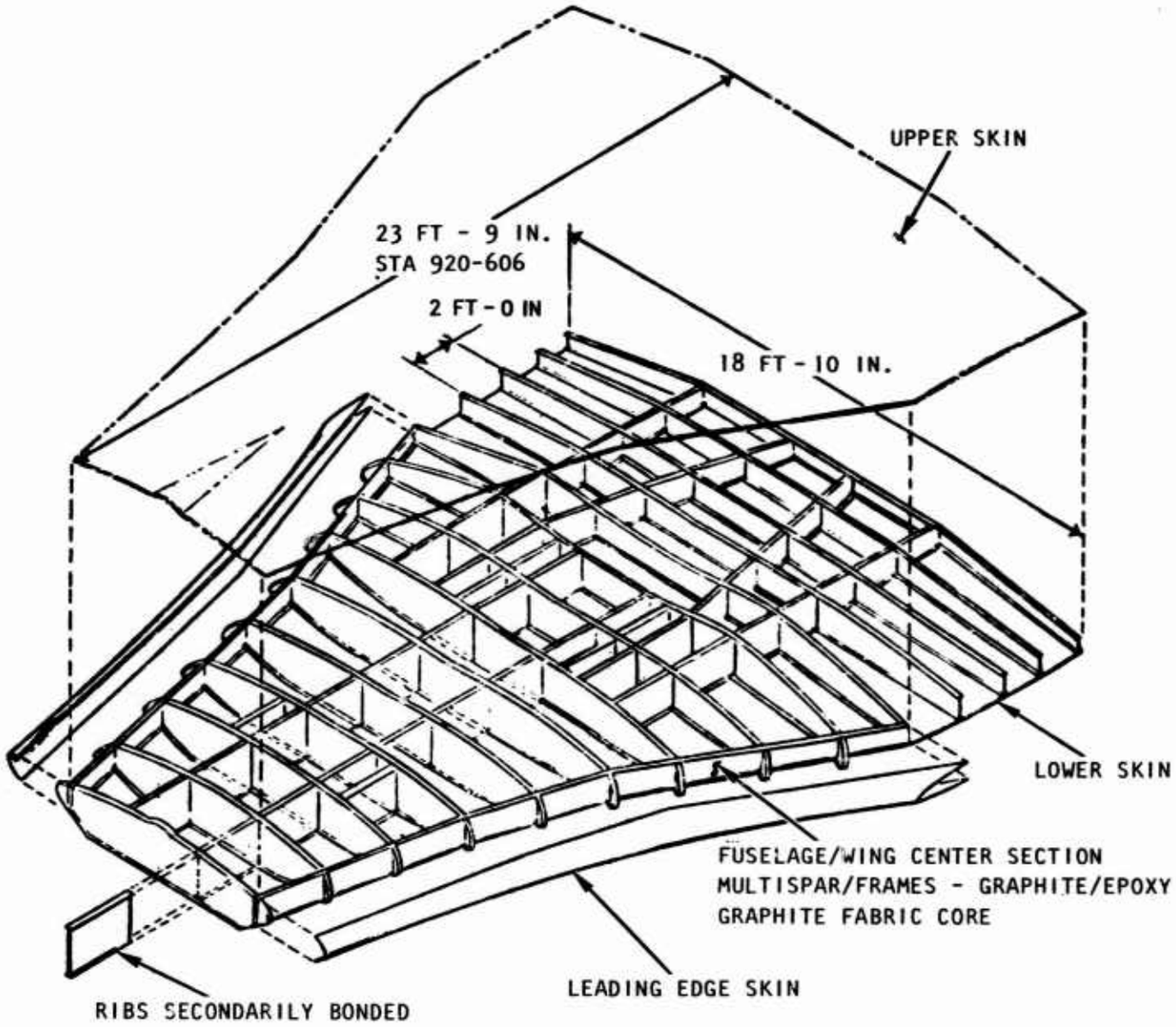

Figure 149. Integrally cured fuselage-wing center section.

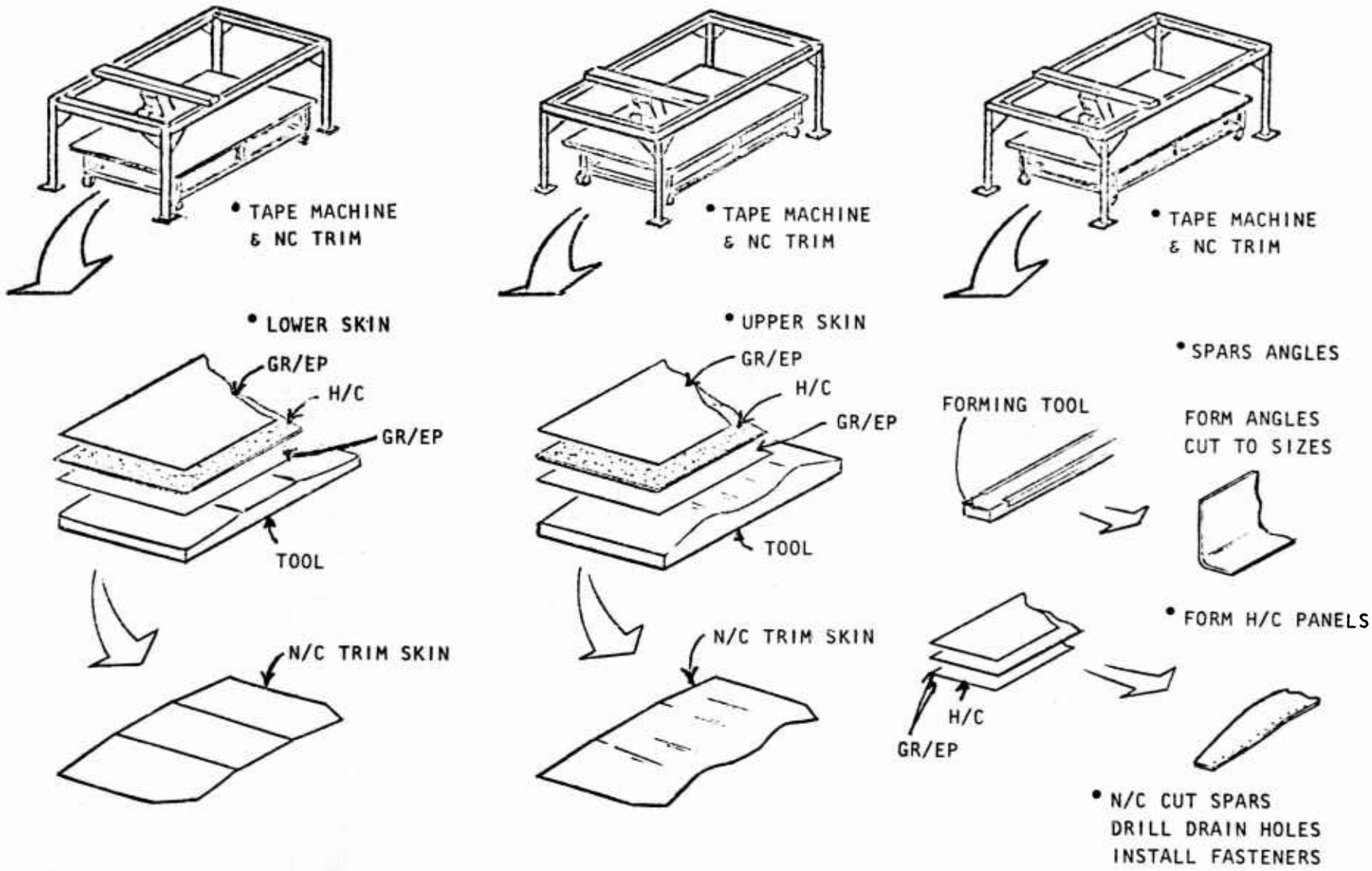

Figure 150. Manufacturing concept, major subcomponents wing carry-through structure baseline design.

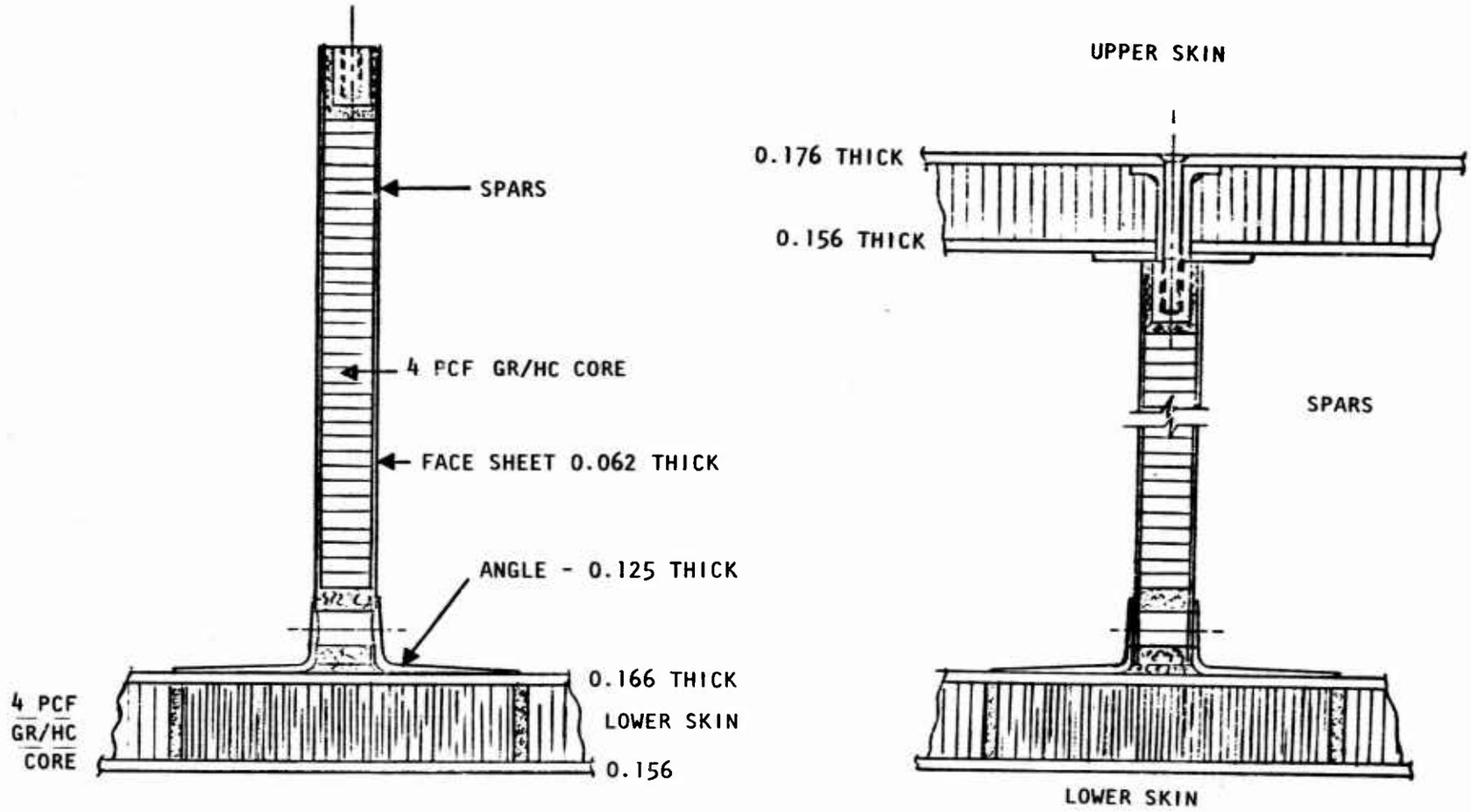

Figure 151. Upper cover assembly wing carry-through structure baseline design.

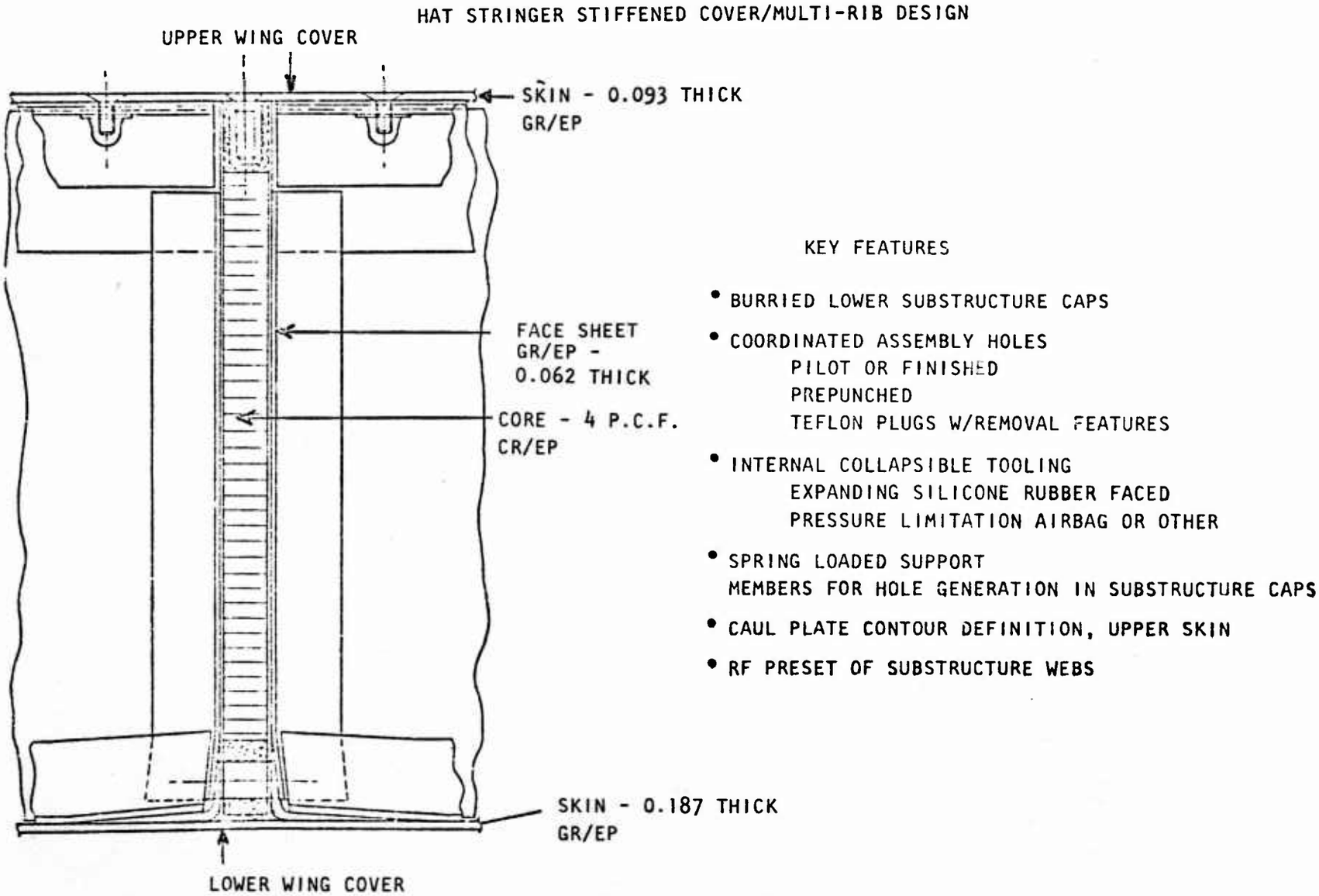

Figure 152. Rib/cover manufacturing detail wing carry-through structure.

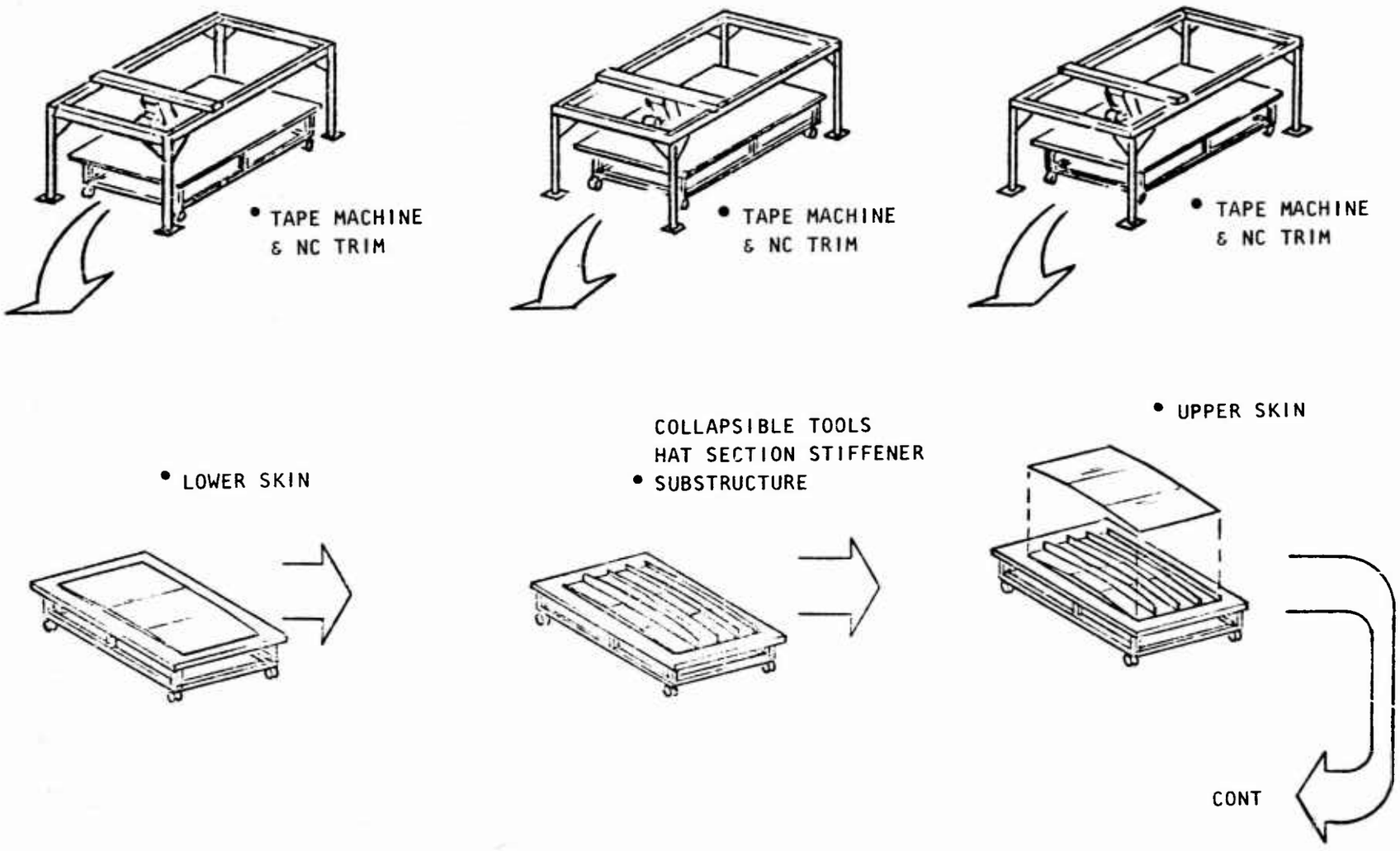

Figure 153. Manufacturing concept wing carry-through structure.

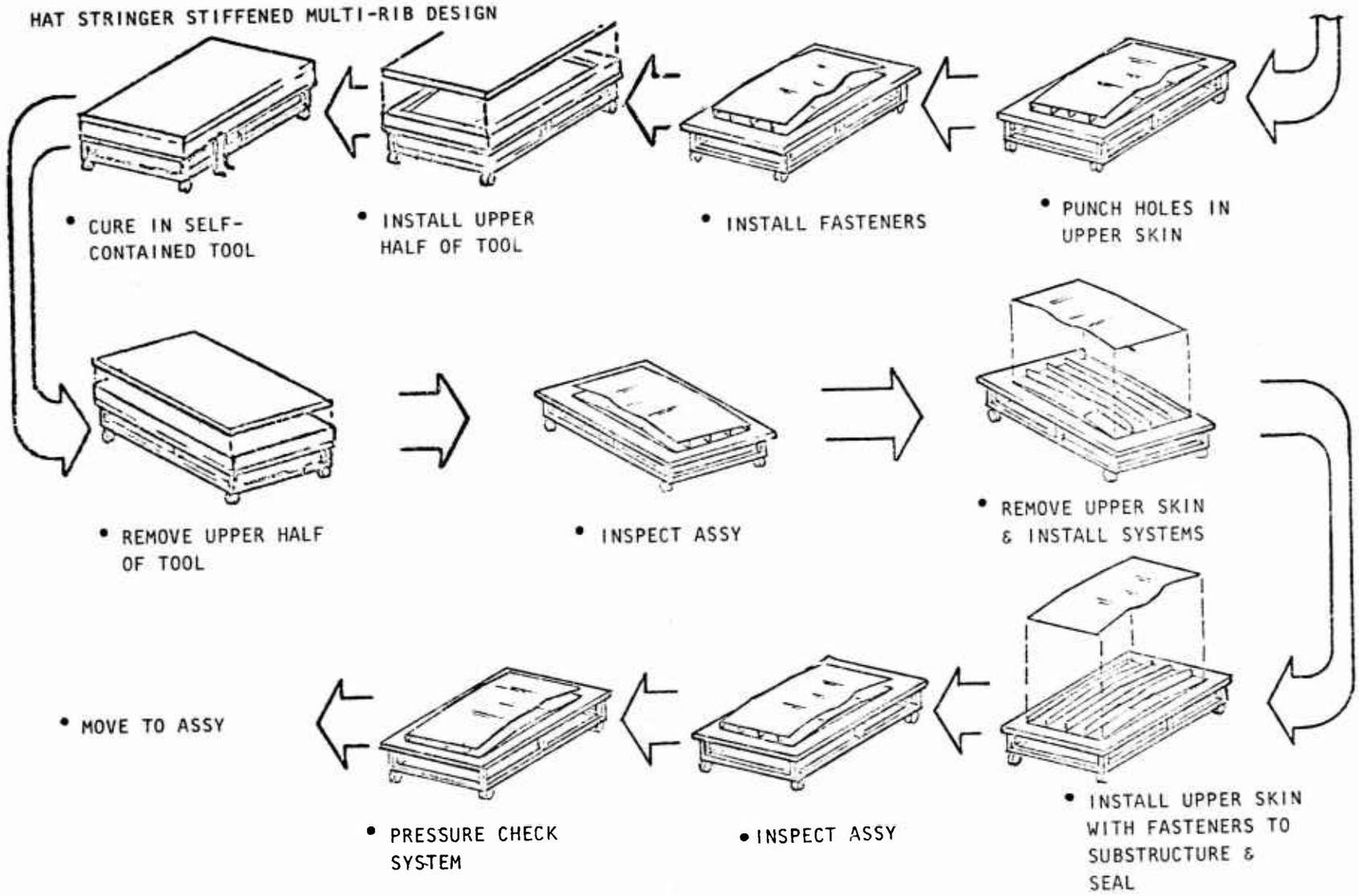

Figure 153. Manufacturing concept wing carry-through structure (concl).

OUTBOARD WING STRUCTURES

The major portion of these structures is conceived as full-depth honeycomb core sandwich with composite facings, Figures 119 and 154. Since it is questionable that single-cycle co-cure will permit adequate mold line definition of both upper and lower air passage surfaces, a modified co-cure approach is proposed for components requiring accurate control of both mold contours. As shown schematically in Figure 154, upper and lower surfaces are individually co-cured in female tools to thickness-wise oversize honeycomb core blankets. The honeycomb core members are machined to matching flat planes and the sections mated with an interposed adhesive system. Space for flanges of closeout structure had been provided by withdrawable Teflon dummy inserts. Caps of the separately fabricated closeout members are faced with sanding plies permitting adjustment to match mating details.

ENGINE NACELLE STRUCTURES

Due to temperature requirements, Gr/PI is the principal baseline material of construction for this component. It is anticipated that process technology for both condensation and addition type PI's will have progressed sufficiently by 1980 to permit reliable and reproducible fabrication of Gr/PI components by techniques essentially identical to those for Gr/Ep. The envisioned fabrication concept for engine nacelle structures, Figure 155, contemplates integral fabrication of the longerons with the bulkhead members and mechanical fastener attachment of the doors.

WEAPONS BAY STRUCTURE

Fabrication of this structure (Figure 156) follows the same principle as the propulsion module. Side and center longerons and bulkheads are integrally fabricated and assembled. Gr/Ep is the planned material candidate.

FINAL ASSEMBLY

Final assembly of the ADCA aircraft is presently visualized as schematically depicted in Figure 157.

COST ANALYSIS SUPPORTING DATA

Manufacturing cost projections for ADCA composite and metal baseline structures considered in the trade studies of Section IV are presented in Table 37.

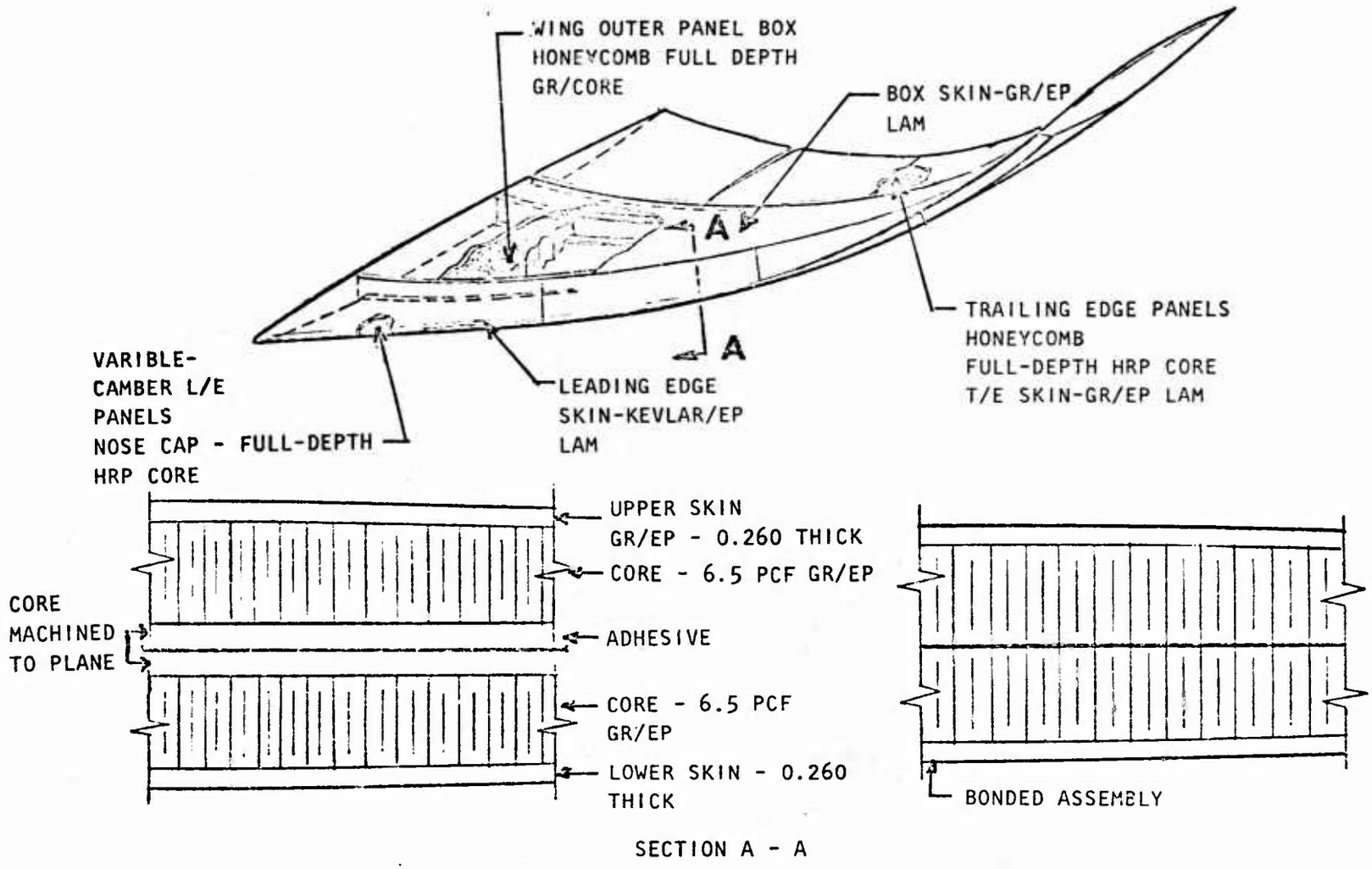

Figure 154. ADCA outer wing structure.

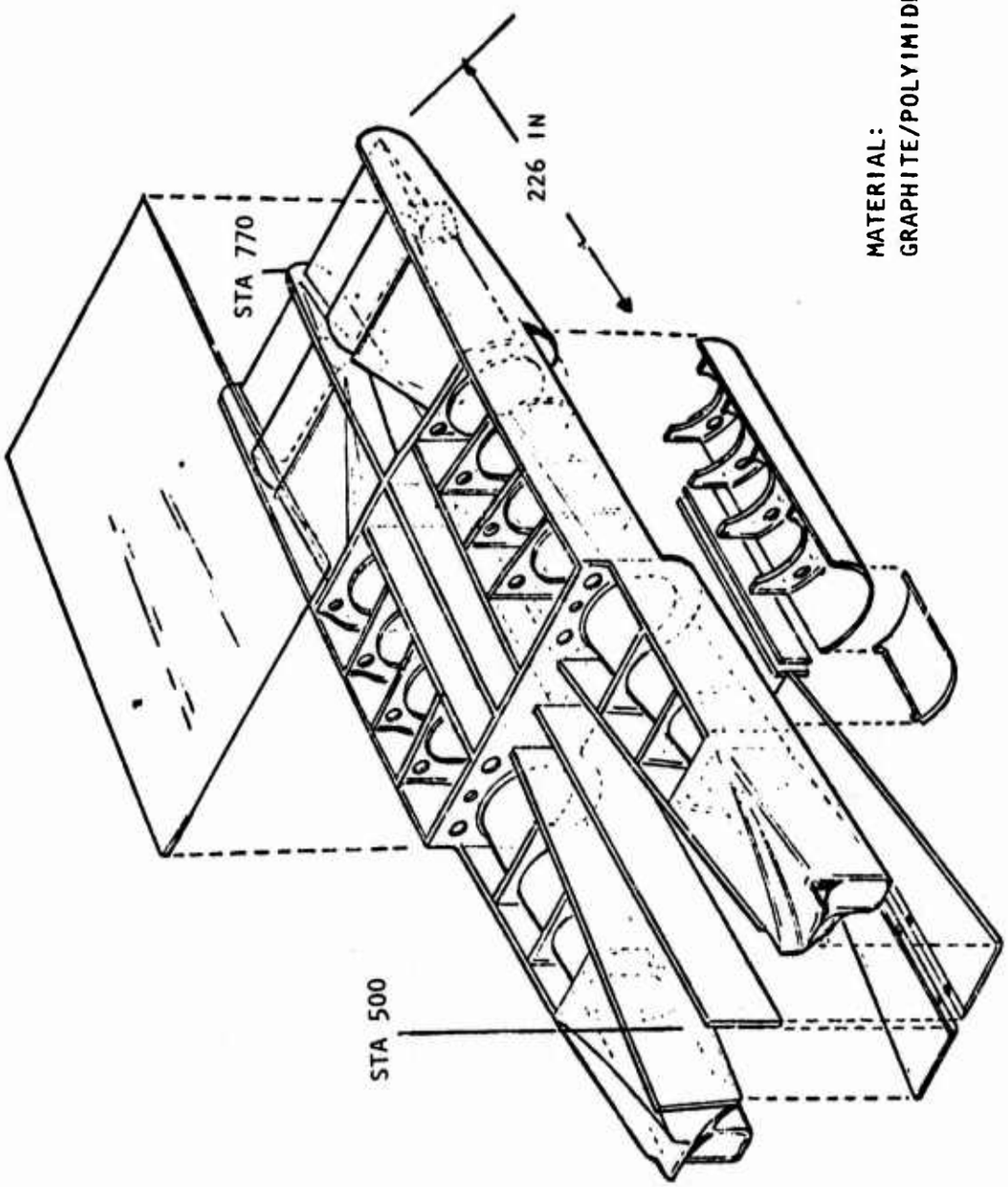

Figure 155. ADCA propulsion module.

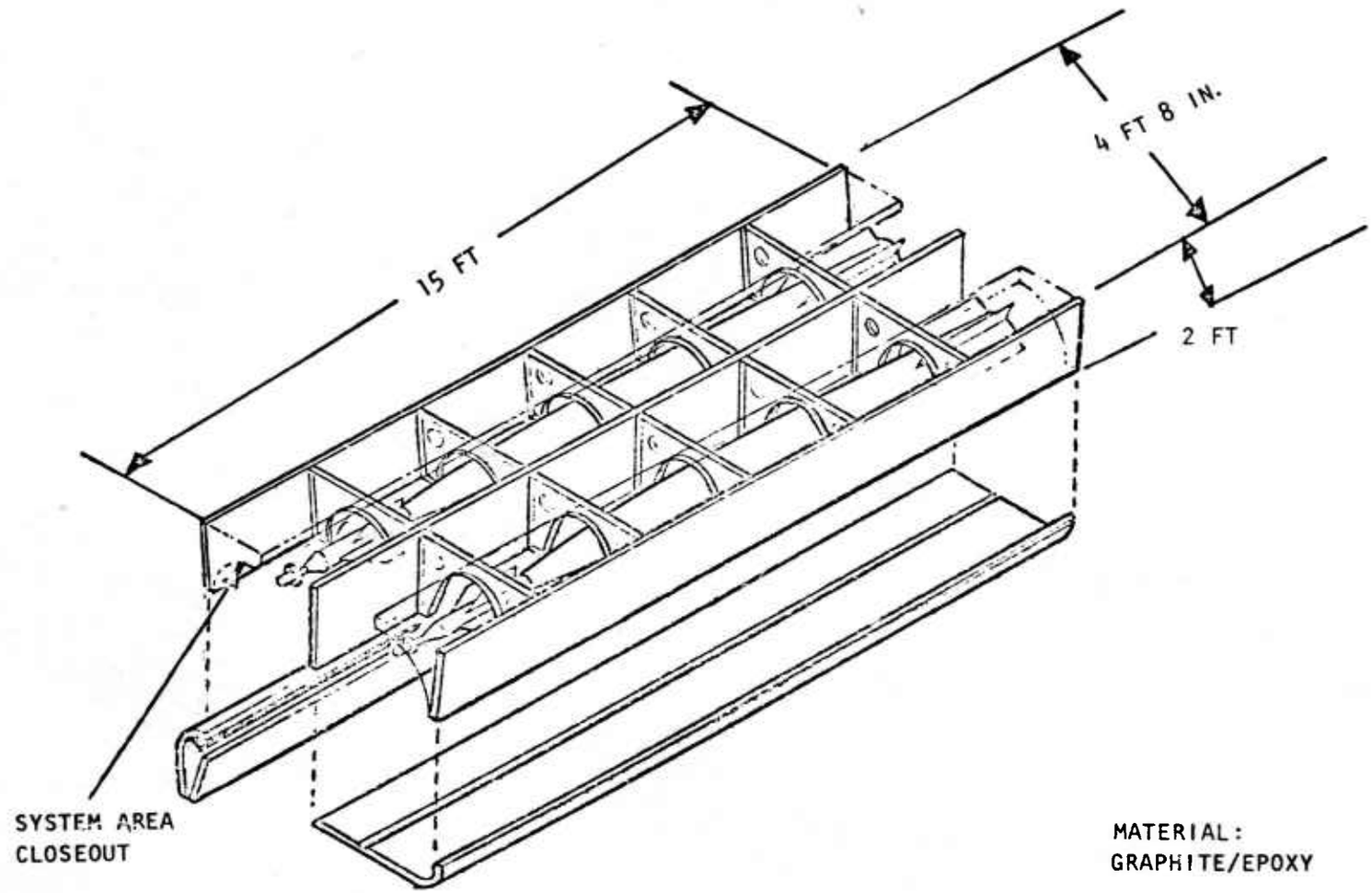

Figure 156. ADCA weapons bay structure.

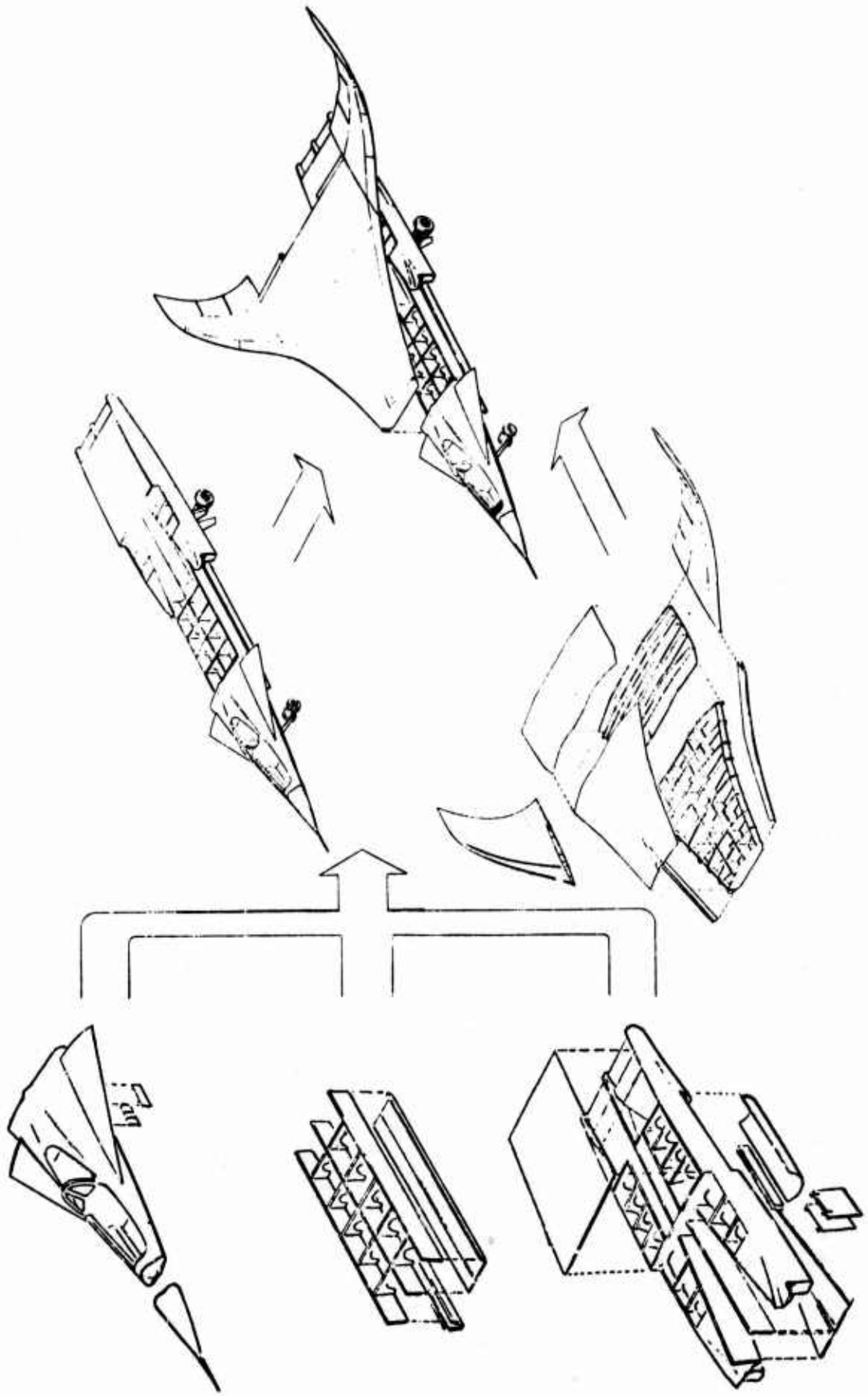

Figure 157. ADCA final assembly.

TABLE 37. ADCA COST TRADE STUDY

	AMPR WEIGHT	PRODUCTION HOURS PER POUND @ T1	FABRICATION & ASSY. PRODUCTION HOURS	TOOLING HOURS PER POUND	BASIC TOOLING HOURS	TOTAL MFG. HOURS T1	TOTAL PRODUCTION HOURS - 300 UNITS 78% CRC	TOTAL TOOLING MAINTENANCE HOURS 300 UNITS 100% SLOPE	PRODUCTION AVERAGE UNIT COST	TOOLING MATERIAL COST T1	PRODUCTION MATERIAL COST T1	TOTAL MATERIAL COST T1	PRODUCTION & TOOLING AVERAGE UNIT COST
FORWARD FUSELAGE													
BASELINE MULTI - SPAR - HONEYCOMB PANELS	504	10	5040	54	27,216	33,264	300,238	24,053	1001	81,648	20,106	101,754	1188
METAL CONFIGURATION	690	14	9660	54	37,260	46,920	575,379	32,930	1918	111,780	33,327	145,107	2152
WING CARRY THRU													
BASELINE HONEYCOMB PANELS MULTI SPAR	1426	10	14,260	54	77,004	91,264	849,370	68,056	2831	231,012	50,489	311,436	3315
OPTION - 1 - MULTI - SPAR MONO - SKIN	1626	12	19,512	54	87,804	107,316	1,162,195	77,601	3874	263,472	53,172	316,584	4425
OPTION - 2 - MULTI - RIB - MONO - SKIN HAT STRINGER	1286	12	15,432	54	69,444	84,876	919,178	61,375	3064	208,332	40,902	249,234	3490
METAL CONFIGURATION	1836	19	34,884	54	99,144	134,028	2,077,794	87,623	6926	297,432	54,797	352,229	7549
WING OUTER PANEL													
BASELINE GRAPHITE/EPOXY HONEYCOMB FULL DEPTH GRAPHITE FABRIC CORE	760	10	7600	54	41,040	48,640	452,680	36,271	1509	123,120	26,904	150,004	1767
OPTION - 1 - MULTI SPAR MONO SKIN	868	12	10,416	54	46,872	57,288	620,409	41,425	2068	140,616	26,040	166,656	2962
METAL CONFIGURATION	1802	19	28,832	54	97,308	126,140	1,717,323	86,000	5724	291,924	38,894	330,818	6335
LEADING EDGE CONTROL PANELS													
BASELINE GRAPHITE/EPOXY NOSE CAP FULL DEPTH CORE	80	10	840	54	4752	5632	52,416	4199	175	14,256	2802	17,058	205
METAL CONFIGURATION	234	10	2340	54	12,636	14,976	139,378	11,168	465	37,908	21,238	59,146	544
TRAILING EDGE CONTROL PANELS													
BASELINE GRAPHITE/EPOXY HONEYCOMB FULL DEPTH CORE	250	10	2500	54	13,500	16,000	148,908	11,931	496	40,230	8850	49,350	581
METAL CONFIGURATION	368	10	3680	54	19,872	23,552	219,192	17,563	731	59,616	28,015	87,631	855
FORWARD INTERMEDIATE FUSELAGE													
BASELINE MULTI SPAR - HONEYCOMB PANELS	1045	10	10,450	54	56,430	66,880	622,435	49,873	2075	169,290	68,475	237,765	2429
OPTION - 1 - SKIN - STRINGER	938	12	11,256	54	50,652	61,908	670,643	44,766	2235	151,956	28,140	180,096	2753
METAL CONFIGURATION	1501	16	24,016	54	81,054	105,070	1,430,467	71,636	4768	243,162	59,028	302,190	5277
AFT INTERMEDIATE FUSELAGE													
BASELINE MULTI - SPAR - HONEYCOMB PANELS	485	10	4,850	54	26,190	31,040	288,881	23,147	963	78,570	18,474	105,054	1127
METAL CONFIGURATION	766	16	12,256	54	41,364	53,620	730,005	36,558	2433	124,092	36,348	160,440	2693
AFT FUSELAGE - NACELLES													
BASELINE FRAMES&TONG'S GRAPHITE/POLYIMIDE HONEYCOMB PANELS - P/I FIBERGLASS CORE	695	13	9035	54	37,530	46,565	538,152	33,169	1794	112,590	29,190	141,768	2030
METAL CONFIGURATION	950	19	18,050	54	51,300	69,350	1,075,114	45,338	3584	153,900	57,815	211,715	3900
WEAPONS BAY DOORS													
BASELINE GRAPHITE/EPOXY HONEYCOMB FABRIC CORE	527	10	5270	54	28,458	33,728	313,898	25,151	1046	85,374	18,654	104,028	1225
METAL CONFIGURATION	559	14	7826	54	30,186	38,012	466,140	26,678	1554	90,558	48,971	139,529	1743
ENGINE DUCT													
BASELINE GRAPHITE/EPOXY HONEYCOMB	300	10	3000	54	16,200	19,200	178,689	14,316	596	48,600	11,160	59,760	697
METAL CONFIGURATION	305	14	4270	54	16,470	21,190	254,334	14,556	848	49,410	13,322	62,732	951
VARIABLE CANARD													
BASELINE GRAPHITE/EPOXY SKINS FULL DEPTH H/C	166	10	1660	54	8964	10,624	98,875	7,922	330	26,892	5,574	32,466	386
METAL CONFIGURATION	250	14	3500	54	13,500	17,000	208,471	11,931	695	40,500	4,849	4,849	780

REVISED 9-12-75

Since sufficient detail was not available to permit estimation of labor costs on an operational basis, a "cost per finished pound of structure" approach was taken. Salient assumptions made are discussed below:

1. The hours per pound shown for composite and metal configurations reflect the estimated fabrication costs through major subassembly only (forward fuselage, wing center section, aft fuselage, etc). Estimates are not included for final assembly, mating, bracketry, subsystems, installations, and checkout.

2. Manufacturing supporting functions, i.e., Planning, Quality Control, Manufacturing Engineering, Order Release, and Scheduling, are not included.

3. The manufacturing and tooling hours per pound of metal baseline structure were derived from Rockwell historical data compiled on similar programs. The F-100 and A3J programs were used for the comparisons. The individual aircraft sections (wing, forward fuselage, control surfaces, etc) were compared to the ADCA design, and weight adjustments were made for the respective sections. The hours per pound were then estimated for the 1980-1985 time span. The forecasted technology advancements were estimated and applied to arrive at the aircraft average hour per pound use for the cost trade in manufacturing and tooling projections.

4. Current data on composite tooling hours per pound experience in IR&D programs were used to establish baseline hours per pound. The projected hours per pound were derived using the baseline hours, new tooling concepts, materials, and quantity. The 1980-1985 composite tooling hours per pound shown in the cost trade study happened to turn out the same as for the metal configuration.

5. The labor hours per pound of composite construction were estimated using Rockwell available experience, as well as that of other aerospace companies, including those in present active cooperative programs with Rockwell. Cost projections schemes generated in internal and Government-sponsored programs were also perused. The projections shown are the best engineering judgement based on analysis of the above data. The cost of advanced technology processes not currently in production status is based on present costs, modified by projections of Rockwell and other aerospace companies and suppliers to the 1980-1985 time period.

6. The materials for the metal configuration were computed by dollars per pound, using current prices plus unknowns escalated to the 1980-1985 time span.

7. Material prices per pound for composite configurations reflect projected price reduction due to the increased demand and usage of composite materials.

Section VI

PRELIMINARY PAYOFF ASSESSMENT

INTRODUCTION

This section contains a discussion of the weight and performance comparison between the Task I all-composite baseline configuration, D572-4C, and the advanced metallic baseline configuration, D572-5B. Also included is a summary of the cost analysis showing cost comparisons between the two baseline configurations. In addition, a discussion is included defining the method to be used during Task IV of the study for payoff assessment of the all-composite configuration in comparison to the advanced metallic configuration.

WEIGHT AND PERFORMANCE COMPARISON

The potential payoff of the Advanced Design Composite Aircraft design approach can be readily seen by comparing performance and weights with its metallic counterpart. (See Table 38.)

The two vehicles selected for the weight and performance comparison table are the parametric -4C composite and -5B metallic aircraft which were presented in the summary of the configuration development section of this report. The most significant payoff of the composite aircraft is the 24.7 percent lighter structural weight. Nearly all of the performance benefits are derived from this weight savings. The only performance decrement, the Battlefield Mission Radius, can be attributed to the smaller fuel load carried aboard the composite aircraft, which can be compensated for by the excess volume contained in the composite wing center section. However, both vehicles exceed the desired radius as configured.

COST ANALYSIS

INTRODUCTION

Production or unit average flyaway cost estimates were generated for the ADCA "all-metal" baseline (design D572-5A), the ADCA composite baseline (design D572-4B), and the various cost/construction-type trade studies. These production costs were estimated using data from Manufacturing and a slightly modified version of the Production Cost Model (PCM).

TABLE 38. WEIGHT AND PERFORMANCE COMPARISON

Parameter	Composite -4C	Metallic -5B	Composite Payoff
Takeoff Gross Weight	34069	37213	9.2%
Wing Area	400	500	-
Wing Loading (PSF)	85.2	74.4	-
Engines	Two	F404-GE-404	Turbofans
Installed Thrust to Weight	0.7012	0.6419	8.4%
Structural Weight	9175	11441	24.7%
Empty Weight	20700	22996	11.1%
Fuel Weight	6962	7865	12.9%
Design Mission Radius	400	400	0 NMI
Battlefield Mission Radius	252	268	-16 NMI
Ferry Mission Range	2667	1937	730 NMI
Takeoff-Maxpwr, Flaps 30°	2404	2532	128 Ft
Landing-Thrust Reverse Flaps 30°	2454	2454	-2 Ft
P_S - 0.9M/30,000 Ft/5 g	-13	-25	12 Ft/Sec
P_S - 1.2M/30,000 Ft/5 g	268	168	100 Ft/Sec

For this portion of the ADCA contract, only airframe costs are considered since the avionics package is undefined and propulsion cost estimates have not been received yet.

The methodology used in costing the two baseline aircraft and the trades will be discussed later in this section, but just as an aid to understanding the cost methodology, a discussion of the structure and operation of the PCM follows.

PRODUCTION COST MODEL

The Production Cost Model (PCM) was developed in 1972 in support of the advanced Tactical Fighter (ATF) study program. This is a statistical/parametric computerized cost model based on Rockwell historical data which is intended to be used to estimate production costs for advanced aircraft systems where only a limited amount of data is available (e.g., preliminary design stage). The PCM is specifically directed toward airframe costs; avionics and propulsion costs are model thru-puts. The production cost estimate is broken down into a Work Breakdown Structure (WBS) consisting of manufacturing, tooling, engineering, planning, quality and reliability assurance, and material cost elements; and cost estimating relationships are employed which are sensitive to numerous design parameters including weights, materials mix, construction type, performance criteria, and production quantity and rates. The model is intended to realistically assess the cost impact of changes in the preceding design parameters.

The heart of this model are matrices containing the "manufacturing hours per pound structure weight" values. These matrices contain hours per pound data for fuselage, wing, nacelle, and empennage. The individual structural element matrices are further broken down by construction type (e.g. skin stringer) and material type. The data contained in these matrices is derived from Rockwell Manufacturing and Pricing history. In the operation of the model, the hours per pound values in this matrix are adjusted for the AMPR weight and the production quantity of the subject aircraft. Hours per pound decreases along an 87-percent slope (Wright) learning curve as AMPR weight increases over 15,000 pounds (the chosen reference AMPR weight) and increases along the same curve as AMPR weight drops below 15,000 pounds. As would be expected, hours per pound decreases along learning curves appropriate to the chosen construction type as production quantity increases. The manufacturing hours total for each structural element is the sum of the products of weights and hours per pound for each material/construction type within each structural element appropriately adjusted for AMPR weight and production quantity.

Assembly costs are broken out into basic structure assembly, final integration and assembly, and material costs for each. Basic structure assembly hours is a function of structure weight; final integration and assembly is a function of subsystem total weight, and increases with the weight of the subsystems to be installed. Final integration and assembly is also adjusted for

the year of production; this is to reflect the increasing complexity of subsystems and subsystem installation as the years go by. The material costs for basic and final assembly are derived from the amount of structural and system hardware (e.g. fasteners, joints, etc) necessary for these assembly processes.

Subsystem costs consist of manufacturing hours and material costs for Rockwell-produced subsystems and material costs for purchased subsystems. Manufacturing hours for Rockwell-produced subsystems are a product of subsystem weight, percentage of the particular subsystem produced at Rockwell, subsystem manufacturing hours per pound, and an appropriate learning curve factor. Purchased subsystem material costs are a product of subsystem weight, percentage of the subsystem purchased from subcontractors, average cost per pound of purchased subsystems, and an appropriate learning curve factor. Subsystem costs and factors again are based on historical data.

Tooling hours for manufacturing and tooling material costs are derived from historical data. Tooling hours is a function of initial production rate, final production rate, total production quantity, aircraft AMPR weight, and RDT&E/production program tooling concurrency or non-concurrency. Total airframe tooling hours are then apportioned over the various structural elements according to ratios derived historically. Tooling material costs are a function of tooling hours and the year of production. The model contains a tooling material factor, again based on historical data, which predicts an increase in tooling material cost due to increased tooling sophistication as the years go by.

Engineering hours through the first unit are derived using regression relationships from the Rockwell RDT&E cost model. To find engineering costs for the entire production run, first-unit costs are extrapolated down a 55-percent-slope (Wright) learning curve for the chosen production quantity.

Planning and quality control and reliability assurance are derived as percentages of the functions they support. Quality control and reliability assurance is a percentage of manufacturing and tooling total hours; planning is a function of manufacturing, tooling, and engineering total hours.

Manufacturing raw material costs are determined as follows: the total weight of each major structural element is broken down into a set of material process (e.g. plate, forging, etc) weights. The set of material process weights is then costed as a function of process type, process type fly-to-buy ratio, process type mortality factor as a function of production quantity, and process type dollars per pound. These calculated dollars are then summed to final total raw material dollars for each structural element.

The elements of the work breakdown structure are summed to find aircraft costs, and then General and Administrative (G&A) and fee are added on to calculate total program cost. Unit average flyaway cost is then calculated by dividing total program cost by production quantity.

PCM MODIFICATIONS AND ASSUMPTIONS

The PCM has built-in manufacturing hours per pound values and construction-type learning curves. For the ADCA study, however, Manufacturing generated hours per pound data and chose the learning curves which would be used in the costing process. The model was modified for this process. Also, the nacelle tooling hours and tooling material costs are now included in the fuselage tooling and tooling material costs. This was deemed appropriate since the nacelle is part of the fuselage in these designs. The historical tooling hours and tooling material cost data in the model are used for both baselines and all trades. While this does not seem to reflect composite tooling costs adequately, this method treats each baseline and trade equally and is in agreement, in spirit, if not in absolute dollar value, with Manufacturing's treatment of tooling hours and material costs.

METHODOLOGY

The following methodology was used in estimating costs for the ADCA baselines and trades:

1. Manufacturing developed hours per pound data and chose learning curves for each baseline and trade.

2. The data from Manufacturing was converted for use by the PCM, and combined with inputs from the Weights and Structure groups to form model inputs.

3. The model was run to estimate production costs.

The development of the hours per pound and learning curve data by Manufacturing is covered in preceding sections of this report.

The data from Manufacturing was converted in the following way. Manufacturing T_1 was adjusted to the model hours per pound reference point of 500 production units and 15,000 pounds AMPR weight. For the two baseline cases, the model was then run. For the trades, however, the hours per pound data was used to adjust the baseline hours per pound values, thereby reflecting the weight and construction type changes due to the trades in the manufacturing

hours and, resultantly, the production cost. This was a "weighted average" adjustment to the baseline hours per pound data in which the weights and hours per pound changes due to the construction-type trades were combined with the baseline weights and hours per pound in a manner which gave the correct statistical "weight" to the changes caused by the trades.

The hours per pound and production costs for the two baseline design, -4B and 5A, and the "weighted average" hours per pound of the trades are presented in Table 39. Baseline production costs and work breakdown structure are presented in Tables 40 through 43.

TABLE 39. WEIGHTED AVERAGE HRS/LB AT 500 UNITS

	Fuselage	Wing/Canard
Composite baseline	1.79	1.68
Trade 1, Wing Carry-Thru	1.79	1.88
Trade 2, Wing Carry-Thru	1.79	1.86
Trade 3, Wing Outer Panel	1.79	1.79
Trade 4, Stringer Fuselage	1.85	1.73
Metal baseline	2.80	2.76

	Production Costs (Millions 1975 $)
Composite baseline	2.746
Metal baseline	4.213

TABLE 40. COMPOSITE BASELINE CONFIGURATION COSTS

AIRCRAFT: D572-4 COMPOSITE ADCA BASELINE
ALL COSTS IN MILLIONS AND IN 1975 DOLLARS

PRODUCTION COST FOR 300 UNITS
UNIT AVG. FLYAWAY COST 2.746

WORK BREAKDOWN STRUCTURE	LABOR COST					MATERIAL COST		TOTAL COST
	MFG.	TOOL.	PLNG.	ENGR.	G&A	MFG.	TOOL.	
TOTAL PROGRAM COST INCLUDING FEE	381.71	71.22	33.79	40.52	51.59	235.66	9.01	823.84
TOTAL PROGRAM COST INCLUDING G&A	347.01	64.74	30.72	36.84	46.90	214.24	8.19	748.97
TOTAL PROGRAM COST LESS G&A	315.95	58.95	27.97	33.54	42.70	195.06	7.46	681.97
AIR VEHICLE	315.95	58.95	27.97	33.54	42.70	195.06	7.46	681.97
AIRFRAME	162.35	52.35	16.99	33.54	24.41	188.91	6.62	485.16
BASIC STRUCTURE	95.02	52.35	10.61	8.11	16.72	58.97	6.62	248.41
FUSELAGE	35.67	33.60	5.05	4.85	7.84	24.31	4.25	115.57
WING	33.22	12.50	3.30	2.53	5.20	32.11	1.58	90.44
CANARDS	1.49	5.19	0.50	0.73	0.75	1.56	0.66	10.89
NACELLES	0.0	0.0	0.0	0.0	0.0	0.0	0.0	0.0
BASIC STRUCTURE ASSEMELY	24.64	1.06	1.76	0.0	2.93	0.99	0.13	31.51
LANDING GEAR	0.0	0.0	0.0	0.60	0.0	13.48	0.0	14.07
FUEL SYSTEM	6.40	0.0	0.56	1.72	0.73	4.61	0.0	14.01
FLIGHT VEHICLE POWER	31.07	0.0	2.55	6.06	3.55	58.12	0.0	101.29
ENVIRONMENTAL CONTROL	0.0	0.0	0.0	2.09	0.0	25.90	0.0	27.99
CREW ACCOMMODATIONS	6.75	0.0	0.52	0.80	0.77	0.0	0.0	8.84
CONTROLS AND DISPLAYS	0.0	0.0	0.0	0.0	0.0	8.56	0.0	8.56
FLIGHT CONTROLS	20.72	0.0	1.42	0.0	2.37	0.0	0.0	24.50
ARMAMENT	0.0	0.0	0.0	0.30	0.0	19.26	0.0	19.55
AIR INDUCTION CONTROL SYSTEM	2.39	0.0	0.21	0.66	0.27	0.0	0.0	3.53
AIRFRAME INTEGRATION & CHECK	0.0	0.0	0.0	16.92	0.0	0.0	0.0	16.92
ENGINEERING TECHNOLOGIES	0.0	0.0	0.0	12.28	0.0	0.0	0.0	12.28
DESIGN SUPPORT TECHNOLOGIES	0.0	0.0	0.0	1.74	0.0	0.0	0.0	1.74
AIRFRAME INSTALL & CHECKOUT	0.0	0.0	0.0	2.89	0.0	0.0	0.0	2.89
PROPULSION (GFE)	0.0	0.0	0.0	0.0	0.0	0.0	0.0	0.33
AVIONICS (GFE)	0.0	0.0	0.0	0.0	0.0	0.0	0.0	0.0
A/V INTEGRATION, ASSY, INSTALL	153.00	6.60	10.99	0.0	18.29	6.16	0.86	196.67

TABLE 41. COMPOSITE BASELINE CONFIGURATION WEIGHTS

AIRCRAFT: D572-4 COMPOSITE ADCA BASELINE

AIRCRAFT WEIGHTS - IN POUNDS

	AL	TI	ST	BO	GR	EG	SA	TOTAL
FUSELAGE	78.	171.	69.	0.	2066.	27.	0.	3236.
FRAME/LONG	0.	171.	69.	0.	695.	0.	0.	935.
SKIN-STRGR	78.	0.	0.	0.	0.	0.	0.	78.
BOND HONEY	0.	0.	0.	0.	1391.	27.	0.	1418.
BRAZE HONEY		0.	0.				0.	0.
DIFF BOND		0.					0.	0.
MISC								805.
WING	125.	25.	0.	0.	2923.	0.	0.	3224.
SKIN-STRGR	0.	0.	0.	0.	0.	0.	0.	0.
MULTI-SPAR	0.	25.	0.	0.	515.	0.	0.	540.
BOND HONEY	125.	0.	0.	0.	2408.	0.	0.	2533.
BRAZE HONEY		0.	0.				0.	0.
DIFF BOND		0.					0.	0.
MISC								151.
CANARDS	0.	16.	2.	0.	117.	0.	0.	145.
SKIN-STRGR	0.	0.	0.	0.	0.	0.	0.	0.
MULTI-SPAR	0.	0.	0.	0.	0.	0.	0.	0.
BOND HONEY	0.	16.	2.	0.	117.	0.	0.	135.
BRAZE HONEY		0.	0.				0.	0.
DIFF BOND		0.					0.	0.
MISC								10.
NACELLE	0.	0.	0.	0.	0.	0.	0.	0.
FRAME/LONG	0.	0.	0.	0.	0.	0.	0.	0.
SKIN-STRGR	0.	0.	0.	0.	0.	0.	0.	0.
BOND HONEY	0.	0.	0.	0.	0.	0.	0.	0.
BRAZE HONEY		0.	0.				0.	0.
DIFF BOND		0.					0.	0.
MISC								0.

WEIGHT DATA - IN POUNDS	
AMPR WEIGHT	13211.
STRUCTURE WT	7885.
STRUCTURAL HDWE WT	133.
SYSTEM HDWE WT	133.
LANDING GEAR WT	1280.
FUEL SYSTEM WT	750.
ELECTRICAL SYSTEM WT	680.
HYDRAULIC SYSTEM WT	430.
AUX POWER SYSTEM WT	310.
ECS WT	530.
CREW ACCOM WT	320.
CONTROL & DISPLAY WT	120.
FLIGHT CONTROL WT	950.
ARMAMENT WT	560.
AICS MECHANISM WT	300.
EQUIPMENT WT	60.
ENGINE WT	5375.
EMPTY WT	19265.
FUEL WT	7060.
TOGW	30432.

DESIGN VARIABLES	
WING AREA-SQ FT	400.
CANARDS AREA-SQ FT	35.
WETTED AREA-SQ FT	1772.
WING + HORIZ AREA	435.
WING SPAN-FT	31.6
HORIZ SPAN-FT	10.0
OVERALL LENGTH-FT	57.0
ASPECT RATIO	2.50
DYNAMIC PRESSURE	2133.

TABLE 42. ADVANCED METALLIC BASELINE CONFIGURATION COSTS

AIRCRAFT: D572-5A ALL-METAL ADCA BASELINE
ALL COSTS IN MILLIONS AND IN 1975 DOLLARS

PRODUCTION COST FOR 300 UNITS
UNIT AVG. FLYAWAY COST 4.213

WORK BREAKDOWN STRUCTURE	LABOR COST					MATERIAL COST		TOTAL
	MFG.	TOOL.	PLNG.	ENGR.	G&A	MFG.	TOOL.	COST
TOTAL PROGRAM COST INCLUDING FEE	705.91	93.50	57.94	46.19	91.12	256.96	11.63	1263.77
TOTAL PROGRAM COST INCLUDING G&A	641.73	85.00	52.67	41.99	82.84	233.60	10.75	1148.91
TOTAL PROGRAM COST LESS G&A	584.30	77.39	47.96	38.23	75.42	212.69	9.79	1046.11
AIR VEHICLE	584.30	77.39	47.96	38.23	75.42	212.69	9.79	1046.11
AIRFRAME	333.56	66.52	30.15	38.23	45.79	203.55	8.67	728.49
BASIC STRUCTURE	263.83	68.52	23.48	10.92	37.82	69.84	8.67	483.07
FUSELAGE	148.82	44.12	13.64	6.64	21.95	38.34	5.58	279.09
WING	77.40	16.41	6.66	3.54	10.68	28.58	2.08	145.34
CANARDS	4.00	6.81	0.78	0.74	1.22	1.70	0.86	16.11
NACELLES	0.0	0.0	0.0	0.0	0.0	0.0	0.0	0.0
BASIC STRUCTURE ASSEMBLY	33.60	1.19	2.39	0.6	3.97	1.23	0.15	42.52
LANDING GEAR	0.0	0.0	0.0	0.79	0.0	18.36	0.0	19.16
FUEL SYSTEM	4.86	0.0	0.45	1.74	0.56	3.50	0.0	11.11
FLIGHT VEHICLE POWER	31.07	0.0	2.59	6.57	3.55	58.12	0.0	101.90
ENVIRONMENTAL CONTROL	0.0	0.0	0.0	2.23	0.0	25.90	0.0	28.13
CREW ACCOMMODATIONS	6.75	0.0	0.52	0.80	0.77	0.0	0.0	8.84
CONTROLS AND DISPLAYS	0.0	0.0	0.0	0.0	0.0	8.56	0.0	8.56
FLIGHT CONTROLS	24.64	0.0	1.69	0.0	2.81	0.0	0.0	29.15
ARMAMENT	0.0	0.0	0.0	0.30	0.0	19.26	0.0	19.55
AIR INDUCTION CONTROL SYSTEM	2.43	0.0	0.25	1.22	0.28	0.0	0.0	4.18
AIRFRAME INTEGRATION & CHECK	0.0	0.0	0.0	18.56	0.0	0.0	0.0	18.56
ENGINEERING TECHNOLOGIES	0.0	0.0	0.0	13.04	0.0	0.0	0.0	13.04
DESIGN SUPPORT TECHNOLOGIES	0.0	0.0	0.0	2.08	0.0	0.0	0.0	2.08
AIRFRAME INSTALL & CHECKOUT	0.0	0.0	0.0	3.44	0.0	0.0	0.0	3.44
PROPULSION (GFE)	0.0	0.0	0.0	0.0	0.0	0.0	0.0	0.33
AVIONICS (GFE)	0.0	0.0	0.0	0.0	0.0	0.0	0.0	0.0
A/V INTEGRATION, ASSY, INSTALL	250.72	8.87	17.80	0.0	29.63	9.14	1.12	317.29

TABLE 43. ADVANCED METALLIC BASELINE CONFIGURATION WEIGHTS

AIRCRAFT: D572-5A ALL-METAL ADCA BASELINE

AIRCRAFT WEIGHTS - IN POUNDS

	AL	TI	SI	BO	GR	EG	SA	TOTAL
FUSELAGE	2473.	796.	71.	0.	310.	43.	0.	4542.
FRAME/LONG	1697.	0.	71.	0.	0.	0.	0.	1768.
SKIN-STRGR	527.	156.	0.	0.	0.	43.	0.	726.
BOND HONEY	249.	0.	0.	0.	310.	0.	0.	559.
BRAZE HONEY		0.	0.				0.	0.
DIFF BOND		640.					0.	640.
MISC								849.
WING	3710.	270.	0.	0.	403.	234.	0.	4834.
SKIN-STRGR	0.	0.	0.	0.	0.	0.	0.	0.
MULTI-SPAR	3710.	270.	0.	0.	0.	202.	0.	4182.
BOND HONEY	0.	0.	0.	0.	403.	32.	0.	435.
BRAZE HONEY		0.	0.				0.	0.
DIFF BOND		0.					0.	0.
MISC								217.
CANARDS	195.	35.	4.	0.	0.	0.	0.	250.
SKIN-STRGR	0.	0.	0.	0.	0.	0.	0.	0.
MULTI-SPAR	0.	0.	0.	0.	0.	0.	0.	0.
BOND HONEY	195.	35.	4.	0.	0.	0.	0.	234.
BRAZE HONEY		0.	0.				0.	0.
DIFF BOND		0.					0.	0.
MISC								16.
NACELLE	0.	0.	0.	0.	0.	0.	0.	0.
FRAME/LONG	0.	0.	0.	0.	0.	0.	0.	0.
SKIN-STRGR	0.	0.	0.	0.	0.	0.	0.	0.
BOND HONEY	0.	0.	0.	0.	0.	0.	0.	0.
BRAZE HONEY		0.	0.				0.	0.
DIFF BOND		0.					0.	0.
MISC								0.

WEIGHT DATA - IN POUNDS	
AMPR WEIGHT	16683.
STRUCTURE WT	11370.
STRUCTURAL HDWE WT	193.
SYSTEM HDWE WT	193.
LANDING GEAR WT	1744.
FUEL SYSTEM WT	570.
ELECTRICAL SYSTEM WT	680.
HYDRAULIC SYSTEM WT	430.
AUX POWER SYSTEM WT	310.
ECS WT	530.
CREW ACCOM WT	320.
CONTROL & DISPLAY WT	120.
FLIGHT CONTROL WT	1130.
ARMAMENT WT	500.
AICS MECHANISM WT	305.
EQUIPMENT WT	50.
ENGINE WT	5375.
EMPTY WT	22745.
FUEL WT	6033.
TOGW	35385.

DESIGN VARIABLES	
WING AREA-SQ FT	500.
CANARDS AREA-SQ FT	42.
WETTED AREA-SQ FT	1883.
WING + HORIZ AREA	542.
WING SPAN-FT	35.3
HORIZ SPAN-FT	10.0
OVERALL LENGTH-FT	57.0
ASPECT RATIO	2.50
DYNAMIC PRESSURE	2133.

RFFERENCES

1. Rockwell LAAD Report NA-66-862, "Theoretical Prediction of Supersonic Pressure Drag," by E. Bonner, October, 1966.

2. NACA RM L551.23, "Drag of Canopies at Transonic and Supersonic Speeds," by Sherwood Hoffman and A. Warner Robins, February, 1956.

3. NACA TN-4405, "Free-Flight Investigation to Determine the Drag of Flat and Vee-Windshield Canopies on a Parabolic Fuselage With and Without Transonic Indentation Between Mach Numbers of 0.75 and 1.35," by W. L. Kovyomjian and Sherwood Hoffman, September 1958.

4. Rockwell LAAD TFD-75-713, "Present Status of the Rockwell International Flexible Unified Distributed Panel Program," by K. M. Dunn, July, 1975.

5. Rockwell LAAD Report NA-75-846, "Analysis of Low Speed Wind Tunnel Test of D572-1 Supersonic Cruise Vehicle," by T. Goebel and D. Sitar, December, 1974.

6. Rockwell LAAD Report NA-75-129, "Analysis of Low Speed Wind Tunnel Test of Revised 0.0625 Scale D572-1 Supercruise Vehicle," by O. M. Sokolsky, July, 1975.

7. NASA Preliminary Supersonic Wind Tunnel Data for D575-2A Configuration (Langley UPWT TSI PRJ1116 Batch No. 1, 2, 3, 4, 5).

8. Rockwell LAAD Report NA-75-596, "Substantiation of the Longitudinal and Laterial/Directional Characteristics of the D572-4B Configuration," by O. M. Sokolsky and B. E. Moore.

9. Rockwell LAAD Report NA-75-597, "Analysis of Supersonic Wind Tunnel Test of 0.085 Scale Model of Supersonic Cruise Configuration D575-2A in Langley UPWT TSI (PRJ 1114 and 1116)," by O. M. Sokolsky.

10. Rockwell LAAD Report NA-75-598, "Stability and Control of Three Supercruiser Wing Shapes," By C. D. Wiler.

11. Jet Flap Exhaust System Design Report, General Electric T.M. No. 75-233, dated 20 April 1975.

12. Kaneshiro, Roy S., "Weight Estimation of Hydraulic Secondary Power System," paper presented at Society of Aeronautical Weight Engineers Conference, Atlanta, Georgia, 1972.

13 Rockwell International, Los Angeles Aircraft Division, A Structural Weight Estimation Program (SWEEP) for Aircraft, ASD/XR 74-10, Aeronautical Systems Division, Wright-Patterson AFB, Ohio.

☆ U. S. GOVERNMENT PRINTING OFFICE: 1976 — 657-630/862